



Technische Universität München

Fakultät für Mathematik

# Well-Posedness of Nonlocal and Mixed-Dimensional Phase-Field Models Applied to Tumor Growth

Marvin Fritz, M.Sc.

Vollständiger Abdruck der von der Fakultät für Mathematik der Technischen Universität München zur Erlangung des akademischen Grades eines

**Doktors der Naturwissenschaften** (Dr. rer. nat.)

genehmigten Dissertation.

**Vorsitzende:** Prof. Dr. Christina Kuttler

**Prüfende der Dissertation:**

1. Prof. Dr. Barbara Wohlmuth
2. Prof. Dr. Daniel Matthes
3. Prof. Dr. Elisabetta Rocca

Die Dissertation wurde am 23.11.2021 bei der Technischen Universität München eingereicht und durch die Fakultät für Mathematik am 11.04.2022 angenommen.



## Zusammenfassung

In der vorliegenden Arbeit werden verschiedene Systeme zur Modellierung von Tumorwachstum vorgestellt. Wir folgen den 'Hallmarks of Cancer' (dt. Schlüsselmerkmale von Krebserkrankung) von Hanahan & Weinberg und beziehen die wichtigsten Charakteristiken von Tumorwachstum in unsere Modelle mit ein. In dieser Hinsicht wählen wir die Herangehensweise der diffusiven Grenzflächenmodelle und beschreiben den Tumor als eine Ansammlung von Zellen unter Verwendung eines Phasenfeldansatzes. Solche Modelle basieren auf einem mehrphasigen Konzept mit konstitutiven Gesetzen und Gleichgewichtsgesetzen für die einzelnen Bestandteile. Wir untersuchen diese Tumormodelle im Hinblick auf ihre mathematische Wohlgestelltheit und die Existenz schwacher Lösungen. Viele biologische Phänomene wie zeitliche und räumliche nichtlokale Effekte, komplexe Nichtlinearitäten und gemischtdimensionale Kopplungen sind in der mathematischen Onkologie involviert. Daher ist eine detaillierte Analysis dieser komplexen Systeme erforderlich, und wir liefern rigorose Beweise dafür. Die Grundidee des Beweises ist die Faedo–Galerkin-Methode, welche besagt, dass wir die partiellen Differentialgleichungen im Raum diskretisieren, approximative Lösungen erhalten, geeignete Energieschätzungen herleiten, die schwach konvergente Teilfolgen ergeben, und dann den Grenzwert nehmen, um das gewünschte kontinuierliche System zu erhalten. Abschließend geben wir einige Ideen zur numerischen Annäherung der Systeme, um die Entwicklung des Tumors unter den verschiedenen biologischen Effekten zu simulieren.

## Abstract

In this thesis, various systems for modeling tumor growth are presented. We follow the 'Hallmarks of Cancer' by Hanahan & Weinberg, and we include the main characteristics of cancer in our models. In this regard, we choose the path of diffusive interface models and describe the tumor as a collection of cells using a phase-field approach. Such systems are based on a multiphase ansatz using constitutive laws and balance laws for single constituents. We investigate these tumor models with respect to their mathematical well-posedness and the existence of weak solutions. Many biological phenomena, such as temporal and spatial nonlocal effects, complex nonlinearities, and mixed-dimensional couplings, are involved in mathematical oncology. As a result, detailed analysis of these complex systems is required, and we provide rigorous proofs for this. The basic idea behind the proof is the Faedo–Galerkin method, which states that we discretize the partial differential equations in space, obtain approximative solutions, derive suitable energy estimates yielding weakly convergent subsequences, and then take the limit to obtain the desired continuous system. Finally, we give some ideas on approximating the models numerically in order to simulate the evolution of the tumor under various biological effects.



## Acknowledgments

*In the broad light of day mathematicians check their equations and their proofs, leaving no stone unturned in their search for rigour. But, at night, under the full moon, they dream, they float among the stars and wonder at the miracle of the heavens. They are inspired. Without dreams there is no art, no mathematics, no life.*  
(Sir Michael Francis Atiyah)

Finally, it is completed, and I am nearing the end of my Ph.D. studies. After 3 year of Bachelor, 2 years of Master, and 4 years as a Ph.D. student, my studies come (seemingly) to an end. Math is amazing. It is clear, it is true, it is honest. I met a lot of wonderful people along the way, and I'd like to thank everyone I remember here.

First and foremost, I'd like to express my gratitude to my supervisor, Prof. Dr. Barbara Wohlmuth, for her patience, advice, and support. I'm also grateful to Prof. Dr. J. Tinsley Oden for his ongoing encouragement and for inviting me to his institute. I am extremely grateful to Prof. Dr. Elisabetta Rocca and Prof. Dr. Daniel Matthes for taking their valuable time and reviewing the thesis. I would also like to thank Prof. Dr. Christina Kuttler for agreeing to chair the examining committee.

Furthermore, I'd like to thank the past and present members of the M2 group. It was a lot of fun. I'd like to thank my office mates Markus Muhr and Dr. Mabel L. Rajendran for their help and productive discussions. I am thankful to Prof. Dr. Rainer Callies and Prof. Dr. Elisabeth Ullmann for their valuable advices. As former Ph.D. students of the chair, I am grateful to Dr. Piotr Swierczynski, Dr. Markus Huber, Dr. Ettore Vidotto, Dr. Jonas Latz, Dr. Mario T. Parente, and Dr. Daniel Drzisga for their assistance in the early and mid stages of my Ph.D. studies. Furthermore, I am grateful to my fellow Ph.D. students, postdocs, and former member of the group for the numerous chats, discussions, and entertaining lunch breaks in both the old and new Mensa. Jenny Radeck deserves special recognition for her helpfulness in dealing with bureaucratic issues. Thank you for making work such a pleasant, productive, and friendly environment.

I'd like to thank Dr. Carl-Friedrich Kreiner for being my mentor and providing valuable advice and counsel throughout my Master's and Ph.D. studies.

During my research, I had the opportunity to work with and learn a lot from many amazing people, especially Dr. Ernesto Lima and Dr. Prashant Jha from the University of Texas at Austin.

I am grateful to all of the proofreaders for the current text. Furthermore, I'd like to thank all of my friends who have helped me in various ways over the years, particularly Christian, Claudio, and Matthias. Furthermore, I'd like to express my heartfelt gratitude to my dear girlfriend Julia, who has always been there for me over the years. Finally, none of this would have been possible without the encouragement and support of my parents, Reiner and Claudia, as well as my brother, Fabian. A special thanks goes to Teddy as well as my cats, Pepe and Sam.

Thank you all, you are amazing.



## List of contributed articles

This thesis is based on the following articles:

### *Core articles as principal author*

- I) Marvin Fritz, Ernesto A.B.F. Lima, J. Tinsley Oden, Barbara Wohlmuth  
**On the unsteady Darcy–Forchheimer–Brinkman equation in local and nonlocal tumor growth models**  
*Mathematical Models and Methods in Applied Sciences*, 29(09):1691–1731, 2019  
(see also article [62] in the bibliography)
- II) Marvin Fritz, Ernesto A.B.F. Lima, Vanja Nikolić, J. Tinsley Oden, Barbara Wohlmuth  
**Local and nonlocal phase-field models of tumor growth and invasion due to ECM degradation**  
*Mathematical Models and Methods in Applied Sciences*, 29(13):2433–2468, 2019  
(see also article [61] in the bibliography)
- III) Marvin Fritz, Prashant K. Jha, Tobias Köppl, J. Tinsley Oden, Barbara Wohlmuth  
**Analysis of a new multispecies tumor growth model coupling 3D phase-fields with a 1D vascular network**  
*Nonlinear Analysis: Real World Applications*, 61:103331, 2021  
(see also article [57] in the bibliography)

### *Further articles*

- IV) Marvin Fritz, Christina Kuttler, Mabel L. Rajendran, Barbara Wohlmuth, Laura Scarabosio  
**On a subdiffusive tumor growth model with fractional time derivative**  
*IMA Journal of Applied Mathematics*, 86(04):688–729, 2021  
(see also article [59] in the bibliography)

I, Marvin Fritz, am the principal author of the articles I, II, III.

## List of further contributed articles

The following selected articles include further contributions by the author which are not part of this thesis. They are included for the sake of completeness only. Note that the author of this thesis does not claim to be the principal author of the following articles.

*Further articles that are not part of this thesis*

- Marvin Fritz, Vanja Nikolić, Barbara Wohlmuth  
**Well-posedness and numerical treatment of the Blackstock equation in nonlinear acoustics**  
*Mathematical Models and Methods in Applied Sciences*, 28(13):2557–2597, 2018  
(see also article [63] in the bibliography)
- Marvin Fritz, Prashant K. Jha, Tobias Köppl, J. Tinsley Oden, Andreas Wagner, Barbara Wohlmuth  
**Modeling and simulation of vascular tumors embedded in evolving capillary networks**  
*Computer Methods in Applied Mechanics and Engineering*, 384:113975, 2021  
(see also article [56] in the bibliography)
- Marvin Fritz, Tobias Köppl, J. Tinsley Oden, Andreas Wagner, Barbara Wohlmuth, Chengyue Wu  
**A 1D-0D-3D coupled model for simulating blood flow and transport processes in breast tissue**  
*International Journal for Numerical Methods in Biomedical Engineering*, 2022  
(see also article [60] in the bibliography)
- Marvin Fritz, Mabel L. Rajendran, Barbara Wohlmuth  
**Time-fractional Cahn–Hilliard equation: Well-posedness, degeneracy, and numerical solutions**  
*Computer & Mathematics with Applications*, 108:66–87, 2022  
(see also article [64] in the bibliography)
- Marvin Fritz, Ustim Khristenko, Barbara Wohlmuth  
**Equivalence between a time-fractional and an integer-order gradient flow: The memory effect reflected in the energy**  
submitted, preprint available at *arXiv: 2106.10985 [math.AP]*  
(see also article [58] in the bibliography)



# Contents

<b>1. Introduction</b>	<b>1</b>
1.1. Open research issues . . . . .	2
1.2. State of the art . . . . .	3
1.3. Outline . . . . .	5
1.4. Summary of results . . . . .	6
<b>2. Mathematical Background</b>	<b>9</b>
2.1. Function spaces, inequalities, and embedding results . . . . .	9
2.2. Fractional derivative . . . . .	10
2.3. Model problem: The Cahn–Hilliard equation . . . . .	12
<b>3. Modeling of Tumor Growth</b>	<b>13</b>
3.1. Multiple constituent model . . . . .	13
3.2. Phase separation in an ECM . . . . .	15
3.3. Nonlocal phenomena . . . . .	18
3.4. Mechanical deformation . . . . .	20
3.5. Chemotherapeutic influence . . . . .	22
3.6. Angiogenesis and mixed-dimensional coupling . . . . .	23
<b>4. Well-Posedness Analysis</b>	<b>25</b>
4.1. Faedo–Galerkin method . . . . .	25
4.2. Analysis of the four-species model . . . . .	26
4.3. Key estimates . . . . .	29
<b>5. Numerical Implementation</b>	<b>37</b>
5.1. Three-dimensional model . . . . .	37
5.2. Nonlocal phenomena . . . . .	37
5.3. Mixed-dimensional coupling . . . . .	39
<b>Acronyms</b>	<b>40</b>
<b>Bibliography</b>	<b>41</b>
<b>A. Core Articles</b>	<b>49</b>
A.1. On the unsteady Darcy–Forchheimer–Brinkman equation in local and nonlocal tumor growth models . . . . .	49
A.2. Local and nonlocal phase-field models of tumor growth and invasion due to ECM degradation . . . . .	95
A.3. Analysis of a new multispecies tumor growth model coupling 3D phase-fields with a 1D vascular network . . . . .	137
<b>B. Further Articles</b>	<b>183</b>
B.1. On a subdiffusive tumor growth model with fractional time derivative . . . . .	183



# 1. Introduction

*As long as a branch of science offers an abundance of problems, so long is it alive.* (David Hilbert)

Partial differential equations (PDEs) are omnipresent in describing the phenomena of the world – they model the flow of liquids and gases (Navier–Stokes equations), the evolution of a quantum state (Schrödinger equation), thermal conduction (heat equation), spinodal decomposition (Cahn–Hilliard equation), and many more. Complex processes evoke complicated models which might contain nonlinearities, temporal and spatial nonlocalities, and mixed-dimensional couplings. Until now, there is no unified theory for the analysis of any nonlinear PDE, and each novel nonlinear system presents its own set of challenges that must be thoroughly investigated.

We are interested in establishing the well-posedness of PDEs describing the growth and decline of tumors under the influence of a variety of complex biological phenomena. The definition of well-posedness goes back to Jacques Hadamard [85] in 1902, saying that a model is well-posed if

1. a solution exists,
2. the solution is unique,
3. the solution depends continuously on the given data.

We give an example that illustrates why it is important to show the well-posedness of a model before investigating it further. Let us assume beforehand that the problem ‘There exists a largest natural number’ is well-posed. Let  $n$  be said unique solution. However, because  $n^2$  is a natural number, it must be less than or equal to  $n$ . We compute  $n^2 - n = n \cdot (n - 1) \leq 0$ , from which we can conclude  $0 \leq n \leq 1$ . Hence,  $n = 1$ , or in other words, 1 is the largest natural number. The contradiction is caused by the incorrect assumption that the problem is well-posed. This example demonstrates the importance of proving the existence of mathematical objects before proceeding to prove things about them. Otherwise, a lot of interesting but illogical conclusions can be reached.

One of the most famous PDEs are the Navier–Stokes equations that describe the evolution of a fluid. This model became known among laymen as it was selected as one of the seven millennium problems [45] by the Clay Mathematics Institute, whose each solution is rewarded with a prize of one million dollars. It has been known since 1934 by Jean Leray’s work [98] that weak solutions exist, but it is not known yet whether they are unique in the three-dimensional case. On the other hand, strong solutions are unique, but their existence is unknown. If one reduces the dimension of the space domain by one and investigates the two-dimensional setting, then everything is perfectly understood. One can already see the fine nuances of mathematical analysis in this particular nonlinear problem. Such open questions in the analysis of PDEs are also included in the 19th and 20th Hilbert problems [142].

There are several known methods for determining whether or not a problem is well-posed. Depending on the difficulty of the problem, they can range from simple to difficult to apply. In the case of ordinary differential equations (ODEs), there are

the Carathéodory, Cauchy–Peano, and Cauchy–Lipschitz theorems providing results on the existence of solutions depending on the regularity of the right-hand side of the ODE. For linear PDEs there are, for example, the Lax–Milgram lemma and the Banach–Nečas–Babuška theorem.

In the following, we look at PDEs arising in the study of mathematical oncology that are highly nonlinear, and there is no standard analytical procedure for these kinds of models. Each model must be investigated individually to determine its analytical properties and to prove or disprove the system’s well-posedness.

### 1.1. Open research issues

Cancer is one of the leading causes of death in the world. There were 19.3 million new cancer cases and 9.96 million cancer-related deaths globally in 2020, see [130]. By 2040, the annual number of new cancer cases is expected to reach 30.2 million, with 16.3 million cancer-related deaths. Each tumor is unique and depends on many parameters. There is no foolproof method for curing cancer, and the cause of cancer is not fully understood. The main goal of mathematical oncology is the use of mathematical models to accurately describe tumor evolution.

Hanahan and Weinberg [86] captured the characteristics of cancer, and a mathematical model should meet the following ‘hallmarks of cancer’:

- **Resisting cell death:** Apoptosis is a form of programmed cell death that can be triggered when a cell is damaged. Malignant cells are able to ignore the apoptotic triggers and bypass this mechanism.
- **Sustaining proliferative signaling:** Cell proliferation is normally regulated by the production and release of growth factors as well as other signals. In contrast, external stimulation is not required for cancer cells to multiply themselves.
- **Evading growth suppressors:** Non-cancerous cells have genes called ‘tumor suppressors’, which prevent tumor formation by preventing excessive growth. These growth-suppressing signals are ineffective against cancer cells.
- **Inducing angiogenesis:** Tumor cells cause the formation of new blood vessels to supply their growth with nutrients and oxygen.
- **Enabling replicative immortality:** Normal cells have a finite lifespan because they go through a certain number of growth and division cycles. Cancer cells, on the other hand, are unaffected by this and can replicate indefinitely.
- **Activating invasion and metastasis:** Cancer cells are immune to the restrictions that normally confine cells to their original tissue. Tumor cells can break away from their origin, infiltrate surrounding tissue, and spread to other parts of the body.

Later, the authors [87] added two more hallmarks and two more characteristics to the list. All of the hallmarks must be met for mathematical oncology to be successful. In this way, cancer can be predicted so that, hopefully, in a few years, doctors will be able

to simply click a button on their computers to start a simulation depicting the patient's tumor and its evolution over the following days and weeks. A targeted therapy that improves the prognosis of the cancer is ideal.

But, first and foremost, one must ensure that the model is well-posed, both mathematically and in terms of capturing the movement of actual cancer. The second point can only be investigated with data and model verification through prediction, see the extensive article of Oden [110] on this subject. This thesis is heading in the direction of the first point. We want to make sure that such models are mathematically sound, that a solution to the model exists, and that nothing illogical occurs. After that, one can start thinking about a numerical scheme for the model that will provide a fast, accurate, and stable representation of the tumor's evolution on the doctor's monitor.

## 1.2. State of the art

There is a vast amount of literature on the mathematical modeling of tumor growth, and this development is in fact a good thing. Different groups establish different models and methods. With this diversification, there is hope that researchers will be able to predict the growth of tumors with sufficient detail. In this section, we want to point out the history of tumor modeling, and in particular with respect to the analysis of well-posedness.

Tumor models were originally stated as a free boundary problem. We refer to Greenspan [83] in 1976, who modeled the tissue as a porous medium and used Darcy's law for the convective velocity field. Such models have been further developed in many articles and we refer to the reviews [11, 117]. Many different models have been formulated since then. We follow the path of diffusive interface models in which the tumor is described as a collection of cells using a fourth-order PDE – the Cahn–Hilliard equation. These models are based on a multiphase approach using constitutive laws, thermodynamic principles, and balance laws for single constituents, which goes back to the work of Cristini, Löwengrub and others, see the articles [26, 27, 47, 137] starting in 2003. Such models have been further derived by the groups of Oden [111] in 2010 and Garcke [73] in 2018 in the case of general multispecies models.

In the work [88] by Hawkins-Daarud and others, the most basic model of tumor growth was formulated and it serves as the starting point of this thesis. The volume fractions of tumor cells, healthy cells, nutrient-rich extracellular water, and nutrient-poor extracellular water were considered. We refer to such a system as 'four-species model'. It was analyzed in [69–71] with respect to its mathematical well-posedness by the group of Garcke in the years 2016 and 2017. The system was also studied in [53, 54] by Frigeri, Rocca, and others for a degenerating mobility function. Since the model is based on a fourth-order PDE with concentration dependent mobilities, the uniqueness of weak solutions is an open problem, even for the prototype model, see the discussion in [39]. The four-species model was studied in [22] in an optimal control problem and in [18, 108] with respect to the solution's long time behavior.

Various velocity models have been added to the four-species model in order to include fluid flow in cancer evolution. The cells are treated as viscous, inertia-less fluids, and one models the velocity in a volume-averaged sense for the fluid mixture. Such an

assumption is justified since the cells are tightly packed. The Darcy law was modeled in the four-species model in [76] and analyzed in [72]. The law was extended to the Darcy–Brinkman equation in [36,37] and to the unsteady Darcy–Forchheimer–Brinkman (DFB) equation in our work [62]. There have also been authors who modeled the velocity as a Stokes flow, see [46,48,49] and one can consider the Darcy–Brinkman equation as an interpolation between Darcy and Stokes flow. The inclusion of a velocity equation in a Cahn–Hilliard system is by itself not novel and has been done without the application to tumor growth in, e.g., [97]. These techniques have been adapted to the new system, which includes nontrivial effects such as chemotaxis, proliferation, and nonlinear source functions.

Although such four-species models are very viable when describing the growth of an early tumor whose evolution is mostly dictated by proliferation, they are limited when tumor cells undergo hypoxia or necrosis. Indeed, a larger and more developed tumor tends to become stratified [117], i.e., the tumor tissue is divided into multiple layers, each with its own set of characteristics. Tumors are typically divided into three phases:

- a rapidly proliferating outer rim,
- an intermediate quiescent layer whose cells suffer from hypoxia,
- a necrotic core with cells that have perished.

Several multiphase models with multiple types of cell species and nutrients have been introduced in the works [3,5,28,42,47,55,73,122,137] and in our articles [56,57,61].

Low oxygen and nutrition levels cause tumor cells to enter the hypoxia phase, during which they remain dormant and release matrix-degrading enzymes (MDEs) that erode the extracellular matrix (ECM) and allows nutrients to flow. This process permits tumor cells to migrate into the tissue and is a first step towards modeling metastasis. Simply put, the ECM functions as a wall around the tumor which regulates the flow of nutrients. The ECM has been considered in [19,41,123,125,126,129] in tumor models of reaction-diffusion type. Our group was the first to analyze the ECM in a Cahn–Hilliard type model, see [61], and it was also included in our subsequent works [56,57].

Hypoxic tumor cells do not only emit MDEs to erode the ECM, but they also release tumor angiogenesis factors (TAFs), which drive endothelial cell proliferation and new vessel development. Angiogenesis is the process of blood vessels sprouting and elongating to supply nutrients to the tumor. The volume of an isolated colony of tumor cells is generally restricted by the size of  $1\text{mm}^3$ , see [109], unless sufficient nutrients and oxygen are supplied for proliferation. Cancerous cells stimulate angiogenesis in order to obtain such nutrients [17,114]. With respect to modeling and numerical simulations of angiogenesis, we refer to [25,26,139]. Angiogenesis has been considered with regards to the mathematical analysis of weak solutions in a Cahn–Hilliard type model by us in [57]. We are not aware of other works since then. Such models are highly complex due to mixed-dimensional couplings and the inclusion of hypoxic tumor cells that release TAFs.

Mathematicians are not just interested in accurately modeling the tumor’s growth but also in treating the tumor and halting it from growing. Currently, tumors are

being treated with chemotherapy, surgery, immunotherapy, and radiotherapy. Anti-angiogenic medications that restrict the production of new vascular structures are typically identified as one of the techniques to delay or arrest cancer growth because angiogenesis is one of the key processes through which cancers grow. As a result, a realistic model of angiogenesis is crucial for evaluating the efficacy of anti-angiogenic medications, see the optimal control problems studied in [23, 24] for the optimal dosage of medication. Chemotherapy has been included in our research [59] with a reaction-diffusion equation (RDE) and subdiffusive tumor growth, as well as in the works [23, 24, 38, 74, 127] on optimal control problems for the ideal dosage of drugs.

Moreover, nonlocal phenomena are involved in the mathematical modeling of cancer cells. Such effects illustrate long-range interactions and can be either of spatial or temporal nature. In the case of spatial nonlocality, cell-matrix and cell-cell adhesion properties are important characterizations in the modeling of tumor growth and promote the growth of tumor cells. These are nonlocal-in-space phenomena and involve a novel mathematical analysis due to the structure of integro-differential systems. We have investigated cell-cell adhesion in [62] and cell-matrix adhesion in [61]. Otherwise, nonlocal cell-cell adhesion properties have been studied analytically in phase-field models with applications to tumor growth in [54, 121].

In the case of temporal nonlocality, not only does the solution from the last step influence the current evolution, but it is taken into account that cells have an intrinsic memory [106]. Consequently, the past influences the present. Memory effects are modeled by a time-fractional derivative and fractional heat equations reflect subdiffusivity in contrast to the typical Fickian diffusion process. Tumors migrate via both traditional Fickian diffusion and subdiffusion, as shown in the *in vitro* and *in vivo* experimental results in [91]. The memory effect was studied by us in [58, 64] in relation to the time-fractional Cahn–Hilliard equation with degenerating mobility. Furthermore, we investigated a fractional tumor model with subdiffusion, nutritional couplings, and mechanical deformation in [59]. The surrounding host tissues increase mechanical stress as the tumor grows, limiting the tumor’s ability to grow further. In the papers [44, 102, 103], mechanical deformation in a tumor development model was first mentioned, and in terms of analysis, it was initially examined by us [59] in a diffusion-type tumor model and later in [75] by the group of Garcke in a Cahn–Hilliard type system. It had previously been included in the Cahn–Hilliard equation without being applied to tumor growth or the conventional source terms in [67, 68]; such models with elasticity are called Cahn–Larché equations.

### 1.3. Outline

This thesis is organized as follows: In Section 2, we give some analytical preliminaries such as Sobolev embeddings and compactness results, which will be used in the proofs of the well-posedness of weak solutions. Moreover, we introduce the core model of our tumor growth systems – the Cahn–Hilliard equation. In this spirit, we also introduce the fractional derivative and elaborate on the memory effect of time-fractional PDEs. In Section 3, we investigate the modeling of tumor growth and present an approach via continuum mixture theory. We introduce a multiphase tumor growth model with

various components and several biological processes. We present some subsystems that we have investigated in our articles [56, 57, 59, 61, 62, 64]. In Section 4, we give the proof ideas of the well-posedness of weak solutions to the subsystems of the previous section. We make use of the Faedo–Galerkin approximation and compactness methods combined with various test functions. Finally, we state the ideas of numerical approximations in Section 5 in order to implement the systems from the previous sections.

#### 1.4. Summary of results

The contributed articles address several systems for modeling tumor growth under the influence of various biological phenomena. Furthermore, these systems are theoretically analyzed in terms of their mathematical well-posedness and numerical simulations are presented. We derive a four-species model with an unsteady fluid flow based on the DFB law in 'Core Article I' (Appendix A.1). We investigate the effects of the ECM in an extended tumor model with stratification in 'Core Article II' (Appendix A.2). In 'Core Article III' (Appendix A.3), we present a mixed-dimensional tumor growth model to investigate the effects of an existing capillary structure in the tumor's vicinity on the release of TAFs. Finally, we combine a diffusion-type tumor model with memory effects and mechanical deformations in 'Article IV' (Appendix B.1); we also look into the effects of chemotherapy on the tumor. The scope and subject matter of each contribution are briefly summarized in the following paragraphs.

*Core articles as principal author*

- 'Core Article I' [62] in Appendix A.1:  
*On the unsteady Darcy–Forchheimer–Brinkman equation in local and nonlocal tumor growth models*

Starting with the four-species model, we derive local and nonlocal phase-field models of tumor growth, as well as a time-dependent DFB equation for convective velocity fields. The model becomes an integro-differential system since the nonlocal-in-space effects are represented by an integral in the space domain. Long-range cell interactions and cell-cell adhesion are represented by this nonlocal effect. The Faedo–Galerkin method provides a complete existence analysis for both the local and nonlocal systems. A parameter-sensitivity analysis is described, which quantifies the sensitivity of model parameters in relation to tumor mass as the quantity of interest. Two sensitivity analyses are investigated: one that uses statistical variances of model outputs and the other that uses active subspaces based on experimental data. The two methods arrive at very similar conclusions about the sensitivity of the chosen quantity of interest. The work concludes with a description of an algorithm based on the finite element method (FEM) for solving the system numerically. Lastly, simulations are conducted to demonstrate the impact of the new velocity model on the tumor.



- 'Core Article II' [61] in Appendix A.2:  
*Local and nonlocal phase-field models of tumor growth and invasion due to ECM degradation*

A multispecies phase-field model of tumor growth and ECM invasion is presented and analyzed. We start with a stratified tumor that divides into two phases: viable (i.e., proliferative and hypoxic cells) and necrotic. Furthermore, as soon as the tumor cells are deprived of nutrients, they release MDEs. A RDE is used to describe this effect. We take into account nonlocal-in-space effects and cell-matrix adhesion, i.e., the tumor cells' long-range interaction with the ECM. Using a coupled PDE-ODE approach, we prove the existence of solutions of the coupled system with both gradient-based and adhesion-based haptotaxis effects. We also present a FEM of the model and show the results of numerical experiments that were designed to demonstrate the relative importance and roles of various effects, such as the generation of MDEs and the degradation of the ECM.

- 'Core Article III' [57] in Appendix A.3:  
*Analysis of a new multispecies tumor growth model coupling 3D phase-fields with a 1D vascular network*

In this paper, we develop a mathematical model for stratified tumor growth that includes ECM erosion, interstitial flow, and the effects of vascular flow and nutrient transport. Multiple phases of cell species and other constituents are separated by smooth evolving interfaces in this phase-field model. One-dimensional equations are used to model flow and transport processes in the vasculature that supplies healthy and cancerous tissue. We obtain a 3D-1D coupled system since the equations governing the transport and flow processes are defined together with cell species models on a three-dimensional domain. We present a thorough examination of the existence of weak solutions for the entire system. Additionally, simulation results are presented that show the evolution of tumors as well as the effects of the mixed-dimensional coupling.

#### *Further articles*

- 'Article IV' [59] in Appendix B.1:  
*On a subdiffusive tumor growth model with fractional time derivative*

We present and analyze a coupled PDE system that models tumor growth under the influence of subdiffusion, mechanical effects, nutrient supply, and chemotherapy. The equation for the volume fraction of the tumor cells contains a time-fractional derivative and models the system's subdiffusion. RDEs are used to model the mass densities of cancer cells, nutrients, and chemotherapeutic agents. We use the Faedo–Galerkin method and appropriate compactness theorems to prove the existence and uniqueness of a weak solution to the model. We propose a fully discretized system based on the FEM for the spatial discretization and a convolution quadrature scheme for the time discretization. Finally, we present several numerical examples to demonstrate the effects of the fractional parameter, the mechanical deformation, and the chemotherapy.



## 2. Mathematical Background

*In most sciences one generation tears down what another has built, and what one has established another undoes. In mathematics alone each generation builds a new story to the old structure.* (Hermann Hankel)

In this section, we present the notation and concepts of the mathematical tools that are the building block of the development of our methods. First, we introduce the function spaces that we consider throughout this work and their corresponding norms and scalar products. Afterwards, we introduce important inequalities for the key estimates in the energy bounds. Moreover, we introduce embedding theorems in order to achieve strong convergence, which is needed for the nonlinear parts of the system during the limit process in the Faedo–Galerkin method. Next, we describe the concept of memory effects and the fractional derivatives of Caputo type. Finally, we present the prototype system for modeling tumor growth – the Cahn–Hilliard equation with concentration-dependent mobility.

### 2.1. Function spaces, inequalities, and embedding results

In this section, we introduce the function spaces that will be used frequently in the following sections. Some excellent introductions on the mathematical analysis of PDEs are given in the textbooks [12, 43, 118]. Let  $\Omega \subset \mathbb{R}^d$ ,  $d \in \mathbb{N}$ , be a bounded domain with a sufficiently smooth boundary  $\partial\Omega$  and  $T > 0$  a fixed time horizon. Further, let  $X$  be a given Banach space with norm  $\|\cdot\|_X$  and we denote the dual pairing by  $\langle \cdot, \cdot \rangle_X$  with its dual space  $X'$ .

Let  $\beta = (\beta_1, \dots, \beta_d) \in \mathbb{N}_0^d$  denote a multi-index. We define the Sobolev space  $W^{k,p}(\Omega)$ ,  $p \in [1, \infty]$ ,  $k \in \mathbb{N}_0$ , by

$$W^{k,p}(\Omega) = \{u \in L^p(\Omega) : \partial^\beta u \in L^p(\Omega) \text{ for } \|\beta\|_{\ell^1} \leq k\},$$

becoming a Banach space with the norm  $\|u\|_{W^{k,p}(\Omega)}^p = \sum_{|\beta| \leq k} \|\partial^\beta u\|_{L^p(\Omega)}^p$ . Here,  $\partial^\beta u$  denotes the weak derivative of  $u$  in the sense of

$$\int_{\Omega} \partial^\beta u(x) \varphi(x) \, dx = (-1)^{|\beta|} \int_{\Omega} u(x) \partial^\beta \varphi(x) \, dx \quad \forall \varphi \in C_c^\infty(\Omega).$$

In the case of  $p = 2$ , the Sobolev space inherits the Hilbert space structure from  $L^2(\Omega)$  and we denote this space by  $H^k(\Omega)$ . In the case of Bochner functions, we introduce the Sobolev–Bochner space,

$$W^{1,p}(0, T; X) = \{u \in L^p(0, T; X) : \partial_t u \in L^p(0, T; X)\},$$

where  $\partial_t u$  denotes the weak derivative of  $u$  in the sense of

$$\int_0^T \partial_t u(t) \varphi(t) \, dt = - \int_0^T u(t) \varphi'(t) \, dt \quad \forall \varphi \in C_c^\infty(0, T).$$

Throughout this thesis,  $C > 0$  stands for a generic constant, which may change from line to line. For brevity, we write  $x \lesssim y$  for  $x \leq Cy$ . We recall the Young convolution, Poincaré–Wirtinger, Korn and Sobolev inequalities [13, 33, 43, 118]

$$\begin{aligned} \|u * v\|_{L^r(\Omega)} &\leq \|u\|_{L^p(\Omega)} \|v\|_{L^q(\Omega)} && \forall u \in L^p(\Omega), v \in L^q(\Omega), \frac{1}{p} + \frac{1}{q} = 1 + \frac{1}{r}, \\ \|u - \langle u \rangle_\Omega\|_{L^p(\Omega)} &\lesssim \|\nabla u\|_{L^p(\Omega)} && \forall u \in W^{1,p}(\Omega), \\ \|\nabla u\|_{L^p(\Omega)}^p &\lesssim \|u\|_{L^p(\Omega)}^p + \|\varepsilon(u)\|_{L^p(\Omega)}^p && \forall u \in W^{1,p}(\Omega), \\ \|u\|_{W^{m,q}(\Omega)} &\lesssim \|u\|_{W^{k,p}(\Omega)} && \forall u \in W^{k,p}(\Omega), k - \frac{d}{p} \geq m - \frac{d}{q}, k \geq m, \end{aligned}$$

where  $\langle u \rangle_\Omega = \frac{1}{|\Omega|} \int_\Omega u$  is the mean of  $u$  with respect to  $\Omega$ , and  $\varepsilon(u) = \frac{1}{2}(\nabla u + \nabla u^\top)$  denotes the strain measure of  $u$ . The last inequality yields the continuous embedding  $W^{k,p}(\Omega) \hookrightarrow W^{m,q}(\Omega)$ , which is also compact due to the Rellich–Kondrachov embedding theorem [2, Section 10.9].

We require compact embeddings of Bochner spaces in order to achieve strong convergence and pass the limit in the nonlinear parts of the given evolutionary PDEs. Let  $X, Y, Z$  be Banach spaces such that  $X$  is compactly embedded in  $Y$ , and  $Y$  is continuously embedded in  $Z$ , i.e.,  $X \hookrightarrow Y \hookrightarrow Z$ . It is not true that the embedding  $L^2(0, T; X)$  is compact in  $L^2(0, T; Y)$ , which already the example  $f_n(t, x) = x \sin(nt)$  shows. One requires an additional information on the time derivative. The Aubin–Lions compactness lemma, see [128, Corollary 4], reads

$$\begin{aligned} L^p(0, T; X) \cap W^{1,1}(0, T; Z) &\hookrightarrow L^p(0, T; Y), && 1 \leq p < \infty, \\ L^\infty(0, T; X) \cap W^{1,r}(0, T; Z) &\hookrightarrow C^0([0, T]; Y), && r > 1, \end{aligned} \tag{2.1}$$

Further, we make use of the following continuous embedding, see [104, Theorem 3.1, Chapter 1],

$$L^2(0, T; Y) \cap H^1(0, T; Z) \hookrightarrow C^0([0, T]; [Y, Z]_{1/2}),$$

where  $[Y, Z]_{1/2}$  denotes the interpolation space between  $Y$  and  $Z$ , see [104, Definition 2.1, Chapter 1] for more details.

## 2.2. Fractional derivative

In this section, we investigate fractional derivatives. We concentrate on the well-known Caputo derivative. There are many other approaches to a fractional derivative besides these two, but many of the newer methods with non-singular kernels have serious shortcomings and should not be used, see the article [35] by Diethelm and others.

We begin by defining the singular kernel function  $g_\alpha \in L^1(0, T)$  as  $g_\alpha(t) = t^{\alpha-1}/\Gamma(\alpha)$  with  $\alpha \in (0, 1)$  and  $\Gamma$  being the Gamma function. The Riemann–Liouville integral operator  $\mathcal{I}_\alpha \in \mathcal{L}(L^1(0, T; X))$  of a function  $u \in L^1(0, T; X)$  reads  $\mathcal{I}_\alpha u = g_\alpha \otimes u$ , where  $\otimes$  denotes the convolution on the positive half-line with respect to the time variable. Note that the operator  $\mathcal{I}_\alpha$  has a complementary element in the sense  $\mathcal{I}_\alpha \mathcal{I}_{1-\alpha} u = \mathcal{I}_1 u = 1 \otimes u$ . The fractional derivative of order  $\alpha \in (0, 1)$  in the sense of Caputo is defined by

$$\partial_t^\alpha u(t) = (\mathcal{I}_{1-\alpha} \partial_t u)(t) = (g_{1-\alpha} \otimes \partial_t u)(t) = \frac{1}{\Gamma(1-\alpha)} \int_0^t \frac{u'(s)}{(t-s)^\alpha} ds,$$

see the textbooks [34, 93]. In the limit cases  $\alpha = 0$  and  $\alpha = 1$ , we define  $\partial_t^0 u = u$  and  $\partial_t^1 u = \partial_t u$ , respectively. The Caputo derivative, as shown in [93, Theorem 2.1], requires a function that is absolutely continuous on  $[0, T)$ . However, this definition can be relaxed to a broader class of functions that are equivalent to the classical definition for absolutely continuous functions, see [64, 99]. Let us remark the inverse convolution property

$$(\mathcal{I}_\alpha \partial_t^\alpha u)(t) = (\mathcal{I}_\alpha \mathcal{I}_{1-\alpha} \partial_t u)(t) = (\mathcal{I}_1 \partial_t u)(t) = u(t) - u(0). \quad (2.2)$$

Similar to before, we define the fractional Sobolev–Bochner space  $W^{\alpha,p}(0, T; X)$  as the functions in  $L^p(0, T; X)$  such that their  $\alpha$ -th fractional weak time derivative is in  $L^p(0, T; X)$ . In the special case of  $p = 2$ , we write  $H^\alpha(0, T; X)$ . As in the integer-order setting, there is a compact embedding result, see [138, Theorem 3.1], which works in the spirit of a fractional Aubin–Lions lemma,

$$L^p(0, T; X) \cap W^{\alpha,p}(0, T; Z) \hookrightarrow L^p(0, T; Y), \quad p \in [1, \infty). \quad (2.3)$$

We note that that the lower order  $\alpha < 1$  of the time-derivative has to be compensated with the power  $p$ , compare the classical Aubin–Lions lemma (2.1). We are not aware of a version with a compact embedding into  $C([0, T]; Y)$  using a  $L^\infty$ -bound in  $X$ . Moreover, it holds the following version of the Grönwall–Bellman inequality in the fractional setting.

**Lemma 1 (cf. [64, Corollary 1])** *Let  $w, v \in L^1(0, T; \mathbb{R}_{\geq 0})$ , and  $a, b \geq 0$ . If  $w$  and  $v$  satisfy the inequality*

$$w(t) + (\mathcal{I}_\alpha v)(t) \leq a + b \cdot (\mathcal{I}_\alpha w)(t) \quad \text{for a.a. } t \in (0, T),$$

*then it holds  $w(t) + v(t) \leq a \cdot C(\alpha, b, T)$  for almost every  $t \in (0, T)$ .*

The traditional chain rule  $\frac{d}{dt} f(u) = f'(u) \frac{d}{dt} u$  does not hold for general functions  $f$  if we replace the derivative by its fractional version. But there is a remedy: for convex functionals  $f : X \rightarrow \mathbb{R}$ , see [99, Proposition 2.18], there is the fractional chain inequality

$$\partial_t^\alpha f(u) \leq \langle f'(u), \partial_t^\alpha u \rangle_{X' \times X} \quad \forall u \in C^1([0, T]; X). \quad (2.4)$$

This is exactly the correct direction of the inequality in order to apply it the typical energy estimates, e.g., testing the time-fractional heat equation with the solution itself gives

$$\partial_t^\alpha \|u\|_{L^2(\Omega)}^2 + \|\nabla u\|_{L^2(\Omega)}^2 \leq \langle \partial_t^\alpha u, u \rangle_{H^1(\Omega)} - \langle \Delta u, u \rangle_{H^1(\Omega)} = 0.$$

Gradient flows, like the Cahn–Hilliard equation, have a  $\lambda$ -convex (or: semiconvex) energy rather than a convex one, see [64]. The fractional chain inequality can be applied to the convex functional  $x \mapsto f(x) - \frac{\lambda}{2} \|x\|_X^2$ , yielding the following result for semiconvex functionals

$$\partial_t^\alpha f(u) \leq \langle f'(u), \partial_t^\alpha u \rangle_X + \frac{\lambda}{2} \partial_t^\alpha \|u\|_X^2 - \lambda \langle \partial_t^\alpha u, u \rangle_X \quad \forall u \in C^1([0, T]; X).$$

### 2.3. Model problem: The Cahn–Hilliard equation

The prototype model of our tumor growth system is the Cahn–Hilliard equation. It is among the phase-field equations of diffuse-interface type, and it has the important property of having a solution that is either 0 or 1, or something smooth in between as a transition phase. As a result, we define the 1-phase as the representation of tumor cells, while the 0-phase reflects the absence of cancerous cells.

Let  $\phi_1, \phi_2$  represent the concentrations of two components with the relationship  $\phi_1 + \phi_2 = 1$ . That means they describe local portions, such as in binary alloys. They adhere to the law of mass conservation

$$\partial_t \phi_i = -\operatorname{div} J_i, \quad i \in \{1, 2\},$$

where  $J_i$  denotes the mass flux of the  $i$ -th component. In order to guarantee  $\partial_t(\phi_1 + \phi_2) = 0$ , the fluxes have to fulfill the condition  $J_1 + J_2 = 0$ . We reduce the equations by setting  $\phi = \phi_1 - \phi_2$  and  $J = J_1 - J_2$ , yielding

$$\partial_t \phi = -\operatorname{div} J.$$

Traditionally, the flux  $J$  is given by the negative of the gradient of the chemical potential  $\mu$ , i.e.,  $J = -\nabla \mu$ . Gurtin [84] proposed a mechanical version of the second law of thermodynamics by introducing a new mass flux with the mobility function  $m$  for interactions at a microscopic level given by

$$J = -m(\phi)\nabla \mu.$$

Following [15], the chemical potential is defined as the first variation (Gâteaux derivative) of the Ginzburg–Landau free energy functional

$$\mathcal{E}(\phi) = \int_{\Omega} \left\{ \Psi(\phi) + \frac{\varepsilon^2}{2} |\nabla \phi|^2 \right\} dx. \quad (2.5)$$

The parameter  $\varepsilon$  denotes the interfacial width, and  $\Psi$  describes a double-well potential with zeros at  $-1$  and  $1$ , e.g., the Landau potential,  $\Psi(\phi) = \frac{1}{4}(1 - \phi^2)^2$ , but also logarithmic variants are possible, see [20], such as the Flory–Huggins logarithmic potential, or potentials of double-obstacle type. A straightforward calculation of the first variation of the Ginzburg–Landau energy yields the so-called Cahn–Hilliard equation with variable mobility:

<p><b>Cahn–Hilliard equation</b></p> $\partial_t \phi = \operatorname{div}(m(\phi)\nabla \mu)$ $\mu = \Psi'(\phi) - \varepsilon^2 \Delta \phi$
------------------------------------------------------------------------------------------------------------------------------------------------

Typically, the mobility function is either constant or of the form  $m(\phi) = M(1 - \phi^2)^2$  for a constant  $M$ , see [16, 133]. The scenario of constant mobility has been thoroughly investigated, and with sufficient assumptions, well-posedness can be demonstrated, see [107]. A proof or counterexample to uniqueness in the case of a degenerate mobility is still an open problem; this is unsolved for the class of fourth-order degenerate parabolic equations, see the discussion in [39].

### 3. Modeling of Tumor Growth

*The greatest challenge to any thinker is stating the problem in a way that will allow a solution.* (Bertrand Russell)

*Everything should be made as simple as possible, but not simpler.* (Albert Einstein)

We postulate models of mathematical oncology that abstract many of the important processes that are known to be involved in tumor growth, decline, and therapeutic treatment in real tissue. The systems are designed to reflect processes at the mesoscale and macroscale, with fields representing volume fractions of mass concentrations of various species, determining tumor constituents. Several writers have developed local versions of multiphase models in the previous decade, including [3, 73, 76, 101, 137]. The model equations are derived from the balance laws of continuum mixture theory [14, 25, 111, 112] and representations of the main mechanisms that govern cancer formation and evolution [87, 101].

In Subsection 3.1, we state a multiple constituent model from the mass balance law and a Ginzburg–Landau energy in a general framework. As an example, we give the classical four-species model by Hawkins–Daarud and others. Next, we include stratification into the model and invasion due to ECM degradation in Subsection 3.2. In the following subsections, we add more and more biological phenomena to the model with a stratified tumor. We add spatial and temporal nonlocalities in Subsection 3.3, mechanical deformation in Subsection 3.4, chemotherapeutic influence in Subsection 3.5, and finally, angiogenesis and mixed-dimensional couplings in Subsection 3.6.

#### 3.1. Multiple constituent model

We apply the framework of continuum mixture theory, in which multiple mechanical and chemical species can exist at a point  $x$  in some given domain  $\Omega \subset \mathbb{R}^d$ ,  $d \in \mathbb{N}$ , at time  $t > 0$ . Thus, for a medium with  $N$  interacting constituents, the volume fraction of each species is represented by a field  $\phi_\alpha$ ,  $1 \leq \alpha \leq N$ , with value  $\phi_\alpha(t, x)$  at  $x \in \Omega$ , and time  $t \geq 0$ . For convenience, we collect the constituents of the model within the following  $N$ -tuple

$$\phi_{\mathbb{A}} = (\phi_\alpha)_{\alpha \in \mathbb{A}},$$

where  $\mathbb{A}$  is an index set that is further disjointly separated between the phase-field index set  $\mathbb{CH}$ , the reaction-diffusion indices  $\mathbb{RD}$ , and the evolution indices  $\mathbb{OD}$  that correspond to abstract ODEs.

The constituents  $\phi_\alpha$ ,  $\alpha \in \mathbb{A}$ , are governed by the following extended mass balance law, see [100, 101],

$$\partial_t \phi_\alpha + \operatorname{div}(\phi_\alpha v_\alpha) = -\operatorname{div} J_\alpha(\phi_{\mathbb{A}}) + S_\alpha(\phi_{\mathbb{A}}). \quad (3.1)$$

Here, the cell velocity of the  $\alpha$ -th constituent is denoted by  $v_\alpha$  and  $S_\alpha$  describes a mass source term depending on all species  $\phi_{\mathbb{A}}$ . We call the system closed if it holds

$\sum_{\alpha \in \mathbb{A}} S_\alpha(\phi_{\mathbb{A}}) = 0$ . Moreover,  $J_\alpha$  denotes the flux of the  $\alpha$ -th constituent, which is given by the negative gradient of the chemical potential scaled by a mobility function

$$J_\alpha(\phi_{\mathbb{A}}) = -m_\alpha(\phi_{\mathbb{A}})\nabla\mu_\alpha. \quad (3.2)$$

Here,  $\mu_\alpha$  denotes the chemical potential of the  $\alpha$ -th species and  $m_\alpha$  the mobility function possibly depending on all constituents. In our applications, we typically consider the mobilities

$$\begin{aligned} m_\alpha(\phi_{\mathbb{A}}) &= M_\alpha\phi_\alpha^2(1-\phi_\alpha)^2, & \alpha \in \mathbb{C}\mathbb{H}, \\ m_\beta(\phi_{\mathbb{A}}) &= M_\beta, & \beta \in \mathbb{R}\mathbb{D}, \\ m_\gamma(\phi_{\mathbb{A}}) &= 0, & \gamma \in \mathbb{O}\mathbb{D}, \end{aligned} \quad (3.3)$$

where  $M_\alpha > 0$  are mobility constants. As in the prototype model, see Subsection 2.3, we define the chemical potential  $\mu_\alpha$  as the first variation of the Ginzburg–Landau free energy with respect to  $\phi_\alpha$ . We propose the energy

$$\mathcal{E}(\phi_{\mathbb{A}}) = \int_{\Omega} \left\{ \Psi(\phi_{\mathbb{C}\mathbb{H}}) + \Phi(\phi_{\mathbb{A}}) + \sum_{\alpha \in \mathbb{C}\mathbb{H}} \frac{\varepsilon_\alpha^2}{2} |\nabla\phi_\alpha|^2 + \sum_{\beta \in \mathbb{R}\mathbb{D}} \frac{D_\beta}{2} \phi_\beta^2 \right\} dx, \quad (3.4)$$

where  $\varepsilon_\alpha$ ,  $\alpha \in \mathbb{C}\mathbb{H}$ , is a parameter associated with the interface thickness separating the different cell species. The function  $\Phi$  describes adhesion processes like chemotaxis and haptotaxis. Lastly,  $\Psi$  represents a double-well potential as in the general Cahn–Hilliard equation, e.g., it can be of Landau type, where we mention the two possibilities

$$\Psi(\phi_{\mathbb{C}\mathbb{H}}) = C_\Psi \left( \sum_{\alpha \in \mathbb{C}\mathbb{H}} \phi_\alpha \right)^2 \left( 1 - \sum_{\alpha \in \mathbb{C}\mathbb{H}} \phi_\alpha \right)^2, \quad \Psi(\phi_{\mathbb{C}\mathbb{H}}) = \sum_{\alpha \in \mathbb{C}\mathbb{H}} C_{\Psi_\alpha} \phi_\alpha^2 (1 - \phi_\alpha)^2,$$

where  $C_\Psi, C_{\Psi_\alpha} > 0$  are appropriate prefactors. Alternatively, one can also select a logarithmic potential of Flory–Huggins type, see [20, 55].

We calculate the first variations of the Ginzburg–Landau energy with respect to the constituents and thus, the chemical potentials read

$$\begin{aligned} \mu_\alpha &= \partial_{\phi_\alpha} \Psi(\phi_{\mathbb{C}\mathbb{H}}) + \partial_{\phi_\alpha} \Phi(\phi_{\mathbb{A}}) - \varepsilon_\alpha^2 \Delta\phi_\alpha, & \alpha \in \mathbb{C}\mathbb{H}, \\ \mu_\beta &= D_\beta \phi_\beta + \partial_{\phi_\beta} \Phi(\phi_{\mathbb{A}}), & \beta \in \mathbb{R}\mathbb{D}, \\ \mu_\gamma &= \partial_{\phi_\gamma} \Phi(\phi_{\mathbb{A}}), & \gamma \in \mathbb{O}\mathbb{D}, \end{aligned}$$

and inserting these into (3.1)–(3.3) yields the multispecies model:

<b>Multiple constituent model</b>		
$\partial_t \phi_\alpha + \operatorname{div}(\phi_\alpha v_\alpha) = \operatorname{div}(M_\alpha \phi_\alpha^2 (1 - \phi_\alpha)^2 \nabla \mu_\alpha) + S_\alpha(\phi_{\mathbb{A}})$	$\alpha \in \mathbb{C}\mathbb{H}$	(3.5)
$\mu_\alpha = \partial_{\phi_\alpha} \Psi(\phi_{\mathbb{C}\mathbb{H}}) + \partial_{\phi_\alpha} \Phi(\phi_{\mathbb{A}}) - \varepsilon_\alpha^2 \Delta\phi_\alpha$	$\alpha \in \mathbb{C}\mathbb{H}$	
$\partial_t \phi_\beta + \operatorname{div}(\phi_\beta v_\beta) = \operatorname{div}(M_\beta \nabla (D_\beta \phi_\beta + \partial_{\phi_\beta} \Phi(\phi_{\mathbb{A}}))) + S_\beta(\phi_{\mathbb{A}})$	$\beta \in \mathbb{R}\mathbb{D}$	
$\partial_t \phi_\gamma = S_\gamma(\phi_{\mathbb{A}})$	$\gamma \in \mathbb{O}\mathbb{D}$	



### 3.1.1. Four-species tumor growth model

We begin with an easy example of a tumor growth model starting from the proposed multiple constituent system (3.5). We choose  $|\mathbb{A}| = 2$  constituents and set  $\mathbb{A} = \{T, \sigma\}$ ,  $\mathbb{CH} = \{T\}$ ,  $\mathbb{RD} = \{\sigma\}$ , and  $\mathbb{OD} = \emptyset$ . The volume fraction of tumor cells  $\phi_T$  is understood to represent an averaged cell concentration, a homogenized depiction over many thousands of cells. The local nutrient concentration is represented by the field  $\phi_\sigma$ . Moreover, we propose the adhesion function  $\Phi(\phi_T, \phi_\sigma) = -\chi_c \phi_T \phi_\sigma$  in the energy (3.4) for some chemotaxis parameter  $\chi_c > 0$ . We assume a volume-averaged velocity  $v$  for the tumor cells and the nutrients. This assumption of a volume-averaged velocity is reasonable since the cells are tightly packed. Inserting all the assumptions into the multispecies model reads the so-called four-species model:

<p><b>Four-species model</b></p> $\begin{aligned} \partial_t \phi_T + \operatorname{div}(\phi_T v) &= \operatorname{div}(M_T \phi_T^2 (1 - \phi_T)^2 \nabla \mu_T) + S_T(\phi_T, \phi_\sigma) \\ \mu_T &= \Psi'(\phi_T) - \chi_c \phi_\sigma - \varepsilon_T^2 \Delta \phi_T \\ \partial_t \phi_\sigma + \operatorname{div}(\phi_\sigma v) &= \operatorname{div}(M_\sigma \nabla (D_\sigma \phi_\sigma - \chi_c \phi_T)) + S_\sigma(\phi_T, \phi_\sigma) \end{aligned} \tag{3.6}$
-----------------------------------------------------------------------------------------------------------------------------------------------------------------------------------------------------------------------------------------------------------------------------------------------------------------------------------------------------------------------------------------------------------------------------------------------------------------------------------

This model is studied mathematically in [70, 71] in the case of a absent velocity  $v = 0$ . For a flow governed by Darcy's law  $v = -K \nabla p + S_v(\phi_T, \phi_\sigma)$ , we refer to [69, 76]. Here, the pressure is denoted by  $p$ , the permeability factor by  $K > 0$ , and  $S_v$  is called the Korteweg force [55]. Alternatively, there have also been used the Brinkman law [36, 37], the unsteady DFB law [62] by us, and the Navier–Stokes equations [89, 96].

Of particular interest are source functions that are formulated as sink and source terms. Tumors absorb the nutrients, and therefore, the tumor increases at the same rate as the nutrients decrease. Further, there is a programmed cell death (or: apoptosis) and these dead cells become nutrients. Therefore, we propose

$$S_T(\phi_T, \phi_\sigma) = -S_\sigma(\phi_T, \phi_\sigma) = \lambda_T^{\text{pro}} \phi_\sigma \phi_T (1 - \phi_T) - \lambda_T^{\text{apo}} \phi_T,$$

where  $\lambda_T^{\text{pro}}$  is called the proliferation rate and  $\lambda_T^{\text{apo}}$  the apoptosis rate.

The system (3.6) is also called 'four-species model', see [88, 101, 111], since it can also be derived from four constituents – namely, the volume fraction of the tumor cells  $\phi_T$ , healthy cells  $\phi_C$ , nutrient-rich extracellular water  $\phi_\sigma$ , and its nutrient-poor counterpart  $\phi_{\sigma_0}$ . Then the four variables are governed by the law of mass balance from before, see (3.1), for  $\mathbb{A} = \{T, C, \sigma, \sigma_0\}$ . One sets  $\phi_T = 1 - \phi_C$  and  $\phi_\sigma = 1 - \phi_{\sigma_0}$ . Therefore, one can eliminate the superfluous constituents  $\phi_C$  and  $\phi_{\sigma_0}$  from the system and recover (3.6).

## 3.2. Phase separation in an ECM

The so-called 'microenvironment' of a solid tumor is a patch of vascularized tissue in a living subject, such as within an organ, that is home to a colony of tumor cells and other elements. The tumor is contained within an open bounded region  $\Omega \subset \mathbb{R}^3$  and is sustained by a network of macromolecules that make up the ECM, which includes collagen, enzymes, and other proteins. We are concentrating on constructing

phenomenological characterizations of tumor cell colony evolution that seek to capture both mesoscale and macroscale events.

The field of the tumor cells  $\phi_T$  can be expressed as the sum

$$\phi_T = \phi_P + \phi_H + \phi_N,$$

of the three components  $\phi_P, \phi_H, \phi_N$ , which describe the volume fractions of the proliferative, hypoxic, and necrotic cells, respectively, and are characterized by:

- proliferative cells are those that have a high chance of going through mitosis, dividing into twin cells, and promoting tumor growth;
- hypoxic cells are tumor cells that have been deprived of enough resources such as oxygen to become or remain proliferative;
- necrotic cells have died owing to nutrient deficiency.

The production of an enzyme by tumor cells in response to hypoxia accumulates, and increases cell mobility, and activates the secretion of angiogenesis-promoting factors characterized by the field  $\phi_{TAF}$ . The most commonly discussed of these factors is vascular endothelial growth factor (VEGF), which causes endothelial cells to sprout and create the tubular structure of blood vessels, which expand into new vessels that feed nutrients to hypoxic cells. Furthermore, hypoxic cells release MDEs, such as urokinase-plasminogen and matrix metalloproteinases, as indicated by the volume fraction  $\phi_{MDE}$ , which erode the ECM, the density of which is denoted by  $\phi_{ECM}$ . This process allows tumor cells to invade, increasing  $\phi_T$  in the ECM domain and increasing the likelihood of metastasis. A simplistic view of the effects of the tumor's evolution is:

1. outer proliferative tumor layer absorbs nutrients and expands ( $\phi_P \uparrow, \phi_\sigma \downarrow$ );
2. inner tumor layer changes to hypoxic ( $\phi_H \uparrow$ );
3. hypoxic cells send out MDE and TAF signaling ( $\phi_{TAF} \uparrow, \phi_{MDE} \uparrow$ );
4. TAFs trigger angiogenesis and new vessels are sprouting ( $\phi_H \downarrow, \phi_P \uparrow$ ), and MDEs erode the ECM, tumor cells migrate ( $\phi_{ECM} \downarrow, \phi_H \downarrow, \phi_P \uparrow$ ).

We collect the constituents within the following 7-tuple:

$$\phi_{\mathbb{A}} = (\phi_\alpha)_{\alpha \in \mathbb{A}} = (\phi_P, \phi_H, \phi_N, \phi_\sigma, \phi_{ECM}, \phi_{MDE}, \phi_{TAF}),$$

with  $\mathbb{A} = \{P, H, N, \sigma, ECM, MDE, TAF\}$ . Using the setting of the multiple constituent model (3.5) in Subsection 3.1, we further distinguish between the tumor phase-field indices  $\mathbb{C}\mathbb{H} = \{P, H, N\}$ , the reaction-diffusion indices  $\mathbb{R}\mathbb{D} = \{\sigma, MDE, TAF\}$  and the evolution index set  $\mathbb{O}\mathbb{D} = \{ECM\}$ . The necrotic cells are non-moving and only gain mass from the nutrient-lacking hypoxic cells. Therefore, the mobility of the necrotic cells is set to zero, i.e.,  $m_N = v_N = 0$ . Still, the necrotic cells are counted as a phase-field variable and are part of  $\mathbb{C}\mathbb{H}$  instead of the ODEs since it influences the double-well potential and inherits its phase-field structure from the hypoxic phase-field variable.

We assume that haptotaxis and chemotaxis are included in the system, and therefore, we take an adhesion force of the form

$$\Phi(\phi_{\mathbb{A}}) = -(\phi_P + \phi_H)(\chi_c \phi_\sigma + \chi_h \phi_{ECM}),$$

where  $\chi_c$  and  $\chi_h$  are the chemotaxis and haptotaxis factors, respectively. We note that the adhesion force only acts on the viable (i.e., proliferative and hypoxic) cells, whereas the necrotic cells are excluded from this process. Therefore, from the multiple constituent model (3.5), we arrive at the equations for the phase-field variables  $(\phi_\alpha)_{\alpha \in \mathbb{CH}}$ :

**Stratified tumor growth model with ECM:  $\mathbb{CH}$**

$$\begin{aligned} \partial_t \phi_P + \operatorname{div}(\phi_P v) &= \operatorname{div}(M_P \phi_P^2 (1 - \phi_P)^2 \nabla \mu_P) + S_P(\phi_{\mathbb{A}}) \\ \mu_P &= \partial_{\phi_P} \Psi(\phi_{\mathbb{CH}}) - \varepsilon_P^2 \Delta \phi_P - \chi_c \phi_\sigma - \chi_h \phi_{ECM} \\ \partial_t \phi_H + \operatorname{div}(\phi_H v) &= \operatorname{div}(M_H \phi_H^2 (1 - \phi_H)^2 \nabla \mu_H) + S_H(\phi_{\mathbb{A}}) \\ \mu_H &= \partial_{\phi_H} \Psi(\phi_{\mathbb{CH}}) - \varepsilon_H^2 \Delta \phi_H - \chi_c \phi_\sigma - \chi_h \phi_{ECM} \\ \partial_t \phi_N &= S_N(\phi_{\mathbb{A}}) \end{aligned} \tag{3.7}$$

Here, we assume a volume-averaged velocity  $v = v_\alpha$  for the fields  $\phi_P$ ,  $\phi_H$ , and  $\phi_\sigma$  governed by the Darcy law. Further, we propose the source functions

$$\begin{aligned} S_P(\phi_{\mathbb{A}}) &= \lambda_P^{\text{pro}} \phi_\sigma \phi_P (1 - \phi_T) - \lambda_P^{\text{apo}} \phi_P - \lambda_{PH} \mathcal{H}(\sigma_{PH} - \phi_\sigma) \phi_P \\ &\quad + \lambda_{HP} \mathcal{H}(\phi_\sigma - \sigma_{HP}) \phi_H, \\ S_H(\phi_{\mathbb{A}}) &= \lambda_H^{\text{pro}} \phi_\sigma \phi_H (1 - \phi_T) - \lambda_H^{\text{apo}} \phi_H + \lambda_{PH} \mathcal{H}(\sigma_{PH} - \phi_\sigma) \phi_P \\ &\quad - \lambda_{HP} \mathcal{H}(\phi_\sigma - \sigma_{HP}) \phi_H - \lambda_{HN} \mathcal{H}(\sigma_{HN} - \phi_\sigma) \phi_H, \\ S_N(\phi_{\mathbb{A}}) &= \lambda_{HN} \mathcal{H}(\sigma_{HN} - \phi_\sigma) \phi_H. \end{aligned}$$

The parameters  $\lambda_\alpha^{\text{pro}}$  and  $\lambda_\alpha^{\text{apo}}$  are the proliferation and apoptosis rates of the  $\alpha$ -th species. Moreover,  $\lambda_{PH}$  denotes the transition rate from the proliferative to the hypoxic phase below the nutrient level  $\sigma_{PH}$ ,  $\lambda_{HP}$  the transition rate from the hypoxic to the proliferative phase above the nutrient level  $\sigma_{HP}$ , and  $\lambda_{HN}$  the transition rate from the hypoxic to the necrotic phase below the nutrient level  $\sigma_{HN}$ . Finally,  $\mathcal{H}$  denotes the Heaviside step function, which might be replaced by the Sigmoid function if a sufficiently smooth right-hand side is needed.

Related models of ECM degradation due to MDEs released by hypoxic cell concentrations and subsequent tumor invasion and metastasis are discussed in [41, 125, 131, 132] for diffusion-type models. Following these references, we introduce the equation for the ECM evolution:

**Stratified tumor growth model with ECM:  $\mathbb{OD}$**

$$\begin{aligned} \partial_t \phi_{ECM} &= S_{ECM}(\phi_{\mathbb{A}}) \\ &= -\lambda_{ECM}^{\text{deg}} \phi_{ECM} \phi_{MDE} + \lambda_{ECM}^{\text{pro}} \phi_\sigma (1 - \phi_{ECM}) \mathcal{H}(\phi_{ECM} - \phi_{ECM}^{\text{pro}}) \end{aligned}$$

Here,  $\lambda_{ECM}^{\text{deg}}$  is the degradation rate of ECM fibers due to the matrix degrading enzymes, and  $\lambda_{ECM}^{\text{pro}}$  is the production rate of ECM fibers above the threshold level  $\phi_{ECM}^{\text{pro}}$  for the ECM density.

Further, for  $(\phi_\beta)_{\beta \in \mathbb{RD}}$  we arrive at the following system of equations:

<p><b>Stratified tumor growth model with ECM: <math>\mathbb{RD}</math></b></p> $\begin{aligned} \partial_t \phi_\sigma + \operatorname{div}(\phi_\sigma v) &= \operatorname{div}(M_\sigma \nabla(D_\sigma \phi_\sigma - \chi_c(\phi_P + \phi_H))) + S_\sigma(\phi_\mathbb{A}) \\ \partial_t \phi_{MDE} &= M_{MDE} D_{MDE} \Delta \phi_{MDE} + S_{MDE}(\phi_\mathbb{A}) \\ \partial_t \phi_{TAF} &= M_{TAF} D_{TAF} \Delta \phi_{TAF} + S_{TAF}(\phi_\mathbb{A}) \end{aligned}$
--------------------------------------------------------------------------------------------------------------------------------------------------------------------------------------------------------------------------------------------------------------------------------------------------------------------------------------------------------------------------------------------------------------------------------------------------------------------------------

The source functions are given by

$$\begin{aligned} S_\sigma(\phi_\mathbb{A}) &= \lambda_P^{\text{apo}} \phi_P + \lambda_H^{\text{apo}} \phi_H - \lambda_P^{\text{pro}} \phi_\sigma \phi_P (1 - \phi_T) - \lambda_H^{\text{pro}} \phi_\sigma \phi_H (1 - \phi_T) \\ &\quad + \lambda_{ECM}^{\text{deg}} \phi_{ECM} \phi_{MDE} - \lambda_{ECM}^{\text{pro}} \phi_\sigma (1 - \phi_{ECM}) \mathcal{H}(\phi_{ECM} - \phi_{ECM}^{\text{pro}}), \\ S_{MDE}(\phi_\mathbb{A}) &= \lambda_{MDE}^{\text{pro}} (\phi_P + \phi_H) \phi_{ECM} \frac{\sigma_{HP}}{\sigma_{HP} + \phi_\sigma} (1 - \phi_{MDE}) - \lambda_{MDE}^{\text{deg}} \phi_{MDE} \\ &\quad - \lambda_{ECM}^{\text{deg}} \phi_{ECM} \phi_{MDE}, \\ S_{TAF}(\phi_\mathbb{A}) &= \lambda_{TAF}^{\text{pro}} (1 - \phi_{TAF}) \phi_H \mathcal{H}(\phi_H - \phi_H^{\text{pro}}) - \lambda_{TAF}^{\text{deg}} \phi_{TAF}. \end{aligned}$$

The parameters  $\lambda_{MDE}^{\text{deg}}$  and  $\lambda_{TAF}^{\text{deg}}$  denote the decay rates of the MDEs and TAFs, respectively,  $\lambda_{MDE}^{\text{pro}}$  the production rate of MDEs, and  $\lambda_{TAF}^{\text{pro}}$  is the production rate of the  $\phi_{TAF}$  due to the release by hypoxic cells above a threshold value of  $\phi_H^{\text{pro}}$ .

We note that the cell species  $\phi_\alpha$ ,  $\alpha \in \{P, H, N, \sigma, ECM\}$ , form a mass conserving subsystem in the sense that their source terms add to zero. The fields  $\phi_{MDE}$  and  $\phi_{TAF}$  do not belong to this mass exchanging closed subsystem since these signals show natural degradation factors that are not absorbed by the other constituents.

### 3.3. Nonlocal phenomena

In this section, we discuss the nonlocal effects in tumor growth models. There are two types of nonlocality: temporal and spatial. The first phenomenon is known as the memory effect and corresponds to a time-fractional derivative in the PDE. In the second case, a space integral has to be treated, and such a term represents long-range interactions.

#### 3.3.1. Nonlocal-in-space: Cell-cell and cell-matrix adhesion

If events or cell concentrations at one site in the tumor domain are dependent on events at other points within a defined neighborhood, the model is said to be nonlocal-in-space. Long-range interactions, such as cell-cell adhesion, are one of the many mechanisms that influence tumor cell mobility and migration. Cell-cell adhesion is a fundamental element in tissue development, stability, breakdown, and is a significant factor that contributes to cancer cell invasion and metastasis.

Following [19, 54], we consider cell-cell adhesion effects, which are responsible for the binding of one or more cells to one another via protein reactions on cell surfaces. It is reasonable to include cell-cell adhesion since the Ginzburg-Landau free energy functional causes separation and surface tension effects [54]. Therefore, tumor cells prefer to stick to one another over healthy cells. The physicists Giacomini & Lebowitz [79, 80]

used statistical mechanics in 1996 to study the problem of phase separation from a microscopic background and derived the Helmholtz free energy functional

$$\mathcal{E}(\phi_T) = \int_{\Omega} \Psi(\phi_T) dx + \frac{1}{4} \int_{\Omega} \int_{\Omega} J(x-y)(\phi_T(x) - \phi_T(y))^2 dy dx.$$

Here,  $J : \mathbb{R}^d \rightarrow \mathbb{R}$  is assumed to be a convolution kernel with  $J(-x) = J(x)$ . One obtains the Ginzburg–Landau energy by selecting a specific kernel function and passing the limit, see [52]. We modify the energy to account for chemotaxis and propose

$$\mathcal{E}(\phi_T, \phi_{\sigma}) = \int_{\Omega} \Psi(\phi_T) + \frac{D_{\sigma}}{2} \phi_{\sigma}^2 - \chi_c \phi_T \phi_{\sigma} dx + \frac{1}{4} \int_{\Omega} \int_{\Omega} J(x-y)(\phi_T(x) - \phi_T(y))^2 dy dx.$$

Therefore, we consider a class of long-range interactions that are classified by chemical potentials of the form,

$$\mu_T = \frac{\delta \mathcal{E}}{\delta \phi_T} = \Psi'(\phi_T) - \chi_c \phi_{\sigma} + \int_{\Omega} J(x-y)(\phi_T(x) - \phi_T(y)) dy.$$

This leads directly to a nonlocal model governed by the system:

<p><b>Four-species model with cell-cell adhesion</b></p> $\begin{aligned} \partial_t \phi_T + \operatorname{div}(\phi_T v) &= \operatorname{div}(M_T \phi_T^2 (1 - \phi_T)^2 \nabla \mu_T) + S_T(\phi_T, \phi_{\sigma}) \\ \mu_T &= \Psi'(\phi_T) - \chi_c \phi_{\sigma} + \phi_T \cdot J * 1 - J * \phi_T \\ \partial_t \phi_{\sigma} + \operatorname{div}(\phi_{\sigma} v) &= \operatorname{div}(M_{\sigma} \nabla (D_{\sigma} \phi_{\sigma} - \chi_c \phi_T)) + S_{\sigma}(\phi_T, \phi_{\sigma}) \end{aligned}$	(3.8)
---------------------------------------------------------------------------------------------------------------------------------------------------------------------------------------------------------------------------------------------------------------------------------------------------------------------------------------------------------------------------------------------------------------------------------------------------------------------------------------------------------------------	-------

Models that account for cell-matrix adhesion effects include MDEs that erode the ECM and therefore, this process allows cells to migrate into tissue. Such systems have been thoroughly examined in [19, 41]. In contrast to the fourth-order Cahn–Hilliard phase-field equation in our situation, the tumor volume fraction is described by a RDE in these works. The cell-matrix adhesion flux can be classified as either a local gradient-based haptotaxis effect [129, 131, 135] or a nonlocal adhesion-based haptotaxis effect [4, 19, 78]. We consider the respective fluxes of the form

$$J_{\alpha}(\phi_{\mathbb{A}}) = \chi_h \phi_V \cdot \begin{cases} \nabla \phi_{ECM}, & \alpha = \text{local}, \\ k * \phi_{ECM}, & \alpha = \text{nonlocal}, \end{cases}$$

where  $k$  is a vector-valued kernel function. This adhesion flux is included in the equation of the mass balance law of the volume fraction of viable cells as:

$$\partial_t \phi_V + \operatorname{div}(\phi_V v) = \operatorname{div}(m_V(\phi_{\mathbb{A}}) \nabla \mu_V) + \operatorname{div} J_{\alpha} + S_V(\phi_{\mathbb{A}})$$

### 3.3.2. Nonlocal-in-time: The memory effect

According to [7, 136, 143], the tumor microenvironment has a significant impact on tumor cell proliferation and migration. Tumor cells migrate using a variety of mechanisms, including Fickian diffusion and subdiffusion. The results of the experiments in [91] indicate evidence of anomalous diffusion in cancer progression. They detected subdiffusion during in vitro trials of developing cultured cells from the breast line, as well as clinical data from patients with adrenal and liver tumors.

The phenomenological law  $J_T = -m_T(\phi_{\mathbb{A}})\nabla\mu_T$  has been used to represent the typical relationship between flow and the gradient of the chemical potential in previous sections. Without violating the conservation law indicated by the continuity equation, a more sophisticated phenomenological connection that could account for putative nonlocal, nonlinear, and memory effects, see [82, 115], may be substituted for this law. Subdiffusion-limited reactions are simulated on a microscopic level in [124, 144] by using fractional derivatives in flux and reaction terms. Therefore, we propose

$$J_T^{\text{rel}}(\phi_{\mathbb{A}}) = -\partial_t(g_\alpha \circledast (m_T(\phi_{\mathbb{A}})\nabla\mu_T)), \quad S_T^{\text{rel}}(\phi_{\mathbb{A}}) = \partial_t(g_\alpha \circledast S_T(\phi_{\mathbb{A}})),$$

for  $\alpha \in (0, 1)$ . Inserting the relaxed flux and source into the law of conservation of mass (3.1) for the tumor species  $\phi_T$  yields

$$\partial_t\phi_T = -\text{div}J_T^{\text{rel}}(\phi_{\mathbb{A}}) + S_T^{\text{rel}}(\phi_{\mathbb{A}}) = \partial_t(g_\alpha \circledast (\text{div}(m_T(\phi_{\mathbb{A}})\nabla\mu_T) + S_T(\phi_{\mathbb{A}}))).$$

We rewrite this system in an equivalent manner by taking the convolution with  $g_{1-\alpha}$  on both sides of the equation and using the inverse convolution property (2.2). This procedure yields:

$$\partial_t^\alpha\phi_T = \text{div}(m_T(\phi_{\mathbb{A}})\nabla\mu_T) + S_T(\phi_{\mathbb{A}}).$$

In the case of the Ginzburg–Landau energy (2.5), the chemical potential writes  $\mu_T = \Psi'(\phi_T) - \varepsilon_T^2\Delta\phi_T$  and this model is called the time-fractional Cahn–Hilliard equation, see our work [58, 64]. Choosing the Dirichlet energy  $\mathcal{E}(\phi_T) = \int_\Omega \phi_T^2 dx$  results in a time-fractional RDE as studied by us in [59] in a tumor growth setting.

### 3.4. Mechanical deformation

The surrounding host tissues increase mechanical stress as the tumor grows, limiting the tumor’s ability to grow further. In the literature [44, 90, 102, 103], RDEs with mechanical coupling have been used to model tumor growth with respect to mathematical modeling and sensitivity analyses. We added mechanical effects in a similar way in our work [59] and studied the well-posedness of the model. The underlying energy functional now includes a new component called the stored energy potential  $W(\phi_T, \varepsilon(u))$ , which is dependent on the tumor volume fraction  $\phi_T$  and the symmetric strain measure  $\varepsilon(u) = \frac{1}{2}(\nabla u + \nabla u^\top)$  of the displacement field  $u$ . Assuming small deformations, we consider the stored energy potential

$$W(\phi_T, \varepsilon(u)) = \frac{1}{2}\varepsilon(u) : T_M(\phi_T)\varepsilon(u) + \varepsilon(u) : T_S(\phi_T), \quad (3.9)$$

where  $T_S(\phi_T) = \lambda\phi_T\mathbb{1}$  denotes the symmetric compositional stress tensor with  $\lambda > 0$ , and  $T_M$  is the linear elastic inhomogeneous material tensor. Here, the symbol  $\mathbb{1}$  denotes the  $(d \times d)$ -dimensional identity matrix. The displacement field  $u$  is governed by the conservation law of linear and angular momentum

$$\begin{aligned}\partial_t(\phi_T v) + \operatorname{div}(\phi_T v \otimes v) &= \operatorname{div} T_C + \phi_T b + p, \\ T_C - T_C^\top &= m,\end{aligned}$$

where  $v$  is the volume-averaged velocity,  $b$  the body force,  $p$  the momentum supplied by other constituents, and  $m$  the intrinsic moment of momentum. The chemical potential  $\mu_T$  and the Cauchy stress tensor  $T_C$  are defined by the first variations of the energy functional  $\mathcal{E}$  with respect to  $\phi_T$  and  $\varepsilon(u)$ , respectively. We reduce the complexity of the system by using common simplifying assumptions as in [102]. In this regard, we assume constant mass density  $m = 0$  and a monopolar material  $b = 0$ . Further, we neglect inertial forces and set  $\operatorname{div}(\phi_T v \otimes v) = p = 0$ . We assume that the mechanical equilibrium is attained on a faster time scale than diffusion takes place, i.e., the time derivative on the left-hand side vanishes. After the simplifications, the equation of the mechanical deformation (3.9) reads

$$0 = \operatorname{div} T_C = \operatorname{div} \frac{\delta \mathcal{E}(\phi_T, \phi_\sigma, \varepsilon(u))}{\delta \varepsilon(u)} = \operatorname{div} \frac{\partial W(\phi_T, \varepsilon(u))}{\partial \varepsilon(u)}.$$

For ease of technical difficulties, we assume that the tumor is an isotropic and homogeneous material, i.e., its material tensor  $C_M(\phi) = C_M$  takes the form

$$C_M \varepsilon(u) = 2G\varepsilon(u) + \frac{2G\nu}{1-2\nu} \operatorname{tr} \varepsilon(u) \mathbb{1},$$

where  $G > 0$  and  $\nu < \frac{1}{2}$  denote the shear modulus and the Poisson ratio, respectively. Therefore, we can write for the stored energy potential

$$W(\phi_T, \varepsilon(u)) = \frac{1}{2} \varepsilon(u) : \left( 2G\varepsilon(u) + \frac{2G\nu}{1-2\nu} \operatorname{tr} \varepsilon(u) \mathbb{1} \right) \varepsilon(u) + \varepsilon(u) : (\lambda\phi_T \mathbb{1}),$$

and its partial derivatives with respect to  $\phi_T$  and  $\varepsilon(u)$  read

$$\frac{\partial W(\phi_T, \varepsilon(u))}{\partial \phi_T} = \lambda \operatorname{div} u, \quad \frac{\partial W(\phi_T, \varepsilon(u))}{\partial \varepsilon(u)} = 2G\varepsilon(u) + \frac{2G\nu}{1-2\nu} \operatorname{tr}(\varepsilon(u)) \mathbb{1} + \lambda\phi_T \mathbb{1}.$$

It yields the four-species model with mechanical deformation:

**Four-species model with mechanical deformation**

$$\begin{aligned}\partial_t \phi_T + \operatorname{div}(\phi_T v) &= \operatorname{div}(M_T \phi_T^2 (1 - \phi_T)^2 \nabla \mu_T) + S_T(\phi_T, \phi_\sigma) \\ \partial_t \phi_\sigma + \operatorname{div}(\phi_\sigma v) &= \operatorname{div}(M_\sigma \nabla(D_\sigma \phi_\sigma - \chi_c \phi_T)) + S_\sigma(\phi_T, \phi_\sigma) \\ 0 &= \operatorname{div} \left( 2G\varepsilon(u) + \frac{2G\nu}{1-2\nu} \operatorname{tr}(\varepsilon(u)) \mathbb{1} + \lambda\phi_T \mathbb{1} \right)\end{aligned}$$

In case of the Ginzburg–Landau energy, we obtain

$$\mu_T = \Psi'(\phi_T) - \chi_c \phi_\sigma - \varepsilon_T^2 \Delta \phi_T + \lambda \operatorname{div} u,$$

whereas it yields  $\mu_T = D_T \phi_T - \chi_c \phi_\sigma + \lambda \operatorname{div} u$  for the Dirichlet energy as done in our work [59], i.e.,

$$\mathcal{E}(\phi_T, \phi_\sigma) = \int_{\Omega} \left\{ \frac{D_T}{2} \phi_T^2 + \frac{D_\sigma}{2} \phi_\sigma^2 - \chi_c \phi_T \phi_\sigma + W(\phi_T, \varepsilon(u)) \right\} dx.$$

### 3.5. Chemotherapeutic influence

We do not only study the growth of tumors, but we also incorporate a constituent that will slow down the tumor's spread. Current tumor treatments are:

- Surgery: Removing the tumor by an operation.
- Immunotherapy: Strengthening the immune system.
- Radiotherapy: Employing radiation to kill tumor cells.
- Chemotherapy: Using drugs to kill the tumor.

Apart from surgery, these therapies are delivered in cycles, with each cycle consisting of a period of therapy followed by a period of rest to allow the patient's body to mend and regenerate new healthy cells. These therapeutic procedures should reduce the tumor to a manageable point where it can be surgically removed.

The mass density of chemotherapy  $\phi_{CMT}$  is assumed to be governed by a RDE that couples to the tumor equation and degrades the tumor if chemotherapy is present. Therefore, we add the index  $CMT$  to  $\mathbb{RD}$  and propose:

**Four-species model with chemotherapy**

$$\begin{aligned} \partial_t \phi_T + \operatorname{div}(\phi_T v) &= \operatorname{div}(M_T \phi_T^2 (1 - \phi_T)^2 \nabla \mu_T) + S_T(\phi_T, \phi_\sigma, \phi_{CMT}) \\ \mu_T &= \Psi'(\phi_T) - \chi_c \phi_\sigma - \varepsilon_T^2 \Delta \phi_T \\ \partial_t \phi_\sigma + \operatorname{div}(\phi_\sigma v) &= \operatorname{div}\left(M_\sigma \nabla (D_\sigma \phi_\sigma - \chi_c \phi_T)\right) + S_\sigma(\phi_T, \phi_\sigma, \phi_{CMT}) \\ \partial_t \phi_{CMT} &= M_{CMT} D_{CMT} \Delta \phi_{CMT} + S_{CMT}(\phi_T, \phi_\sigma, \phi_{CMT}). \end{aligned}$$

Here, the mobility of chemotherapeutic agents is denoted by  $M_{CMT}$  and the source  $S_{CMT}$  is of the form

$$S_{CMT}(\phi_T, \phi_\sigma, \phi_{CMT}) = -\lambda_{CMT}^{\operatorname{deg}} \phi_{CMT} - \lambda_{CMT}^{\operatorname{kill}} \frac{\phi_T (1 - \phi_T) \phi_{CMT}}{K_{CMT} + \phi_{CMT}},$$

where  $\lambda_{CMT}^{\operatorname{deg}}$  is the degradation factor of chemotherapeutic agents and  $\lambda_{CMT}^{\operatorname{kill}}$  is the rate at which chemotherapeutic agents act and are blocked later by killing tumor cells. The killing term includes a saturation effect, so that mainly cells in a certain growth phase are sensible to chemotherapy. The parameter  $K_{CMT} > 0$  is the density of chemotherapeutic agents when they reach their half-maximum value. Similarly, the source term of the tumor volume fraction will include a term of the form

$$-\lambda_T^{\operatorname{kill}} \frac{\phi_T (1 - \phi_T) \phi_{CMT}}{K_{CMT} + \phi_{CMT}},$$



which represents the killing effect of the chemotherapy at some rate  $\lambda_T^{\text{kill}}$ . In our work [59], we provide the chemotherapeutic agents in cycles by a Dirichlet boundary of the form

$$\phi_{CMT}(t, x)|_{x \in \partial\Omega} = \begin{cases} 1, & \text{for } t \leq 2 \text{ or } 6 < t \leq 8 \text{ or } 12 < t \leq 14, \\ 0, & \text{else.} \end{cases}$$

That is, during the times  $t \in [0, 2] \cup (6, 8] \cup (12, 14]$  chemotherapy is provided and in between, the body is allowed to rest.

### 3.6. Angiogenesis and mixed-dimensional coupling

The effect of angiogenesis in models of stratified tumor growth is presented in the works [101, 119, 120, 137, 139–141]. In contrast to their previous approaches using, e.g., agent-based systems, we model the network of blood arteries giving nutrition to a solid tumor mass in our papers [56, 57] as a network of 1D capillaries within a 3D tissue domain. In this regard, tumor growth is regarded as a phase-field system incorporating several cell species and other constituents. The microvascular network in the tumor-bearing tissue is represented by a graph structure with 1D filaments through which nutrient-rich blood can flow. This microvascular network is denoted by  $\Lambda$  and the single edges are denoted by  $\Lambda_i$  such that  $\Lambda$  is given by the union  $\Lambda = \bigcup_{i=1}^N \Lambda_i$ . An edge  $\Lambda_i$  is parameterized by a curve parameter  $s_i$  as follows:

$$\Lambda_i = \{x \in \Omega : x = \Lambda_i(s_i) = x_{i,1} + s_i \cdot (x_{i,2} - x_{i,1}), s_i \in (0, 1)\}.$$

We propose a global curve parameter  $s$  for the total 1D network  $\Lambda$ , defined as  $s = s_i$  if  $x = \Lambda(s) = \Lambda_i(s_i)$ . We look for 1D elements that couple to their 3D counterparts in  $\Omega$  for each value of the curve parameter  $s$ . We assume that the surface of a single vessel is a cylinder with a constant radius, and the radius of a vessel connected with  $\Lambda_i$  is given by  $R_i$ . We write  $\Gamma_i$  as the cylinder's surface, with  $\Lambda_i$  as its center line, and the total surface  $\Gamma$  is given by the union of the single vessel surfaces  $\Gamma_i$ .

On the 1D network  $\Lambda$ , we consider the constituents  $\phi_v$ ,  $v_v$  and  $p_v$ , which represent the 1D counterparts of the local nutrient concentration  $\phi_\sigma$ , the volume-averaged velocity  $v$  and the pressure  $p$ . We introduce a new source term  $S_{\sigma v}$  in the equation of  $\phi_\sigma$  for coupling the 1D constituents  $\phi_v$  and  $p_v$ . Therefore, this source term is responsible for the connection between the constituents in  $\Omega$  and  $\Lambda$ .

To quantify the flux of nutrients across the vessel surface, we use the Kedem–Katchalsky law [81] and write the flux  $J_{\sigma v}$  between the nutrients on the network and tissue as

$$J_{\sigma v}(\bar{\phi}_\sigma, \bar{p}, \phi_v, p_v) = (1 - r_\sigma) f(\phi_\sigma, \phi_v) L_p (p_v - \bar{p}) + L_\sigma (\phi_v - \bar{\phi}_\sigma), \quad (3.10)$$

where  $r_\sigma > 0$  is reflection parameter,  $L_\sigma, L_p > 0$  denote the permeabilities of the vessel wall, and the function  $f$  is either  $\phi_\sigma$  or  $\phi_v$  depending on the values of  $p$  and  $p_v$ . Moreover,  $\bar{p}$  denotes an averaged pressure over the circumference of cylinder cross-sections. From a physical standpoint, the averaging reflects the fact that the 3D-1D coupling is a reduced model, whereas the exchange occurs through the surface in a fully coupled 3D-3D model. The first part of the Kedem–Katchalsky law calculates the nutritional

flux generated by blood plasma flowing from arteries into tissue or vice versa. It is determined by Starling's law that is given by the pressure difference between  $p_v$  and  $p$  weighted by a parameter  $L_p$  for the vessel wall permeability. The second part of the law is a Fickian type law, accounting for the tendency of nutrients to balance out their concentration levels.

Since the exchange processes between the vascular network and the tissue occur at the vessel surface  $\Gamma$ , we concentrate the flux  $J_{\sigma v}$  by means of the Dirac measure  $\delta_\Gamma$ , i.e., with the distributional space  $(C_c^\infty(\Omega))'$  we define

$$\langle \delta_\Gamma, \varphi \rangle_{C_c^\infty(\Omega)} = \int_\Gamma \varphi|_\Gamma(x) \, dS \quad \forall \varphi \in C_c^\infty(\Omega).$$

This yields the following new source term in the nutrient equation

$$S_{\sigma v}(\phi_\sigma, p, \phi_v, p_v) = J_{\sigma v}(\phi_\sigma, p, \Pi_\Gamma \phi_v, \Pi_\Gamma p_v) \delta_\Gamma,$$

where  $\Pi_\Gamma \in \mathcal{L}(L^2(\Lambda); L^2(\Gamma))$  is the projection of the 1D quantities onto the cylindrical surface  $\Gamma$  via extending the function value  $\Pi_\Gamma \phi_v(s) = \phi_v(s_i)$  for all  $s \in \partial B_{R_i}(s_i)$ .

The 3D model reads:

<b>Angiogenesis model: 3D</b>	
$\partial_t \phi_\alpha + \operatorname{div}(\phi_\alpha v) = \operatorname{div}(m_\alpha(\phi_\mathbb{A}) \nabla \mu_\alpha) + S_\alpha(\phi_\mathbb{A})$	$\alpha \in \{P, H\}$
$\mu_\alpha = \partial_{\phi_\alpha} \Psi(\phi_{\text{CH}}) - \varepsilon_\alpha^2 \Delta \phi_\alpha - \chi_c \phi_\sigma - \chi_h \phi_{ECM}$	$\alpha \in \{P, H\}$
$\partial_t \phi_\beta = S_\beta(\phi_\mathbb{A})$	$\beta \in \{N, ECM\}$
$\partial_t \phi_\gamma = \operatorname{div}(m_\gamma(\phi_\mathbb{A}) D_\gamma \nabla \phi_\gamma) + S_\gamma(\phi_\mathbb{A})$	$\gamma \in \{MDE, TAF\}$
$\partial_t \phi_\sigma + \operatorname{div}(\phi_\sigma v) = \operatorname{div}(m_\sigma(\phi_\mathbb{A}) \nabla (D_\sigma \phi_\sigma - \chi_c(\phi_P + \phi_H))) + S_\sigma(\phi_\mathbb{A})$	
$\quad + J_{\sigma v}(\operatorname{tr}_\Gamma \phi_\sigma, \operatorname{tr}_\Gamma p, \Pi_\Gamma \phi_v, \Pi_\Gamma p_v) \delta_\Gamma$	
$v = -K(\nabla p - S_p(\phi_\mathbb{A}, \mu_P, \mu_H))$	
$\operatorname{div} v = L_p(\Pi_\Gamma p_v - p) \delta_\Gamma$	

Since the vascular network typically forms a system of small inclusions, we average all the physical units across the cross-sections of the single blood vessels and set them to a constant with respect to the angular and radial components. In other words, the 1D variables  $\phi_v$  and  $p_v$  on a 1D vessel  $\Lambda_i$  depend only on  $s_i$ . For further details related to the derivation of 1D pipe flow and transport models, we refer to [95]. Accordingly, the 1D model equations for flow and transport on  $\Lambda_i$  read as follows:

<b>Angiogenesis model: 1D</b>	
$\partial_t \phi_v + \partial_{s_i}(v_v \phi_v) = \partial_{s_i}(m_v(\phi_v) D_v \partial_{s_i} \phi_v) - 2\pi R_i J_{\sigma v}(\bar{\phi}_\sigma, \bar{p}, \phi_v, p_v)$	
$- \partial_{s_i}(R_i^2 \pi K_{v,i} \partial_{s_i} p_v) = -2\pi R_i J_{pv}(\bar{p}, p_v)$	
$v_v = -R_i^2 \pi K_{v,i} \partial_{s_i} p_v$	

In order to interconnect the different solutions on  $\Lambda_i$  at inner network nodes on intersections  $x \in \partial \Lambda_i \setminus \partial \Lambda$ , we require the continuity of pressure and concentration as well as the conservation of mass to obtain a physically relevant solution, see [56].

## 4. Well-Posedness Analysis

*The analysis of PDE is a beautiful subject, combining the rigour and technique of modern analysis and geometry with the very concrete real-world intuition of physics, biology, and other sciences.* (Terence Tao)

In this section, we describe the techniques that we apply to prove the well-posedness of weak solutions to the nonlinear systems of equations induced by the problems presented in the previous section. We analyze a prototype tumor growth model, which is a Cahn–Hilliard type phase-field equation with complex couplings. We combine it with homogeneous Neumann boundary and consider the setting of the Gelfand triple

$$V = H^1(\Omega) \hookrightarrow H = L^2(\Omega) \hookrightarrow V'.$$

We also investigate different effects like mixed-dimensional couplings and nonlocal influences, as well as the key estimates in the Faedo–Galerkin setting. The method’s basic concept is outlined in the following subsection.

### 4.1. Faedo–Galerkin method

- (FG1) **Approximate problem.** Because  $V$  is separable, there exists a linearly independent sequence  $\{v_k\}_{k \in \mathbb{N}}$  in  $V$ , whose span is dense in  $V$ . We approximate the Cahn–Hilliard equation via a problem in the finite-dimensional space  $V_k = \text{span}\{v_1, v_2, \dots, v_k\}$ . This reduces the problem to an ODE and we can apply standard theory to ensure the existence of a solution of this finite-dimensional problem. As a result, we obtain a sequence of solutions  $\{\phi_k\}_{k \in \mathbb{N}}$  of the respective finite-dimensional problem in  $\{V_k\}_{k \in \mathbb{N}}$ .
- (FG2) **Energy estimates.** In this step, one shows that the sequence of solutions  $\{\phi_k\}_{k \in \mathbb{N}}$  is uniformly bounded in the typical solution space  $L^\infty(0, T; V)$  of the Cahn–Hilliard equation. According to the theorem of Banach–Alaoglu, there is a subsequence  $\{\phi_{k_j}\}_{j \in \mathbb{N}}$  that converges weakly-\* to some element  $\phi$  in this space.
- (FG3) **Compactness.** We prove that the derivative of  $\phi_{k_j}$ ,  $j \in \mathbb{N}$ , is bounded in the Bochner space  $L^2(0, T; V')$  and thus, we can apply the Aubin–Lions lemma, see (2.1), to conclude that  $\{\phi_{k_j}\}_{j \in \mathbb{N}}$  converges strongly in  $C([0, T]; H)$ . This strong convergence is essential for the limit process in (FG5). Otherwise, we would not be able to conclude the convergence of the nonlinear functions  $m$  and  $\Psi$  in the Cahn–Hilliard equation.
- (FG4) **Initial condition.** We show that the limit function  $\phi$  also fulfills the imposed initial condition  $\phi(0) = \phi_0$  in  $V'$ . This is performed using the strong convergence at  $t = 0$  and the uniqueness of limits.
- (FG5) **Limit process.** In (FG1), we proved the existence of functions  $\phi_{k_j}$ ,  $j \in \mathbb{N}$ , fulfilling the  $k_j$ -th Faedo–Galerkin equations, respectively. In this step, we take the limit  $j \rightarrow \infty$  of the  $k_j$ -th Faedo–Galerkin equations to obtain the variational Cahn–Hilliard equation. Thus, the weak-\* limit of a subsequence of  $\{\phi_k\}_{k \in \mathbb{N}}$  turns out to be a solution of the variational Cahn–Hilliard equation.

## 4.2. Analysis of the four-species model

In this section, we follow through the steps of the Faedo–Galerkin method in an explaining manner. For more information on the technical details, we refer to our papers [57, 59, 61, 62]. We consider the four-species model of (3.6) with an incompressible volume-averaged velocity that is governed by Darcy’s law  $v = -K\nabla p + K(\mu_T + \chi_c\phi_\sigma)\nabla\phi_T$ . Together, we analyze the model:

$$\begin{aligned} \partial_t\phi_T + \operatorname{div}(\phi_T v) &= \operatorname{div}(m_T(\phi_T, \phi_\sigma)\nabla\mu_T) + S_T(\phi_T, \phi_\sigma) \\ \mu_T &= \Psi'(\phi_T) - \varepsilon_T^2\Delta\phi_T - \chi_c\phi_\sigma \\ \partial_t\phi_\sigma + \operatorname{div}(\phi_\sigma v) &= \operatorname{div}(M_\sigma\nabla(D_\sigma\phi_\sigma - \chi_c\phi_T)) + S_\sigma(\phi_T, \phi_\sigma) \\ v &= -K\nabla p + K(\mu_T + \chi_c\phi_\sigma)\nabla\phi_T \\ \operatorname{div}v &= 0 \end{aligned}$$

We couple this system to the initial data  $\phi_T(0) = \phi_{T,0}$ ,  $\phi_\sigma(0) = \phi_{\sigma,0}$ , and the homogeneous Neumann boundary data

$$\nabla\phi_T \cdot n = \nabla\mu_T \cdot n = \nabla\phi_\sigma \cdot n = v \cdot n = 0 \quad \text{on } \partial\Omega.$$

Since we are interested in weak solutions, we formulate the system as a variational form and look for functions  $\phi_T$ ,  $\mu_T$ ,  $\phi_\sigma$  and  $v$  such that it holds:

$$\begin{aligned} (\partial_t\phi_T, \varphi_T)_H + (m_T(\phi_T, \phi_\sigma)\nabla\mu_T, \nabla\varphi_T)_H &= (\phi_T v, \nabla\varphi_T)_H + (S_T(\phi_T, \phi_\sigma), \varphi_T)_H \\ (\Psi'(\phi_T), \varphi_\mu)_H + \varepsilon_T^2(\nabla\phi_T, \nabla\varphi_\mu)_H &= (\mu_T, \varphi_\mu)_H + \chi_c(\phi_\sigma, \varphi_\mu)_H \\ (\partial_t\phi_\sigma, \varphi_\sigma)_H + M_\sigma D_\sigma(\nabla\phi_\sigma, \varphi_\sigma)_H &= M_\sigma \chi_c(\nabla\phi_T, \varphi_\sigma)_H + (\phi_\sigma v, \nabla\varphi_\sigma)_H \\ &\quad + (S_\sigma(\phi_T, \phi_\sigma), \varphi_\sigma)_H \\ (v, \varphi_v)_H &= K(\mu + \chi_c\phi_\sigma, \nabla\phi_T \cdot \varphi_v)_H \end{aligned}$$

for all test functions  $\varphi_T, \varphi_\mu, \varphi_\sigma \in V$  and  $\varphi_v \in V_{\operatorname{div}} = \{\varphi \in V : \operatorname{div}v = 0\}$ .

As a first step in the Faedo–Galerkin method, see (FG1), we introduce discrete spaces  $V_k$  and  $V_{\operatorname{div},k}$ , which are spans of eigenfunctions to the Neumann–Laplace problem. This has the advantage that the eigenfunctions form an orthonormal basis in  $H$  and a orthogonal one in  $V$ . Then one postulates the Faedo–Galerkin approximation system with test functions in the discrete spaces. One proposes ansatz functions for the approximate solutions in terms of a linear combination of the eigenfunctions, which reduces the system to ODEs with continuous right-hand sides. Therefore, the system has a continuous solution in finite time due to the Cauchy–Peano theorem, i.e.,

$$\phi_T^k, \mu_T^k, \phi_\sigma^k \in C^1([0, T_k]; V_k), \quad v^k \in C^1([0, T_k]; V_{\operatorname{div},k}).$$

In the next step, (FG2), the main difficulty appears – the energy estimates. One has to perform clever testing and absorb the right-hand sides by the left-hand sides of the inequalities. The goal is a uniform energy inequality in order to extract weakly convergent subsequences. In the Cahn–Hilliard equation, one typically tests the phase-field equation by its chemical potential, and the equation of the chemical potential by

the negative time-derivative of the phase-field variable. In this manner, the mixed terms  $(\partial_t \phi_T^k, \mu_T^k)_H$  negate each other. In addition, we test the phase-field equation by  $\chi_c \phi_\sigma^k$  to cancel the chemotaxis term in the equation of the chemical potential. We test the velocity equation with  $v^k$  itself and now we can see why the Korteweg force  $S_p$  in the Darcy equation was chosen in this manner. It cancels exactly with the tested convection terms in the tumor and nutrient equations. Therefore, the initially difficult-looking nonlinear terms got canceled away.

All in all, we take the test functions  $\varphi_T = \mu_T^k + \chi_c \phi_\sigma^k$ ,  $\varphi_\mu = -\partial_t \phi_T^k$ ,  $\varphi_\sigma = C_\sigma \phi_\sigma^k$ ,  $\varphi_v = v^k$ , which yields the tested and added system

$$\begin{aligned} & \frac{d}{dt} \left[ \|\Psi(\phi_T^k)\|_{L^1(\Omega)} + \frac{\varepsilon_T^2}{2} \|\nabla \phi_T^k\|_H^2 + \frac{C_\sigma}{2} \|\phi_\sigma^k\|_H^2 \right] + C_\sigma D_\sigma M_\sigma \|\nabla \phi_\sigma^k\|_H^2 + M_0 \|\nabla \mu_T^k\|_H^2 \\ & + \frac{1}{K} \|v^k\|_H^2 \\ & \leq -\chi_c (m_T^k \nabla \mu_T^k, \nabla \phi_\sigma^k)_H + (S_T^k, \mu^k + \chi_c \phi_\sigma^k)_H + \chi_c C_\sigma M_\sigma (\nabla \phi_T^k, \nabla \phi_\sigma^k)_H + C_\sigma (S_\sigma^k, \phi_\sigma^k)_H. \end{aligned}$$

We can already state the assumptions that we need in order to achieve a uniform energy bound. We require that the mobility function  $m_T$  is bounded from below by some positive constant  $M_0 > 0$ . Of course, the typical mobility function  $m(x) = x^2(1-x)^2$  does not satisfy this assumption, but it can be shifted slightly upwards by some small parameter  $\delta > 0$ . To consider degenerate mobility functions, one first proves the existence of a bounded mobility and then, one approximates the degenerating mobility by some sequence  $m_\delta$  with  $m_\delta(x) > M(\delta) > 0$  and  $m_\delta \rightarrow m$  as  $\delta \rightarrow 0$ . We refer to the papers [39, 54, 64] on this subject.

In the case of the third term on the right side, it is straightforward to estimate it using the  $\varepsilon$ -Young inequality and reduce the prefactor of  $\|\nabla \phi_\sigma^k\|_H^2$  sufficiently to absorb it by the left side. A large prefactor for  $\|\nabla \phi_T^k\|_H^2$  is not a problem because we can absorb it later by the Grönwall–Bellman lemma. The first term is more difficult in this spirit. Both the terms  $\|\nabla \mu_T^k\|_H^2$  and  $\|\nabla \phi_\sigma^k\|_H^2$  in the first term should be sufficiently small. We can compensate for this by using the prefactor of  $\|\nabla \phi_\sigma^k\|_H^2$  on the inequality's left side. We scaled the test function for the nutrient equation by an open parameter  $C_\sigma > 0$  and now we choose it big enough to absorb the large prefactor after giving  $\|\nabla \mu_T^k\|_H^2$  a small one.

We need some well-behaved source terms, e.g., some kind of linear growth estimate like

$$|S_T^k|, |S_\sigma^k| \leq C(1 + |\phi_T^k| + |\phi_\sigma^k|).$$

More general source functions can be treated in a second approximation by first linearizing the source functions, e.g., see [28]. Now, we only miss the term of  $\mu_T^k$  on the right-hand side. Up to now, we can control the gradient of the chemical potential, but not the potential itself. We can achieve this by testing the equation of the chemical potential with 1 and applying the Poincaré–Wirtinger inequality. In order to estimate the upcoming term  $\|\Psi'(\phi_T^k)\|_{L^1(\Omega)}$  on the right-hand side, we have to assume some growth estimate on the double-well potential. One can either bound the derivative by the solution itself, or uses some power estimate, i.e.,

$$|\Psi'(\phi_T^k)| \leq C(1 + |\Psi(\phi_T^k)|), \quad |\Psi'(\phi_T^k)| \leq C(1 + |\phi_T^k|^q),$$

and  $q > 1$  is determined by the Sobolev embedding theorem in order to absorb this term by the gradient term on the left-hand side.

After taking care of the right-hand side and the necessary absorptions and integrating over the time-interval  $(0, t)$ ,  $t \leq T_k$ , we end up with the inequality

$$\begin{aligned} & \|\Psi(\phi_T^k(t))\|_{L^1(\Omega)} + \|\nabla \phi_T^k(t)\|_H^2 + \|\phi_\sigma^k(t)\|_H^2 + \|\nabla \phi_\sigma^k\|_{L^2(0,t;H)}^2 + \|\nabla \mu_T^k\|_{L^2(0,t;H)}^2 \\ & + \|v^k\|_{L^2(0,t;H)}^2 \lesssim 1 + \|\Psi(\phi_T^k(0))\|_{L^1(\Omega)} + \|\nabla \phi_T^k(0)\|_H^2 + \|\phi_\sigma^k(0)\|_H^2. \end{aligned}$$

We use the Grönwall–Bellman lemma and take advantage of the fact that the approximation's initial  $\phi_T^k(0) = \Pi_k \phi_0$  can be bounded by the PDE's initial because the operator norm of the orthogonal projection  $\Pi_k : V \rightarrow V_k$  is bounded by 1. Therefore, we achieve the energy estimate

$$\begin{aligned} & \|\Psi(\phi_T^k)\|_{L^\infty(0,T;L^1(\Omega))} + \|\nabla \phi_T^k\|_{L^\infty(0,T;H)}^2 + \|\phi_\sigma^k\|_{L^\infty(0,T;H)}^2 + \|\nabla \phi_\sigma^k\|_{L^2(0,T;H)}^2 \\ & + \|\nabla \mu_T^k\|_{L^2(0,T;H)}^2 + \|v^k\|_{L^2(0,T;H)}^2 \lesssim 1 + \|\nabla \phi_T(0)\|_H^2 + \|\phi_\sigma(0)\|_H^2, \end{aligned}$$

where also already took the essential supremum over  $t$  and extended the time-interval by setting  $T_k = T$  due to the no-blow-up criteria and the right-hand side being independent of  $k$ .

All our spaces are reflexive and due to the Banach–Alaoglu and Eberlein–Šmulian theorems [2, 13], there are functions  $\phi_T, \mu_T, \phi_\sigma, v$  such that it holds

$$\begin{aligned} \phi_T^{k_j} & \rightharpoonup \phi_T \text{ weakly-* in } L^\infty(0, T; V), \\ \mu^{k_j} & \rightharpoonup \mu \text{ weakly in } L^2(0, T; V), \\ \phi_\sigma^{k_j} & \rightharpoonup \phi_\sigma \text{ weakly-* in } L^\infty(0, T; H) \cap L^2(0, T; V), \\ v^{k_j} & \rightharpoonup v \text{ weakly in } L^2(0, T; H). \end{aligned}$$

as  $j \rightarrow \infty$ . The weak convergence is not enough to pass the limit in the nonlinear functions in the Faedo–Galerkin system and therefore, strong convergences are required. We bound the time-derivative of  $\phi_T^k$  and  $\phi_\sigma^k$  in the step (FG3) in order to apply the Aubin–Lions lemma (2.1).

Let us fix an arbitrary function  $\varphi \in L^2(0, T; V)$ . We must test the Faedo–Galerkin system with a function in the discrete space  $V_{k_j}$ , so we test with the orthogonal projection of  $\varphi$  onto  $V_{k_j}$ . We take advantage of the fact that the adjoint of this function is invariant under the time derivative and its operator norm equals 1, see [12]. Therefore, we get after testing

$$\int_0^T \langle \partial_t \phi_T^{k_j}, \varphi \rangle_V dt = \int_0^T (\phi_T^{k_j} v^{k_j} - m_T^{k_j} \nabla \mu_T^{k_j}, \nabla \Pi_{k_j} \varphi)_H + (S_T^{k_j}, \Pi_{k_j} \varphi)_H dt,$$

which directly gives a uniform bound of  $\partial_t \phi_T^{k_j}$  in the space  $L^2(0, T; V')$  after applying the Hölder inequality and using the energy estimate from before. By using the Aubin–Lions lemma (2.1) on the Gelfand triple  $V \hookrightarrow H \hookrightarrow V'$ , it yields the compact embedding

$$L^\infty(0, T; V) \cap H^1(0, T; V') \hookrightarrow C([0, T]; H).$$

Therefore, we obtain the new convergences

$$\begin{aligned}\partial_t \phi_T^{k_j} &\rightharpoonup \partial_t \phi_T \text{ weakly in } L^2(0, T; V'), \\ \phi_T^{k_j} &\longrightarrow \phi_T \text{ strongly in } C([0, T]; H),\end{aligned}$$

as  $j \rightarrow \infty$ . We also know from the strong convergence that  $\phi_T^{k_j}(0) \rightarrow \phi_T(0)$  in  $H$ , which implies  $\phi_T(0) = \phi_{T,0}$  in  $H$ , i.e., step (FG4) is completed.

We multiply the Faedo–Galerkin system by a function  $\eta \in C_c^\infty(0, T)$  and integrate the system on  $(0, T)$  which yields for the tumor equation

$$\int_0^T \langle \partial_t \phi_T^{k_j}, \varphi_T \rangle_V \eta + (m_T^{k_j} \nabla \mu_T^{k_j}, \varphi_T)_H \eta \, dt = \int_0^T (\phi_T^{k_j} v^{k_j}, \nabla \varphi_T)_H \eta + (S_T^{k_j}, \varphi_T) \eta \, dt,$$

for all  $\varphi_T \in V_{k_j}$ . In order to complete step (FG5), we take the limit  $j \rightarrow \infty$  in the equation and use the density of  $\cup_j V_{k_j}$  in  $V$ . The linear terms follow directly from the given weak convergence. For the nonlinear terms, we apply the Lebesgue dominated convergence and exploit the boundedness assumptions of the nonlinear functions. Further, we use the weak-strong convergence lemma to pass the limit in the term involving the mobility function. In fact, by the strong convergence and the boundedness of  $m_T$ , we obtain on the one hand

$$m_T(\phi_T^{k_j}) \varphi_T \eta \longrightarrow m_T(\phi_T) \varphi_T \eta \quad \text{in } L^2((0, T) \times \Omega).$$

We have, on the other hand, derived the weak convergence  $\nabla \mu_T^{k_j} \rightharpoonup \nabla \mu$  in  $L^2((0, T) \times \Omega)$ , which means that their product converges strongly in  $L^1((0, T) \times \Omega)$ .

### 4.3. Key estimates

In this section, we analyze the key estimates in the step (FG2) of the Faedo–Galerkin method of the systems that we have derived in Section 3. We need to take care of the new complex couplings and nonlocalities. We derive the key estimates in the continuous setting in order to drop the index  $k$ . For the proof to be rigorous, the estimates must still be obtained at a discrete level, see, e.g., our works [57, 59, 61, 62].

#### 4.3.1. Stratified tumor growth model

In the case of a stratified tumor that has undergone phase separation and admits a proliferative, hypoxic, and necrotic phase, it leads to couplings between several Cahn–Hilliard equations. This results to difficulties in the definition of the potential function  $\Psi$  and in the choice of the correct test functions. We are in the setting of the system as in (3.7) and choose  $\mathbb{A} = \mathbb{C}\mathbb{H} = \{P, H, N\}$ .

$\begin{aligned}\partial_t \phi_P &= \operatorname{div}(m_P(\phi_{\mathbb{A}}) \nabla \mu_P) + S_P(\phi_{\mathbb{A}}) \\ \mu_P &= \partial_{\phi_P} \Psi(\phi_{\mathbb{C}\mathbb{H}}) - \varepsilon_P^2 \Delta \phi_P \\ \partial_t \phi_H &= \operatorname{div}(m_H(\phi_{\mathbb{A}}) \nabla \mu_H) + S_H(\phi_{\mathbb{A}}) \\ \mu_H &= \partial_{\phi_H} \Psi(\phi_{\mathbb{C}\mathbb{H}}) - \varepsilon_H^2 \Delta \phi_H \\ \partial_t \phi_N &= S_N(\phi_{\mathbb{A}})\end{aligned}$
---------------------------------------------------------------------------------------------------------------------------------------------------------------------------------------------------------------------------------------------------------------------------------------------------------------------------------------------------------------------------------------------------------------------------------------------------------------------------------------------

We use a Landau-type potential function as described in 3.1. In this system, we explicitly exclude chemotaxis and haptotaxis in order to concentrate on the multiphase system. Similarly, we set the velocity to zero. We take the typical test functions of the Cahn–Hilliard equation and achieve

$$\begin{aligned}
& (\partial_t \phi_P, \mu_P)_H + (m_P(\phi_{\mathbb{A}}), |\nabla \mu_P|^2)_H = (S_P(\phi_{\mathbb{A}}), \mu_P)_H, \\
& (\partial_{\phi_P} \Psi(\phi_{\text{CH}}), \partial_t \phi_P)_H + \varepsilon_P^2 (\nabla \phi_P, \partial_t \nabla \phi_P)_H = (\mu_P, \partial_t \phi_P)_H, \\
& (\partial_t \phi_H, \mu_H)_H + (m_H(\phi_{\mathbb{A}}), |\nabla \mu_H|^2)_H = (S_H(\phi_{\mathbb{A}}), \mu_H)_H, \\
& (\partial_{\phi_H} \Psi(\phi_{\text{CH}}), \partial_t \phi_H)_H + \varepsilon_H^2 (\nabla \phi_H, \partial_t \nabla \phi_H)_H = (\mu_H, \partial_t \phi_H)_H, \\
& (\partial_t \phi_N, \partial_{\phi_N} \Psi(\phi_{\text{CH}}) - \varepsilon_N^2 \Delta \phi_N)_H = (S_N(\phi_{\mathbb{A}}), \partial_{\phi_N} \Psi(\phi_{\text{CH}}) - \varepsilon_N^2 \Delta \phi_N)_H.
\end{aligned}$$

Only the test function of  $\phi_N$  may seem unusual. This is caused by the irregular character of the necrotic cells. Despite the fact that it is a tumor component, influences the potential function  $\Psi$ , and is a phase-field variable, its mobility is zero, and thus its analytical regularity is lost. As a result, we test it with its Laplacian  $-\Delta \phi_N$  and assume more regularity on its source function  $S_N$ . Moreover, we test with the partial derivative of  $\Psi$  in order to get the total derivative of  $\Psi$  on the left-hand side of the energy inequality. By adding and canceling, we get

$$\begin{aligned}
& \frac{d}{dt} \left[ \|\Psi(\phi_{\text{CH}})\|_{L^1(\Omega)} + \sum_{\alpha \in \text{CH}} \frac{\varepsilon_{\alpha}^2}{2} \|\nabla \phi_{\alpha}\|_H^2 \right] + \|\sqrt{m_P(\phi_{\mathbb{A}})} \nabla \mu_P\|_H^2 + \|\sqrt{m_H(\phi_{\mathbb{A}})} \nabla \mu_H\|_H^2 \\
& = (S_P(\phi_{\mathbb{A}}), \mu_P)_H + (S_H(\phi_{\mathbb{A}}), \mu_H)_H + (S_N(\phi_{\mathbb{A}}), \partial_{\phi_N} \Psi(\phi_{\text{CH}}) - \varepsilon_N^2 \Delta \phi_N)_H.
\end{aligned}$$

In the case of the last term, we need a new assumption on the growth character of the potential's partial derivative such as linear growth. Moreover, the chain rule yields

$$-(S_N(\phi_{\mathbb{A}}), \Delta \phi_N)_H = \sum_{\alpha \in \mathbb{A}} (\partial_{\phi_{\alpha}} S_N(\phi_{\mathbb{A}}), \nabla \phi_{\alpha} \cdot \nabla \phi_N)_H,$$

which suggests an additional assumption on the partial derivatives of the source  $S_N$ . We do not need a smallness assumption here, since we can give  $\|\nabla \phi_N\|_H^2$  a large prefactor anyway due to the structure for the application of the Grönwall–Bellman lemma.

#### 4.3.2. Nonlocal-in-space effect

We investigate both nonlocal cell-cell and cell-matrix adhesion effects in our papers [61, 62]. The first one is concerned with the nonlocal adhesion flux between the tumor cells and the ECM. The second paper introduces long-range interactions directly in a modified Ginzburg–Landau energy and such nonlocal Cahn–Hilliard equations have also been analyzed in [8–10, 65, 66] without the application to tumor modeling. In [21, 50–52], the nonlocal Cahn–Hilliard equation has been coupled to the Navier–Stokes equation, in [31] to the Darcy equation, and in [32] to the Brinkman equation. In the work [54] by Frigeri and others, a nonlocal tumor growth system was studied with respect to its well-posedness. We briefly discuss the modifications in the energy estimates of the



nonlocal model (3.8) in contrast to the estimates of the local system. For convenience, we state the system:

$$\begin{cases} \partial_t \phi_T = \operatorname{div}(m_T(\phi_T, \phi_\sigma) \nabla \mu_T) + S_T(\phi_T, \phi_\sigma) \\ \mu_T = \Psi'(\phi_T) - \chi_c \phi_\sigma + \phi_T \cdot J * 1 - J * \phi_T \\ \partial_t \phi_\sigma = \operatorname{div}(m_\sigma(\phi_T, \phi_\sigma)(D_\sigma \nabla \phi_\sigma - \chi_c \nabla \phi_T)) + S_\sigma(\phi_T, \phi_\sigma) \end{cases}$$

Due to the integro-differential structure, we cannot expect  $\phi_T \in L^\infty(0, T; V)$  since no Laplacian appears in the equation of the chemical potential. Therefore, the term  $\chi_c \operatorname{div}(m_\sigma \nabla \phi_T)$  in the nutrient equation has to be treated again, and we will see that we require an additional assumption on the chemotaxis parameter  $\chi_c$ . We take the typical test functions of the four-species model as before and achieve

$$\begin{aligned} & \frac{d}{dt} \left[ \|\Psi(\phi_T)\|_{L^1(\Omega)} + \frac{1}{2} \|(J * 1)^{1/2} \phi_T\|_H^2 - \frac{1}{2} (\phi_T, J * \phi_T)_H + \frac{C_\sigma}{2} \|\phi_\sigma\|_H^2 \right] \\ & + (m_T(\phi_T, \phi_\sigma), |\nabla \mu_T|^2)_H + C_\sigma D_\sigma (m_\sigma(\phi_T, \phi_\sigma), |\nabla \phi_\sigma|^2)_H \\ & = -\chi_c (m_T(\phi_T, \phi_\sigma) \nabla \mu_T, \nabla \phi_\sigma)_H + (S_T(\phi_T, \phi_\sigma), \mu_T + \chi_c \phi_\sigma)_H \\ & + \chi_c C_\sigma (m_\sigma(\phi_T, \phi_\sigma) \nabla \phi_T, \nabla \phi_\sigma)_H + C_\sigma (S_\sigma(\phi_T, \phi_\sigma), \phi_\sigma)_H. \end{aligned} \quad (4.1)$$

We estimate the right-hand side as in the four-species model from before, which results in terms  $\|\nabla \phi_T\|_H^2$  with large prefactors. At this point, there is no information on  $\frac{d}{dt} \|\nabla \phi_T\|_H^2$  on the left-hand side of (4.1), which is crucially needed to absorb the terms from the right-hand side. Due to a growth estimate on  $\Psi$  and the Young convolution inequality, we can derive

$$\begin{aligned} & \|\Psi(\phi_T)\|_{L^1(\Omega)} + \frac{1}{2} \|(J * 1)^{1/2} \phi_T\|_H^2 - \frac{1}{2} (\phi_T, J * \phi_T)_H \\ & \geq \int_\Omega \left[ C + \frac{1}{2} (J * 1)(x) - \frac{1}{2} \|J\|_{L^1(\Omega)} \right] |\phi_T(x)|^2 dx - C|\Omega| \\ & \geq C(\|\phi_T\|_H^2 - 1). \end{aligned} \quad (4.2)$$

This estimate will give us  $\phi_T \in L^\infty(0, T; H)$ . Indeed, integrating (4.1) with respect to time on the interval  $(0, s)$ ,  $0 < s < T$ , and introducing the result into (4.2) and employing the estimates of the source terms gives

$$\begin{aligned} & C \|\phi_T(s)\|_H^2 + \frac{C_\sigma}{2} \|\phi_\sigma(s)\|_H^2 + \frac{m_0}{2} \|\nabla \mu_T\|_{L^2(0, T; H)}^2 \\ & + \left( C_\sigma D_\sigma m_0 - \frac{\chi_c^2 m_\infty^2}{m_0} - \frac{\chi_c m_\infty}{2} \right) \|\nabla \phi_\sigma\|_{L^2(0, T; H)}^2 - \frac{\chi_c K^2 m_\infty}{2} \|\nabla \phi_T\|_{L^2(0, T; H)}^2 \\ & \lesssim 1 + \|\phi_T\|_{L^2(0, T; H)}^2 + \|\phi_\sigma\|_{L^2(0, T; H)}^2, \end{aligned} \quad (4.3)$$

where we have put the initial values into the constant since we are not interested in them at this point. Note that we have the term  $\|\nabla \phi_T\|_{L^2(0, T; H)}^2$  with a negative sign on the left-hand side in the inequality (4.3). To apply the Grönwall–Bellman lemma, we must overpower this term, so we use  $-\Delta \phi_T$  as a test function in the  $\mu$ -equation. On

one hand, using a suitable growth estimate on  $\Psi''$  such as  $\Psi''(x) \geq C_\Psi$  and again the Young convolution inequality, we deduce that

$$\begin{aligned}
(\nabla\mu_T, \nabla\phi_T)_H &= (\Psi''(\phi_T), |\nabla\phi_T|^2)_H + (|\nabla\phi_T|^2, J * 1)_H + (\nabla(J * 1), \phi_T \nabla\phi_T)_H \\
&\quad - (\nabla J * \phi_T, \nabla\phi_T)_H - \chi_c (\nabla\phi_\sigma, \nabla\phi_T)_H \\
&\geq C_\Psi \|\nabla\phi_T\|_H^2 - \|\nabla J\|_{L^1(\Omega)} \|\phi_T\|_H \|\nabla\phi_T\|_H - \chi_c \|\nabla\phi_\sigma\|_H \|\nabla\phi_T\|_H \\
&\geq \frac{C_\Psi}{2} \|\nabla\phi_T\|_H^2 - C \|\phi_T\|_H^2 - \frac{\chi_c^2}{C_\Psi} \|\nabla\phi_\sigma\|_H^2.
\end{aligned}$$

On the other hand, we have by the Hölder inequality

$$(\nabla\mu_T, \nabla\phi_T)_H \leq \frac{1}{C_T} \|\nabla\mu_T\|_H^2 + \frac{C_T}{4} \|\nabla\phi_T\|_H^2,$$

for some constant  $C_T$ . Combining these two inequalities gives the following estimate

$$\frac{m_0 C_\Psi^2}{16} \|\nabla\phi_T\|_H^2 \leq \frac{m_0}{4} \|\nabla\mu_T\|_H^2 + C \|\phi_T\|_H^2 + \frac{m_0 \chi_c^2}{4} \|\nabla\phi_\sigma\|_H^2.$$

Adding this inequality to (4.3) results in

$$\begin{aligned}
&C \|\phi_T(s)\|_H^2 + \frac{C_\sigma}{2} \|\phi_\sigma(s)\|_H^2 + \frac{m_0}{2} \|\nabla\mu_T\|_{L^2(0,T;H)}^2 \\
&+ \left( \frac{C_\sigma m_0}{\delta_\sigma} - \frac{\chi_c^2 m_\infty^2}{m_0} - \frac{\chi_c m_\infty}{2} - \frac{m_0 \chi_c^2}{4} \right) \|\nabla\phi_\sigma\|_{L^2(0,T;H)}^2 \\
&+ \left( \frac{m_0 C_T^2}{16} - \frac{\chi_c C_\sigma^2 m_\infty}{2} \right) \|\nabla\phi_T\|_{L^2(0,T;H)}^2 \\
&\lesssim 1 + \|\phi_T\|_{L^2(0,T;H)}^2 + \|\phi_\sigma\|_{L^2(0,T;H)}^2.
\end{aligned}$$

We set  $C_\sigma$  to a sufficiently large value so that the prefactor of  $\|\nabla\phi_\sigma\|_{L^2(0,T;H)}^2$  is strictly positive. Furthermore, the prefactor of  $\|\nabla\phi_T\|_{L^2(0,T;H)}^2$  is positive if  $C_\Psi$  is large enough or the chemotaxis factor  $\chi_c$  is sufficiently small. The Grönwall–Bellman lemma gives the final energy estimate.

### 4.3.3. Nonlocal-in-time effect

In this section, we point out the differences in the proof of the existence of weak solutions if a time-fractional derivative is involved. The Faedo–Galerkin system is reduced to a fractional differential equation (FDE) instead of an ODE. Similar to the classical theorems of Cauchy–Peano and Cauchy–Lipschitz, there is standard theory on the well-posedness of FDEs, see [34, 93]. It leads to the existence of approximative solutions in the solution space  $H^\alpha(0, T_k; V_k)$ .

Typically, the same test functions are taken. For example, in the case of the time-fractional Cahn–Hilliard equation

$$\begin{aligned}
\partial_t^\alpha \phi &= \operatorname{div}(m(\phi) \nabla \mu) + S(\phi), \\
\mu &= \Psi'(\phi) - \varepsilon^2 \Delta \phi,
\end{aligned}$$

we test the  $\phi$ -equation by  $\mu$  and the  $\mu$ -equation by  $-\partial_t^\alpha \phi$ , which yields

$$\varepsilon^2(\nabla\phi, \partial_t^\alpha \nabla\phi)_H + (\Psi'(\phi), \partial_t^\alpha \phi)_H + (m(\phi), |\nabla\mu|^2)_H = (S(\phi), \mu)_H.$$

We can apply the fractional chain inequality (2.4) to obtain the lower estimates

$$\frac{\varepsilon^2}{2} \partial_t^\alpha \|\nabla\phi\|_H^2 + \partial_t^\alpha \|\Psi'(\phi)\|_{L^1(\Omega)} \leq \varepsilon^2(\nabla\phi, \partial_t^\alpha \nabla\phi)_H + (\Psi'(\phi), \partial_t^\alpha \phi)_H,$$

where we have assumed that  $\Psi$  is convex. Afterwards, one convolves the inequality with the kernel function  $g_\alpha$  and use the inverse convolution property  $g_\alpha \otimes \partial_t^\alpha \phi = \phi - \phi_0$ , see (2.2), to achieve

$$\begin{aligned} & \frac{\varepsilon^2}{2} \|\nabla\phi(t)\|_H^2 + \|\Psi(\phi(t))\|_{L^1(\Omega)} + M_0(g_\alpha \otimes \|\nabla\mu\|_H^2)(t) \\ & \leq \frac{\varepsilon^2}{2} \|\nabla\phi(0)\|_H^2 + \|\Psi(\phi(0))\|_{L^1(\Omega)} + g_\alpha \otimes (S(\phi), \mu)_H. \end{aligned}$$

The term on the right-hand side involving  $\mu$  can be estimated as usual, and with the generalized Grönwall–Bellman lemma, see Lemma 1, one can obtain a uniform energy estimate. Assuming that we derived this inequality in a discrete setting, by the Banach–Alaoglu and Eberlein–Šmulian there is a subsequence  $(\phi^{k_j}, \mu^{k_j})$  that converges weakly in the respective spaces to some element  $(\phi, \mu)$ . We obtain strong convergence via the fractional Aubin–Lions lemma (2.3)

$$L^2(0, T; V) \cap H^\alpha(0, T; V') \hookrightarrow L^2(0, T; H),$$

in order to pass the limits in the nonlinear functions  $\Psi$  and  $m$ . Since fractional problems have less regularity in time, the continuity in time is lost for small values of  $\alpha$ . Therefore, the given initial data  $\phi_0 \in H$  is interpreted in the sense  $(g_{1-\alpha} \otimes (\phi - \phi_0))(t) \rightarrow 0$  in  $H$  as  $t \rightarrow 0$ .

#### 4.3.4. Mechanical deformation

We consider the system stated in Subsection 3.4 without the effect of a volume-averaged velocity, that is:

$$\begin{aligned} \partial_t \phi_T &= \operatorname{div}(m_T(\phi_T, \phi_\sigma) \nabla \mu_T) + S_T(\phi_T, \phi_\sigma) \\ \mu_T &= \Psi'(\phi_T) - \chi_c \phi_\sigma - \varepsilon_T^2 \Delta \phi_T + \lambda \operatorname{div} u \\ \partial_t \phi_\sigma &= \operatorname{div}(M_\sigma \nabla (D_\sigma \phi_\sigma - \chi_c \phi_T)) + S_\sigma(\phi_T, \phi_\sigma) \\ 0 &= \operatorname{div} \left( 2G\varepsilon(u) + \frac{2G\nu}{1-2\nu} \operatorname{tr}(\varepsilon(u)) \mathbb{1} + \lambda \phi_T \mathbb{1} \right) \end{aligned}$$

We consider the variational form of the deformation field

$$2G(\varepsilon(u), \varepsilon(\varphi))_H + \frac{2G\nu}{1-2\nu} (\operatorname{div} u, \operatorname{div} \varphi)_H = -\lambda(\phi_T, \operatorname{div} \varphi)_H,$$

for all  $\varphi \in V$ . We take the test function  $\varphi = u$  and achieve

$$2G\|\varepsilon(u)\|_H^2 + \frac{2G\nu}{1-2\nu} \|\operatorname{div} u\|_H^2 = -\lambda(\phi_T, \operatorname{div} u)_H,$$

which gives after an application of the  $\varepsilon$ -Young and Korn inequalities, see Subsection 2.1,

$$C\|u\|_V^2 \leq 2G\|\varepsilon(u)\|_H^2 + \frac{G\nu}{1-2\nu}\|\operatorname{div}u\|_H^2 \leq \frac{\lambda^2(1-2\nu)}{4G\nu}\|\phi_T\|_H^2.$$

We take the typical test functions and add it to this inequality, which gives the energy bound

$$\begin{aligned} & \frac{d}{dt} \left[ \|\Psi(\phi_T)\|_{L^1(\Omega)} + \frac{\varepsilon_T^2}{2}\|\nabla\phi_T\|_H^2 + \frac{C_\sigma}{2}\|\phi_\sigma\|_H^2 \right] + C_\sigma D_\sigma M_\sigma \|\nabla\phi_\sigma\|_H^2 \\ & + M_0\|\nabla\mu\|_H^2 + C\|u\|_V^2 + \lambda(\operatorname{div}u, \partial_t\phi)_H \\ & \leq -\chi_c(m_T\nabla\mu_T, \nabla\phi_\sigma^k)_H + (S_T, \mu_T + \chi_c\phi_\sigma)_H + \chi_c C_\sigma M_\sigma (\nabla\phi_T, \nabla\phi_\sigma)_H \\ & + C_\sigma(S_\sigma, \phi_\sigma)_H + \frac{\lambda^2(1-2\nu)}{2G\nu}\|\phi_T\|_H^2. \end{aligned}$$

In contrast to the energy bounds from before, the mixed term  $\lambda(\operatorname{div}u, \partial_t\phi)_H$  on the left-hand side is new. After integrating this inequality, it gives for this term after integration by parts in time

$$\int_0^t \lambda(\operatorname{div}u, \partial_t\phi_T)_H dt = \lambda(\operatorname{div}u_0, \phi_{T,0})_H - \int_0^t \lambda(\operatorname{div}\partial_t u, \phi_T)_H dt.$$

We observe that testing with  $\varphi = \partial_t u$  in the deformation equation gives

$$G \frac{d}{dt} \|\varepsilon(u)\|_H^2 + \frac{G\nu}{1-2\nu} \frac{d}{dt} \|\operatorname{div}u\|_H^2 = -\lambda(\phi_T, \operatorname{div}\partial_t u)_H,$$

and the right-hand side is exactly the term from above. Therefore, the integrated energy inequality reads

$$\begin{aligned} & \|\Psi(\phi_T(t))\|_{L^1(\Omega)} + \frac{\varepsilon_T^2}{2}\|\nabla\phi_T(t)\|_H^2 + \frac{C_\sigma}{2}\|\phi_\sigma(t)\|_H^2 + G\|\varepsilon(u(t))\|_H^2 + \frac{G\nu}{1-2\nu}\|\operatorname{div}u(t)\|_H^2 \\ & + C_\sigma D_\sigma M_\sigma \|\nabla\phi_\sigma\|_{L^2(0,t;H)}^2 + M_0\|\nabla\mu_T\|_{L^2(0,t;H)}^2 + C\|u\|_{L^2(0,t;V)}^2 \\ & \leq C + \int_0^t \left\{ -\chi_c(m_T\nabla\mu_T, \nabla\phi_\sigma^k)_H + (S_T, \mu_T + \chi_c\phi_\sigma)_H + \chi_c C_\sigma M_\sigma (\nabla\phi_T, \nabla\phi_\sigma)_H \right. \\ & \left. + C_\sigma(S_\sigma, \phi_\sigma)_H + \frac{\lambda^2(1-2\nu)}{2G\nu}\|\phi_T\|_H^2 \right\} dt, \end{aligned}$$

where we have put the initial values again into the constant. The right-hand side can be estimated as usual by overpowering the prefactors and applying the Grönwall–Bellman inequality.

#### 4.3.5. Mixed-dimensional coupling

We consider a 3D-1D coupled model as described in Subsection 3.6. Such mixed-dimensional models with a dimension difference of greater than one have a ‘high-dimensional gap’. Such a name is justified because the trace operator as a mapping  $\operatorname{tr}_\Lambda : H^1(\Omega) \rightarrow L^2(\Lambda)$  is not well-defined, see [30]. Therefore, one cannot use the

typical Hilbert space setting and consequently, such problems are particularly difficult to analyze. One can use a Petrov–Galerkin setting and apply the well-defined trace operator on weighted Sobolev spaces or on  $W^{1,p}(\Omega)$  with  $p > 2$ . Then the test functions are more regular than the solution space, see [29, 30].

As already described in Subsection 3.6, we use a different approach. We consider a 3D-1D problem, but we do the couplings between the constituents on different domains through the two-dimensional cylinder surface  $\Gamma$ . Therefore, the trace operator  $\text{tr}_\Gamma : H^1(\Omega) \rightarrow L^2(\Gamma)$  is well-defined and the model can be analyzed in the typical solution spaces.

For the sake of simplicity, we consider the variational form of the 3D nutrients  $\phi_\sigma$  and investigate the new source term with the coupling to the 1D constituents. We have

$$\partial_t \phi_\sigma = \text{div}(M_\sigma \nabla (D_\sigma \phi_\sigma - \chi_c(\phi_P + \phi_H))) + S_\sigma(\phi_\mathbb{A}) + J_{\sigma v}(\text{tr}_\Gamma \phi_\sigma, \text{tr}_\Gamma p, \Pi_\Gamma \phi_v, \Pi_\Gamma p_v) \delta_\Gamma.$$

Then we test the RDE with its own solution to achieve

$$\begin{aligned} \frac{1}{2} \frac{d}{dt} \|\phi_\sigma\|_H^2 + M_\sigma D_\sigma \|\nabla \phi_\sigma\|_H^2 &= M_\sigma \chi_c (\nabla(\phi_P + \phi_H), \nabla \phi_\sigma)_H + (S_\sigma(\phi_\mathbb{A}), \phi_\sigma)_H \\ &\quad + \langle J_{\sigma v}(\text{tr}_\Gamma \phi_\sigma, \text{tr}_\Gamma p, \Pi_\Gamma \phi_v, \Pi_\Gamma p_v) \delta_\Gamma, \phi_\sigma \rangle_{V' \times V}, \end{aligned}$$

The last term can be written via the well-defined trace operator  $\text{tr}_\Gamma : H^1(\Omega) \rightarrow L^2(\Gamma)$

$$\langle J_{\sigma v} \delta_\Gamma, \phi_\sigma \rangle_{V' \times V} = \int_\Gamma J_{\sigma v} \text{tr}_\Gamma \phi_\sigma(s) ds \leq \|J_{\sigma v}\|_{L^2(\Gamma)} \|\text{tr}_\Gamma \phi_\sigma\|_{L^2(\Gamma)} \leq C_{\text{tr}} \|J_{\sigma v}\|_{L^2(\Gamma)} \|\phi_\sigma\|_V.$$

We recall the flux  $J_{\sigma v}$  that is governed by the Kedem–Katchalsky law, see (3.10),

$$J_{\sigma v} = (1 - r_\sigma) L_p (\Pi_\Gamma p_v - \text{tr}_\Gamma p) f(\phi_\sigma, \phi_v) + L_\sigma (\Pi_\Gamma \phi_v - \text{tr}_\Gamma \phi_\sigma),$$

and assume that  $f$  is a bounded function. Then it gives

$$\begin{aligned} \|J_{\sigma v}\|_{L^2(\Gamma)} &\leq |1 - r_\sigma| \cdot L_p \cdot \|\Pi_\Gamma p_v - \text{tr}_\Gamma p\|_{L^2(\Gamma)} \cdot \|f\|_\infty + L_\sigma \cdot \|\Pi_\Gamma \phi_v - \text{tr}_\Gamma \phi_\sigma\|_{L^2(\Gamma)} \\ &\leq |1 - r_\sigma| \cdot \|f\|_\infty \cdot L_p \left( \|\Pi_\Gamma\|_{\mathcal{L}(L^2(\Lambda); L^2(\Gamma))} \|p_v\|_{L^2(\Lambda)} + C_{\text{tr}} \|p\|_{H^1(\Omega)} \right) \\ &\quad + L_\sigma \left( C_{\text{tr}} \|\phi_\sigma\|_{H^1(\Omega)} + \|\Pi_\Gamma\|_{\mathcal{L}(L^2(\Lambda); L^2(\Gamma))} \|\phi_v\|_{L^2(\Lambda)} \right). \end{aligned}$$

Finally, we can apply the  $\varepsilon$ -Young inequality to absorb the right-hand sides of the energy inequality by its left side. Then we obtain the final energy estimate by the Grönwall–Bellman lemma.



## 5. Numerical Implementation

*I have no satisfaction in formulas unless I feel their numerical magnitude.*  
(Sir William Thomson, Lord Kelvin)

In our articles, we focused on deriving tumor growth models and establishing the existence of weak solutions to the governing equations. Besides this, we were interested in showing numerical simulations and studying the influence of the new features and effects of the models. How useful is a well-posed model that does not reflect real biological processes? In this section, we briefly describe the techniques that we used for the implementation of the PDEs in the last sections. Our code is based on the finite element libraries `libMesh` [94] and `FEniCS` [1]. We started with `FEniCS` since it is written in the accessible `Python` language and variational forms are straightforward to implement. For the more recent papers on mixed-dimensional couplings, we moved to `libMesh`, which is a high performance computing (HPC) library written in `C++` and therefore, yields higher potential for code optimization and saving runtimes than in `FEniCS`. We refer to our `GitHub`

<https://github.com/CancerModeling/Angiogenesis3D1D>

where our code is freely accessible. In particular, the settings for the simulations in our two recent papers [56, 57] on multispecies tumor growth are given.

### 5.1. Three-dimensional model

We implemented the 3D models with the FEM. The code solves the system in a sequential way, see [56, Algorithm 2.1] for the algorithm of the full model. We use the classical energy splitting method for the potential  $\Psi = \Psi_e + \Psi_c$ , which provides unconditional energy stability, see [40]. That is, we treat the expansive part  $\Psi_e$  explicitly and the contractive part  $\Psi_c$  implicitly. We present the results of numerical experiments in [56, 57] and show the relative importance and roles of various biological effects, including cell mobility, proliferation, necrosis, hypoxia, and nutrient concentration, on the generation of MDEs and the degradation of the ECM.

### 5.2. Nonlocal phenomena

Nonlocal effects are not only difficult from an analytical point of view, but they also cause problems in numerical methods and increase the computational burden. The FEM is based on a local element concept, which is in contrast to the character of spatial nonlocality. Cells should not only exchange information within their element but also with elements in the neighborhood around them. In the case of time-fractional PDEs, not only the solution from the previous time step is of relevance, but one has to save all the solutions starting from the initial condition.

#### 5.2.1. Nonlocal-in-space effects

In our work [61], we investigate the evolution of the tumor volume fraction in both local and nonlocal four-species models. That is, in the local model we choose the gradient-

based haptotaxis flux  $J_{\text{loc}} = \chi_h \phi_V \nabla \theta$  and for the nonlocal model  $J_{\text{nonloc}} = \chi_h \phi_V k * \theta$ . Following [19, 77, 78], we select a kernel function  $k_\varepsilon$ ,  $\varepsilon > 0$ , such that it approximates the gradient-based haptotaxis effect as  $\varepsilon \rightarrow 0$ . This also implies that a higher  $\varepsilon$ -value corresponds to a larger nonlocal effect. Particularly, we use the approximation

$$\begin{aligned} (k * \theta)(x) - \theta(x) \cdot (k * 1)(x) &= \int_{\mathbb{R}^d} k(x-y)(\theta(y) - \theta(x)) dy \\ &\approx \int_{\mathbb{R}^d} k(x-y)(\nabla \theta(x) \cdot (y-x)) dy \\ &= \nabla \theta(x) \int_{\mathbb{R}^d} (y-x) \cdot k(x-y) dy \\ &= \nabla \theta(x), \end{aligned}$$

where we choose  $k$  such that  $xk(-x)$  is a Dirac sequence with the typical property  $\int_{\mathbb{R}^d} xk(-x) dx = 1$ . We impose the representation  $k(x) = -\omega(\varepsilon)x\chi_{[0,\varepsilon]}(|x|_\infty)$ , which gives in the 2D case after integrating  $xk(-x)$  over  $\mathbb{R}^2$  the weight  $\omega(\varepsilon) = \frac{3}{8}\varepsilon^{-4}$ .

We compare both the local and nonlocal models in [61, Figure 5] and observe a larger adhesion effect in the local model in the sense that the tumor mass moves further towards the right-hand side of the boundary where the nutrition is placed. We also notice that the local model can imitate the nonlocal model for a fixed value of  $\varepsilon$  by choosing a smaller haptotaxis parameter.

### 5.2.2. Nonlocal-in-time effects

We mention the review article [35] that describes the relevant methods for treating time-fractional PDEs numerically. Even though there are more efficient methods available, see [58, 92], which reduce the time-fractional PDE to a system of ODEs, the L1 scheme [113] is often chosen since it is simple to understand, widely accepted, and direct to implement.

Consider the mesh  $0 = t_0 < t_1 < \dots < t_{N-1} = t_N = T$  of the time interval  $[0, T]$ . Then, the  $\alpha$ -th Caputo derivative of some function  $\phi$  at  $t_n$  reads

$$\partial_t^\alpha \phi(t_n) = \frac{1}{\Gamma(1-\alpha)} \int_0^{t_n} \frac{\phi'(s)}{(t-s)^\alpha} ds.$$

Using the approximation formula  $f'(s) \approx \frac{f(t_{j+1})-f(t_j)}{t_{j+1}-t_j}$  for  $s \in (t_j, t_{j+1})$  gives the L1 approximation

$$\partial_t^\alpha \phi(t_n) \approx \frac{1}{\Gamma(2-\alpha)} \sum_{j=0}^{n-1} w_{n-j-1,n} (\phi(t_{n-j}) - \phi(t_{n-j-1})),$$

where the weights  $w_{m,n}$  for  $n, m \in [0, N]$  are given by

$$w_{m,n} = \frac{(t_n - t_m)^{1-\alpha} - (t_n - t_{m+1})^{1-\alpha}}{t_{n-m} - t_{n-m-1}}.$$



The L1 scheme's convergence is  $\mathcal{O}((\Delta t)^{2-\alpha})$ , and the memory effect can be seen on the right-hand side as the history from the previous time steps  $\phi(t_{n-j})$ . Exactly this step involves a huge computational burden in storing all the history in the memory storage of the computer. The computational complexity can be reduced by storing, for example, only the previous 20 solutions. This appears to be reasonable given that the weights on previous solutions decrease the further back the previous solution is. But then nothing about convergence can be said anymore.

In our publications on time-fractional tumor growth models [59, 64], we use a fractional linear multistep method [105] based on a convolution quadrature scheme. Such approaches generalize the standard linear multistep method for ODEs. A special case of this class of methods generalizes the backward Euler method to a fractional setting and approximates the Caputo derivative by

$$\partial_t^\alpha \phi(t_n) \approx \frac{1}{(\Delta t)^\alpha} \sum_{j=0}^{n-1} (-1)^j \binom{-\alpha}{j} (\phi(t_{n-j}) - \phi(0)).$$

Indeed, setting  $\alpha = 1$  gives the backward Euler scheme. Similar to the classical L1 method, one has to store all the previous solutions. The quadrature weights can also be computed recursively and such schemes are known as Grünwald–Letnikov approximations [6, 34].

We refer to our simulation result [59, Figure 1] that shows the influence of the fractional derivative in the form of a subdiffusive evolution of the tumor mass.

### 5.3. Mixed-dimensional coupling

In the case of our 3D-1D tumor growth models, we have to implement the new 1D constituents into the code and create the connection to the 3D variables. We use the implicit Euler method for the time integration of the 1D equations. The vascular graph method is used for the spatial discretization of the 1D equations, which corresponds to a node centered finite volume method, see [116, 134] for further details.

We decouple the 1D and 3D pressure equations at each time step and solve the two systems using block Gauß–Seidel iterations until the 3D pressure converges. The nutrient equation is discretized in a similar way, with the main difference being the addition of an upwinding procedure for the convective term. At each time step, the nutrient equations are solved with block Gauß–Seidel iterations. The described numerical method, as well as the discretization of the terms that arise in the context of the 3D-1D coupling, is detailed in our work [56].

## Acronyms

<b>DFB</b> Darcy–Forchheimer–Brinkman .....	4
<b>ECM</b> extracellular matrix.....	4
<b>FEM</b> finite element method.....	6
<b>FDE</b> fractional differential equation.....	32
<b>HPC</b> high performance computing.....	37
<b>MDE</b> matrix-degrading enzyme.....	4
<b>ODE</b> ordinary differential equation .....	1
<b>PDE</b> partial differential equation .....	1
<b>RDE</b> reaction-diffusion equation .....	5
<b>TAF</b> tumor angiogenesis factor.....	4
<b>VEGF</b> vascular endothelial growth factor .....	16

## References

- [1] M. Alnæs, J. Blechta, J. Hake, A. Johansson, B. Kehlet, A. Logg, C. Richardson, J. Ring, M. E. Rognes, and G. N. Wells. The FEniCS project version 1.5. *Archive of Numerical Software*, 3(100):9–23, 2015.
- [2] H. W. Alt. *Linear Functional Analysis: An Application-Oriented Introduction*. Springer, 2016.
- [3] R. P. Araujo and D. S. McElwain. A history of the study of solid tumour growth: the contribution of mathematical modelling. *Bulletin of Mathematical Biology*, 66(5):1039–1091, 2004.
- [4] N. J. Armstrong, K. J. Painter, and J. A. Sherratt. A continuum approach to modelling cell-cell adhesion. *Journal of Theoretical Biology*, 243(1):98–113, 2006.
- [5] S. Astanin and L. Preziosi. Multiphase models of tumour growth. In E. Angelis, M. Chaplain, and N. Bellomo, editors, *Selected Topics in Cancer Modeling*, pages 1–31. Springer, 2008.
- [6] D. Baleanu, K. Diethelm, and E. Scalas. *Fractional Calculus: Models and Numerical Methods*, volume 3. World Scientific, 2012.
- [7] F. R. Balkwill, M. Capasso, and T. Hagemann. The tumor microenvironment at a glance. *Journal of Cell Science*, 125(23):5591–5596, 2012.
- [8] P. W. Bates. On some nonlocal evolution equations arising in materials science. In H. Brunner, X.-Q. Zhao, and X. Zou, editors, *Nonlinear Dynamics and Evolution Equations*, volume 48, pages 13–52. American Mathematical Society, 2006.
- [9] P. W. Bates and J. Han. The Dirichlet boundary problem for a nonlocal Cahn–Hilliard equation. *Journal of Mathematical Analysis and Applications*, 311(1):289–312, 2005.
- [10] P. W. Bates and J. Han. The Neumann boundary problem for a nonlocal Cahn–Hilliard equation. *Journal of Differential Equations*, 212(2):235–277, 2005.
- [11] N. Bellomo and L. Preziosi. Modelling and mathematical problems related to tumor evolution and its interaction with the immune system. *Mathematical and Computer Modelling*, 32(3-4):413–452, 2000.
- [12] F. Boyer and P. Fabrie. *Mathematical Tools for the Study of the Incompressible Navier–Stokes Equations and Related Models*. Springer, 2012.
- [13] H. Brezis. *Functional Analysis, Sobolev Spaces and Partial Differential Equations*. Springer, 2010.
- [14] H. M. Byrne and L. Preziosi. Modelling solid tumour growth using the theory of mixtures. *Mathematical Medicine and Biology*, 20(4):341–366, 2003.
- [15] J. W. Cahn and J. E. Hilliard. Free energy of a nonuniform system: I. Interfacial free energy. *The Journal of Chemical Physics*, 28(2):258–267, 1958.
- [16] J. W. Cahn and J. E. Hilliard. Spinodal decomposition: A reprise. *Acta Metallurgica*, 19(2):151–161, 1971.
- [17] P. Carmeliet and R. K. Jain. Molecular mechanisms and clinical applications of angiogenesis. *Nature*, 473(7347):298–307, 2011.
- [18] C. Cavaterra, C. G. Gal, and M. Grasselli. Cahn–Hilliard equations with memory and dynamic boundary conditions. *Asymptotic Analysis*, 71(3):123–162, 2011.
- [19] M. A. Chaplain, M. Lachowicz, Z. Szymańska, and D. Wrzosek. Mathematical modelling of cancer invasion: The importance of cell-cell adhesion and cell-matrix adhesion. *Mathematical Models and Methods in Applied Sciences*, 21(04):719–743, 2011.
- [20] L. Cherfils, A. Miranville, and S. Zelik. The Cahn–Hilliard equation with logarithmic potentials. *Milan Journal of Mathematics*, 79(2):561–596, 2011.
- [21] P. Colli, S. Frigeri, and M. Grasselli. Global existence of weak solutions to a nonlocal Cahn–Hilliard–Navier–Stokes system. *Journal of Mathematical Analysis and Applications*, 386(1):428–444, 2012.
- [22] P. Colli, G. Gilardi, E. Rocca, and J. Sprekels. Optimal distributed control of a diffuse interface model of tumor growth. *Nonlinearity*, 30(6):2518, 2017.

- [23] P. Colli, H. Gomez, G. Lorenzo, G. Marinoschi, A. Reali, and E. Rocca. Mathematical analysis and simulation study of a phase-field model of prostate cancer growth with chemotherapy and antiangiogenic therapy effects. *Mathematical Models and Methods in Applied Sciences*, 30(07):1253–1295, 2020.
- [24] P. Colli, H. Gomez, G. Lorenzo, G. Marinoschi, A. Reali, and E. Rocca. Optimal control of cytotoxic and antiangiogenic therapies on prostate cancer growth. *Mathematical Models and Methods in Applied Sciences*, 31(7):1419–1468, 2021.
- [25] V. Cristini, X. Li, J. Lowengrub, and S. M. Wise. Nonlinear simulations of solid tumor growth using a mixture model: invasion and branching. *Journal of Mathematical Biology*, 58(723–763), 2009.
- [26] V. Cristini and J. Lowengrub. *Multiscale Modeling of Cancer: An Integrated Experimental and Mathematical Modeling Approach*. Cambridge University Press, 2010.
- [27] V. Cristini, J. Lowengrub, and Q. Nie. Nonlinear simulation of tumor growth. *Journal of Mathematical Biology*, 46(3):191–224, 2003.
- [28] M. Dai, E. Feireisl, E. Rocca, G. Schimperna, and M. E. Schonbek. Analysis of a diffuse interface model of multispecies tumor growth. *Nonlinearity*, 30(4):1639, 2017.
- [29] C. D’Angelo. Finite element approximation of elliptic problems with Dirac measure terms in weighted spaces: Applications to one-and three-dimensional coupled problems. *SIAM Journal on Numerical Analysis*, 50(1):194–215, 2012.
- [30] C. D’Angelo and A. Quarteroni. On the coupling of 1D and 3D diffusion-reaction equations: application to tissue perfusion problems. *Mathematical Models and Methods in Applied Sciences*, 18(08):1481–1504, 2008.
- [31] F. Della Porta, A. Giorgini, and M. Grasselli. The nonlocal Cahn–Hilliard–Hele–Shaw system with logarithmic potential. *Nonlinearity*, 31(10):4851, 2018.
- [32] F. Della Porta and M. Grasselli. On the nonlocal Cahn–Hilliard–Brinkman and Cahn–Hilliard–Hele–Shaw systems. *Communications in Mathematical Sciences*, 13(6):1541–1567, 2015.
- [33] F. Demengel, G. Demengel, and R. Ern . *Functional spaces for the Theory of Elliptic Partial Differential Equations*. Springer, 2012.
- [34] K. Diethelm. *The Analysis of Fractional Differential Equations: An Application-Oriented Exposition using Differential Operators of Caputo Type*. Springer, 2010.
- [35] K. Diethelm, R. Garrappa, and M. Stynes. Good (and Not So Good) Practices in Computational Methods for Fractional Calculus. *Mathematics*, 8(3):324, 2020.
- [36] M. Ebenbeck and H. Garcke. Analysis of a Cahn–Hilliard–Brinkman model for tumour growth with chemotaxis. *Journal of Differential Equations*, 266(9):5998–6036, 2019.
- [37] M. Ebenbeck and H. Garcke. On a Cahn–Hilliard–Brinkman Model for Tumor Growth and Its Singular Limits. *SIAM Journal on Mathematical Analysis*, 51(3):1868–1912, 2019.
- [38] M. Ebenbeck and P. Knopf. Optimal medication for tumors modeled by a Cahn–Hilliard–Brinkman equation. *Calculus of Variations and Partial Differential Equations*, 58(4):1–31, 2019.
- [39] C. M. Elliott and H. Garcke. On the Cahn–Hilliard equation with degenerate mobility. *SIAM Journal on Mathematical Analysis*, 27(2):404–423, 1996.
- [40] C. M. Elliott and A. Stuart. The global dynamics of discrete semilinear parabolic equations. *SIAM Journal on Numerical Analysis*, 30(6):1622–1663, 1993.
- [41] C. Engwer, C. Stinner, and C. Surulescu. On a structured multiscale model for acid-mediated tumor invasion: The effects of adhesion and proliferation. *Mathematical Models and Methods in Applied Sciences*, 27(07):1355–1390, 2017.
- [42] J. Escher, A.-V. Matioc, and B.-V. Matioc. Analysis of a mathematical model describing necrotic tumor growth. In E. Stephan and P. Wriggers, editors, *Modelling, Simulation and Software Concepts for Scientific-Technological Problems*, pages 237–250. Springer, 2011.
- [43] L. C. Evans. *Partial Differential Equations*. American Mathematical Society, 2010.

- [44] D. Faghihi, X. Feng, E. Lima, J. T. Oden, and T. E. Yankeelov. A Coupled Mass Transport and Deformation Theory of Multi-constituent Tumor Growth. *Journal of the Mechanics and Physics of Solids*, 139:103936, 2020.
- [45] C. L. Fefferman. Existence and smoothness of the Navier–Stokes equation. In J. Carlson, A. Jaffe, and A. Wiles, editors, *The Millennium Prize Problems*, pages 57–67. Clay Mathematics Institute, 2006.
- [46] S. Franks and J. King. Interactions between a uniformly proliferating tumour and its surroundings: Uniform material properties. *Mathematical Medicine and Biology*, 20(1):47–89, 2003.
- [47] H. B. Frieboes, F. Jin, Y.-L. Chuang, S. M. Wise, J. Lowengrub, and V. Cristini. Three-dimensional multispecies nonlinear tumor growth – II: Tumor invasion and angiogenesis. *Journal of Theoretical Biology*, 264(4):1254–1278, 2010.
- [48] A. Friedman. A free boundary problem for a coupled system of elliptic, hyperbolic, and Stokes equations modeling tumor growth. *Interfaces and Free boundaries*, 8(2):247–261, 2006.
- [49] A. Friedman. Free boundary problems for systems of Stokes equations. *Discrete & Continuous Dynamical Systems Series B*, 21(5):1455, 2016.
- [50] S. Frigeri and M. Grasselli. Nonlocal Cahn–Hilliard–Navier–Stokes systems with singular potentials. *Dynamics of Partial Differential Equations*, 9(4):273–304, 2012.
- [51] S. Frigeri, M. Grasselli, and P. Krejčí. Strong solutions for two-dimensional nonlocal Cahn–Hilliard–Navier–Stokes systems. *Journal of Differential Equations*, 255(9):2587–2614, 2013.
- [52] S. Frigeri, M. Grasselli, and E. Rocca. A diffuse interface model for two-phase incompressible flows with non-local interactions and non-constant mobility. *Nonlinearity*, 28:1257–1293, 2015.
- [53] S. Frigeri, M. Grasselli, and E. Rocca. On a diffuse interface model of tumour growth. *European Journal of Applied Mathematics*, 26(2):215–243, 2015.
- [54] S. Frigeri, K. F. Lam, and E. Rocca. On a diffuse interface model for tumour growth with non-local interactions and degenerate mobilities. In P. Colli, A. Favini, E. Rocca, G. Schimperna, and J. Sprekels, editors, *Solvability, Regularity, and Optimal Control of Boundary Value Problems for PDEs*, pages 217–254. Springer, 2017.
- [55] S. Frigeri, K. F. Lam, E. Rocca, and G. Schimperna. On a multi-species Cahn–Hilliard–Darcy tumor growth model with singular potentials. *Communications in Mathematical Sciences*, 16(3):821–856, 2018.
- [56] M. Fritz, P. K. Jha, T. Köppl, J. T. Oden, A. Wagner, and B. Wohlmuth. Modeling and simulation of vascular tumors embedded in evolving capillary networks. *Computer Methods in Applied Mechanics and Engineering*, 384:113975, 2021.
- [57] M. Fritz, P. K. Jha, T. Köppl, J. T. Oden, and B. Wohlmuth. Analysis of a new multispecies tumor growth model coupling 3D phase-fields with a 1D vascular network. *Nonlinear Analysis: Real World Applications*, 61:103331, 2021.
- [58] M. Fritz, U. Khristenko, and B. Wohlmuth. Equivalence between a time-fractional and an integer-order gradient flow: The memory effect reflected in the energy. arXiv:2106.10985 [math.AP], 2021.
- [59] M. Fritz, C. Kuttler, M. L. Rajendran, B. Wohlmuth, and L. Scarabosio. On a subdiffusive tumour growth model with fractional time derivative. *IMA Journal of Applied Mathematics*, 86(04):688–729, 2021.
- [60] M. Fritz, T. Köppl, J. T. Oden, A. Wagner, B. Wohlmuth, and C. Wu. A 1D-0D-3D coupled model for simulating blood flow and transport processes in breast tissue. *International Journal for Numerical Methods in Biomedical Engineering*, page e3612.
- [61] M. Fritz, E. Lima, V. Nikolić, J. T. Oden, and B. Wohlmuth. Local and nonlocal phase-field models of tumor growth and invasion due to ECM degradation. *Mathematical Models and Methods in Applied Sciences*, 29(13):2433–2468, 2019.
- [62] M. Fritz, E. Lima, J. T. Oden, and B. Wohlmuth. On the unsteady Darcy–Forchheimer–Brinkman equation in local and nonlocal tumor growth models. *Mathematical Models and Methods in Applied Sciences*, 29(09):1691–1731, 2019.

- [63] M. Fritz, V. Nikolić, and B. Wohlmuth. Well-posedness and numerical treatment of the Blackstock equation in nonlinear acoustics. *Mathematical Models and Methods in Applied Sciences*, 28(13):2557–2597, 2018.
- [64] M. Fritz, M. L. Rajendran, and B. Wohlmuth. Time-fractional Cahn–Hilliard equation: Well-posedness, degeneracy, and numerical solutions. *Computer & Mathematics with Applications*.
- [65] H. Gajewski and K. Zacharias. On a nonlocal phase separation model. *Journal of Mathematical Analysis and Applications*, 286(1):11–31, 2003.
- [66] C. G. Gal, A. Giorgini, and M. Grasselli. The nonlocal Cahn–Hilliard equation with singular potential: Well-posedness, regularity and strict separation property. *Journal of Differential Equations*, 263(9):5253–5297, 2017.
- [67] H. Garcke. On Cahn–Hilliard systems with elasticity. *Proceedings of the Royal Society of Edinburgh Section A: Mathematics*, 133(2):307–331, 2003.
- [68] H. Garcke. On a Cahn–Hilliard model for phase separation with elastic misfit. *Annales de l’IHP Analyse Non Linéaire*, 22(2):165–185, 2005.
- [69] H. Garcke and K. F. Lam. Global weak solutions and asymptotic limits of a Cahn–Hilliard–Darcy system modelling tumour growth. *AIMS Mathematics*, 1(3):318–360, 2016.
- [70] H. Garcke and K. F. Lam. Analysis of a Cahn–Hilliard system with non-zero Dirichlet conditions modeling tumor growth with chemotaxis. *Discrete & Continuous Dynamical Systems Series A*, 37(8):4277–4308, 2017.
- [71] H. Garcke and K. F. Lam. Well-posedness of a Cahn–Hilliard system modelling tumour growth with chemotaxis and active transport. *European Journal of Applied Mathematics*, 28(2):284–316, 2017.
- [72] H. Garcke and K. F. Lam. On a Cahn–Hilliard–Darcy system for tumour growth with solution dependent source terms. In E. Rocca, U. Stefanelli, L. Truskinovsky, and A. Visintin, editors, *Trends in Applications of Mathematics to Mechanics*, pages 243–264. Springer, 2018.
- [73] H. Garcke, K. F. Lam, R. Nürnberg, and E. Sitka. A multiphase Cahn–Hilliard–Darcy model for tumour growth with necrosis. *Mathematical Models and Methods in Applied Sciences*, 28(03):525–577, 2018.
- [74] H. Garcke, K. F. Lam, and E. Rocca. Optimal control of treatment time in a diffuse interface model of tumor growth. *Applied Mathematics & Optimization*, 78(3):495–544, 2018.
- [75] H. Garcke, K. F. Lam, and A. Signori. On a phase field model of Cahn–Hilliard type for tumour growth with mechanical effects. *Nonlinear Analysis: Real World Applications*, 57:103192, 2021.
- [76] H. Garcke, K. F. Lam, E. Sitka, and V. Styles. A Cahn–Hilliard–Darcy model for tumour growth with chemotaxis and active transport. *Mathematical Models and Methods in Applied Sciences*, 26(06):1095–1148, 2016.
- [77] A. Gerisch. On the approximation and efficient evaluation of integral terms in PDE models of cell adhesion. *IMA Journal of Numerical Analysis*, 30(1):173–194, 2010.
- [78] A. Gerisch and M. Chaplain. Mathematical modelling of cancer cell invasion of tissue: Local and non-local models and the effect of adhesion. *Journal of Theoretical Biology*, 250(4):684–704, 2008.
- [79] G. Giacomin and J. L. Lebowitz. Exact macroscopic description of phase segregation in model alloys with long range interactions. *Physical Review Letters*, 76(7):1094, 1996.
- [80] G. Giacomin and J. L. Lebowitz. Phase segregation dynamics in particle systems with long range interactions. I. Macroscopic limits. *Journal of Statistical Physics*, 87(1-2):37–61, 1997.
- [81] B. Ginzburg and A. Katchalsky. The frictional coefficients of the flows of non-electrolytes through artificial membranes. *The Journal of General Physiology*, 47(2):403–418, 1963.
- [82] R. Gorenflo, F. Mainardi, D. Moretti, and P. Paradisi. Time fractional diffusion: A discrete random walk approach. *Nonlinear Dynamics*, 29:129–143, 2002.
- [83] H. Greenspan. On the growth and stability of cell cultures and solid tumors. *Journal of Theoretical Biology*, 56(1):229–242, 1976.

- [84] M. E. Gurtin. Generalized Ginzburg–Landau and Cahn–Hilliard equations based on a microforce balance. *Physica D: Nonlinear Phenomena*, 92(3-4):178–192, 1996.
- [85] J. Hadamard. Sur les problèmes aux dérivées partielles et leur signification physique. *Princeton University Bulletin*, 13:49–52, 1902.
- [86] D. Hanahan and R. A. Weinberg. The hallmarks of cancer. *Cell*, 100(1):57–70, 2000.
- [87] D. Hanahan and R. A. Weinberg. Hallmarks of cancer: The next generation. *Cell*, 144(5):646–674, 2011.
- [88] A. Hawkins-Daarud, K. G. van der Zee, and J. T. Oden. Numerical simulation of a thermodynamically consistent four-species tumor growth model. *International Journal for Numerical Methods in Biomedical Engineering*, 28(1):3–24, 2012.
- [89] J. He. Global weak solutions to a Navier–Stokes–Cahn–Hilliard system with chemotaxis and singular potential. *Nonlinearity*, 34(4):2155, 2021.
- [90] D. A. Hormuth, S. L. Eldridge, J. A. Weis, M. I. Miga, and T. E. Yankeelov. Mechanically coupled reaction-diffusion model to predict glioma growth: Methodological details. In L. von Stechow, editor, *Cancer Systems Biology*, pages 225–241. Springer, 2018.
- [91] C. Jiang, C. Cui, L. Li, and Y. Shao. The anomalous diffusion of a tumor invading with different surrounding tissues. *PloS one*, 9(10):e109784, 2014.
- [92] U. Khristenko and B. Wohlmuth. Solving time-fractional differential equation via rational approximation. arXiv:2102.05139 [math.NA], 2021.
- [93] A. A. Kilbas, H. M. Srivastava, and J. J. Trujillo. *Theory and Applications of Fractional Differential Equations*. Elsevier, Usa, 2006.
- [94] B. S. Kirk, J. W. Peterson, R. H. Stogner, and G. F. Carey. libMesh: A C++ Library for Parallel Adaptive Mesh Refinement/Coarsening Simulations. *Engineering with Computers*, 22(3-4):237–254, 2006.
- [95] T. Köppl, E. Vidotto, and B. Wohlmuth. A 3D-1D coupled blood flow and oxygen transport model to generate microvascular networks. *International Journal for Numerical Methods in Biomedical Engineering*, 36(10):e3386, 2020.
- [96] K. F. Lam and H. Wu. Thermodynamically consistent Navier–Stokes–Cahn–Hilliard models with mass transfer and chemotaxis. *European Journal of Applied Mathematics*, 29(4):595–644, 2017.
- [97] H.-G. Lee, J. Lowengrub, and J. Goodman. Modeling pinchoff and reconnection in a Hele-Shaw cell. I. The models and their calibration. *Physics of Fluids*, 14(2):492–513, 2002.
- [98] J. Leray. On the motion of a viscous liquid filling space. *Acta Mathematica*, 63(1):193–248, 1934.
- [99] L. Li and J.-G. Liu. Some compactness criteria for weak solutions of time fractional PDEs. *SIAM Journal on Mathematical Analysis*, 50(4):3963–3995, 2018.
- [100] E. Lima, R. C. Almeida, and J. T. Oden. Analysis and numerical solution of stochastic phase-field models of tumor growth. *Numerical Methods for Partial Differential Equations*, 31(2):552–574, 2015.
- [101] E. Lima, J. T. Oden, and R. Almeida. A hybrid ten-species phase-field model of tumor growth. *Mathematical Models and Methods in Applied Sciences*, 24(13):2569–2599, 2014.
- [102] E. Lima, J. T. Oden, D. Hormuth, T. Yankeelov, and R. Almeida. Selection, calibration, and validation of models of tumor growth. *Mathematical Models and Methods in Applied Sciences*, 26(12):2341–2368, 2016.
- [103] E. Lima, J. T. Oden, B. Wohlmuth, A. Shahmoradi, D. Hormuth II, T. Yankeelov, L. Scarabosio, and T. Horger. Selection and validation of predictive models of radiation effects on tumor growth based on noninvasive imaging data. *Computer Methods in Applied Mechanics and Engineering*, 327:277–305, 2017.
- [104] J.-L. Lions and E. Magenes. *Non-Homogeneous Boundary Value Problems and Applications*. Springer, 2012.

- [105] C. Lubich. Discretized fractional calculus. *SIAM Journal on Mathematical Analysis*, 17(3):704–719, 1986.
- [106] Z. Meir, Z. Mukamel, E. Chomsky, A. Lifshitz, and A. Tanay. Single-cell analysis of clonal maintenance of transcriptional and epigenetic states in cancer cells. *Nature Genetics*, 52(7):709–718, 2020.
- [107] A. Miranville. *The Cahn–Hilliard Equation: Recent Advances and Applications*. Society for Industrial and Applied Mathematics, 2019.
- [108] A. Miranville, E. Rocca, and G. Schimperna. On the long time behavior of a tumor growth model. *Journal of Differential Equations*, 267(4):2616–2642, 2019.
- [109] N. Nishida, H. Yano, T. Nishida, T. Kamura, and M. Kojiro. Angiogenesis in cancer. *Vascular Health and Risk Management*, 2(3):213–219, 2006.
- [110] J. T. Oden. Adaptive multiscale predictive modelling. *Acta Numerica*, 27:353–450, 2018.
- [111] J. T. Oden, A. Hawkins, and S. Prudhomme. General diffuse-interface theories and an approach to predictive tumor growth modeling. *Mathematical Models and Methods in Applied Sciences*, 20(03):477–517, 2010.
- [112] J. T. Oden, E. Lima, R. C. Almeida, Y. Feng, M. N. Rylander, D. Fuentes, D. Faghihi, M. M. Rahman, M. DeWitt, M. Gadde, et al. Toward predictive multiscale modeling of vascular tumor growth. *Archives of Computational Methods in Engineering*, 23(4):735–779, 2016.
- [113] K. B. Oldham and J. Spanier. *The Fractional Calculus: Theory and Applications of Differentiation and Integration to Arbitrary Order*. Academic Press, 1974.
- [114] C. Patsch, L. Challet-Meylan, E. C. Thoma, E. Urich, T. Heckel, J. F. O’Sullivan, S. J. Grainger, F. G. Kapp, L. Sun, K. Christensen, et al. Generation of vascular endothelial and smooth muscle cells from human pluripotent stem cells. *Nature Cell Biology*, 17(8):994–1003, 2015.
- [115] Y. Povstenko and T. Kyrylych. Two approaches to obtaining the space-time fractional advection-diffusion equation. *Entropy*, 19(7):297, 2017.
- [116] J. Reichold, M. Stampanoni, A. L. Keller, A. Buck, P. Jenny, and B. Weber. Vascular graph model to simulate the cerebral blood flow in realistic vascular networks. *Journal of Cerebral Blood Flow & Metabolism*, 29(8):1429–1443, 2009.
- [117] T. Roose, S. J. Chapman, and P. K. Maini. Mathematical models of avascular tumor growth. *SIAM Review*, 49(2):179–208, 2007.
- [118] T. Roubíček. *Nonlinear Partial Differential Equations with Applications*. Springer, 2013.
- [119] R. Santagiuliana, M. Ferrari, and B. Schrefler. Simulation of angiogenesis in a multiphase tumor growth model. *Computer Methods in Applied Mechanics and Engineering*, 304:197–216, 2016.
- [120] R. Santagiuliana, M. Milosevic, B. Milicevic, G. Sciumè, V. Simic, A. Ziemys, M. Kojic, and B. A. Schrefler. Coupling tumor growth and bio distribution models. *Biomedical Microdevices*, 21(2):1–18, 2019.
- [121] L. Scarpa and A. Signori. On a class of non-local phase-field models for tumor growth with possibly singular potentials, chemotaxis, and active transport. *Nonlinearity*, 34(5):3199, 2021.
- [122] G. Sciumè, W. Gray, F. Hussain, M. Ferrari, P. Decuzzi, and B. Schrefler. Three phase flow dynamics in tumor growth. *Computational Mechanics*, 53(3):465–484, 2014.
- [123] G. Sciumè, R. Santagiuliana, M. Ferrari, P. Decuzzi, and B. Schrefler. A tumor growth model with deformable ECM. *Physical Biology*, 11(6):065004, 2014.
- [124] K. Seki, M. Wojcik, and M. Tachiya. Recombination kinetics in subdiffusive media. *The Journal of Chemical Physics*, 119(14):7525–7533, 2003.
- [125] N. Sfakianakis, A. Madzvamuse, and M. A. Chaplain. A hybrid multiscale model for cancer invasion of the extracellular matrix. *Multiscale Modeling & Simulation*, 18(2):824–850, 2020.
- [126] R. Shuttleworth and D. Trucu. Cell-scale degradation of peritumoural extracellular matrix fibre network and its role within tissue-scale cancer invasion. *Bulletin of Mathematical Biology*, 82(65):1–47, 2020.



- [127] A. Signori. Penalisation of long treatment time and optimal control of a tumour growth model of Cahn–Hilliard type with singular potential. *Discrete & Continuous Dynamical Systems*, 41(6):2519–2542, 2021.
- [128] J. Simon. Compact sets in the space  $L^p(0, T; B)$ . *Annali di Matematica Pura ed Applicata*, 146(1):65–96, 1986.
- [129] C. Stinner, C. Surulescu, and M. Winkler. Global weak solutions in a PDE-ODE system modeling multiscale cancer cell invasion. *SIAM Journal on Mathematical Analysis*, 46(3):1969–2007, 2014.
- [130] H. Sung, J. Ferlay, R. L. Siegel, M. Laversanne, I. Soerjomataram, A. Jemal, and F. Bray. Global cancer statistics 2020: GLOBOCAN estimates of incidence and mortality worldwide for 36 cancers in 185 countries. *CA: A Cancer Journal for Clinicians*, 71(3):209–249, 2021.
- [131] Y. Tao and M. Winkler. A chemotaxis-haptotaxis model: the roles of nonlinear diffusion and logistic source. *SIAM Journal on Mathematical Analysis*, 43(2):685–704, 2011.
- [132] Y. Tao and M. Winkler. Energy-type estimates and global solvability in a two-dimensional chemotaxis–haptotaxis model with remodeling of non-diffusible attractant. *Journal of Differential Equations*, 257(3):784–815, 2014.
- [133] J. E. Taylor and J. W. Cahn. Linking anisotropic sharp and diffuse surface motion laws via gradient flows. *Journal of Statistical Physics*, 77(1-2):183–197, 1994.
- [134] E. Vidotto, T. Koch, T. Köppl, R. Helmig, and B. Wohlmuth. Hybrid models for simulating blood flow in microvascular networks. *Multiscale Modeling & Simulation*, 17(3):1076–1102, 2019.
- [135] C. Walker and G. F. Webb. Global existence of classical solutions for a haptotaxis model. *SIAM Journal on Mathematical Analysis*, 38(5):1694–1713, 2007.
- [136] M. Wang, J. Zhao, L. Zhang, F. Wei, Y. Lian, Y. Wu, Z. Gong, S. Zhang, J. Zhou, K. Cao, et al. Role of tumor microenvironment in tumorigenesis. *Journal of Cancer*, 8(5):761, 2017.
- [137] S. M. Wise, J. Lowengrub, H. B. Frieboes, and V. Cristini. Three-dimensional multispecies nonlinear tumor growth – I: Model and numerical method. *Journal of Theoretical Biology*, 253(3):524–543, 2008.
- [138] P. Wittbold, P. Wolejko, and R. Zacher. Bounded weak solutions of time-fractional porous medium type and more general nonlinear and degenerate evolutionary integro-differential equations. *Journal of Mathematical Analysis and Applications*, 499(1):125007, 2020.
- [139] J. Xu, G. Vilanova, and H. Gomez. A mathematical model coupling tumor growth and angiogenesis. *PLoS One*, 11(2), 2016.
- [140] J. Xu, G. Vilanova, and H. Gomez. Full-scale, three-dimensional simulation of early-stage tumor growth: The onset of malignancy. *Computer Methods in Applied Mechanics and Engineering*, 314:126–146, 2017.
- [141] J. Xu, G. Vilanova, and H. Gomez. Phase-field model of vascular tumor growth: Three-dimensional geometry of the vascular network and integration with imaging data. *Computer Methods in Applied Mechanics and Engineering*, 359:112648, 2020.
- [142] B. Yandell. *The Honors Class: Hilbert’s Problems and their Solvers*. CRC Press, 2001.
- [143] Y. Yuan, Y.-C. Jiang, C.-K. Sun, and Q.-M. Chen. Role of the tumor microenvironment in tumor progression and the clinical applications. *Oncology Reports*, 35(5):2499–2515, 2016.
- [144] S. Yuste, L. Acedo, and K. Lindenberg. Reaction front in an  $A + B \rightarrow C$  reaction-subdiffusion process. *Physical Review E*, 69:036126, 2004.



## A. Core Articles

### A.1. On the unsteady Darcy–Forchheimer–Brinkman equation in local and nonlocal tumor growth models

#### On the unsteady Darcy–Forchheimer–Brinkman equation in local and nonlocal tumor growth models

Marvin Fritz, Ernesto Lima, J. Tinsley Oden, Barbara Wohlmuth

---

In this work, we study a PDE system for modeling the growth of a tumor cell colony under the influence of a convective velocity field. The four-species model of Hawkins–Daarud and others [88] serves as the system’s foundation. We use the Cahn–Hilliard equations for the tumor volume fraction  $\phi_T$  and a RDE for the nutrients  $\phi_\sigma$ . We assume that the cells are tightly packed and therefore, we add a volume-averaged velocity field regulated by the unsteady DFB equation to this system. The model is an expansion of the articles [69, 72, 73, 76] that considered a four-species model with Darcy’s law. Furthermore, the publications [36, 37] of a coupled Brinkman-four-species model were taken into consideration at the same time. We also consider the case of a nonlocal model, in which the Laplacian in the equation of the chemical potential was replaced by a convolution. This results in cell–cell adhesion effects that are responsible for the binding of one or more cells to each other via protein reactions on cell surfaces. Instead of taking the conventional Ginzburg–Landau energy functional, we pick the nonlocal Helmholtz free energy functional. This has been analyzed previously in [8–10, 65, 66], but not in combination with a velocity-driven tumor growth system. Our contributions are the modeling, analysis, and numerical simulation of the entire system.

In Section 2, we exploit the mass and momentum balance laws based on continuum mixture theory and the Ginzburg–Landau free energy functional to build a generic class of multispecies phase-field models. In particular, we derive the system with an unsteady DFB equation. We present some primary results on the mathematical analysis in Section 3, e.g., we introduce some analytical tools such as the Sobolev embedding theorem that we need in the upcoming sections. A comprehensive mathematical examination of the existence of weak solutions to the local system is done in Section 4. We use the Faedo–Galerkin method to derive an energy inequality. We briefly discuss nonlocal cell-cell adhesion effects for long-range interactions in Section 5 and analyze the nonlocal model in terms of its weak solution. In Section 6, we investigate the model’s parameters using a sensitivity analysis. We introduce both the variance-based analysis and one using active subspaces. Both strategies are compared, and matching results are concluded. In Section 7, we present a numerical algorithm for solving the local system, as well as various numerical illustrations demonstrating the nonlinear flow’s influence.

I was heavily involved in the brainstorming of ideas and was in charge of establishing the mathematical foundation and carrying out the scientific effort described in this article. Additionally, I was in charge of writing the article while the co-authors contributed by making corrective changes.

## Permission to include:

Marvin Fritz, Ernesto Lima, J. Tinsley Oden, Barbara Wohlmuth

**On the unsteady Darcy–Forchheimer–Brinkman equation in local and non-local tumor growth models**

*Mathematical Models and Methods in Applied Sciences* 29(09):1691–1731, 2019

(see also article [62] in the bibliography)

The following pages on copyright are excerpts from copies of the website

<https://www.worldscientific.com/page/authors/author-rights>

(Accessed on 21 November 2021)

## Author Rights

All articles published on the World Scientific website are protected by copyright held by World Scientific Publishing Company (or its subsidiaries). This copyright covers the exclusive rights to share, reproduce and distribute the article, including in electronic forms, reprints, translations, photographic reproductions, or similar. Except for articles published on an [open access basis](#), the transfer of copyright to World Scientific (or its subsidiaries) becomes effective when an article is accepted for publication.

As author of a journal article, you retain the rights detailed in the following:

### Publisher-created version

1. The publisher-created version can only be posted where a gold open access fee has been paid and the article contains an OpenAccess logo.

### Preprint version

2. Authors may post their submitted manuscript (preprint) at any time on their personal website, in their company or institutional repository, in not-for-profit subject-based preprint servers or repositories, and on scholarly collaboration networks (SCNs) which have [signed up to the STM sharing principles](#). Please provide the following acknowledgement along with a link to the article via its DOI if available.

- *Preprint of an article submitted for consideration in [Journal] © [Year] [copyright World Scientific Publishing Company] [Journal URL]*
- *Preprint of an article published in [Journal, Volume, Issue, Year, Pages] [Article DOI] © [copyright World Scientific Publishing Company] [Journal URL]*

### Author accepted manuscript

3. After an embargo of 12 months, you may post the accepted author manuscript on your personal website, your company or institutional repository, not-for-profit subject-based preprint servers or repositories of your own choice or as stipulated by the Funding Agency and may share the article in private research groups including those on SCNs which have [signed up to the STM sharing principles](#).

The private research groups must be formed by invitation for a specific research purpose and be of a size that is typical for research groups within the discipline. Sharing of articles must be limited to members of the group only. The SCNs which have signed up to the sharing principles are required to provide COUNTER compliant usage data to World Scientific by agreement. Please provide the following acknowledgement along with a link to the article via its DOI if available:

- *Electronic version of an article published as [Journal, Volume, Issue, Year, Pages] [Article DOI] © [copyright World Scientific Publishing Company] [Journal URL]*

The [Digital Object Identifier \(DOI\)](#) of your article can be found on the relevant webpage of WorldSciNet where your article is posted.

The above permissions apply to authors whose articles are to be published by World Scientific and authors who have purchased a copy or received a complimentary copy of their published article.

This policy does not apply to pay-per-view customers and subscribers, who should adhere to their respective agreed policies

#### Definitions:

- "preprint" - a version of an article created prior to peer review
- "accepted author manuscript" - an author-created version of the final journal article (to reflect changes made in peer review and editing)
- "publisher-created version" - the definitive final record of published research that appears in the journal and embodies all value-adding publisher activities including copy-editing, formatting and pagination.



#### Resources

[For Authors](#)  
[For Booksellers](#)  
[For Librarians](#)  
[Copyright & Permissions](#)  
[Translation Rights](#)  
[How to Order](#)  
[Contact Us](#)  
[Sitemap](#)

#### About Us & Help

[About Us](#)  
[News](#)  
[Help](#)

#### Links

[World Scientific Europe](#)  
[World Scientific China 世界科技](#)  
[WS Education](#)  
[Global Publishing 八方文化](#)  
[Asia-Pacific Biotech News](#)  
[World Century](#)

[Privacy policy](#)

© 2021 World Scientific Publishing Co Pte Ltd

Powered by Atypon® Literatum

## **Notice of publication and copyright**

First Published in "On the unsteady Darcy–Forchheimer–Brinkman equation in local and nonlocal tumor growth models" in *Mathematical Models and Methods in Applied Sciences*, 29(09):1691–1731 (2019), published by World Scientific.

DOI: <https://doi.org/10.1142/S0218202519500519>

## On the unsteady Darcy–Forchheimer–Brinkman equation in local and nonlocal tumor growth models

Marvin Fritz\*

*Department of Mathematics,  
Technical University of Munich,  
Boltzmannstraße 3, 85748 Garching, Germany  
marvin.fritz@ma.tum.de*

Ernesto A. B. F. Lima<sup>†</sup> and J. Tinsley Oden<sup>‡</sup>

*Oden Institute for Computational Engineering and Sciences,  
The University of Texas at Austin,  
201 East 24th St, Austin, TX 78712-1229, USA  
<sup>†</sup>lima@oden.utexas.edu  
<sup>‡</sup>oden@oden.utexas.edu*

Barbara Wohlmuth

*Department of Mathematics,  
Technical University of Munich,  
Boltzmannstraße 3, 85748 Garching, Germany  
wohlmuth@ma.tum.de*

Received 20 December 2018

Revised 30 March 2019

Accepted 12 April 2019

Published 4 July 2019

Communicated by N. Bellomo

A mathematical analysis of local and nonlocal phase-field models of tumor growth is presented that includes time-dependent Darcy–Forchheimer–Brinkman models of convective velocity fields and models of long-range cell interactions. A complete existence analysis is provided. In addition, a parameter-sensitivity analysis is described that quantifies the sensitivity of key quantities of interest to changes in parameter values. Two sensitivity analyses are examined; one employing statistical variances of model outputs and another employing the notion of active subspaces based on existing observational data. Remarkably, the two approaches yield very similar conclusions on sensitivity for certain quantities of interest. The work concludes with the presentation of numerical approximations of solutions of the governing equations and results of numerical experiments on tumor growth produced using finite element discretizations of the full tumor model for representative cases.

*Keywords:* Tumor growth; nonlocal; existence; sensitivity analysis; finite elements.

AMS Subject Classification: 35K35, 76D07, 35A01, 35D30, 35Q92, 65C60, 65M60

\*Corresponding author



## 1. Introduction

In this exposition, we present a mathematical analysis of a general class of local and nonlocal multispecies phase-field models of tumor growth, derived using the balance laws of continuum mixture theory and employing mesoscale versions of the Ginzburg–Landau energy functional involving cell-species volume fractions. The model class involves nonlinear characterizations of cell velocity obeying a time-dependent Darcy–Forchheimer–Brinkman law. In addition, to account for long-range interactions characterizing such effects as cell-to-cell adhesion, a class of nonlocal models of tumor growth is considered, which involves systems of integro-differential equations.

This contribution generalizes the analyses of Cahn–Hilliard–Darcy models studied in Refs. 34 and 36 and includes a detailed analysis of existence of weak solutions of the governing system of fourth-order integro-partial-differential equations. Beyond the mathematical analysis of this class of models, we also explore the sensitivity of model outputs to perturbations in parameters for the local models. These analyses draw from active subspace methods when observational data are available and on variance sensitivity analysis when models outputs due to parameter variations are considered. Finite element approximations of the general local tumor models are presented and the results of numerical experiments are given that depict the role of linear and nonlinear flow laws on the evolution and structure of solid tumors.

This study is intended to contribute to a growing body of mathematical and computational work accumulated over the last two decades on tumor growth, decline, and invasion in living organisms. To date, the bulk of the models proposed are phenomenological models, designed to depict phenomena at the macro- or meso-scale where microenvironmental constituents are represented by fields describing volume fractions or mass concentrations of various species. The models studied here are in this category. Reviews and surveys of recent literature of tumor growth modeling can be found in Refs. 5, 63 and 21, and in surveys of work of the last decade in Refs. 47, 65, 10, 42, 68 and 84.

Prominent among more recent proposed models are those involving diffuse-interface or phase-field representations designed to capture morphological instabilities in the form of phase changes driven by cell necrosis and non-uniform cell proliferation. These effects result in tumor growth made possible by increases in the surface areas at the interface of cell species.<sup>84</sup> Models that can replicate such phenomena usually involve Ginzburg–Landau free energy functionals<sup>45</sup> of species concentrations or volume fractions, nutrient concentrations, and, importantly, gradients of species concentrations as a representation of surface energies, a feature that leads to Cahn–Hilliard type models. The use of such phase-field formulations eliminates the need for enforcing conditions across interfaces between species and for tracking the interface, the locations of which are intrinsic features of the solution. Such non-sharp interfaces are often better characterizations of the actual moving

interfaces between multiple species within a tumor than models employing sharp interfaces.

Multiphase models of tumor growth have been proposed by several authors over the last decade. We mention as examples the multicomponent models of Araujo and McElwain<sup>1</sup> and the four, six, and 10 species models of Refs. 48, 53 and 55, respectively, the Cahn–Hilliard–Darcy models of Garcke *et al.*<sup>34,36</sup> and the three-dimensional nonlinear multispecies models of Wise *et al.*<sup>84</sup> Additional references can be found in these works.

Following this introduction, we introduce a general class of multispecies, phase-field models developed from balance laws and accepted cell-biological phenomena observed in cancer, in which cell velocity, present in mass convection, is modeled via a time-dependent, nonlinear flow field governed by a Darcy–Forchheimer–Brinkman law,<sup>9,43,46,51,86</sup> which can be obtained by the means of mixture theory.<sup>66,77</sup> In Secs. 3–5, we develop a complete mathematical analysis of these classes of models proving existence of weak solutions through compactness arguments. We first consider the so-called local theory with nonlinear flow in which the evolution of the tumor volume fractions is influenced only by events in the neighborhood of each spatial point in the tumor mass and then we address nonlocal effects to depict long-range interactions of cell species.

To address the fundamental question of sensitivity of solutions of such nonlinear systems to variation in model parameters, we provide a detailed analysis of sensitivity for local models in Sec. 6, calling on both statistical methods<sup>62,71–73</sup> of sensitivity analysis and data-dependent methods based on the notion of active subspaces.<sup>16,18</sup> In Sec. 7, we take up representative finite element approximations and numerical algorithms and present the results of numerical experiments, particularly focusing on the effects of time-dependent nonlinear flow regimes on the evolution of tumor morphology. In a final section, we provide concluding remarks of the study.

## 2. A Class of Local Models of Tumor Growth

We consider a solid tumor mass  $\mathcal{T}$  evolving in the interior of a bounded Lipschitz domain  $\Omega \subset \mathbb{R}^d$ ,  $d \leq 3$ , over a time period  $[0, T]$ . At each point  $x \in \Omega$ , several cell species and other constituents exist which are differentiated according to their volume fractions,  $\phi_\alpha$ ,  $\alpha = 1, 2, \dots, N$ . The volume fractions of tumor cells is given by the scalar-valued field  $\phi_T = \phi_T(x, t)$  and the volume-averaged velocity is denoted by  $v$ . The mass density of all  $N$  species is assumed to be a single constant field, and the evolution of the tumor cells is governed by the evolution of proliferative cells with volume fraction  $\phi_P$ , hypoxic cells  $\phi_H$ , and necrotic cells  $\phi_N$ . The nutrient supply to the tumor is characterized by a constituent with volume fraction  $\phi_\sigma = \phi_\sigma(x, t)$ .

The tumor mass is conserved during its evolution, and this is assumed to be captured by the convective phase-field equation<sup>53,55</sup>

$$\partial_t \phi_T + \operatorname{div}(\phi_T v) = \operatorname{div}(m_T(\phi_T, \phi_\sigma) \nabla \mu) + \lambda_T \phi_\sigma \phi_T (1 - \phi_T) - \lambda_A \phi_T, \quad (2.1)$$

where  $m_T$  is the mobility function,  $\mu$  the chemical potential, and  $\lambda_T, \lambda_A$  are the proliferation and apoptosis rates, respectively. Following Refs. 48, 53, 55 and 84, we consider

$$\mu = \frac{\delta \mathcal{E}}{\delta \phi_T} = \Psi'(\phi_T) - \varepsilon_T^2 \Delta \phi_T - \chi_0 \phi_\sigma, \tag{2.2}$$

where  $\delta \mathcal{E} / \delta \phi_T$  denotes the first variation of the Ginzburg–Landau free energy functional,

$$\mathcal{E}(\phi_T, \phi_\sigma) = \int_\Omega \Psi(\phi_T) + \frac{\varepsilon_T^2}{2} |\nabla \phi_T|^2 - \chi_0 \phi_\sigma \phi_T \, dx. \tag{2.3}$$

In (2.3),  $\Psi$  is a double-well potential with a prefactor  $\bar{E}$  (such as  $\Psi(\phi_T) = \bar{E} \phi_T^2 (1 - \phi_T)^2$ ),  $\varepsilon_T$  is a parameter associated with the interface thickness separating cell species, and  $\chi_0$  is the chemotaxis parameter. The velocity  $v$  is assumed to obey the time-dependent incompressible Darcy–Forchheimer–Brinkman law<sup>9,43,46,51,86</sup>

$$\begin{aligned} \partial_t v + \alpha v &= \operatorname{div}(\nu(\phi_T, \phi_\sigma) Dv) - F_1 |v|v - F_2 |v|^2 v - \nabla p + (\mu + \chi_0 \phi_\sigma) \nabla \phi_T, \\ \operatorname{div} v &= 0, \end{aligned} \tag{2.4}$$

where  $Dv = \frac{1}{2}(\nabla v + (\nabla v)^\top)$  denotes the deformation-rate tensor. The nutrient concentration  $\phi_\sigma$  is assumed to obey a convection–reaction–diffusion equation of the form:

$$\partial_t \phi_\sigma + \operatorname{div}(\phi_\sigma v) = \operatorname{div}(m_\sigma(\phi_T, \phi_\sigma)(\delta_\sigma^{-1} \nabla \phi_\sigma - \chi_0 \nabla \phi_T)) - \lambda_\sigma \phi_T \phi_\sigma, \tag{2.5}$$

with  $m_\sigma$  a mobility function and  $\delta_\sigma$  and  $\lambda_\sigma$  positive parameters.

Collecting (2.1), (2.2), (2.4) and (2.5), we arrive at a model governed by the system,

$$\begin{aligned} \partial_t \phi_T + \operatorname{div}(\phi_T v) &= \operatorname{div}(m_T(\phi_T, \phi_\sigma) \nabla \mu) + S_T(\phi_T, \phi_\sigma), \\ \mu &= \Psi'(\phi_T) - \varepsilon_T^2 \Delta \phi_T - \chi_0 \phi_\sigma, \\ \partial_t \phi_\sigma + \operatorname{div}(\phi_\sigma v) &= \operatorname{div}(m_\sigma(\phi_T, \phi_\sigma)(\delta_\sigma^{-1} \nabla \phi_\sigma - \chi_0 \nabla \phi_T)) + S_\sigma(\phi_T, \phi_\sigma), \\ \partial_t v + \alpha v &= \operatorname{div}(\nu(\phi_T, \phi_\sigma) Dv) - F_1 |v|v - F_2 |v|^2 v - \nabla p + S_v(\phi_T, \phi_\sigma), \\ \operatorname{div} v &= 0, \end{aligned} \tag{2.6}$$

in the time-space domain  $(0, T) \times \Omega$  with source functions  $S_T, S_\sigma, S_v$  with properties laid down in Theorem 4.1 of Sec. 4. We supplement the system with the following boundary and initial conditions,

$$\begin{aligned} \partial_n \phi_T = \partial_n \mu &= 0 && \text{on } (0, T) \times \partial\Omega, \\ \phi_\sigma &= 1 && \text{on } (0, T) \times \partial\Omega, \\ v &= 0 && \text{on } (0, T) \times \partial\Omega, \\ \phi_T(0) &= \phi_{T,0} && \text{in } \Omega, \\ \phi_\sigma(0) &= \phi_{\sigma,0} && \text{in } \Omega, \\ v(0) &= v_0 && \text{in } \Omega, \end{aligned} \tag{2.7}$$

where  $\phi_{T,0}, \phi_{\sigma,0}, v_0$  are given functions. Here,  $\partial_n f = \nabla f \cdot n$  denotes the normal derivative of a function  $f$  at the boundary  $\partial\Omega$  with the outer unit normal  $n$ .

### 3. Notation and Auxiliary Results

Notationally, we suppress the domain  $\Omega$  when denoting various Banach spaces and write simply  $L^p, H^m, W^{m,p}$ . We equip these spaces with the norms  $|\cdot|_{L^p}, |\cdot|_{H^m}, |\cdot|_{W^{m,p}}$ , and, to simplify notation, we denote by  $(\cdot, \cdot)$  the scalar product in  $L^2$ . The brackets  $\langle \cdot, \cdot \rangle_{H^1}$  denote the duality pairing on  $(H^1)' \times H^1$  and in the same way for the other spaces. In the case of  $d$ -dimensional vector functions, we write  $[L^p]^d$  and in the same way for the other Banach spaces, but we do not make this distinction in the notation of norms, scalar products and applications with its dual.

Throughout this paper,  $C < \infty$  stands for a generic constant. We recall the Poincaré and Korn inequalities,<sup>69</sup>

$$\begin{aligned} |f - \bar{f}|_{L^2} &\leq C|\nabla f|_{L^2} \quad \text{for all } f \in H^1, \\ |f|_{L^2} &\leq C|\nabla f|_{L^2} \quad \text{for all } f \in H_0^1, \\ |\nabla f|_{L^2} &\leq C|Df|_{L^2} \quad \text{for all } f \in H_0^1, \end{aligned}$$

where  $\bar{f} = \frac{1}{|\Omega|} \int_{\Omega} f(x)dx$  is the mean of  $f$ . We define the spaces  $H, V, V^\perp, L_0^2$  as follows:

$$\begin{aligned} H &= \{u \in [L^2]^d : \operatorname{div} u = 0, u \cdot n|_{\partial\Omega} = 0\}, \\ V &= \{u \in [H_0^1]^d : \operatorname{div} u = 0\}, \\ V^\perp &= \{f \in [H^{-1}]^d : \langle f, u \rangle_{H^{-1} \times H_0^1} = 0 \text{ for all } u \in V\}, \\ L_0^2 &= \{u \in L^2 : \bar{u} = 0\}, \end{aligned}$$

where, for  $u \in H$ , the divergence is meant in a distributional sense and its trace operator is well-defined; see Ref. 41. For a given Banach space  $X$ , we define the Bochner space<sup>26,69</sup>

$$L^p(0, T; X) = \left\{ u : (0, T) \rightarrow X : u \text{ Bochner measurable, } \int_0^T |u(t)|_X^p dt < \infty \right\},$$

where  $1 \leq p < \infty$ , with the norm  $\|u\|_{L^p X}^p = \int_0^T |u(t)|_X^p dt$ . For  $p = \infty$ , we equip  $L^\infty(0, T; X)$  with the norm  $\|u\|_{L^\infty X} = \operatorname{ess\,sup}_{t \in (0, T)} |u(t)|_X$ . We introduce the Sobolev–Bochner space,

$$W^{1,p}(0, T; X) = \{u \in L^p(0, T; X) : \partial_t u \in L^p(0, T; X)\},$$

and the inverse Sobolev–Bochner space

$$W^{-1,p}(0, T; X) = \mathcal{L}(W_0^{1,q}(0, T); X),$$

where  $q = 1/(1 - 1/p)$  is the Hölder conjugate of  $p$ .

Let  $X, Y, Z$  be Banach spaces such that  $X$  is compactly embedded in  $Y$  and  $Y$  is continuously embedded in  $Z$ , i.e.  $X \hookrightarrow Y \hookrightarrow Z$ . In the proof of the existence

theorem below we make use of the Aubin–Lions compactness lemma, see Corollary 4 in Ref. 74,

$$\begin{aligned} L^p(0, T; X) \cap W^{1,1}(0, T; Z) &\hookrightarrow L^p(0, T; Y), \quad 1 \leq p < \infty, \\ L^\infty(0, T; X) \cap W^{1,r}(0, T; Z) &\hookrightarrow C([0, T]; Y), \quad r > 1, \end{aligned} \tag{3.1}$$

and of the following continuous embeddings, see Theorem 3.1, Chap. 1 in Ref. 56 and Theorem 2.1 in Ref. 79,

$$L^2(0, T; Y) \cap H^1(0, T; Z) \hookrightarrow C([0, T]; [Y, Z]_{1/2}), \tag{3.2}$$

$$L^\infty(0, T; Y) \cap C_w([0, T]; Z) \hookrightarrow C_w([0, T]; Y), \tag{3.3}$$

where  $[Y, Z]_{1/2}$  denotes the interpolation space between  $Y$  and  $Z$ ; see Definition 2.1, Chap. 1 in Ref. 56 for a precise definition. Here,  $C_w([0, T]; Y)$  denotes the space of the weakly continuous functions on the interval  $[0, T]$  with values in  $Y$ .

**Lemma 3.1.** (Gronwall, cf. Lemma 3.1 in Ref. 35) *Let  $u, v \in C([0, T]; \mathbb{R}_{\geq 0})$ . If there are constants  $C_1, C_2 < \infty$  such that*

$$u(t) + v(t) \leq C_1 + C_2 \int_0^t u(s) ds \quad \text{for all } t \in [0, T],$$

*then it holds that  $u(t) + v(t) \leq C_1 e^{C_2 T}$  for all  $t \in [0, T]$ .*

**Lemma 3.2.** (De Rham, cf. Lemma 7 in Ref. 81) *If  $f \in V^\perp$ , then there is a unique  $q \in L_0^2$  such that  $f = \nabla q$  and  $|q|_{L^2} \leq C|f|_{H^{-1}}$ . In other words, there exists an operator  $L \in \mathcal{L}(V^\perp, L_0^2)$  such that  $\nabla \circ L = \text{Id}$ .*

Introducing the Nemyzki operator of  $L$ ,

$$\begin{aligned} \mathcal{N}_L : W^{-1,\infty}(0, T; V^\perp) &\rightarrow W^{-1,\infty}(0, T; L_0^2), \\ (\mathcal{N}_L w)(\eta) &= L(w(\eta)) \quad \text{for all } \eta \in W_0^{1,1}(0, T), \end{aligned}$$

we get the following corollary of the de Rham lemma.

**Corollary 3.1.** *If  $w \in W^{-1,\infty}(0, T; V^\perp)$ , then there exists a unique element  $p \in W^{-1,\infty}(0, T; L_0^2)$  such that  $w = \nabla p$  in  $W^{-1,\infty}(0, T; H^{-1})$ .*

**Proof.** Since  $w(\eta) \in V^\perp$  for all  $\eta \in W_0^{1,1}(0, T)$ , we have

$$w(\eta) = \nabla L(w(\eta)) = \nabla(\mathcal{N}_L w)(\eta),$$

and we define  $p = \mathcal{N}_L w \in W^{-1,\infty}(0, T; L_0^2)$ , which is clearly unique. □

#### 4. Analysis of the Local Model

In this section, we first state the definition of a weak solution to the system (2.6) with the boundary and initial conditions (2.7), and then we establish the existence of a weak solution by employing the Faedo–Galerkin method.

To simplify notation, we introduce the abbreviations

$$m_T = m_T(\phi_T, \phi_\sigma), \quad m_\sigma = m_\sigma(\phi_T, \phi_\sigma), \quad \nu = \nu(\phi_T, \phi_\sigma),$$

$$S_T = S_T(\phi_T, \phi_\sigma), \quad S_\sigma = S_\sigma(\phi_T, \phi_\sigma), \quad S_v = S_v(\phi_T, \phi_\sigma).$$

**Definition 4.1.** (Weak solution) We call a quadruple  $(\phi_T, \mu, \phi_\sigma, v)$  a weak solution of system (2.6) if the functions  $\phi_T, \mu, \phi_\sigma : (0, T) \times \Omega \rightarrow \mathbb{R}, v : (0, T) \times \Omega \rightarrow \mathbb{R}^d$  have the regularity

$$\begin{aligned} \phi_T &\in H^1(0, T; (H^1)') \cap L^2(0, T; H^1), \\ \mu &\in L^2(0, T; H^1), \\ \phi_\sigma &\in W^{1, \frac{4}{d}}(0, T; H^{-1}) \cap (1 + L^2(0, T; H_0^1)), \\ v &\in W^{1, \frac{4}{d}}(0, T; V') \cap L^4(0, T; [L^4]^d) \cap L^2(0, T; V), \end{aligned}$$

fulfill the initial data  $\phi_T(0) = \phi_{T,0}, \phi_\sigma(0) = \phi_{\sigma,0}, v(0) = v_0$ , and satisfy the following variational form of (2.6),

$$\begin{aligned} \langle \partial_t \phi_T, \varphi_1 \rangle_{H^1} &= (\phi_T v, \nabla \varphi_1) - (m_T \nabla \mu, \nabla \varphi_1) + (S_T, \varphi_1), \\ (\mu, \varphi_2) &= (\Psi'(\phi_T), \varphi_2) + \varepsilon_T^2 (\nabla \phi_T, \nabla \varphi_2) - \chi_0(\phi_\sigma, \varphi_2), \\ \langle \partial_t \phi_\sigma, \varphi_3 \rangle_{H_0^1} &= (\phi_\sigma v, \nabla \varphi_3) - \delta_\sigma^{-1} (m_\sigma \nabla \phi_\sigma, \nabla \varphi_3) + \chi_0(m_\sigma \nabla \phi_T, \nabla \varphi_3) + (S_\sigma, \varphi_3), \\ \langle \partial_t v, \varphi_4 \rangle_V &= -\alpha(v, \varphi_4) - (\nu Dv, D\varphi_4) - F_1(|v|v, \varphi_4) - F_2(|v|^2 v, \varphi_4) + (S_v, \varphi_4), \end{aligned} \tag{4.1}$$

for all  $\varphi_1, \varphi_2 \in H^1, \varphi_3 \in H_0^1, \varphi_4 \in V$ .

In the variational form, we use the divergence-free space  $V$  as the test function space of the Darcy–Forchheimer–Brinkman equation. Therefore, the pressure  $p$  is eliminated from the equation. After proving the existence of a weak solution, we can associate a distributional pressure to the solution quadruple using the de Rham lemma; see Lemma 3.2.

A first principal result of this paper involves stating the existence of a weak solution to the model (2.6) in the sense of Definition 4.1.

**Theorem 4.1.** (Existence of a global weak solution) *Let the following assumptions hold:*

- (A1)  $\Omega \subset \mathbb{R}^d, d \in \{2, 3\}$ , is a bounded Lipschitz domain and  $T > 0$ .
- (A2)  $\phi_{T,0} \in H^1, \phi_{\sigma,0} \in L^2, v_0 \in H$ .
- (A3)  $m_T, m_\sigma, \nu \in C_b(\mathbb{R}^2)$  such that  $m_0 \leq m_T(x), m_\sigma(x), \nu(x) \leq m_\infty$  for positive constants  $m_0, m_\infty < \infty$ .
- (A4)  $S_T, S_\sigma, S_v$  are of the form  $S_T = \lambda_T \phi_\sigma g(\phi_T) - \lambda_A \phi_T, S_\sigma = -\lambda_\sigma \phi_\sigma h(\phi_T)$  for  $g, h \in C_b(\mathbb{R})$ , and  $S_v = (\mu + \chi_0 \phi_\sigma) \nabla \phi_T, \lambda_T, \lambda_A, \lambda_\sigma \geq 0$ .
- (A5)  $\Psi \in C^2(\mathbb{R})$  is such that  $\Psi(x) \geq C(|x|^2 - 1), |\Psi'(x)| \leq C(|x| + 1)$ , and  $|\Psi''(x)| \leq C(|x|^4 + 1)$ .

Then there exists a weak solution quadruple  $(\phi_T, \mu, \phi_\sigma, v)$  to (2.6) in the sense of Definition 4.1. Moreover, the solution quadruple has the regularity:

$$\begin{aligned} \phi_T &\in C([0, T]; L^2) \cap C_w([0, T]; H^1), \\ \phi_\sigma &\in \begin{cases} C([0, T]; L^2), & d = 2, \\ C([0, T]; H^{-1}) \cap C_w([0, T]; L^2), & d = 3, \end{cases} \\ v &\in \begin{cases} C([0, T]; H), & d = 2, \\ C([0, T]; V') \cap C_w([0, T]; H), & d = 3. \end{cases} \end{aligned}$$

Additionally, there is a unique  $p \in W^{-1,\infty}(0, T; L^2_0)$  such that  $(\phi_T, \mu, \phi_\sigma, v, p)$  is a solution quintuple to (2.6) in the distributional sense.

**Proof.** To prove the existence of a weak solution, we use the Faedo–Galerkin method<sup>26,70</sup> and semi-discretize the original problem in space. The discretized model can be formulated as an ordinary differential equation system and by the Cauchy–Peano theorem we conclude the existence of a discrete solution. Having energy estimates, we deduce from the Banach–Alaogulu theorem the existence of limit functions which eventually form a weak solution. This method has fared popularly in the analysis of tumor models, e.g. see Refs. 30, 34, 37, 36, 24, 35, 49, 50 and 58.

#### 4.1. Discretization in space

We introduce the discrete spaces

$$\begin{aligned} W_k &= \text{span}\{w_1, \dots, w_k\}, \\ Y_k &= \text{span}\{y_1, \dots, y_k\}, \\ Z_k &= \text{span}\{z_1, \dots, z_k\}, \end{aligned}$$

where  $w_j, y_j : \Omega \rightarrow \mathbb{R}, z_j : \Omega \rightarrow \mathbb{R}^d$  are the eigenfunctions to the eigenvalues  $\lambda_j^w, \lambda_j^y, \lambda_j^z \in \mathbb{R}$  of the following respective problems

$$\begin{cases} -\Delta w_j = \lambda_j^w w_j & \text{in } \Omega, \\ \partial_n w_j = 0 & \text{on } \partial\Omega, \end{cases} \begin{cases} -\Delta y_j = \lambda_j^y y_j & \text{in } \Omega, \\ y_j = 0 & \text{on } \partial\Omega, \end{cases} \begin{cases} -\Delta z_j = \lambda_j^z z_j & \text{in } \Omega, \\ \text{div } z_j = 0 & \text{in } \Omega, \\ z_j = 0 & \text{on } \partial\Omega. \end{cases}$$

Since the Laplace operator is a compact, self-adjoint, injective operator, we conclude by the spectral theorem<sup>7,8,67</sup> that

- $\{w_j\}_{j \in \mathbb{N}}$  is an orthonormal basis in  $L^2$  and orthogonal in  $H^1$ ,
- $\{y_j\}_{j \in \mathbb{N}}$  is an orthonormal basis in  $L^2$  and orthogonal in  $H_0^1$ ,
- $\{z_j\}_{j \in \mathbb{N}}$  is an orthonormal basis in  $H$  and orthogonal in  $V$ .

Exploiting orthonormality of the eigenfunctions, we deduce that  $W_k$  and  $Y_k$  are dense in  $L^2$ , and  $Z_k$  is dense in  $H$ . We introduce the orthogonal projections,

$$\Pi_{W_k} : L^2 \rightarrow W_k, \quad \Pi_{Y_k} : L^2 \rightarrow Y_k, \quad \Pi_{Z_k} : H \rightarrow Z_k,$$

which can be written as

$$\Pi_{W_k} u = \sum_{j=1}^k (u, w_j) w_j \quad \text{for all } u \in H^1,$$

and analogously for  $\Pi_{Y_k}$  and  $\Pi_{Z_k}$ .

We next consider the Galerkin approximations

$$\begin{aligned} \phi_T^k(t, x) &= \sum_{j=1}^k \alpha_j(t) w_j(x), & \mu^k(t, x) &= \sum_{j=1}^k \beta_j(t) w_j(x), \\ \phi_\sigma^k(t, x) &= 1 + \sum_{j=1}^k \gamma_j(t) y_j(x), & v^k(t, x) &= \sum_{j=1}^k \delta_j(t) z_j(x), \end{aligned} \tag{4.2}$$

where  $\alpha_j, \beta_j, \gamma_j, \delta_j : (0, T) \rightarrow \mathbb{R}$  are coefficient functions for  $j \in \{1, \dots, k\}$ . To simplify the notation we set

$$\begin{aligned} m_T^k &= m_T(\phi_T^k, \phi_\sigma^k), & m_\sigma^k &= m_\sigma(\phi_T^k, \phi_\sigma^k), & \nu^k &= \nu(\phi_T^k, \phi_\sigma^k), \\ S_T^k &= S_T(\phi_T^k, \phi_\sigma^k), & S_\sigma^k &= S_\sigma(\phi_T^k, \phi_\sigma^k), & S_v^k &= S_v(\phi_T^k, \phi_\sigma^k). \end{aligned}$$

The Galerkin system of the model (4.1) then reads

$$\langle \partial_t \phi_T^k, w_j \rangle_{H^1} = (\phi_T^k v^k, \nabla w_j) - (m_T^k \nabla \mu^k, \nabla w_j) + (S_T^k, w_j), \tag{4.3a}$$

$$(\mu^k, w_j) = (\Psi'(\phi_T^k), w_j) + \varepsilon_T^2 (\nabla \phi_T^k, \nabla w_j) - \chi_0 (\phi_\sigma^k, w_j), \tag{4.3b}$$

$$\begin{aligned} \langle \partial_t \phi_\sigma^k, y_j \rangle_{H_0^1} &= (\phi_\sigma^k v^k, \nabla y_j) - \delta_\sigma^{-1} (m_\sigma^k \nabla \phi_\sigma^k, \nabla y_j) + \chi_0 (m_\sigma^k \nabla \phi_T^k, \nabla y_j) \\ &\quad + (S_\sigma^k, y_j), \end{aligned} \tag{4.3c}$$

$$\begin{aligned} \langle \partial_t v^k, z_j \rangle_V &= -\alpha(v^k, z_j) - (\nu^k \mathbf{D} v^k, \mathbf{D} z_j) - F_1(|v^k| v^k, z_j) \\ &\quad - F_2(|v^k|^2 v^k, z_j) + (S_v^k, z_j), \end{aligned} \tag{4.3d}$$

for all  $j \in \{1, \dots, k\}$ . We equip this system with the initial data

$$\begin{aligned} \phi_T^k(0) &= \Pi_{W_k} \phi_{T,0} && \text{in } L^2, \\ \phi_\sigma^k(0) &= 1 + \Pi_{Y_k} \phi_{\sigma,0} && \text{in } L^2, \\ v^k(0) &= \Pi_{Z_k} v_0 && \text{in } H. \end{aligned} \tag{4.4}$$



After inserting the Galerkin ansatz functions (4.2) into the system (4.3), one can see that the Galerkin system is equivalent to a system of nonlinear ordinary differential equations in the  $4k$  unknowns  $\{\alpha_j, \beta_j, \gamma_j, \delta_j\}_{1 \leq j \leq k}$  with the initial data

$$\begin{aligned} \alpha_j(0) &= (\phi_{T,0}, w_j) && \text{in } \Omega, \\ \gamma_j(0) &= (\phi_{\sigma,0}, y_j) && \text{in } \Omega, \\ \delta_j(0) &= (v_0, z_j) && \text{in } \Omega. \end{aligned}$$

Due to the continuity of the nonlinear functions  $\Psi', m_T, m_\sigma, \nu$ , the existence of solutions to (4.3) with data (4.4) follows from the standard theory of ordinary differential equations, according to the Cauchy–Peano theorem, see Theorem 1.2, Chap. 1 in Ref. 14. We thus have local-in-time existence of a continuously differentiable solution quadruple,

$$\begin{aligned} (\phi_T^k, \mu^k, \phi_\sigma^k, v^k) &\in C^1([0, T_k]; W_k) \times C^1([0, T_k]; W_k) \\ &\times (1 + C^1([0, T_k]; Y_k)) \times C^1([0, T_k]; Z_k) \end{aligned}$$

to the Galerkin problem (4.3) on some sufficiently short time interval  $[0, T_k]$ .

### 4.2. Energy estimates

Next, we extend the existence interval to  $[0, T]$  by deriving  $k$ -independent estimates. In particular, these estimates allow us to deduce that the solution sequences converge to some limit functions as  $k \rightarrow \infty$ . It will turn out that exactly these limit functions will form a weak solution to our model (2.6) in the sense of Definition 4.1.

Testing (4.3a) with  $\mu^k + \chi_0 \phi_\sigma^k$ , (4.3b) with  $-\partial_t \phi_T^k$ , (4.3c) with  $K(\phi_\sigma^k - 1)$ ,  $K > 0$  to be specified, and (4.3d) with  $v^k$ , gives the equation system,

$$\begin{aligned} \langle \partial_t \phi_T^k, \mu^k \rangle_{H^1} + \chi_0 \langle \partial_t \phi_T^k, \phi_\sigma^k \rangle_{H^1} &= (\phi_T^k v^k, \nabla \mu^k + \chi_0 \nabla \phi_\sigma^k) \\ &\quad - (m_T^k \nabla \mu^k, \nabla \mu^k + \chi_0 \nabla \phi_\sigma^k) + (S_T^k, \mu^k + \chi_0 \phi_\sigma^k), \\ - \langle \partial_t \phi_T^k, \mu^k \rangle_{H^1} &= - \langle \partial_t \phi_T^k, \Psi'(\phi_T^k) \rangle_{H^1} + \chi_0 \langle \partial_t \phi_T^k, \phi_\sigma^k \rangle_{H^1} \\ &\quad - \varepsilon_T^2 \langle \nabla \partial_t \phi_T^k, \nabla \phi_T^k \rangle_{H^1}, \\ \langle \partial_t \phi_\sigma^k, K(\phi_\sigma^k - 1) \rangle_{H_0^1} &= (\phi_\sigma^k v^k, K \nabla \phi_\sigma^k) \\ &\quad - K(m_\sigma^k (\delta_\sigma^{-1} \nabla \phi_\sigma^k - \chi_0 \nabla \phi_T^k), \nabla \phi_\sigma^k) \\ &\quad + K(S_\sigma^k, \phi_\sigma^k - 1), \\ \langle \partial_t v^k, v^k \rangle_V &= -(\nu^k Dv^k, Dv^k) - F_1(|v^k| v^k, v^k) \\ &\quad - F_2(|v^k|^2 v^k, v^k) - (\alpha v^k, v^k) + (S_v^k, v^k). \end{aligned}$$

We observe that the tested convective terms cancel each other together with the tested source term in the velocity equation. Indeed, noting that  $v^k$  is divergence-free,

we have by integration by parts

$$\begin{aligned}
 & (\phi_T^k v^k, \nabla \mu^k + \chi_0 \nabla \phi_\sigma^k) + (\phi_\sigma^k v^k, K \nabla \phi_\sigma^k) \\
 &= -(v^k \cdot \nabla \phi_T^k, \mu^k + \chi_0 \phi_\sigma^k) - K(v^k \cdot \nabla \phi_\sigma^k, \phi_\sigma^k) = -(v^k, S_v^k),
 \end{aligned}$$

see also (A4) of Theorem 4.1 for the assumed form of  $S_v^k$ . Here, we also used that  $(\phi_\sigma^k v^k, \nabla \phi_\sigma^k) = -(v^k \cdot \nabla \phi_\sigma^k, \phi_\sigma^k)$  and therefore this term vanishes.

Adding the four tested equations results in

$$\begin{aligned}
 & \frac{d}{dt} \left[ |\Psi(\phi_T^k)|_{L^1} + \frac{\varepsilon_T^2}{2} |\nabla \phi_T^k|_{L^2}^2 + \frac{K}{2} |\phi_\sigma^k - 1|_{L^2}^2 + \frac{1}{2} |v^k|_{L^2} \right] + \delta_\sigma^{-1} K(m_\sigma^k, |\nabla \phi_\sigma^k|^2) \\
 &+ (m_T^k, |\nabla \mu^k|^2) + (\nu^k, |Dv^k|^2) + F_1 |v^k|_{L^3}^3 + F_2 |v^k|_{L^4}^4 + \alpha |v^k|_{L^2}^2 \\
 &= -\chi_0 (m_T^k \nabla \mu^k, \nabla \phi_\sigma^k) + (S_T^k, \mu^k + \chi_0 \phi_\sigma^k) + \chi_0 K(m_\sigma^k \nabla \phi_T^k, \nabla \phi_\sigma^k) \\
 &+ K(S_\sigma^k, \phi_\sigma^k), \tag{4.5}
 \end{aligned}$$

where  $K > 0$  can still be chosen appropriately.

We now estimate the terms on the right-hand side of this inequality. The Poincaré inequality applied to  $\mu^k$  and  $\phi_\sigma^k$  gives

$$\begin{aligned}
 |\mu^k|_{L^2} &\leq |\mu^k - \overline{\mu^k}|_{L^2} + |\overline{\mu^k}|_{L^2} \leq C |\nabla \mu^k|_{L^2} + |\Omega|^{-1/2} |\mu^k|_{L^1}, \\
 |\phi_\sigma^k|_{L^2} &\leq |\phi_\sigma^k - 1|_{L^2} + |1|_{L^2} \leq C |\nabla \phi_\sigma^k|_{L^2} + |\Omega|^{1/2}.
 \end{aligned}$$

Therefore, we can estimate the tested source term  $S_T^k$  using its assumed representation, see (A4) of Theorem 4.1, the Poincaré inequality, and the  $\varepsilon$ -Young inequality,

$$\begin{aligned}
 (S_T^k, \mu^k + \chi_0 \phi_\sigma^k) &= (\lambda_T \phi_\sigma^k g(\phi_T^k) - \lambda_A \phi_T^k, \mu^k + \chi_0 \phi_\sigma^k) \\
 &= \lambda_T (\phi_\sigma^k g(\phi_T^k), \mu^k) + \lambda_T \chi_0 (|\phi_\sigma^k|^2, g(\phi_T^k)) - \lambda_A (\phi_T^k, \mu^k) \\
 &\quad - \lambda_A \chi_0 (\phi_T^k, \phi_\sigma^k) \\
 &\leq C (|\phi_\sigma^k|_{L^2} |\mu^k|_{L^2} + |\phi_\sigma^k|_{L^2}^2 + |\phi_T^k|_{L^2} |\mu^k|_{L^2} + |\phi_T^k|_{L^2} |\phi_\sigma^k|_{L^2}) \\
 &\leq \frac{m_0}{4} |\nabla \mu^k|_{L^2}^2 + C(1 + |\phi_\sigma^k|_{L^2}^2 + |\mu^k|_{L^1}^2 + |\phi_T^k|_{L^2}^2). \tag{4.6}
 \end{aligned}$$

Testing (4.3b) with  $1 \in H^1$ , gives, together with the growth assumption (A5) on  $\Psi'$ ,

$$|\mu^k|_{L^1} \leq |\Psi'(\phi_T^k)|_{L^1} + \chi_0 |\phi_\sigma^k|_{L^1} \leq C(1 + |\phi_T^k|_{L^2} + |\phi_\sigma^k|_{L^2}). \tag{4.7}$$

Similarly, using the representation of  $S_\sigma^k$ , see (A4), we get

$$K(S_\sigma^k, \phi_\sigma^k) = -K \lambda_\sigma (h(\phi_T^k), |\phi_\sigma^k|^2) \leq CK |\phi_\sigma^k|_{L^2}^2, \tag{4.8}$$

$K$  being a positive constant appearing in (4.5) to be chosen below.

Now, using (4.6)–(4.8), the Hölder inequality and the  $\varepsilon$ -Young inequality, we can estimate the right-hand side in (4.5) as follows:

$$(\text{RHS}) \leq \chi_0 m_\infty |\nabla \mu^k|_{L^2} |\nabla \phi_\sigma^k|_{L^2} + \frac{m_0}{4} |\nabla \mu^k|_{L^2}^2 + C(1 + |\phi_\sigma^k|_{L^2}^2 + |\phi_T^k|_{L^2}^2)$$

$$\begin{aligned}
 & + \chi_0 K m_\infty |\nabla \phi_T^k|_{L^2} |\nabla \phi_\sigma^k|_{L^2} + CK |\phi_\sigma^k|_{L^2}^2 \\
 & \leq \frac{m_0}{2} |\nabla \mu^k|_{L^2}^2 + CK(1 + |\phi_\sigma^k - 1|_{L^2}^2 + |\nabla \phi_T^k|_{L^2}^2) + C(1 + |\nabla \phi_\sigma^k|_{L^2}^2 + |\phi_T^k|_{L^2}^2).
 \end{aligned}$$

We note that in this inequality  $C$  is independent of  $K$ . This is important since we choose  $K$  such that  $\delta_\sigma^{-1} K m_0 > C$  so that we can absorb  $|\nabla \phi_\sigma^k|_{L^2}$  from the right-hand side. Indeed, we get the following inequality from (4.5),

$$\begin{aligned}
 & \frac{d}{dt} \left[ |\Psi(\phi_T^k)|_{L^1} + \frac{\varepsilon_T^2}{2} |\nabla \phi_T^k|_{L^2}^2 + \frac{K}{2} |\phi_\sigma^k - 1|_{L^2}^2 + \frac{1}{2} |v^k|_{L^2}^2 \right] \\
 & \quad + \left( \frac{K m_0}{\delta_\sigma} - C \right) |\nabla \phi_\sigma^k|_{L^2}^2 + \frac{m_0}{2} |\nabla \mu^k|_{L^2}^2 + m_0 |Dv^k|_{L^2}^2 + F_2 |v^k|_{L^4}^4 \\
 & \leq C(1 + |\nabla \phi_T^k|_{L^2}^2 + |\phi_\sigma^k - 1|_{L^2}^2 + |\phi_T^k|_{L^2}^2).
 \end{aligned}$$

Integrating this inequality over  $(0, t)$ ,  $t \in (0, T_k)$ , and using the growth assumption (A5) on  $\Psi$  give

$$\begin{aligned}
 & |\phi_T^k(t)|_{L^2}^2 + |\nabla \phi_T^k(t)|_{L^2}^2 + |\phi_\sigma^k(t) - 1|_{L^2}^2 + |v^k(t)|_{L^2}^2 + \|\nabla \phi_\sigma^k\|_{L^2(0,t;L^2)}^2 \\
 & \quad + \|\nabla \mu^k\|_{L^2(0,t;L^2)}^2 + \|Dv^k\|_{L^2(0,t;L^2)}^2 + \|v^k\|_{L^4(0,t;L^4)}^4 \\
 & \quad - C(\|\nabla \phi_T^k\|_{L^2(0,t;L^2)}^2 + \|\phi_\sigma^k - 1\|_{L^2(0,t;L^2)}^2 + \|\phi_T^k\|_{L^2(0,t;L^2)}^2) \\
 & \leq C(1 + |\Psi(\phi_T^k(0))|_{L^1} + |\nabla \phi_T^k(0)|_{L^2}^2 + |\phi_\sigma^k(0) - 1|_{L^2}^2 + |v^k(0)|_{L^2}^2).
 \end{aligned}$$

Applying the Gronwall lemma and taking the essential supremum over  $t \in (0, T_k)$ , give

$$\begin{aligned}
 & \|\phi_T^k\|_{L^\infty(0,T_k;L^2)}^2 + \|\nabla \phi_T^k\|_{L^\infty(0,T_k;L^2)}^2 + \|\phi_\sigma^k - 1\|_{L^\infty(0,T_k;L^2)}^2 + \|v^k\|_{L^\infty(0,T_k;L^2)}^2 \\
 & \quad + \|\nabla \phi_\sigma^k\|_{L^2(0,T_k;L^2)}^2 + \|\nabla \mu^k\|_{L^2(0,T_k;L^2)}^2 + \|Dv^k\|_{L^2(0,T_k;L^2)}^2 + \|v^k\|_{L^4(0,T_k;L^4)}^4 \\
 & \leq C(1 + |\Psi(\phi_T^k(0))|_{L^1} + |\nabla \phi_T^k(0)|_{L^2}^2 + |\phi_\sigma^k(0) - 1|_{L^2}^2 + |v^k(0)|_{L^2}^2) e^{CT}. \tag{4.9}
 \end{aligned}$$

We have chosen the initial values of the Galerkin approximations as the orthogonal projections of the initial values of their counterpart, see (4.4). The operator norm of an orthogonal projection is bounded by 1 and, therefore, uniform estimates are obtained in (4.9); for example

$$|v^k(0)|_{L^2}^2 = |\Pi_{Z_k} v_0|_{L^2}^2 \leq |v_0|_{L^2}^2.$$

We note that we have to invoke the growth estimate (A5) to treat the term involving  $\Psi$  in the following way:

$$|\Psi(\phi_T^k(0))|_{L^1} \leq C + C|\phi_T^k(0)|_{L^2}^2 = C + C|\Pi_{W_k} \phi_{T,0}|_{L^2}^2 \leq C + C|\phi_{T,0}|_{L^2}^2.$$

Now, these  $k$ -independent estimates allow us to extend the time interval by setting  $T_k = T$  for all  $k \in \mathbb{N}$ . Therefore, we have the final uniform energy estimate,

$$\|\phi_T^k\|_{L^\infty H^1}^2 + \|\mu^k\|_{L^2 H^1}^2 + \|\phi_\sigma^k\|_{L^\infty L^2}^2 + \|\phi_\sigma^k - 1\|_{L^2 H^1}^2$$

$$\begin{aligned}
 & + \|v^k\|_{L^\infty H}^2 + \|v^k\|_{L^2 V}^2 + \|v^k\|_{L^4 L^4}^4 \\
 & \leq C \times (1 + |\phi_{T,0}|_{H^1}^2 + |\phi_{\sigma,0}|_{L^2}^2 + |v_0|_{L^2}^2) \times \exp(CT).
 \end{aligned}
 \tag{4.10}$$

### 4.3. Weak convergence

Next, we prove that there are subsequences of  $\phi_T^k, \mu^k, \phi_\sigma^k, v^k$ , which converge to a weak solution of our model (2.6) in the sense of Definition 4.1. From the energy estimate (4.10) we deduce that

$$\begin{aligned}
 \{\phi_T^k\}_{k \in \mathbb{N}} & \text{ is bounded in } L^\infty(0, T; H^1), \\
 \{\mu^k\}_{k \in \mathbb{N}} & \text{ is bounded in } L^2(0, T; H^1), \\
 \{\phi_\sigma^k\}_{k \in \mathbb{N}} & \text{ is bounded in } L^\infty(0, T; L^2) \cap (1 + L^2(0, T; H_0^1)), \\
 \{v^k\}_{k \in \mathbb{N}} & \text{ is bounded in } L^\infty(0, T; H) \cap L^2(0, T; V) \cap L^4(0, T; [L^4]^d),
 \end{aligned}
 \tag{4.11}$$

and, by the Banach–Alaoglu theorem, these bounded sequences have weakly convergent subsequences. By a typical abuse of notation, we drop the subsequence index. Consequently, there are functions  $\phi_T, \mu, \phi_\sigma : (0, T) \times \Omega \rightarrow \mathbb{R}, v : (0, T) \times \Omega \rightarrow \mathbb{R}^d$  such that

$$\begin{aligned}
 \phi_T^k & \rightharpoonup \phi_T \quad \text{weakly-* in } L^\infty(0, T; H^1), \\
 \mu^k & \rightharpoonup \mu \quad \text{weakly in } L^2(0, T; H^1), \\
 \phi_\sigma^k & \rightharpoonup \phi_\sigma \quad \text{weakly-* in } L^\infty(0, T; L^2) \cap (1 + L^2(0, T; H_0^1)), \\
 v^k & \rightharpoonup v \quad \text{weakly-* in } L^\infty(0, T; H) \cap L^2(0, T; V) \cap L^4(0, T; [L^4]^d),
 \end{aligned}
 \tag{4.12}$$

as  $k \rightarrow \infty$ .

### 4.4. Strong convergence

We now consider taking the limit  $k \rightarrow \infty$  in the Galerkin system (4.3) in hopes to attain the initial variational system (4.1). Since the equations in (4.3) are nonlinear in  $\phi_T^k, \phi_\sigma^k, v^k$ , we want to achieve strong convergence of these sequences before we take the limit in (4.3). Therefore, our goal is to bound their time derivatives and applying the Aubin–Lions lemma (3.1).

Let  $(\zeta, \eta, \xi)$  be such that  $\zeta \in L^2(0, T; H^1), \eta \in L^{4/(4-d)}(0, T; H_0^1), \xi \in L^{4/(4-d)}(0, T; V)$  and

$$\Pi_{W_k} \zeta = \sum_{j=1}^k \zeta_j^k w_j, \quad \Pi_{Y_k} \varphi = \sum_{j=1}^k \eta_j^k y_j, \quad \Pi_{Z_k} \xi = \sum_{j=1}^k \xi_j^k z_j,$$

with coefficients  $\{\zeta_j^k\}_{j=1}^k, \{\eta_j^k\}_{j=1}^k, \{\xi_j^k\}_{j=1}^k$ . Multiplying Eq. (4.3a) by  $\zeta_j^k$ , (4.3c) by  $\eta_j^k$  and (4.3d) by  $\xi_j^k$ , we sum up each equation from  $j = 1$  to  $k$  and integrate in time over  $(0, T)$ , to obtain the equation system,

$$\begin{aligned}
 \int_0^T \langle \partial_t \phi_T^k, \zeta \rangle_{H^1} dt & = \int_0^T (\phi_T^k v^k, \nabla \Pi_{W_k} \zeta) - (m_T^k \nabla \mu^k, \nabla \Pi_{W_k} \zeta) \\
 & + (S_T^k, \Pi_{W_k} \zeta) dt,
 \end{aligned}
 \tag{4.13a}$$

$$\begin{aligned} \int_0^T \langle \partial_t \phi_\sigma^k, \varphi \rangle_{H_0^1} dt &= \int_0^T (\phi_\sigma^k v^k, \nabla \Pi_{Y_k} \varphi) - \delta_\sigma^{-1} (m_\sigma^k \nabla \phi_\sigma^k, \nabla \Pi_{Y_k} \varphi) \\ &\quad + \chi_0 (m_\sigma^k \nabla \phi_T^k, \nabla \Pi_{Y_k} \varphi) + (S_\sigma^k, \Pi_{Y_k} \varphi) dt, \end{aligned} \tag{4.13b}$$

$$\begin{aligned} \int_0^T \langle \partial_t v^k, \xi \rangle_V dt &= \int_0^T -\alpha (v^k, \Pi_{Z_k} \xi) - (\nu^k \mathbf{D} v^k, \mathbf{D} \Pi_{Z_k} \xi) \\ &\quad - F_1 (|v^k| v^k, \Pi_{Z_k} \xi) - F_2 (|v^k|^2 v^k, \Pi_{Z_k} \xi) \\ &\quad + (S_v^k, \Pi_{Z_k} \xi) dt. \end{aligned} \tag{4.13c}$$

Each equation in (4.13) can be estimated using the typical inequalities and the boundedness of the orthogonal projection. From (4.13a), we find

$$\begin{aligned} &\langle \partial_t \phi_T^k, \zeta \rangle_{L^2(H^1)' \times L^2 H^1} \\ &\leq \|\nabla \phi_T^k\|_{L^\infty L^2} \|v\|_{L^2 L^4} \|\Pi_{W_k} \zeta\|_{L^2 L^4} + m_\infty \|\nabla \mu^k\|_{L^2 L^2} \|\nabla \Pi_{W_k} \zeta\|_{L^2 L^2} \\ &\quad + \|S_T^k\|_{L^2 L^2} \|\Pi_{W_k} \zeta\|_{L^2 L^2} \\ &\leq C \|\zeta\|_{L^2 H^1}, \end{aligned} \tag{4.14}$$

and from (4.13b), we get

$$\begin{aligned} &\langle \partial_t \phi_\sigma^k, \varphi \rangle_{L^{4/d} H^{-1} \times L^{4/(4-d)} H_0^1} \\ &\leq \|\phi_\sigma^k\|_{L^2 L^4} \|v\|_{L^4 L^4} \|\nabla \Pi_{Y_k} \varphi\|_{L^4 L^2} + \|S_\sigma^k\|_{L^2 L^2} \|\Pi_{Y_k} \varphi\|_{L^2 L^2} \\ &\quad + m_\infty (\delta_\sigma^{-1} \|\nabla \phi_\sigma^k\|_{L^2 L^2} + \chi_0 \|\nabla \phi_T^k\|_{L^2 L^2}) \|\nabla \Pi_{Y_k} \varphi\|_{L^2 L^2} \\ &\leq C \|\varphi\|_{L^{4/(4-d)} H_0^1}, \end{aligned} \tag{4.15}$$

and (4.13c) results in

$$\begin{aligned} &\langle \partial_t v^k, \xi \rangle_{L^{4/3} V' \times L^4 V} \\ &\leq C (\alpha \|v^k\|_{L^2 L^2} + m_\infty \|\mathbf{D} v^k\|_{L^2 L^2} + F_1 \| |v^k| v^k \|_{L^2 L^2} + F_2 \| |v^k|^2 v^k \|_{L^{4/3} L^{4/3}} \\ &\quad + \|\mu^k\|_{L^2 L^4} \|\nabla \phi_T^k\|_{L^\infty L^2} + \chi_0 \|\phi_\sigma^k\|_{L^2 L^4} \|\nabla \phi_T^k\|_{L^\infty L^2}) \|\xi\|_{L^4 V} \\ &= C (\alpha \|v^k\|_{L^2 L^2} + m_\infty \|\mathbf{D} v^k\|_{L^2 L^2} + F_1 \|v^k\|_{L^4 L^4}^2 + F_2 \|v^k\|_{L^4 L^4}^3 \\ &\quad + \|\mu^k\|_{L^2 L^4} \|\nabla \phi_T^k\|_{L^\infty L^2} + \chi_0 \|\phi_\sigma^k\|_{L^2 L^4} \|\nabla \phi_T^k\|_{L^\infty L^2}) \|\xi\|_{L^4 V} \\ &\leq C \|\xi\|_{L^4 V}. \end{aligned} \tag{4.16}$$

We note that we could have estimated the convective term in the nutrient equation without using the fact that  $\{v^k\}_{k \in \mathbb{N}}$  is bounded in  $L^4(0, T; [L^4]^d)$ . This is particularly interesting for the case  $F_2 = 0$  where that regularity is missing; see Remark 4.2. As a substitute, we apply the Gagliardo–Nirenberg inequality<sup>69</sup>

$$|f|_{L^3} \leq C |\nabla f|_{L^2}^{1/2} |f|_{L^2}^{1/2} \quad \text{for all } f \in H_0^1,$$

on  $v^k$  and use the Sobolev embedding  $H^1 \hookrightarrow L^6$  for  $d \leq 3$  to get

$$\begin{aligned} \int_0^T (\phi_\sigma^k v^k, \nabla \Pi_{Y_k} \xi) dt &\leq \int_0^T |\nabla \phi_\sigma^k|_{L^2} |v^k|_{L^3} |\xi|_{L^6} dt \\ &\leq \|\phi_\sigma^k\|_{L^2 H^1}^2 \|v^k\|_{L^2 V}^{1/2} \|v^k\|_{L^\infty H}^{1/2} \|\xi\|_{L^4 H^1}. \end{aligned}$$

From the inequalities (4.14)–(4.16) and the bounds derived earlier, see (4.11), we conclude that

$$\begin{aligned} \{\phi_T^k\}_{k \in \mathbb{N}} &\text{ is bounded in } L^\infty(0, T; H^1) \cap H^1(0, T; (H^1)'), \\ \{\phi_\sigma^k\}_{k \in \mathbb{N}} &\text{ is bounded in } L^\infty(0, T; L^2) \cap (1 + L^2(0, T; H_0^1)) \cap W^{1, \frac{4}{d}}(0, T; H^{-1}), \\ \{v^k\}_{k \in \mathbb{N}} &\text{ is bounded in } L^\infty(0, T; H) \cap L^4(0, T; [L^4]^d) \cap L^2(0, T; V) \cap W^{1, \frac{4}{d}}(0, T; V). \end{aligned}$$

Making use of the Aubin–Lions compactness lemma (3.1), giving compact embeddings to achieve the strong convergences, we have

$$\begin{aligned} \phi_T^k &\rightarrow \phi_T \text{ strongly in } C([0, T]; L^2), \\ \phi_\sigma^k &\rightarrow \phi_\sigma \text{ strongly in } L^2(0, T; L^2) \cap C([0, T]; H^{-1}), \\ v^k &\rightarrow v \text{ strongly in } L^2(0, T; H) \cap C([0, T]; V'), \end{aligned} \tag{4.17}$$

as  $k \rightarrow \infty$ . The strong convergence  $\phi_T^k \rightarrow \phi_T$  in  $C([0, T]; L^2)$  implies  $\phi_T(0) = \phi_{T,0}$  in  $L^2$  and similarly  $\phi_\sigma(0) = \phi_{\sigma,0}$  in  $H^{-1}$  and  $v(0) = v_0$  in  $V'$ . Therefore, the limit functions  $(\phi_T, \mu, \phi_\sigma, v)$  of the Galerkin approximations already fulfill the initial data of the system (2.6).

In the case of  $d = 2$ , we can also conclude  $\phi_\sigma \in C([0, T]; L^2)$  and  $v \in C([0, T]; H)$  due to the continuous embedding (3.2). Here, we used  $[H^1, (H^1)']_{1/2} = L^2$  and  $[V, V']_{1/2} = H$ . In contrast, in the three-dimensional case, we deduce the respective weak continuities of  $\phi_\sigma$  and  $v$  due to the continuous embedding (3.3).

### 4.5. Limit process

It remains to be shown that the limit functions also fulfill the variational form (4.1), as defined in Definition 4.1. Multiplying the Galerkin system (4.3) by  $\eta \in C_c^\infty(0, T)$  and integrating from 0 to  $T$ , gives

$$\begin{aligned} \int_0^T \langle \partial_t \phi_T^k, w_j \rangle_{H^1} \eta(t) dt &= \int_0^T (-m_T^k \nabla \mu^k + \phi_T^k v^k, \nabla w_j) \eta(t) + (S_T^k, w_j)_{L^2} \eta(t) dt, \\ \int_0^T (\mu^k, w_j) \eta(t) dt &= \int_0^T (\Psi'(\phi_T^k) - \chi_0 \phi_\sigma^k, w_j)_{L^2} \eta(t) + \varepsilon_T^2 (\nabla \phi_T^k, \nabla w_j)_{L^2} \eta(t) dt, \\ \int_0^T \langle \partial_t \phi_\sigma^k, y_j \rangle_{H_0^1} \eta(t) dt &= \int_0^T (-m_\sigma^k (\delta_\sigma^{-1} \nabla \phi_\sigma^k - \chi_0 \nabla \phi_T^k) + \phi_\sigma^k v^k, \nabla y_j)_{L^2} \eta(t) \\ &\quad + (S_\sigma^k, y_j)_{L^2} \eta(t) dt, \end{aligned}$$

$$\int_0^T \langle \partial_t v^k, z_j \rangle_V \eta(t) dt = \int_0^T (\nu^k Dv^k, Dz_j) \eta(t) + (F_1 |v^k| v^k + F_2 |v_k|^2 v_k, z_j) \eta(t) + (\alpha v^k + S_v^k, z_j) \eta(t) dt,$$

for each  $j \in \{1, \dots, k\}$ . We take the limit  $k \rightarrow \infty$  in each equation. The linear terms can be treated directly in the limit process since they can be justified via the weak convergences (4.12), e.g. the functional

$$\mu^k \mapsto \int_0^T (\mu^k, w_j) \eta(t) dt \leq \|\mu^k\|_{L^2 L^2} |w_j|_{L^2} |\eta|_{L^2}$$

is linear and continuous on  $L^2(0, T; L^2)$  and, hence, as  $k \rightarrow \infty$

$$\int_0^T (\mu^k, w_j) \eta(t) dt \rightarrow \int_0^T (\mu, w_j) \eta(t) dt.$$

Thus, it remains to examine the nonlinear terms. We do so in the steps (i)–(vi) as follows.

(i) We have derived the convergences, see (4.17),

$$\begin{aligned} \phi_T^k &\rightarrow \phi_T && \text{in } L^2(0, T; L^2) \cong L^2((0, T) \times \Omega), \\ \phi_\sigma^k &\rightarrow \phi_\sigma && \text{in } L^2(0, T; L^2) \cong L^2((0, T) \times \Omega) \end{aligned}$$

as  $k \rightarrow \infty$  and, consequently, we have by the continuity and boundedness of  $m_T$ ,  $m_T^k = m_T(\phi_T^k(t, x), \phi_\sigma^k(t, x)) \rightarrow m_T(\phi_T(t, x), \phi_\sigma(t, x)) =: m_T$  a.e. in  $(0, T) \times \Omega$  as  $k \rightarrow \infty$ . Applying the Lebesgue dominated convergence theorem gives

$$m_T^k \nabla w_j \eta \rightarrow m_T \nabla w_j \eta \quad \text{in } L^2((0, T) \times \Omega; \mathbb{R}^d)$$

as  $k \rightarrow \infty$  and, together with  $\nabla \mu^k \rightharpoonup \nabla \mu$  weakly in  $L^2((0, T) \times \Omega; \mathbb{R}^d)$  as  $k \rightarrow \infty$ , we have

$$m_T(\phi_T^k) \eta \nabla w_j \cdot \nabla \mu^k \rightarrow m_T(\phi_T) \eta \nabla w_j \cdot \nabla \mu \quad \text{in } L^1((0, T) \times \Omega)$$

as  $k \rightarrow \infty$ . We use here the fact that the product of a strongly and a weakly converging sequence in  $L^2$  converges strongly in  $L^1$ . The same procedure can be used with terms which involve the functions  $m_\sigma^k$  and  $\nu^k$ .

(ii) By (4.17), we have  $\phi_T^k \rightarrow \phi_T$  in  $L^2((0, T) \times \Omega)$  and  $v^k \rightarrow v$  in  $L^2((0, T) \times \Omega; \mathbb{R}^d)$  as  $k \rightarrow \infty$ , hence, as  $k \rightarrow \infty$ ,

$$\phi_T^k v^k \cdot \nabla w_j \eta \rightarrow \phi_T v \cdot \nabla w_j \eta \quad \text{in } L^1((0, T) \times \Omega).$$

(iii) By the continuity and the growth assumptions on  $\Psi'$ , we have

$$\begin{aligned} \Psi'(\phi_T^k(t, x)) &\rightarrow \Psi'(\phi_T(t, x)) \quad \text{a.e. in } (0, T) \times \Omega \text{ as } k \rightarrow \infty, \\ |\Psi'(\phi_T^k) \eta w_j| &\leq C(1 + |\phi_T^k|) |\eta w_j|, \end{aligned}$$

and the Lebesgue dominated convergence theorem yields as  $k \rightarrow \infty$ ,

$$\Psi'(\phi_T^k) \eta w_j \rightarrow \Psi'(\phi_T) \eta w_j \quad \text{in } L^1((0, T) \times \Omega).$$

(iv) Using the triangle inequality, we conclude that

$$\begin{aligned} \left| |v^k|v^k - |v|v \right| &= \left| |v^k|v^k - |v^k|v + |v^k|v - |v|v \right| \\ &\leq |v^k| \cdot |v^k - v| + |v| \cdot \left| |v^k| - |v| \right| \\ &\leq |v^k - v|(|v^k| + |v|). \end{aligned}$$

and, thus, taking the limit  $k \rightarrow \infty$ , results in

$$|v^k|v^k \cdot z_j \eta \rightarrow |v|v \cdot z_j \eta \quad \text{in } L^1((0, T) \times \Omega).$$

(v) Similarly to (iv), we apply the triangle inequality to deduce that

$$\begin{aligned} \left| |v_k|^2 v_k - |v|^2 v \right| &= \left| |v_k|^2 v_k - |v_k|^2 v + |v_k|^2 v - |v|^2 v_k + |v|^2 v_k - |v|^2 v \right| \\ &\leq |v^k - v|(|v_k|^2 + |v|^2 + |v^k| \cdot |v|) \end{aligned}$$

and, again, taking the limit as  $k \rightarrow \infty$  gives

$$|v^k|^2 v^k \cdot z_j \eta \rightarrow |v|^2 v \cdot z_j \eta \quad \text{in } L^1((0, T) \times \Omega).$$

(vi) We have the strong convergence of  $\mu^k$  and  $\phi_\sigma^k$  in  $L^2((0, T) \times \Omega)$ . Together with the weak convergence of  $\nabla \phi_T^k$  in  $L^2((0, T) \times \Omega; \mathbb{R}^d)$  it is enough to conclude the convergence of the term involving  $S_v^k = (\mu + \chi_0 \phi_\sigma^k) \nabla \phi_T^k$ .

Using the density of  $\bigcup_{k \in \mathbb{N}} W_k$  in  $H^1$ ,  $\bigcup_{k \in \mathbb{N}} Y_k$  in  $H_0^1$ ,  $\bigcup_{k \in \mathbb{N}} Z_k$  in  $V$  and the fundamental lemma of the calculus of variations, we obtain a solution  $(\phi_T, \mu, \phi_\sigma, v)$  to our model (2.6) in the weak sense as defined in Definition 4.1.  $\square$

**Remark 4.1.** We can associate a pressure function to the velocity so that we have a quintuple  $(\phi_T, \mu, \phi_\sigma, v, p)$ , which solves (2.6) in distributional sense. See also Refs. 82 and 75 for a similar argument. Let

$$w = -\partial_t v + \operatorname{div}(\nu Dv) - \alpha v - F_1 |v|v - F_2 |v|^2 v + S_v.$$

Then  $w \in W^{-1, \infty}(0, T; H^{-1}) = \mathcal{L}(W_0^{1,1}(0, T); H^{-1})$  and  $\langle w(\psi), \xi \rangle_V = 0$  for all  $\psi \in W_0^{1,1}(0, T), \xi \in V$ . Thus, by the corollary of the de Rham lemma, see Corollary 3.1, there is a unique  $p \in W^{-1, \infty}(0, T; L_0^2)$  such that  $\nabla p = w$ .

**Remark 4.2.** If  $F_2 = 0$ , then we only have  $u \in L^3(0, T; [L^3]^d)$  instead of  $L^4(0, T; [L^4]^d)$ . We have to control

$$\int_0^T (|v|v, \zeta) dt \leq \int_0^t |v|^2 |\zeta| dt \leq |v^2|_{L^{3/2}L^{3/2}} |\zeta|_{L^3L^3} \leq C |v|_{L^3L^3}^2 |\zeta|_{L^3H^1}.$$

Hence, we are even able to bound  $\partial_t v$  in  $L^{3/2}(0, T; V')$  instead of only  $L^{4/3}(0, T; V')$ . That means the velocity itself has less regularity, but its derivative’s regularity is larger. Still, via the Aubin–Lions lemma, we are able to extract a subsequence of the Galerkin approximation  $\{v^k\}_{k \in \mathbb{N}}$ , which converges strongly to a function  $v$  in  $L^2(0, T; H)$ .



## 5. Nonlocal Effects

In this section, we consider nonlocal effects in a tumor growth model with a convective velocity, which obeys the unsteady Darcy–Forchheimer–Brinkman law. In biological models nonlocal terms are used to describe competition for space,<sup>80</sup> cell-to-cell adhesion and cell-to-matrix adhesion,<sup>12,38</sup> and the inclusion of such nonlocal effects in mesoscale models of tumor growth leads to systems of nonlinear integro-differential equations.

Models, that account for cell–matrix adhesion effects, involve matrix degrading enzymes, which erode the extracellular matrix and therefore, allow the migration of cells into tissue. Such systems have been analyzed in-depth in Refs. 78, 25 and 12. There, the tumor volume fraction is modeled by a reaction–diffusion equation, in contrast to the fourth order Cahn–Hilliard phase field equation in our setting.

Following Refs. 12 and 31, we consider cell–cell adhesion effects, which are responsible for the binding of one or more cells to each other through the reaction of proteins on the cell surfaces. It is reasonable to take cell-to-cell adhesion into account since the Ginzburg–Landau free energy functional (2.3) leads to separation and surface tension effects,<sup>31</sup> which implies that the tumor cells prefer to adhere to each other rather than to the healthy cells. Moreover, cell-to-cell adhesion is a key factor in tissue formation, stability, and the breakdown of tissue.

The well-known local Cahn–Hilliard equation has an phenomenological background<sup>11</sup> and in the search for a physical derivation Giacomini and Lebowitz studied the problem of phase separation from a microscopic background using the methods of statistical mechanics, see Refs. 39 and 40. They obtained a nonlocal version of the Cahn–Hilliard equation with the underlying free energy functional

$$\int_{\Omega} \Psi(\phi_T(x))dx + \frac{1}{4} \int_{\Omega} \int_{\Omega} J(x-y)(\phi_T(x) - \phi_T(y))^2 dydx, \quad (5.1)$$

which is also called the nonlocal Helmholtz free energy functional.<sup>13,33</sup> Here,  $J : \mathbb{R}^d \rightarrow \mathbb{R}$  is assumed to be a convolution kernel such that  $J(x) = J(-x)$ . One can obtain the classical Ginzburg–Landau free energy functional from (5.1) by choosing the kernel function  $J(x, y) = k^{d+2} \chi_{[0,1]}(|k(x-y)|^2)$  and letting  $k \rightarrow \infty$ , see Refs. 29 and 44, and therefore, the well-known Cahn–Hilliard model can be interpreted as an approximation of its nonlocal version.

We modify the nonlocal Helmholtz free energy functional (5.1) to account for chemotactic effects,

$$\begin{aligned} \mathcal{E}(\phi_T, \phi_{\sigma}) &= \int_{\Omega} \Psi(\phi_T(x))dx + \frac{1}{4} \int_{\Omega} \int_{\Omega} J(x-y)(\phi_T(x) - \phi_T(y))^2 dydx \\ &\quad - \chi_0 \int_{\Omega} \phi_{\sigma}(x)\phi_T(x)dx. \end{aligned}$$

The chemical potential is given by the first variation of the system’s underlying free energy functional  $\mathcal{E}$  and therefore, we consider a class of long-range interactions in

which nonlocal effects are characterized by chemical potentials of the form,

$$\mu = \frac{\delta \mathcal{E}}{\delta \phi_T} = \Psi'(\phi_T) + \int_{\Omega} J(x - y)(\phi_T(x) - \phi_T(y))dy - \chi_0 \phi_{\sigma},$$

and recalling the convolution operator, which we denote by  $*$ , we can rewrite the chemical potential as

$$\mu = \Psi'(\phi_T) + \phi_T \cdot J * 1 - J * \phi_T - \chi_0 \phi_{\sigma}.$$

This leads directly to a nonlocal model governed by the system,

$$\begin{aligned} \partial_t \phi_T + \operatorname{div}(\phi_T v) &= \operatorname{div}(m_T(\phi_T, \phi_{\sigma}) \nabla \mu) + S_T(\phi_T, \phi_{\sigma}), \\ \mu &= \Psi'(\phi_T) + \phi_T \cdot J * 1 - J * \phi_T - \chi_0 \phi_{\sigma}, \\ \partial_t \phi_{\sigma} + \operatorname{div}(\phi_{\sigma} v) &= \operatorname{div}(m_{\sigma}(\phi_T, \phi_{\sigma})(\delta_{\sigma}^{-1} \nabla \phi_{\sigma} - \chi_0 \nabla \phi_T)) + S_{\sigma}(\phi_T, \phi_{\sigma}), \\ \partial_t v + \alpha v &= \operatorname{div}(\nu(\phi_T, \phi_{\sigma}) Dv) - F_1 |v|v - F_2 |v|^2 v - \nabla p + S_v(\phi_T, \phi_{\sigma}), \\ \operatorname{div} v &= 0, \end{aligned} \tag{5.2}$$

with the initial-boundary data as before, see (2.7).

The nonlocal Cahn–Hilliard equation has been analyzed in Refs. 4, 3, 2, 32 and 33. In Refs. 15, 27, 28 and 29, it has been coupled to the Navier–Stokes equation, in Ref. 22 to the Darcy equation, in Ref. 23 to the Brinkman equation and in Ref. 31 to a reaction–diffusion equation. We briefly discuss modifications in the energy estimates of the nonlocal model (5.2) in contrast to the estimates derived in the proof of Theorem 4.1 for the local model. Due to the integro-differential structure, some inequalities have to be analyzed again, but overall the existence of a weak solution remains valid for the nonlocal problem. Notice that we cannot expect  $\phi_T \in L^{\infty}(0, T; H^1)$  since no Laplacian appears in the potential equation. Therefore, the term  $\chi_0 \operatorname{div}(m_{\sigma} \nabla \phi_T)$  has to be treated again in the estimates with an additional assumption on the chemotaxis constant  $\chi_0$ .

**Definition 5.1.** (Weak solution) We call a quadruple  $(\phi_T, \mu, \phi_{\sigma}, v)$  a weak solution of the system (5.2) if the functions  $\phi_T, \mu, \phi_{\sigma} : (0, T) \times \Omega \rightarrow \mathbb{R}, v : (0, T) \times \Omega \rightarrow \mathbb{R}^d$  have the regularity

$$\begin{aligned} \phi_T &\in W^{1, \frac{4}{d}}(0, T; (H^1)') \cap L^{\infty}(0, T; L^2) \cap L^2(0, T; H^1), \\ \mu &\in L^2(0, T; H^1), \\ \phi_{\sigma} &\in W^{1, \frac{4}{d}}(0, T; H^{-1}) \cap (1 + L^2(0, T; H_0^1)), \\ v &\in W^{1, \frac{4}{d}}(0, T; V') \cap L^4(0, T; [L^4]^d) \cap L^2(0, T; V), \end{aligned}$$

fulfill the initial data  $\phi_T(0) = \phi_{T,0}, \phi_{\sigma}(0) = \phi_{\sigma,0}, v(0) = v_0$  and satisfy the following variational form of (2.6)

$$\langle \partial_t \phi_T, \varphi_1 \rangle_{H^1} = (\phi_T v, \nabla \varphi_1) - (m_T \nabla \mu, \nabla \varphi_1) + (S_T, \varphi_1), \tag{5.3a}$$

$$(\mu, \varphi_2) = (\Psi'(\phi_T), \varphi_2) + (\phi_T \cdot J * 1, \varphi_2) - (J * \phi_T, \varphi_2) - \chi_0 (\phi_{\sigma}, \varphi_2), \tag{5.3b}$$

$$\begin{aligned} \langle \partial_t \phi_\sigma, \varphi_3 \rangle_{H_0^1} &= (\phi_\sigma v, \nabla \varphi_3) - \delta_\sigma^{-1} (m_\sigma \nabla \phi_\sigma, \nabla \varphi_3) + \chi_0 (m_\sigma \nabla \phi_T, \nabla \varphi_3) \\ &\quad + (S_\sigma, \varphi_3), \end{aligned} \tag{5.3c}$$

$$\begin{aligned} \langle \partial_t v, \varphi_4 \rangle_V &= -\alpha(v, \varphi_4) - (\nu Dv, D\varphi_4) - F_1(|v|v, \varphi_4) - F_2(|v|^2 v, \varphi_4) \\ &\quad + (S_v, \varphi_4), \end{aligned} \tag{5.3d}$$

for all  $\varphi_1, \varphi_2 \in H^1, \varphi_3 \in H_0^1, \varphi_4 \in V$ .

**Theorem 5.1.** (Existence of a global weak solution) *Let (A1)–(A4) hold and additionally:*

(A6)  $\Psi \in C^2(\mathbb{R})$  is such that  $|\Psi(x)| \geq C_1|x|^2 - C_2$ ,  $\Psi''(x) \geq C_3 - (J * 1)(x)$ , and  $|\Psi'(x)| \leq C_4(|x| + 1)$  for  $C_2, C_4 > 0$ ,  $C_1 > \frac{1}{2}|J|_{L^1} - \frac{1}{2}(J * 1)(x)$  for a.e.  $x \in \Omega$  and

$$C_3 > \sqrt{\frac{2\chi_0 m_\infty}{m_0}} \cdot \frac{4\chi_0^2 m_\infty^2 \delta_\sigma + 2m_0 \chi_0 m_\infty \delta_\sigma + \chi_0^2 \delta_\sigma m_0^2}{2m_0^2}.$$

(A7)  $J \in W^{1,1}(\mathbb{R}^d)$  is even and  $(J * 1)(x) \geq 0$  for a.e.  $x \in \Omega$ .

Then there exists a solution quadruple  $(\phi_T, \mu, \phi_\sigma, v)$  to (5.2) in the sense of Definition 5.1. Moreover, the solution quadruple has the regularity

$$\begin{aligned} \phi_T &\in \begin{cases} C([0, T]; L^2), & d = 2, \\ C([0, T]; (H^1)') \cap C_w([0, T]; L^2), & d = 3, \end{cases} \\ \phi_\sigma &\in \begin{cases} C([0, T]; L^2), & d = 2, \\ C([0, T]; H^{-1}) \cap C_w([0, T]; L^2), & d = 3, \end{cases} \\ v &\in \begin{cases} C([0, T]; H), & d = 2, \\ C([0, T]; V') \cap C_w([0, T]; H), & d = 3. \end{cases} \end{aligned}$$

Additionally, there is a unique  $p \in W^{-1,\infty}(0, T; L_0^2)$  such that  $(\phi_T, \mu, \phi_\sigma, v, p)$  is a solution quintuple to (5.2) in the distributional sense.

**Proof.** Since the approach is similar to the proof of Theorem 4.1, we will directly derive an energy estimate in the continuous setting. We take, as the test function in (5.3b),  $\varphi_2 = -\partial_t \phi_T$ , which gives

$$\begin{aligned} -(\mu, \partial_t \phi_T) &= -\frac{dt}{dt} \left( |\Psi(\phi_T)|_{L^1} + \frac{1}{2} |(J * 1)^{1/2} \phi_T|_{L^2}^2 - \frac{1}{2} (\phi_T, J * \phi_T) \right) \\ &\quad + \chi_0 (\phi_\sigma, \partial_t \phi_T) \\ &= -\frac{d}{dt} \left( |\Psi(\phi_T)|_{L^1} + \frac{1}{4} \int_\Omega \int_\Omega J(x - y) (\phi_T(x) - \phi_T(y))^2 dx dy \right) \\ &\quad + \chi_0 (\phi_\sigma, \partial_t \phi_T), \end{aligned}$$

where we used the fact that

$$\begin{aligned} & \frac{d}{dt} \int_{\Omega} \int_{\Omega} J(x-y)(\phi_T(x) - \phi_T(y))^2 dy dx \\ &= 2 \int_{\Omega} \int_{\Omega} J(x-y)[\phi_T(x) - \phi_T(y)] \cdot [\partial_t \phi_T(x) - \partial_t \phi_T(y)] dy dx \\ &= 4 \int_{\Omega} \int_{\Omega} J(x-y)[\phi_T(x) - \phi_T(y)] \partial_t \phi_T(x) dy dx, \end{aligned}$$

since  $J$  is assumed to be even, see (A7) in Theorem 5.1. As in the local model, we use the test functions  $\varphi_1 = \mu + \chi_0 \phi_{\sigma}$ ,  $\varphi_3 = K(\phi_{\sigma} - 1)$  and  $\varphi_4 = v$  in (5.3), which gives, after adding the equations,

$$\begin{aligned} & \frac{d}{dt} \left[ |\Psi(\phi_T)|_{L^1} + \frac{1}{4} \int_{\Omega} \int_{\Omega} J(x-y)(\phi_T(x) - \phi_T(y))^2 dx dy + \frac{K}{2} |\phi_{\sigma} - 1|_{L^2}^2 + \frac{1}{2} |v|_{L^2}^2 \right] \\ &+ (m_T, |\nabla \mu|^2) + K \delta_{\sigma}^{-1} (m_{\sigma}, |\nabla \phi_{\sigma}|^2) + (\nu, |Dv|^2) + F_1 |v|_{L^3}^3 + F_2 |v|_{L^4}^4 + \alpha |v|_{L^2}^2 \\ &= -\chi_0 (m_T \nabla \mu, \nabla \phi_{\sigma}) + (S_T, \mu + \chi_0 \phi_{\sigma}) + \chi_0 K (m_{\sigma} \nabla \phi_T, \nabla \phi_{\sigma}) + K (S_{\sigma}, \phi_{\sigma}), \end{aligned} \tag{5.4}$$

where we again used that the tested convective terms cancel with  $S_v$ . We estimate the terms involving the source functions  $S_T, S_{\sigma}$  as before in the local case, see (4.6) and (4.8). Also, as before in the local model, we additionally test with  $\varphi_2 = 1$  in (5.3b) to deduce the following estimate on  $\mu$ :

$$|\mu|_{L^1} \leq |\Psi'(\phi_T)|_{L^1} + \chi_0 |\phi_{\sigma}|_{L^1} \leq C(1 + |\phi_T|_{L^2} + |\phi_{\sigma}|_{L^2}).$$

Here, we used the fact that  $(\phi_T, J * 1) = (J * \phi_T, 1)$ , since  $J$  is assumed to be even, see (A7) in Theorem 5.1. Therefore, we can estimate the right-hand side in (5.4) as

$$\begin{aligned} \text{(RHS)} &\leq \frac{m_0}{2} |\nabla \mu|_{L^2}^2 + \frac{\chi_0^2 m_{\infty}^2}{m_0} |\nabla \phi_{\sigma}|_{L^2}^2 + C(1 + |\phi_{\sigma}|_{L^2}^2 + |\phi_T|_{L^2}^2) \\ &+ \frac{\chi_0 K^2 m_{\infty}}{2} |\nabla \phi_T|_{L^2}^2 + \frac{\chi_0 m_{\infty}}{2} |\nabla \phi_{\sigma}|_{L^2}^2. \end{aligned}$$

Notice that at this point we have no information on  $\phi_T$  on the left-hand side of (5.4), which is crucially needed to absorb the terms from the right-hand side. We can do the following calculation due to the growth estimate on  $\Psi$ , see (A6),

$$\begin{aligned} & |\Psi(\phi_T)|_{L^1} + \frac{1}{4} \int_{\Omega} \int_{\Omega} J(x-y)(\phi_T(x) - \phi_T(y))^2 dx dy \\ &= |\Psi(\phi_T)|_{L^1} + \frac{1}{2} |(J * 1)^{1/2} \phi_T|_{L^2}^2 - \frac{1}{2} (\phi_T, J * \phi_T) \\ &\geq \int_{\Omega} \left[ C_1 + \frac{1}{2} (J * 1)(x) - \frac{1}{2} |J|_{L^1} \right] |\phi_T(x)|^2 dx - C_2 |\Omega| \\ &\geq C(|\phi_T|_{L^2}^2 - 1), \end{aligned} \tag{5.5}$$

where we used the Young convolution inequality<sup>52</sup> to get

$$(\phi_T, J * \phi_T) \leq |\phi_T|_{L^2} |J * \phi_T|_{L^2} \leq |\phi_T|_{L^2}^2 |J|_{L^1}.$$

This estimate will give us  $\phi_T \in L^\infty(0, T; L^2)$ . Indeed, integrating (5.4) with respect to time on the interval  $(0, s)$ ,  $0 < s < T$ , and introducing the result into (5.5) and employing the estimates of the source terms give

$$\begin{aligned} & C|\phi_T(s)|_{L^2}^2 + \frac{K}{2}|\phi_\sigma(s)|_{L^2}^2 + \frac{1}{2}|v(s)|_{L^2}^2 + \frac{m_0}{2}\|\nabla\mu\|_{L^2L^2}^2 + m_0\|Dv\|_{L^2L^2}^2 \\ & + F_2\|v\|_{L^4L^4}^4 + \left(\frac{Km_0}{\delta_\sigma} - \frac{\chi_0^2m_\infty^2}{m_0} - \frac{\chi_0m_\infty}{2}\right) \\ & \times \|\nabla\phi_\sigma\|_{L^2L^2}^2 - \frac{\chi_0K^2m_\infty}{2}\|\nabla\phi_T\|_{L^2L^2}^2 \\ & \leq C(1 + \text{IC} + \|\phi_T\|_{L^2L^2}^2 + \|\phi_\sigma\|_{L^2L^2}^2), \end{aligned} \tag{5.6}$$

where

$$\begin{aligned} \text{IC} &= |\Psi(\phi_{T,0})|_{L^1} + \frac{1}{4} \int_\Omega \int_\Omega J(x-y)(\phi_{T,0}(x) - \phi_{T,0}(y))^2 dx dy \\ &+ \frac{K}{2}|\phi_{\sigma,0} - 1|_{L^2}^2 + \frac{1}{2}|v_0|_{L^2}^2, \end{aligned}$$

and, due to assumption (A6), we have  $|\Psi(\phi_{T,0})|_{L^1} \leq C(|\phi_{T,0}|_{L^2}^2 + 1)$ . Note that we have a negative term on the left-hand side in the inequality (5.6), which we still have to overpower so that we can apply the Gronwall lemma. We have, on one hand,

$$(\nabla\mu, \nabla\phi_T) \leq \frac{1}{C_3}|\nabla\mu|_{L^2}^2 + \frac{C_3}{4}|\nabla\phi_T|_{L^2}^2,$$

and, on the other hand, using the growth estimate on  $\Psi''$ , see (A6), and again the Young convolution inequality, we deduce that

$$\begin{aligned} (\nabla\mu, \nabla\phi_T) &= (\Psi''(\phi_T), |\nabla\phi_T|^2) + (|\nabla\phi_T|^2, J * 1) + (\nabla(J * 1), \phi_T \nabla\phi_T) \\ &\quad - (\nabla J * \phi_T, \nabla\phi_T) - \chi_0(\nabla\phi_\sigma, \nabla\phi_T) \\ &\geq C_3|\nabla\phi_T|_{L^2}^2 - |\nabla J|_{L^1}|\phi_T|_{L^2}|\nabla\phi_T|_{L^2} - \chi_0|\nabla\phi_\sigma|_{L^2}|\nabla\phi_T|_{L^2} \\ &\geq \frac{C_3}{2}|\nabla\phi_T|_{L^2}^2 - C|\phi_T|_{L^2}^2 - \frac{\chi_0^2}{C_3}|\nabla\phi_\sigma|_{L^2}^2. \end{aligned}$$

Combining these two inequalities gives the following estimate on  $\nabla\phi_T$ :

$$\frac{m_0C_3^2}{16}|\nabla\phi_T|_{L^2}^2 \leq \frac{m_0}{4}|\nabla\mu|_{L^2}^2 + C|\phi_T|_{L^2}^2 + \frac{m_0\chi_0^2}{4}|\nabla\phi_\sigma|_{L^2}^2.$$

Adding this inequality to (5.6) results in

$$C|\phi_T(s)|_{L^2}^2 + \frac{K}{2}|\phi_\sigma(s)|_{L^2}^2 + \frac{1}{2}|v(s)|_{L^2}^2 + \frac{m_0}{2}\|\nabla\mu\|_{L^2L^2}^2 + m_0\|Dv\|_{L^2L^2}^2$$

$$\begin{aligned}
 &+ F_2 \|v\|_{L^4 L^4}^4 + \left( \frac{K m_0}{\delta_\sigma} - \frac{\chi_0^2 m_\infty^2}{m_0} - \frac{\chi_0 m_\infty}{2} - \frac{m_0 \chi_0^2}{4} \right) \|\nabla \phi_\sigma\|_{L^2 L^2}^2 \\
 &+ \left( \frac{m_0 C_3^2}{16} - \frac{\chi_0 K^2 m_\infty}{2} \right) \|\nabla \phi_T\|_{L^2 L^2}^2 \\
 &\leq C(1 + \text{IC} + \|\phi_T\|_{L^2 L^2}^2 + \|\phi_\sigma\|_{L^2 L^2}^2). \tag{5.7}
 \end{aligned}$$

We choose  $K$  large enough such that the prefactor of  $\|\nabla \phi_\sigma\|_{L^2 L^2}^2$  is strictly positive. As a consequence, the prefactor of  $\|\nabla \phi_T\|_{L^2 L^2}^2$  is also strictly positive due to the assumption on  $C_3$ , see (A6). Hence, by applying the Gronwall lemma, see Lemma 3.1, we can deduce the final energy estimate

$$\begin{aligned}
 &\|\phi_T\|_{L^\infty L^2}^2 + \|\phi_\sigma\|_{L^\infty L^2}^2 + \|v\|_{L^\infty L^2}^2 \\
 &\quad + \|\nabla \mu\|_{L^2 L^2}^2 + \|Dv\|_{L^2 L^2}^2 + \|v\|_{L^4 L^4}^4 + \|\nabla \phi_\sigma\|_{L^2 L^2}^2 + \|\nabla \phi_T\|_{L^2 L^2}^2 \\
 &\leq C(1 + \text{IC})e^{CT}.
 \end{aligned}$$

In the same way as before, we can bound the time derivatives of  $\phi_T, \phi_\sigma, v$  and conclude existence of strongly converging sequences in the discrete case. The only difference to the local model in the limit process is the integral term, but it can be treated immediately since the functional

$$\phi_T \mapsto \int_0^T (\phi_T \cdot J * 1 - J * \phi_T, w_j) \eta(t) dt \leq 2|\eta|_\infty |w_j|_{L^2} \|\phi_T\|_{L^2 L^2} |J|_{L^1}$$

is linear and continuous on  $L^2(0, T; L^2)$ . □

The first steps in deriving the energy estimate were the same as in the local case. The lack of regularity on  $\phi_T$ , which is caused by the new chemical potential, required us to derive additional estimates as a replacement. We achieved the regularity  $\phi_T \in L^\infty(0, T; L^2) \cap L^2(0, T; H^1)$  instead of  $L^\infty(0, T; H^1)$  as in the local case. Nonetheless, this regularity is enough to prove the existence of weak solutions.

The new assumptions in Theorem 5.1 were crucial for the proof to be completed. We assumed a lower bound assumption on  $\Psi''$ , directly involving the new constant  $C_3$ , which has to be sufficiently large. In the case of a sufficiently small chemotaxis constant  $\chi_0$ , the assumption on  $C_3$  is fulfilled. Moreover, we introduce assumptions on properties for the new function  $J$  in the chemical potential, which are fulfilled by a typical kernel function.

### 6. Sensitivity Analysis

The relative effects of model parameters in determining key quantities of interest (QoIs), such as the evolution of tumor mass over time, are very important in the development of predictive models of tumor growth. Accordingly, in this section we address the question of sensitivity of solutions of our system (2.6) to variations in model parameters, and we provide a sensitivity analyses using both statistical

methods<sup>62,71–73</sup> and data-dependent methods based on the notion of active subspaces.<sup>16,18</sup> We first introduce each method and then compare the sensitivities of the parameters

$$\theta = (\varepsilon_T, \chi_0, \delta_\sigma, \lambda_T, \lambda_\sigma, \lambda_A, M_T, M_\sigma, \bar{E}, \alpha, \nu, F_1, F_2)^\top \in \mathbb{R}^{13}$$

in our model for each method.

As the quantity of interest in the sensitivity analysis of both methods, we choose the volume of the tumor mass at different times  $t \in \mathcal{I}$ , i.e.

$$Q(\theta) = \left[ \frac{1}{|\Omega|} \int_{\Omega} \phi_T(t, x) dx \right]_{t \in \mathcal{I}} \in \mathbb{R}^{\dim(\mathcal{I})},$$

which depends on the choice of the parameter setting  $p$ . Further, we choose the following uniformly distributed priors,

$$\begin{aligned} \varepsilon_T &\sim \mathcal{U}(0.01, 0.10), & \lambda_T &\sim \mathcal{U}(0.01, 1.00), & M_T &\sim \mathcal{U}(0.10, 1.00), \\ \chi_0 &\sim \mathcal{U}(0.10, 1.00), & \lambda_\sigma &\sim \mathcal{U}(0.01, 1.00), & M_\sigma &\sim \mathcal{U}(0.10, 1.00), \\ \delta_\sigma &\sim \mathcal{U}(0.01, 0.10), & \lambda_A &\sim \mathcal{U}(0.00, 0.05), & \bar{E} &\sim \mathcal{U}(0.25, 1.00), \\ \alpha &\sim \mathcal{U}(0.10, 10.0), & \nu &\sim \mathcal{U}(0.10, 10.0), & F_1, F_2 &\sim \mathcal{U}(0.10, 10.0). \end{aligned} \tag{6.1}$$

### 6.1. Variance-based method

The statistical method of sensitivity analysis employed in this work is a variance-based method, developed by Ref. 76, and described in detail by Ref. 73. The variance-based method takes into account uncertainties from the input factors, showing how the variance of the output is dependent on these uncertainties. The main drawback of this method is the high computational cost, which is  $N(k + 2)$ , where  $N$  is the number of samples and  $k$  is the number of parameters (here  $k = 13$ ).

The algorithm implementing the variance-based method consists of initially generating two matrices,  $A$  and  $B$ , with size  $N \times k$ , given as:

$$A = \begin{pmatrix} \theta_1^{(A1)} & \theta_2^{(A1)} & \dots & \theta_i^{(A1)} & \dots & \theta_k^{(A1)} \\ \theta_1^{(A2)} & \theta_2^{(A2)} & \dots & \theta_i^{(A2)} & \dots & \theta_k^{(A2)} \\ \vdots & \vdots & \ddots & \vdots & \ddots & \vdots \\ \theta_1^{(AN)} & \theta_2^{(AN)} & \dots & \theta_i^{(AN)} & \dots & \theta_k^{(AN)} \end{pmatrix},$$

$$B = \begin{pmatrix} \theta_1^{(A1)} & \theta_2^{(B1)} & \dots & \theta_i^{(B1)} & \dots & \theta_k^{(B1)} \\ \theta_1^{(B2)} & \theta_2^{(B2)} & \dots & \theta_i^{(B2)} & \dots & \theta_k^{(B2)} \\ \vdots & \vdots & \ddots & \vdots & \ddots & \vdots \\ \theta_1^{(BN)} & \theta_2^{(BN)} & \dots & \theta_i^{(BN)} & \dots & \theta_k^{(BN)} \end{pmatrix}.$$

Each row represents one set of values from the vector of parameters sampled from the priors given in (6.1). The following step is to generate  $k$  matrices  $C_i$ ,

where column  $i$  comes from matrix  $B$  and all other  $k$  columns come from matrix  $A$ , such as:

$$C_i = \begin{pmatrix} \theta_1^{(A1)} & \theta_2^{(A1)} & \dots & \theta_i^{(B1)} & \dots & \theta_k^{(A1)} \\ \theta_1^{(A2)} & \theta_2^{(A2)} & \dots & \theta_i^{(B2)} & \dots & \theta_k^{(A2)} \\ \vdots & \vdots & \ddots & \vdots & \ddots & \vdots \\ \theta_1^{(AN)} & \theta_2^{(AN)} & \dots & \theta_i^{(BN)} & \dots & \theta_k^{(AN)} \end{pmatrix}.$$

The output for all the sample matrices, that means  $A$ ,  $B$  and  $C_i$ , are computed, and stored as the vectors  $Y_A$ ,  $Y_B$  and  $Y_{C_i}$ . Each line of the vectors  $Y_J$ ,  $J \in \{A, B, C_i\}$ , of size  $N$  represents the QoI computed for each row of the matrix  $J$ . The last step from the variance-based method is to compute the first-order sensitivity indices,  $S_i$ , and the total effect indices,  $S_{T_i}$ . The first-order sensitivity indices are computed as

$$S_i = \frac{Y_A \cdot Y_C - f_0^2}{Y_A \cdot Y_B - f_0^2},$$

where

$$f_0^2 = \left( \frac{1}{N} \sum_{n=1}^N Y_A^{(n)} \right)^2.$$

These indices are always between 0 and 1. High values of  $S_i$  indicate a sensitive parameter, and low  $S_i$ , for additive models, indicates a low-sensitive parameter. For non-additive models, the total effect indices take the first-order effects and the contribution of higher-order effects into account due to interactions between the model parameters. These indices are given as:

$$S_{T_i} = 1 - \frac{Y_B \cdot Y_{C_i} - f_0^2}{Y_A \cdot Y_A - f_0^2}.$$

According to Ref. 73, for  $\theta_i$  to be a non-influential parameter, it is necessary and sufficient that  $S_{T_i} = 0$ . If the total effect index from the  $i$ th parameter is close to zero, then the parameter can be fixed to any value within the uncertainty range without affecting the variance of the QoI.<sup>73</sup>

### 6.2. Active subspace method

The active subspace method is used for dimensional reduction of subspaces of probability distributions of model parameters and identifies the directions of the sensitive parameters.<sup>16,18</sup> Let  $\rho$  be the probability density function corresponding to the distribution of the parameters  $\theta$  as chosen in (6.1) and let  $f$  be the data misfit function, which is given by

$$f : \mathbb{R}^{13} \rightarrow \mathbb{R}, \quad p \mapsto \frac{1}{2} \|\Gamma^{-1/2}(d - Q(p))\|_2^2,$$



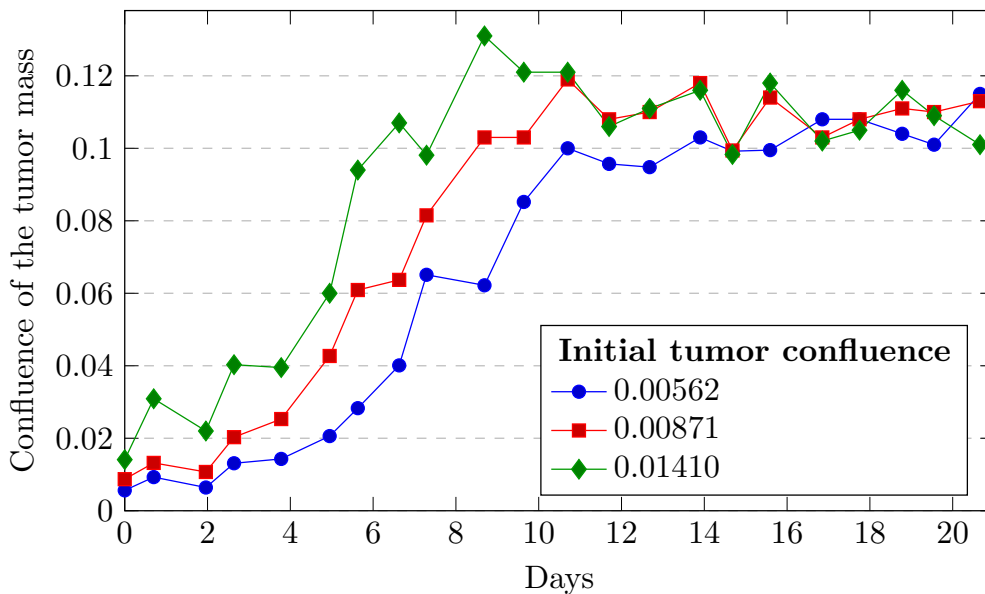


Fig. 1. Data of the evolution of the tumor confluence over the duration of 21 days for three different initial tumor confluences.

where  $d = Q(\theta) + \eta$  is some data for a zero-centered Gaussian noise  $\eta \sim \mathcal{N}(0, \Gamma)$  with covariance  $\Gamma$ . Our data<sup>54</sup> consists of *in vitro* data observed during the evolution of tumor cells with different initial tumor confluences without any treatment in a well with radius 0.32 cm over the course of 21 days, see Fig. 1.

We selected initial tumor cells corresponding to confluences of 0.00562, 0.00871 and 0.01410. For example, an initial confluence of 0.00562 corresponds to an initial tumor volume of  $A_{\text{init}} = 0.00562 \cdot \pi \cdot 0.32^2 \text{ cm}^2 \approx 0.00181 \text{ cm}^2$  with radius  $r_{\text{init}} = \sqrt{0.00562 \cdot 0.32^2} \text{ cm} \approx 0.0240 \text{ cm}$ .

The covariance matrix  $V$  of  $f$  is given by the integral of the outer product of the gradient of  $f$  weighted with  $\rho$ ,

$$V = \int_{\mathbb{R}^{13}} \nabla f(x)(\nabla f(x))^\top \rho(x) dx.$$

In our algorithm we approximate the covariance matrix  $V$  by

$$V \approx \frac{1}{N} \sum_{j=1}^N \nabla f(X_j)(\nabla f(X_j))^\top, \quad X_j \sim \rho,$$

whose eigenvalues are close to the true eigenvalues of  $V$  for a sufficiently large  $N$ , see Refs. 18 and 16.

We consider an orthogonal eigen decomposition of  $V$ ; that means for the eigenvalue matrix  $\Lambda = \text{diag}(\lambda_1, \dots, \lambda_{13})$  with descending eigenvalues and the corresponding eigenvector matrix  $W = [w_1 \cdots w_{13}]$  we have

$$V = W\Lambda W^\top.$$

Since  $V$  is a symmetric and positive semi-definite matrix, its eigenvectors can be chosen to form an orthonormal basis in  $\mathbb{R}^n$  and its eigenvalues are non-negative. In particular, the  $i$ th eigenvalue is given by

$$\lambda_i = w_i^\top V w_i = \int_{\mathbb{R}^{13}} (w_i^\top \nabla f(x))^2 \rho(x) dx,$$

from which we can see that it reflects the sensitivity of  $f$  in the direction of the  $i$ th eigenvector. In other words, on average  $f$  changes a little in the direction of an eigenvector with a small corresponding eigenvalue, and  $f$  may change significantly in the direction of an eigenvector with a large corresponding eigenvalue. But this is not enough to identify the sensitivity of each parameter. Following Ref. 17, we define the activity score  $\alpha_i$  for the  $i$ th parameter  $p_i$  as

$$\alpha_i = \sum_{j=1}^{13} \lambda_j w_{i,j}^2, \quad i = 1, \dots, 13,$$

and use the resulting number to rank the importance of each parameter. As discussed in Ref. 17 this metric has fared well in comparison to other standard sensitivity metrics such as the Sobol’ sensitivity index<sup>76</sup> when adequate data is available.

### 6.3. Comparison of the sensitivity methods

In Fig. 2, we list the relative sensitivity of each parameter for each method. We see that the proliferation rate  $\lambda_T$  is highly sensitive for both methods. For the active subspace method the effects of other parameters besides  $\lambda_T$  and  $\lambda_A$  are nearly zero for this choice of QoI. Therefore, to notice the difference, we also listed the comparison of the sensitives in Fig. 3 with a logarithmic scale.

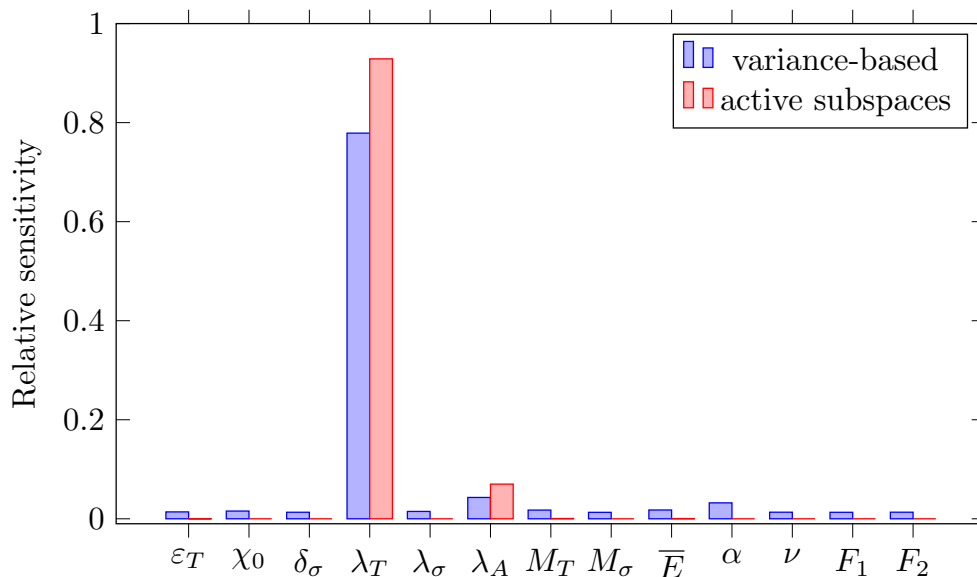


Fig. 2. Comparison of the relative sensitivities for the variance-based and the active subspaces method; linear scale.

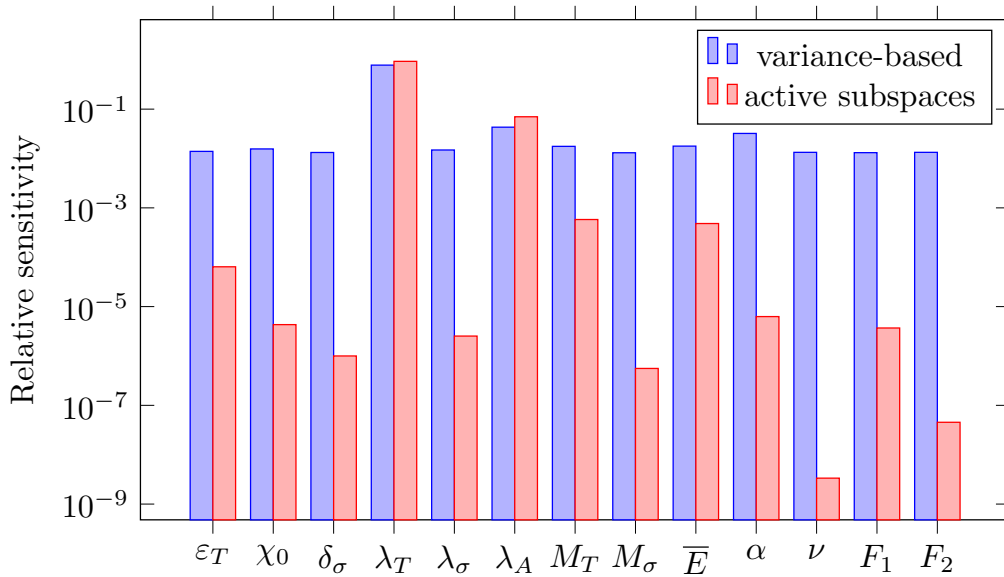


Fig. 3. Comparison of the relative sensitivities for the variance-based and the active subspaces method; logarithmic scale.

We remark that the dominance of the proliferation rate  $\lambda_T$  in the results shown is largely due to the choice of the QoI; other choices favor different parameters of the model. For example, numerical simulations described in the next section suggest that the velocity parameters play an important role in determining the evolution of tumor shape and, for example, surface area.

### 7. Numerical Discretization and Examples

We choose a similar computational framework as in Refs. 55 and 53 to solve the deterministic system (2.6) with the initial and boundary data (2.7). This framework includes a discrete-time local semi-implicit scheme with an energy convex–nonconvex splitting. Here, the stable contractive part is treated implicitly and the expansive part explicitly. In particular, introducing the Ginzburg–Landau energy<sup>45</sup>

$$E = \int_{\Omega} \Psi(\phi_T) + \frac{\varepsilon_T^2}{2} |\nabla \phi_T|^2 + \frac{1}{2\delta_\sigma} \phi_\sigma^2 - \chi_0 \phi_T \phi_\sigma \, dx$$

we can rewrite the chemical potential in the following way,

$$\mu = \frac{\delta E}{\delta \phi_T},$$

where  $\frac{\delta E}{\delta \phi_T}$  is the first variation of  $E$  with respect to  $\phi_T$ . We split the energy in its contractive and expansive parts via  $E = E_c - E_e$ .

Let the time domain be divided into the steps  $\Delta t_n = t_{n+1} - t_n$  for  $n \in \{0, 1, \dots\}$ . We assume  $\Delta t_n = \Delta t$  for all  $n$ . We write  $\phi_{T_n}$  for the approximation of  $\phi_T^h(t_n)$  and likewise for the other variables. The backward Euler method applied to the system

(2.6) reads

$$\begin{aligned}
 \frac{\phi_{T_{n+1}} - \phi_{T_n}}{\Delta t} + \operatorname{div}(\phi_{T_{n+1}} v_{n+1}) &= \operatorname{div}(m_T(\phi_{T_{n+1}}, \phi_{\sigma_{n+1}}) \nabla \mu_{n+1}) - \lambda_A \phi_{T_{n+1}} \\
 &\quad + \lambda_T \phi_{\sigma_{n+1}} \mathcal{C}(\phi_{T_{n+1}}(1 - \phi_{T_{n+1}})), \\
 \mu_{n+1} &= D_{\phi_T} E_c(\phi_{T_{n+1}}, \phi_{\sigma_{n+1}}) - D_{\phi_T} E_e(\phi_{T_n}, \phi_{\sigma_n}), \\
 \frac{\phi_{\sigma_{n+1}} - \phi_{\sigma_n}}{\Delta t} + \operatorname{div}(\phi_{\sigma_{n+1}} v_{n+1}) &= \operatorname{div}(m_\sigma(\phi_{T_{n+1}}, \phi_{\sigma_{n+1}})(\delta_\sigma^{-1} \nabla \phi_{\sigma_{n+1}} - \chi_0 \nabla \phi_{T_{n+1}})) \\
 &\quad - \lambda_\sigma \phi_{\sigma_{n+1}} \mathcal{C}(\phi_{T_{n+1}}), \\
 \frac{v_{n+1} - v_n}{\Delta t} + \alpha v_{n+1} + \nabla p_{n+1} &= \operatorname{div}(\nu(\phi_{T_{n+1}}, \phi_{\sigma_{n+1}}) \nabla v_{n+1}) - F_1 |v_{n+1}| v_{n+1} \\
 &\quad - F_2 |v_{n+1}|^2 v_{n+1} + (\mu_{n+1} + \chi_0 \phi_{\sigma_{n+1}}) \phi_{T_{n+1}}, \\
 \operatorname{div} v_{n+1} &= 0, \tag{7.1}
 \end{aligned}$$

where  $\mathcal{C}(\phi_{T_{n+1}}) = \max(0, \min(1, \phi_{T_{n+1}}))$  is the cut-off operator.

We uncouple the equations and use an iterative Gauß–Seidel method for solving each equation. In Algorithm 1 below, the subscript 0 stands for the initial solution,  $k$  the iteration index,  $n_{\text{iter}}$  the maximum number of iterations at each time step and TOL the tolerance for the iteration process. In each iterative loop three linear systems are solved and the convergence of the nonlinear solution is achieved at each time if  $\max |\phi_{T_{n+1}}^{k+1} - \phi_{T_{n+1}}^k| < \text{TOL}$ . We obtain the algebraic systems using a Galerkin finite element approach. In this regard, let  $\mathcal{T}^h$  be a quasiuniform family of triangulations of  $\Omega$  and let the piecewise linear finite element space be given by

$$\mathcal{V}^h = \{v \in H^1(\bar{\Omega}) : v|_T \in P_1(T) \text{ for all } T \in \mathcal{T}^h\} \subset H^1(\Omega),$$

where  $P_1(T)$  denotes the set of all affine linear function on  $T$ . Moreover, we introduce the piecewise linear finite element space with homogeneous Dirichlet boundary

$$\mathcal{V}_0^h = \{v \in \mathcal{V}^h : v = 0 \text{ on } \partial\Omega\},$$

and for the divergence-free space  $V$  we consider the Brezzi–Douglas–Marini (BDM) space of order 1, see Ref. 6. In Ref. 64 it was shown that the mixed finite element space  $\text{BDM}_1\text{-DG}_0$  is stable for the mixed formulation of the Darcy–Forchheimer equation.

We formulate the discrete problem as follows: for each  $k$ , find

$$\phi_{T_{n+1}}^{k+1} \in \mathcal{V}^h, \quad \mu_{n+1}^{k+1} \in \mathcal{V}^h, \quad \phi_{\sigma_{n+1}}^{k+1} \in 1 + \mathcal{V}_0^h, \quad v_{n+1}^{k+1} \in \text{BDM}_1, \quad p_{n+1}^{k+1} \in \text{DG}_0,$$

for all

$$\varphi_T \in \mathcal{V}^h, \quad \varphi_\mu \in \mathcal{V}^h, \quad \varphi_\sigma \in \mathcal{V}_0^h, \quad \varphi_v \in \text{BDM}_1, \quad \varphi_p \in \text{DG}_0,$$

such that:

$$(v_{n+1}^{k+1} - v_n, \varphi_v) + \Delta t \alpha (v_{n+1}^{k+1}, \varphi_v) + \Delta t (\nu(\phi_{T_{n+1}}^k, \phi_{\sigma_{n+1}}^k) \nabla v_{n+1}^{k+1}, \nabla \varphi_v)$$

$$\begin{aligned}
 & + \Delta t F_1(|v_{n+1}^{k+1}|v_{n+1}^{k+1}, \varphi_v) + \Delta t F_2(|v_{n+1}^{k+1}|^2v_{n+1}^{k+1}, \varphi_v) - \Delta t(p_{n+1}^{k+1}, \operatorname{div} \varphi_v) \\
 & = -\Delta t((\mu_{n+1}^k + \chi_0 \phi_{\sigma_{n+1}}^k) \phi_{T_{n+1}}^k, \varphi_v);
 \end{aligned} \tag{7.2}$$

$$(v_{n+1}^{k+1}, \nabla \varphi_p) = 0; \tag{7.3}$$

$$\begin{aligned}
 & (\phi_{\sigma_{n+1}}^{k+1} - \phi_{\sigma_n}, \varphi_\sigma) - \Delta t(\phi_{\sigma_{n+1}}^{k+1} v_{n+1}^{k+1}, \nabla \varphi_\sigma) \\
 & + \Delta t(m_\sigma(\phi_{T_{n+1}}^k, \phi_{\sigma_{n+1}}^{k+1}) \cdot (\delta_\sigma^{-1} \nabla \phi_{\sigma_{n+1}}^{k+1} - \chi_0 \nabla \phi_{T_{n+1}}^k), \nabla \varphi_\sigma) \\
 & + \Delta t \lambda_\sigma(\phi_{\sigma_{n+1}}^{k+1} \mathcal{C}(\phi_{T_{n+1}}^k), \varphi_\sigma) = 0;
 \end{aligned} \tag{7.4}$$

$$\begin{aligned}
 & (\phi_{T_{n+1}}^{k+1} - \phi_{T_n}, \varphi_T) - \Delta t(\phi_{T_{n+1}}^{k+1} v_{n+1}^{k+1}, \nabla \varphi_T) \\
 & + \Delta t(m_T(\phi_{T_{n+1}}^{k+1}, \phi_{\sigma_{n+1}}^{k+1}) \nabla \mu_{n+1}^{k+1}, \nabla \varphi_T) \\
 & - \Delta t \lambda_T(\phi_{\sigma_{n+1}}^{k+1} \mathcal{C}(\phi_{T_{n+1}}^{k+1} (1 - \phi_{T_{n+1}}^{k+1})), \varphi_T) = 0;
 \end{aligned} \tag{7.5}$$

$$(\mu_{n+1}^{k+1}, \varphi_\mu) - (D_{\phi_T} E_c(\phi_{T_{n+1}}^{k+1}, \phi_{\sigma_{n+1}}^{k+1}), \varphi_\mu) = (D_{\phi_T} E_e(\phi_{T_n}, \phi_{\sigma_n}), \varphi_\mu). \tag{7.6}$$

**Algorithm 1.** Semi-implicit scheme for (7.1)

```

1 Input:  $\phi_{T_0}, \phi_{\sigma_0}, v_0, \Delta t, T, \text{TOL}$ 
2 Output:  $\phi_{T_n}, \mu_n, \phi_{\sigma_n}, v_n$  for all  $n$ 
3  $t = 0, n = 0$ 
4 while  $t \leq T$  do
5    $\phi_{T_{n+1}}^0 = \phi_{T_n}$ 
6   while  $\max\|\phi_{T_{n+1}}^{k+1} - \phi_{T_{n+1}}^k\| > \text{TOL}$  do
7      $\phi_{T_{n+1}}^k = \phi_{T_{n+1}}^{k-1}$ 
8     solve  $v_{n+1}^{k+1}, p_{n+1}^{k+1}$  using (7.2) and (7.3), given  $\phi_{\sigma_n}, \phi_{T_{n+1}}^k$ 
9     solve  $\phi_{\sigma_{n+1}}^{k+1}$  using (7.4), given  $\phi_{\sigma_n}, \phi_{T_{n+1}}^k$ 
10    solve  $\phi_{T_{n+1}}^{k+1}, \mu_{n+1}^{k+1}$  using (7.5) and (7.6), given  $\phi_{T_n}, \phi_{T_{n+1}}^k, \phi_{\sigma_{n+1}}^{k+1}$ 
11     $k \mapsto k + 1$ 
12  end
13   $\phi_{T_{n+1}} = \phi_{T_{n+1}}^{k+1}$ 
14   $\mu_{n+1} = \mu_{n+1}^{k+1}$ 
15   $\phi_{\sigma_{n+1}} = \phi_{\sigma_{n+1}}^{k+1}$ 
16   $v_{n+1} = v_{n+1}^{k+1}$ 
17   $n \mapsto n + 1, t \mapsto t + \Delta t$ 
18 end

```

We implemented Algorithm 1 in FEniCS,<sup>57</sup> an open-source computing platform for solving partial differential equations using finite element methods. We use this implementation to obtain the numerical results below.

### 7.1. Spherically symmetric case

For specificity and demonstration purposes, we assume a spherically symmetric tumor volume and use polar coordinates to transform our model (2.6) to a system of equations depending solely on time  $t$  and radius  $r$ . We consider the domain  $R = [0, 0.32]$  imitating our data setting as described in Sec. 6. We choose parameters matching the priors we used in (6.1); in particular we choose the dimensionless values

$$\begin{aligned} \varepsilon_T &= 0.01, & \lambda_T &= 1.0, & M_T &= 1.0, & \alpha &= 1.0, \\ \chi_0 &= 0.5, & \lambda_\sigma &= 1.0, & M_\sigma &= 1.0, & \nu &= 10.0, \\ \delta_\sigma &= 0.05, & \lambda_A &= 0.01, & \bar{E} &= 0.25, & F_1, F_2 &= 10.0. \end{aligned} \tag{7.7}$$

We consider a smooth approximation of the Heaviside function matching the initial tumor confluence 0.00562 of our data setting, as it can be seen in Fig. 4(a) below. The approximation is given by

$$\phi_T(0, r) = \frac{1}{1 + \exp(M(r - r_{\text{init}}))},$$

where a larger  $M > 0$  is increasing the steepening of the function around zero, and  $r_{\text{init}} = 0.32\sqrt{0.00562}$  again represents the radius of the initial tumor cell.

In Fig. 4, the simulation of the tumor cell  $\phi_T$  is shown at different time spots. First, the initial tumor cell is illustrated, then after 7, 14 and 21 days. We plot

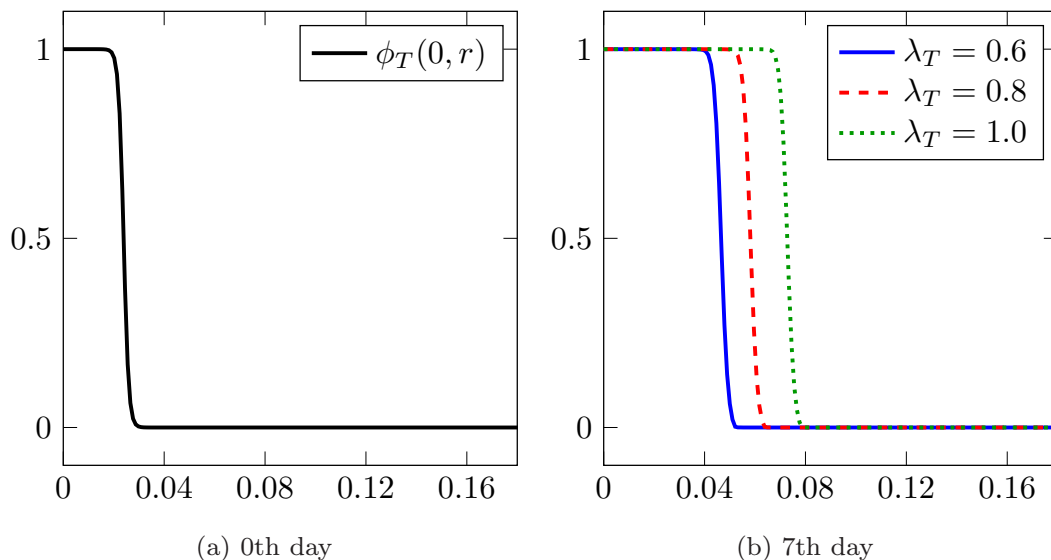


Fig. 4. Simulation of the evolution of the tumor cell volume fraction  $\phi_T$  over the duration of 21 days for three different proliferation rates.

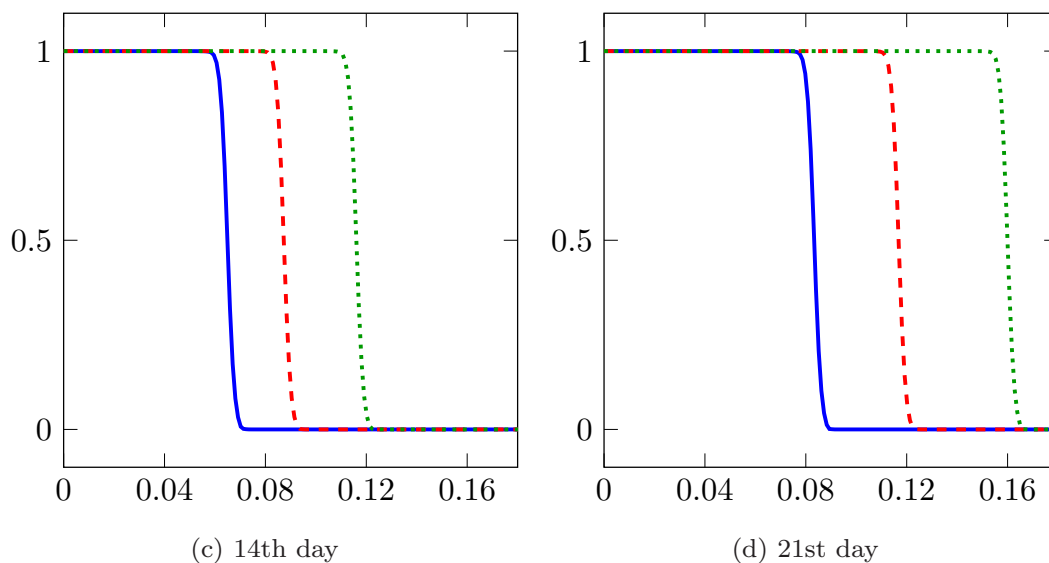


Fig. 4. (Continued)

three different curves for different proliferation rates, 0.6, 0.8, and 1.0. We observe that a higher proliferation rate is increasing the expansion of the tumor cell volume fraction  $\phi_T$ , and the tumor cell is continuously growing over time.

The simulation of the evolution of the tumor confluence is depicted in Fig. 5 below. We observe that the confluence grows continuously in time with an increasing rate.

### 7.2. Two-dimensional case

We simulate the tumor growth on the circular domain

$$\Omega = \{x \in \mathbb{R}^2 : x_1^2 + x_2^2 = 0.32^2\}$$

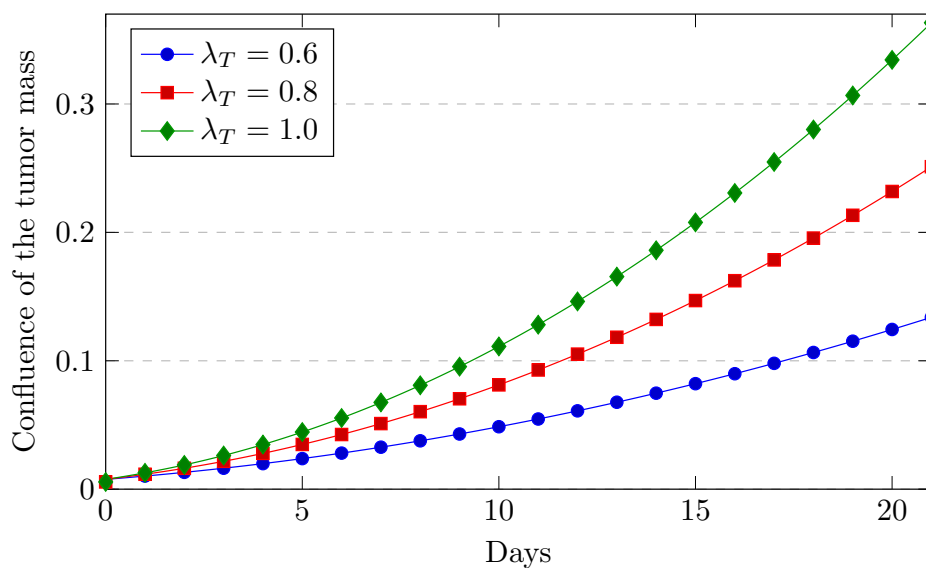


Fig. 5. Simulation of the tumor confluence for three different proliferation rates  $\lambda_T$  over the duration of 21 days.

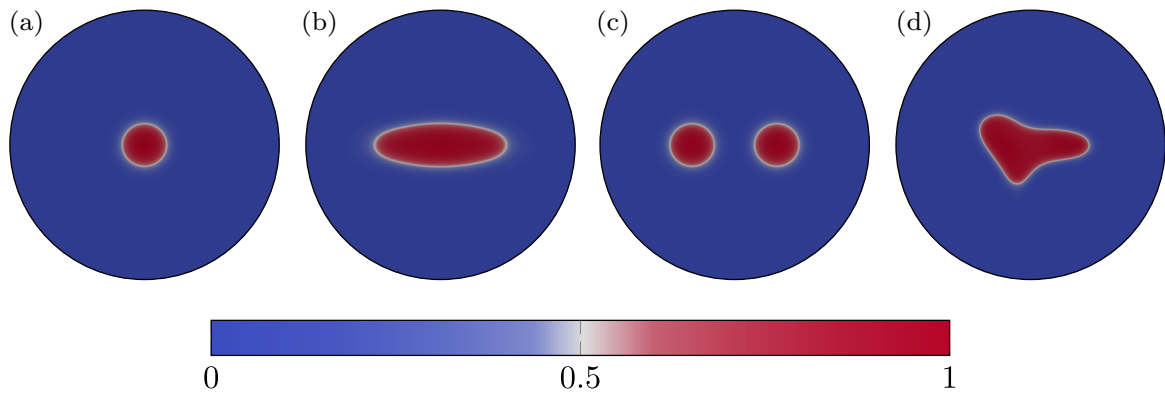


Fig. 6. Choices for the initial tumor mass  $\phi_{T,0}$ , (a) slightly elliptic, (b) highly elliptic, (c) separated, (d) irregularly perturbed.

with the same parameters as chosen in the one-dimensional setting; see (7.7). For the initial tumor volume we select the following four possibilities, which are depicted in Fig. 6:

$$\begin{aligned}
 \text{(a)} \quad \phi_T(0, x) &= \begin{cases} 1, & \text{if } 0.9 \cdot x_1^2 + x_2^2 \leq r_{\text{init}}^2, \\ 0, & \text{else,} \end{cases} \\
 \text{(b)} \quad \phi_T(0, x) &= \begin{cases} 1, & \text{if } 0.15 \cdot x_1^2 + x_2^2 \leq r_{\text{init}}^2, \\ 0, & \text{else,} \end{cases} \\
 \text{(c)} \quad \phi_T(0, x) &= \begin{cases} 1, & \text{if } 0.9 \cdot (x_1 \pm 0.05)^2 + x_2^2 \leq r_{\text{init}}^2, \\ 0, & \text{else,} \end{cases} \\
 \text{(d)} \quad \phi_T(0, x) &= \begin{cases} 1, & \text{if } (\sin(7.2x_1 + 5.6x_2) + 1) \cdot (4x_1 - 0.2)^2 \\ & + (\sin(8x_1) + 1) \cdot 64x_2^2 \leq 1, \\ 0, & \text{else.} \end{cases}
 \end{aligned}$$

In Fig. 7, we show the evolution of the slightly elliptic initial tumor mass (a) using

- I model (2.6) without any influence of the velocity, that means we set  $v \equiv 0$  and neglect the convection terms in the equations of  $\phi_T$  and  $\phi_\sigma$ ;
- II model (2.6) without the effect of the Forchheimer law, that means we set  $F_1 = F_2 = 0$  in the velocity equation;
- III the full model (2.6) without any restrictions.

Afterwards, we simulate the entire model III together with the initial tumor volumes (b), (c) and (d), see Fig. 8 below for the results.

The simulation of the full local model III with a slightly elliptic initial tumor mass (a) is depicted in the bottom row of Fig. 7. Similar to Cristini *et al.*<sup>19,20,83–85</sup> Macklin *et al.*<sup>59–61</sup> and Garcke *et al.*<sup>37</sup> we notice an evolving shape instability. Starting from the slightly elliptic initial tumor mass, the ellipticity is enforced at the beginning and on the 10th day we see a clearly elliptic tumor volume. At the



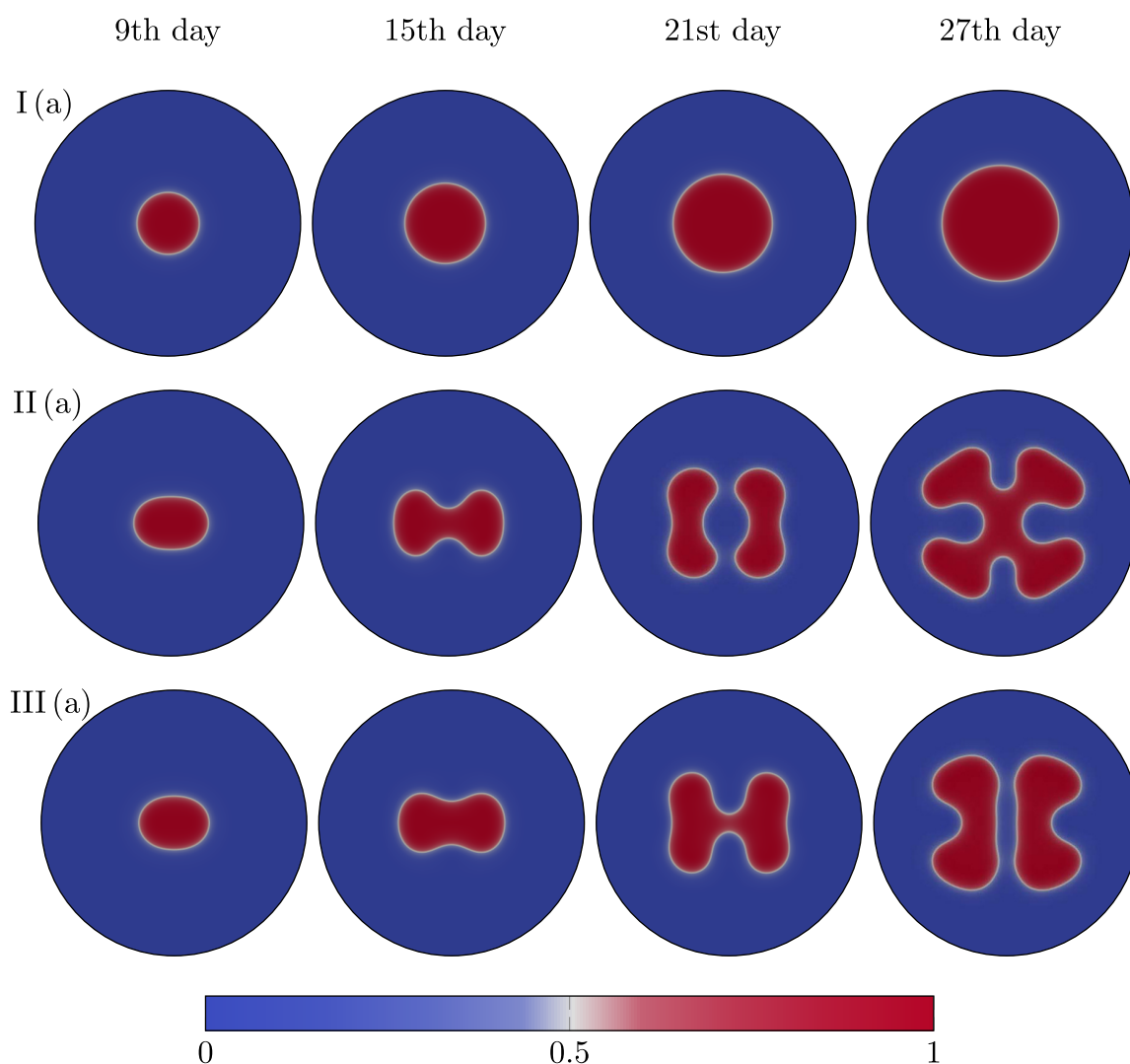


Fig. 7. Evolution of the tumor volume fraction  $\phi_T$  starting from the initial slightly elliptic tumor mass (a) using the models, I without velocity, II without the Forchheimer law, III full model.

15th day, a slight bulge forms along the horizontal direction and two buds form at the horizontal end points. These buds continue to evolve vertically with a new bulge oriented along the vertical directions and therefore, for each bud two new buds are forming, see the simulation on the 21st day. This behavior of the tumor cells implies that the instability repeats itself and this highly complex evolution in tumor shape is captured by the high-order phase-field structure of the model and is indicative of examples in tumor growth in living tissue.

To inspect the effects of the velocity itself in the model, we redo the first simulation with the same initial data (a) but without the presence of any velocity, which means we are in the case of model I as described above. We depict the results of the simulation in the first row of Fig. 7. We observe that the tumor stays in its symmetric shape, resembling the results in Ref. 48. We conclude that the velocity highly influences the shape of the tumor, even though the velocity parameters do not mainly impact the tumor volume as the sensitivity analysis has shown in Sec. 6.

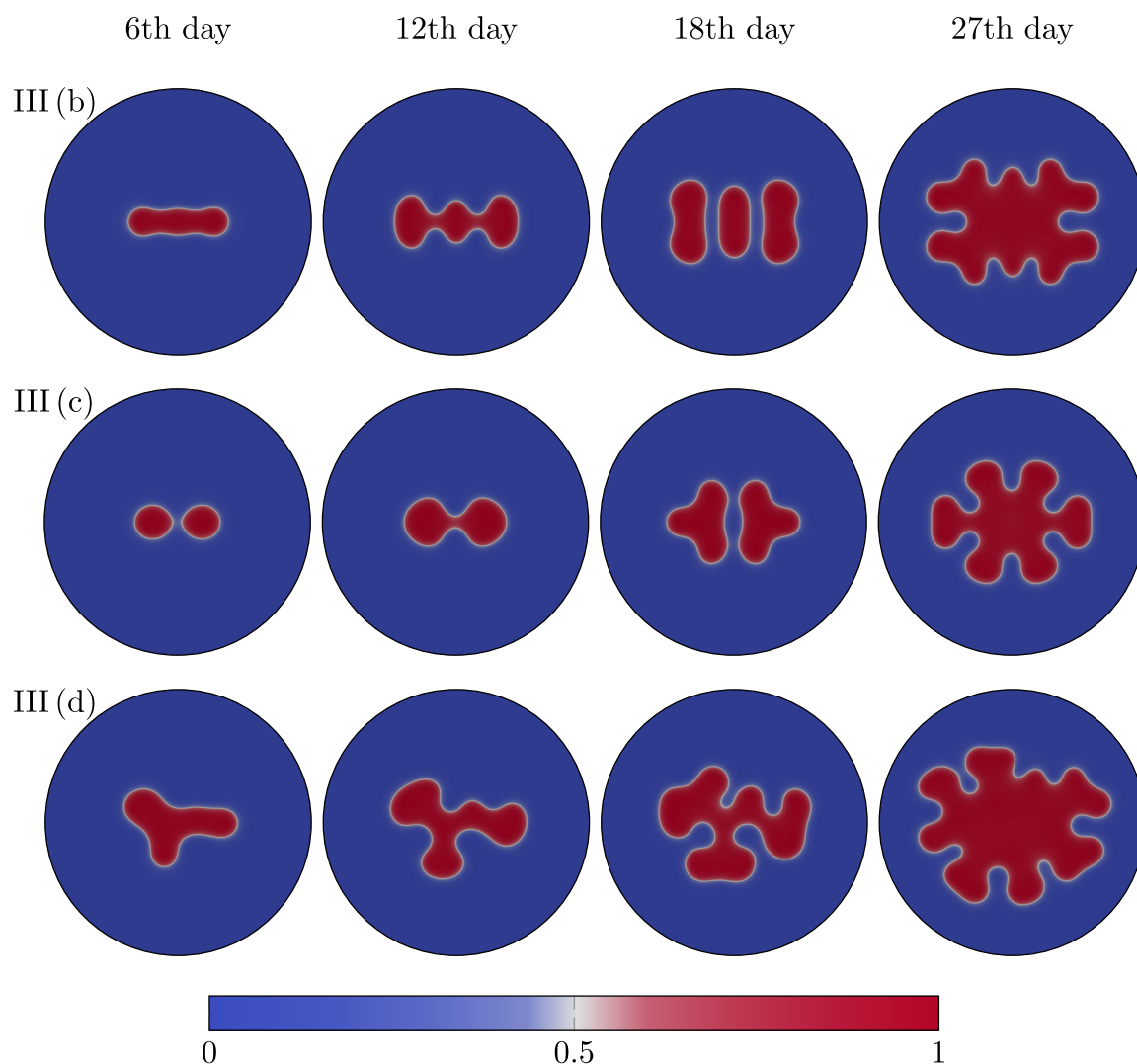


Fig. 8. Evolution of the tumor volume fraction  $\phi_T$  using the full model III, starting from (b) a highly elliptic tumor mass, (c) two separated tumor masses, (d) an irregularly perturbed tumor mass.

In the next simulation, see the middle row of Fig. 7 for the result, we use the slightly elliptic initial data (a) and model II, that means we set the Forchheimer constants  $F_1$  and  $F_2$  equal to zero. We observe that the result largely resembles the simulation of the full case III (a), in the sense that the Forchheimer terms delay the tumor evolution. We notice that the tumor mass splits into two parts, which begin to approach each other on the lower and upper bulbs. Eventually, these buds reconnect and therefore, trapping the healthy tissue within the tumor, which has also been observed in Ref. 20.

Next, we start from the three initial conditions (b)–(d), which have been depicted in Fig. 6, and simulate the evolution of the tumor cell volume fraction using the full model III. See Fig. 8 for the simulation results.

In the case of the highly elliptic initial tumor shape (b), we observe on the 6th day that three buds are forming, two at the end points of the horizontal shape and

one in the middle. These buds continue to evolve vertically and eventually separate from each other, see the result on the 18th day. The lower and upper parts of the buds will connect again, and therefore, trapping the health tissue in between. Finally on the 27th day, we observe that the tumor shape has formed a simply connected domain.

In the middle row of Fig. 8, we see the results of the simulation of model III starting with the separated initial tumor shape (c). We observe on the 6th day that the tumor cells are moving toward each other, until they connect, form buds and separate again. As in the case of the highly elliptic initial tumor shape (b), eventually, the tumor mass is forming a simply connected domain.

Lastly, we simulate model III together with the irregularly perturbed tumor mass (d), see the last row of Fig. 8. Before, we always used for the initial tumor mass a symmetric shape. Now, the tumor volume fraction is starting irregularly and it keeps this form while growing in the evolving buds.

## 8. Concluding Remarks

In this paper, we present a mathematical analysis of a class of phase-field models of the growth and decline of tumors in living organisms, in which convective velocities of tumor cells are assumed to obey a time-dependent Darcy–Forchheimer–Brinkman flow and in which long-range interactions of cell species are accounted for through nonlocal integro-differential operators. Under some mild assumptions on mathematical properties of the governing operators, we are able to establish existence of weak solutions in the topologies of the underlying function spaces.

In addition, we explore the sensitivity of key quantities of interest, such as the evolving tumor volume, on model parameters. We demonstrate that when observational data are available, the method of active subspaces can be used to estimate parameter sensitivity. In parallel, we consider methods of output-variance-sensitivity as an alternative measure of parameter-sensitivity. Remarkably, for certain quantities of interest, such as tumor volume or mass, these two approaches yield very similar estimates. In the case in which the tumor volume is selected as the quantity of interest, the tumor proliferation parameter of the model was found to be, by far, the dominant factor compared to other parameters.

To determine the effects of various flow terms in the evolution of tumor shape and growth, we performed numerical experiments using finite-element approximations of the model for representative cases. These numerical results reveal that nonlinear flow regimes, expected to be relevant in certain types of tumors, can apparently affect the shape, connectivity, and distribution of tumors.

## Acknowledgments

The authors gratefully acknowledge the support of the German Science Foundation (DFG) for funding part of this work through grant WO 671/11-1, the Cancer Prevention Research Institute of Texas (CPRIT) under grant number RR160005,

the NIH through the grants NCI U01CA174706 and NCI R01CA186193, and the US Department of Energy, Office of Science, Office of Advanced Scientific Computing Research, Mathematical Multifaceted Integrated Capability Centers (MMICCS) program, under award number DE-SC0019393.

## References

1. R. P. Araujo and D. S. McElwain, A history of the study of solid tumour growth: The contribution of mathematical modelling, *Bull. Math. Biol.* **66** (2014) 1039–1091.
2. P. W. Bates, On some nonlocal evolution equations arising in materials science, in *Nonlinear Dynamics and Evolution Equations* (Amer. Math. Soc., 2006), pp. 13–52.
3. P. W. Bates and J. Han, The Dirichlet boundary problem for a nonlocal Cahn–Hilliard equation, *J. Math. Anal. Appl.* **311** (2015) 289–312.
4. P. W. Bates and J. Han, The Neumann boundary problem for a nonlocal Cahn–Hilliard equation, *J. Differential Equations* **212** (2005) 235–277.
5. N. Bellomo, N. Li and P. K. Maini, On the foundations of cancer modelling: Selected topics, speculations, and perspectives, *Math. Models Methods Appl. Sci.* **18** (2008) 593–646.
6. D. Boffi, F. Brezzi and M. Fortin, *Mixed Finite Element Methods and Applications*, Springer Series in Computational Mathematics (Springer-Verlag, 2013).
7. F. Boyer and P. Fabrie, *Mathematical Tools for the Study of the Incompressible Navier–Stokes Equations and Related Models*, Applied Mathematical Sciences (Springer-Verlag, 2012).
8. H. Brezis, *Functional Analysis, Sobolev Spaces and Partial Differential Equations* (Springer-Verlag, 2010).
9. H. Burcharth and O. Andersen, On the one-dimensional steady and unsteady porous flow equations, *Coast. Eng.* **24** (1995) 233–257.
10. H. M. Byrne, M. R. Owen, T. Alarcon, J. Murphy and P. K. Maini, Modelling the response of vascular tumours to chemotherapy: A multiscale approach, *Math. Models Methods Appl. Sci.* **16** (2006) 1219–1241.
11. J. W. Cahn and J. E. Hilliard, Free energy of a nonuniform system. I. Interfacial free energy, *J. Chem. Phys.* **28** (1958) 258–267.
12. M. A. Chaplain, M. Lachowicz, Z. Szymańska and D. Wrzosek, Mathematical modelling of cancer invasion: The importance of cell–cell adhesion and cell–matrix adhesion, *Math. Models Methods Appl. Sci.* **21** (2011) 719–743.
13. Z. Chen, S. L. Lyons and G. Qin, Derivation of the Forchheimer law via homogenization, *Transp. Porous Media* **44** (2001) 325–335.
14. E. A. Coddington and N. Levinson, *Theory of Ordinary Differential Equations* (McGraw-Hill, 1984).
15. P. Colli, S. Frigeri and M. Grasselli, Global existence of weak solutions to a nonlocal Cahn–Hilliard–Navier–Stokes system, *J. Math. Anal. Appl.* **386** (2012) 428–444.
16. P. G. Constantine, *Active Subspaces: Emerging Ideas for Dimension Reduction in Parameter Studies* (SIAM, 2015).
17. P. G. Constantine and P. Diaz, Global sensitivity metrics from active subspaces, *Reliab. Eng. Syst. Safe.* **162** (2017) 1–13.
18. P. G. Constantine, E. Dow and Q. Wang, Active subspace methods in theory and practice: Applications to kriging surfaces, *SIAM J. Sci. Comput.* **36** (2014) A1500–A1524.

19. V. Cristini, X. Li, J. S. Lowengrub and S. M. Wise, Nonlinear simulations of solid tumor growth using a mixture model: Invasion and branching, *J. Math. Biol.* **58** (2009) 723–763.
20. V. Cristini, J. Lowengrub and Q. Nie, Nonlinear simulation of tumor growth, *J. Math. Biol.* **46** (2003) 191–224.
21. T. S. Deisboeck and G. S. Stamatakos, *Multiscale Cancer Modeling* (CRC Press, 2010).
22. F. Della Porta, A. Giorgini and M. Grasselli, The nonlocal Cahn–Hilliard–Hele–Shaw system with logarithmic potential, *Nonlinearity* **31** (2018) 4851–4881.
23. F. Della Porta and M. Grasselli, On the nonlocal Cahn–Hilliard–Brinkman and Cahn–Hilliard–Hele–Shaw systems, *Commun. Math. Sci.* **13** (2015) 1541–1567.
24. M. Ebenbeck and H. Garcke, Analysis of a Cahn–Hilliard–Brinkman model for tumour growth with chemotaxis, *J. Differential Equations* **266** (2018) 5998–6036.
25. C. Engwer, C. Stinner and C. Surulescu, On a structured multiscale model for acid-mediated tumor invasion: The effects of adhesion and proliferation, *Math. Models Methods Appl. Sci.* **27** (2017) 1355–1390.
26. L. C. Evans, *Partial Differential Equations*, Graduate Studies in Mathematics (Amer. Math. Soc., 2010).
27. S. Frigeri and M. Grasselli, Nonlocal Cahn–Hilliard–Navier–Stokes systems with singular potentials, *Dyn. Partial Differential Equations* **9** (2012) 273–304.
28. S. Frigeri, M. Grasselli and P. Krejčí, Strong solutions for two-dimensional nonlocal Cahn–Hilliard–Navier–Stokes systems, *J. Differential Equations* **255** (2013) 2587–2614.
29. S. Frigeri, M. Grasselli and E. Rocca, A diffuse interface model for two-phase incompressible flows with non-local interactions and non-constant mobility, *Nonlinearity* **28** (2015) 1257–1293.
30. S. Frigeri, M. Grasselli and E. Rocca, On a diffuse interface model of tumour growth, *European J. Appl. Math.* **26** (2015) 215–243.
31. S. Frigeri, K. F. Lam and E. Rocca, On a diffuse interface model for tumour growth with non-local interactions and degenerate mobilities, in *Solvability, Regularity, and Optimal Control of Boundary Value Problems for PDEs* (Springer, 2017), pp. 217–254.
32. H. Gajewski and K. Zacharias, On a nonlocal phase separation model, *J. Math. Anal. Appl.* **286** (2003) 11–31.
33. C. G. Gal, A. Giorgini and M. Grasselli, The nonlocal Cahn–Hilliard equation with singular potential: Well-posedness, regularity and strict separation property, *J. Differential Equations* **263** (2017) 5253–5297.
34. H. Garcke and K. F. Lam, Global weak solutions and asymptotic limits of a Cahn–Hilliard–Darcy system modelling tumour growth, *AIMS Math.* **1** (2016) 318–360.
35. H. Garcke and K. F. Lam, Well-posedness of a Cahn–Hilliard system modelling tumour growth with chemotaxis and active ort, *European J. Appl. Math.* **28** (2017) 284–316.
36. H. Garcke and K. F. Lam, On a Cahn–Hilliard–Darcy system for tumour growth with solution dependent source terms, in *Trends in Applications of Mathematics to Mechanics* (Springer, 2018), pp. 243–264.
37. H. Garcke, K. F. Lam, E. Sitka and V. Styles, A Cahn–Hilliard–Darcy model for tumour growth with chemotaxis and active transport, *Math. Models Methods Appl. Sci.* **26** (2016) 1095–1148.
38. A. Gerisch and M. Chaplain, Mathematical modelling of cancer cell invasion of tissue: Local and non-local models and the effect of adhesion, *J. Theor. Biol.* **250** (2008) 684–704.

39. G. Giacomini and J. L. Lebowitz, Exact macroscopic description of phase segregation in model alloys with long range interactions, *Phys. Rev. Lett.* **76** (1996) 1094–1097.
40. G. Giacomini and J. L. Lebowitz, Phase segregation dynamics in particle systems with long range interactions. I. Macroscopic limits, *J. Stat. Phys.* **87** (1997) 37–61.
41. V. Girault and P.-A. Raviart, *Finite Element Approximation of the Navier–Stokes Equations*, Lecture Notes in Mathematics (Springer-Verlag, 1979).
42. L. Graziano and L. Preziosi, Mechanics in tumor growth, in *Modeling of Biological Materials* (Springer, 2007), pp. 263–321.
43. Z. Gu and H. Wang, Gravity waves over porous bottoms, *Coast. Eng.* **15** (1991) 497–524.
44. Z. Guan, C. Wang and S. M. Wise, A convergent convex splitting scheme for the periodic nonlocal Cahn–Hilliard equation, *Numer. Math.* **128** (2014) 377–406.
45. M. E. Gurtin, Generalized Ginzburg–Landau and Cahn–Hilliard equations based on a microforce balance, *Physica D.* **92** (1996) 178–192.
46. K. R. Hall, G. M. Smith and D. J. Turcke, Comparison of oscillatory and stationary flow through porous media, *Coast. Eng.* **24** (1995) 217–232.
47. H. Hatzikirou, A. Deutsch, C. Schaller, M. Simon and K. Swanson, Mathematical modelling of glioblastoma tumour development: A review, *Math. Models Methods Appl. Sci.* **15** (2005) 1779–1794.
48. A. Hawkins-Daarud, K. G. van der Zee and T. J. Oden, Numerical simulation of a thermodynamically consistent four-species tumor growth model, *Int. J. Numer. Methods Biomed. Eng.* **28** (2021) 3–24.
49. J. Jiang, H. Wu and S. Zheng, Well-posedness and long-time behavior of a non-autonomous Cahn–Hilliard–Darcy system with mass source modeling tumor growth, *J. Differential Equations* **259** (2015) 3032–3077.
50. K. F. Lam and H. Wu, Thermodynamically consistent Navier–Stokes–Cahn–Hilliard models with mass transfer and chemotaxis, *European J. Appl. Math.* **29** (2018) 595–644.
51. L. M. Laushey and L. V. Papat, Darcy’s law during unsteady flow, in *Ground Water: General Assembly of Bern*, Vol. 77 (1957), pp. 284–299.
52. E. H. Lieb and M. Loss, *Analysis*, Graduate Studies in Mathematics (Amer. Math. Soc., 2001).
53. E. A. Lima, R. C. Almeida and J. T. Oden, Analysis and numerical solution of stochastic phase-field models of tumor growth, *Numer. Methods Partial Differential Equations* **31** (2015) 552–574.
54. E. A. Lima, N. Ghousifam, A. Ozkan, J. T. Oden, A. Shahmoradi, M. N. Rylander, B. Wohlmuth and T. E. Yankeelov, Calibration of multi-parameter models of avascular tumor growth using time resolved microscopy data, *Sci. Rep.* **8** (2018) Report number 14558.
55. E. A. Lima, J. T. Oden and R. C. Almeida, A hybrid ten-species phase-field model of tumor growth, *Math. Models Methods Appl. Sci.* **24** (2014) 2569–2599.
56. J. L. Lions and E. Magenes, *Non-Homogeneous Boundary Value Problems and Applications I*, Grundlehren der mathematischen Wissenschaften (Springer-Verlag, 2012).
57. A. Logg, K.-A. Mardal and G. Wells, *Automated Solution of Differential Equations by the Finite Element Method: The FEniCS Book* (Springer-Verlag 2012).
58. J. Lowengrub, E. Titi and K. Zhao, Analysis of a mixture model of tumor growth, *European J. Appl. Math.* **24** (2013) 691–734.
59. P. Macklin and J. Lowengrub, Evolving interfaces via gradients of geometry-dependent interior poisson problems: Application to tumor growth, *J. Comput. Phys.* **203** (2005) 191–220.

60. P. Macklin and J. Lowengrub, An improved geometry-aware curvature discretization for level set methods: Application to tumor growth, *J. Comput. Phys.* **215** (2006) 392–401.
61. P. Macklin and J. S. Lowengrub, A new ghost cell/level set method for moving boundary problems: Application to tumor growth, *J. Sci. Comput.* **35** (2008) 266–299.
62. J. T. Oden, Adaptive multiscale predictive modelling, *Acta Numer.* **27** (2018) 353–450.
63. J. T. Oden *et al.*, Toward predictive multiscale modeling of vascular tumor growth, *Arch. Comput. Methods Eng.* **23** (2016) 735–779.
64. H. Pan and H. Rui, Mixed element method for two-dimensional Darcy–Forchheimer model, *J. Sci. Comput.* **52** (2012) 563–587.
65. V. Quaranta, A. M. Weaver, P. T. Cummings and A. R. Anderson, Mathematical modeling of cancer: The future of prognosis and treatment, *Clin. Chim. Acta* **357** (2005) 173–179.
66. K. Rajagopal, On a hierarchy of approximate models for flows of incompressible fluids through porous solids, *Math. Models Methods Appl. Sci.* **17** (2007) 215–252.
67. J. C. Robinson, *Infinite-Dimensional Dynamical Systems: An Introduction to Dissipative Parabolic PDEs and the Theory of Global Attractors*, Cambridge Texts in Applied Mathematics (Cambridge Univ. Press, 2001).
68. T. Roose, S. J. Chapman and P. K. Maini, Mathematical models of avascular tumor growth, *SIAM Rev.* **49** (2007) 179–208.
69. T. Roubíček, *Nonlinear Partial Differential Equations with Applications*, International Series of Numerical Mathematics (Birkhäuser, 2013).
70. S. Salsa, *Partial Differential Equations in Action: From Modelling to Theory* (Springer-Verlag, 2016).
71. A. Saltelli, P. Annoni, I. Azzini, F. Campolongo, M. Ratto and S. Tarantola, Variance based sensitivity analysis of model output: Design and estimator for the total sensitivity index, *Comput. Phys. Commun.* **181** (2010) 259–270.
72. A. Saltelli *et al.*, *Sensitivity Analysis* (Wiley, 2000).
73. A. Saltelli, M. Ratto, T. Andres, F. Campolongo, J. Cariboni, D. Gatelli, M. Saisana and S. Tarantola, *Global Sensitivity Analysis: The Primer* (Wiley, 2008).
74. J. Simon, Compact sets in the space  $L^p(0, T; B)$ , *Ann. Math. Pura Appl.* **146** (1986) 65–96.
75. J. Simon, On the existence of the pressure for solutions of the variational Navier–Stokes equations, *J. Math. Fluid Methods* **1** (1999) 225–234.
76. I. M. Sobol, Global sensitivity indices for nonlinear mathematical models and their Monte–Carlo estimates, *Math. Comput. Simul.* **55** (2001) 271–280.
77. S. Srinivasan and K. Rajagopal, A thermodynamic basis for the derivation of the Darcy, Forchheimer and Brinkman models for flows through porous media and their generalizations, *Int. J. Nonlinear Mech.* **58** (2014) 162–166.
78. C. Stinner, C. Surulescu and M. Winkler, Global weak solutions in a PDE–ODE system modeling multiscale cancer cell invasion, *SIAM J. Math. Anal.* **46** (2014) 1969–2007.
79. W. Strauss, On continuity of functions with values in various Banach spaces, *Pacific J. Math.* **19** (1966) 543–551.
80. Z. Szymańska, C. M. Rodrigo, M. Lachowicz and M. A. Chaplain, Mathematical modelling of cancer invasion of tissue: The role and effect of nonlocal interactions, *Math. Models Methods Appl. Sci.* **19** (2009) 257–281.
81. L. Tartar, Nonlinear Partial Differential Equations using Compactness Method, Report 1584, Mathematics Research Center, University of Wisconsin (1976)

82. R. Temam, *Navier–Stokes Equations: Theory and Numerical Analysis* (Amer. Math. Soc., 2001).
83. S. M. Wise, J. S. Lowengrub and V. Cristini, An adaptive multigrid algorithm for simulating solid tumor growth using mixture models, *Math. Comput. Model.* **53** (2011) 1–20.
84. S. M. Wise, J. S. Lowengrub, H. B. Frieboes and V. Cristini, Three-dimensional multispecies nonlinear tumor growth I: Model and numerical method, *J. Theor. Biol.* **253** (2008) 524–543.
85. X. Zheng, S. Wise and V. Cristini, Nonlinear simulation of tumor necrosis, neo-vascularization and tissue invasion via an adaptive finite-element/level-set method, *Bull. Math. Biol.* **67** (2005) 211–259.
86. T. Zhu, C. Waluga, B. Wohlmuth and M. Manhart, A study of the time constant in unsteady porous media flow using direct numerical simulation, *Transp. Porous Media* **104** (2014) 161–179.



## A.2. Local and nonlocal phase-field models of tumor growth and invasion due to ECM degradation

### Local and nonlocal phase-field models of tumor growth and invasion due to ECM degradation

Marvin Fritz, Ernesto Lima, Vanja Nikolić, J. Tinsley Oden, Barbara Wohlmuth

---

In this article, we consider a system of PDEs for modelling the growth of a tumor cell colony inside an ECM. The ECM is an important factor in mathematical oncology since it functions as a regulator around the tumor and controls the flow of nutrients. The goal of the tumor cells is the erosion of the ECM in order to get to the nutrients outside of it. The basis of our model is a multiphase system with the Cahn–Hilliard equation for the viable tumor volume fraction  $\phi_V$ . Here, we included the proliferative and hypoxic cells in one variable. It is particularly important to single out the necrotic cells since many processes, such as chemotaxis and haptotaxis, do not involve the dead cancer cells. We propose two ODEs for the evolution of necrotic cells  $\phi_N$  and extracellular matrix density  $\theta$ , as well as two RDE for the nutrients  $\phi_\sigma$  and the MDEs  $\phi_{MDE}$ . In our analysis, we treat both the cases of a local gradient-based and a nonlocal-based cell-matrix adhesion effect. These two have been used in the literature before, and we compared both of them in numerical simulations. Our contribution is the modeling, analysis, and numerics of the full system.

In Section 2, we explore two types of haptotaxis effects in tumor modeling – the local gradient-based haptotaxis and the nonlocal one. We investigate the modeling of the new variables  $\theta$  and  $\phi_{MDE}$  in contrast to our first paper [62] on this subject. In Section 3, we state some mathematical preliminaries that we need in the further sections, e.g., the Aubin–Lions compactness lemma. Section 4 presents a thorough mathematical analysis of the local and nonlocal systems. We show the existence of weak solutions in both cases, and we prove both of the cases at the same time by introducing a parameter that indicates whether we are in the local or nonlocal setting. Interestingly, we need to assume a higher regularity on the initial condition of the ECM density in the local system. In fact, we had to assume that the initial is in  $H^1(\Omega) \cap L^\infty(\Omega)$  instead of  $L^2(\Omega)$  in the nonlocal setting. In Section 5, we present a fully discrete scheme of the systems based on the FEM and write a complete algorithm for solving the system. Finally, we collect the findings of numerical experiments in Section 6 and compare both the local and nonlocal models from a numerical point of view. In Section 7, we give some concluding remarks.

I was heavily involved in the idea generation process and was principally responsible for establishing the mathematical framework and carrying out the scientific work described in this article. Additionally, I was responsible for authoring the essay, while my co-authors participated by providing corrections.

## Permission to include:

Marvin Fritz, Ernesto Lima, Vanja Nikolić, J. Tinsley Oden, Barbara Wohlmuth  
**Local and nonlocal phase-field models of tumor growth and invasion due to ECM degradation**  
*Mathematical Models and Methods in Applied Sciences*, 29(13):2433–2468, 2019  
(see also article [61] in the bibliography)

The following pages on copyright are excerpts from copies of the website

<https://www.worldscientific.com/page/authors/author-rights>

(Accessed on 21 November 2021)

## Author Rights

All articles published on the World Scientific website are protected by copyright held by World Scientific Publishing Company (or its subsidiaries). This copyright covers the exclusive rights to share, reproduce and distribute the article, including in electronic forms, reprints, translations, photographic reproductions, or similar. Except for articles published on an [open access basis](#), the transfer of copyright to World Scientific (or its subsidiaries) becomes effective when an article is accepted for publication.

As author of a journal article, you retain the rights detailed in the following:

### Publisher-created version

1. The publisher-created version can only be posted where a gold open access fee has been paid and the article contains an OpenAccess logo.

### Preprint version

2. Authors may post their submitted manuscript (preprint) at any time on their personal website, in their company or institutional repository, in not-for-profit subject-based preprint servers or repositories, and on scholarly collaboration networks (SCNs) which have [signed up to the STM sharing principles](#). Please provide the following acknowledgement along with a link to the article via its DOI if available.

- *Preprint of an article submitted for consideration in [Journal] © [Year] [copyright World Scientific Publishing Company] [Journal URL]*
- *Preprint of an article published in [Journal, Volume, Issue, Year, Pages] [Article DOI] © [copyright World Scientific Publishing Company] [Journal URL]*

### Author accepted manuscript

3. After an embargo of 12 months, you may post the accepted author manuscript on your personal website, your company or institutional repository, not-for-profit subject-based preprint servers or repositories of your own choice or as stipulated by the Funding Agency and may share the article in private research groups including those on SCNs which have [signed up to the STM sharing principles](#).

The private research groups must be formed by invitation for a specific research purpose and be of a size that is typical for research groups within the discipline. Sharing of articles must be limited to members of the group only. The SCNs which have signed up to the sharing principles are required to provide COUNTER compliant usage data to World Scientific by agreement. Please provide the following acknowledgement along with a link to the article via its DOI if available:

- *Electronic version of an article published as [Journal, Volume, Issue, Year, Pages] [Article DOI] © [copyright World Scientific Publishing Company] [Journal URL]*

The [Digital Object Identifier \(DOI\)](#) of your article can be found on the relevant webpage of WorldSciNet where your article is posted.

The above permissions apply to authors whose articles are to be published by World Scientific and authors who have purchased a copy or received a complimentary copy of their published article.

This policy does not apply to pay-per-view customers and subscribers, who should adhere to their respective agreed policies

#### Definitions:

- "preprint" - a version of an article created prior to peer review
- "accepted author manuscript" - an author-created version of the final journal article (to reflect changes made in peer review and editing)
- "publisher-created version" - the definitive final record of published research that appears in the journal and embodies all value-adding publisher activities including copy-editing, formatting and pagination.



#### Resources

[For Authors](#)  
[For Booksellers](#)  
[For Librarians](#)  
[Copyright & Permissions](#)  
[Translation Rights](#)  
[How to Order](#)  
[Contact Us](#)  
[Sitemap](#)

#### About Us & Help

[About Us](#)  
[News](#)  
[Help](#)

#### Links

[World Scientific Europe](#)  
[World Scientific China 世界科技](#)  
[WS Education](#)  
[Global Publishing 八方文化](#)  
[Asia-Pacific Biotech News](#)  
[World Century](#)

[Privacy policy](#)

© 2021 World Scientific Publishing Co Pte Ltd

Powered by Atypon® Literatum

## **Notice of publication and copyright**

First Published in "Local and nonlocal phase-field models of tumor growth and invasion due to ECM degradation" in *Mathematical Models and Methods in Applied Sciences*, 29(13):2433–2468 (2019), published by World Scientific.

DOI: <https://doi.org/10.1142/S0218202519500519>

## Local and nonlocal phase-field models of tumor growth and invasion due to ECM degradation

Marvin Fritz\*

*Technical University of Munich,  
Department of Mathematics,  
Boltzmannstraße 3, 85748 Garching, Germany  
marvin.fritz@ma.tum.de*

Ernesto A. B. F. Lima

*The University of Texas at Austin,  
Oden Institute for Computational Engineering and Sciences,  
201 East 24th St, Austin, TX 78712-1229, USA  
lima@oden.utexas.edu*

Vanja Nikolić

*Technical University of Munich,  
Department of Mathematics,  
Boltzmannstraße 3, 85748 Garching, Germany  
vanja.nikolic@ma.tum.de*

J. Tinsley Oden

*The University of Texas at Austin,  
Oden Institute for Computational Engineering and Sciences,  
201 East 24th St, Austin, TX 78712-1229, USA  
oden@oden.utexas.edu*

Barbara Wohlmuth

*Technical University of Munich,  
Department of Mathematics,  
Boltzmannstraße 3, 85748 Garching, Germany  
wohlmuth@ma.tum.de*

Received 18 June 2019

Accepted 18 August 2019

Published 25 October 2019

Communicated by N. Bellomo

We present and analyze new multi-species phase-field mathematical models of tumor growth and ECM invasion. The local and nonlocal mathematical models describe the evolution of volume fractions of tumor cells, viable cells (proliferative and hypoxic cells),

\*Corresponding author

necrotic cells, and the evolution of matrix-degenerative enzyme (MDE) and extracellular matrix (ECM), together with chemotaxis, haptotaxis, apoptosis, nutrient distribution, and cell-to-matrix adhesion. We provide a rigorous proof of the existence of solutions of the coupled system with gradient-based and adhesion-based haptotaxis effects. In addition, we discuss finite element discretizations of the model, and we present the results of numerical experiments designed to show the relative importance and roles of various effects, including cell mobility, proliferation, necrosis, hypoxia, and nutrient concentration on the generation of MDEs and the degradation of the ECM.

*Keywords:* Tumor growth; ECM degradation; nonlocal adhesion; existence of solutions; energy method; finite elements.

AMS Subject Classification: 35K35, 35A01, 35D30, 35Q92, 65M60

## 1. Introduction

An important factor in tumor growth and invasion of healthy tissue in humans, and a first step toward metastasis, is the over expression by tumor cells of matrix-degenerative enzymes (MDEs) that erode the extracellular matrix (ECM) and allow the migration of tumor cells into the tissue. The expression of MDEs such as urokinase-plasminogen activator and matrix metalloproteinases lead to the activation of plasminogen and the degrading protein plasmin (see, e.g. Refs. 8, 46 and 42). According to Ref. 42, “matrix degradation is central to tumor pathogenesis”, and the degradation of ECM “makes room for migration as cells cannot move into regions of the tissue which are too dense”, see Ref. 46.

This study complements and extends recent work on general phase-field models reported in Refs. 21, 40 and 38. The models developed and analyzed there are intended to depict phenomena at the mesoscale and macroscale where tumor constituents are determined by fields representing volume fractions of mass concentrations of various species. Local versions of multiphase models have been proposed by several authors over the last decade, and we mention as examples the papers of Araujo and McElwain,<sup>2</sup> Garcke *et al.*,<sup>25,26</sup> Wise *et al.*,<sup>59</sup> and Lima *et al.*<sup>39</sup> Recent literature on models of tumor growth is surveyed in, for example, Refs. 4, 11 and 47. Among studies of phenomenological models of tumor cell invasion and tumor-host interaction, we mention Refs. 1, 8, 27, 31, 42, 43, 46, 48–50. Typically, in these works, the models are characterized by systems of reaction–diffusion partial differential equations describing the evolution of concentrations of densities of tumor cells, ECM, and some form of matrix-degradation agent, such as MDE.

Among other factors influencing tumor cell mobility and migration are long-range interactions due to such phenomena as cell-to-cell adhesion. Cell-to-cell adhesion involves the binding of one or more cells to each other through the reaction of proteins on the cell surfaces and is a key factor in tissue formation, stability, and the breakdown of tissue. This adhesion related deterioration of tissue is a factor contributing to the invasion and metastasis of cancer cells (see, e.g. Refs. 3, 7 and 8). Several nonlocal mathematical models of adhesion (meaning models in which events or cell concentrations at a point  $x$  in the tumor domain depend on events at points

distinct from  $x$  but within a finite neighborhood of  $x$ ) have been proposed in the literature. For an example of such cell-to-cell adhesion models, see Armstrong *et al.*,<sup>3</sup> Chaplain *et al.*,<sup>1,8</sup> Engwer *et al.*,<sup>17</sup> and Stinner *et al.*,<sup>54</sup> the latter two references addressing the effects of adhesion on tumor-cell invasion.

The inclusion of such nonlocal effects in mesoscale models of tumor growth leads to convolution terms in the Ginzburg–Landau free energy functional of the tumor and gives rise to models involving systems of nonlinear integro-differential equations. An analysis of a class of such models is discussed in a recent study, see Ref. 21.

In this work, we introduce new nonlocal, multi-species, phase-field mathematical models of tumor growth and invasion due to ECM degradation. The models depict the evolution of volume fractions of tumor cells, viable cells (proliferative and hypoxic cells), necrotic cells and the evolution of MDE and ECM, together with chemotaxis, haptotaxis, apoptosis, and nutrient distribution.

We then provide a rigorous analysis of existence of solutions of the full model system. To the authors' best knowledge, there has been no prior analytical treatment of a phase-field tumor system with ECM degradation. In Refs. 7, 17 and 54, diffusion-type tumor models with invasion due to ECM degradation are analyzed. Phase-field tumor systems without ECM degradation are treated in Garcke *et al.*<sup>23,24</sup> We combine these two aspects in one tumor growth model. The main challenge in the analysis is to control the ECM density without having a maximum principle for the phase-field tumor equations, as can be done for diffusion-type tumor models; see, e.g. Ref. 54.

In this work, we also discuss efficient finite element discretizations of the model. We present the results of numerical experiments designed to show the relative importance and roles of various effects, including cell mobility, proliferation, necrosis, hypoxia, and nutrient concentration on the generation of MDEs and the degradation of the ECM.

Following this introduction, we describe two families of haptotaxis effects in tumor models in Sec. 2, and include discussions of the role and interpretation of key terms in mass balance laws and the models of MDE production, and the evolution of ECM. After the mathematical notation is introduced in Sec. 3, a complete mathematical analysis of a local and nonlocal model is presented in Sec. 4. Finite element approximations and time-marching schemes are presented in Sec. 5 and results of numerical experiments are collected in Sec. 6. Concluding comments are provided in Sec. 7.

## 2. Models of Tumor Growth and ECM Degradation

We begin with a generalization of the setting described in Ref. 47 in which a tumor mass, contained in a region  $\Omega \subset \mathbb{R}^d$ ,  $d \in \{2, 3\}$ , at time  $t \in [0, T]$ , is viewed as a mixture of constituents of constant and equal mass density  $\varrho_0$  characterized by volume fractions  $\phi_\beta : \bar{\Omega} \times [0, T] \rightarrow \mathbb{R}$ ,  $\beta \in \{T, P, H, N\}$ . The volume fraction of



tumor cells  $\phi_T$  is made of proliferative cells ( $\phi_P$ ), which have a high probability of migration or growing in density (e.g. through mitosis and cell-to-cell and cell-to-matrix adhesion) in  $\Omega$ , hypoxic cells ( $\phi_H$ ) that are in a harsh environment with low nutrient availability, and necrotic cells ( $\phi_N$ ) that are cells that died due to the lack of nutrients. The total tumor cell volume fraction is then the sum  $\phi_T = \phi_P + \phi_H + \phi_N$ . We assume that the tumor growth is logistic, with a proliferation rate  $\lambda_T^{\text{pro}}$ , and thus the viable cells ( $\phi_V = \phi_P + \phi_H = \phi_T - \phi_N$ ) can proliferate until the capacity of the domain is reached (i.e.  $\phi_T = 1$ ). The tumor volume fraction can decrease due to two phenomena: (1) natural cell death (apoptosis) of viable cells at a rate  $\lambda_T^{\text{apo}}$ ; (2) degradation of necrotic cells at a rate  $\lambda_N^{\text{deg}}$ .

The tumor is supplied with nutrients,  $\phi_\sigma$ , such as oxygen or glucose by the vascular system that nourishes both healthy and tumor cells and which dictates the process of chemotaxis whereby cells migrate in the direction of increasing gradient of the nutrient. Here, we characterize the nutrient concentration over  $\bar{\Omega} \times [0, T]$  by a scalar field  $\phi_\sigma = \phi_\sigma(x, t)$  governed by a reaction–diffusion equation.

The tumor is embedded in a network of macromolecules called the ECM, the density of which is represented by a scalar-valued field  $\theta = \theta(x, t)$ . The ECM is non-diffusible<sup>46</sup> and its evolution can be modeled by a logistic-type evolution equation which captures the degradation of ECM due to the action of certain MDEs. When the local nutrient supply (indicated by  $\phi_\sigma$ ) drops below a certain threshold, tumor cells may enter a state of hypoxia in which enzymes are released by hypoxic cells that make room for cell migration by eroding the ECM. This process is called haptotaxis. The concentration of MDEs is characterized here by a field  $\phi_M = \phi_M(x, t)$ .

The mechanical behavior of the tumor mass must obey the balance laws of mechanics, namely the laws of conservation of mass, momentum, and energy. We will ignore thermal effects, and also, for the moment, mechanical deformations, see, e.g. Ref. 40, as well as convective flow velocities in the material time derivatives, see, e.g. Ref. 21, concentrating on mass conservation.

Under these assumptions, tumor mass ( $m_T = \int_\Omega \rho_0 \phi_T dx$ ) is conserved ( $dm_T/dt = \Gamma$ ,  $\Gamma$  being the mass supplied to by other constituents). This leads to the evolution equation,

$$\partial_t \phi_T = \text{div} J - \text{div} J_\alpha + \lambda_T^{\text{pro}} \phi_\sigma \phi_V (1 - \phi_T) - \lambda_T^{\text{apo}} \phi_V - \lambda_N^{\text{deg}} \phi_N. \quad (2.1)$$

Here,  $J$  is the mass flux,  $\lambda_T^{\text{pro}}$  and  $\lambda_T^{\text{apo}}$  are non-negative parameters governing the rate of growth and decline of tumor cell volume due to cell proliferation and apoptosis, respectively,  $\lambda_N^{\text{deg}}$  is the rate in reduction of  $\phi_N$  due to the natural removal of necrotic cells and  $J_\alpha$  is the adhesion flux (cf. Ref. 3) representing the influx of tumor mass due to cell-to-matrix effects, such as haptotaxis and cell-ECM adhesion. We refer to both  $J$  and  $J_\alpha$  as “mass” fluxes recognizing that they are actually characterized by volume fractions of constituents rather than mass concentrations because the constituent mass densities are assumed to be equal and constant and thus do not appear in the mass balance law.

According to well-established thermodynamics arguments, the mass flux is of the form,

$$J = m_T(\phi_V)\nabla\mu, \tag{2.2}$$

where  $m_T$  is the cell mobility matrix (such as  $m_T(\phi_V) = M_T\phi_V^2(1 - \phi_V)^2$ ,  $M_T > 0$ ) and  $\mu$  is the chemical potential,

$$\mu = \frac{\delta\mathcal{E}}{\delta\phi_T} = \Psi'(\phi_T) - \varepsilon_T^2\Delta\phi_T - \chi_C\phi_\sigma + \delta_T\phi_T, \tag{2.3}$$

$\mathcal{E}$  being the Ginzburg–Landau free energy functional,

$$\mathcal{E}(\phi_T, \phi_\sigma) = \int_\Omega \left( \Psi(\phi_T) + \frac{\varepsilon_T^2}{2}|\nabla\phi_T|^2 - \chi_C\phi_\sigma\phi_T + \frac{1}{2\delta_\sigma}\phi_\sigma^2 + \frac{\delta_T}{2}\phi_T^2 \right) dx. \tag{2.4}$$

$\delta\mathcal{E}/\delta\phi_T$  denotes the variational or Gateaux derivative of  $\mathcal{E}$  with respect to  $\phi_T$ . In (2.4),  $\delta_T$  is a positive parameter relating to the level of cell diffusion,  $\Psi$  is a double-well potential (such as  $\Psi(\phi_T) = \bar{E}\phi_T^2(1 - \phi_T)^2$ ,  $\bar{E} > 0$ ),  $\varepsilon_T$  is a parameter characterizing surface energy of domains separated by large gradients in  $\phi_T$ , and  $\chi_C$  is the chemotaxis parameter. If  $\mu$  is simply  $\delta_T\phi_T$ , then  $\text{div}(J)$  in (2.1) collapses to a classical diffusion term  $J = \text{div}(m_T(\phi_V)\delta_T\nabla\phi_T)$ . The potential  $\Psi$  penalizes the energy (increases it to move the system away from a minimum energy point) when  $\phi_T \notin [0, 1]$ . The presence of the Laplacian in (2.3) leads to a fourth-order evolution equation of the Cahn–Hilliard type when  $\mu$  is introduced into (2.1). The resulting model is a diffused-interface or phase-field model in which the boundary between “phases” ( $\phi_T, \phi_V, \phi_N, \dots$ ) is an implicit part of the solution.

The adhesion flux  $J_\alpha$  in (2.1) represents either a *local* gradient-based (cf. Refs. 54, 56 and 57) or a *nonlocal* adhesion-based haptotaxis effect; cf. Refs. 3, 7 and 29. Therefore, we consider the cases  $\alpha \in \{\text{loc}, \text{nonloc}\}$  with respective fluxes of the form

$$J_\alpha = \chi_H\phi_V \cdot \begin{cases} \nabla\theta, & \alpha = \text{loc}, \\ k * \theta, & \alpha = \text{nonloc}, \end{cases} \tag{2.5}$$

where  $\chi_H$  is the so-called haptotaxis parameter,  $k$  is a vector-valued kernel function and  $*$  denotes the convolution operator, which is set to zero outside of the domain  $\Omega$ . We will specify assumptions on  $k$  needed in the analysis later.

The rate-of-change of the volume fraction of necrotic cells,  $\phi_N$ , is assumed to be non-diffusive and increases when the nutrient drops below a threshold  $\sigma_{VN}$ . Also, some of the necrotic cells are removed from the tumor domain and leave as waste products. We propose to capture these phenomena by the evolution equation,

$$\partial_t\phi_N = \lambda_{VN}\mathcal{H}(\sigma_{VN} - \phi_\sigma)\phi_V - \lambda_N^{\text{deg}}\phi_N, \tag{2.6}$$

where  $\lambda_{VN}$  is a non-negative parameters and  $\mathcal{H}$  is the Heaviside step function.

To the mass balance (2.1), we add the equations governing the evolution of the nutrient, the MDE, and the ECM,

$$\partial_t \phi_\sigma = \operatorname{div}(D_\sigma(\phi_\sigma)(\delta_\sigma^{-1} \nabla \phi_\sigma - \chi_C \nabla \phi_T)) - \lambda_T^{\text{pro}} \phi_V \frac{\phi_\sigma}{\phi_\sigma + \lambda_\sigma^{\text{sat}}}, \tag{2.7}$$

$$\begin{aligned} \partial_t \phi_M &= \operatorname{div}(D_M(\phi_M) \nabla \phi_M) - \lambda_M^{\text{dec}} \phi_M \\ &\quad + \lambda_M^{\text{pro}} \phi_V \theta \frac{\sigma_H}{\sigma_H + \phi_\sigma} (1 - \phi_M) - \lambda_\theta^{\text{dec}} \theta \phi_M, \end{aligned} \tag{2.8}$$

$$\partial_t \theta = -\lambda_\theta^{\text{deg}} \theta \phi_M. \tag{2.9}$$

In (2.7)–(2.9), we assume that the nutrient volume fraction decreases as it is consumed by viable tumor cells. The production of MDE by the viable cells is proportional to the nutrient and ECM concentrations at a rate  $\lambda_M^{\text{pro}}$ . We assume that the production is higher at low-nutrient<sup>46</sup> and high ECM concentration environments. The MDE concentration decreases due to a natural decay,  $\lambda_M^{\text{dec}}$ , and the decay of the ECM,  $\lambda_\theta^{\text{dec}}$ . The quantities  $\lambda_M^{\text{pro}}$ ,  $\lambda_M^{\text{dec}}$ ,  $\lambda_\theta^{\text{dec}}$ , and  $\lambda_\theta^{\text{deg}}$  are non-negative parameters governing the rate of growth or decay of the MDE and ECM, as indicated.

### 3. Notation and Auxiliary Results

For notational simplicity, we omit the spatial domain  $\Omega$  when denoting various Banach spaces and write only  $L^p, H^m, W^{m,p}$ , where  $1 \leq p \leq \infty$  and  $1 \leq m < \infty$ . These spaces are equipped with the norms  $|\cdot|_{L^p}$ ,  $|\cdot|_{H^m}$ , and  $|\cdot|_{W^{m,p}}$ . We denote by  $(\cdot, \cdot)$  the scalar product in  $L^2$ . The brackets  $\langle \cdot, \cdot \rangle$  stand for the duality pairing on  $(H^1)' \times H^1$ . In the case of  $d$ -dimensional vector functions, we write  $[L^p]^d$ ,  $[H^m]^d$  and  $[W^{m,p}]^d$ .

For a given Banach space  $X$ , we define the Bochner space

$$L^p(0, T; X) = \left\{ u : (0, T) \rightarrow X : u \text{ Bochner measurable, } \int_0^T |u(t)|_X^p dt < \infty \right\},$$

where  $1 \leq p < \infty$ , with the norm

$$\|u\|_{L^p X} = \|u\|_{L^p(0, T; X)} = \left( \int_0^T |u(t)|_X^p dt \right)^{1/p},$$

see Refs. 18 and 52. For  $p = \infty$ , we equip  $L^\infty(0, T; X)$  with the norm

$$\|u\|_{L^\infty X} = \|u\|_{L^\infty(0, T; X)} = \operatorname{ess\,sup}_{t \in (0, T)} |u(t)|_X$$

and we introduce the Sobolev-Bochner space as

$$W^{1,p}(0, T; X) = \{u \in L^p(0, T; X) : \partial_t u \in L^p(0, T; X)\}.$$

Throughout this paper,  $C < \infty$  stands for a generic positive constant.

### 3.1. Helpful inequalities

We recall the Poincaré inequality,

$$|f - \bar{f}|_{L^2} \leq C_P |\nabla f|_{L^2} \quad \text{for all } f \in H^1, \quad (3.1)$$

where  $C_P < \infty$  and  $\bar{f} = \frac{1}{|\Omega|} \int_{\Omega} f(x) dx$  is the mean of  $f$ ; cf. Ref. 52. We also recall Young's inequality for convolutions,

$$|f * g|_{L^r} \leq |f|_{L^p} |g|_{L^q}, \quad p, q, r \geq 1, \quad 1 + \frac{1}{r} = \frac{1}{p} + \frac{1}{q}, \quad (3.2)$$

where  $f \in L^p$ ,  $g \in L^q$ ; see Theorem 4.2 in Ref. 37. Gronwall's inequality will be often employed as well.

**Lemma 3.1.** (Gronwall, cf. Lemma 3.1 in Ref. 23) *Let  $u, v \in C([0, T]; \mathbb{R}_{\geq 0})$ . If there are positive constants  $C_1, C_2 < \infty$  such that*

$$u(t) + v(t) \leq C_1 + C_2 \int_0^t u(s) ds \quad \text{for all } t \in [0, T],$$

*then it holds that*

$$u(t) + v(t) \leq C_1 e^{C_2 T} \quad \text{for all } t \in [0, T].$$

### 3.2. Embedding results

Let  $X, Y, Z$  be Banach spaces such that  $X$  is compactly embedded in  $Y$  and  $Y$  is continuously embedded in  $Z$ , i.e.  $X \hookrightarrow Y \hookrightarrow Z$ . In the proof of the existence theorem below we will rely on the Aubin–Lions compactness lemma, see Corollary 4 in Ref. 53,

$$L^p(0, T; X) \cap W^{1,1}(0, T; Z) \hookrightarrow L^p(0, T; Y), \quad 1 \leq p < \infty, \quad (3.3)$$

$$L^\infty(0, T; X) \cap W^{1,r}(0, T; Z) \hookrightarrow C([0, T]; Y), \quad r > 1.$$

Furthermore, we make use of the following continuous embeddings:

$$L^2(0, T; Y) \cap H^1(0, T; Z) \hookrightarrow C([0, T]; [Y, Z]_{1/2}), \quad (3.4)$$

$$L^\infty(0, T; Y) \cap C_w([0, T]; Z) \hookrightarrow C_w([0, T]; Y), \quad (3.5)$$

where  $[Y, Z]_{1/2}$  denotes the interpolation space between  $Y$  and  $Z$ ; cf. Theorem 3.1 in Chap. 1 in Ref. 41 and Theorem 2.1 in Ref. 55. We refer to Definition 2.1 in Chap. 1 in Ref. 41 for the definition of the interpolation space. In (3.5),  $C_w([0, T]; Y)$  denotes the space of weakly continuous functions on the interval  $[0, T]$  with values in  $Y$ .

### 3.3. General assumptions

We make the following assumptions on the domain and parameters throughout the paper.

- (A1)  $\Omega \subset \mathbb{R}^d$ , where  $d \in \{2, 3\}$ , is a bounded domain with Lipschitz boundary and  $T > 0$  is a fixed time horizon.

(A2) The mobility  $m_T \in C_b(\mathbb{R}^2)$  satisfies

$$(\exists m_0, m_\infty > 0) (\forall x \in \mathbb{R}^2) : m_0 \leq m_T(x) \leq m_\infty.$$

(A3) The functions  $D_\sigma, D_M \in C_b(\mathbb{R})$  satisfy

$$(\exists D_0, D_\infty > 0) (\forall x \in \mathbb{R}) : D_0 \leq D_\sigma(x) \leq D_\infty, \quad D_0 \leq D_M(x) \leq D_\infty.$$

(A4) The constants  $\varepsilon_T, \delta_\sigma, \lambda_M^{\text{pro}}$  are positive and fixed, while  $\chi_C, \delta_T, \sigma_{VN}, \lambda_T^{\text{apo}}, \lambda_N^{\text{deg}}$  are non-negative fixed constants.

(A5) The potential  $\Psi \in C^{1,1}(\mathbb{R})$  is non-negative, continuously differentiable, with globally Lipschitz derivative, and satisfies

$$(\exists R_1, R_2, R_3 > 0) (\forall x \in \mathbb{R}) : \Psi(x) \geq R_1|x|^2 - R_2, \quad |\Psi'(x)| \leq R_3(1 + |x|).$$

(A6) The adhesion flux  $J_\alpha$ , where  $\alpha \in \{\text{loc}, \text{nonloc}\}$ , is of the form

$$J_\alpha(\phi_T, \phi_N, \theta) = g(\phi_T, \phi_N)G(\theta)$$

with  $g \in C_b(\mathbb{R}^2)$  and  $G \in \mathcal{L}(X_\alpha; [L^2]^d)$ . The space  $X_\alpha$  is defined as

$$X_\alpha = \begin{cases} H^1 \cap L^\infty, & \alpha = \text{loc}, \\ L^2, & \alpha = \text{nonloc}. \end{cases} \tag{3.6}$$

The assumptions (A1)–(A5) are typical in tumor growth models; see, e.g. Refs. 21–24 and 26. Assumption (A6) is satisfied if we modify the adhesion flux in (2.5) by replacing  $\phi_V$  with the bounded cut-off functional  $\mathcal{C}(\phi_V) = \max(0, \min(1, \phi_V))$ . This approach is also common in tumor modeling; cf. Refs. 21 and 24. We define  $g(\phi_T, \phi_N) = \mathcal{C}(\phi_T - \phi_N)$  and

$$G(\theta) = \begin{cases} \nabla\theta, & \alpha = \text{loc}, \\ k * \theta, & \alpha = \text{nonloc}, \end{cases}$$

for a kernel function  $k \in L^1(\mathbb{R}^d)$ , which gives the following estimate on the adhesion flux:

$$\begin{aligned} |J_{\text{loc}}|_{L^2} &\leq \chi_H |\nabla\theta|_{L^2} \leq \chi_H |\theta|_{H^1 \cap L^\infty}, \\ |J_{\text{nonloc}}|_{L^2} &\leq \chi_H |k * \theta|_{L^2} \leq \chi_H |k|_{L^1} |\theta|_{L^2}, \end{aligned}$$

where we applied Young’s inequality for convolutions (3.2) in the case  $\alpha = \text{nonloc}$ . Here, we equip the intersection space  $X_{\text{loc}} = H^1 \cap L^\infty$  with the norm  $|\cdot|_{H^1 \cap L^\infty} := |\cdot|_{H^1} + |\cdot|_{L^\infty}$ .

### 3.4. Comparison to other tumor growth models

In Sec. 4, we provide a rigorous analysis of existence of solutions to a modification of the system governed by Eqs. (2.1), (2.3), (2.6)–(2.9). In our model, we combine the effects of tumor growth and invasion, ECM degradation and the separation of tumor phases into viable and necrotic cells.

The basis of phase-field tumor models, i.e. a Cahn–Hilliard equation for the tumor volume fraction  $\phi_T$  and a reaction–diffusion equation for the nutrient concentration  $\phi_\sigma$ , has been proposed in Ref. 30 and has been extended to general multiphase models in Ref. 25. The existence analysis for this model is provided in Refs. 9 and 23 and additionally, several flow models for the velocity field of the mixture have been proposed and analyzed, e.g. flow models by Darcy,<sup>10,22,24,26,32</sup> Brinkman,<sup>15,16</sup> Darcy–Forchheimer–Brinkman<sup>21</sup> and Navier–Stokes.<sup>35</sup>

To account for cell-to-matrix and cell-to-cell adhesion effects, nonlocal models have been proposed, see, e.g. Refs. 7 and 20. For the analysis of cell-to-cell adhesion models, we refer to Refs. 12, 13 and 21. To account for cell-to-matrix adhesion, one has to introduce the ECM, and up to the authors’ knowledge, there has been no coupling of the ECM density to a phase-field type tumor growth model. In Refs. 7, 17 and 54, diffusion-type tumor models with ECM degradation have been considered and analyzed.

Our model combines both the phase-field type and the effect of ECM degradation into one system. The main challenge in the analysis of our system is to control the ECM density without having a maximum principle for the phase-field tumor equations, as can be done for diffusion-type tumor models, see Ref. 54.

#### 4. Analysis of the Local and Nonlocal Model

We consider the system given by Eqs. (2.1), (2.3), (2.6)–(2.9) and modify it to perform the analysis. Since the equation for the ECM density (2.9) is given by an operator-valued ordinary differential equation, its solution can be expressed via the integral

$$\theta(x, t) = \theta(x, 0) \exp \left\{ - \int_0^t \phi_M(x, s) ds \right\} \quad \text{a.e. in } \Omega \times (0, T). \quad (4.1)$$

We will employ equation (4.1) going forward. Next, we eliminate the viable cell volume fraction  $\phi_V$  from the system by expressing it in terms of  $\phi_T$  and  $\phi_N$ , i.e.  $\phi_V = \phi_T - \phi_N$ , which yields the system

$$\begin{aligned} \partial_t \phi_T &= \operatorname{div}(m_T(\phi_T, \phi_N) \nabla \mu) - \operatorname{div}(J_\alpha(\phi_T, \phi_N, \theta)) + \phi_\sigma f_1(\phi_T, \phi_N) \\ &\quad - \lambda_T^{\text{apo}} \phi_T - \lambda_N^{\text{dec}} \phi_N, \\ \mu &= \Psi'(\phi_T) - \varepsilon_T^2 \Delta \phi_T - \chi_C \phi_\sigma + \delta_T \phi_T, \\ \partial_t \phi_N &= \mathcal{S}(\sigma_{VN} - \phi_\sigma) f_2(\phi_T, \phi_N) - \lambda_N^{\text{deg}} \phi_N, \\ \partial_t \phi_\sigma &= \operatorname{div}(D_\sigma(\phi_\sigma) (\delta_\sigma^{-1} \nabla \phi_\sigma - \chi_C \nabla \phi_T)) + (\phi_T - \phi_N) f_3(\phi_\sigma), \\ \partial_t \phi_M &= \operatorname{div}(D_M(\phi_M) \nabla \phi_M) + \theta f_4(\phi_T, \phi_N, \phi_\sigma, \phi_M) - \lambda_M^{\text{pro}} \phi_M, \\ \theta(x, t) &= \theta(x, 0) \exp \left\{ - \int_0^t f_5(\phi_M(x, s)) ds \right\}, \end{aligned} \quad (4.2)$$

where  $\lambda_N^{\text{dec}} := \lambda_N^{\text{deg}} - \lambda_T^{\text{apo}}$ . Note that we have additionally modified the equation for  $\phi_N$  by introducing the Sigmoid function  $\mathcal{S}$  as a smooth approximation of the Heaviside step function  $\mathcal{H}$ . This modification is necessary to derive  $H^1$ -estimates in space of the necrotic tumor volume fraction  $\phi_N$ . Furthermore, we have generalized the right-hand side terms in (2.1), (2.3), (2.6)–(2.8), (4.1) by introducing functions  $f_i, i \in \{1, \dots, 5\}$ , on which we make the following assumptions:

(A7<sub>nonloc</sub>) The functions  $f_1 \in C_b(\mathbb{R}^2), f_2 \in \text{Lip}(\mathbb{R}^2) \cap PC^1(\mathbb{R}^2), f_3 \in C_b(\mathbb{R}), f_4 \in C_b(\mathbb{R}^4)$ , and  $f_5 \in C_b(\mathbb{R}; \mathbb{R}_{\geq 0})$  satisfy

$$(\exists f_\infty, \bar{f}_\infty > 0) (\forall x) : |f_i(x)| \leq f_\infty, \quad \forall i \in \{1, \dots, 5\}, \quad |D_x f_2(x)| \leq \bar{f}_\infty \text{ a.e.},$$

in the case of the nonlocal model ( $\alpha = \text{nonloc}$ ), or

(A7<sub>loc</sub>) Let (A7<sub>nonloc</sub>) hold. Additionally, let  $f_5 \in \text{Lip}(\mathbb{R}; \mathbb{R}_{\geq 0})$  such that  $|D_x f_5(x)| \leq \bar{f}_\infty$  a.e.,

in case of the local model ( $\alpha = \text{loc}$ ).

Here,  $PC^1$  denotes the space of piecewise continuously differentiable functions, which ensure together with Lipschitz continuity the validity of the chain rule in the situation of a composition with a vector-valued Sobolev function; see Refs. 36 and 45. We note that the assumption on  $f_5$  is strengthened in the local case from continuity to Lipschitz continuity. Since Lipschitz continuous functions are almost everywhere differentiable, the expression  $D_x f_5$  is well-defined a.e. for  $f_5 \in \text{Lip}(\mathbb{R}; \mathbb{R}_{\geq 0})$ .

In Sec. 5, we give specific and practically relevant examples of functions  $f_1, \dots, f_5$ , which satisfy the assumptions given in (A7 $_\alpha$ ) and relate the system (4.2) to the model given by (2.1), (2.3), (2.6)–(2.9).

We couple the system of equations (4.2) to the initial data and homogeneous Neumann boundary conditions

$$\begin{cases} \partial_n \phi_T = \partial_n \phi_\sigma = \partial_n \phi_M \\ \quad = m_T(\phi_T, \phi_N) \partial_n \mu - J_\alpha(\phi_T, \phi_N, \theta) \cdot n = 0 \quad \text{on } \partial\Omega \times (0, T), \\ (\phi_T, \phi_N, \phi_\sigma, \phi_M)|_{t=0} = (\phi_{T,0}, \phi_{N,0}, \phi_{\sigma,0}, \phi_{M,0}), \end{cases} \quad (4.3)$$

where  $n$  denotes the outer unit normal of  $\partial\Omega$ .

We next define the notion of a weak solution to our system.

**Definition 4.1.** (Weak solution) Let  $\alpha \in \{\text{loc}, \text{nonloc}\}$  and  $\theta_0 \in X_\alpha$ , with  $X_\alpha$  defined as in (3.6). We call  $(\phi_T, \mu, \phi_N, \phi_\sigma, \phi_M, \theta)$  a weak solution of the initial-boundary value problem (4.2), (4.3) if

$$\begin{aligned} \phi_T &\in L^\infty(0, T; H^1) \cap H^1(0, T; (H^1)'), \quad \mu \in L^2(0, T; H^1), \\ \phi_N &\in L^\infty(0, T; H^1) \cap H^1(0, T; L^2), \\ \phi_\sigma, \phi_M &\in L^2(0, T; H^1) \cap L^\infty(0, T; L^2) \cap H^1(0, T; (H^1)'), \\ \theta &\in \begin{cases} W^{1,\infty}(0, T; L^\infty) \cap H^1(0, T; H^1) & \text{for } \alpha = \text{loc}, \\ W^{1,\infty}(0, T; L^2) & \text{for } \alpha = \text{nonloc}, \end{cases} \end{aligned}$$

and it holds that

$$\begin{aligned} &\langle \partial_t \phi_T, \varphi_1 \rangle + (m_T(\phi_T, \phi_N) \nabla \mu, \nabla \varphi_1) - (J_\alpha(\phi_T, \phi_N, \theta), \nabla \varphi_1) \\ &\quad - (\phi_\sigma f_1(\phi_T, \phi_N), \varphi_1) + (\lambda_T^{\text{apo}} \phi_T + \lambda_N^{\text{dec}} \phi_N, \varphi_1) = 0, \end{aligned} \tag{4.4a}$$

$$\begin{aligned} &-(\mu, \varphi_2) + (\Psi'(\phi_T), \varphi_2) + \varepsilon_T^2 (\nabla \phi_T, \nabla \varphi_2) \\ &\quad - \chi_C(\phi_\sigma, \varphi_2) + \delta_T(\phi_T, \varphi_2) = 0, \end{aligned} \tag{4.4b}$$

$$(\partial_t \phi_N, \varphi_3) - (\mathcal{S}(\sigma_{VN} - \phi_\sigma) f_2(\phi_T, \phi_N), \varphi_3) + \lambda_N^{\text{deg}}(\phi_N, \varphi_3) = 0, \tag{4.4c}$$

$$\begin{aligned} &\langle \partial_t \phi_\sigma, \varphi_4 \rangle + (D_\sigma(\phi_\sigma) \nabla \varphi_4, \delta_\sigma^{-1} \nabla \phi_\sigma - \chi_C \nabla \phi_T) \\ &\quad + ((\phi_T - \phi_N) f_3(\phi_\sigma), \varphi_4) = 0, \end{aligned} \tag{4.4d}$$

$$\begin{aligned} &\langle \partial_t \phi_M, \varphi_5 \rangle + (D_M(\phi_M) \nabla \phi_M, \nabla \varphi_5) - (\theta f_4(\phi_T, \phi_N, \phi_M, \phi_\sigma), \varphi_5) \\ &\quad + \lambda_M^{\text{pro}}(\phi_M, \varphi_5) = 0, \end{aligned} \tag{4.4e}$$

a.e. in time, for all test functions  $\varphi_1, \varphi_2, \varphi_4, \varphi_5 \in H^1$ ,  $\varphi_3 \in L^2$ , and

$$\theta(x, t) = \theta_0(x) \exp \left\{ - \int_0^t f_5(\phi_M(x, s)) ds \right\} \text{ a.e. in } \Omega \times (0, T), \tag{4.4f}$$

where

$$(\phi_T, \phi_N, \phi_\sigma, \phi_M)|_{t=0} = (\phi_{T,0}, \phi_{N,0}, \phi_{\sigma,0}, \phi_{M,0}).$$

#### 4.1. Existence of solutions

Our first goal is to prove existence of solutions for the local and nonlocal model.

**Theorem 4.1.** (Existence of weak solutions) *Let  $\alpha \in \{\text{loc}, \text{nonloc}\}$  and  $\theta_0 \in X_\alpha$ , with  $X_\alpha$  defined as in (3.6). Furthermore, let assumptions (A1)–(A6), (A7 $_\alpha$ ) hold and let the initial data have the following regularity:*

$$\phi_{T,0} \in H^1, \quad \phi_{N,0} \in H^1, \quad \phi_{\sigma,0} \in L^2, \quad \phi_{M,0} \in L^2.$$

*Then there exists a solution  $(\phi_T, \mu, \phi_N, \phi_\sigma, \phi_M, \theta)$  of the problem (4.2) in the sense of Definition 4.1. Additionally, the following energy estimate holds:*

$$\begin{aligned} &\|\phi_T\|_{L^\infty H^1}^2 + \|\mu\|_{L^2 H^1}^2 + \|\phi_N\|_{L^\infty H^1}^2 + \|\phi_\sigma\|_{L^\infty L^2}^2 + \|\phi_\sigma\|_{L^2 H^1}^2 \\ &\quad + \|\phi_M\|_{L^\infty L^2}^2 + \|\phi_M\|_{L^2 H^1}^2 + \|\theta\|_{L^\infty X_\alpha}^2 \leq C(T)(1 + \text{IC}), \end{aligned}$$

where

$$\text{IC} = |\phi_{T,0}|_{H^1}^2 + |\phi_{N,0}|_{H^1}^2 + |\phi_{\sigma,0}|_{L^2}^2 + |\phi_{M,0}|_{L^2}^2 + |\theta_0|_{X_\alpha}^2.$$



**4.2. Galerkin approximations in space**

To prove existence of solutions, we employ Galerkin approximations in space, following the strategy in e.g., Refs. 21, 23 and 26. We construct approximate solutions by considering eigenfunctions  $\{w_k\}_{k \in \mathbb{N}}$  of the Neumann-Laplacian:

$$\begin{cases} -\Delta w_k = \lambda_k w_k, & \text{in } \Omega, \\ \frac{\partial w_k}{\partial n} = 0, & \text{on } \partial\Omega. \end{cases} \tag{4.5}$$

It is known that the eigenfunctions of the Neumann-Laplacian form an orthonormal basis of  $L^2$  and an orthogonal basis of  $H^1$ ; cf. Theorem II.6.6 in Ref. 5. We then define the discrete space by

$$V_n = \text{span}\{w_1, \dots, w_n\}. \tag{4.6}$$

We seek approximate solutions of the form

$$\begin{aligned} \phi_T^n(x, t) &= \sum_{j=1}^n \alpha_j(t) w_j(x), & \phi_N^n(x, t) &= \sum_{j=1}^n \beta_j(t) w_j(x), \\ \phi_\sigma^n(x, t) &= \sum_{j=1}^n \gamma_j(t) w_j(x), & \phi_M^n(x, t) &= \sum_{j=1}^n \delta_j(t) w_j(x), \end{aligned} \tag{4.7}$$

where  $\alpha_j, \beta_j, \gamma_j, \delta_j : (0, T) \rightarrow \mathbb{R}$  will be determined by a system of ordinary differential equations. We choose the approximations of the initial conditions as follows:

$$\begin{aligned} \phi_{T,0}^n &= \Pi_{V_n} \phi_{T,0}, & \phi_{N,0}^n &= \Pi_{V_n} \phi_{N,0}, \\ \phi_{\sigma,0}^n &= \Pi_{V_n} \phi_{\sigma,0}, & \phi_{M,0}^n &= \Pi_{V_n} \phi_{M,0}. \end{aligned} \tag{4.8}$$

Above,  $\Pi_{V_n}$  denotes the  $L^2$  projection operator:  $(\Pi_{V_n} u, v) = (u, v)$  for all  $v \in V_n$ . Note that for all  $n \in \mathbb{N}$  it holds that

$$\begin{aligned} |\phi_{T,0}^n|_{H^1} &\leq |\phi_{T,0}|_{H^1}, & |\phi_{N,0}^n|_{H^1} &\leq |\phi_{N,0}|_{H^1}, \\ |\phi_{\sigma,0}^n|_{L^2} &\leq |\phi_{\sigma,0}|_{L^2}, & |\phi_{M,0}^n|_{L^2} &\leq |\phi_{M,0}|_{L^2}, \end{aligned} \tag{4.9}$$

see, e.g. Lemma 7.5 in Ref. 51.

The semi-discretization of the problem (4.2) is then given by

$$\begin{aligned} (\partial_t \phi_T^n, \varphi^n) &+ (m_T(\phi_T^n, \phi_N^n) \nabla \mu^n, \nabla \varphi^n) - (J_\alpha(\phi_T^n, \phi_N^n, \theta^n), \nabla \varphi^n) \\ &- (\phi_\sigma^n f_1(\phi_T^n, \phi_N^n), \varphi^n) + (\lambda_T^{\text{apo}} \phi_T^n + \lambda_N^{\text{dec}} \phi_N^n, \varphi^n) = 0, \end{aligned} \tag{4.10a}$$

$$\begin{aligned} -(\mu^n, \varphi^n) &+ (\Psi'(\phi_T^n), \varphi^n) + \varepsilon_T^2 (\nabla \phi_T^n, \nabla \varphi^n) - \chi_C(\phi_\sigma^n, \varphi^n) \\ &+ \delta_T(\phi_T^n, \varphi^n) = 0, \end{aligned} \tag{4.10b}$$

$$(\partial_t \phi_N^n, \varphi^n) - (\mathcal{S}(\sigma_{VN} - \phi_\sigma^n) f_2(\phi_T^n, \phi_N^n), \varphi^n) + \lambda_N^{\text{deg}}(\phi_N^n, \varphi^n) = 0, \tag{4.10c}$$

$$\begin{aligned} (\partial_t \phi_\sigma^n, \varphi^n) &+ (D_\sigma(\phi_\sigma^n)(\delta_\sigma^{-1} \nabla \phi_\sigma^n - \chi_C \nabla \phi_T^n), \nabla \varphi^n) \\ &+ ((\phi_T^n - \phi_N^n) f_3(\phi_\sigma^n), \varphi^n) = 0, \end{aligned} \tag{4.10d}$$

$$\begin{aligned}
 &(\partial_t \phi_M^n, \varphi^n) + (D_M(\phi_M^n) \nabla \phi_M^n, \nabla \varphi^n) - (\theta^n f_4(\phi_T^n, \phi_N^n, \phi_\sigma^n, \phi_M^n), \varphi^n) \\
 &+ \lambda_M^{\text{pro}}(\phi_M^n, \varphi^n) = 0,
 \end{aligned} \tag{4.10e}$$

$$\theta^n(x, t) = \theta_0(x) \exp \left\{ - \int_0^t f_5(\phi_M^n(x, s)) ds \right\}, \tag{4.10f}$$

for all  $\varphi^n \in V_n$ , with

$$(\phi_T^n, \phi_N^n, \phi_\sigma^n, \phi_M^n)|_{t=0} = (\phi_{T,0}^n, \phi_{N,0}^n, \phi_{\sigma,0}^n, \phi_{M,0}^n). \tag{4.11}$$

The system (4.10)–(4.11) is equivalent to an initial value problem for a system of integro-differential equations for the unknown function  $\xi = (\xi_1, \dots, \xi_n)$ , where  $\xi_i = (\alpha_i, \beta_i, \gamma_i, \delta_i)$ ,  $i \in \{1, \dots, n\}$ , which can be equivalently written as

$$\begin{aligned}
 \partial_t \xi_i(t) &= F^i(t, \xi(t), K\xi(t)) \\
 &= \widehat{F}^i(t, \xi(t)) + \widetilde{F}^i(t, \xi(t), K\xi(t)),
 \end{aligned}$$

for all  $i \in \{1, \dots, n\}$ , where  $K\xi(t) = \int_0^t f_5(\sum_{j=1}^n \delta_j(s) w_j) ds$  and

$$\begin{aligned}
 \widetilde{F}_1^i &= \int_\Omega g(\phi_T^n(x, t), \phi_N^n(x, t)) G(\theta_0 \exp\{-K\xi(t)\}) \cdot \nabla w_i \, dx, \\
 \widetilde{F}_2^i &= \widetilde{F}_3^i = 0, \\
 \widetilde{F}_4^i &= \int_\Omega \theta_0 \exp\{-K\xi(t)\} f_4(\phi_T^n(x, t), \phi_N^n(x, t), \phi_\sigma^n(x, t), \phi_M^n(x, t)) w_i \, dx.
 \end{aligned}$$

We note that the given functions  $\Psi'$ ,  $m_T$ ,  $D_M$ ,  $D_\sigma$ ,  $f_1, \dots, f_5$  are all continuous. Therefore, on account of an extension of the Cauchy–Peano theorem for integro-differential equations, see Theorem 7.1 in Appendix A below, we obtain a solution of (4.10)–(4.11) such that

$$\begin{aligned}
 &(\phi_T^n, \mu^n, \phi_N^n, \phi_\sigma^n, \phi_M^n, \theta^n) \in C^1([0, T_n]; V_n) \times C([0, T_n]; V_n) \\
 &\quad \times (C^1([0, T_n]; V_n))^3 \times C([0, T_n]; X_\alpha),
 \end{aligned}$$

for sufficiently short time  $T_n \leq T$ . The upcoming energy estimate will allow us to extend the existence interval to  $[0, T]$ .

### 4.3. Energy estimates

Our next goal is to derive an energy estimate for solutions of (4.10a)–(4.10f), (4.11) that is uniform with respect to  $n$ . To this end, we test Eqs. (4.10a)–(4.10e) with different test functions.

#### Estimates for $\theta^n$ .

Since the integral and the exponential function are continuous and the function  $f_5$  is non-negative by assumption (A7 $_\alpha$ ), we conclude

$$|\theta^n(t)|_{L^p} \leq |\theta_0|_{L^p}, \tag{4.12}$$

for all  $t \leq T_n$ . Above,  $p \in [1, 2]$  for  $\theta_0 \in X_{\text{nonloc}} = L^2$  and  $p \in [1, \infty]$  for  $\theta_0 \in X_{\text{loc}} = H^1 \cap L^\infty$ .

In the nonlocal case, this uniform bound of  $\theta^n$  is already enough for the upcoming energy estimates. We recall that the term  $J_\alpha(\phi_T^n, \phi_N^n, \theta^n)$  in the equation for  $\phi_T^n$  can be expressed as  $g(\phi_T^n, \phi_N^n)G(\theta^n)$  on account of assumption (A6). Since the operator  $G$  requires an argument in  $X_\alpha$ , we still have to derive an estimate of  $\theta^n$  in  $H^1$  when  $\alpha = \text{loc}$ .

$\alpha = \text{loc}$ : By the product rule and the chain rule for the composition of a bounded Lipschitz continuous function with a Sobolev function, see Ref. 60, we further infer that

$$\nabla\theta^n(t) = \left( \nabla\theta_0 - \theta_0 \int_0^t f_5'(\phi_M^n(s)) \nabla\phi_M^n(s) ds \right) \cdot \exp \left\{ - \int_0^t f_5(\phi_M^n(s)) ds \right\}, \tag{4.13}$$

for all  $t \in [0, T_n]$ . From here, using assumption (A7<sub>loc</sub>), we obtain the bound for the gradient of the ECM density

$$|\nabla\theta^n(t)|_{L^2} \leq |\nabla\theta_0|_{L^2} + |\theta_0|_{L^\infty} \sqrt{T_n} \bar{f}_\infty \|\nabla\phi_M^n\|_{L_t^2 L^2},$$

for  $t \in [0, T_n]$ , where we have used the abbreviation  $L_t^2 L^2$  for  $L^2(0, t; L^2(\Omega))$ . By combining this estimate and the estimate (4.12) with  $p = 2$ , it follows for all  $t \in [0, T_n]$  that

$$|\theta^n(t)|_{H^1}^2 \leq 2|\theta_0|_{H^1}^2 + 2T \bar{f}_\infty^2 |\theta_0|_{L^\infty}^2 \|\nabla\phi_M^n\|_{L_t^2 L^2}^2. \tag{4.14}$$

**Estimates for  $\phi_M^n$ .**

Testing equation (4.10e) with  $\varphi^n = \phi_M^n(t) \in V_n$  and recalling assumption (A3) as well as the bound (4.12) for  $\theta^n$  yields

$$\frac{1}{2} \frac{d}{dt} |\phi_M^n|_{L^2}^2 + D_0 |\nabla\phi_M^n|_{L^2}^2 + \lambda_M^{\text{pro}} |\phi_M^n|_{L^2}^2 \leq \frac{f_\infty}{2} (|\theta_0|_{L^2}^2 + |\phi_M^n|_{L^2}^2). \tag{4.15}$$

After integrating over  $(0, t)$ , where  $t \leq T_n$ , we conclude by the Gronwall lemma that

$$|\phi_M^n(t)|_{L^2}^2 + \|\nabla\phi_M^n\|_{L_t^2 L^2}^2 + \|\phi_M^n\|_{L_t^2 L^2}^2 \leq C(T_n) (|\phi_{M,0}^n|_{L^2}^2 + |\theta_0|_{L^2}^2). \tag{4.16}$$

Adding to this estimate (4.12) and (4.14) for  $\alpha = \text{loc}$ , or (4.12) for  $\alpha = \text{nonloc}$ , we get

$$|\theta^n(t)|_{X_\alpha}^2 + |\phi_M^n(t)|_{L^2}^2 + \|\phi_M^n\|_{L_t^2 H^1}^2 \leq C(T_n) (|\theta_0|_{X_\alpha}^2 + |\phi_{M,0}^n|_{L^2}^2). \tag{4.17}$$

Note that above we have also employed the uniform bound for the approximate initial data  $\phi_{M,0}^n$  given in (4.9).

**Estimates for  $\phi_T^n, \mu^n, \phi_\sigma^n$ .**

Testing equation (4.10a) with  $\mu^n(t) + \chi_C \phi_\sigma^n(t)$ , Eq. (4.10b) with  $-\partial_t \phi_T^n(t)$ , and Eq. (4.10d) with  $K_1 \phi_\sigma^n(t)$ , where  $K_1 > 0$ , and adding the resulting equations yields

$$\begin{aligned} & \frac{d}{dt} \left[ |\Psi(\phi_T^n)|_{L^1} + \frac{\varepsilon_T^2}{2} |\nabla \phi_T^n|_{L^2}^2 + \frac{\delta_T}{2} |\phi_T^n|_{L^2}^2 + \frac{K_1}{2} |\phi_\sigma^n|_{L^2}^2 \right] \\ & + \left| \sqrt{m_T(\phi_T^n, \phi_N^n)} \nabla \mu^n \right|_{L^2}^2 + K_1 \delta_\sigma^{-1} \left| \sqrt{D_\sigma(\phi_\sigma^n)} \nabla \phi_\sigma^n \right|_{L^2}^2 \\ & = -\chi_C (m_T(\phi_T^n, \phi_N^n) \nabla \mu^n, \nabla \phi_\sigma^n) + (J_\alpha(\phi_T^n, \phi_N^n, \theta^n), \nabla(\mu^n + \chi_C \phi_\sigma^n)) \\ & + (f_1(\phi_T^n, \phi_N^n) \phi_\sigma^n - \lambda_T^{\text{apo}} \phi_T^n - \lambda_N^{\text{dec}} \phi_N^n, \mu^n + \chi_C \phi_\sigma^n) \\ & + K_1 \chi_C (D_\sigma(\phi_\sigma^n) \nabla \phi_T^n, \nabla \phi_\sigma^n) - K_1 ((\phi_T^n - \phi_N^n) f_3(\phi_\sigma^n), \phi_\sigma^n) =: \text{RHS}. \end{aligned} \tag{4.18}$$

We can then estimate the right-hand side of (4.18) by using assumptions (A2), (A6), (A7 $_\alpha$ ), and Hölder’s inequality as follows:

$$\begin{aligned} \text{RHS} & \leq \chi_C m_\infty |\nabla \mu^n|_{L^2} |\nabla \phi_\sigma^n|_{L^2} + C |\theta^n|_{X_\alpha} (|\nabla \mu^n|_{L^2} + \chi_C |\nabla \phi_\sigma^n|_{L^2}) \\ & + (f_\infty |\phi_\sigma^n|_{L^2} + \lambda_T^{\text{apo}} |\phi_T^n|_{L^2} + |\lambda_N^{\text{dec}}| \cdot |\phi_N^n|_{L^2}) (|\mu^n|_{L^2} + \chi_C |\phi_\sigma^n|_{L^2}) \\ & + K_1 \chi_C D_\infty |\nabla \phi_T^n|_{L^2} |\nabla \phi_\sigma^n|_{L^2} + K_1 f_\infty (|\phi_T^n|_{L^2} + |\phi_N^n|_{L^2}) |\phi_\sigma^n|_{L^2}. \end{aligned} \tag{4.19}$$

We note that we need a bound on  $|\mu^n|_{L^2}$  to further estimate (4.19). Testing (4.10b) with  $1 \in H^1$  and taking into account assumption (A7) on the function  $\Psi$  results in

$$\begin{aligned} |\mu^n|_{L^1} & \leq \int_\Omega |\Psi'(\phi_T^n)| dx + \chi_C |\phi_\sigma^n|_{L^1} + \delta_T |\phi_T^n|_{L^1} \\ & \leq R_3 (|\Omega| + |\phi_T^n|_{L^1}) + \chi_C |\phi_\sigma^n|_{L^1} + \delta_T |\phi_T^n|_{L^1} \\ & \leq R_3 |\Omega| + (R_3 + \delta_T) |\Omega|^{1/2} |\phi_T^n|_{L^2} + \chi_C |\Omega|^{1/2} |\phi_\sigma^n|_{L^2}, \end{aligned}$$

we refer also to Ref. 22 where a similar argument is employed. By the Poincaré inequality (3.1), we then conclude

$$\begin{aligned} |\mu^n|_{L^2} & \leq |\mu^n - \overline{\mu^n}|_{L^2} + |\overline{\mu^n}|_{L^2} \leq C_P |\nabla \mu^n|_{L^2} + \frac{1}{|\Omega|} |\mu^n|_{L^1} \\ & \leq C_P |\nabla \mu^n|_{L^2} + R_3 + (R_3 + \delta_T) |\Omega|^{-1/2} |\phi_T^n|_{L^2} + \chi_C |\Omega|^{-1/2} |\phi_\sigma^n|_{L^2}. \end{aligned} \tag{4.20}$$

Therefore, by using (4.20), we can further estimate the right-hand side of (4.18) as follows:

$$\begin{aligned} \text{RHS} & \leq \chi_C m_\infty |\nabla \mu^n|_{L^2} |\nabla \phi_\sigma^n|_{L^2} + C |\theta^n|_{X_\alpha} (|\nabla \mu^n|_{L^2} + \chi_C |\nabla \phi_\sigma^n|_{L^2}) \\ & + (f_\infty |\phi_\sigma^n|_{L^2} + \lambda_T^{\text{apo}} |\phi_T^n|_{L^2} + |\lambda_N^{\text{dec}}| \cdot |\phi_N^n|_{L^2}) \{ C_P |\nabla \mu^n|_{L^2} + R_3 \\ & + (R_3 + \delta_T) |\Omega|^{-1/2} |\phi_T^n|_{L^2} + \chi_C |\Omega|^{-1/2} |\phi_\sigma^n|_{L^2} + \chi_C |\phi_\sigma^n|_{L^2} \} \\ & + K_1 \chi_C D_\infty |\nabla \phi_T^n|_{L^2} |\nabla \phi_\sigma^n|_{L^2} + K_1 f_\infty (|\phi_T^n|_{L^2} + |\phi_N^n|_{L^2}) |\phi_\sigma^n|_{L^2}. \end{aligned}$$

By employing Young’s inequality, we get

$$\begin{aligned} \text{RHS} &\leq \left(\frac{m_0}{2} + 4\varepsilon\right) |\nabla\mu^n|_{L^2}^2 + \left(\frac{\chi_C^2 m_\infty^2}{2m_0} + \varepsilon\right) |\nabla\phi_\sigma^n|_{L^2}^2 \\ &\quad + C(1 + |\phi_\sigma^n|_{L^2}^2 + |\phi_T^n|_{L^2}^2 + |\nabla\phi_T^n|_{L^2}^2 + |\phi_N^n|_{L^2}^2 + |\theta^n|_{X_\alpha}^2), \end{aligned}$$

where  $\varepsilon > 0$ . Introducing this estimate of the right-hand side into (4.18) and recalling assumptions (A2) and (A3) yields

$$\begin{aligned} &\frac{d}{dt} \left[ |\Psi(\phi_T^n)|_{L^1} + \frac{\varepsilon_T^2}{2} |\nabla\phi_T^n|_{L^2}^2 + \frac{\delta_T}{2} |\phi_T^n|_{L^2}^2 + \frac{K_1}{2} |\phi_\sigma^n|_{L^2}^2 \right] \\ &\quad + \left(\frac{m_0}{2} - 4\varepsilon\right) |\nabla\mu^n|_{L^2}^2 + \left(K_1 D_0 \delta_\sigma^{-1} - \frac{\chi_C^2 m_\infty^2}{2m_0} - \varepsilon\right) |\nabla\phi_\sigma^n|_{L^2}^2 \\ &\leq C(1 + |\theta^n|_{X_\alpha}^2 + |\phi_\sigma^n|_{L^2}^2 + |\Psi(\phi_T^n)|_{L^1} + |\nabla\phi_T^n|_{L^2}^2 + |\phi_N^n|_{L^2}^2), \end{aligned} \tag{4.21}$$

where we have first picked  $\varepsilon \in (0, m_0/8)$  and then chosen  $K_1$  sufficiently large so that

$$K_2 := K_1 D_0 \delta_\sigma^{-1} - \frac{\chi_C^2 m_\infty^2}{2m_0} - \varepsilon > 0. \tag{4.22}$$

**Estimates for  $\phi_N^n$ .**

Testing equation (4.10c) with  $\phi_N^n(t) \in V_n$  yields, after some standard manipulations,

$$\frac{1}{2} \frac{d}{dt} |\phi_N^n|_{L^2}^2 + \lambda_N^{\text{deg}} |\phi_N^n|_{L^2}^2 \leq \frac{f_\infty}{2} (|\phi_N|_{L^2}^2 + |\Omega|). \tag{4.23}$$

This estimate would be enough to absorb the  $\phi_N^n$  term on the right-hand side of (4.21). However, we here also derive an estimate of  $\phi_N^n$  in the space  $L^\infty(0, T; H^1)$ , which will enable us to perform the limit process as  $n \rightarrow \infty$  later on. Testing (4.10c) with  $-\Delta\phi_N^n(t) \in V_n$  and performing integration by parts results in

$$\begin{aligned} &\frac{1}{2} \frac{d}{dt} |\nabla\phi_N^n|_{L^2}^2 + \lambda_N^{\text{deg}} |\nabla\phi_N^n|_{L^2}^2 \\ &\quad = \lambda_{VN} (\nabla(\mathcal{S}(\sigma_{VN} - \phi_\sigma^n) f_2(\phi_T^n, \phi_N^n)), \nabla\phi_N^n) \\ &\quad = (-\nabla\phi_\sigma^n \mathcal{S}'(\sigma_{VN} - \phi_\sigma) f_2(\phi_T^n, \phi_N^n), \nabla\phi_N^n) \\ &\quad \quad + (\mathcal{S}(\sigma_{VN} - \phi_\sigma^n) \nabla\phi_T^n \partial_1 f_2(\phi_T^n, \phi_N^n), \nabla\phi_N^n) \\ &\quad \quad + (\mathcal{S}(\sigma_{VN} - \phi_\sigma^n) \nabla\phi_N^n \partial_2 f_2(\phi_T^n, \phi_N^n), \nabla\phi_N^n), \end{aligned}$$

where we have applied the chain rule for the composition of a bounded Lipschitz, piecewise continuously differentiable function and a vector-valued Sobolev function; see Refs. 36 and 45. After employing the same type of arguments as before, this

estimate implies that

$$\frac{d}{dt} |\nabla \phi_N^n|_{L^2}^2 + |\nabla \phi_N^n|_{L^2}^2 \leq \frac{K_2}{2} |\nabla \phi_\sigma^n|_{L^2}^2 + C(K_2) \cdot (|\nabla \phi_N^n|_{L^2}^2 + |\nabla \phi_T^n|_{L^2}^2), \quad (4.24)$$

where  $K_2$  is the positive constant in (4.22).

**Final energy estimate.**

Combining the upper bounds (4.20), (4.21), (4.23), and (4.24) yields

$$\begin{aligned} & \frac{d}{dt} [|\Psi(\phi_T^n)|_{L^1} + |\nabla \phi_T^n|_{L^2}^2 + |\phi_T^n|_{L^2}^2 + |\phi_\sigma^n|_{L^2}^2 + |\phi_N^n|_{H^1}^2] + |\mu^n|_{H^1}^2 + |\nabla \phi_\sigma^n|_{L^2}^2 \\ & \leq C(1 + |\theta^n|_{X_\alpha}^2 + |\phi_\sigma^n|_{L^2}^2 + |\Psi(\phi_T^n)|_{L^1} + |\nabla \phi_T^n|_{L^2}^2 + |\phi_N^n|_{H^1}^2). \end{aligned} \quad (4.25)$$

After integrating (4.25) over  $(0, t)$ , where  $t \leq T_n$  and taking into account estimate (4.17), we have

$$\begin{aligned} & |\Psi(\phi_T^n(t))|_{L^1} + |\nabla \phi_T^n(t)|_{L^2}^2 + |\phi_\sigma^n(t)|_{L^2}^2 + |\phi_N^n(t)|_{H^1}^2 + \|\mu^n\|_{L_t^2 H^1}^2 + \|\nabla \phi_\sigma^n\|_{L_t^2 L^2}^2 \\ & \leq IC^n + C(T_n) \cdot (1 + |\phi_\sigma^n|_{L^2}^2 + |\Psi(\phi_T^n)|_{L^1} + |\nabla \phi_T^n|_{L^2}^2 + |\phi_N^n|_{H^1}^2). \end{aligned} \quad (4.26)$$

Above, we have introduced the following constant that depends on the approximate initial data to simplify the notation:

$$IC^n = |\phi_{T,0}^n|_{H^1}^2 + |\Psi(\phi_{T,0}^n)|_{L^1} + |\phi_{\sigma,0}^n|_{L^2}^2 + |\phi_{N,0}^n|_{L^2}^2 + |\phi_{M,0}^n|_{L^2}^2 + |\theta_0|_{X_\alpha}^2.$$

We can employ the fact that

$$|\Psi(\phi_{T,0}^n)|_{L^1} \leq C + C|\phi_{T,0}^n|_{L^2}^2 \leq C + C|\phi_{T,0}|_{L^2}^2,$$

and thus,  $IC^n$  can be estimated in terms of the initial data as follows:

$$IC^n \leq IC = |\phi_{T,0}|_{H^1}^2 + C + C|\phi_{T,0}|_{L^2}^2 + |\phi_{\sigma,0}|_{L^2}^2 + |\phi_{N,0}|_{H^1}^2 + |\phi_{M,0}|_{L^2}^2 + |\theta_0|_{X_\alpha}^2,$$

where the constant  $C$  does not depend on  $n$ . By adding (4.17) to (4.26), applying Gronwall’s inequality to the resulting estimate, and taking the supremum over  $(0, T_n)$ , we get

$$\begin{aligned} & \|\Psi(\phi_T^n)\|_{L_t^\infty L^1} + \|\nabla \phi_T^n\|_{L_t^\infty L^2}^2 + \|\phi_\sigma^n\|_{L_t^\infty L^2}^2 + \|\phi_N^n\|_{L_t^\infty H^1}^2 + \|\theta^n\|_{L_t^\infty X_\alpha}^2 \\ & \quad + \|\phi_M^n\|_{L_t^\infty L^2}^2 + \|\phi_M^n\|_{L_t^2 H^1}^2 + \|\mu^n\|_{L_t^2 H^1}^2 + \|\phi_\sigma^n\|_{L_t^2 H^1}^2 \\ & \leq C(T)(1 + IC), \end{aligned} \quad (4.27)$$

for all  $t \in [0, T_n]$ . The right-hand side of this estimate is independent of  $T_n$ , which allows to extend the existence interval to  $[0, T]$ ; see also Sec. I.6.VI in Ref. 58.

We remark that from (4.27) we can get a uniform bound for  $\phi_T^n$  in  $L^\infty(0, T; H^1)$  by noting that

$$\begin{aligned} |\phi_T^n(t)|_{L^2}^2 & \leq 2C_P^2 |\nabla \phi_T^n(t)|_{L^2}^2 + 2 \frac{1}{|\Omega|^2} |\phi_T^n(t)|_{L^1}^2 \\ & \leq 2C_P^2 |\nabla \phi_T^n(t)|_{L^2}^2 + 2 \frac{1}{|\Omega|^2} \frac{1}{R_1} (|\Psi(\phi_T^n(t))|_{L^1} + R_2), \end{aligned} \quad (4.28)$$

for all  $t \in [0, T]$ . Above, we have made use of the Poincaré inequality (3.1) and assumption (A5) on the potential  $\Psi$ .

**Additional estimates of the time derivatives of  $\theta^n$ ,  $\phi_N^n$ ,  $\phi_T^n$ , and  $\phi_\sigma^n$ .**

The derived energy estimate (4.27) implies the boundedness of the Galerkin solution  $(\phi_T^n, \mu^n, \phi_N^n, \phi_\sigma^n, \phi_M^n)$  and of  $\theta^n$  in appropriate Banach spaces, which in turn implies the weak and weak-\* convergence of subsequences. We consider taking the limit  $n \rightarrow \infty$  in the Galerkin system (4.10). Since the equations in our system are nonlinear in  $\phi_T^n$ ,  $\phi_N^n$ ,  $\phi_\sigma^n$  and  $\phi_M^n$ , we want to acquire strong convergence of the respective subsequences. We can obtain strong convergence from compact embeddings (3.3), which requires the boundedness of the respective time derivative. We derive these estimates in this section.

Testing equation (4.10c) with  $\partial_t \phi_N^n(t) \in V_n$  and employing Young’s inequality yields

$$(1 - \varepsilon) \|\partial_t \phi_N^n\|_{L^2 L^2}^2 + \frac{\lambda_N^{\text{deg}}}{2} \|\phi_N\|_{L^\infty L^2}^2 \leq C(T, \varepsilon) + \frac{\lambda_N^{\text{deg}}}{2} |\phi_{N,0}|_{L^2}^2, \tag{4.29}$$

where  $\varepsilon \in (0, 1)$ . Furthermore, from Eq. (4.10d) we find that for all  $\varphi \in L^2(0, T; H^1)$  it holds that

$$\begin{aligned} \int_0^T \int_\Omega \partial_t \phi_\sigma^n \varphi \, dx dt &\leq (D_\infty \delta_\sigma^{-1} \|\nabla \phi_\sigma^n\|_{L^2 L^2} + D_\infty \chi_C \|\nabla \phi_T^n\|_{L^2 L^2} \\ &\quad + f_\infty (\|\phi_N^n\|_{L^2 L^2} + \|\phi_T^n\|_{L^2 L^2})) \|\varphi\|_{L^2 H^1}, \end{aligned}$$

from which we also get that

$$\|\partial_t \phi_\sigma^n\|_{L^2(H^1)'} \leq C(\|\nabla \phi_\sigma^n\|_{L^2 L^2} + \|\nabla \phi_T^n\|_{L^2 L^2} + \|\phi_N^n\|_{L^2 L^2}), \tag{4.30}$$

where the constant  $C > 0$  does not depend on  $n$ . Similarly, from Eq. (4.10a) we have

$$\begin{aligned} \int_0^T \int_\Omega \partial_t \phi_T^n \varphi \, dx dt &\leq (m_\infty \|\nabla \mu^n\|_{L^2 L^2} + C \|\theta^n\|_{L^2 L^2} + f_\infty \|\phi_\sigma^n\|_{L^2 L^2} \\ &\quad + \lambda_T^{\text{apo}} \|\phi_T^n\|_{L^2 L^2} + |\lambda_N^{\text{dec}}| \cdot \|\phi_N^n\|_{L^2 L^2}) \|\varphi\|_{L^2 H^1}, \end{aligned}$$

and from Eq. (4.10e)

$$\int_0^T \int_\Omega \partial_t \phi_M^n \varphi \, dx dt \leq (D_\infty \|\nabla \phi_M^n\|_{L^2 L^2} + f_\infty \|\theta^n\|_{L^2 L^2} + \lambda_M^{\text{pro}} \|\phi_M^n\|_{L^2 L^2}) \|\varphi\|_{L^2 H^1},$$

for all  $\varphi \in L^2(0, T; H^1)$ . From the above two estimates it follows that

$$\begin{aligned} \|\partial_t \phi_T^n\|_{L^2(H^1)'} &\leq C(\|\nabla \mu^n\|_{L^2 L^2} + \|\nabla \theta^n\|_{L^2 L^2} + \|\phi_\sigma^n\|_{L^2 L^2} \\ &\quad + \|\phi_T^n\|_{L^2 L^2} + \|\phi_N^n\|_{L^2 L^2}), \\ \|\partial_t \phi_M^n\|_{L^2(H^1)'} &\leq C(\|\nabla \phi_M^n\|_{L^2 L^2} + \|\theta^n\|_{L^2 L^2} + \|\phi_M^n\|_{L^2 L^2}). \end{aligned} \tag{4.31}$$

Lastly, we note that from the integral representation of the ECM density  $\theta^n$  we can directly derive a uniform bound of  $\partial_t \theta^n$  in  $L^\infty(0, T; L^2)$  for  $\alpha = \text{nonloc}$  and in  $L^\infty(0, T; L^\infty) \cap L^2(0, T; H^1)$  for  $\alpha = \text{loc}$ .

**4.4. Passing to the limit**

On account of the final estimate (4.26) for Galerkin approximations and estimates (4.28)–(4.31), we can conclude that

$$\begin{aligned}
 \{\phi_T^n\}_{n \in \mathbb{N}} & \text{ is bounded in } L^\infty(0, T; H^1) \cap H^1(0, T; (H^1)'), \\
 \{\mu^n\}_{n \in \mathbb{N}} & \text{ is bounded in } L^2(0, T; H^1), \\
 \{\phi_N^n\}_{n \in \mathbb{N}} & \text{ is bounded in } L^\infty(0, T; H^1) \cap H^1(0, T; L^2), \\
 \{\phi_\sigma^n\}_{n \in \mathbb{N}} & \text{ is bounded in } L^\infty(0, T; L^2) \cap L^2(0, T; H^1) \cap H^1(0, T; (H^1)'), \quad (4.32) \\
 \{\phi_M^n\}_{n \in \mathbb{N}} & \text{ is bounded in } L^\infty(0, T; L^2) \cap L^2(0, T; H^1) \cap H^1(0, T; (H^1)'), \\
 \{\theta^n\}_{n \in \mathbb{N}} & \text{ is bounded in } \begin{cases} W^{1,\infty}(0, T; L^2), & \alpha = \text{nonloc}, \\ W^{1,\infty}(0, T; L^\infty) \cap H^1(0, T; H^1), & \alpha = \text{loc}, \end{cases}
 \end{aligned}$$

uniformly with respect to  $n$ . This implies the existence of weakly/weakly-\* converging subsequences, indexed again by  $n$ , to some limit functions  $(\phi_T, \mu, \phi_N, \phi_\sigma, \phi_M, \theta)$  in the respective spaces and the following strong convergences due to the Aubin–Lions Compactness lemma, see (3.3),

$$\begin{aligned}
 \phi_T^n & \rightarrow \phi_T \quad \text{strongly in } C([0, T]; L^2), \\
 \phi_N^n & \rightarrow \phi_N \quad \text{strongly in } C([0, T]; L^2), \\
 \phi_\sigma^n & \rightarrow \phi_\sigma \quad \text{strongly in } L^2(0, T; L^2), \\
 \phi_M^n & \rightarrow \phi_M \quad \text{strongly in } L^2(0, T; L^2),
 \end{aligned} \tag{4.33}$$

as  $n \rightarrow \infty$  and the following weak convergence:

$$\theta^n \rightharpoonup \theta \quad \text{weakly in } L^2(0, T; X_\alpha). \tag{4.34}$$

We next show that the limit functions  $(\phi_T, \mu, \phi_N, \phi_\sigma, \phi_M, \theta)$  are a solution of the problem (4.2) in the sense of Definition 4.1. In particular, for the ECM density  $\theta$  we have to prove that it possesses the integral representation given in (4.4f). Due to the strong convergence of  $\phi_M^n$  to  $\phi_M$  in  $L^2(\Omega \times (0, T))$ , there is a subsequence, for notational simplicity indexed again by  $n$ , such that

$$\phi_M^n(x, t) \rightarrow \phi_M(x, t) \quad \text{for a.e. } (x, t) \in \Omega \times (0, T),$$

for  $n \rightarrow \infty$ . On account of the exponential function being continuous, the Lebesgue dominated convergence theorem, and  $f_5$  being continuous and bounded, we have

$$\theta^n(x, t) = \theta_0(x) \exp \left\{ - \int_0^t f_5(\phi_M^n(x, s)) ds \right\} \rightarrow \theta_0(x) \exp \left\{ - \int_0^t f_5(\phi_M(x, s)) ds \right\}$$

almost everywhere as  $n \rightarrow \infty$ . Applying the Lebesgue dominated convergence theorem again yields

$$\theta^n \rightarrow \left( (x, t) \mapsto \theta_0(x) \exp \left\{ - \int_0^t f_5(\phi_M(x, s)) ds \right\} \right) \quad \text{in } L^2(\Omega \times (0, T)),$$



as  $n \rightarrow \infty$ . Since strong convergence implies weak convergence and weak limits are unique, we have proven that  $\theta$ , given in (4.34), is of the required form.

For the other solution functions, we multiply the Galerkin system (4.10) by an arbitrary test function  $\eta \in C_c^\infty(0, T)$  and integrate from 0 to  $T$ , which gives for all  $j \in \{1, \dots, n\}$ ,

$$\begin{aligned}
 & \int_0^T [\langle \partial_t \phi_T^n, w_j \rangle + (m_T(\phi_T^n, \phi_N^n) \nabla \mu^n, \nabla w_j) - (J_\alpha(\phi_T^n, \phi_N^n, \theta^n), \nabla w_j) \\
 & \quad - (\phi_\sigma^n f_1(\phi_T^n, \phi_N^n), w_j) + (\lambda_T^{\text{apo}} \phi_T^n + \lambda_N^{\text{dec}} \phi_N^n, w_j)] \eta(t) dt = 0, \\
 & \int_0^T [-(\mu^n, w_j) + (\Psi'(\phi_T^n), w_j) + \varepsilon_T^2 (\nabla \phi_T^n, \nabla w_j) - \chi_C(\phi_\sigma^n, w_j) \\
 & \quad + \delta_T(\phi_T^n, w_j)] \eta(t) dt = 0, \\
 & \int_0^T [(\partial_t \phi_N^n, \varphi^n) - (\mathcal{S}(\sigma_{VN} - \phi_\sigma^n) f_2(\phi_T^n, \phi_N^n), w_j) \\
 & \quad + \lambda_N^{\text{deg}}(\phi_N^n, w_j)] \eta(t) dt = 0, \tag{4.35} \\
 & \int_0^T [\langle \partial_t \phi_\sigma^n, w_j \rangle + (D_\sigma(\phi_\sigma^n)(\delta_\sigma^{-1} \nabla \phi_\sigma^n - \chi_C \nabla \phi_T^n), \nabla w_j) \\
 & \quad + ((\phi_T^n - \phi_N^n) f_3(\phi_\sigma^n), w_j)] \eta(t) dt = 0, \\
 & \int_0^T [\langle \partial_t \phi_M^n, w_j \rangle + (D_M(\phi_M^n) \nabla \phi_M^n, \nabla w_j) - (\theta^n f_4(\phi_T^n, \phi_N^n, \phi_\sigma^n, \phi_M^n), w_j) \\
 & \quad + \lambda_M^{\text{pro}}(\phi_M^n, w_j)] \eta(t) dt = 0.
 \end{aligned}$$

We take the limit  $n \rightarrow \infty$  in each equation. The convergence of the linear terms follows directly from the definition of weak convergence. For instance, the functional

$$\mu^n \mapsto \int_0^T (\mu^n, w_j) \eta(t) dt \leq \|\mu^n\|_{L^2 L^2} |w_j|_{L^2} |\eta|_{L^2(0, T)},$$

is linear and continuous on  $L^2(0, T; L^2)$  and therefore, we conclude that

$$\int_0^T (\mu^n, w_j) \eta(t) dt \rightarrow \int_0^T (\mu, w_j) \eta(t) dt,$$

as  $n \rightarrow \infty$ . It remains to treat the nonlinear terms. We note that a similar limit process is performed in Ref. 21 for a tumor growth system which also includes a nonlinear mobility, diffusion, and potential function with the same assumptions as in (A2), (A3), and (A5). The same arguments can be applied to our model; we therefore omit the details here.

We focus on the treatment of the adhesion flux  $J_\alpha$  and the nonlinear functions  $f_1, \dots, f_5$ . We employ the following three arguments.

(i) By assumption (A6), the adhesion flux has the representation

$$J_\alpha(\phi_T^n, \phi_N^n, \theta^n) = g(\phi_T^n, \phi_N^n) G(\theta^n),$$

for  $g \in C_b(\mathbb{R}^2)$  and  $G \in \mathcal{L}(X_\alpha; [L^2]^d)$ . On the one hand, we know  $\theta^n \rightharpoonup \theta$  weakly in  $L^2(0, T; X_\alpha)$  as  $n \rightarrow \infty$  by (4.32), which implies by the weak sequential continuity of  $G$ ,

$$G\theta^n \rightharpoonup G\theta \quad \text{weakly in } L^2(\Omega \times (0, T); \mathbb{R}^d),$$

as  $n \rightarrow \infty$ . On the other hand, we have derived  $\phi_T^n \rightarrow \phi_T$  and  $\phi_N^n \rightarrow \phi_N$  strongly in  $L^2(\Omega \times (0, T))$  in (4.33). Therefore, applying the Lebesgue dominated convergence theorem yields

$$g(\phi_T^n, \phi_N^n) \nabla w_j \eta \rightarrow g(\phi_T, \phi_N) \nabla w_j \eta \quad \text{strongly in } L^2(\Omega \times (0, T); \mathbb{R}^d),$$

as  $n \rightarrow \infty$ . Putting these two results together, we finally have, as  $n \rightarrow \infty$ ,

$$J_\alpha(\phi_T^n, \phi_N^n, \theta^n) \nabla w_j \eta \rightarrow J_\alpha(\phi_T, \phi_N, \theta) \nabla w_j \eta \quad \text{strongly in } L^1(\Omega \times (0, T)).$$

(ii) Since  $\mathcal{S}$  and  $f_2$  are bounded, continuous functions, we obtain analogously to (i), as  $n \rightarrow \infty$ ,

$$\mathcal{S}(\sigma_{VN} - \phi_\sigma^n) f_2(\phi_T^n, \phi_N^n) w_j \eta \rightarrow \mathcal{S}(\sigma_{VN} - \phi_\sigma^n) f_2(\phi_T, \phi_N) w_j \eta,$$

strongly in  $L^2(\Omega \times (0, T))$ .

(iii) Similar to (i), we employ that  $\theta^n \rightharpoonup \theta$  weakly in  $L^2(\Omega \times (0, T))$  and

$$f_4(\phi_T^n, \phi_N^n, \phi_\sigma^n, \phi_M^n) w_j \eta \rightarrow f_4(\phi_T, \phi_N, \phi_\sigma, \phi_M) w_j \eta \quad \text{strongly in } L^2(\Omega \times (0, T)),$$

as  $n \rightarrow \infty$ , which implies the convergence of their product in  $L^1(\Omega \times (0, T))$ . Convergence of the terms involving  $f_1$ ,  $f_3$ , and  $f_5$  follows in the same manner.

Finally, by taking the limit  $n \rightarrow \infty$  in the system (4.35), using the density of  $\text{span}\{w_1, w_2, \dots\}$  in  $H^1$ , and the fundamental lemma of calculus of variations, we obtain a solution  $(\phi_T, \mu, \phi_N, \phi_\sigma, \phi_M, \theta)$  of the system (4.4) in the sense of Definition 4.1.

We note that on account of the standard Sobolev embeddings, we have the following regularity in time of our solution:

$$\phi_T, \phi_N \in C([0, T]; L^2) \cap C_w([0, T]; H^1),$$

$$\phi_\sigma, \phi_M \in C([0, T]; L^2),$$

and, thus, initial conditions are meaningful and the Galerkin approximations fulfill the initial data. This completes the proof.

### 5. Finite Element Approximations

We select a similar algorithmic framework as in Refs. 21, 39 and 38 to solve the deterministic systems of the respective local and nonlocal model with the initial and boundary data (4.3). This framework contains a discrete-time local semi-implicit scheme with an energy convex-nonconvex splitting; that means the stable contractive part is treated implicitly and the expansive part explicitly. In particular,

recalling the Ginzburg–Landau energy  $\mathcal{E}$  in (2.4), we split its contractive part  $\mathcal{E}_c$  and expansive part  $\mathcal{E}_e$  via  $\mathcal{E}_e = \mathcal{E} - \mathcal{E}_c$ , see also Refs. 30 and 38.

Let the time domain be divided into the steps  $\Delta t_n = t_{n+1} - t_n$  for  $n \in \{0, 1, \dots\}$ . To simplify exposition, we assume  $\Delta t_n = \Delta t$  for all  $n$ . We write  $\phi_{T_n}$  for the approximation of  $\phi_T^h(t_n)$  and likewise for the other variables. The backward Euler method applied to the system (4.2) reads

$$\begin{aligned} \frac{\phi_{T_{n+1}} - \phi_{T_n}}{\Delta t} &= \operatorname{div}(m_T(\phi_{T_{n+1}}, \phi_{N_{n+1}})\nabla\mu_{n+1}) + \phi_{\sigma_{n+1}}f_{1,n+1} \\ &\quad - \lambda_T^{\text{apo}}\phi_{T_{n+1}} - \operatorname{div}(J_\alpha(\phi_{T_{n+1}}, \phi_{N_{n+1}}, \theta_{n+1})) - \lambda_N^{\text{dec}}\phi_{N_{n+1}} \\ \mu_{n+1} &= D_{\phi_T}\mathcal{E}_c(\phi_{T_{n+1}}, \phi_{\sigma_{n+1}}) - D_{\phi_T}\mathcal{E}_e(\phi_{T_n}, \phi_{\sigma_n}), \\ \frac{\phi_{N_{n+1}} - \phi_{N_n}}{\Delta t} &= \mathcal{S}(\sigma_{VN} - \phi_{\sigma_{n+1}})f_{2,n+1} - \lambda_N^{\text{deg}}\phi_{N_{n+1}}, \\ \frac{\phi_{\sigma_{n+1}} - \phi_{\sigma_n}}{\Delta t} &= \operatorname{div}(D_\sigma(\theta_{n+1})(\delta_\sigma^{-1}\nabla\phi_{\sigma_{n+1}} - \chi_C\nabla\phi_{T_{n+1}})) \\ &\quad + (\phi_{T_{n+1}} - \phi_{N_{n+1}})f_{3,n+1}, \\ \frac{\phi_{M_{n+1}} - \phi_{M_n}}{\Delta t} &= \operatorname{div}(D_M(\theta_{n+1})\nabla\phi_{M_{n+1}}) + \theta_{n+1}f_{4,n+1} - \lambda_M^{\text{dec}}\phi_{M_{n+1}}, \\ \frac{\theta_{n+1} - \theta_n}{\Delta t} &= -\theta f_{5,n+1}. \end{aligned} \tag{5.1}$$

The functions  $f_{i,n+1}$ ,  $i \in \{1, \dots, 5\}$ , are given by

$$\begin{aligned} f_{1,n+1} &= \lambda_T^{\text{pro}}(\mathcal{C}(\phi_{T_{n+1}}) - \mathcal{C}(\phi_{N_{n+1}})) \cdot (1 - \mathcal{C}(\phi_{T_{n+1}})), \\ f_{2,n+1} &= \lambda_{VN}(\mathcal{C}(\phi_{T_{n+1}}) - \mathcal{C}(\phi_{N_{n+1}})), \\ f_{3,n+1} &= \lambda_T^{\text{pro}}(\mathcal{C}(\phi_{T_{n+1}}) - \mathcal{C}(\phi_{N_{n+1}}))\frac{\mathcal{C}(\phi_{\sigma_{n+1}})}{\mathcal{C}(\phi_{\sigma_{n+1}}) + \lambda_\sigma^{\text{sat}}}, \\ f_{4,n+1} &= \lambda_M^{\text{pro}}(\mathcal{C}(\phi_{T_{n+1}}) - \mathcal{C}(\phi_{N_{n+1}}))\frac{\sigma_H}{\sigma_H + \mathcal{C}(\phi_{\sigma_{n+1}})}(1 - \mathcal{C}(\phi_{M_{n+1}})) \\ &\quad - \lambda_\theta^{\text{dec}}\mathcal{C}(\phi_{M_{n+1}}), \\ f_{5,n+1} &= \lambda_\theta^{\text{deg}}\mathcal{C}(\phi_{M_{n+1}}), \end{aligned} \tag{5.2}$$

where  $\mathcal{C}$  denotes the cut-off operator,

$$\mathcal{C}(\sigma) = \max(0, \min(1, \sigma)).$$

The functions  $f_{i,n+1}$ ,  $i \in \{1, \dots, 5\}$ , are selected so that the model given in (2.1), (2.6)–(2.9) is replicated besides the cut-off operator and the Sigmoid function  $\mathcal{S}$  approximating the Heaviside step function  $\mathcal{H}$ . Furthermore, the functions satisfy the assumptions given in (A7<sub>loc</sub>).

We solve the highly nonlinear coupled system (5.1) by decoupling the equations and using an iterative Gauß–Seidel method. In Algorithm 1, the subscript 0 stands

for the initial solution,  $k$  the iteration index,  $n_{\text{iter}}$  the maximum number of iterations at each time step and TOL the tolerance for the iteration process. In each iterative loop, three linear systems are solved and the convergence of the nonlinear solution is achieved at each time if  $\max|\phi_{T_{n+1}}^{k+1} - \phi_{T_{n+1}}^k| < \text{TOL}$ .

We obtain the algebraic systems using a Galerkin finite element approach. Let  $\mathcal{T}^h$  be a quasiuniform family of triangulations of  $\Omega$  and let the piecewise linear finite element space be given by

$$\mathcal{V}^h = \{v \in C(\bar{\Omega}) : v|_T \in P_1(K) \text{ for all } K \in \mathcal{T}^h\} \subset H^1(\Omega),$$

where  $P_1(T)$  denotes the set of all affine linear functions on  $T$ .

We formulate the discrete problem as follows: for each  $k$ , find

$$(\phi_{T_{n+1}}^{k+1}, \mu_{n+1}^{k+1}, \phi_{N_{n+1}}^{k+1}, \phi_{\sigma_{n+1}}^{k+1}, \phi_{M_{n+1}}^{k+1}, \theta_{n+1}^{k+1}) \in (\mathcal{V}^h)^6,$$

for all

$$(\varphi_T, \varphi_\mu, \varphi_N, \varphi_\sigma, \varphi_M, \varphi_\theta) \in (\mathcal{V}^h)^6,$$

such that

$$\begin{aligned} & (\phi_{\sigma_{n+1}}^{k+1} - \phi_{\sigma_n}, \varphi_\sigma) + \Delta t (D_M(\theta_{n+1}^k) \cdot (\delta_\sigma^{-1} \nabla \phi_{\sigma_{n+1}}^{k+1} - \chi_C \nabla \phi_{T_{n+1}}^k), \nabla \varphi_\sigma) \\ & - \Delta t \lambda_T^{\text{pro}} \left( (\phi_{T_{n+1}}^k - \phi_{N_{n+1}}^k) (\mathcal{C}(\phi_{T_{n+1}}^k) - \mathcal{C}(\phi_{N_{n+1}}^k)) \frac{\mathcal{C}(\phi_{\sigma_{n+1}}^{k+1})}{\mathcal{C}(\phi_{\sigma_{n+1}}^{k+1}) + \lambda_\sigma^{\text{sat}}}, \varphi_\sigma \right) \\ & = 0, \end{aligned} \tag{5.3}$$

$$\begin{aligned} & (\phi_{T_{n+1}}^{k+1} - \phi_{T_n}, \varphi_T) + \Delta t (m_T(\phi_{T_{n+1}}^{k+1}, \phi_{N_{n+1}}^{k+1}) \nabla \mu_{n+1}^{k+1}, \nabla \varphi_T) \\ & - \Delta t (J_\alpha(\phi_{T_{n+1}}^{k+1}, \phi_{N_{n+1}}^k, \theta_{n+1}^k), \nabla \varphi_T) \\ & - \Delta t \lambda_T^{\text{pro}} ((\mathcal{C}(\phi_{T_{n+1}}^{k+1}) - \mathcal{C}(\phi_{N_{n+1}}^k)) \cdot (1 - \mathcal{C}(\phi_{T_{n+1}}^{k+1})), \phi_{\sigma_{n+1}}^{k+1} \varphi_T) \\ & + \Delta t (\lambda_T^{\text{apo}} \phi_{T_{n+1}}^{k+1} + \lambda_N^{\text{dec}} \phi_{N_{n+1}}^k, \varphi_T) = 0, \end{aligned} \tag{5.4}$$

$$(\mu_{n+1}^{k+1}, \varphi_\mu) - (D_{\phi_T} \mathcal{E}_c(\phi_{T_{n+1}}^{k+1}, \phi_{\sigma_{n+1}}^{k+1}), \varphi_\mu) = (D_{\phi_T} \mathcal{E}_e(\phi_{T_n}, \phi_{\sigma_n}), \varphi_\mu), \tag{5.5}$$

$$\begin{aligned} & (\phi_{N_{n+1}}^{k+1} - \phi_{N_n}, \varphi_N) - \Delta t (\mathcal{C}(\phi_{T_{n+1}}^{k+1} - \phi_{N_{n+1}}^{k+1}), \mathcal{S}(\sigma_{VN} - \phi_{\sigma_{n+1}}^{k+1}) \varphi_N) \\ & + \Delta t \lambda_N^{\text{deg}} (\phi_{N_{n+1}}^{k+1}, \varphi_N) = 0, \end{aligned} \tag{5.6}$$

$$\begin{aligned} & (\phi_{M_{n+1}}^{k+1} - \phi_{M_n}, \varphi_M) + \Delta t (D_M(\theta_{n+1}^k) \nabla \phi_{M_{n+1}}^{k+1}, \nabla \varphi_M) \\ & - \Delta t \lambda_M^{\text{pro}} \left( \theta_{n+1}^k (\mathcal{C}(\phi_{T_{n+1}}^{k+1}) - \mathcal{C}(\phi_{N_{n+1}}^{k+1})) \frac{\sigma_H}{\sigma_H + \mathcal{C}(\phi_{\sigma_{n+1}}^{k+1})} (1 - \mathcal{C}(\phi_{M_{n+1}}^{k+1})), \varphi_M \right) \\ & + \Delta t \lambda_\theta^{\text{dec}} (\theta_{n+1}^k \mathcal{C}(\phi_{M_{n+1}}^{k+1}), \varphi_M) + \Delta t \lambda_M^{\text{dec}} (\phi_{M_{n+1}}^{k+1}, \varphi_M) = 0, \end{aligned} \tag{5.7}$$

$$(\theta_{n+1}^{k+1} - \theta_n, \varphi_\theta) + \Delta t \lambda_\theta^{\text{deg}} (\theta_{n+1}^{k+1} \mathcal{C}(\phi_{M_{n+1}}^{k+1}), \varphi_\theta) = 0. \tag{5.8}$$

**Algorithm 1.** Semi-implicit scheme for (5.1).

---

**Input:**  $\phi_{T_0}, \phi_{N_0}, \phi_{\sigma_0}, \phi_{M_0}, \theta_0, \Delta t, T, \text{TOL}$

**Output:**  $\phi_{T_n}, \mu_n, \phi_{N_n}, \phi_{\sigma_n}, \phi_{M_n}, \theta_n$  for all  $n$

$n = 0$

$t = 0$

**while**  $t \leq T$  **do**

$\phi_{T_{n+1}}^0 = \phi_{T_n}, \phi_{N_{n+1}}^0 = \phi_{N_n}, \phi_{\sigma_{n+1}}^0 = \phi_{\sigma_n}, \phi_{M_{n+1}}^0 = \phi_{M_n}, \theta_{n+1}^0 = \theta_n$

**while**  $\max\|\phi_{T_{n+1}}^{k+1} - \phi_{T_{n+1}}^k\| > \text{TOL}$  **do**

$\phi_{T_{n+1}}^k = \phi_{T_{n+1}}^{k-1}, \phi_{N_{n+1}}^k = \phi_{N_{n+1}}^{k-1}, \phi_{\sigma_{n+1}}^k = \phi_{\sigma_{n+1}}^{k-1}, \phi_{M_{n+1}}^k = \phi_{M_{n+1}}^{k-1},$   
 $\theta_{n+1}^k = \theta_{n+1}^{k-1}$

**solve**  $\phi_{\sigma_{n+1}}^{k+1}$  **using** (5.3), **given**  $\phi_{\sigma_n}, \phi_{T_{n+1}}^k, \phi_{N_{n+1}}^k$

**solve**  $\phi_{T_{n+1}}^{k+1}, \mu_{n+1}^{k+1}$  **using** (5.4) and (5.5), **given**  
 $\phi_{T_n}, \phi_{T_{n+1}}^k, \phi_{N_{n+1}}^k, \phi_{\sigma_{n+1}}^{k+1}, \theta_{n+1}^k$

**solve**  $\phi_{N_{n+1}}^{k+1}$  **using** (5.6), **given**  $\phi_{N_n}, \phi_{T_{n+1}}^{k+1}, \phi_{\sigma_{n+1}}^{k+1}$

**solve**  $\phi_{M_{n+1}}^{k+1}$  **using** (5.7), **given**  $\phi_{M_n}, \phi_{T_{n+1}}^{k+1}, \phi_{\sigma_{n+1}}^{k+1}, \theta_{n+1}^k$

**solve**  $\theta_{n+1}^{k+1}$  **using** (5.8), **given**  $\theta_n, \phi_{M_{n+1}}^{k+1}$

$k \mapsto k + 1$

**end**

$\phi_{T_{n+1}}^{k+1} = \phi_{T_{n+1}}^k, \mu_{n+1}^{k+1} = \mu_{n+1}^k, \phi_{N_{n+1}}^{k+1} = \phi_{N_{n+1}}^k$

$\phi_{\sigma_{n+1}}^{k+1} = \phi_{\sigma_{n+1}}^k, \phi_{M_{n+1}}^{k+1} = \phi_{M_{n+1}}^k, \theta_{n+1}^{k+1} = \theta_{n+1}^k$

$n \mapsto n + 1$

$t \mapsto t + \Delta t$

**end**

---

We implemented Algorithm 1 in libMesh,<sup>33</sup> an open-source computing platform for solving partial differential equations using finite element methods. We use this implementation to obtain the numerical results as follows.

## 6. Numerical Simulations

In this section, numerical approximations of the growth of the tumor volume fractions  $\phi_T$  and the simulation of the other variables in the local and nonlocal model (4.2) obtained by implementing Algorithm 1 are presented. We present a numerical experiment of the local model both in two and three dimension in the domain  $\Omega = (-1, 1)^d$ ,  $d \in \{2, 3\}$ . Afterwards, we compare the growth of the tumor volume fraction in the local and nonlocal model in two dimensions.

We impose for the nutrient concentrations an inhomogeneous Dirichlet boundary condition at  $x_1 = 1$ , namely  $\phi_\sigma = 1$ . This is a slight modification to the analyzed model in Sec. 4, but the existence proof can be adapted in a straightforward way, see Ref. 21.

We choose for the parameters in our system (4.2) the dimensionless values

$$\begin{aligned} \varepsilon_T &= 0.005, & \chi_C &= 0, & \chi_H &= 0.001, & \delta_\sigma &= 0.01, & \delta_T &= 0, \\ \lambda_T^{\text{pro}} &= 2, & \lambda_T^{\text{apo}} &= 0.005, & \lambda_N^{\text{deg}} &= 0, & \lambda_{VN} &= 1, & \lambda_\sigma^{\text{sat}} &= 0, \\ \lambda_M^{\text{dec}} &= 1, & \lambda_M^{\text{pro}} &= 1, & \lambda_\theta^{\text{dec}} &= 0.1, & \lambda_\theta^{\text{deg}} &= 1, & \bar{E} &= 0.045, \\ \sigma_H &= 0.6, & \sigma_{VN} &= 0.44, & M_T &= 2, & D_\sigma &= 0.001, & D_M &= 0.1. \end{aligned}$$

### 6.1. Local model in two dimensions

In Fig. 1, the computed simulations of the volume fractions of tumor cells ( $\phi_T$ ), necrotic cells ( $\phi_N$ ) and viable cells ( $\phi_V$ ) for a local model in a two-dimensional domain are shown at four different time points  $t \in \{0, 5, 10, 15\}$ . For the initial

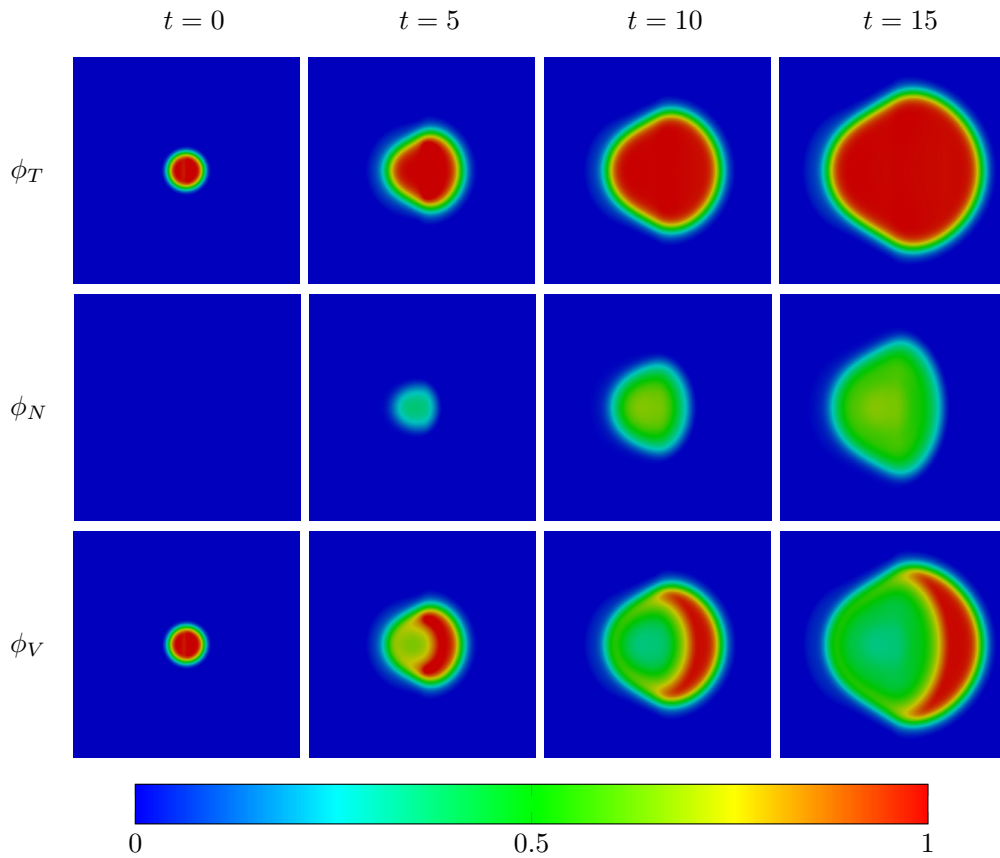


Fig. 1. Simulation of the volume fractions  $\phi_T$ ,  $\phi_N$ ,  $\phi_V$  in the local model in the 2D domain  $\Omega = (-1, 1)^2$ ; the evolution of the tumor, necrotic and viable cells is shown at the times  $t \in \{0, 5, 10, 15\}$ .

conditions, we start off from a small circular concentration of tumor cells without a necrotic part, that means  $\phi_T = \phi_V$  at  $t = 0$ .

In the first row of Fig. 1, one observes that the tumor volume fraction  $\phi_T$  evolves towards the nutrient-rich part of the domain, see also Fig. 2 below for the simulation of  $\phi_\sigma$ . As the transition between tumor phenotypes is guided by the nutrient concentration, the necrotic concentration increases in the nutrient-poor region, see the second row in Fig. 1. Moreover, in the third row in Fig. 1, the viable tumor cells, responsible for the tumor growth, are concentrated closer to the right side of the domain, which is the region with higher nutrient concentration.

In the first row of Fig. 2, the ECM density ( $\theta$ ) is degraded over time by the matrix degrading enzymes ( $\phi_M$ ). These enzymes are released by the tumor cells, mainly at regions with low nutrient and high ECM density. The nutrient concentration decreases as the tumor grows, with a higher value of  $\phi_\sigma$  towards the boundary on the right-hand side of the domain  $\Omega = (-1, 1)^2$ , due to the imposed Dirichlet boundary condition  $\phi_\sigma = 1$  at  $x_1 = 1$ .

**6.2. Local model in three dimensions**

The simulation of the ECM density in the three-dimensional domain  $\Omega = (-1, 1)^3$  at the times  $t \in \{8, 11\}$  is illustrated in Fig. 3. Additionally, an isosurface of the tumor volume fraction  $\phi_T$  at 0.7 is shown in the same plots.

At time  $t = 0$ , the top part of the domain has a higher ECM density  $\theta = 1$  than the lower part with  $\theta = 0.5$ , similarly to the initial data in the two-dimensional

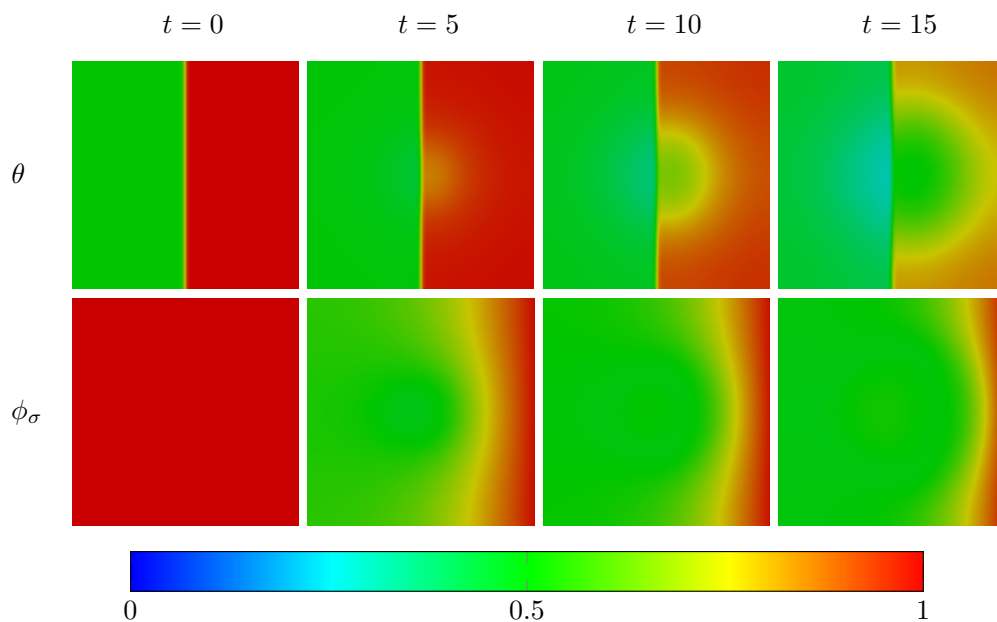


Fig. 2. Simulation of the ECM density  $\theta$  and the nutrient concentration  $\phi_\sigma$  in the local model in two dimensions; their evolution is shown at the times  $t \in \{0, 5, 10, 15\}$ .

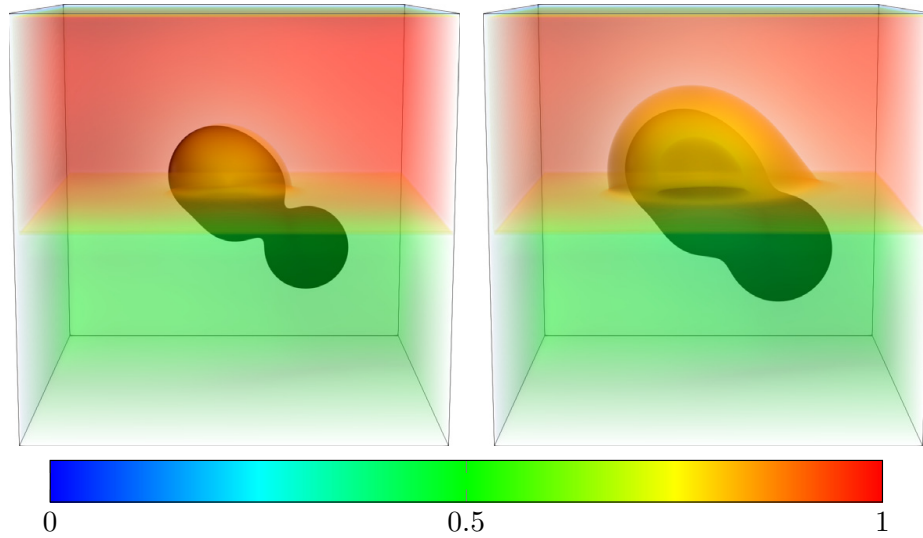


Fig. 3. Simulation of the ECM density  $\theta$  in the three-dimensional domain  $\Omega = (-1, 1)^3$  together with the isosurface of the tumor volume fraction  $\phi_T$  at 0.7, at the times  $t = 8$  (left plot) and  $t = 11$  (right plot).

case, see Fig. 2. At  $t = 8$  and  $t = 11$ , one observes in Fig. 3 that the ECM density has degraded around the tumor volume, similar to the two-dimensional case.

The evolution of the volume fractions of tumor cells  $\phi_T$  and necrotic cell  $\phi_N$  in the three-dimensional case is depicted in Fig. 4 below. As initial data we take two separated elliptic-shaped tumor volume fractions, which start to connect at  $t = 5$ . At the initial time there are no necrotic cells. They begin to form at  $t = 6.5$  and already inhabit a large portion of the tumor volume fraction at  $t = 11$ , as seen in Fig. 4.

### 6.3. Comparison to the nonlocal model

In this section, we compare the simulation of the tumor volume fraction  $\phi_T$  in the local and nonlocal model (4.2), that means in the local model we choose for the adhesion flux  $J_{\text{loc}} = \chi_H \phi_V \nabla \theta$  and for the nonlocal model  $J_{\text{nonloc}} = \chi_H \phi_V k * \theta$ , as introduced in (2.5). In the case of the nonlocal adhesion-based haptotaxis effect, we have to select an appropriate vector-valued kernel function  $k$ . In the existence proof of the nonlocal model we only had to assume  $k \in L^1(\mathbb{R}^d)$  and no additional requirements on its representation. Following Refs. 7, 28 and 29, we choose a kernel function  $k_\varepsilon$ ,  $\varepsilon > 0$  indicating some parameter, such that it approximates the gradient-based haptotaxis effect as  $\varepsilon \rightarrow 0$ . See also Refs. 14 and 44 for different choices for nonlocal gradient operators.

In tumor growth models involving nonlocal cell-to-cell adhesion effects, it is a standard procedure to replace the term  $\frac{1}{2} \varepsilon_T^2 |\nabla \phi_T(x)|^2$  in the Ginzburg–Landau free



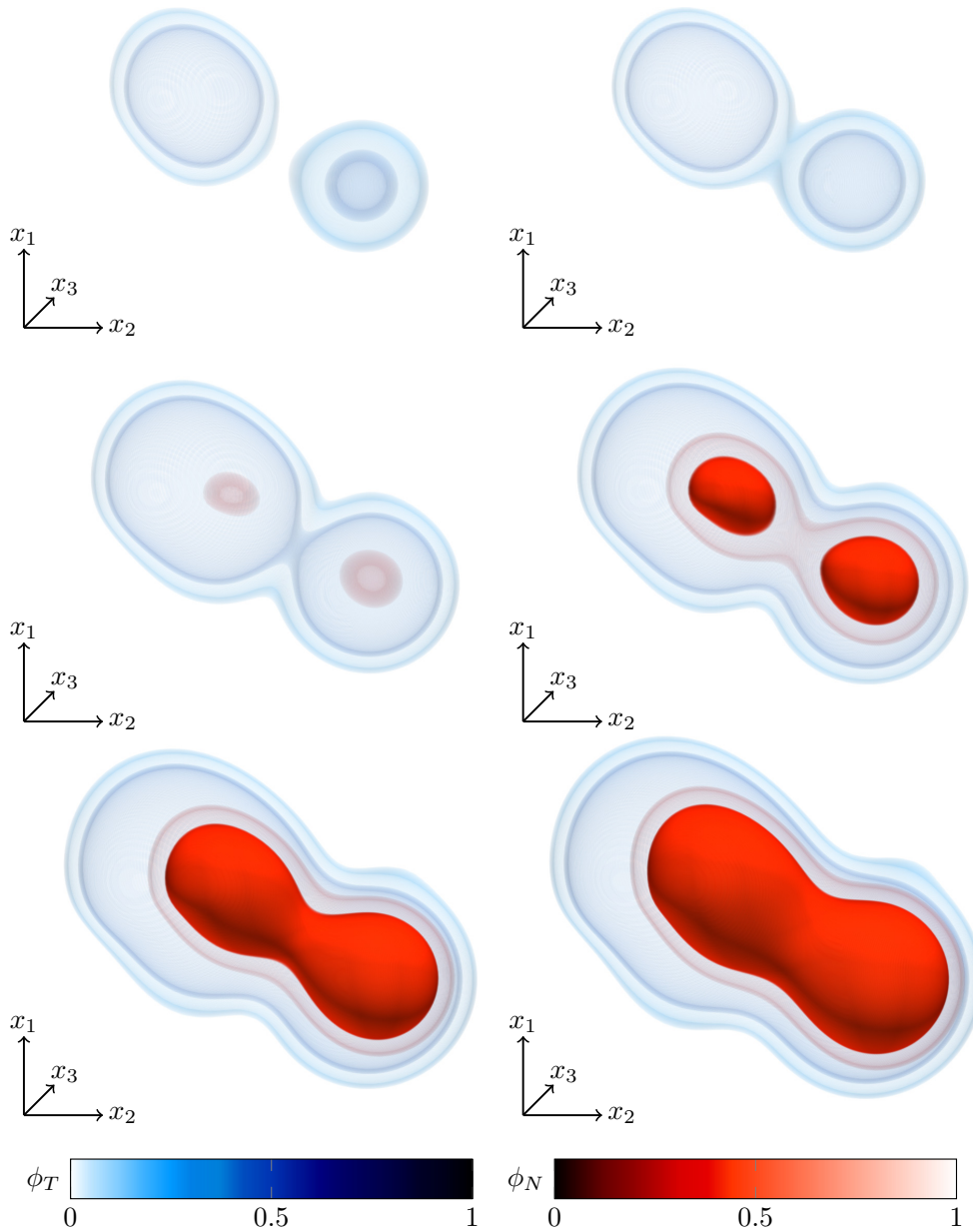


Fig. 4. Simulation of volume fractions of tumor cells  $\phi_T$  and necrotic cells  $\phi_N$  in a three-dimensional domain, the isosurfaces of 0.2 and 0.4 of each volume fraction at times  $t \in \{3.5, 5, 6.5, 8, 9.5, 11\}$  are shown.

energy functional (2.4) by

$$\frac{1}{4} \int_{\Omega} J(x - y) (\phi_T(x) - \phi_T(y))^2 dy. \tag{6.1}$$

As shown in Ref. 19, choosing  $J(x - y) = j^{d+2} \chi_{[0,1]}(|j(x - y)|^2)$  and letting  $j \rightarrow \infty$ , one returns to the Ginzburg–Landau free energy functional, where the interfacial parameter is expressed by  $\varepsilon_T^2 = \frac{2}{d} \int_{\mathbb{R}^d} J(|z|^2) |z|^2 dz$ . Therefore, one can interpret the classical Cahn–Hilliard equation as an approximation of its nonlocal version.

Taking the Gateaux derivative of the nonlocal energy functional results in the chemical potential  $\mu$ . In particular, the term in (6.1) becomes

$$\phi_T \cdot J * 1 - J * \phi_T,$$

instead of  $-\varepsilon_T^2 \Delta \phi_T$  in the case of the local Ginzburg–Landau free energy functional. This suggests for the gradient operator the following approximation:

$$\begin{aligned} k \otimes \theta(x) &:= (k * \theta)(x) - \theta(x) \cdot (k * 1)(x) \\ &= \int_{\mathbb{R}^d} k(x - y)(\theta(y) - \theta(x))dy \\ &\approx \int_{\mathbb{R}^d} k(x - y)(\nabla\theta(x) \cdot (y - x))dy \\ &= \nabla\theta(x) \int_{\mathbb{R}^d} (y - x) \cdot k(x - y)dy \\ &= \nabla\theta(x), \end{aligned}$$

where we chose  $k$  such that  $xk(-x)$  is a Dirac sequence with the typical property  $\int_{\mathbb{R}^d} xk(-x)dx = 1$ . We impose the representation

$$k(x) = -\omega(\varepsilon)x\chi_{[0,\varepsilon]}(|x|_\infty), \tag{6.2}$$

which gives in the two-dimensional case

$$\int_{\mathbb{R}^2} xk(-x) dx = \omega(\varepsilon) \int_{-\varepsilon}^\varepsilon \int_{-\varepsilon}^\varepsilon (x_1^2 + x_2^2)dx_1dx_2 = \omega(\varepsilon)\frac{8}{3}\varepsilon^4,$$

and defining  $\omega(\varepsilon) = \frac{3}{8}\varepsilon^{-4}$  yields the desired normalization property.

Note that  $k(x) = -\omega(\varepsilon)x\chi_{[0,\varepsilon]}(|x|_\infty)$  is an odd function and therefore,

$$(k * 1)(x) = \int_{\mathbb{R}^d} k(x - y)dy = 0,$$

and we can write  $k \otimes \theta = k * \theta$ .

In the following, we numerically investigate the effects of the different haptotaxis parameters  $\chi_H$  on the growth of the tumor volume fraction. We distinguish between three different values for  $\chi_H$ ,  $\chi_H \in \{5 \cdot 10^{-4}, 10^{-3}, 2 \cdot 10^{-3}\}$ . We can observe in Fig. 5 that a lower haptotaxis parameter results in a more circular shape than for a higher  $\chi_H$ , e.g. for  $\chi_H = 10^{-3}$ , we see that the tumor shape forms a bump at the vertical axis. Moreover, we compare the local gradient-based ( $\varepsilon = 0$ ) and the nonlocal adhesion-based haptotaxis effect, for which we select  $\varepsilon \in \{2.75 \cdot 10^{-2}, 5.25 \cdot 10^{-2}\}$  in the definition of the kernel function (6.2).

The larger  $\varepsilon$ , the less sensitive the results are on the three considered values for  $\chi_H$ . However as we can see in the last column in Fig. 5, different  $(\varepsilon, \chi_H)$  pairings can also yield quite similar results. A larger  $\varepsilon$  requires a larger  $\chi_H$  to show similar effects as a pairing with smaller  $\varepsilon$  and  $\chi_H$  values.

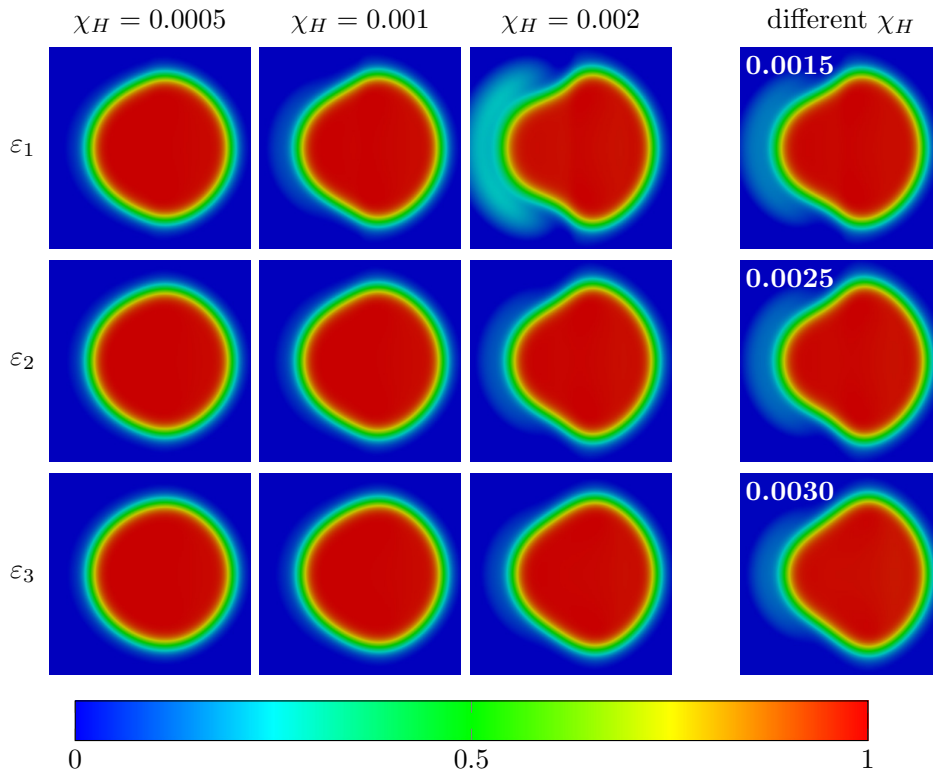


Fig. 5. Simulation of the tumor volume fraction  $\phi_T$  for three different haptotaxis parameters  $\chi_H \in \{5 \cdot 10^{-4}, 10^{-3}, 2 \cdot 10^{-3}\}$  and different kernel functions  $k_\varepsilon$  for  $\varepsilon \in \{\varepsilon_1, \varepsilon_2, \varepsilon_3\} := \{0, 2.75 \cdot 10^{-2}, 5.25 \cdot 10^{-2}\}$  for a fixed time  $t = 12$ ; also three different parameters  $\chi_H$  are selected such that the shapes are in accordance with each other.

The larger  $\chi_H$ , the more the local and nonlocal model differ from each other. This results from the fact that for  $\varepsilon > 0$  in the nonlocal model terms involving  $\varepsilon^2$  play a more significant role.

## 7. Concluding Comments

In this study, we have presented and analyzed new local and nonlocal mathematical models of growth and of invasion of tumors in healthy tissue that depict the erosion of the ECM by MDEs and the affects of long-range interactions such as cell-to-cell adhesion. Under reasonable assumptions on the forms of the total energy of the system, potentials, and cell mobility behavior, we proved the existence of solutions to systems of phase-field models characterized by nonlinear integro-partial differential equations derived using the balance laws of mechanics and principal biological mechanisms know to control the growth and decline of tumor masses. The results of several numerical experiments based on two- and three-dimensional finite element approximations of the models are presented which demonstrate that the models provide realistic simulations of the effects of nonlocal interactions and MDE concentrations on erosion of the ECM and corresponding invasion of tumor cells for various distributions of nutrient concentration.

**Appendix A. An Existence Result for Integro-Differential Equations**

We study the initial value problem for integro-differential systems in the form

$$\begin{cases} x'(t) = f(t, x(t), Kx(t)), \\ x(0) = x_0, \end{cases} \tag{7.1}$$

where  $f \in C([0, T] \times \mathbb{R}^n \times \mathbb{R}^n; \mathbb{R}^n)$ ,  $Kx(t) = \int_0^t k(s, x(s))ds$ , and prove a local existence theorem. To this end, we employ the Schauder fixed-point theorem; see, e.g. Theorem 3 in Chap. 9.2 in Ref. 18. The proof below can be considered as an extension of the Cauchy–Peano theorem and Theorem 1.1.1 in Ref. 34, where a similar integro-differential equation is considered. We note that since  $f$  is continuous on  $[0, T]$  with respect to  $t$ , (7.1) can be equivalently rewritten as

$$x(t) = x_0 + \int_0^t f(s, x(s), Kx(s))ds,$$

for  $t \in [0, T]$ .

**Theorem 7.1.** (Local existence of solutions of (7.1)) *Let  $f \in C([0, T] \times \mathbb{R}^n \times \mathbb{R}^n; \mathbb{R}^n)$  and  $k \in C([0, T] \times \mathbb{R}^n; \mathbb{R}^n)$ . Then the initial value problem (7.1) has a solution  $x$  on the interval  $[0, \tilde{T}]$  for some  $\tilde{T} \in (0, T]$ .*

**Proof.** The proof follows the general outline of Theorem 1.1.1 in Ref. 34. Let  $b > 0$ . The continuous function  $k$  is bounded on the compact set  $D = [0, T] \times \bar{B}_b(x_0)$ ,

$$|k(t, x)| \leq C_k, \quad (t, x) \in D.$$

Here,  $\bar{B}_b(x_0)$  denotes the closed ball around  $x_0$  with radius  $b$  in the Euclidean norm. We then have the estimate

$$|K\phi(s)| \leq \int_0^s |k(\sigma, \phi(\sigma))|d\sigma \leq TC_k =: r.$$

Therefore,  $f$  is a continuous function on the compact set  $\tilde{D} = [0, T] \times \bar{B}_b(x_0) \times \bar{B}_r(0)$ . Then there exists  $0 < C_f < \infty$  such that

$$|f(y)| \leq C_f \quad \text{for all } y \in \tilde{D}.$$

At this point, we introduce the space

$$Y = \{\phi \in C([0, \tilde{T}]; \mathbb{R}^n) : \phi(0) = x_0 \text{ and } \|\phi - x_0\|_\infty \leq b\},$$

for  $\tilde{T} = \min\{T, b/C_f\}$ , where  $\|x\|_\infty = \max_{t \in [0, \tilde{T}]} |x(t)|$  for  $x \in C([0, \tilde{T}]; \mathbb{R}^n)$ . This particular choice of  $\tilde{T}$  will be justified below.

Let  $\phi \in Y$ . We consider the mapping  $\mathcal{T} : \phi \mapsto w$  such that

$$w(t) := \mathcal{T}\phi(t) = x_0 + \int_0^t f(s, \phi(s), K\phi(s))ds, \tag{7.2}$$

where  $t \in [0, \tilde{T}]$ . We intend to prove that  $\mathcal{T}$  is a continuous self-mapping on the compact and convex set  $Y$ , which yields the existence of a fixed point  $\phi \in Y$  of  $\mathcal{T}$  on account of the Schauder fixed-point theorem.

Firstly, we prove that the convexity of  $Y$  holds. For arbitrary  $\phi, \psi \in Y$ , and  $\lambda \in [0, 1]$ , we have  $\lambda\phi + (1 - \lambda)\psi \in C([0, \tilde{T}]; \mathbb{R}^n)$  and  $\lambda\phi(0) + (1 - \lambda)\psi(0) = x_0$ . Furthermore, it holds that

$$\|\lambda\phi + (1 - \lambda)\psi - x_0\|_\infty = \|\lambda(\phi - x_0) + (1 - \lambda)(\psi - x_0)\|_\infty \leq \lambda b + (1 - \lambda)b = b.$$

Secondly, we show the compactness of  $Y$  by employing the theorem of Arzelà–Ascoli; see, e.g. Theorem 4.25 in Ref. 6. For all  $t_1, t_2 \in [0, \tilde{T}]$ , we have the uniform equicontinuity of  $\mathcal{T}$ ,

$$|\mathcal{T}\phi(t_2) - \mathcal{T}\phi(t_1)| \leq \int_{t_1}^{t_2} |f(s, \phi(s), K\phi(s))| ds \leq C_f |t_2 - t_1|.$$

Thirdly, we prove that  $\mathcal{T}$  is a self-mapping, i.e.  $T\phi \in Y$  for  $\phi \in Y$ . We have  $T\phi(0) = w(0) = x_0$  by definition of  $\mathcal{T}$ . Thanks to our choice of  $\tilde{T}$ , we can conclude that

$$|\mathcal{T}\phi(t) - x_0| \leq \int_0^t |f(s, \phi(s), K\phi(s))| ds \leq \tilde{T}C_f \leq b,$$

for all  $t \in [0, \tilde{T}]$ .

Finally, we show the continuity of  $\mathcal{T}$ . Let  $\varepsilon > 0$  and  $\phi, \psi \in Y$  be arbitrary. Since  $f$  is uniformly continuous on the compact set  $\tilde{D}$ , there exists a  $\delta > 0$  with

$$|\phi(s) - \psi(s)| + |K\phi(s) - K\psi(s)| < \delta,$$

such that

$$|f(s, \phi(s), K\phi(s)) - f(s, \psi(s), K\psi(s))| < \frac{\varepsilon}{\tilde{T}}, \tag{7.3}$$

holds true for all  $s \in [0, \tilde{T}]$ . Moreover,  $k$  is uniformly continuous on  $D$  and hence, there is a  $\tilde{\delta} > 0$  with  $|\phi(s) - \psi(s)| < \tilde{\delta}$  such that

$$|K\phi(s) - K\psi(s)| < \frac{\delta}{2},$$

which remains true for  $|\phi(s) - \psi(s)| < \min\{\tilde{\delta}, \delta/2\} =: \hat{\delta}$ . Hence, we have derived the existence of a parameter  $\hat{\delta} > 0$  with  $|\phi(s) - \psi(s)| < \hat{\delta}$  such that (7.3) is fulfilled. Therefore, we conclude

$$\|\mathcal{T}\phi - \mathcal{T}\psi\|_\infty \leq \varepsilon,$$

which completes the proof. □

## Acknowledgments

The authors gratefully acknowledge the support of the German Science Foundation (DFG) for funding part of this work through grant WO 671/11-1, the Cancer Prevention Research Institute of Texas (CPRIT) under grant number RR160005, the NIH through the grants NCI U01CA174706 and NCI R01CA186193, and the US Department of Energy, Office of Science, Office of Advanced Scientific Computing Research, Mathematical Multifaceted Integrated Capability Centers (MMICCS) program, under award number DE-SC0019393.

## References

1. A. R. Anderson, M. A. Chaplain, E. L. Newman, R. J. Steele and A. M. Thompson, Mathematical modelling of tumour invasion and metastasis, *Comput. Math. Methods Med.* **2** (2000) 129–154.
2. R. P. Araujo and D. S. McElwain, A history of the study of solid tumour growth: The contribution of mathematical modelling, *Bull. Math. Biol.* **66** (2014) 1039–1091.
3. N. J. Armstrong, K. J. Painter and J. A. Sherratt, A continuum approach to modelling cell–cell adhesion, *J. Theoret. Biol.* **243** (2006) 98–113.
4. N. Bellomo, N. Li and P. K. Maini, On the foundations of cancer modelling: Selected topics, speculations, and perspectives, *Math. Models Methods Appl. Sci.* **18** (2008) 593–646.
5. F. Boyer and P. Fabrie, *Mathematical Tools for the Study of the Incompressible Navier–Stokes Equations and Related Models* (Springer-Verlag, 2012).
6. H. Brezis, *Functional Analysis, Sobolev Spaces and Partial Differential Equations* (Springer-Verlag, 2010).
7. M. A. Chaplain, M. Lachowicz, Z. Szymańska and D. Wrzosek, Mathematical modelling of cancer invasion: The importance of cell–cell adhesion and cell–matrix adhesion, *Math. Models Methods Appl. Sci.* **21** (2011) 719–743.
8. M. A. Chaplain and G. Lolas, Mathematical modelling of cancer cell invasion of tissue: The role of the urokinase plasminogen activation system, *Math. Models Methods Appl. Sci.* **15** (2005) 1685–1734.
9. P. Colli, G. Gilardi and D. Hilhorst, On a Cahn–Hilliard type phase field system related to tumor growth, *Discrete Contin. Dyn. Syst. – A* **35** (2015) 2423–2442.
10. M. Dai, E. Feireisl, E. Rocca, G. Schimperna and M. E. Schonbek, Analysis of a diffuse interface model of multispecies tumor growth, *Nonlinearity* **30** (2017) 1639–1658.
11. T. S. Deisboeck and G. S. Stamatakos, *Multiscale Cancer Modeling* (CRC Press, 2010).
12. F. Della Porta, A. Giorgini and M. Grasselli, The nonlocal Cahn–Hilliard–Hele–Shaw system with logarithmic potential, *Nonlinearity* **31** (2018) 4851–4881.
13. F. Della Porta and M. Grasselli, On the nonlocal Cahn–Hilliard–Brinkman and Cahn–Hilliard–Hele–Shaw systems, *Commun. Math. Sci.* **13** (2015) 1541–1567.
14. Q. Du, M. Gunzburger, R. B. Lehoucq and K. Zhou, A nonlocal vector calculus, nonlocal volume-constrained problems, and nonlocal balance laws, *Math. Models Methods Appl. Sci.* **23** (2013) 493–540.
15. M. Ebenbeck and H. Garcke, Analysis of a Cahn–Hilliard–Brinkman model for tumour growth with chemotaxis, *J. Differential Equations* **266** (2019) 5998–6036.
16. M. Ebenbeck and H. Garcke, On a Cahn–Hilliard–Brinkman model for tumor growth and its singular limits, *SIAM J. Math. Anal.* **51** (2019) 1868–1912.

17. C. Engwer, C. Stinner and C. Surulescu, On a structured multiscale model for acid-mediated tumor invasion: The effects of adhesion and proliferation, *Math. Models Methods Appl. Sci.* **27** (2017) 1355–1390.
18. L. C. Evans, *Partial Differential Equations* (Amer. Math. Soc., 2010).
19. S. Frigeri, M. Grasselli and E. Rocca, A diffuse interface model for two-phase incompressible flows with nonlocal interactions and non-constant mobility, *Nonlinearity* **28** (2015) 1257–1293.
20. S. Frigeri, K. F. Lam and E. Rocca, On a diffuse interface model for tumour growth with nonlocal interactions and degenerate mobilities, in *Solvability, Regularity, and Optimal Control of Boundary Value Problems for PDEs* (Springer, 2017), pp. 217–254.
21. M. Fritz, E. A. Lima, J. T. Oden and B. Wohlmuth, On the unsteady Darcy–Forchheimer–Brinkman equation in local and nonlocal tumor growth models, *Math. Models Methods Appl. Sci.* **29** (2019) 1691–1731.
22. H. Garcke and K. F. Lam, Global weak solutions and asymptotic limits of a Cahn–Hilliard–Darcy system modelling tumour growth, *AIMS Math.* **1** (2016) 318–360.
23. H. Garcke and K. F. Lam, Well-posedness of a Cahn–Hilliard system modelling tumour growth with chemotaxis and active ort, *European J. Appl. Math.* **28** (2017) 284–316.
24. H. Garcke and K. F. Lam, On a Cahn–Hilliard–Darcy system for tumour growth with solution dependent source terms, in *Trends in Applications of Mathematics to Mechanics* (Springer, 2018), pp. 243–264.
25. H. Garcke, K. F. Lam, R. Nürnberg and E. Sitka, A multiphase Cahn–Hilliard–Darcy model for tumour growth with necrosis, *Math. Models Methods Appl. Sci.* **28** (2018) 525–577.
26. H. Garcke, K. F. Lam, E. Sitka and V. Styles, A Cahn–Hilliard–Darcy model for tumour growth with chemotaxis and active transport, *Math. Models Methods Appl. Sci.* **26** (2016) 1095–1148.
27. R. A. Gatenby, Models of tumor–host interaction as competing populations: Implications for tumor biology and treatment, *J. Theoret. Biol.* **176** (1995) 447–455.
28. A. Gerisch, On the approximation and efficient evaluation of integral terms in pde models of cell adhesion, *IMA J. Numer. Anal.* **30** (2010) 173–194.
29. A. Gerisch and M. Chaplain, Mathematical modelling of cancer cell invasion of tissue: Local and nonlocal models and the effect of adhesion, *J. Theoret. Biol.* **250** (2008) 684–704.
30. A. Hawkins-Daarud, K. G. van der Zee and T. J. Oden, Numerical simulation of a thermodynamically consistent four-species tumor growth model, *Int. J. Numer. Methods Biomed. Eng.* **28** (2021) 3–24.
31. T. Hillen, K. J. Painter and M. Winkler, Convergence of a cancer invasion model to a logistic chemotaxis model, *Math. Models Methods Appl. Sci.* **23** (2013) 165–198.
32. J. Jiang, H. Wu and S. Zheng, Well-posedness and long-time behavior of a non-autonomous Cahn–Hilliard–Darcy system with mass source modeling tumor growth, *J. Differential Equations* **259** (2015) 3032–3077.
33. B. S. Kirk, J. W. Peterson, R. H. Stogner and G. F. Carey, libMesh: A C++ library for parallel adaptive mesh refinement/coarsening simulations, *Eng. Comput.* **22** (2006) 237–254.
34. V. Lakshmikantham and M. Rama Mohana Rao, *Theory of Integro-Differential Equations* (Gordon and Breach Sci. Publ., 1995).
35. K. F. Lam and H. Wu, Thermodynamically consistent Navier–Stokes–Cahn–Hilliard models with mass transfer and chemotaxis, *European J. Appl. Math.* **29** (2018) 595–644.

36. G. Leoni and M. Morini, Necessary and sufficient conditions for the chain rule in  $W_{\text{loc}}^{1,1}(\mathbb{R}^n; \mathbb{R}^d)$  and  $BV_{\text{loc}}(\mathbb{R}^n; \mathbb{R}^d)$ , *J. Eur. Math. Soc.* **9** (2007) 219–252.
37. E. H. Lieb and M. Loss, *Analysis* (Amer. Math. Soc., 2001).
38. E. A. Lima, R. C. Almeida and J. T. Oden, Analysis and numerical solution of stochastic phase-field models of tumor growth, *Numer. Methods Partial Differential Equations* **31** (2015) 552–574.
39. E. A. Lima, J. T. Oden and R. C. Almeida, A hybrid ten-species phase-field model of tumor growth, *Math. Models Methods Appl. Sci.* **24** (2014) 2569–2599.
40. E. Lima, J. Oden, B. Wohlmuth, A. Shahmoradi, D. Hormuth II, T. Yankeelov, L. Scarabosio and T. Horger, Selection and validation of predictive models of radiation effects on tumor growth based on noninvasive imaging data, *Comput. Methods Appl. Mech. Engrg.* **327** (2017) 277–305.
41. J. L. Lions and E. Magenes, *Non-Homogeneous Boundary Value Problems and Applications I* (Springer-Verlag, 2012).
42. D. H. Madsen and T. H. Bugge, The source of matrix-degrading enzymes in human cancer: Problems of research reproducibility and possible solutions, *J. Cell. Biol.* **209** (2015) 195–198.
43. B. Marchant, J. Norbury and J. Sherratt, Travelling wave solutions to a haptotaxis-dominated model of malignant invasion, *Nonlinearity* **14** (2001) 1653–1671.
44. T. Mengesha and D. Spector, Localization of nonlocal gradients in various topologies, *Calc. Var. Partial Differential Equations* **52** (2015) 253–279.
45. F. Murat and C. Trombetti, A chain rule formula for the composition of a vector-valued function by a piecewise smooth function, *Boll. Unione Mat. Ital.* **6** (2003) 581–595.
46. N. Nargis and R. Aldredge, Effects of matrix metalloproteinase on tumour growth and morphology via haptotaxis, *J. Bioengineer and Biomedical Sci.* **6** (2016), doi:10.4172/2155-9538.1000207
47. J. T. Oden *et al.*, Toward predictive multiscale modeling of vascular tumor growth, *Arch. Comput. Methods Eng.* **23** (2016) 735–779.
48. L. Peng, D. Trucu, P. Lin, A. Thompson and M. A. Chaplain, A multiscale mathematical model of tumour invasive growth, *Bull. Math. Biol.* **79** (2017) 389–429.
49. A. Perumpanani, B. Marchant and J. Norbury, Traveling shock waves arising in a model of malignant invasion, *SIAM J. Appl. Math.* **60** (2000) 463–476.
50. B. Perumpani, A. Sherratt, J. Norbury and H. Byrne, Biological inferences from a mathematical model for malignant invasion, *Invasion Metastasis* **16** (1996) 209–221.
51. J. C. Robinson, *Infinite-Dimensional Dynamical Systems: An Introduction to Dissipative Parabolic PDEs and the Theory of Global Attractors* (Cambridge Univ. Press, 2001).
52. T. Roubíček, *Nonlinear Partial Differential Equations with Applications* (Birkhäuser, 2013).
53. J. Simon, Compact sets in the space  $L^p(0, T; B)$ , *Ann. Math. Pura Appl.* **146** (1986) 65–96.
54. C. Stinner, C. Surulescu and M. Winkler, Global weak solutions in a PDE-ODE system modeling multiscale cancer cell invasion, *SIAM J. Math. Anal.* **46** (2014) 1969–2007.
55. W. Strauss, On continuity of functions with values in various Banach spaces, *Pacific J. Math.* **19** (1966) 543–551.
56. Y. Tao and M. Winkler, A chemotaxis-haptotaxis model: The roles of nonlinear diffusion and logistic source, *SIAM Math. Anal.* **43** (2011) 685–704.



57. C. Walker and G. F. Webb, Global existence of classical solutions for a haptotaxis model, *SIAM J. Math. Anal.* **38** (2007) 1694–1713.
58. W. Walter, *Ordinary Differential Equations* (Springer-Verlag 1998).
59. S. M. Wise, J. S. Lowengrub, H. B. Frieboes and V. Cristini, Three-dimensional multispecies nonlinear tumor growth I: Model and numerical method, *J. Theoret. Biol.* **253** (2008) 524–543.
60. W. P. Ziemer, *Weakly Differentiable Functions: Sobolev Spaces and Functions of Bounded Variation* (Springer-Verlag, 1989).



### **A.3. Analysis of a new multispecies tumor growth model coupling 3D phase-fields with a 1D vascular network**

## **Analysis of a new multispecies tumor growth model coupling 3D phase-fields with a 1D vascular network**

Marvin Fritz, Prashant K. Jha, Tobias Köppl, J. Tinsley Oden, Barbara Wohlmuth

---

The major purpose of this research is to offer a holistic approach to tumor growth that includes analysis and numerics of a novel model of mathematical oncology. The model depicts ECM degradation, interstitial flow, and the influence of vascular flow and nutrition delivery on the growth of tumors. One-dimensional equations are used to model flow and transport mechanisms in the vasculature feeding healthy and malignant tissue. We establish a new 3D-1D coupled model that has not previously been studied and examined in the literature. The transport and flow processes are combined with cell-species models on a three-dimensional domain. For the modeling and prediction of tumor growth, mathematical analysis and numerical treatment of the system of PDEs are useful methods. We apply the Faedo–Galerkin approach and compactness theorems to conduct a rigorous analysis and prove the existence of weak solutions. Due to the unusual nonlinear coupling of the equations and non-standard function spaces, the analysis is not done in a straightforward manner. For the solution tuple, we also derive an energy inequality. A combined finite element/volume technique is used in our numerical treatment. Several numerical experiments in three dimensions are used to demonstrate the evolution of the tumor and the stratification into its proliferative, hypoxic, and necrotic phases. Section 2 introduces the 3D tissue domain, the 1D network domain, and the constituents in the multispecies phase-field model, among other components of the entire model. The controlling PDEs are derived from balance laws and the Ginzburg–Landau free energy functional. The resultant model is a nonlinear coupled system of PDEs with a high degree of nonlinearity and mixed-dimensional coupling. We introduce the cylinder surface  $\Gamma$  and propose a mixed-dimensional coupling through the 2D surface in order to avoid the high-dimensional gap. Section 3 introduces certain analytical preliminaries such as Sobolev embeddings and interpolation inequalities in Bochner spaces that will be utilized in the subsequent sections. In Section 4, we give a theorem stating the existence of weak solutions to the coupled nonlinear 3D-1D model under some given assumptions. We prove the theorem in Section 5 using the Faedo–Galerkin approximation and compactness approaches. Finally, in Section 6, we present numerical data indicating tumor cell development inside a tissue with a vascular network.

I was heavily involved in the generation of concepts and was principally responsible for establishing the mathematical framework and carrying out the analytical effort described in this paper. I took charge in the implementation of the 3D model and the co-authors handled the coupling to the 1D constituents in the code. I was in charge of writing the article, while the co-authors helped by making revisions.

## Permission to include:

Marvin Fritz, Prashant K. Jha, Tobias Köppl, J. Tinsley Oden, Barbara Wohlmuth  
**Analysis of a new multispecies tumor growth model coupling 3D phase-fields  
with a 1D vascular network**

*Nonlinear Analysis: Real World Applications*, 61:103331, 2021

(see also article [57] in the bibliography)

The following pages on copyright are excerpts from copies of the website

<https://www.elsevier.com/about/policies/copyright>

(Accessed on 21 November 2021)



# Copyright

Overview Author rights Institution rights Government rights Find out more

## Overview

In order for Elsevier to publish and disseminate research articles, we need certain publishing rights from authors, which are determined by a publishing agreement between the author and Elsevier.

For articles published open access, the authors license exclusive publishing rights to Elsevier.

For articles published under the subscription model, the authors transfer copyright to Elsevier.

Regardless of whether they choose to publish open access or subscription with Elsevier, authors have many of the same rights under our publishing agreement, which support their need to share, disseminate and maximize the impact of their research.

For open access articles, authors will also have additional rights, depending on the Creative Commons end user license that they select. This Creative Commons license sets out the rights that readers (as well as the authors) have to re-use and share the article: please see [here](#) for more information on how articles can be re-used and shared under these licenses.

This page aims to summarise authors' rights when publishing with Elsevier; these are explained in more detail in the [publishing agreement](#) between the author and Elsevier.

Irrespective of how an article is published, Elsevier is committed to protect and defend authors' works and their reputation. We take allegations of infringement, plagiarism, ethical disputes, and fraud very seriously.

## Author rights

The below table explains the rights that authors have when they publish with Elsevier, for authors who choose to publish either open access or subscription. These apply to the corresponding author and all co-authors.

Author rights in Elsevier's proprietary journals	Published open access	Published subscription
Retain patent and trademark rights	√	√
Retain the rights to use their research data freely without any restriction	√	√
Receive proper attribution and credit for their published work	√	√
Re-use their own material in new works without permission or payment (with full acknowledgement of the original article): 1. Extend an article to book length 2. Include an article in a subsequent compilation of their own work 3. Re-use portions, excerpts, and their own figures or tables in other works.	√	√
Use and share their works for scholarly purposes (with full acknowledgement of the original article): 1. In their own classroom teaching. Electronic and physical distribution of copies is permitted 2. If an author is speaking at a conference, they can present the article and distribute copies to the attendees 3. Distribute the article, including by email, to their students and to research colleagues who they know for their personal use 4. Share and publicize the article via Share Links, which offers 50 days' free access for anyone, without signup or registration 5. Include in a thesis or dissertation (provided this is not published commercially) 6. Share copies of their article privately as part of an invitation-only work group on commercial sites with which the publisher has a hosting agreement	√	√

Publicly share the preprint on any website or repository at any time.	√	√
Publicly share the accepted manuscript on non-commercial sites	√	√ using a CC BY-NC-ND license and usually only after an embargo period (see <a href="#">Sharing Policy</a> for more information)
Publicly share the final published article	√ in line with the author's choice of end user license	×
Retain copyright	√	×

## Institution rights

Regardless of how the author chooses to publish with Elsevier, their institution has the right to use articles for classroom teaching and internal training. Articles can be used for these purposes throughout the author's institution, not just by the author:

Institution rights in Elsevier's proprietary journals (providing full acknowledgement of the original article is given)	All articles
Copies can be distributed electronically as well as in physical form for classroom teaching and internal training purposes	√
Material can be included in coursework and courseware programs for use within the institution (but not in Massive Open Online Courses)	√
Articles can be included in applications for grant funding	√
Theses and dissertations which contain embedded final published articles as part of the formal submission can be posted publicly by the awarding institution with DOI links back to the formal publication on ScienceDirect	√

## Government rights

For US government employees, works created within the scope of their employment are considered to be public domain and Elsevier's publishing agreements do not require a transfer or license of rights for such works.

In the UK and certain commonwealth countries, a work created by a government employee is copyrightable, but the government may own the copyright (Crown copyright). Click [here](#) for information about UK government employees publishing open access.

## Find out more

- Download a sample publishing agreement for articles financed by journal subscriptions in [↓ English](#) and [↓ French](#).
- Download a sample publishing agreement for articles published open access with a [↓ commercial user license](#) (CC BY) and a [↓ non-commercial user license](#) (CC BY-NC-ND)
- For authors who wish to self-archive see our [sharing guidelines](#).
- See our [author pages](#) for further details about how to promote your article.
- See our [hosting](#) page for additional information on hosting research published by Elsevier.
- For use of Elsevier material not defined here please see our [permissions page](#) or visit the [Permissions Support Center](#) ↗ .
- If an author has become aware of a possible plagiarism, fraud or infringement we recommend contacting their Elsevier publishing contact who can then liaise with our in-house legal department.
- If you are publishing in a society or third party owned journal, they may have different publishing agreements. Please see the journal's Guide for Authors for journal specific copyright information.

[Scopus](#)  
[ScienceDirect](#)  
[Mendeley](#)  
[Evolve](#)  
[Knovel](#)  
[Reaxys](#)  
[ClinicalKey](#)

[Submit your paper](#)  
[Find books & journals](#)  
[Visit Author Hub](#)  
[Visit Editor Hub](#)  
[Visit Librarian Hub](#)  
[Visit Reviewer Hub](#)

[About](#)  
[Careers](#)  
[Newsroom](#)  
[Events](#)  
[Publisher relations](#)  
[Advertising, reprints and supplements](#)

[Support and Contact](#)

Follow Elsevier



Select location/language

 Global - English



Copyright © 2021 Elsevier, except certain content provided by third parties

Cookies are used by this site.

[Terms and Conditions](#) [Privacy Policy](#) [Cookie Notice](#) [Sitemap](#)



## **Notice of publication and copyright**

First Published in "Analysis of a new multispecies tumor growth model coupling 3D phase-fields with a 1D vascular network" in *Nonlinear Analysis: Real World Applications* 61:103331 (2021), published by Elsevier.

DOI: <https://doi.org/10.1016/j.nonrwa.2021.103331>





Contents lists available at ScienceDirect

## Nonlinear Analysis: Real World Applications

[www.elsevier.com/locate/nonrwa](http://www.elsevier.com/locate/nonrwa)


# Analysis of a new multispecies tumor growth model coupling 3D phase-fields with a 1D vascular network



Marvin Fritz<sup>a,\*</sup>, Prashant K. Jha<sup>b</sup>, Tobias Köppl<sup>a</sup>, J. Tinsley Oden<sup>b</sup>,  
Barbara Wohlmuth<sup>a</sup>

<sup>a</sup> Department of Mathematics, Technical University of Munich, Germany

<sup>b</sup> Oden Institute for Computational Engineering and Sciences, The University of Texas at Austin, USA

## ARTICLE INFO

*Article history:*

Received 30 October 2020

Received in revised form 17 March 2021

Accepted 21 March 2021

Available online xxxx

*Keywords:*

Tumor growth

3D–1D coupled blood flow models

ECM degradation

Existence of weak solutions

Energy inequality

Galerkin method

## ABSTRACT

In this work, we present and analyze a mathematical model for tumor growth incorporating ECM erosion, interstitial flow, and the effect of vascular flow and nutrient transport. The model is of phase-field or diffused-interface type in which multiple phases of cell species and other constituents are separated by smooth evolving interfaces. The model involves a mesoscale version of Darcy's law to capture the flow mechanism in the tissue matrix. Modeling flow and transport processes in the vasculature supplying the healthy and cancerous tissue, one-dimensional (1D) equations are considered. Since the models governing the transport and flow processes are defined together with cell species models on a three-dimensional (3D) domain, we obtain a 3D–1D coupled model.

© 2021 Elsevier Ltd. All rights reserved.

## 1. Introduction

We develop and analyze a mathematical model of vascular tumor growth designed to simulate abstractions of many of the key phenomena known to be involved in the growth–decline of tumors and therapeutic treatment in living tissue. The complex vascular structure of tissue and the network of blood vessels supplying nutrients to a solid tumor mass embedded in the tissue are modeled as a network of one-dimensional capillaries within a three-dimensional tissue domain, while the growth of the tumor is represented by a phase-field model involving multiple cell species and other constituents. Our tumor models may be regarded as mesoscale depictions of physical and biological events employing continuum mixture theory to construct general forms of the Ginzburg–Landau–Helmholtz free energy of biological materials in terms of volume fractions or mass concentrations of the cell phenotypes and principal mechanical and chemical fields. The equations governing the tumor growth are derived from the balance laws of continuum mixture theory as

\* Corresponding author.

*E-mail addresses:* [fritzm@ma.tum.de](mailto:fritzm@ma.tum.de) (M. Fritz), [pjha@utexas.edu](mailto:pjha@utexas.edu) (P.K. Jha), [koepplto@ma.tum.de](mailto:koepplto@ma.tum.de) (T. Köppl), [oden@oden.utexas.edu](mailto:oden@oden.utexas.edu) (J.T. Oden), [wohlmuth@ma.tum.de](mailto:wohlmuth@ma.tum.de) (B. Wohlmuth).

in e.g. [1–5], and representations of the principal mechanisms governing the development and evolution of cancer [5,6]. In the tissue containing the tumor cells, the microvascular network is represented by a graph structure with 1D filaments through which nutrient-containing blood may flow. The exchange of nutrients between the network and tissue is depicted by a Kedem–Katalchsky type law [7]. We briefly describe the construction of approximations of these models, see also [8–13].

There is a significant and growing volume of published work on various aspects of this subject. Continuum mixture theory as a framework for developing meaningful models of materials with many interacting constituents is proposed in [3–5,10,14,15]. Of particular interest are the comprehensive developments of diffuse-interface multispecies models described in [16,17], the four- and ten species models presented in [5,14], and the multispecies nonlocal models of adhesion and tumor invasion described in [12]. The book compiled by Lowengrub and Cristini [10] contains over 700 references to relevant cancer cell biology and mathematical models of cancer growth. The complex processes underlying angiogenesis which are key to vascular tumor growth present formidable challenges to the goal of predictive computer modeling. Angiogenesis models embedded in models of hypoxic and cell growth or decline were presented in [5,16,18–22]. More recent developments have included models of the vascular network interwoven in tissue containing solid tumors, and the sprouting of capillaries in response to concentrations of various tumor angiogenesis factors so as to supply nutrients to hypoxic tumor cells. Such network-tissue models are discussed in [18,23,24]. These models generalized the lattice-probabilistic network models of [25].

This article is organized as follows: In Section 2, we introduce various components of the complete model, such as the tissue domain, the 1D network domain, the species in the multi-species phase-field model. Further, we present the governing partial differential equations. The resulting model is a highly non-linear coupled system of partial differential equations. We give some analytical preliminaries in Section 3, e.g. Sobolev embeddings and interpolation inequalities in Bochner spaces, which will be used in the following sections. In Section 4, we state a theorem for the existence of weak solutions of the coupled non-linear 3D–1D model under certain given assumptions. In Section 5, we give the proof of the theorem via the Faedo–Galerkin approximation and compactness methods.

## 2. Derivation of the model

### 2.1. Setup and notation

We consider a region of vascularized tissue in a living subject, e.g., within an organ, which is host to a colony of tumor cells and other constituents that make up the so-called microenvironment of a solid tumor. The tumor is contained in an open bounded domain  $\Omega \subset \mathbb{R}^3$  and is supported by a network of macromolecules within  $\Omega$  consisting of collagen, enzymes, and various proteins, that constitute the extracellular matrix (ECM). We focus on developing phenomenological characterizations of the evolutions of the tumor cell colony that attempt to capture mesoscale and macroscale events.

The primary feature of our model of tumor growth is that it employs the framework of continuum mixture theory in which multiple mechanical and chemical species can exist at a point  $x \in \Omega$  at time  $t > 0$ . Thus, for a medium with  $N$  interacting constituents, the volume fraction of each species  $\phi_\alpha$ ,  $1 \leq \alpha \leq N$ , is represented by a field  $\phi_\alpha$  with value  $\phi_\alpha(t, x)$  at  $x \in \Omega$ , and time  $t \geq 0$ , and  $\sum_\alpha \phi_\alpha(t, x) = 1$ . Setting  $\alpha = 1 = T$ , the volume fraction of tumor cells  $\phi_T(t, x)$  is understood to represent an averaged cell concentration, a homogenized depiction over many thousands of cells, since in volumes as small as a voxel in modern tumor imaging techniques,  $4 - 5 \times 10^4$  cells can exist.

We could also develop equivalent models in terms of mass concentration,  $c_\alpha = \rho_\alpha \phi_\alpha$ ,  $\rho_\alpha$  being the mass density of species  $\alpha$ . Moreover, we assume that  $\rho_\alpha = \rho_0 = \text{constant}$ ,  $1 \leq \alpha \leq N$ , and thus,  $C_\alpha$  and  $\phi_\alpha$

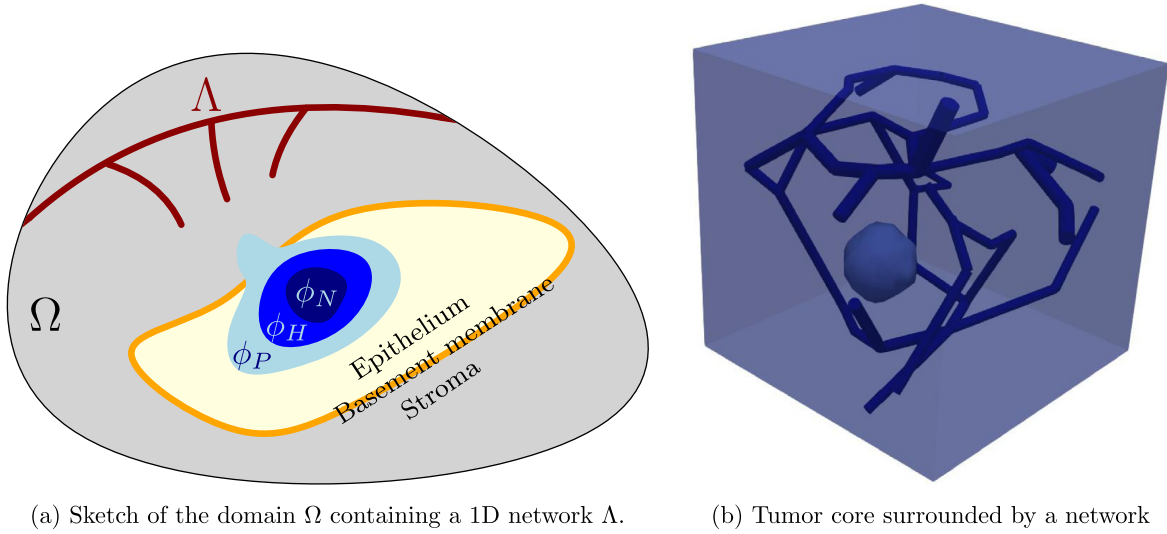


**Fig. 1.** Setup of the domain  $\Omega$  with the microvascular network  $\Lambda = \cup A_i$  and a tumor mass, which is composed in its proliferative ( $\phi_P$ ), hypoxic ( $\phi_H$ ) and necrotic ( $\phi_N$ ) phase (left). Three dimensional presentation of a given tumor core surrounded by a capillary network (right).

are up to a fixed scaling equivalent. This simplification is regarded as a reasonable assumption in many investigations since the mass densities of species are generally close to that of water at room temperature.

As another important feature of our model, we depict the evolving interfaces in which a smooth boundary layer exists and which is defined intrinsically as a feature of the solution of the forward problem. This feature is a property of phase-field or diffuse-interface models and avoids complex interface tracking while producing characterizations of interfaces between cell species which are in good agreement with actual observations (see Fig. 1).

Moreover, we consider a one-dimensional graph-like structure  $\Lambda$  inside of  $\Omega$  forming a microvascular network. The single edges of  $\Lambda$  are denoted by  $A_i$  such that  $\Lambda$  is given by  $\Lambda = \cup_{i=1}^N A_i$ . The edge  $A_i$  is parameterized by a curve parameter  $s_i$ , such that  $A_i$  is given by:

$$A_i = \{x \in \Omega \mid x = A_i(s_i) = x_{i,1} + s_i \cdot (x_{i,2} - x_{i,1}), s_i \in (0, 1)\}.$$

Thereby,  $x_{i,1} \in \Omega$  and  $x_{i,2} \in \Omega$  mark the boundary nodes of  $A_i$ , see Fig. 2. For the total 1D network  $\Lambda$ , we introduce a global curve parameter  $s$ , which has to be interpreted in the following way:  $s = s_i$ , if  $x = \Lambda(s) = A_i(s_i)$ . At each value of the curve parameter  $s$ , we study 1D constituents, which couple to their respective 3D counter-part in  $\Omega$ . In order to formulate the coupling between 3D and 1D constituents in Sections 2.3 and 2.4, we need to introduce the surface  $\Gamma$  of the microvascular network. For simplicity, it is assumed that the surface for a single vessel is approximated by a cylinder with a constant radius, see Fig. 2. The radius of a vessel that is associated with  $A_i$ , is given by  $R_i$  and the corresponding surface is denoted by  $\Gamma_i$ . In fact,  $\Gamma_i$  is the surface of the cylinder whose center line is given by  $A_i$ , i.e.,

$$\Gamma_i = \{x \in \Omega \mid \text{dist}(x, A_i(s_i)) = R_i, s_i \in (0, 1)\}.$$

According to the definition of  $\Lambda$ , the total surface  $\Gamma$  is given by the union of the single vessel surfaces, i.e.,  $\Gamma = \cup_{i=1}^N \Gamma_i$ .

## 2.2. Constituents

After introducing the domains on which the 1D and 3D models are defined, we describe in a next step all the dependent variables occurring in our model.

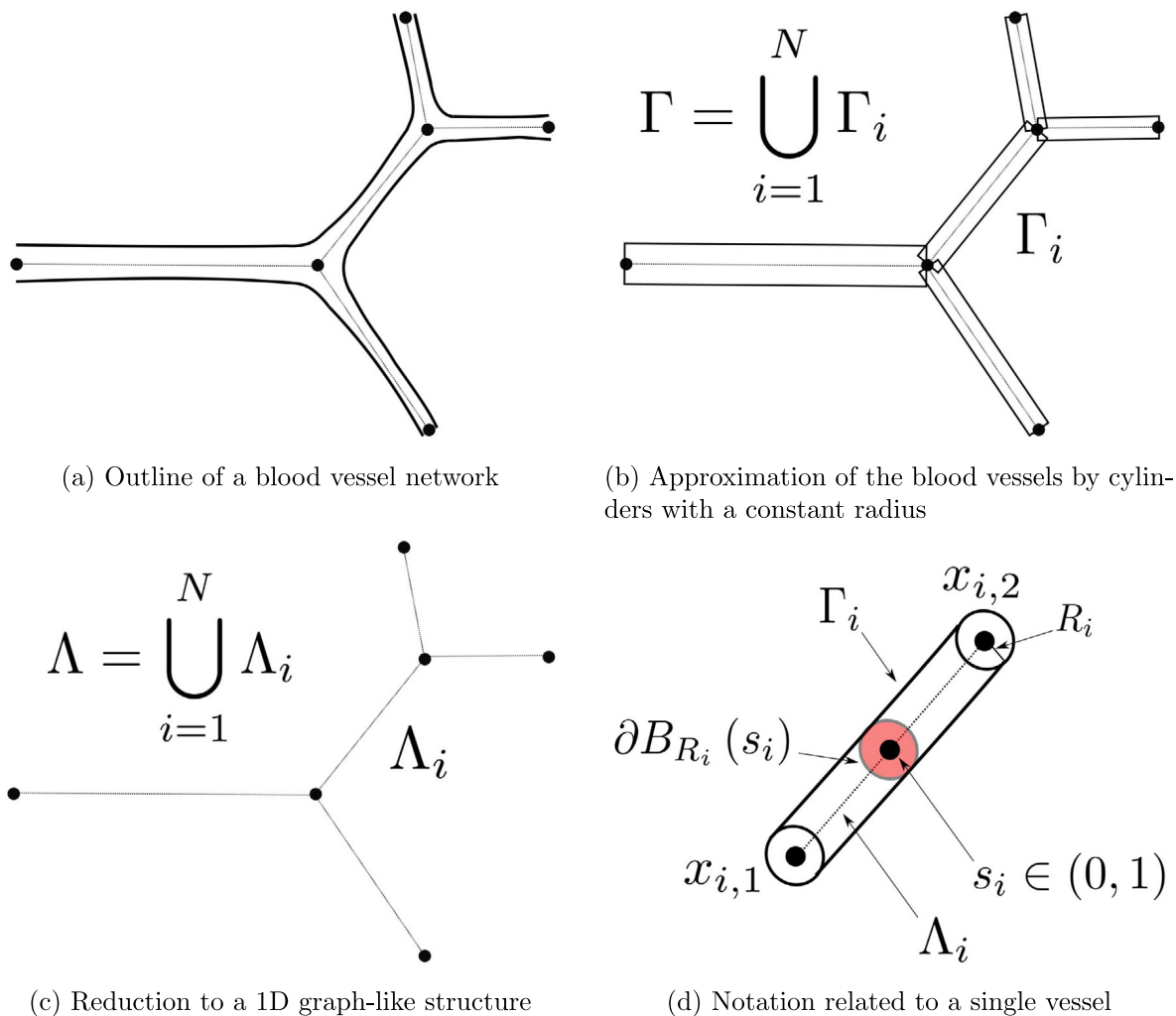


**Fig. 2.** Modeling a blood vessel network (A) by means of a 1D graph-like structure (C). At first the surface of the blood vessels is approximated by cylinders with constant radius whose surfaces are denoted by  $\Gamma_i$ , see (B). Then, the blood vessels are lumped to the center lines  $\Lambda_i$  of the cylinders.

The tumor cell's field,  $\phi_T = \phi_T(t, x)$ , can be represented as the sum of three components,  $\phi_T = \phi_P + \phi_H + \phi_N$ , where  $\phi_P = \phi_P(t, x)$  is the volume fraction of proliferative cells,  $\phi_H = \phi_H(t, x)$  that of hypoxic cells, and  $\phi_N = \phi_N(t, x)$  is the volume fraction of necrotic cells. Proliferative cells are those which have a high probability of mitosis, division into twin cells, and to produce growth of tumor. Hypoxic cells are those tumor cells deprived of sufficient nutrient (e.g., oxygen) to become or remain proliferative and necrotic cells have died due to the lack of nutrients. The local nutrient concentration is represented by a field  $\phi_\sigma = \phi_\sigma(t, x)$ . The tumor cells response to hypoxia (e.g., low oxygen), i.e.,  $\phi_\sigma$  is below a certain threshold, by the production of an enzyme (hypoxia-inducible factor) that accumulates and increases cell mobility and activates the secretion of angiogenesis promoting factors characterized by another field,  $\phi_{TAF} = \phi_{TAF}(t, x)$ , tumor angiogenesis factor. Of several such factors, that most frequently addressed, is VEGF, Vascular Endothelial Growth Factor, which induces sprouting of endothelial cells forming the tubular structure of blood vessels, the lumens, which grow into new vessels that supply nutrient to the hypoxic cells. In this article, we treat a stationary network of endothelial cells and neglect the sprouting.

Moreover, at lower oxygen levels the hypoxic cells release matrix-degenerative enzymes such urokinase-plasminogen and matrix metalloproteinases, labeled MDEs, with volume fraction denoted by  $\phi_{MDE} =$

$\phi_{MDE}(t, x)$ , that can erode the extracellular matrix, whose density is denoted by  $\phi_{ECM} = \phi_{ECM}(t, x)$ , and make room for invasion of tumor cells, increasing  $\phi_T$  in the ECM domain and increasing the likelihood of metastasis. Below a certain level of nutrient, or sustained periods of hypoxia, cells may die and enter the necrotic phase represented by the field  $\phi_N$ . In many forms of cancer, necrotic cells undergo calcification and become inert and can be removed as waste from the organism.

On the one-dimensional network  $\Lambda$ , we consider the constituents  $\phi_v = \phi_v(t, s)$  and  $v_v = v_v(t, s)$ , which represent the one-dimensional counter-part of the local nutrient concentration  $\phi_\sigma$  and the volume-averaged velocity  $v$ . In addition, we consider both in the vascular system and the tissue domain pressure variables that are denoted by  $p_v$  and  $p$ , respectively. The different constituents are coupled by the source terms of the different partial differential equations governing the behavior of the constituents.

For convenience, we collect the constituents within the following 7-tuple:

$$\phi = (\phi_P, \phi_H, \phi_N, \phi_\sigma, \phi_{MDE}, \phi_{TAF}, \phi_{ECM}) = (\phi_\alpha)_{\alpha \in \mathcal{A}},$$

where  $\mathcal{A} = \{P, H, N, \sigma, ECM, MDE, TAF\}$ , and further, we distinguish between the tumor phase-field indices  $\mathcal{CH} = \{P, H, N\}$ , the reaction–diffusion indices  $\mathcal{RD} = \{\sigma, MDE, TAF\}$  and the evolution index  $\{ECM\}$ , which corresponds to an abstract ordinary differential equation.

### 2.3. Three-dimensional model

The constituents  $\phi_\alpha$ ,  $\alpha \in \mathcal{A}$ , are governed by the following mass balance law, see e.g., [5,26],

$$\partial_t \phi_\alpha + \operatorname{div}(\phi_\alpha v_\alpha) = -\operatorname{div} J_\alpha(\phi) + S_\alpha(\phi), \tag{1}$$

for all  $\alpha \in \mathcal{A}$ , where  $v_\alpha$  is the cell velocity of the  $\alpha$ th constituent, and  $S_\alpha$  describes a mass source term depending on all species  $\phi$ . Moreover,  $J_\alpha$  denotes the flux of the  $\alpha$ th constituent, which is given by

$$J_\alpha(\phi) = -m_\alpha(\phi) \nabla \mu_\alpha. \tag{2}$$

Here,  $\mu_\alpha$  denotes the chemical potential of the  $\alpha$ th species and  $m_\alpha$  the mobility function of it. In our applications, we consider the mobilities

$$\begin{aligned} m_\alpha(\phi) &= M_\alpha \phi_\alpha^2 (1 - \phi_\alpha)^2 I_d, & \alpha \in \mathcal{CH}, \\ m_\beta(\phi) &= M_\beta I_d, & \beta \in \mathcal{RD}, \\ m_{ECM}(\phi) &= 0, \end{aligned}$$

where  $M_\alpha$  are mobility constants and  $I_d$  is the  $(d \times d)$ -dimensional identity matrix. Especially, we choose  $m_{ECM} = 0$  in accordance to the non-diffusivity of the ECM, see [27]. Following [5,14,16,26], we define the chemical potential as

$$\mu_\alpha = \frac{\delta \mathcal{E}(\phi)}{\delta \phi_\alpha},$$

where  $\delta \mathcal{E} / \delta \phi_\alpha$  denotes the first variation (Gâteaux derivative) of the Ginzburg–Landau–Helmholtz free energy functional,

$$\mathcal{E}(\phi) = \int_\Omega \left\{ \Psi(\phi_P, \phi_H, \phi_N) + \sum_{\alpha \in \mathcal{CH}} \frac{\varepsilon_\alpha^2}{2} |\nabla \phi_\alpha|^2 + \sum_{\beta \in \mathcal{RD}} \frac{D_\beta}{2} \phi_\beta^2 - (\chi_c \phi_\sigma + \chi_h \phi_{ECM}) \sum_{\alpha \in \{P, H\}} \phi_\alpha \right\} dx. \tag{3}$$

Here,  $\chi_c$  is the chemotaxis parameter, see [28],  $\chi_h$  represents the haptotaxis parameter, see [12,29], and  $\varepsilon_\alpha$ ,  $\alpha \in \mathcal{CH}$ , is a parameter associated with the interface thickness separating the different cell species. Lastly,  $\Psi$  represents a double-well potential, e.g., it can be of Landau type, where we mention the three possibilities

$$\begin{aligned} \Psi(\phi_P, \phi_H, \phi_N) &= C_{\psi_T} \phi_T^2 (1 - \phi_T)^2, \\ \Psi(\phi_P, \phi_H, \phi_N) &= C_{\psi_P} \phi_P^2 (1 - \phi_P)^2 + C_{\psi_H} \phi_H^2 (1 - \phi_H)^2 + C_{\psi_N} \phi_N^2 (1 - \phi_N)^2 + C_{\psi_T} \phi_T^2 (1 - \phi_T)^2, \\ \Psi(\phi_P, \phi_H, \phi_N) &= C_{\psi_P} \phi_P^2 (1 - \phi_T)^2 + C_{\psi_H} \phi_H^2 (1 - \phi_T)^2 + C_{\psi_N} \phi_N^2 (1 - \phi_T)^2, \end{aligned}$$

where  $C_{\psi_\alpha}$  are appropriate prefactors. Alternatively, one can also select a logarithmic potential of Flory–Huggins type, e.g., see [30,31],

$$\begin{aligned} \Psi(\phi_P, \phi_H, \phi_N) &= C_{\psi_P} \phi_P \log \phi_P + C_{\psi_H} \phi_H \log \phi_H + C_{\psi_N} \phi_N \log \phi_N + C_{\psi_T} (1 - \phi_T) \log(1 - \phi_T) \\ &\quad + \frac{1}{2} (C_{\psi_P} \phi_P (1 - \phi_P) + C_{\psi_H} \phi_H (1 - \phi_H) + C_{\psi_N} \phi_N (1 - \phi_N) + C_{\psi_T} \phi_T (1 - \phi_T)). \end{aligned}$$

Lastly, we also mention potentials, which are used for abstract multiphase models, see [15],

$$\Psi(\phi_P, \phi_H, \phi_N) = C_{\psi_P} \phi_P^2 \phi_H^2 + C_{\psi_H} \phi_H^2 \phi_N^2 + C_{\psi_N} \phi_N^2 \phi_P^2,$$

The chemical potentials read

$$\begin{aligned} \mu_\alpha &= \partial_{\phi_\alpha} \Psi(\phi_P, \phi_H, \phi_N) - \varepsilon_\alpha^2 \Delta \phi_\alpha - \chi_c \phi_\sigma - \chi_h \phi_{ECM}, & \alpha \in \mathcal{CH} \setminus \{N\}, \\ \mu_\beta &= D_\beta \phi_\beta, & \beta \in \mathcal{RD} \setminus \{\sigma\}, \\ \mu_N &= \partial_{\phi_N} \Psi(\phi_P, \phi_H, \phi_N) - \varepsilon_N^2 \Delta \phi_N, & (4) \\ \mu_\sigma &= D_\sigma \phi_\sigma - \chi_c (\phi_P + \phi_H), \\ \mu_{ECM} &= -\chi_h (\phi_P + \phi_H). \end{aligned}$$

The necrotic cells are non-moving and only gain mass from the nutrient-lacking hypoxic cells. Therefore, the mobility of the necrotic cells is set to zero. Consequently, we have  $m_N = v_N = 0$ . Consequently, inserting (2) and (4) into the mass balance equation (1), we arrive at the equations for  $(\phi_\alpha)_{\alpha \in \mathcal{CH}}$

$$\begin{aligned} \partial_t \phi_P + \operatorname{div}(\phi_P v) &= \operatorname{div}(m_P(\phi) \nabla \mu_P) + S_P(\phi), \\ \mu_P &= \partial_{\phi_P} \Psi(\phi_P, \phi_H, \phi_N) - \varepsilon_P^2 \Delta \phi_P - \chi_c \phi_\sigma - \chi_h \phi_{ECM}, \\ \partial_t \phi_H + \operatorname{div}(\phi_H v) &= \operatorname{div}(m_H(\phi) \nabla \mu_H) + S_H(\phi), & (5) \\ \mu_H &= \partial_{\phi_H} \Psi(\phi_P, \phi_H, \phi_N) - \varepsilon_H^2 \Delta \phi_H - \chi_c \phi_\sigma - \chi_h \phi_{ECM}, \\ \partial_t \phi_N &= S_N(\phi). \end{aligned}$$

Further, we propose the source functions

$$\begin{aligned} S_P(\phi) &= \lambda_P \phi_\sigma \phi_P (1 - \phi_T) - \lambda_A \phi_P - \lambda_{PH} \mathcal{H}(\sigma_{PH} - \phi_\sigma) \phi_P + \lambda_{HP} \mathcal{H}(\phi_\sigma - \sigma_{HP}) \phi_H, \\ S_H(\phi) &= \lambda_{P_h} \phi_\sigma \phi_H (1 - \phi_T) - \lambda_{A_h} \phi_H + \lambda_{PH} \mathcal{H}(\sigma_{PH} - \phi_\sigma) \phi_P - \lambda_{HP} \mathcal{H}(\phi_\sigma - \sigma_{HP}) \phi_H \\ &\quad - \lambda_{HN} \mathcal{H}(\sigma_{HN} - \phi_\sigma) \phi_H, & (6) \\ S_N(\phi) &= \lambda_{HN} \mathcal{H}(\sigma_{HN} - \phi_\sigma) \phi_H. \end{aligned}$$

In (5),  $v = v_\alpha$  is a volume-averaged velocity for the fields  $\phi_P$  and  $\phi_H$ . In (6),  $\lambda_P$  is the rate of cellular mitosis of tumor cells,  $\lambda_A$  and  $\lambda_{A_h}$  are the apoptosis rates of the proliferative and hypoxic cells, respectively,  $\lambda_{P_h}$  is the proliferation rate of hypoxic cells,  $\lambda_{PH}$  the transition rate from the proliferative to the hypoxic phase below the nutrient level  $\sigma_{PH}$ ,  $\lambda_{HP}$  the transition rate from the hypoxic to the proliferative phase above the nutrient level  $\sigma_{HP}$ , and  $\lambda_{HN}$  the transition rate from the hypoxic to the necrotic phase below the nutrient level  $\sigma_{HN}$ . Finally,  $\mathcal{H}$  denotes the Heaviside step function.

Related models of extracellular matrix (ECM) degradation due to matrix-degenerative enzymes (MDEs) released by hypoxic cell concentrations and subsequent tumor invasion and metastasis are discussed in [32–37]. Following these references, we introduce the equation for the ECM evolution,

$$\begin{aligned} \partial_t \phi_{ECM} &= S_{ECM}(\phi) \\ &= -\lambda_{ECM_D} \phi_{ECM} \phi_{MDE} + \lambda_{ECM_P} \phi_\sigma (1 - \phi_{ECM}) \mathcal{H}(\phi_{ECM} - \phi_{ECM_P}), & (7) \end{aligned}$$

where  $\lambda_{ECM_D}$  is the degradation rate of ECM fibers due to the matrix degrading enzymes, and  $\lambda_{ECM_P}$  is the production rate of ECM fibers above the threshold level  $\phi_{ECM_P}$  for the ECM density.

Further, for  $(\phi_\beta)_{\beta \in \mathcal{RD}}$  we arrive at the following system of equations

$$\begin{aligned} \partial_t \phi_\sigma + \operatorname{div}(\phi_\sigma v) &= \operatorname{div}(m_\sigma(\phi))(D_\sigma \nabla \phi_\sigma - \chi_c \nabla(\phi_P + \phi_H)) + S_\sigma(\phi) + S_{\sigma v}(\phi_\sigma, p, \phi_v, p_v), \\ \partial_t \phi_{MDE} &= \operatorname{div}(m_{MDE}(\phi) D_{MDE} \nabla \phi_{MDE}) + S_{MDE}(\phi), \\ \partial_t \phi_{TAF} &= \operatorname{div}(m_{TAF}(\phi) D_{TAF} \nabla \phi_{TAF}) + S_{TAF}(\phi), \end{aligned} \tag{8}$$

with source functions

$$\begin{aligned} S_\sigma(\phi) &= -\lambda_P \phi_\sigma \phi_P (1 - \phi_T) - \lambda_{P_h} \phi_\sigma \phi_H (1 - \phi_T) + \lambda_A \phi_P + \lambda_{A_h} \phi_H + \lambda_{ECM_D} \phi_{ECM} \phi_{MDE} \\ &\quad - \lambda_{ECM_P} \phi_\sigma (1 - \phi_{ECM}) \mathcal{H}(\phi_{ECM} - \phi_{ECM_P}), \\ S_{MDE}(\phi) &= -\lambda_{MDE_D} \phi_{MDE} + \lambda_{MDE_P} (\phi_P + \phi_H) \phi_{ECM} \frac{\sigma_{HP}}{\sigma_{HP} + \phi_\sigma} (1 - \phi_{MDE}) - \lambda_{ECM_D} \phi_{ECM} \phi_{MDE}, \\ S_{TAF}(\phi) &= \lambda_{TAF_P} (1 - \phi_{TAF}) \phi_H \mathcal{H}(\phi_H - \phi_{H_P}) - \lambda_{TAF_D} \phi_{TAF}. \end{aligned} \tag{9}$$

Here,  $\lambda_{MDE_D}$  and  $\lambda_{TAF_D}$  denote the decay rates of the MDEs and TAFs, respectively,  $\lambda_{MDE_P}$  the production rate of MDEs, and  $\lambda_{TAF_P}$  is the production rate of the  $\phi_{TAF}$  due to the release by hypoxic cells above a threshold value of  $\phi_{H_P}$ . We note that the cell species  $\phi_\alpha$ ,  $\alpha \in \{P, H, N, \sigma, ECM\}$ , form a mass conserving subsystem in the sense that their source terms add to zero. The fields  $\phi_{MDE}$  and  $\phi_{TAF}$  do not belong to this mass exchanging closed subsystem system since they show natural degradation factors.

Additionally, we have introduced a source term  $S_{\sigma v}$  in (8) for the nutrient volume fraction  $\phi_\sigma$ , which depends on the 1D constituents  $\phi_v$  and  $p_v$ , and therefore, this source term is responsible for the coupling between the constituents in  $\Omega$  and  $\Lambda$ . In particular, it governs the exchange of nutrients between the vascular network and the tissue. In order to quantify the flux of nutrients across the vessel surface, we use the Kedem–Katchalsky law, see e.g., [7],

$$J_{\sigma v}(\bar{\phi}_\sigma, \bar{p}, \phi_v, p_v) = (1 - r_\sigma) J_{pv}(\bar{p}, p_v) \phi_\sigma^v + L_\sigma (\phi_v - \bar{\phi}_\sigma), \tag{10}$$

where  $J_{\sigma v}$  represents the flux of nutrients between the vascular network and the tissue. The Kedem–Katchalsky law (10) consists of two parts: The first part quantifies the nutrient flux caused by the flux of blood plasma  $J_{pv}$  from the vessels into the tissue or vice versa. It is determined by Starling’s law, which is given by the pressure difference between  $p_v$  and  $p$  weighted by a parameter  $L_p$  for the permeability of the vessel wall,

$$J_{pv}(\bar{p}, p_v) = L_p (p_v - \bar{p}). \tag{11}$$

Here,  $\bar{p}$  denotes an averaged pressure over the circumference of cylinder cross-sections. For each parameter  $s_i$ , we consider a point on the curve  $A_i(s_i)$ . Around this point a circle  $\partial B_{R_i}(s_i)$  of radius  $R_i$  and perpendicular to  $A_i$  is constructed and the tissue pressure  $p$  is averaged with respect to  $\partial B_{R_i}(s_i)$ ,

$$\bar{p}(s_i) = \frac{1}{2\pi R_i} \int_{\partial B_{R_i}(s_i)} p|_\Gamma(x) \, dS.$$

From a physical point of view, the averaging reflects the fact that the 3D–1D coupling is a reduced model, whereas in a fully coupled 3D–3D model, the exchange occurs through the surface.

In order to account for the permeability of the vessel wall with respect to the nutrients,  $J_{pv} \phi_\sigma^v$  is weighted by a factor  $1 - r_\sigma$ , where  $r_\sigma$  is considered as a reflection parameter. The value of  $\phi_\sigma^v$  is either set to  $\bar{\phi}_\sigma$  or  $\phi_v$  depending on the sign of  $J_{pv}$ ,

$$\phi_\sigma^v = \begin{cases} \phi_v, & p_v \geq \bar{p}, \\ \bar{\phi}_\sigma, & p_v < \bar{p}. \end{cases}$$

The second part of the law (10) is a Fickian type law, accounting for the tendency of the nutrients to balance out their concentration levels. Again, the 3D quantity  $\phi_\sigma$  has to be averaged such that it can be related to the 1D quantity  $\phi_v$ ,

$$\bar{\phi}_\sigma(s_i) = \frac{1}{2\pi R_i} \int_{\partial B_{R_i}(s_i)} \phi_\sigma|_\Gamma(x) \, dS.$$

The permeability of the vessel wall is represented by another parameter  $L_\sigma$ .

Since the exchange processes between the vascular network and the tissue occur at the vessel surface  $\Gamma$ , we concentrate the flux  $J_{\sigma v}$  by means of the Dirac measure  $\delta_\Gamma$ , i.e., with the distributional space  $\mathcal{D}' = (C_c^\infty(\Omega))'$  we define

$$\langle \delta_\Gamma, \varphi \rangle_{\mathcal{D}' \times \mathcal{D}} = \int_\Gamma \varphi|_\Gamma(x) \, dS \quad \text{for all } \varphi \in \mathcal{D}.$$

This yields the following source term in (8),

$$S_{\sigma v}(\phi_\sigma, p, \phi_v, p_v) = J_{\sigma v}(\phi_\sigma, p, \Pi_\Gamma \phi_v, \Pi_\Gamma p_v) \delta_\Gamma,$$

where  $\Pi_\Gamma \in \mathcal{L}(L^2(\Lambda); L^2(\Gamma))$  is the projection of the 1D quantities onto the cylindrical surface  $\Gamma$  via extending the function value  $\Pi_\Gamma \phi_v(s) = \phi_v(s_i)$  for all  $s \in \partial B_{R_i}(s_i)$ . In particular, we have

$$\int_{\partial B_{R_i}(s_i)} \Pi_\Gamma \phi_v(x) \, dS = 2\pi R_i \phi_v(s_i).$$

We assume a volume-averaged velocity  $v$  for the proliferative cells, hypoxic cells, and the nutrients. This assumption of a volume-averaged velocity is reasonable since the cells are tightly packed. Therefore, we assume  $v$  to obey the compressible Darcy law

$$\begin{aligned} v &= -K(\nabla p - S_p(\phi, \mu_P, \mu_H)), \\ -\operatorname{div}(K\nabla p) &= J_{pv}(p, \Pi_\Gamma p_v) \delta_\Gamma - \operatorname{div}(KS_p(\phi, \mu_P, \mu_H)), \end{aligned} \tag{12}$$

where  $K > 0$  is the permeability and  $J_{pv}(p, \Pi_\Gamma p_v) \delta_\Gamma$  models the flux between the vascular system and the tissue. Moreover, the source  $S_p$  is assumed to represent a form of the elastic Korteweg force, e.g., see [30], and we correct the chemical potential by the haptotaxis and chemotaxis adhesion terms as done in [15], giving

$$S_p(\phi, \mu_P, \mu_H) = -(\nabla \mu_P + \chi_c \nabla \phi_\sigma + \chi_h \nabla \phi_{ECM}) \phi_P - (\nabla \mu_H + \chi_c \nabla \phi_\sigma + \chi_h \nabla \phi_{ECM}) \phi_H. \tag{13}$$

Collecting (5)–(12), we arrive at a model governed by the system,

$$\begin{aligned} \partial_t \phi_P + \operatorname{div}(\phi_P v) &= \operatorname{div}(m_P(\phi) \nabla \mu_P) + S_P(\phi), \\ \mu_P &= \partial_{\phi_P} \Psi(\phi_P, \phi_H, \phi_N) - \varepsilon_P^2 \Delta \phi_P - \chi_c \phi_\sigma - \chi_h \phi_{ECM}, \\ \partial_t \phi_H + \operatorname{div}(\phi_H v) &= \operatorname{div}(m_H(\phi) \nabla \mu_H) + S_H(\phi), \\ \mu_H &= \partial_{\phi_H} \Psi(\phi_P, \phi_H, \phi_N) - \varepsilon_H^2 \Delta \phi_H - \chi_c \phi_\sigma - \chi_h \phi_{ECM}, \\ \partial_t \phi_N &= S_N(\phi), \\ \partial_t \phi_\sigma + \operatorname{div}(\phi_\sigma v) &= \operatorname{div}(m_\sigma(\phi))(D_\sigma \nabla \phi_\sigma - \chi_c \nabla(\phi_P + \phi_H)) + S_\sigma(\phi) + J_{\sigma v}(\phi_\sigma, p, \Pi_\Gamma \phi_v, \Pi_\Gamma p_v) \delta_\Gamma, \\ \partial_t \phi_{MDE} &= \operatorname{div}(m_{MDE}(\phi) D_{MDE} \nabla \phi_{MDE}) + S_{MDE}(\phi), \\ \partial_t \phi_{TAF} &= \operatorname{div}(m_{TAF}(\phi) D_{TAF} \nabla \phi_{TAF}) + S_{TAF}(\phi), \\ \partial_t \phi_{ECM} &= S_{ECM}(\phi), \\ v &= -K(\nabla p - S_p(\phi, \mu_P, \mu_H)), \\ -\operatorname{div}(K\nabla p) &= J_{pv}(p, \Pi_\Gamma p_v) \delta_\Gamma - \operatorname{div}(KS_p(\phi, \mu_P, \mu_H)), \end{aligned} \tag{14}$$

in the time–space domain  $(0, T) \times \Omega$  with source functions  $S_P, S_H, S_N, S_\sigma, S_{MDE}, S_{TAF}, S_{ECM}, S_p$ , recall (6), (9) and (13), with properties laid down in Assumption 1 of Section 4. We supplement the system with the following boundary and initial conditions,

$$\begin{aligned} m_\alpha(\phi) \partial_n \mu_\alpha - \phi_\alpha v \cdot n &= m_\beta(\phi) \partial_n \phi_\beta = \partial_n \phi_\gamma = 0 && \text{on } (0, T) \times \partial\Omega, \\ p &= p_\infty && \text{on } (0, T) \times \partial\Omega_D, \\ \partial_n p &= 0 && \text{on } (0, T) \times \partial\Omega \setminus \partial\Omega_D, \\ \phi_\delta(0) &= \phi_{\delta,0} && \text{in } \Omega, \end{aligned} \tag{15}$$



for  $\alpha \in \{P, H\}$ ,  $\beta \in \mathcal{RD}$ ,  $\gamma \in \mathcal{CH} \cup \{ECM\}$ , and  $\delta \in \mathcal{A}$ . Here,  $\phi_{\delta,0}$  are given functions with regularity as in Assumption 1 of Section 4,  $\partial_n f = \nabla f \cdot n$  denotes the normal derivative of a function  $f$  at the boundary  $\partial\Omega$  with the outer unit normal  $n$  and  $\partial\Omega_D$  is a part of the boundary with positive measure representing an inlet where the pressure is set to the time-dependent function  $p_\infty : (0, T) \times \Omega \rightarrow \mathbb{R}$ .

2.4. One-dimensional model for flow and nutrient transport in the vascular network

Since the vascular network typically forms a system of small inclusions, we average all the physical units across the cross-sections of the single blood vessels and set them to a constant with respect to the angular and radial component. This means that the 1D variables  $\phi_v$  and  $p_v$  on a 1D vessel  $\Lambda_i$  depend only on  $s_i$ . For further details related to the derivation of 1D pipe flow and transport models, we refer to [38]. Accordingly, the 1D model equations for flow and transport on  $\Lambda_i$  read as follows,

$$\begin{aligned} \partial_t \phi_v + \partial_{s_i}(v_v \phi_v) &= \partial_{s_i}(m_v(\phi_v) D_v \partial_{s_i} \phi_v) - 2\pi R_i J_{\sigma v}(\bar{\phi}_\sigma, \bar{p}, \phi_v, p_v), \\ - \partial_{s_i}(R_i^2 \pi K_{v,i} \partial_{s_i} p_v) &= -2\pi R_i J_{pv}(\bar{p}, p_v). \end{aligned} \tag{16}$$

As in (14), the fluxes  $J_{\sigma v}$  and  $J_{pv}$  account for the exchange processes between the blood vessels and the tissue. The permeability is given by the relation  $K_{v,i} = \frac{R_i^2}{8\mu_{bl}}$ , where  $\mu_{bl}$  represents the viscosity of blood. For convenience, we fix it to a constant value, i.e., the non-Newtonian behavior of blood is not considered in this work. The diffusivity parameter  $D_v$  is the same as the one of the nutrients in the blood. The blood velocity  $v_v$  is calculated as follows via a Darcy-type model,

$$v_v = -R_i^2 \pi K_{v,i} \partial_{s_i} p_v.$$

In order to interconnect the different solutions on  $\Lambda_i$  at inner networks nodes on intersections  $x \in \partial\Lambda_i \setminus \partial\Lambda$ , we require the continuity of pressure and concentration as well as the conservation of mass to obtain a physically relevant solution. To formulate these coupling conditions in a mathematical way, we define for each bifurcation point  $x$  an index set  $N(x) \subset \{1, \dots, N\}$ :

$$N(x) = \{i \mid x \in \partial\Lambda_i, i \in \{1, \dots, N\}\}.$$

Using this notation, we have for  $p_v$  and  $\phi_v$  four different coupling conditions at an inner node  $x \in \partial\Lambda_i$ :

1. Continuity of  $p_v$ :

$$p_v|_{\Lambda_i}(x) = p_v|_{\Lambda_j}(x) \quad \text{for all } j \in N(x) \setminus \{i\}.$$

2. Mass conservation with respect to  $p_v$ :

$$\sum_{j \in N(x)} -\frac{R_j^4 \pi}{8\mu_{bl}} \frac{\partial p_v}{\partial s_j} \Big|_{\Lambda_j}(x) = 0.$$

3. Continuity of  $\phi_v$ :

$$\phi_v|_{\Lambda_i}(x) = \phi_v|_{\Lambda_j}(x) \quad \text{for all } j \in N(x) \setminus \{i\}.$$

4. Mass conservation with respect to  $\phi_v$ :

$$\sum_{j \in N(x)} \left( v_v \phi_v - m_v(\phi_v) D_v \frac{\partial \phi_v}{\partial s_j} \right) \Big|_{\Lambda_j}(x) = 0.$$

Further, we decompose the boundary of  $\Lambda$  into a Dirichlet boundary  $\partial\Lambda_D$  and a Neumann boundary  $\partial\Lambda_N$  such that  $\partial\Lambda = \partial\Lambda_D \dot{\cup} \partial\Lambda_N$ . We introduce the inlet functions  $\phi_{v,\infty}, p_{v,\infty} : (0, T) \rightarrow \mathbb{R}$  on  $\partial\Lambda_D$  and prescribe the following boundary data for  $\phi_v$  and  $p_v$ ,

$$\begin{aligned} \phi_v - \phi_{v,\infty} = p_v - p_{v,\infty} &= 0 \quad \text{on } (0, T) \times \partial\Lambda_D, \\ \partial_{n_\Lambda} \phi_v = \partial_{n_\Lambda} p_v &= 0 \quad \text{on } (0, T) \times \partial\Lambda_N. \end{aligned} \tag{17}$$

### 3. Analytical preliminaries

Notationally, we equip the function spaces  $L^p(\Omega)$ ,  $L^p(\Lambda)$ ,  $W^{m,p}(\Omega)$ ,  $W^{m,p}(\Lambda)$  with the norms  $|\cdot|_{L^p(\Omega)}$ ,  $|\cdot|_{L^p(\Lambda)}$ ,  $|\cdot|_{W^{m,p}(\Omega)}$ ,  $|\cdot|_{W^{m,p}(\Lambda)}$ . In the case of  $d$ -dimensional vector functions, we write  $L^p(\Omega; \mathbb{R}^d)$  and in the same way for the other Banach spaces, but we do not make this distinction in the notation of norms, scalar products and applications with its dual.

Throughout this paper,  $C < \infty$  stands for a generic constant, which may change from line to line. For brevity, we write  $x \lesssim y$  for  $x \leq Cy$ . We recall the Poincaré–Wirtinger and Sobolev inequalities, see [39–41],

$$\begin{aligned} |f - f_\Omega|_{L^p(\Omega)} &\lesssim |\nabla f|_{L^p(\Omega)} \quad \text{for all } f \in W^{1,p}(\Omega), \\ |f|_{L^p(\Omega)} &\lesssim |\nabla f|_{L^p(\Omega)} \quad \text{for all } f \in W_0^{1,p}(\Omega), \\ |f|_{W^{m,q}(\Omega)} &\lesssim |f|_{W^{k,p}(\Omega)} \quad \text{for all } f \in W^{k,p}(\Omega), \quad k - \frac{d}{p} \geq m - \frac{d}{q}, \quad k \geq m, \end{aligned} \tag{18}$$

where  $p, q \in [1, \infty)$  and  $f_\Omega = \frac{1}{|\Omega|} \int_\Omega f(x) dx$  denotes the mean of  $f$  with respect to  $\Omega$ . Also, the last inequality yields the continuous embedding  $W^{k,p}(\Omega) \hookrightarrow W^{m,q}(\Omega)$ .

For a given Banach space  $X$ , we define the Bochner space, see e.g., [42],

$$L^p(0, T; X) = \{u : (0, T) \rightarrow X : u \text{ is strongly measurable, } \int_0^T |u(t)|_X^p dt < \infty\},$$

where  $1 \leq p < \infty$ , with the norm  $\|u\|_{L^p X}^p = \int_0^T |u(t)|_X^p dt$ . For  $p = \infty$ , we equip  $L^\infty(0, T; X)$  with the norm  $\|u\|_{L^\infty X} = \text{ess sup}_{t \in (0, T)} |u(t)|_X$ . Moreover, we introduce the Sobolev–Bochner space,

$$W^{1,p}(0, T; X) = \{u \in L^p(0, T; X) : \partial_t u \in L^p(0, T; X)\}.$$

Let  $X, Y, Z$  be Banach spaces such that  $X$  is compactly embedded in  $Y$ , and  $Y$  is continuously embedded in  $Z$ , i.e.,  $X \hookrightarrow Y \hookrightarrow Z$ . In the proof of the existence theorem below, we make use of the Aubin–Lions–Simon compactness lemma, see [43, Corollary 4],

$$\begin{aligned} L^p(0, T; X) \cap W^{1,1}(0, T; Z) &\hookrightarrow L^p(0, T; Y), \quad 1 \leq p < \infty, \\ L^\infty(0, T; X) \cap W^{1,r}(0, T; Z) &\hookrightarrow C^0([0, T]; Y), \quad r > 1, \end{aligned} \tag{19}$$

where we equip an intersection space  $X \cap Y$  with the norm  $\|\cdot\|_{X \cap Y} = \max\{\|\cdot\|_X, \|\cdot\|_Y\}$ . Further, we make use of the following continuous embeddings, see [44, Theorem 3.1, Chapter 1],

$$\begin{aligned} L^2(0, T; Y) \cap H^1(0, T; Z) &\hookrightarrow C^0([0, T]; [Y, Z]_{1/2}), \\ L^\infty(0, T; Y) \cap C_w([0, T]; Z) &\hookrightarrow C_w([0, T]; Y), \end{aligned} \tag{20}$$

where  $[Y, Z]_{1/2}$  denotes the interpolation space between  $Y$  and  $Z$ , see [44, Definition 2.1, Chapter 1] for more details. Also,  $C_w([0, T]; Y)$  denotes the space of the weakly continuous functions on the interval  $[0, T]$  with values in  $Y$ .

We note the following special case of the Gagliardo–Nirenberg inequality, see [45, Lemma II.2.33],

$$|f|_{L^p(\Omega)} \lesssim |f|_{H^1(\Omega)}^\alpha |f|_{L^2(\Omega)}^{1-\alpha} \quad \text{for all } f \in H^1(\Omega), \quad \frac{1}{p} = \frac{1}{2} - \frac{\alpha}{3}, \quad \alpha \in [0, 1],$$

which gives in a time-dependent setting, choosing  $\alpha = 2/q$  with  $q \geq 2$ ,

$$\begin{aligned} \|u\|_{L^q(0, T; L^p(\Omega))}^q &= \int_0^T |u(t)|_{L^p(\Omega)}^q dt \lesssim \int_0^T |u(t)|_{H^1(\Omega)}^{q\alpha} |u(t)|_{L^2(\Omega)}^{q(1-\alpha)} dt \\ &= \int_0^T |u(t)|_{H^1(\Omega)}^2 |u(t)|_{L^2(\Omega)}^{q-2} dt \\ &\leq \|u\|_{L^2(0, T; H^1(\Omega))}^2 \|u\|_{L^\infty(0, T; L^2(\Omega))}^{q-2} \\ &\leq (\max\{\|u\|_{L^\infty(0, T; L^2(\Omega))}, \|u\|_{L^2(0, T; H^1(\Omega))}\})^q. \end{aligned} \tag{21}$$

In particular, it yields the continuous embedding

$$L^\infty(0, T; L^2(\Omega)) \cap L^2(0, T; H^1(\Omega)) \hookrightarrow L^q(0, T; L^p(\Omega)), \quad \frac{1}{p} + \frac{2}{3q} = \frac{1}{2}.$$

We also make use of the classical Grönwall–Bellman lemma in the energy estimates to absorb solution-dependent terms on the right hand side of the energy inequalities.

**Lemma 1** (Grönwall–Bellman, cf. [45, Lemma II.4.10]). *Let  $u \in L^\infty(0, T)$ ,  $g \in L^1(0, T; \mathbb{R}_{\geq 0})$  and  $u_0 \in \mathbb{R}$ . If we have*

$$u(t) \leq u_0 + \int_0^t g(s)u(s) \, ds \quad \text{for a.e. } t \in (0, T),$$

*then it holds  $u(t) \leq u_0 \exp(\int_0^t g(s) \, ds)$  for almost every  $t \in (0, T)$ .*

#### 4. Existence of solutions

In this section, we lay down some general assumptions on the model that are in force throughout this paper. Under these assumptions, we state the definition of a weak solution, and we then state a theorem, which provides the existence of a weak solution.

For simplicity, we write

$$S_\alpha = S_\alpha(\phi), \quad m_\beta = m_\beta(\phi), \quad \Psi = \Psi(\phi_P, \phi_H, \phi_N),$$

$$J_{pv} = J_{pv}(\bar{p}, p_v), \quad J_{pv, \Gamma} = J_{pv}(p, \Pi_\Gamma p_v), \quad J_{\sigma v} = J_{\sigma v}(\bar{\phi}_\sigma, \bar{p}, \phi_v, p_v), \quad J_{\sigma v, \Gamma} = J_{\sigma v}(\phi_\sigma, p, \Pi_\Gamma \phi_v, \Pi_\Gamma p_v),$$

where  $\alpha \in \mathcal{A}$  and  $\beta \in \mathcal{A} \setminus \{N, ECM\}$ . We introduce the scaled parameters  $\tilde{R} = 2\pi R_i$  and  $\tilde{K}_v = R_i^2 \pi K_{v,i}$  in order to express the 1D model (16) in a shorter way. Moreover, we define the cut-off operator

$$\mathcal{C}(x) = \max\{0, \min\{1, x\}\}. \tag{22}$$

Moreover, we introduce the following abbreviations for frequently appearing function spaces,

$$\begin{aligned} V &= H^1(\Omega) & \hookrightarrow & H = L^2(\Omega) & \hookrightarrow & V' = (H^1(\Omega))', \\ V_0 &= H_D^1(\Omega) & \hookrightarrow & H = L^2(\Omega) & \hookrightarrow & V'_0 = (H_D^1(\Omega))', \\ W &= W^{1,3/2}(\Omega) & \hookrightarrow & H = L^2(\Omega) & \hookrightarrow & W' = (W^{1,3/2}(\Omega))', \\ X &= H^1(\Lambda) & \hookrightarrow & Y = L^2(\Lambda) & \hookrightarrow & X' = (H^1(\Lambda))', \\ X_0 &= H_D^1(\Lambda) & \hookrightarrow & Y = L^2(\Lambda) & \hookrightarrow & X'_0 = (H_D^1(\Lambda))', \end{aligned}$$

where we have denoted the Sobolev space of vanishing trace on  $\partial\Omega_D \subset \partial\Omega$  by  $H_D^1(\Omega) = \{u \in H^1(\Omega) : u|_{\partial\Omega_D} = 0\}$  and in the same way  $H_D^1(\Lambda) = \{u \in H^1(\Lambda) : u|_{\partial\Lambda_D} = 0\}$ . We equip these spaces of vanishing trace with the norms  $|\cdot|_{V_0} = |\nabla \cdot|_H$  and  $|\cdot|_{X_0} = |\nabla_\Lambda \cdot|_Y$ , respectively. Here, we use the notation  $\nabla_\Lambda$  for the space derivative of the 1D fields.

The space  $W$  with the Lebesgue order 3/2 becomes useful in the application of the Hölder inequality. Indeed, we have the relation  $\frac{2}{3} = \frac{1}{6} + \frac{1}{2}$ , and therefore, we obtain

$$|u\varphi|_{L^{3/2}(\Omega)} \leq |u|_{L^6(\Omega)}|\varphi|_H \lesssim |u|_V|\varphi|_H \quad \text{for all } u \in V, \varphi \in H,$$

where we also applied the Sobolev embedding theorem  $V \hookrightarrow L^6(\Omega)$  in the three-dimensional domain  $\Omega$ . Hence, we have for all  $u, \varphi \in V$ ,

$$|u\varphi|_W = \left( |u\varphi|_{L^{3/2}(\Omega)}^{3/2} + |\nabla(u\varphi)|_{L^{3/2}(\Omega)}^{3/2} \right)^{2/3} \leq |u\varphi|_{L^{3/2}(\Omega)} + |\nabla(u\varphi)|_{L^{3/2}(\Omega)} \lesssim |u|_V|\varphi|_V, \tag{23}$$

where we used the Bernoulli inequality to obtain  $(a + b)^r \leq a^r + b^r$  with  $a, b \geq 0, r \in [0, 1]$ .

**Assumption 1.**

- (A1)  $\Omega \subset \mathbb{R}^3$  is a bounded domain with  $C^{1,1}$ -boundary,  $\Lambda$  is a 1D structure as depicted in Fig. 2c,  $\Gamma$  is the 2D associated cylindrical surface, see Fig. 2d, and  $T > 0$  denotes a finite time horizon,
- (A2)  $\phi_{\alpha,0} \in V$  for all  $\alpha \in \mathcal{CH} \cup \{ECM\}$ ,  $\phi_{\beta,0} \in H$  for all  $\beta \in \mathcal{RD}$ ,  $\phi_{v,0} \in Y$ ,  $\phi_{v,\infty}, p_{v,\infty} \in H^1(0, T) \subset C([0, T])$  and  $p_\infty \in H^1(0, T; H) \cap L^2(0, T; V) \subset C([0, T]; H)$ ,
- (A3)  $\chi_c, \chi_h \geq 0$  and  $\varepsilon_\alpha, D_\beta, C_\sigma, \tilde{K}_v, \tilde{R} > 0$  for  $\alpha \in \{P, H\}$ ,  $\beta \in \mathcal{RD}$ ,
- (A4)  $S_\alpha$  are of the form

$$\begin{aligned}
 S_\alpha(\phi) &= \sum_{\gamma \in \mathcal{A}} \phi_\gamma f_{\alpha,\gamma}(\phi), & \alpha \in \mathcal{A} \setminus \{N, ECM\}, \\
 S_\beta(\phi) &= f_\beta(\phi), & \beta \in \{N, ECM\}, \\
 S_p(\phi, \mu_P, \mu_H) &= -\mathcal{C}(\phi_P)(\nabla \mu_P + \chi_c \nabla \phi_\sigma + \chi_h \nabla \phi_{ECM}) \\
 &\quad - \mathcal{C}(\phi_H)(\nabla \mu_H + \chi_c \nabla \phi_\sigma + \chi_h \nabla \phi_{ECM}),
 \end{aligned}$$

where  $f_{\alpha,\gamma} \in C_b(\mathbb{R}^{|\mathcal{A}|})$ ,  $f_\beta \in \text{Lip}(\mathbb{R}^{|\mathcal{A}|}) \cap PC^1(\mathbb{R}^{|\mathcal{A}|})$ , such that  $|f_{\alpha,\gamma}|, |f_\beta|, |\partial_{\phi_\gamma} f_\beta| \leq f_\infty$  for all  $\alpha \in \mathcal{A} \setminus \{N, ECM\}$ ,  $\beta \in \{N, ECM\}$ ,  $\gamma \in \mathcal{A}$ ,

- (A5)  $J_{pv}$  and  $J_{\sigma v}$  are of the form

$$\begin{aligned}
 J_{pv}(y_1, y_2) &= L_p(y_2 - y_1), \\
 J_{\sigma v}(x_1, y_1, x_2, y_2) &= f_{\sigma,v}(x_1, x_2)J_{pv}(y_1, y_2) + L_\sigma(x_2 - x_1),
 \end{aligned}$$

where  $f_{\sigma,v} \in C_b(\mathbb{R}^2)$  such that  $|f_{\sigma,v}(x)| \leq f_\infty$  for all  $x \in \mathbb{R}^2$  and  $L_p, L_\sigma, K \geq 0$  are sufficiently small in the sense that the prefactors in (53) are positive,

- (A6)  $m_\alpha \in C_b(\mathbb{R}^{|\mathcal{A}|})$  such that  $0 < m_0 \leq m_\alpha(x) \leq m_\infty$  for all  $x \in \mathbb{R}^{|\mathcal{A}|}$  for all  $\alpha \in \mathcal{A} \setminus \{N, ECM\}$ ,
- (A7)  $\Psi \in C^1(\mathbb{R}^3)$  non-negative such that  $\Psi(0, 0, 0) = \Psi'(0, 0, 0) = 0$ , and there are constants  $C_{\Psi_j}$ ,  $j \in \{1, \dots, 3\}$ , such that for all  $(x, y, z) \in \mathbb{R}^3$  it holds

$$\begin{aligned}
 \Psi(x, y, z) &\geq C_{\Psi_1}(|x|^2 + |y|^2 + |z|^2) - C_{\Psi_2}, \\
 |\partial_x \Psi(x, y, z)|, |\partial_y \Psi(x, y, z)|, |\partial_z \Psi(x, y, z)| &\leq C_{\Psi_3}(1 + |x| + |y| + |z|).
 \end{aligned}$$

Remarks on the assumptions:

- (A4) After a suitable reformulation of the source functions (6) and (9) with the cut-off operator  $\mathcal{C}$ , see (22), and replacing the Heaviside functions by the continuous Sigmoid function, the source functions can be brought into the form as stated in assumption (A4). Further, the assumption  $f_\beta \in \text{Lip}(\mathbb{R}^{|\mathcal{A}|}) \cap PC^1(\mathbb{R}^{|\mathcal{A}|})$ ,  $\beta \in \{N, ECM\}$ , ensures the validity of the chain rule if  $f_\beta$  is composed with a vector-valued Sobolev function; see [46,47]. In particular, we have for all  $\alpha \in \mathcal{A}$ ,

$$(\nabla f_\beta(\phi), \nabla \phi_\alpha)_H = \sum_{\gamma \in \mathcal{A}} (\partial_{\phi_\gamma} f_\beta(\phi) \nabla \phi_\gamma, \nabla \phi_\alpha)_H \leq f_\infty \sum_{\gamma \in \mathcal{A}} |\nabla \phi_\gamma|_H |\nabla \phi_\alpha|_H.$$

- (A5) We consider the unique, linear and continuous trace operator, see [48],

$$\text{tr}_\Gamma : W \rightarrow W^{1/3,3/2}(\Gamma) \text{ such that } \text{tr}_\Gamma u = u|_\Gamma \text{ for } u \in C^\infty(\Omega),$$

onto the two dimensional associated cylindrical surface  $\Gamma$  of the one-dimensional network  $\Lambda$ , see Fig. 2. In two dimensions, we can apply the Sobolev embedding theorem to obtain  $W^{1/3,3/2}(\Gamma) \hookrightarrow L^2(\Gamma)$ ,

see (18). Note that this embedding does not hold in three dimensions. Consequently, we have

$$\begin{aligned} \|\delta_\Gamma\|_{W'} &= \sup_{|\varphi|_W \leq 1} |\langle \delta_\Gamma, \varphi \rangle_W| = \sup_{|\varphi|_W \leq 1} \left| \int_\Gamma \text{tr}_\Gamma \varphi(s) \, ds \right| \leq \sup_{|\varphi|_W \leq 1} |\text{tr}_\Gamma \varphi|_{L^1(\Gamma)} \\ &\leq C_{W^{1/3,3/2}(\Gamma)}^{L^1(\Gamma)} |\text{tr}_\Gamma|_{\mathcal{L}(W; W^{1/3,3/2}(\Gamma))}, \end{aligned}$$

where  $C_{W^{1/3,3/2}(\Gamma)}^{L^1(\Gamma)}$  denotes the embedding constant from  $W^{1/3,3/2}(\Gamma) \hookrightarrow L^1(\Gamma)$ . Therefore, we have  $\delta_\Gamma \in W'$  and in the following existence proof we often apply the estimate for  $\varphi \in W$

$$\langle \delta_\Gamma, J_{\alpha v, \Gamma} \varphi \rangle_W = \int_\Gamma J_{\alpha v, \Gamma} \text{tr}_\Gamma \varphi(s) \, ds \leq |J_{\alpha v, \Gamma}|_{L^2(\Gamma)} |\text{tr}_\Gamma \varphi|_{L^2(\Gamma)} \leq C_\Gamma |J_{\alpha v, \Gamma}|_{L^2(\Gamma)} |\varphi|_W, \tag{24}$$

for  $\alpha \in \{\sigma, p\}$ , where

$$C_\Gamma = C_{W^{1/3,3/2}(\Gamma)}^{L^2(\Gamma)} |\text{tr}_\Gamma|_{\mathcal{L}(W; W^{1/3,3/2}(\Gamma))}.$$

Further, we can estimate the fluxes by

$$\begin{aligned} |J_{pv, \Gamma}|_{L^2(\Gamma)} &\leq L_p(C_\Gamma |p|_W + |\Pi_\Gamma|_{\mathcal{L}(Y; L^2(\Gamma))} |p_v|_Y), \\ |J_{\sigma v, \Gamma}|_{L^2(\Gamma)} &\leq f_\infty L_p(C_\Gamma |p|_W + |\Pi_\Gamma|_{\mathcal{L}(Y; L^2(\Gamma))} |p_v|_Y) + L_\sigma(C_\Gamma |\phi_\sigma|_W + |\Pi_\Gamma|_{\mathcal{L}(Y; L^2(\Gamma))} |\phi_v|_Y). \end{aligned} \tag{25}$$

The assumption of smallness of  $L_p$  and  $L_\sigma$  is generally accepted in the analysis of very weak solution of the stationary Navier–Stokes equation. There, one also considers a distributional divergence, which should be sufficiently small, see [49]. Additionally, in [50] the authors have shown well-posedness of an abstract stationary 3D–1D model if the prefactor of the Dirac delta functional is sufficiently small.

(A7) The assumption on the potential  $\Psi$  is quite typical in the analysis of Cahn–Hilliard equations, see also [12,13]. In order to take the fourth order polynomial  $(x + y + z)^2(1 - x - y - z)^2$ , we have to extend it by a quadratic function outside of the interval  $[0, 1]$ , i.e.,

$$\Psi(x, y, z) = \begin{cases} (x + y + z)^2, & x + y + z < 0, \\ (x + y + z)^2(1 - x - y - z)^2, & x + y + z \in [0, 1], \\ (1 - x - y - z)^2, & x + y + z > 1, \end{cases}$$

and one can show that  $\Psi \in C^2(\mathbb{R}^3; \mathbb{R})$ .

We invoke from (A7) and the fundamental lemma of calculus the upper estimate

$$\begin{aligned} \Psi(x, y, z) &= \Psi(0, y, z) + \int_0^x \partial_x \Psi(\tilde{x}, y, z) \, d\tilde{x} \\ &= \Psi(0, 0, 0) + \int_0^x \partial_x \Psi(\tilde{x}, y, z) \, d\tilde{x} + \int_0^y \partial_y \Psi(0, \tilde{y}, z) \, d\tilde{y} + \int_0^z \partial_z \Psi(0, 0, \tilde{z}) \, d\tilde{z} \\ &\lesssim 1 + |x|^2 + |y|^2 + |z|^2. \end{aligned} \tag{26}$$

We define a weak solution of the coupled 3D–1D system, see (14) and (16), in the following way.

**Definition 1 (Weak Solution).** We call the tuple  $(\phi, \mu_P, \mu_H, v, p, \phi_v, v_v, p_v)$  a weak solution of (14) and (16) with boundary data (15) and (17) if the functions  $\phi : (0, T) \times \Omega \rightarrow \mathbb{R}^{|\mathcal{A}|}$ ,  $\mu_P, \mu_H, v, p, \phi_v, v_v, p_v : (0, T) \times \Omega \rightarrow \mathbb{R}$  have the regularity

$$\begin{aligned} \phi_\alpha &\in H^1(0, T; V') \cap L^\infty(0, T; V), & \alpha &\in \{P, H\}, \\ \mu_\alpha &\in L^2(0, T; V), & \alpha &\in \{P, H\}, \\ \phi_\beta &\in H^1(0, T; H) \cap L^\infty(0, T; V), & \beta &\in \{N, ECM\}, \\ \phi_\gamma &\in H^1(0, T; V') \cap L^\infty(0, T; H) \cap L^2(0, T; V), & \gamma &\in \mathcal{RD}, \\ (v, p - p_\infty) &\in L^2((0, T) \times \Omega; \mathbb{R}^3) \times L^2(0, T; V_0), \\ \phi_v - \phi_{v, \infty} &\in H^1(0, T; X'_0) \cap L^\infty(0, T; Y) \cap L^2(0, T; X_0), \\ (v_v, p_v - p_{v, \infty}) &\in L^2(0, T; Y) \times L^2(0, T; X_0), \end{aligned} \tag{27}$$

fulfill the initial data  $\phi_\alpha(0) = \phi_{\alpha,0}$ ,  $\alpha \in \mathcal{A}$ ,  $\phi_v(0) = \phi_{v,0}$ , and satisfy the following variational form of (14),

$$\begin{aligned}
 \langle \partial_t \phi_P, \varphi_1 \rangle_{W^{1,3}(\Omega)} - (\mathcal{C}(\phi_P)v, \nabla \varphi_1)_H + (m_P \nabla \mu_P, \nabla \varphi_1)_H &= (S_P, \varphi_1)_H, \\
 -(\mu_P, \varphi_2)_H + (\partial_{\phi_P} \Psi, \varphi_2)_H + \varepsilon_P^2 (\nabla \phi_P, \nabla \varphi_2)_H &= \chi_c(\phi_\sigma, \varphi_2)_H + \chi_h(\phi_{ECM}, \varphi_2)_H, \\
 \langle \partial_t \phi_H, \varphi_3 \rangle_{W^{1,3}(\Omega)} - (\mathcal{C}(\phi_H)v, \nabla \varphi_3)_H + (m_H \nabla \mu_H, \nabla \varphi_3)_H &= (S_H, \varphi_3)_H, \\
 -(\mu_H, \varphi_4)_H + (\partial_{\phi_H} \Psi, \varphi_4)_H + \varepsilon_H^2 (\nabla \phi_H, \nabla \varphi_4)_H &= \chi_c(\phi_\sigma, \varphi_4)_H + \chi_h(\phi_{ECM}, \varphi_4)_H, \\
 (\partial_t \phi_N, \varphi_5)_H &= (S_N, \varphi_5)_H, \\
 \langle \partial_t \phi_\sigma, \varphi_6 \rangle_{W^{1,3}(\Omega)} - (\mathcal{C}(\phi_\sigma)v, \nabla \varphi_6)_H + D_\sigma(m_\sigma \nabla \phi_\sigma, \nabla \varphi_6)_H &= (S_\sigma, \varphi_6)_H + \langle \delta_\Gamma, J_{\sigma v, \Gamma} \varphi_6 \rangle_W \\
 &\quad - \chi_c(m_\sigma \nabla(\phi_P + \phi_H), \nabla \varphi_6)_H, \\
 \langle \partial_t \phi_{MDE}, \varphi_7 \rangle_V + D_{MDE}(m_{MDE} \nabla \phi_{MDE}, \nabla \varphi_7)_H &= (S_{MDE}, \varphi_7)_H, \\
 \langle \partial_t \phi_{TAF}, \varphi_8 \rangle_V + D_{TAF}(m_{TAF} \nabla \phi_{TAF}, \nabla \varphi_8)_H &= (S_{TAF}, \varphi_8)_H, \\
 \langle \partial_t \phi_{ECM}, \varphi_9 \rangle_V &= (S_{ECM}, \varphi_9)_H, \\
 (v, \varphi_{10})_H &= -K(\nabla p, \varphi_{10})_H + K(S_p, \varphi_{10})_H, \\
 K(\nabla p, \nabla \varphi_{11})_H &= \langle \delta_\Gamma, J_{pv, \Gamma} \varphi_{11} \rangle_W + K(S_p, \nabla \varphi_{11})_H,
 \end{aligned} \tag{28}$$

for all  $\varphi_j \in V$ ,  $j \in \{1, \dots, 9\}$ ,  $\varphi_{10} \in L^2(\Omega; \mathbb{R}^3)$ ,  $\varphi_{11} \in V_0$ , and the variational form of (16),

$$\begin{aligned}
 \langle \partial_t \phi_v, \varphi_{12} \rangle_X - (\mathcal{C}(\phi_v)v_v, \nabla_\Lambda \varphi_{12})_Y + D_v(m_v \nabla_\Lambda \phi_v, \nabla_\Lambda \varphi_{12})_Y &= -\tilde{R}(J_{\sigma v}, \varphi_{12})_Y, \\
 (v_v, \varphi_{13})_Y &= -\tilde{K}_v(\nabla_\Lambda p_v, \varphi_{13})_Y, \\
 \tilde{K}_v(\nabla_\Lambda p_v, \nabla_\Lambda \varphi_{14})_Y &= -\tilde{R}(J_{pv}, \varphi_{14})_Y,
 \end{aligned} \tag{29}$$

for all  $\varphi_j \in X_0$ ,  $j \in \{12, 14\}$ ,  $\varphi_{13} \in Y$ .

The initial data  $\phi_\alpha(0) = \phi_{\alpha,0}$ ,  $\alpha \in \mathcal{A}$ , are well-defined with assumption (A2) on the regularity of the initial data. Indeed, from the regularity given in (27), we achieve, by the embeddings (20), the continuity-in-time regularity

$$\begin{aligned}
 \phi_\alpha &\in C^0([0, T]; H) \cap C_w([0, T]; V), \quad \alpha \in \mathcal{CH} \cup \{ECM\}, \\
 \phi_\beta &\in C^0([0, T]; V') \cap C_w([0, T]; H), \quad \beta \in \mathcal{RD}, \\
 \phi_v &\in C^0([0, T]; X'_0) \cap C_w([0, T]; Y),
 \end{aligned}$$

and therefore,  $\phi_\alpha(0)$  is well-defined in  $H$ ,  $\phi_\beta(0)$  in  $V'$  and  $\phi_v(0)$  in  $X'_0$ .

We use a mixed boundary approach for  $p, \phi_v, p_v$ , e.g., for the pressure  $p$  we define  $\tilde{p} = p - p_\infty$  with  $\tilde{p}|_{\partial\Omega_D} = 0$  and  $(\partial_n \tilde{p} + \partial_n p_\infty)_{\partial\Omega \setminus \partial\Omega_D} = 0$ . Hence, we consider the partial differential equation

$$-\operatorname{div}(K \nabla \tilde{p}) - \operatorname{div}(K \nabla p_\infty) = \delta_\Gamma J_{pv, \Gamma} - \operatorname{div} S_p,$$

with the weak form with the test function  $q \in V_0$

$$K(\nabla \tilde{p} + \nabla p_\infty, \nabla q)_H - K(\partial_n \tilde{p} + \partial_n p_\infty, q)_{L^2(\partial\Omega)} = \langle \delta_\Gamma, J_{pv, \Gamma} q \rangle_W + (K S_p, \nabla q)_H - (K S_p \cdot n, q)_{L^2(\partial\Omega)},$$

or, after the cancellation of the boundary terms,

$$K(\nabla p, \nabla q)_H = \langle \delta_\Gamma, J_{pv, \Gamma} q \rangle_W + (K S_p, \nabla q)_H.$$

The main result of this paper involves stating the existence of a weak solution of the 3D–1D model, see (14) and (16), in the sense of Definition 1.

**Theorem 1** (Existence of a Global Weak Solution). *Let Assumption 1 hold. Then there exists a weak solution tuple  $(\phi, \mu_P, \mu_H, p, \phi_v, p_v)$  to the 3D–1D model in the sense of Definition 1, which additionally satisfies the energy inequality*

$$\begin{aligned} & \|\Psi\|_{L^\infty(0,T;L^1(\Omega))} + \sum_{\alpha \in \mathcal{CH} \cup \{ECM\}} \|\phi_\alpha\|_{L^\infty(0,T;V)}^2 + \sum_{\beta \in \{P,H\}} \|\mu_\beta\|_{L^2(0,T;V)}^2 + \sum_{\gamma \in \mathcal{RD}} \|\phi_\gamma\|_{L^\infty(0,T;H) \cap L^2(0,T;V)}^2 \\ & + \|v\|_{L^2(0,T;H)}^2 + \|p\|_{L^2(0,T;V)}^2 + \|\phi_v\|_{L^\infty(0,T;Y) \cap L^2(0,T;X)}^2 + \|v_v\|_{L^2(0,T;Y)}^2 + \|p_v\|_{L^2(0,T;X)}^2 \\ & \lesssim 1 + |\phi_{v,0}|_Y^2 + \sum_{\alpha \in \mathcal{CH} \cup \{ECM\}} |\phi_{\alpha,0}|_V^2 + \sum_{\beta \in \mathcal{RD}} |\phi_{\beta,0}|_H^2 + \|p_\infty\|_{L^2(0,T;V)}^2 + |\phi_{v,\infty}|_{H^1(0,T)}^2 + |p_{v,\infty}|_{L^2(0,T)}^2. \end{aligned} \tag{30}$$

### 5. Proof of Theorem 1

To prove the existence of a weak solution, we use the Faedo–Galerkin method [41] and semi-discretize the original problem in space. The discretized model can be formulated as an ordinary differential equation system and by the Cauchy–Peano theorem [51], we conclude the existence of a discrete solution, see Section 5.1. Having derived energy estimates in Section 5.2, we deduce from the Banach–Alaoglu theorem the existence of limit functions which eventually form a weak solution, see Section 5.3. This method is by now standard in the analysis of tumor growth models, e.g., see [30,52–54]. Nevertheless, the novel nonlinear coupling of the equations requires a thorough proof of the existence of a solution to the system.

#### 5.1. Faedo–Galerkin discretization

We introduce the discrete spaces

$$\begin{aligned} H_k &= \text{span}\{h_1, \dots, h_k\}, \\ H_k^0 &= \text{span}\{h_1^0, \dots, h_k^0\}, \\ Y_k &= \text{span}\{y_1, \dots, y_k\}, \end{aligned}$$

where  $h_j : \Omega \rightarrow \mathbb{R}$ ,  $h_j^0 : \Omega \rightarrow \mathbb{R}$ ,  $y_j : \Lambda \rightarrow \mathbb{R}$ ,  $j \in \{1, \dots, k\}$ , are the eigenfunctions to the eigenvalues  $\lambda_{h,j}, \lambda_{h^0,j}, \lambda_{y,j} \in \mathbb{R}$  of the following respective problems

$$\begin{aligned} (\nabla h_j, \nabla v)_H &= \lambda_{h,j} (h_j, v)_H \quad \forall v \in V, \\ (\nabla h_j^0, \nabla v)_H &= \lambda_{h^0,j} (h_j^0, v)_H \quad \forall v \in V_0, \\ (\nabla y_j, \nabla v)_Y &= \lambda_{y,j} (y_j, v)_Y \quad \forall v \in X_0. \end{aligned}$$

Since the inverse Neumann–Laplace operator is a compact, self-adjoint, injective, positive operator on  $L^2_0(\Omega)$ , we conclude by the spectral theorem, see e.g., [55, 12.12 and 12.13], that

$$\{h_j\}_{j \in \mathbb{N}} \text{ is an orthonormal basis in } H \text{ and orthogonal in } V.$$

Therefore,  $\cup_{k \in \mathbb{N}} H_k$  is dense in  $V$ . Additionally,  $\{h_j\}_{j \in \mathbb{N}}$  is a basis in  $H^2_N(\Omega) = \{u \in H^2(\Omega) : \partial_n u = 0 \text{ on } \partial\Omega\}$ , see [8].

Next, we investigate the inverse Dirichlet–Neumann Laplacian  $(-\Delta)^{-1}|_H : H \rightarrow H$ , see, e.g., [56] for the consideration of the Dirichlet–Neumann Laplacian in a Faedo–Galerkin approach. According to the Lax–Milgram theorem, for all  $f \in H$  there exists a unique solution  $u_f \in V_0$  to the problem

$$(\nabla u_f, \nabla v)_H = (u_f, f)_H \quad \forall v \in V_0.$$

Additionally, it holds  $|u_f|_{V_0} \lesssim |f|_H$  for all  $f \in H$  and we can construct an operator  $T \in \mathcal{L}(H; V_0)$  with  $Tf = u_f$ . Since  $V_0$  is compactly embedded in  $H$ , we conclude the compactness of  $T \in \mathcal{L}(H; H)$ . Taking the test function  $v = Tg$  for an arbitrary element  $g \in H$ , we obtain the self-adjointness of  $T$ ,

$$(Tg, f)_H = (\nabla Tf, \nabla Tg)_H = (g, Tf)_H,$$

and taking  $g = f$  yields the positivity of  $T$ ,

$$(Tf, f)_H = |\nabla Tf|_H^2 \geq 0.$$

Additionally,  $T$  is injective, since  $Tf = 0$  yields  $(f, v)_H = 0$  for all  $v \in H$  and hence,  $f = 0$  almost everywhere. Similarly, we can derive the same results for an operator  $\tilde{T} \in \mathcal{L}(Y; Y)$  corresponding to the eigenvalue problem on  $Y$ . Hence, by the spectral theorem we conclude

$$\begin{aligned} \{h_j^0\}_{j \in \mathbb{N}} &\text{ is an orthonormal basis in } H \text{ and orthogonal in } V_0, \\ \{y_j\}_{j \in \mathbb{N}} &\text{ is an orthonormal basis in } Y \text{ and orthogonal in } X_0. \end{aligned}$$

Additionally, we deduce that  $\cup_{k \in \mathbb{N}} H_k^0$  is dense in  $V_0$  and  $\cup_{k \in \mathbb{N}} Y_k$  is dense in  $X_0$ .

We consider the Faedo–Galerkin approximations,  $\alpha \in \mathcal{A}$ ,  $\beta \in \{P, H\}$ ,

$$\begin{aligned} \phi_\alpha^k(t) &= \sum_{j=1}^k \xi_{\alpha,j}(t) h_j, & \mu_\beta^k(t) &= \sum_{j=1}^k \zeta_{\beta,j}(t) h_j, & \phi_v^k(t) &= \phi_{v,\infty}(t) + \sum_{j=1}^k \xi_{v,j}(t) y_j, \\ p^k(t) &= p_\infty(t) + \sum_{j=1}^k \zeta_{p,j}(t) h_j^0, & p_v^k(t) &= p_{v,\infty}(t) + \sum_{j=1}^k \zeta_{p_v,j}(t) y_j, \end{aligned} \tag{31}$$

where  $(\xi_{\alpha,j})_{\alpha \in \mathcal{A}} : (0, T) \rightarrow \mathbb{R}^{|\mathcal{A}|}$ ,  $(\zeta_{\beta,j})_{\beta \in \{P, H\}} : (0, T) \rightarrow \mathbb{R}^2$  and  $\xi_{v,j}, \zeta_{p,j}, \zeta_{p_v,j} : (0, T) \rightarrow \mathbb{R}$  are coefficient functions for all  $j \in \{1, \dots, k\}$ . To simplify the notation, we set  $\phi^k = (\phi_\alpha^k)_{\alpha \in \mathcal{A}}$ , and

$$\begin{aligned} S_\alpha^k &= S_\alpha(\phi^k), & m_\beta^k &= m_\beta(\phi^k), & \Psi^k &= \Psi(\phi_P^k, \phi_H^k, \phi_N^k), \\ J_{pv}^k &= J_{pv}(\bar{p}^k, p_v^k), & J_{pv,\Gamma}^k &= J_{pv}(p^k, \Pi_\Gamma p_v^k), & J_{\sigma v}^k &= J_{\sigma v}(\bar{\phi}_\sigma^k, \bar{p}^k, \phi_v^k, p_v^k), \\ & & J_{\sigma v,\Gamma}^k &= J_{\sigma v}(\phi_\sigma^k, p^k, \Pi_\Gamma \phi_v^k, \Pi_\Gamma p_v^k), \end{aligned}$$

where  $\alpha \in \mathcal{A}$  and  $\beta \in \mathcal{A} \setminus \{N, ECM\}$ . The Faedo–Galerkin system of the model then reads

$$\begin{aligned} (\partial_t \phi_P^k, \varphi_1)_H - (\mathcal{C}(\phi_P^k) v^k, \nabla \varphi_1)_H + (m_P^k \nabla \mu_P^k, \nabla \varphi_1)_H &= (S_P^k, \varphi_1)_H, \\ -(\mu_P^k, \varphi_2)_H + (\partial_{\phi_P^k} \Psi^k, \varphi_2)_H + \varepsilon_P^2 (\nabla \phi_P^k, \nabla \varphi_2)_H &= \chi_c(\phi_\sigma^k, \varphi_2)_H + \chi_h(\phi_{ECM}^k, \varphi_2)_H, \\ (\partial_t \phi_H^k, \varphi_3)_H - (\mathcal{C}(\phi_H^k) v^k, \nabla \varphi_3)_H + (m_H^k \nabla \mu_H^k, \nabla \varphi_3)_H &= (S_H^k, \varphi_3)_H, \\ -(\mu_H^k, \varphi_4)_H + (\partial_{\phi_H^k} \Psi^k, \varphi_4)_H + \varepsilon_H^2 (\nabla \phi_H^k, \nabla \varphi_4)_H &= \chi_c(\phi_\sigma^k, \varphi_4)_H + \chi_h(\phi_{ECM}^k, \varphi_4)_H, \\ (\partial_t \phi_N^k, \varphi_5)_H &= (S_N^k, \varphi_5)_H, \\ (\partial_t \phi_\sigma^k, \varphi_6)_H - (\mathcal{C}(\phi_\sigma^k) v^k, \nabla \varphi_6)_H + D_\sigma (m_\sigma^k \nabla \phi_\sigma^k, \nabla \varphi_6)_H &= (S_\sigma^k, \varphi_6)_H + \langle \delta_\Gamma, J_{\sigma v,\Gamma}^k \varphi_6 \rangle_W \\ &\quad - \chi_c(m_\sigma^k \nabla (\phi_P^k + \phi_H^k), \nabla \varphi_6)_H, \\ (\partial_t \phi_{MDE}^k, \varphi_7)_H + D_{MDE} (m_{MDE}^k \nabla \phi_{MDE}^k, \nabla \varphi_7)_H &= (S_{MDE}^k, \varphi_7)_H, \\ (\partial_t \phi_{TAF}^k, \varphi_8)_H + D_{TAF} (m_{TAF}^k \nabla \phi_{TAF}^k, \nabla \varphi_8)_H &= (S_{TAF}^k, \varphi_8)_H, \\ (\partial_t \phi_{ECM}^k, \varphi_9)_H &= (S_{ECM}^k, \varphi_9)_H, \\ K (\nabla p^k, \nabla \varphi_{10})_H &= \langle \delta_\Gamma, J_{pv,\Gamma}^k \varphi_{10} \rangle_W + K (S_p^k, \nabla \varphi_{10})_H, \end{aligned} \tag{32}$$



for all  $\varphi_i \in H_k, i \in \{1, \dots, 9\}, \varphi_{10} \in H_k^0$ , and

$$\begin{aligned} (\partial_t \phi_v^k, \varphi_{11})_Y + D_v(m_v^k \nabla_\Lambda \phi_v^k, \nabla_\Lambda \varphi_{11})_Y &= (\mathcal{C}(\phi_v^k)v_v^k, \nabla_\Lambda \varphi_{11})_Y - \tilde{R}(J_{\sigma v}^k, \varphi_{11})_Y, \\ \tilde{K}_v(\nabla_\Lambda p_v^k, \nabla_\Lambda \varphi_{12})_Y &= -\tilde{R}(J_{pv}^k, \varphi_{12})_Y, \end{aligned} \tag{33}$$

for all  $\varphi_j \in Y_k, j \in \{11, 12\}$ , where we define the Faedo–Galerkin ansatz for the velocities  $v^k, v_v^k$  by

$$\begin{aligned} v^k &= -K(\nabla p^k - S_p^k), \\ v_v^k &= -\tilde{K}_v \nabla_\Lambda p_v^k. \end{aligned} \tag{34}$$

We equip the system with the initial data,

$$\begin{aligned} \phi_\alpha^k(0) &= \Pi_{H_k} \phi_{\alpha,0}, & \alpha \in \mathcal{A}, \\ \phi_v^k(0) &= \phi_{v,\infty}(0) + \Pi_{Y_k} \phi_{v,0}, \end{aligned} \tag{35}$$

where  $\Pi_{H_k} : H \rightarrow H_k$  and  $\Pi_{Y_k} : Y \rightarrow Y_k$  are the orthogonal projections onto the finite dimensional spaces, which can be written as

$$\Pi_{H_k} h = \sum_{j=1}^k (h, h_j)_H h_j, \quad \text{and} \quad \Pi_{Y_k} y = \sum_{j=1}^k (y, y_j)_Y y_j.$$

After inserting the Faedo–Galerkin ansatz functions (31) into the system (32)–(33), one can see that the Faedo–Galerkin system is equivalent to a system of nonlinear ordinary differential equations in the unknowns  $((\xi_{\alpha,j})_{\alpha \in \mathcal{A} \cup \{v\}}, (\zeta_{\beta,j})_{\beta \in \mathcal{CH} \cup \{p,p_v\}})_{1 \leq j \leq k}$  with the initial data,

$$\begin{aligned} \xi_{\alpha,j}(0) &= (\phi_{\alpha,0}, h_j)_H, & \alpha \in \mathcal{A}, \\ \xi_{v,j}(0) &= (\phi_{v,0}, y_j)_Y. \end{aligned}$$

Due to the continuity of the involved nonlinear functions the existence of solutions to (32)–(33) with the initial data (35) follows from the standard theory of ordinary differential equations, according to the Cauchy–Peano theorem [51]. We thus have local-in-time existence of a continuously differentiable solution,

$$\begin{aligned} (\phi^k, \mu_P^k, \mu_H^k, p^k - p_\infty, \phi_v^k - \phi_{v,\infty}, p_v^k - p_{v,\infty}) &\in [C^1([0, T_k]; H_k)]^{|\mathcal{A}|} \times [C^0([0, T_k]; H_k)]^2 \times C^0([0, T_k]; H_k^0) \\ &\times C^1([0, T_k]; Y_k) \times C^0([0, T_k]; Y_k), \end{aligned}$$

to the Faedo–Galerkin problem (32)–(33) on some sufficiently short time interval  $[0, T_k]$ . Further, we obtain  $\text{div} S_p^k \in H$  by the representation of  $S_p^k$ , see (A4), and therefore,  $v^k \in H$  with  $\text{div} v^k = -K(\Delta p^k - \text{div} S_p^k) = J_{pv,\Gamma}^k \delta_\Gamma$ . Similarly,  $v_v^k \in Y$  with  $\text{div} v_v^k = -R J_{pv}^k$ .

### 5.2. Energy estimates

Next, we extend the existence interval to  $[0, T]$  by deriving  $T_k$ -independent estimates. In particular, these estimates allow us to deduce that the solution sequences converge to some limit functions as  $k \rightarrow \infty$ . It will turn out that exactly these limit functions will form a weak solution to our 3D–1D model (14)–(16) in the sense of Definition 1.

#### Step 1 (Testing)

We derive energy estimates of the model (32)–(33) by choosing suitable test functions in the variational form. For the Cahn–Hilliard type equations, we choose  $\varphi_1 = \mu_P^k + \chi_c \phi_\sigma^k + \chi_h \phi_{ECM}^k, \varphi_2 = \partial_t \phi_P^k - \mu_P^k$ ,

$\varphi_3 = \mu_H^k + \chi_c \phi_\sigma^k + \chi_h \phi_{ECM}^k$ ,  $\varphi_4 = \partial_t \phi_H^k - \mu_H^k$ ,  $\varphi_5 = \Pi_{H_k} \partial_{\phi_N^k} \Psi^k - \varepsilon_N^2 \Delta \phi_N^k$ , and we arrive at the system of equations,

$$\begin{aligned}
 (\partial_t \phi_P^k, \mu_P^k + \chi_c \phi_\sigma^k + \chi_h \phi_{ECM}^k)_H + \left| \sqrt{m_P^k} \nabla \mu_P^k \right|_H^2 &= (\mathcal{C}(\phi_P^k) v^k, \nabla \mu_P^k + \chi_c \nabla \phi_\sigma^k + \chi_h \nabla \phi_{ECM}^k)_H \\
 &\quad - (m_P^k \nabla \mu_P^k, \chi_c \nabla \phi_\sigma^k + \chi_h \nabla \phi_{ECM}^k)_H \\
 &\quad + (S_P^k, \mu_P^k + \chi_c \phi_\sigma^k + \chi_h \phi_{ECM}^k)_H, \\
 (\partial_{\phi_P^k} \Psi^k, \partial_t \phi_P^k)_H + \frac{\varepsilon_P^2}{2} \frac{d}{dt} |\nabla \phi_P^k|_H^2 + |\mu_P^k|_H^2 &= (\mu_P^k + \chi_c \phi_\sigma^k + \chi_h \phi_{ECM}^k, \partial_t \phi_P^k)_H + (\partial_{\phi_P^k} \Psi^k, \mu_P^k)_H \\
 &\quad - (\chi_c \phi_\sigma^k + \chi_h \phi_{ECM}^k, \mu_P^k)_H + \varepsilon_P^2 (\nabla \phi_P^k, \nabla \mu_P^k)_H, \\
 (\partial_t \phi_H^k, \mu_H^k + \chi_c \phi_\sigma^k + \chi_h \phi_{ECM}^k)_H + \left| \sqrt{m_H^k} \nabla \mu_H^k \right|_H^2 &= (\mathcal{C}(\phi_H^k) v^k, \nabla \mu_H^k + \chi_c \nabla \phi_\sigma^k + \chi_h \nabla \phi_{ECM}^k)_H \\
 &\quad - (m_H^k \nabla \mu_H^k, \chi_c \nabla \phi_\sigma^k + \chi_h \nabla \phi_{ECM}^k)_H \\
 &\quad + (S_H^k, \mu_H^k + \chi_c \phi_\sigma^k + \chi_h \phi_{ECM}^k)_H, \\
 (\partial_{\phi_H^k} \Psi^k, \partial_t \phi_H^k)_H + \frac{\varepsilon_H^2}{2} \frac{d}{dt} |\nabla \phi_H^k|_H^2 + |\mu_H^k|_H^2 &= (\mu_H^k + \chi_c \phi_\sigma^k + \chi_h \phi_{ECM}^k, \partial_t \phi_H^k)_H + (\partial_{\phi_H^k} \Psi^k, \mu_H^k)_H \\
 &\quad - (\chi_c \phi_\sigma^k + \chi_h \phi_{ECM}^k, \mu_H^k)_H + \varepsilon_H^2 (\nabla \phi_H^k, \nabla \mu_H^k)_H, \\
 (\partial_t \phi_N^k, \Pi_{H_k} \partial_{\phi_N^k} \Psi^k)_H + \frac{\varepsilon_N^2}{2} \frac{d}{dt} |\nabla \phi_N^k|_H^2 &= (S_N^k, \Pi_{H_k} \partial_{\phi_N^k} \Psi^k)_H + \varepsilon_N^2 (\nabla S_N^k, \nabla \phi_N^k)_H.
 \end{aligned} \tag{36}$$

We exploit that the time derivative operator is invariant under the adjoint of the orthogonal projection.

Further, for the reaction–diffusion type equations, we choose  $\varphi_6 = C_\sigma \phi_\sigma^k$ ,  $C_\sigma > 0$  to be determined,  $\varphi_7 = \phi_{MDE}^k$ ,  $\varphi_8 = \phi_{TAF}^k$ ,  $\varphi_9 = \phi_{ECM}^k - \Delta \phi_{ECM}^k$ , which yields the system,

$$\begin{aligned}
 \frac{C_\sigma}{2} \frac{d}{dt} |\phi_\sigma^k|_H^2 + C_\sigma D_\sigma \left| \sqrt{m_\sigma^k} \nabla \phi_\sigma^k \right|_H^2 &= \chi_c C_\sigma (m_\sigma^k \nabla (\phi_P^k + \phi_H^k), \nabla \phi_\sigma^k)_H + C_\sigma (S_\sigma^k, \phi_\sigma^k)_H \\
 &\quad + C_\sigma (\mathcal{C}(\phi_\sigma^k) v^k, \nabla \phi_\sigma^k)_H + C_\sigma \langle \delta_\Gamma, J_{\sigma v, \Gamma}^k \phi_\sigma^k \rangle_W, \\
 \frac{1}{2} \frac{d}{dt} |\phi_{MDE}^k|_H^2 + D_{MDE} \left| \sqrt{m_{MDE}^k} \nabla \phi_{MDE}^k \right|_H^2 &= (S_{MDE}^k, \phi_{MDE}^k)_H, \\
 \frac{1}{2} \frac{d}{dt} |\phi_{TAF}^k|_H^2 + D_{TAF} \left| \sqrt{m_{TAF}^k} \nabla \phi_{TAF}^k \right|_H^2 &= (S_{TAF}^k, \phi_{TAF}^k)_H, \\
 \frac{1}{2} \frac{d}{dt} |\phi_{ECM}^k|_H^2 + \frac{1}{2} \frac{d}{dt} |\nabla \phi_{ECM}^k|_H^2 &= (S_{ECM}^k, \phi_{ECM}^k)_H + (\nabla S_{ECM}^k, \nabla \phi_{ECM}^k)_H,
 \end{aligned} \tag{37}$$

and for the equations in  $Y_k$ , we choose  $\varphi_{12} = C_v (\phi_v^k - \phi_{v, \infty})$ ,  $C_v > 0$  to be determined, giving

$$\frac{C_v}{2} \frac{d}{dt} |\phi_v^k - \phi_{v, \infty}|_Y^2 + C_v D_v \left| \sqrt{m_v^k} \nabla \phi_v^k \right|_Y^2 = C_v (\mathcal{C}(\phi_v^k) v_v^k, \nabla \phi_v^k)_Y - C_v (R J_{\sigma v}^k + \phi'_{v, \infty}, \phi_v^k - \phi_{v, \infty})_Y, \tag{38}$$

Similarly, we test Eqs. (34)<sub>2</sub> by  $\frac{1}{K_v} v_v^k$  to obtain

$$\frac{1}{\tilde{K}_v} |v_v^k|_H^2 = -(\nabla \Lambda (p_v^k - p_{v, \infty}), v_v^k)_Y = -\tilde{R} (J_{p v}^k, p_v^k - p_{v, \infty})_Y. \tag{39}$$

We test (34)<sub>1</sub> by  $\frac{1}{K} v^k$  and simplify the first term on the right hand side by comparing it with Eq. (34)<sub>1</sub> for the velocity  $v^k$  and the pressure equation (32), which is tested by  $\varphi_{10} = p^k - p_\infty$ . This procedure yields

$$\begin{aligned}
 \frac{1}{K} |v^k|_H^2 &= -(\nabla (p^k - p_\infty), v^k)_H + (\nabla p_\infty, v^k)_H + (S_p^k, v^k)_H \\
 &= K (\nabla p^k - S_p^k, \nabla (p^k - p_\infty))_H + (\nabla p_\infty, v^k)_H + (S_p^k, v^k)_H \\
 &= \langle \delta_\Gamma, J_{p v, \Gamma}^k (p^k - p_\infty) \rangle_W - (\nabla p_\infty, v^k)_H + (S_p^k, v^k)_H.
 \end{aligned} \tag{40}$$

Step 2 (Estimates)

We separate this step into three sub-steps by deriving the energy estimates separately for (36)–(38).

Step 2.1 (Estimate for (36))

Adding the equations in (36) and (40) gives

$$\begin{aligned}
 & \frac{d}{dt} |\Psi^k|_{L^1(\Omega)} + \frac{\varepsilon_P^2}{2} \frac{d}{dt} |\nabla \phi_P^k|_H^2 + \frac{\varepsilon_H^2}{2} \frac{d}{dt} |\nabla \phi_H^k|_H^2 + \frac{\varepsilon_N^2}{2} \frac{d}{dt} |\nabla \phi_N^k|_H^2 + \left| \sqrt{m_P^k} \nabla \mu_P^k \right|_H^2 + \left| \sqrt{m_H^k} \nabla \mu_H^k \right|_H^2 \\
 & + |\mu_P^k|_H^2 + |\mu_H^k|_H^2 + \frac{1}{K} |v^k|_H^2 \\
 & = (\mathcal{C}(\phi_P^k) v^k, \nabla \mu_P^k + \chi_c \nabla \phi_\sigma^k + \chi_h \nabla \phi_{ECM}^k)_H - (m_P^k \nabla \mu_P^k, \chi_c \nabla \phi_\sigma^k + \chi_h \nabla \phi_{ECM}^k)_H \\
 & + (S_P^k, \mu_P^k + \chi_c \phi_\sigma^k + \chi_h \phi_{ECM}^k)_H + (\partial_{\phi_P^k} \Psi^k - \chi_c \phi_\sigma^k - \chi_h \phi_{ECM}^k, \mu_P^k)_H + \varepsilon_P^2 (\nabla \phi_P^k, \nabla \mu_P^k)_H \\
 & + (\mathcal{C}(\phi_H^k) v^k, \nabla \mu_H^k + \chi_c \nabla \phi_\sigma^k + \chi_h \nabla \phi_{ECM}^k)_H - (m_H^k \nabla \mu_H^k, \chi_c \nabla \phi_\sigma^k + \chi_h \nabla \phi_{ECM}^k)_H \\
 & + (S_H^k, \mu_H^k + \chi_c \phi_\sigma^k + \chi_h \phi_{ECM}^k)_H + (\partial_{\phi_H^k} \Psi^k - \chi_c \phi_\sigma^k - \chi_h \phi_{ECM}^k, \mu_H^k)_H + \varepsilon_H^2 (\nabla \phi_H^k, \nabla \mu_H^k)_H \\
 & + (S_N^k, \Pi_{H_k} \partial_{\phi_N^k} \Psi^k)_H + \varepsilon_N^2 (\nabla S_N^k, \nabla \phi_N^k)_H + \langle \delta_\Gamma, J_{pv,\Gamma}^k(p^k - p_\infty) \rangle_W - (\nabla p_\infty, v^k)_H + (S_p^k, v^k)_H \\
 & = \text{RHS}_{\mathcal{CH}}.
 \end{aligned} \tag{41}$$

We note that the two convection terms cancel together with the last term  $(S_p^k, v^k)_H$  on the right hand side. We apply the Hölder inequality on the terms on the right hand side, and use the assumptions (A4) and (A6), which gives

$$\begin{aligned}
 \text{RHS}_{\mathcal{CH}} & \leq m_\infty |\nabla \mu_P^k|_H (\chi_c |\nabla \phi_\sigma^k|_H + \chi_h |\nabla \phi_{ECM}^k|_H) + |S_P^k|_H (|\mu_P^k|_H + \chi_c |\phi_\sigma^k|_H + \chi_h |\phi_{ECM}^k|_H) \\
 & + |\mu_P^k|_H (|\partial_{\phi_P^k} \Psi^k|_H + \chi_c |\phi_\sigma^k|_H + \chi_h |\phi_{ECM}^k|_H) + \varepsilon_P^2 |\nabla \phi_P^k|_H |\nabla \mu_P^k|_H \\
 & + m_\infty |\nabla \mu_H^k|_H (\chi_c |\nabla \phi_\sigma^k|_H + \chi_h |\nabla \phi_{ECM}^k|_H) + |S_H^k|_H (|\mu_H^k|_H + \chi_c |\phi_\sigma^k|_H + \chi_h |\phi_{ECM}^k|_H) \\
 & + |\mu_H^k|_H (|\partial_{\phi_H^k} \Psi^k|_H + \chi_c |\phi_\sigma^k|_H + \chi_h |\phi_{ECM}^k|_H) + \varepsilon_H^2 |\nabla \phi_H^k|_H |\nabla \mu_H^k|_H \\
 & + |S_N^k|_H |\Pi_{H_k} \partial_{\phi_N^k} \Psi^k|_H + \varepsilon_N^2 |\nabla S_N^k|_H |\nabla \phi_N^k|_H + \langle \delta_\Gamma, J_{pv,\Gamma}^k(p^k - p_\infty) \rangle_W + |\nabla p_\infty|_H |v^k|_H.
 \end{aligned} \tag{42}$$

We note that the norm of the orthogonal projection is bounded by 1. We use a similar argument as in (24) and (25) to estimate the term involving the Dirac delta functional  $\delta_\Gamma$ , i.e., with the assumption on the form of  $J_{pv,\Gamma}^k$ , see (A5), we obtain

$$\begin{aligned}
 & \langle \delta_\Gamma, J_{pv,\Gamma}^k(p^k - p_\infty) \rangle_W \\
 & \leq C_\Gamma |p^k - p_\infty|_W |J_{pv,\Gamma}^k|_{L^2(\Gamma)} \\
 & \leq C_\Gamma L_p |p^k - p_\infty|_W (C_\Gamma |p^k - p_\infty|_W + C_\Gamma |p_\infty|_W + |\Pi_\Gamma|_{\mathcal{L}(Y;L^2(\Gamma))} |p_v^k - p_{v,\infty}|_Y + |\Pi_\Gamma|_{\mathcal{L}(Y;L^2(\Gamma))} |p_{v,\infty}|_Y) \\
 & \leq C_1 L_p (|\nabla p^k|_H^2 + |\nabla p^k|_Y^2 + |p_\infty|_V^2 + |p_{v,\infty}|^2),
 \end{aligned}$$

where we also applied the Poincaré inequality on  $p^k - p_\infty \in V_0$  and  $p_v^k - p_{v,\infty} \in X_0$  with the Poincaré constants  $C_{P,\Omega}$  and  $C_{P,A}$ , giving the constant

$$C_1 = \max\{2C_\Gamma^2 (C_W^V)^2 (C_{P,\Omega}^2 + 1); |\Pi_\Gamma|_{\mathcal{L}(Y;L^2(\Gamma))}^2 C_{P,A}^2; |\Pi_\Gamma|_{\mathcal{L}(Y;L^2(\Gamma))} |\Lambda|\}.$$

Further, using the form on  $v^k$  and  $v_v^k$  gives

$$\langle \delta_\Gamma, J_{pv,\Gamma}^k(p^k - p_\infty) \rangle_W \leq C_1 L_p (K^{-2} |v^k|_H^2 + |S_p^k|_H^2 + \tilde{K}_v^{-2} |v_v^k|_Y^2 + |p_\infty|_V^2 + |p_{v,\infty}|^2).$$

We apply Young’s inequality on the norm products to separate the terms. Here, the goal is to make the terms involving  $|\mu_P^k|_V, |\mu_H^k|_V, |\nabla \phi_\sigma^k|_H$  small, since we cannot absorb them with the Grönwall–Bellman

lemma later on. We only track the important constants, which are used to absorb the terms on the right hand side with the left hand side, the other ones we simply denote by the generic constant  $C$ . We have

$$\begin{aligned}
 \text{RHS}_{\mathcal{CH}} \leq & \frac{m_0}{4} |\nabla \mu_P^k|_H^2 + \frac{2m_\infty^2 \chi_c^2}{m_0} |\nabla \phi_\sigma^k|_H^2 + \frac{2m_\infty^2 \chi_h^2}{m_0} |\nabla \phi_{ECM}^k|_H^2 + 3|S_P^k|_H^2 + \frac{1}{4} (|\mu_P^k|_H^2 + \chi_c^2 |\phi_\sigma^k|_H^2 \\
 & + \chi_h^2 |\phi_{ECM}^k|_H^2) + \frac{1}{4} |\mu_P^k|_H^2 + 3(|\partial_{\phi_P^k} \Psi^k|_H^2 + \chi_c^2 |\phi_\sigma^k|_H^2 + \chi_h^2 |\phi_{ECM}^k|_H^2) + \frac{\varepsilon_P^4}{m_0} |\nabla \phi_P^k|_H^2 \\
 & + \frac{m_0}{4} |\nabla \mu_P^k|_H^2 + \frac{m_0}{4} |\nabla \mu_H^k|_H^2 + \frac{2m_\infty^2 \chi_c^2}{m_0} |\nabla \phi_\sigma^k|_H^2 + \frac{2m_\infty^2 \chi_h^2}{m_0} |\nabla \phi_{ECM}^k|_H^2 + 3|S_H^k|_H^2 \\
 & + \frac{1}{4} (|\mu_H^k|_H^2 + \chi_c^2 |\phi_\sigma^k|_H^2 + \chi_h^2 |\phi_{ECM}^k|_H^2) + \frac{1}{4} |\mu_H^k|_H^2 + 3(|\partial_{\phi_H^k} \Psi^k|_H^2 + \chi_c^2 |\phi_\sigma^k|_H^2 + \chi_h^2 |\phi_{ECM}^k|_H^2) \\
 & + \frac{\varepsilon_H^4}{m_0} |\nabla \phi_H^k|_H^2 + \frac{m_0}{4} |\nabla \mu_H^k|_H^2 + \frac{1}{2} |S_N^k|_H^2 + \frac{1}{2} |\partial_{\phi_N^k} \Psi^k|_H^2 + \varepsilon |\nabla S_N^k|_H^2 + \frac{\varepsilon_N^4}{4\varepsilon} |\nabla \phi_N^k|_H^2 \\
 & + C_1 L_p (K^{-2} |v^k|_H^2 + |S_P^k|_H^2 + \tilde{K}_v^{-2} |v_v^k|_Y^2 + |p_\infty|_V^2 + |p_{v,\infty}|^2) + \frac{K}{2} |\nabla p_\infty|_H^2 + \frac{1}{2K} |v^k|_H^2,
 \end{aligned} \tag{43}$$

where  $\varepsilon > 0$  is a constant, which will be determined later on, see (52) for more details. We estimate the terms involving the potential  $\Psi$  via assumption (A7) and afterwards, we collect the terms with the same norms, which yields

$$\begin{aligned}
 \text{RHS}_{\mathcal{CH}} \leq & \frac{m_0}{2} (|\nabla \mu_P^k|_H^2 + |\nabla \mu_H^k|_H^2) + \frac{1}{2} (|\mu_P^k|_H^2 + |\mu_H^k|_H^2) + \frac{4m_\infty^2 \chi_c^2}{m_0} |\nabla \phi_\sigma^k|_H^2 + \varepsilon |\nabla S_N^k|_H^2 \\
 & + \frac{1}{2K} |v^k|_H^2 + C_1 L_p (K^{-2} |v^k|_H^2 + |S_P^k|_H^2 + \tilde{K}_v^{-2} |v_v^k|_Y^2 + |p_\infty|_V^2 + |p_{v,\infty}|^2) \\
 & + C (|\phi_\sigma^k|_H^2 + |\phi_P^k|_V^2 + |\phi_H^k|_V^2 + |\phi_N^k|_V^2 + |\phi_{ECM}^k|_V^2 + |p_\infty|_V^2 + |S_P^k|_H^2 + |S_H^k|_H^2 + |S_N^k|_H^2).
 \end{aligned} \tag{44}$$

We insert this estimate into (41), and absorb the terms involving the chemical potentials, and arrive at the upper bound

$$\begin{aligned}
 & \frac{d}{dt} \left[ |\Psi^k|_{L^1(\Omega)} + \frac{\varepsilon_P^2}{2} |\nabla \phi_P^k|_H^2 + \frac{\varepsilon_H^2}{2} |\nabla \phi_H^k|_H^2 + \frac{\varepsilon_N^2}{2} |\nabla \phi_N^k|_H^2 \right] + \frac{m_0}{2} |\nabla \mu_P^k|_H^2 + \frac{m_0}{2} |\nabla \mu_H^k|_H^2 + \frac{1}{2} |\mu_P^k|_H^2 \\
 & + \frac{1}{2} |\mu_H^k|_H^2 + \left( \frac{1}{2K} - \frac{C_1 L_p}{K^2} \right) |v^k|_H^2 \\
 & \leq \frac{4m_\infty^2 \chi_c^2}{m_0} |\nabla \phi_\sigma^k|_H^2 + \varepsilon |\nabla S_N^k|_H^2 + C_1 L_p (|S_P^k|_H^2 + \tilde{K}_v^{-2} |v_v^k|_Y^2) + C (|\phi_\sigma^k|_H^2 + |\phi_P^k|_V^2 + |\phi_H^k|_V^2 \\
 & + |\phi_N^k|_V^2 + |\phi_{ECM}^k|_V^2 + |\phi_v^k|_Y^2 + |p_\infty|_V^2 + |p_{v,\infty}|^2 + |S_P^k|_H^2 + |S_H^k|_H^2 + |S_N^k|_H^2).
 \end{aligned} \tag{45}$$

Step 2.2 (Estimate for (37))

Adding the equations in (37) gives

$$\begin{aligned}
 & \frac{C_\sigma}{2} \frac{d}{dt} |\phi_\sigma^k|_H^2 + C_\sigma D_\sigma \left| \sqrt{m_\sigma^k} \nabla \phi_\sigma^k \right|_H^2 + \frac{1}{2} \frac{d}{dt} |\phi_{MDE}^k|_H^2 + D_{MDE} \left| \sqrt{m_{MDE}^k} \nabla \phi_{MDE}^k \right|_H^2 + \frac{1}{2} \frac{d}{dt} |\phi_{TAF}^k|_H^2 \\
 & + D_{TAF} \left| \sqrt{m_{TAF}^k} \nabla \phi_{TAF}^k \right|_H^2 + \frac{1}{2} \frac{d}{dt} |\phi_{ECM}^k|_H^2 + \frac{1}{2} \frac{d}{dt} |\nabla \phi_{ECM}^k|_H^2 \\
 & = \chi_c C_\sigma (m_\sigma^k \nabla (\phi_P^k + \phi_H^k), \nabla \phi_\sigma^k)_H + C_\sigma (S_\sigma^k, \phi_\sigma^k)_H + C_\sigma (\mathcal{C}(\phi_\sigma^k) v^k, \nabla \phi_\sigma^k)_H + C_\sigma \langle \delta_\Gamma, J_{\sigma v, \Gamma}^k \phi_\sigma^k \rangle_W \\
 & + (S_{MDE}^k, \phi_{MDE}^k)_H + (S_{TAF}^k, \phi_{TAF}^k)_H + (S_{ECM}^k, \phi_{ECM}^k)_H + (\nabla S_{ECM}^k, \nabla \phi_{ECM}^k)_H \\
 & = \text{RHS}_{\mathcal{RD}}.
 \end{aligned} \tag{46}$$

We estimate the term involving the Dirac delta functional as before, i.e., we use assumption (A5) and the inequalities (24) and (25) to obtain

$$\begin{aligned} & C_\sigma \langle \delta_\Gamma, J_{\sigma v, \Gamma}^k \phi_\sigma^k \rangle_W \\ & \leq C_\sigma C_\Gamma |\phi_\sigma^k|_W \left( f_\infty L_p (C_\Gamma |p^k|_W + |\Pi_\Gamma|_{\mathcal{L}(Y; L^2(\Gamma))} |p_v^k|_Y) + L_\sigma (C_\Gamma |\phi_\sigma^k|_W + |\Pi_\Gamma|_{\mathcal{L}(Y; L^2(\Gamma))} |\phi_v^k|_Y) \right) \\ & \leq C_2 C_\sigma \max\{L_p; L_\sigma\} (|\phi_\sigma^k|_V^2 + |\phi_v^k|_Y^2 + K^{-2} |v^k|_H^2 + |S_p^k|_H^2 + \tilde{K}_v^{-2} |v_v^k|_Y^2 + |p_\infty|_V^2 + |p_{v, \infty}|^2), \end{aligned}$$

where

$$C_2 = \max\{2^4 C_\Gamma^2 (C_W^V)^2; f_\infty^2 C_\Gamma^2 (C_W^V)^2 (C_{P, \Omega}^2 + 1); f_\infty^2 |\Pi_\Gamma|_{\mathcal{L}(Y; L^2(\Gamma))}^2 C_{P, \Lambda}^2; f_\infty^2 |\Pi_\Gamma|_{\mathcal{L}(Y; L^2(\Gamma))}^2 |A|; |\Pi_\Gamma|_{\mathcal{L}(Y; L^2(\Gamma))}^2\}.$$

In a similar way to the estimates before, we apply Hölder’s and Young’s inequalities on the terms on the right hand side, which results in

$$\begin{aligned} \text{RHS}_{\mathcal{RD}} & \leq \frac{C_\sigma m_\infty^2 \chi_c^2}{D_\sigma m_0} |\nabla(\phi_P^k + \phi_H^k)|_H^2 + \frac{C_\sigma D_\sigma m_0}{4} |\nabla \phi_\sigma^k|_H^2 + C (|S_\sigma^k|_H^2 + |\phi_\sigma^k|_H^2) \\ & \quad + \frac{C_\sigma D_\sigma m_0}{4} |\nabla \phi_\sigma^k|_H^2 + \frac{C_\sigma}{D_\sigma m_0} |v^k|_H^2 + C_2 C_\sigma \max\{L_p; L_\sigma\} (|\phi_\sigma^k|_V^2 + |\phi_v^k|_Y^2 + K^{-2} |v^k|_H^2 \\ & \quad + |S_p^k|_H^2 + \tilde{K}_v^{-2} |v_v^k|_Y^2 + |p_\infty|_V^2 + |p_{v, \infty}|^2) + C (|S_{MDE}^k|_H^2 + |\phi_{MDE}^k|_H^2 + |S_{TAF}^k|_H^2 \\ & \quad + |\phi_{TAF}^k|_H^2 + |S_{ECM}^k|_H^2 + |\phi_{ECM}^k|_H^2) + \varepsilon |\nabla S_{ECM}^k|_H^2 + \frac{1}{4\varepsilon} |\nabla \phi_{ECM}^k|_H^2, \end{aligned} \tag{47}$$

where we used the same constant  $\varepsilon$  as before in (41) and applied the assumption on the form of  $J_{\sigma v, \Gamma}^k$ , see (A5). Again, collecting the terms on the right hand side and absorbing the terms with their counterparts, we have

$$\begin{aligned} & \frac{1}{2} \frac{d}{dt} \left[ C_\sigma |\phi_\sigma^k|_H^2 + |\phi_{MDE}^k|_H^2 + |\phi_{TAF}^k|_H^2 + |\phi_{ECM}^k|_H^2 + |\nabla \phi_{ECM}^k|_H^2 \right] + D_{MDE} m_0 |\nabla \phi_{MDE}^k|_H^2 \\ & \quad + D_{TAF} m_0 |\nabla \phi_{TAF}^k|_H^2 + \frac{C_\sigma}{2} (D_\sigma m_0 - 2C_2 \max\{L_p; L_\sigma\}) |\nabla \phi_\sigma^k|_H^2 \\ & \leq \left( \frac{C_\sigma}{D_\sigma m_0} + \frac{C_2 C_\sigma \max\{L_p; L_\sigma\}}{K^2} \right) |v^k|_H^2 + C_2 C_\sigma \max\{L_p; L_\sigma\} (|S_p^k|_H^2 + \tilde{K}_v^{-2} |v_v^k|_Y^2) + \varepsilon |\nabla S_{ECM}^k|_H^2 \\ & \quad + C (|\phi_P|_V^2 + |\phi_H|_V^2 + |\phi_\sigma^k|_H^2 + |\phi_{MDE}^k|_H^2 + |\phi_{TAF}^k|_H^2 + |\phi_{ECM}^k|_V^2 + |\phi_v^k|_Y^2 + |p_\infty|_V^2 \\ & \quad + |p_{v, \infty}|^2 + |S_\sigma^k|_H^2 + |S_{MDE}^k|_H^2 + |S_{TAF}^k|_H^2 + |S_{ECM}^k|_H^2). \end{aligned} \tag{48}$$

Step 2.3 (Estimate for (38))

Lastly, adding the equations in (38) and (39) gives

$$\begin{aligned} & \frac{C_v}{2} \frac{d}{dt} |\phi_v^k - \phi_{v, \infty}|_Y^2 + C_v D_v \left| \sqrt{m_v^k} \nabla_\Lambda \phi_v^k \right|_Y^2 + \frac{1}{\tilde{K}_v} |v_v^k|_Y^2 \\ & = C_v (C(\phi_v^k) v_v^k, \nabla_\Lambda \phi_v^k)_Y - C_v (R J_{\sigma v}^k + \phi'_{v, \infty}, \phi_v^k - \phi_{v, \infty})_Y - \tilde{R} (J_{pv}^k, p_v^k - p_{v, \infty})_Y. \end{aligned} \tag{49}$$

We estimate the last term on the right hand side with the Poincaré–Wirtinger inequality (18) with constant  $C_P$ , the Darcy law (34) and the Young inequality as follows

$$-\tilde{R} (J_{pv}^k, p_v^k - p_{v, \infty})_Y \leq \tilde{R} C_P |J_{pv}^k|_Y |\nabla p_v^k|_Y = \frac{R^2 C_P^2}{\tilde{K}_v} |J_{pv}^k|_Y |v_v^k|_Y \leq \frac{R^2 C_P^2}{\tilde{K}_v} |J_{pv}^k|_Y^2 + \frac{1}{4\tilde{K}_v} |v_v^k|_Y^2.$$

Additionally, repeating the steps from before and using the assumption on the forms on  $J_{pv}^k$  and  $J_{\sigma v}^k$ , see (A5), we arrive at

$$\begin{aligned} & \frac{C_v}{2} \frac{d}{dt} |\phi_v^k - \phi_{v,\infty}|_Y^2 + C_v D_v m_0 |\nabla_\Lambda \phi_v^k|_Y^2 + \frac{1}{\tilde{K}_v} |v_v^k|_Y^2 \\ & \leq \frac{C_v}{D_v m_0} |v_v^k|_Y^2 + \frac{C_v D_v m_0}{4} |\nabla_\Lambda \phi_v^k|_Y^2 + R^2 |J_{\sigma v}^k|_Y^2 + C(|\phi'_{v,\infty}|^2 + |\phi_v^k - \phi_{v,\infty}|_Y^2) + \frac{R^2 C_P^2}{\tilde{K}_v} |J_{pv}^k|_Y^2 + \frac{1}{4\tilde{K}_v} |v_v^k|_Y^2 \\ & \leq \frac{C_v}{D_v m_0} |v_v^k|_Y^2 + \frac{C_v D_v m_0}{4} |\nabla_\Lambda \phi_v^k|_Y^2 + C(|\phi'_{v,\infty}|^2 + |\phi_v^k - \phi_{v,\infty}|_Y^2) + \frac{1}{4\tilde{K}_v} |v_v^k|_Y^2 + (1 + C_P^2 \tilde{K}_v^{-1}) \cdot \\ & \quad R^2 C_2 \max\{L_p; L_\sigma\} (|\phi_\sigma^k|_V^2 + |\phi_v^k|_Y^2 + K^{-2} |v^k|_H^2 + |S_p^k|_H^2 + \tilde{K}_v^{-2} |v_v^k|_Y^2 + |p_\infty|_V^2 + |p_{v,\infty}|^2), \end{aligned}$$

which gives after choosing  $C_v > \frac{4\tilde{K}_v}{D_v m_0}$  and absorbing

$$\begin{aligned} & \frac{C_v}{2} \frac{d}{dt} |\phi_v^k - \phi_{v,\infty}|_Y^2 + \frac{3C_v D_v m_0}{4} |\nabla_\Lambda \phi_v^k|_Y^2 + \left( \frac{1}{2\tilde{K}_v} - \frac{(1 + C_P^2 \tilde{K}_v^{-1}) R^2 C_2 \max\{L_p; L_\sigma\}}{\tilde{K}_v^2} \right) |v_v^k|_Y^2 \\ & \leq (1 + C_P^2 \tilde{K}_v^{-1}) R^2 C_2 \max\{L_p; L_\sigma\} (|\phi_\sigma^k|_V^2 + |\phi_v^k - \phi_{v,\infty}|_Y^2 + |\phi_{v,\infty}|^2 + K^{-2} |v^k|_H^2 + |S_p^k|_H^2 \\ & \quad + |p_\infty|_V^2 + |p_{v,\infty}|^2) + C(|\phi'_{v,\infty}|^2 + |\phi_v^k - \phi_{v,\infty}|_Y^2). \end{aligned} \tag{50}$$

Step 3 (Adding)

We add Eqs. (45), (48) and (50) to arrive at

$$\begin{aligned} & \frac{1}{2} \frac{d}{dt} \left[ 2|\Psi^k|_{L^1(\Omega)} + \varepsilon_P^2 |\nabla \phi_P^k|_H^2 + \varepsilon_H^2 |\nabla \phi_H^k|_H^2 + \varepsilon_N^2 |\nabla \phi_N^k|_H^2 + C_\sigma |\phi_\sigma^k|_H^2 + |\phi_{MDE}^k|_H^2 + |\phi_{TAF}^k|_H^2 \right. \\ & \quad \left. + |\phi_{ECM}^k|_V^2 + C_v |\phi_v^k - \phi_{v,\infty}|_Y^2 \right] + \frac{m_0}{2} |\nabla \mu_P^k|_H^2 + \frac{m_0}{2} |\nabla \mu_H^k|_H^2 + \frac{1}{2} |\mu_P^k|_H^2 + \frac{1}{2} |\mu_H^k|_H^2 \\ & \quad + \left( \frac{1}{2K} - \frac{C_1 L_p}{K^2} - \frac{C_\sigma}{D_\sigma m_0} - \frac{(C_\sigma + R^2 + R^2 C_P^2 \tilde{K}_v^{-1}) C_2 \max\{L_p; L_\sigma\}}{K^2} \right) |v^k|_H^2 \\ & \quad + \left( \frac{C_\sigma D_\sigma m_0}{2} - \frac{4m_\infty^2 \chi_c^2}{m_0} - (C_\sigma + \tilde{K}_v + 1) C_2 \max\{L_p; L_\sigma\} \right) |\nabla \phi_\sigma^k|_H^2 \\ & \quad + D_{MDE} m_0 |\nabla \phi_{MDE}^k|_H^2 + D_{TAF} m_0 |\nabla \phi_{TAF}^k|_H^2 + \frac{3C_v D_v m_0}{4} |\nabla_\Lambda \phi_v^k|_Y^2 \\ & \quad + \left( \frac{1}{2\tilde{K}_v} - \frac{C_1 L_p}{\tilde{K}_v^2} - \frac{(C_\sigma + R^2 + R^2 C_P^2 \tilde{K}_v^{-1}) C_2 \max\{L_p; L_\sigma\}}{\tilde{K}_v^2} \right) |v_v^k|_Y^2 \\ & \leq \varepsilon (|\nabla S_N^k|_H^2 + |\nabla S_{ECM}^k|_H^2) + (C_1 + (C_\sigma + R^2 + R^2 C_P^2 \tilde{K}_v^{-1}) C_2) \max\{L_p; L_\sigma\} |S_p^k|_H^2 + C (1 + |\phi_P|_V^2 \\ & \quad + |\phi_H^k|_V^2 + |\phi_N^k|_V^2 + |\phi_v^k|_Y^2 + |\phi_\sigma^k|_H^2 + |\phi_{MDE}^k|_H^2 + |\phi_{TAF}^k|_H^2 + |\phi_{ECM}^k|_V^2 + |\phi_v - \phi_{v,\infty}|_Y^2 + |p_\infty|_V^2 + |p_{v,\infty}|^2 \\ & \quad + |\phi_{v,\infty}|^2 + |\phi'_{v,\infty}|^2 + |S_P^k|_H^2 + |S_H^k|_H^2 + |S_N^k|_H^2 + |S_\sigma^k|_H^2 + |S_{MDE}^k|_H^2 + |S_{TAF}^k|_H^2 + |S_{ECM}^k|_H^2). \end{aligned} \tag{51}$$

By assumption (A4) on the source functions, we have the three estimates

- $\sum_{\alpha \in \mathcal{A}} |S_\alpha^k|_H^2 \lesssim \sum_{\alpha \in \mathcal{A}} |\phi_\alpha|_H^2,$
- $|\nabla S_N^k|_H^2 + |\nabla S_{ECM}^k|_H^2 \leq 2^{|\mathcal{A}|} f_\infty^2 |\mathcal{A}| \sum_{\alpha \in \mathcal{A}} |\nabla \phi_\alpha|_H^2,$
- $|S_p^k|_H^2 \leq 8(|\nabla \mu_P^k|_H^2 + |\nabla \mu_H^k|_H^2 + 2\chi_c^2 |\nabla \phi_\sigma^k|_H^2 + 2\chi_h^2 |\nabla \phi_{ECM}^k|_H^2),$

and insert these estimates into (51). Further, in order to treat the factor  $|\nabla S_N^k|_H^2 + |\nabla S_{ECM}^k|_H^2$ , we choose the constant

$$\varepsilon = \frac{m_0}{2^{|\mathcal{A}|+2} f_\infty^2 |\mathcal{A}|^2} \min\{C_\sigma D_\sigma, D_{MDE}, D_{TAF}\}, \tag{52}$$

so that we can conclude

$$\begin{aligned} \varepsilon(|\nabla S_N^k|_H^2 + |\nabla S_{ECM}^k|_H^2) &\leq \frac{m_0}{4} \min\{C_\sigma D_\sigma, D_{MDE}, D_{TAF}\} \sum_{\alpha \in \mathcal{A}} |\nabla \phi_\alpha|^2_H \\ &\leq \frac{C_\sigma D_\sigma m_0}{4} |\nabla \phi_\sigma^k|_H^2 + \frac{D_{MDE} m_0}{4} |\nabla \phi_{MDE}^k|_H^2 + \frac{D_{TAF} m_0}{4} |\nabla \phi_{TAF}^k|_H^2 \\ &\quad + C(|\phi_P^k|_V^2 + |\phi_H^k|_V^2 + |\phi_N^k|_V^2 + |\phi_{ECM}^k|_V^2). \end{aligned}$$

We absorb, collect and summarize the constants, giving

$$\begin{aligned} &\frac{1}{2} \frac{d}{dt} \left[ 2|\Psi^k|_{L^1(\Omega)} + \varepsilon_P^2 |\nabla \phi_P^k|_H^2 + \varepsilon_H^2 |\nabla \phi_H^k|_H^2 + \varepsilon_N^2 |\nabla \phi_N^k|_H^2 + C_\sigma |\phi_\sigma^k|_H^2 + |\phi_{MDE}^k|_H^2 + |\phi_{TAF}^k|_H^2 \right. \\ &\quad \left. + |\phi_{ECM}^k|_V^2 + |\phi_v^k - \phi_{v,\infty}|_Y^2 \right] + \frac{1}{2} |\mu_P^k|_H^2 + \frac{1}{2} |\mu_H^k|_H^2 \\ &\quad + \left( \frac{m_0}{2} - 8(C_1 + (C_\sigma + R^2 + R^2 C_P^2 \tilde{K}_v^{-1}) C_2) \max\{L_p; L_\sigma\} \right) (|\nabla \mu_P^k|_H^2 + |\nabla \mu_H^k|_H^2) \\ &\quad + \left( \frac{1}{2K} - \frac{C_1 L_p}{K^2} - \frac{C_\sigma}{D_\sigma m_0} - \frac{(C_\sigma + R^2 + R^2 C_P^2 \tilde{K}_v^{-1}) C_2 \max\{L_p; L_\sigma\}}{K^2} \right) |v^k|_H^2 \\ &\quad + \left( \frac{C_\sigma D_\sigma m_0}{2} - \frac{4m_\infty^2 \chi_c^2}{m_0} - (C_\sigma + R^2 + R^2 C_P^2 \tilde{K}_v^{-1}) C_2 \max\{L_p; L_\sigma\} \right) |\nabla \phi_\sigma^k|_H^2 \\ &\quad + \frac{3m_0}{4} (D_{MDE} |\nabla \phi_{MDE}^k|_H^2 + D_{TAF} |\nabla \phi_{TAF}^k|_H^2 + D_v |\nabla \phi_v^k|_Y^2) \\ &\quad + \left( \frac{1}{2\tilde{K}_v} - \frac{C_1 L_p}{\tilde{K}_v^2} - \frac{(C_\sigma + R^2 + R^2 C_P^2 \tilde{K}_v^{-1}) C_2 \max\{L_p; L_\sigma\}}{\tilde{K}_v^2} \right) |v_v^k|_Y^2 \\ &\leq C \left( 1 + |\phi_P^k|_V^2 + |\phi_H^k|_V^2 + |\phi_N^k|_V^2 + |\phi_v^k|_Y^2 + |\phi_\sigma^k|_H^2 + |\phi_{MDE}^k|_H^2 + |\phi_{TAF}^k|_H^2 + |\phi_{ECM}^k|_V^2 + |\phi_v^k - \phi_{v,\infty}|_Y^2 \right. \\ &\quad \left. + |p_\infty|_V^2 + |p_{v,\infty}|^2 + |\phi_{v,\infty}|^2 + |\phi'_{v,\infty}|^2 \right), \end{aligned} \tag{53}$$

and we choose  $C_\sigma$  and  $L_p, L_\sigma, K$  such that the prefactors are positive, see also assumption (A5). In particular, we have to ensure the condition

$$\frac{8m_\infty^2 \chi_c^2}{m_0^2 D_\sigma} < C_\sigma < \frac{D_\sigma m_0}{2K}.$$

*Step 4 (Grönwall–Bellman lemma)*

First, we eliminate the prefactors on the left hand side of the energy inequality (53) by estimating it with the minimum of all prefactors and bringing it to the right hand side to the generic constant  $C$ . Afterwards, we integrate the inequality over the time interval  $(0, t)$  with  $t \in (0, T_k)$ , apply the growth assumption (A7), and obtain

$$\begin{aligned} &|\Psi^k(t)|_{L^1(\Omega)} + |\phi_P^k(t)|_V^2 + |\phi_H^k(t)|_V^2 + |\phi_N^k(t)|_V^2 + |\phi_\sigma^k(t)|_H^2 + |\phi_{MDE}^k(t)|_H^2 + |\phi_{TAF}^k(t)|_H^2 + |\phi_{ECM}^k(t)|_V^2 \\ &\quad + |\phi_v^k(t) - \phi_{v,\infty}|_Y^2 + \|\phi_\sigma^k\|_{L^2(0, T_k; V)}^2 + \|\mu_P^k\|_{L^2(0, T_k; V)}^2 + \|\mu_H^k\|_{L^2(0, T_k; V)}^2 + \|\phi_{MDE}^k\|_{L^2(0, T_k; V)}^2 \\ &\quad + \|\phi_{TAF}^k\|_{L^2(0, T_k; V)}^2 + \|\phi_v^k - \phi_{v,\infty}\|_{L^2(0, T_k; X_0)}^2 + \|v^k\|_{L^2(0, T_k; H)}^2 + \|v_v^k\|_{L^2(0, T_k; Y)}^2 \\ &\quad - C \left( \|\phi_P^k\|_{L^2(0, T_k; V)}^2 + \|\phi_H^k\|_{L^2(0, T_k; V)}^2 + \|\phi_N^k\|_{L^2(0, T_k; V)}^2 + \|\phi_v^k\|_{L^2(0, T_k; Y)}^2 + \|\phi_\sigma^k\|_{L^2(0, T_k; H)}^2 \right. \\ &\quad \left. + \|\phi_{MDE}^k\|_{L^2(0, T_k; H)}^2 + \|\phi_{TAF}^k\|_{L^2(0, T_k; H)}^2 + \|\phi_{ECM}^k\|_{L^2(0, T_k; V)}^2 + \|\phi_v^k - \phi_{v,\infty}\|_{L^2(0, T_k; Y)}^2 \right) \\ &\leq C(T_k) \cdot \left( 1 + |\Psi^k(0)|_{L^1(\Omega)} + |\nabla \phi_{P,0}^k|_H^2 + |\nabla \phi_{H,0}^k|_H^2 + |\nabla \phi_{N,0}^k|_H^2 + |\phi_{\sigma,0}^k|_H^2 + |\phi_{MDE,0}^k|_H^2 + |\phi_{TAF,0}^k|_H^2 \right. \\ &\quad \left. + |\phi_{ECM,0}^k|_V^2 + |\phi_{v,0}^k|_Y^2 + \|p_\infty\|_{L^2(0, T; V)}^2 + \|p_{v,\infty}\|_{L^2(0, T)}^2 + |\phi_{v,\infty}|_{H^1(0, T)}^2 \right). \end{aligned}$$

By applying the Grönwall–Bellman lemma, see Lemma 1, we obtain

$$\begin{aligned} & \|\Psi^k\|_{L^\infty(0,T_k;L^1(\Omega))} + \sum_{\alpha \in \mathcal{CH} \cup \{ECM\}} \|\phi_\alpha^k\|_{L^\infty(0,T_k;V)}^2 + \sum_{\alpha \in \{P,H\}} \|\mu_\alpha^k\|_{L^2(0,T_k;V)}^2 + \sum_{\beta \in \mathcal{RD}} \|\phi_\beta^k\|_{L^\infty(0,T_k;H) \cap L^2(0,T_k;V)}^2 \\ & + \|v^k\|_{L^2(0,T_k;H)}^2 + \|\phi_v^k - \phi_{v,\infty}\|_{L^\infty(0,T_k;Y) \cap L^2(0,T_k;X_0)}^2 + \|v_v^k\|_{L^2(0,T_k;Y)}^2 \\ & \leq C(T_k) \cdot \left( 1 + |\phi_{v,0}^k|_Y^2 + \sum_{\alpha \in \mathcal{CH} \cup \{ECM\}} |\phi_{\alpha,0}^k|_V^2 + \sum_{\beta \in \mathcal{RD}} |\phi_{\beta,0}^k|_H^2 + |\Psi(\phi_{P,0}^k, \phi_{H,0}^k, \phi_{N,0}^k)|_{L^1(\Omega)} \right) \\ & + \|p_\infty\|_{L^2(0,T;V)}^2 + |p_{v,\infty}|_{L^2(0,T)}^2 + |\phi_{v,\infty}|_{H^1(0,T)}^2. \end{aligned} \tag{54}$$

We have chosen the initial values of the Faedo–Galerkin approximations as the orthogonal projections of the initial values of their counterpart, see (35). The operator norm of an orthogonal projection is bounded by 1 and, therefore, uniform estimates are obtained in (54); for example

$$|\phi_{P,0}^k|_V^2 = |\Pi_{H_k} \phi_{P,0}|_V^2 \leq |\phi_{P,0}|_V^2.$$

Using the upper bound (26) of  $\Psi$ , we treat the term involving the potential function on the right hand side in the following way:

$$\begin{aligned} |\Psi(\phi_{P,0}^k, \phi_{H,0}^k, \phi_{N,0}^k)|_{L^1(\Omega)} & \lesssim 1 + |\phi_{P,0}^k|_H^2 + |\phi_{H,0}^k|_H^2 + |\phi_{N,0}^k|_H^2 \\ & = 1 + |\Pi_{H_k} \phi_{P,0}|_H^2 + |\Pi_{H_k} \phi_{H,0}|_H^2 + |\Pi_{H_k} \phi_{N,0}|_H^2 \\ & \leq 1 + |\phi_{P,0}|_H^2 + |\phi_{H,0}|_H^2 + |\phi_{N,0}|_H^2. \end{aligned}$$

Now, the  $k$ -independent right hand side in the estimate allows us to extend the time interval by setting  $T_k = T$  for all  $k \in \mathbb{N}$ . Therefore, we have the final uniform energy estimate,

$$\begin{aligned} & \|\Psi^k\|_{L^\infty(0,T;L^1(\Omega))} + \sum_{\alpha \in \mathcal{CH} \cup \{ECM\}} \|\phi_\alpha^k\|_{L^\infty(0,T;V)}^2 + \sum_{\alpha \in \{P,H\}} \|\mu_\alpha^k\|_{L^2(0,T;V)}^2 + \sum_{\beta \in \mathcal{RD}} \|\phi_\beta^k\|_{L^\infty H \cap L^2(0,T;V)}^2 \\ & + \|v^k\|_{L^2(0,T;H)}^2 + \|\phi_v^k - \phi_{v,\infty}\|_{L^\infty(0,T;Y) \cap L^2(0,T;X_0)}^2 + \|v_v^k\|_{L^2(0,T;Y)}^2 \\ & \leq C(T) \cdot \left( 1 + |\phi_{v,0}|_Y^2 + \sum_{\alpha \in \mathcal{CH} \cup \{ECM\}} |\phi_{\alpha,0}|_V^2 + \sum_{\beta \in \mathcal{RD}} |\phi_{\beta,0}|_H^2 \right. \\ & \left. + \|p_\infty\|_{L^2(0,T;V)}^2 + |p_{v,\infty}|_{L^2(0,T)}^2 + |\phi_{v,\infty}|_{H^1(0,T)}^2 \right). \end{aligned} \tag{55}$$

From this energy inequality and (34) we also get bounds for the pressures  $p^k$  and  $p_v^k$  in the following way

$$\|p^k - p_\infty\|_{L^2(0,T;V_0)} + \|p_v^k - p_{v,\infty}\|_{L^2(0,T;X_0)} \leq C.$$



### 5.3. Limit process

#### Weak convergence

Next, we prove that there are subsequences of  $\phi^k, \mu_P^k, \mu_H^k, p^k, \phi_v^k, p_v^k$ , which converge to a weak solution of our model (14)–(16) in the sense of Definition 1. From the energy estimate (55) we deduce that

$$\begin{aligned}
 \{\phi_\alpha^k\}_{k \in \mathbb{N}} &\text{ is bounded in } L^\infty(0, T; V), & \alpha \in \mathcal{CH} \cup \{ECM\}, \\
 \{\mu_\alpha^k\}_{k \in \mathbb{N}} &\text{ is bounded in } L^2(0, T; V), & \alpha \in \{P, H\}, \\
 \{\phi_\beta^k\}_{k \in \mathbb{N}} &\text{ is bounded in } L^\infty(0, T; H) \cap L^2(0, T; V), & \beta \in \mathcal{RD}, \\
 \{v^k\}_{k \in \mathbb{N}} &\text{ is bounded in } L^2(0, T; L^2(\Omega; \mathbb{R}^3)), \\
 \{p^k\}_{k \in \mathbb{N}} &\text{ is bounded in } (p_\infty + L^2(0, T; V_0)), \\
 \{\phi_v^k\}_{k \in \mathbb{N}} &\text{ is bounded in } L^\infty(0, T; Y) \cap (\phi_{v,\infty} + L^2(0, T; X_0)), \\
 \{v_v^k\}_{k \in \mathbb{N}} &\text{ is bounded in } L^2(0, T; Y), \\
 \{p_v^k\}_{k \in \mathbb{N}} &\text{ is bounded in } (p_{v,\infty} + L^2(0, T; X_0)),
 \end{aligned} \tag{56}$$

and, by the Banach–Alaoglu theorem, these bounded sequences have weakly/weakly-\* convergent subsequences. By a standard abuse of notation, we drop the subsequence index. Consequently, there are functions  $\phi : (0, T) \times \Omega \rightarrow \mathbb{R}^{|\mathcal{A}|}$ ,  $\mu_P, \mu_H, p : (0, T) \times \Omega \rightarrow \mathbb{R}$ ,  $v : (0, T) \times \Omega \rightarrow \mathbb{R}^3$ ,  $\phi_v, v_v, p_v : (0, T) \times \Lambda \rightarrow \mathbb{R}$  such that, for  $k \rightarrow \infty$ ,

$$\begin{aligned}
 \phi_\alpha^k &\rightharpoonup \phi_\alpha \text{ weakly-* in } L^\infty(0, T; V), & \alpha \in \mathcal{CH} \cup \{ECM\}, \\
 \mu_\alpha^k &\rightharpoonup \mu_\alpha \text{ weakly in } L^2(0, T; V), & \alpha \in \mathcal{CH} \setminus \{N\}, \\
 \phi_\beta^k &\rightharpoonup \phi_\beta \text{ weakly-* in } L^\infty(0, T; H) \cap L^2(0, T; V), & \beta \in \mathcal{RD}, \\
 v^k &\rightharpoonup v \text{ weakly in } L^2(0, T; L^2(\Omega; \mathbb{R}^3)), \\
 p^k &\rightharpoonup p \text{ weakly in } (p_\infty + L^2(0, T; V_0)), \\
 \phi_v^k &\rightharpoonup \phi_v \text{ weakly-* in } L^\infty(0, T; Y) \cap (\phi_{v,\infty} + L^2(0, T; X_0)), \\
 v_v^k &\rightharpoonup v_v \text{ weakly in } L^2(0, T; Y), \\
 p_v^k &\rightharpoonup p_v \text{ weakly in } (p_{v,\infty} + L^2(0, T; X_0)).
 \end{aligned} \tag{57}$$

#### Strong convergence

We now consider taking the limit  $k \rightarrow \infty$  in the Faedo–Galerkin system (32)–(33) in the hope to attain the initial variational system (28)–(29). Since the equations in (32)–(33) are nonlinear in  $\phi^k$  and  $\phi_v^k$ , we want to achieve strong convergence of these sequences before we take the limit in (32)–(33). Therefore, our goal is to bound their time derivatives and to apply the Aubin–Lions–Simon compactness lemma (19).

Let  $(\varphi, \hat{\varphi}, \tilde{\varphi})$  be such that  $\varphi \in L^2(0, T; V)$ ,  $\hat{\varphi} \in L^2(0, T; H)$ ,  $\tilde{\varphi} \in L^2(0, T; X_0)$ , and

$$\Pi_{H_k} \varphi = \sum_{j=1}^k \varphi_j^k h_j, \quad \Pi_{H_k} \hat{\varphi} = \sum_{j=1}^k \hat{\varphi}_j^k h_j, \quad \Pi_{Y_k} \tilde{\varphi} = \sum_{j=1}^k \tilde{\varphi}_j^k y_j,$$

with time-dependent coefficient functions  $\varphi_j^k, \hat{\varphi}_j^k, \tilde{\varphi}_j^k : (0, T) \rightarrow \mathbb{R}$ ,  $j \in \{1, \dots, k\}$ . We multiply Eqs. (32) and (33) by  $\tilde{\varphi}_j^k$  by the appropriate coefficient functions, sum up each equation from  $j = 1$  to  $k$  and integrate in

time over  $(0, T)$ , to obtain the equation system,

$$\begin{aligned}
 \int_0^T \langle \partial_t \phi_\alpha^k, \varphi \rangle_V dt &= \int_0^T (\mathcal{C}(\phi_\alpha^k) v^k, \nabla \Pi_{H_k} \varphi)_H - (m_\alpha^k \nabla \mu_\alpha^k, \nabla \Pi_{H_k} \varphi)_H + (S_\alpha^k, \Pi_{H_k} \varphi)_H dt, \\
 \int_0^T \langle \partial_t \phi_\beta^k, \hat{\varphi} \rangle_V dt &= \int_0^T (S_\beta^k, \Pi_{H_k} \hat{\varphi})_H dt, \\
 \int_0^T \langle \partial_t \phi_\sigma^k, \varphi \rangle_V dt &= \int_0^T (\mathcal{C}(\phi_\sigma^k) v^k, \nabla \Pi_{H_k} \varphi)_H - D_\sigma (m_\sigma^k \nabla \phi_\sigma^k, \nabla \Pi_{H_k} \varphi)_H + (S_\sigma^k, \Pi_{H_k} \varphi)_H \\
 &\quad + \langle \delta_\Gamma, J_{\sigma v, \Gamma}^k \Pi_{H_k} \varphi \rangle_W - \chi_c (m_\sigma^k \nabla (\phi_P^k + \phi_H^k + \phi_N^k), \nabla \Pi_{H_k} \varphi)_H dt, \\
 \int_0^T \langle \partial_t \phi_\gamma^k, \varphi \rangle_V dt &= \int_0^T -D_\gamma (m_\gamma^k \nabla \phi_\gamma^k, \nabla \Pi_{H_k} \varphi)_H + (S_\gamma^k, \Pi_{H_k} \varphi)_H dt, \\
 \int_0^T \langle \partial_t \phi_v^k, \tilde{\varphi} \rangle_X dt &= \int_0^T (\mathcal{C}(\phi_v^k) v_v^k, \nabla_\Lambda \Pi_{Y_k} \tilde{\varphi})_Y - D_v (m_v^k \nabla_\Lambda \phi_v^k, \nabla_\Lambda \Pi_{Y_k} \tilde{\varphi})_Y - \tilde{R} (J_{\sigma v}^k, \Pi_{Y_k} \tilde{\varphi})_Y dt,
 \end{aligned} \tag{58}$$

where  $\alpha \in \{P, H\}$ ,  $\beta \in \{N, ECM\}$ ,  $\gamma \in \{MDE, TAF\}$ . Each equation in (58) can be treated using standard inequalities and the estimate involving the trace operator, see (24), the boundedness of the orthogonal projection and the energy estimate (55), e.g., we find

$$\begin{aligned}
 \int_0^T \langle \partial_t \phi_\sigma^k, \varphi \rangle_V dt &\lesssim \int_0^T |v^k|_H |\varphi|_V + |\phi_\sigma^k|_V |\varphi|_V + \sum_{\alpha \in \mathcal{A}} |\phi_\alpha^k|_H |\varphi|_H + |J_{\sigma v, \Gamma}^k|_{L^2(\Gamma)} |\varphi|_V + \sum_{\beta \in \mathcal{CH}} |\phi_\beta^k|_V |\varphi|_V dt \\
 &\lesssim \|\varphi\|_{L^2(0, T; V)}.
 \end{aligned}$$

From this inequality and the bounds derived earlier, see (56), we conclude that

$$\begin{aligned}
 \{\phi_\alpha^k\}_{k \in \mathbb{N}} &\text{ is bounded in } H^1(0, T; V') \cap L^\infty(0, T; V), & \alpha \in \{P, H\}, \\
 \{\phi_\beta^k\}_{k \in \mathbb{N}} &\text{ is bounded in } H^1(0, T; H) \cap L^\infty(0, T; V), & \beta \in \{N, ECM\}, \\
 \{\phi_\gamma^k\}_{k \in \mathbb{N}} &\text{ is bounded in } H^1(0, T; V') \cap L^\infty(0, T; H) \cap L^2(0, T; V), & \gamma \in \mathcal{RD}, \\
 \{\phi_v^k\}_{k \in \mathbb{N}} &\text{ is bounded in } H^1(0, T; X'_0) \cap L^\infty(0, T; Y) \cap (\phi_{v, \infty} + L^2(0, T; X_0)).
 \end{aligned}$$

We apply the Aubin–Lions–Simon compactness lemma (19), yielding the strong convergences as  $k \rightarrow \infty$

$$\begin{aligned}
 \phi_\alpha^k &\longrightarrow \phi_\alpha \text{ strongly in } C^0([0, T]; H), & \alpha \in \mathcal{CH} \cup \{ECM\}, \\
 \phi_\beta^k &\longrightarrow \phi_\beta \text{ strongly in } L^2(0, T; H) \cap C^0([0, T]; V'), & \beta \in \mathcal{RD}, \\
 \phi_v^k &\longrightarrow \phi_v \text{ strongly in } L^2(0, T; Y) \cap C^0([0, T]; X'_0).
 \end{aligned} \tag{59}$$

The strong convergence  $\phi_\alpha^k \rightarrow \phi_\alpha$  in  $C^0([0, T]; H)$  implies  $\phi_\alpha(0) = \phi_{\alpha, 0}$  in  $H$  and similarly  $\phi_\beta(0) = \phi_{\beta, 0}$  in  $V'$  and  $\phi_v(0) = \phi_{v, 0}$  in  $X'_0$ . Therefore, the limit functions  $(\phi, \phi_v)$  of the Faedo–Galerkin approximations fulfill the initial conditions for the system (14)–(17).

*Limit process*

We show that the limit functions also satisfy the variational form (28)–(29), as defined in Definition 1. Multiplying the Faedo–Galerkin system (32)–(33) by  $\eta \in C_c^\infty(0, T)$  and integrating from 0 to  $T$ , gives

$$\begin{aligned}
 \int_0^T \langle \partial_t \phi_\alpha^k, h_j \rangle_V \eta(t) dt &= \int_0^T ((\mathcal{C}(\phi_\alpha^k) v^k, \nabla h_j)_H - (m_\alpha^k \nabla \mu_\alpha^k, \nabla h_j)_H + (S_\alpha^k, h_j)_H) \eta(t) dt, \\
 \int_0^T (\mu_\alpha^k, h_j)_H \eta(t) dt &= \int_0^T ((\partial_{\phi_\alpha} \Psi^k - \chi_c \phi_\sigma^k - \chi_h \phi_{ECM}^k, h_j)_H + \varepsilon_\alpha^2 (\nabla \phi_\alpha^k, \nabla h_j)_H) \eta(t) dt, \\
 \int_0^T \langle \partial_t \phi_\beta^k, h_j \rangle_H \eta(t) dt &= \int_0^T (S_\beta^k, h_j)_H \eta(t) dt,
 \end{aligned} \tag{60}$$

and

$$\begin{aligned}
 \int_0^T \langle \partial_t \phi_\sigma^k, h_j \rangle_V dt &= \int_0^T \left( (\mathcal{C}(\phi_\sigma^k) v^k, \nabla h_j)_H - D_\sigma(m_\sigma^k \nabla \phi_\sigma^k, \nabla h_j)_H + (S_\sigma^k, h_j)_H \right. \\
 &\quad \left. + \langle \delta_\Gamma, J_{\sigma v, \Gamma}^k h_j \rangle_W - \chi_c(m_\sigma^k \nabla(\phi_P^k + \phi_H^k + \phi_N^k), \nabla h_j)_H \right) \eta(t) dt, \\
 \int_0^T \langle \partial_t \phi_\gamma^k, h_j \rangle_V \eta(t) dt &= \int_0^T \left( -D_\gamma(m_\gamma^k \nabla \phi_\gamma^k, \nabla h_j)_H + (S_\gamma^k, h_j)_H \right) \eta(t) dt, \\
 \int_0^T (v^k, h_j)_H \eta(t) dt &= \int_0^T \left( -K(\nabla p, h_j)_H + (S_p, \nabla h_j)_H \right) \eta(t) dt, \\
 \int_0^T K(\nabla p^k, \nabla h_j)_H \eta(t) dt &= \int_0^T \left( \langle \delta_\Gamma, J_{pv, \Gamma}^k h_j \rangle_W + (S_p, \nabla h_j)_H \right) \eta(t) dt,
 \end{aligned} \tag{61}$$

and

$$\begin{aligned}
 \int_0^T \langle \partial_t \phi_v^k, y_j \rangle_X \eta(t) dt &= \int_0^T \left( (\mathcal{C}(\phi_v^k) v_v^k, \nabla y_j)_Y - D_v(m_v^k \nabla \Lambda \phi_v^k, \nabla \Lambda y_j)_Y - \tilde{R}(J_{\sigma v}^k, y_j)_Y \right) \eta(t) dt, \\
 \int_0^T (v_v^k, y_j)_Y \eta(t) dt &= \int_0^T -\tilde{K}_v(\nabla \Lambda p_v^k, y_j)_Y \eta(t) dt, \\
 \int_0^T \tilde{K}_v(\nabla \Lambda p_v^k, \nabla \Lambda y_j)_Y \eta(t) dt &= \int_0^T -\tilde{R}(J_{pv}^k, y_j)_Y \eta(t) dt,
 \end{aligned} \tag{62}$$

for each  $j \in \{1, \dots, k\}$ ,  $\alpha \in \{P, H\}$ ,  $\beta \in \{N, ECM\}$ ,  $\gamma \in \{MDE, TAF\}$ . We take the limit  $k \rightarrow \infty$  in each equation. The linear terms can be treated directly in the limit process since they can be justified via the weak convergences (57), e.g., the functional

$$\mu_P^k \mapsto \int_0^T (\mu_P^k, h_j)_H \eta(t) dt \leq \|\mu_P^k\|_{L^2(0, T; H)} |h_j|_H |\eta|_{L^2(0, T)},$$

is linear and continuous on  $L^2(0, T; H)$  and hence, as  $k \rightarrow \infty$ ,

$$\int_0^T (\mu_P^k, h_j)_H \eta(t) dt \longrightarrow \int_0^T (\mu_P, h_j) \eta(t) dt.$$

Thus, it remains to examine the nonlinear terms. We do so in the steps (i)–(v) as follows.

(i) We have derived the convergence, see (59),

$$\phi_\alpha^k \longrightarrow \phi_\alpha \text{ in } L^2(0, T; H) \cong L^2((0, T) \times \Omega), \quad \alpha \in \mathcal{A},$$

for  $k \rightarrow \infty$  and, consequently, we have by the continuity and boundedness of  $m_\alpha$ ,

$$m_\alpha^k = m_\alpha(\phi^k(t, x)) \longrightarrow m_\alpha(\phi(t, x)) =: m_\alpha \text{ a.e. in } (0, T) \times \Omega \text{ for } k \rightarrow \infty.$$

Applying the Lebesgue dominated convergence theorem, gives for  $k \rightarrow \infty$

$$m_\alpha^k \nabla h_j \eta \longrightarrow m_\alpha \nabla h_j \eta \text{ in } L^2((0, T) \times \Omega; \mathbb{R}^d),$$

and, together with  $\nabla \mu_\alpha^k \rightharpoonup \nabla \mu_\alpha$  weakly in  $L^2((0, T) \times \Omega; \mathbb{R}^d)$  as  $k \rightarrow \infty$ , we have for  $k \rightarrow \infty$

$$m_\alpha(\phi^k) \eta \nabla h_j \cdot \nabla \mu_\alpha^k \longrightarrow m_\alpha(\phi) \eta \nabla h_j \cdot \nabla \mu_\alpha \text{ in } L^1((0, T) \times \Omega).$$

We use here the fact that the product of a strongly and a weakly converging sequence in  $L^2$  converges strongly in  $L^1$ .

(ii) By (59), we have  $\phi_\alpha^k \rightarrow \phi_\alpha$  in  $L^2((0, T) \times \Omega)$  and  $v^k \rightharpoonup v$  in  $L^2((0, T) \times \Omega; \mathbb{R}^d)$  as  $k \rightarrow \infty$ , hence for  $k \rightarrow \infty$

$$\mathcal{C}(\phi_\alpha^k)v^k \cdot \nabla h_j \eta \longrightarrow \mathcal{C}(\phi_\alpha)v \cdot \nabla h_j \eta \text{ in } L^1((0, T) \times \Omega).$$

(iii) By the continuity and the growth assumptions on  $\partial_{\phi_\alpha} \Psi$ , we have for  $k \rightarrow \infty$

$$\begin{aligned} \partial_{\phi_\alpha} \Psi(\phi_P^k(t, x), \phi_H^k(t, x), \phi_N^k(t, x)) &\longrightarrow \partial_{\phi_\alpha} \Psi(\phi_P(t, x), \phi_H(t, x), \phi_N(t, x)) \text{ a.e. in } (0, T) \times \Omega, \\ |\partial_{\phi_\alpha} \Psi(\phi_P^k, \phi_H^k, \phi_N^k)\eta h_j| &\leq C(1 + |\phi_P^k| + |\phi_H^k| + |\phi_N^k|)|\eta h_j|, \end{aligned}$$

and the Lebesgue dominated convergence theorem yields for  $k \rightarrow \infty$

$$\partial_{\phi_\alpha} \Psi(\phi_P^k, \phi_H^k, \phi_N^k)\eta h_j \longrightarrow \partial_{\phi_\alpha} \Psi(\phi_P, \phi_H, \phi_N)\eta h_j \text{ in } L^1((0, T) \times \Omega).$$

(iv) We have the strong convergence of  $\phi_P^k$  and  $\phi_H^k$  in  $L^2((0, T) \times \Omega)$  and the continuity and boundedness of  $\mathcal{C}$ . Together with the weak convergence of  $\nabla \phi_\sigma^k$  and  $\nabla \mu^k$  in  $L^2((0, T) \times \Omega; \mathbb{R}^d)$  it is enough to conclude the convergence of the term involving

$$S_p^k = -\mathcal{C}(\phi_P^k)(\nabla \mu_P^k + \chi_c \nabla \phi_\sigma^k) - \mathcal{C}(\phi_H^k)(\nabla \mu_H^k + \chi_c \nabla \phi_\sigma^k).$$

(v) We have  $\phi_v^k \rightarrow \phi_v$  in  $L^2((0, T) \times \Lambda)$  and  $\phi_\sigma^k \rightarrow \phi_\sigma$  in  $L^2((0, T) \times \Omega)$  as  $k \rightarrow \infty$  and therefore, also  $\Pi_\Gamma \phi_v^k \rightarrow \Pi_\Gamma \phi_v$  in  $L^2((0, T) \times \Gamma)$ . Since  $f_{\sigma, v}$  is a continuous and bounded function, we conclude

$$\int_0^T \int_\Gamma |f_{\sigma, v}(\phi_v^k, \Pi_\Gamma \phi_\sigma^k) \text{tr}_\Gamma h_j \eta(t)|^2 \, dS \, dt \lesssim \|f_{\sigma, v}(\Pi_\Gamma \phi_v^k, \phi_\sigma^k)\|_{L^\infty((0, T) \times \Gamma)}^2 \|h_j|_V\|_{L^2(0, T)}^2,$$

and the Lebesgue dominated convergence theorem gives for  $k \rightarrow \infty$

$$f_{\sigma, v}(\phi_v^k, \Pi_\Gamma \phi_\sigma^k) \text{tr}_\Gamma h_j \eta(t) \longrightarrow f_{\sigma, v}(\phi_v, \Pi_\Gamma \phi_\sigma) \text{tr}_\Gamma h_j \eta(t) \text{ in } L^2((0, T) \times \Gamma).$$

Together with the weak convergence of  $\Pi_\Gamma p_v^k$  and  $p^k$  we have for  $k \rightarrow \infty$

$$\begin{aligned} \int_0^T \langle \delta_\Gamma, J_{\sigma v, \Gamma}^k h_j \rangle_W \eta(t) \, dt &= \int_0^T \int_\Gamma \left( f_{\sigma, v}(\phi_\sigma^k, \Pi_\Gamma \phi_v^k) L_p(\Pi_\Gamma p_v^k - p^k) + L_\sigma(\Pi_\Gamma \phi_v^k - \phi_\sigma^k) \right) \text{tr}_\Gamma h_j \eta(t) \, dS \, dt \\ &\rightarrow \int_0^T \langle \delta_\Gamma, J_{\sigma v, \Gamma} h_j \rangle_W \eta(t) \, dt. \end{aligned}$$

Using the densities of  $\cup_{k \in \mathbb{N}} H_k$  in  $V$ ,  $\cup_{k \in \mathbb{N}} H_k^0$  in  $V_0$  and  $\cup_{k \in \mathbb{N}} Y_k$  in  $X$ , and the fundamental lemma of the calculus of variations, we obtain a solution tuple  $(\phi, \mu_P, \mu_H, v, p, \phi_v, v_v, p_v)$  to our model (14) and (16) in the weak sense as defined in Definition 1.

*Energy inequality*

It remains to prove that found solution tuple satisfies the energy inequality (30). First, we note that norms are weakly/weakly-\* lower semicontinuous, e.g., we have  $\mu_P^k \rightharpoonup \mu_P$  in  $L^2(0, T; V)$  and therefore, we infer

$$\|\mu_P\|_{L^2(0, T; V)} \leq \liminf_{k \rightarrow \infty} \|\mu_P^k\|_{L^2(0, T; V)}.$$

We apply the Fatou lemma on the continuous and non-negative function  $\Psi$  to obtain

$$\int_\Omega \Psi(\phi_P, \phi_H, \phi_N) \, dx \leq \liminf_{k \rightarrow \infty} \int_\Omega \Psi(\phi_P^k, \phi_H^k, \phi_N^k) \, dx.$$

Consequently, passing the limit  $k \rightarrow \infty$  in the discrete energy inequality (55) leads to (30).  $\square$

## 6. Numerical simulations

We present in this section two applications of the theory presented earlier. The first is the simple scenario in which two straight and idealized blood vessels are considered, one representing an artery and the other a vein. This means that the tissue block containing the two vessels is supplied nutrients by a single artery and drained of nutrients by a single vein. In between the two vessels, a tumor core is present which accepts nutrients injected through an inlet of the artery. The second scenario deals with a small blood vessel network described by data in [57] and on the following web page: <https://physiology.arizona.edu/sites/default/files/brain99.txt>. At four inlets of this network, nutrients are injected and transported through the network. As in the first scenario, the impact of the nutrients on a small tumor core surrounded by the network is investigated. We note that in all cases we consider a stationary vessel structure; for evolving and bifurcating vessels we refer to the further work [58].

To solve the one-dimensional partial differential equations (16) numerically, the vascular graph model (VGM) is employed [59,60]. This method corresponds in principle to a vertex centered finite volume method with a two-point flux approximation. For the three-dimensional partial differential equations presented in Section 2.3 a mixed finite volume-finite element discretization method is employed. The equations governing the pressure and nutrients in tissue, which are directly coupled with the one-dimensional system, are solved by a standard cell-centered finite volume scheme. Since the permeability of the cancerous and healthy tissue is given by a scalar field, a two-point flux approximation of the fluxes is used. For the remaining species, we consider a continuous and piecewise linear finite element approximation over a uniform cubic mesh. The coupled nonlinear partial differential equations are discretized in time using the semi-implicit Euler method. To solve the nonlinear system of equations arising in each time step, a fixed point iteration method is applied. We consider following double-well potential in free energy functional in (3)

$$\Psi(\phi_P, \phi_H, \phi_N) = C_{\Psi_T} \phi_T^2 (1 - \phi_T)^2. \quad (63)$$

### 6.1. Tumor between two straight vessels

We consider a tissue domain  $\Omega = (0, 2)^3$  containing two blood vessels aligned along the  $z$ -axis. The center lines of the vessels are located diagonally opposite to each other. The center line of the Vessel 1 and 2 pass through  $(0.2, 0.2, 1)$  and  $(1.8, 1.8, 1)$ , respectively. We choose a radius of  $R = 0.08$  and  $R = 0.1$  for Vessel 1 and 2. At the inlets of Vessel 1, located at  $(0.2, 0.2, 0)$  and  $(0.2, 0.2, 2)$ , pressure values of 10 000 and 5000 are prescribed. The inlets of Vessel 2 are located at  $(1.8, 1.8, 0)$  and  $(1.8, 1.8, 2)$ . Here, we consider the pressure values 1000 and 2000, respectively. Thus, Vessel 2 will act as a vein taking up nutrients and blood plasma from the tissue domain. On the other hand Vessel 1 has the function of an artery transporting nutrients into the tissue block  $\Omega$ . We note that we choose the boundary values such that the velocities are sufficiently large in order to ensure that the transport processes are visible in the simulations. Based on the pressure boundary conditions, we choose the boundary conditions for the nutrients as follows:

- $\phi_v = \phi_{v,inlet} = 1$  at  $(0.2, 0.2, 0)$ .
- $\phi_v = 0$  at  $(1.8, 1.8, 2)$ .
- At all the remaining boundaries, we consider free flow boundary conditions.

The initial tumor core is given by a ball of radius 0.3 and centered at  $(1, 1, 1)$ . Within the tumor core, the total tumor volume fraction,  $\phi_T$ , decays smoothly from 1 in the center to 0 on the boundary of the ball. Thereby, the necrotic and hypoxic volume fractions,  $\phi_N$  and  $\phi_H$ , are set to zero. In the rest of the domain all the volume fractions for the tumor species are set to 0 at  $t = 0$ . The nutrient volume fraction, in the tissue domain  $\Omega$ , is initially fixed to a constant initial value of 0.6, which is below the threshold values for

**Table 1**

List of parameters and their values for the numerical experiments described in Sections 6.1 and 6.2. Parameters not mentioned below are set to zero.

Parameter	Value	Parameter	Value	Parameter	Value
$\lambda_P$	5	$\lambda_{P_h}$	0.5	$\lambda_A$	0.005
$\lambda_{A_h}$	0.005	$\lambda_{PH}$	1	$\lambda_{HP}$	1
$\lambda_{HN}$	1	$\sigma_{PH}$	0.55	$\sigma_{HP}$	0.65
$\sigma_{HN}$	0.44	$\varepsilon_P$	0.005	$\varepsilon_H$	0.005
$M_P$	50	$M_H$	25	$\lambda_{TAF_P}$	10
$D_{TAF}$	0.5	$m_{TAF}$	1	$L_p$	$10^{-7}$
$D_\sigma$	1	$m_\sigma$	1	$K$	$10^{-9}$
$D_{MDE}$	0.5	$m_{MDE}$	1	$D_v$	0.1
$\mu_{bl}$	1	$L_\sigma$	10	$\lambda_{ECM_D}$	5
$\lambda_{ECM_P}$	0.01	$\lambda_{MDE_D}$	1	$\lambda_{MDE_D}$	1
$\phi_{ECM_P}$	0.5	$C_{\Psi_T}$	0.045	–	–

proliferic-to-hypoxic transition and above the threshold value for hypoxic-to-proliferic transition. We also set  $\phi_{ECM} = 1$  at  $t = 0$ . According to (15) homogeneous Neumann boundary conditions are prescribed on  $\partial\Omega$ .

As a simulation time period, the interval  $(0, T)$  with  $T = 5$  is considered and the size of the time step is given by  $\Delta t = 0.025$ . The spatial domain  $\Omega$  is discretized by cubic elements with an edge length of  $h = 0.025$ . We choose the parameters as listed in Table 1.

Plots of the tumor species  $\phi_T, \phi_P, \phi_H$  at the  $z = 1$  plane in the domain  $\Omega$  at time points  $t \in \{3, 4, 5\}$  are shown in Fig. 3. In Fig. 4, the tumor phases are shown along a one-dimensional line. It can be observed that the tumor separates into its three phases and moves towards the nutrient-rich regions of the domain. Moreover, the contour lines of the total tumor and its phases is presented at different times in Fig. 5. We see that tumor is growing towards the artery. As expected, the proliferation is higher near the artery. In Fig. 6, plots of TAF, MDE, ECM at the time point  $t = 5$  in the  $z = 1$  plane of  $\Omega$  are shown (see Fig. 7).

Fig. 8 contains simulation results for the different values of parameters at  $t = T = 5$ . Among the numerous model parameters, we focused on the chemotactic constant  $\chi_c$ , mobility  $M_P$ , proliferation rate  $\lambda_P$ , nutrient diffusion coefficient  $D_\sigma$ , and permeability constant  $L_\sigma$ . We vary one of these parameters while keeping other parameters fixed to their respective values listed in Table 1.

It can be observed that all selected parameters strongly affect the tumor growth. Except for the parameter  $D_\sigma$ , the larger the remaining parameters, the faster the tumor cells move away from the vein and towards the nutrient rich artery. This means that for the chosen parameter values, the fluxes  $J_\alpha$ ,  $\alpha \in \mathcal{CH}$  given by (2), dominate the corresponding convective terms in (14) so that the tumor cells can move against the velocity field. It can be stated that for these parameter choices, the model simulates the migration of tumor cells towards the nutrient sources in the vicinity.

Fig. 9 shows the pressure distribution in the vessels as well as the tissue pressure and velocity field within a plane that is perpendicular to the  $z$ -axis and located at  $z = 1$ . The tissue pressure ranges between 1500 and 7500, which means that it is bounded by the extreme pressures in the vascular system. Furthermore, a gradient in the tissue pressure can be detected pointing from the artery to the vein. As a result, the velocity field is orientated from the artery to the vein.

### 6.2. Tumor surrounded by a network

In the second subsection, we consider a small capillary network given by the data in [57]. To keep the same computational domain as in the previous subsection, the network is scaled such that it fits into  $\Omega = (0, 2)^3$ . After scaling, the resulting network has maximum, minimum, and mean vessel radius 0.0613, 0.0307, 0.0418 respectively. At the inlets that are marked by an arrow, see Fig. 10, we prescribe the pressure  $p_{in} = 25\,000$ , while for all the other inlets, we use  $p_{out} = 10\,000$  as a boundary value. Again, we choose the boundary values synthetically in order to ensure that the transport processes are visible in the simulations. Further,

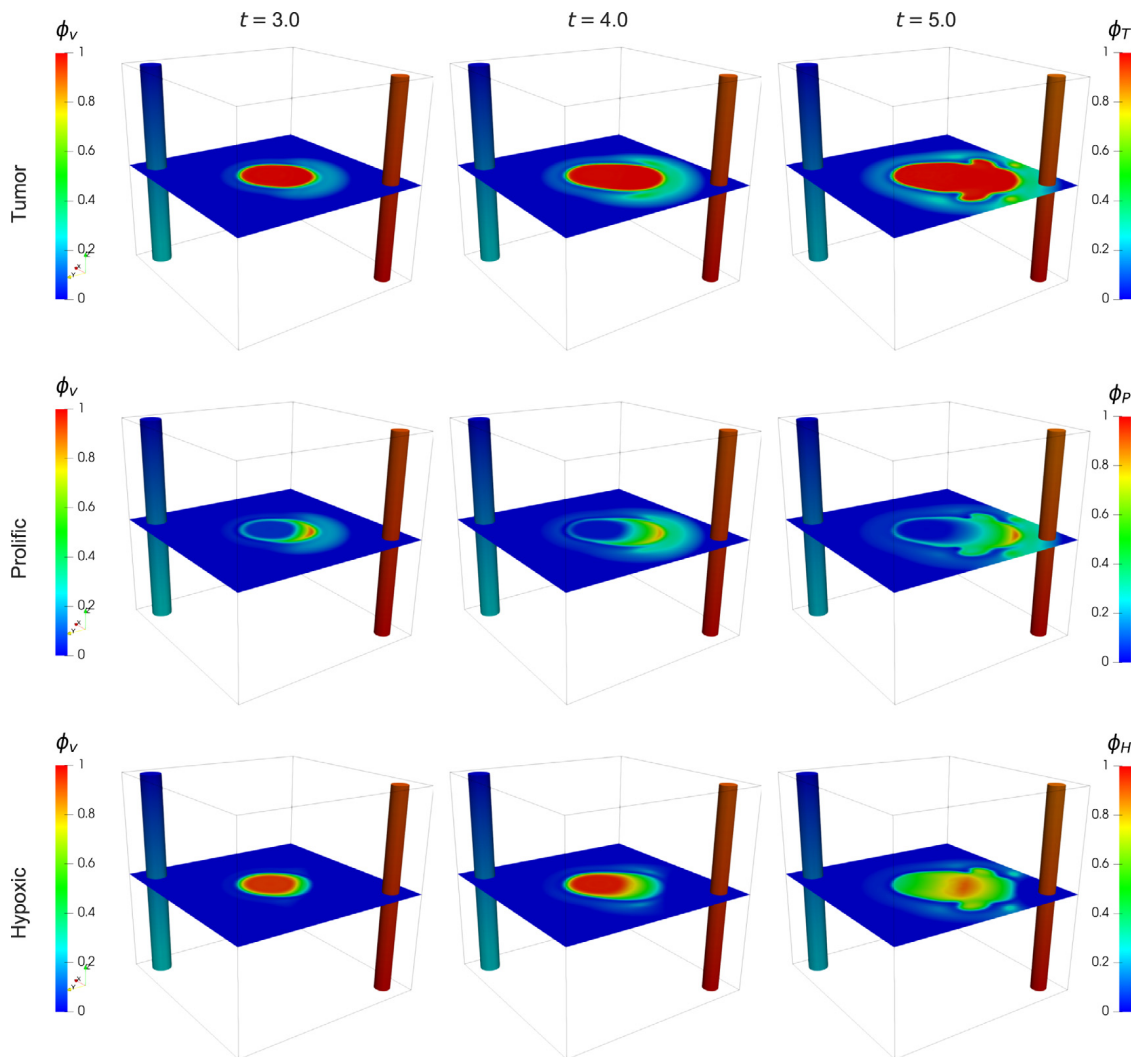


**Fig. 3.** Evolution of the total tumor  $\phi_T$  (top), prolific  $\phi_P$  (middle), and hypoxic  $\phi_H$  (bottom) volume fractions at the times  $t \in \{3, 4, 5\}$  (left, middle, right) in the  $z = 1$  plane of the domain  $\Omega$ . On the two vessels the nutrients are described by the 1D constituent  $\phi_v$ .

the boundary condition for  $\phi_v$  is given by  $\phi_v = \phi_{v,inlet} = 1$  if it holds  $p_v = p_{in}$ , and free outflow boundary if  $p_v = p_{out}$ .

Contrary to the previous subsection, the spherical tumor core has a radius of 0.25 and the center (1.3, 0.9, 0.7). The same model parameters are employed. The domain  $\Omega$  is discretized using cubic elements of mesh size 0.025 and final time and time step of the simulation are  $T = 5$  and  $\Delta t = 0.025$ .

In Fig. 11, the tumor cell volume fraction  $\phi_T$ , prolific cell volume fraction  $\phi_P$ , and hypoxic cell volume fraction  $\phi_H$  are shown at  $z = 0.8$  plane and at time points  $t \in \{3, 4, 5\}$ . Finally in Fig. 12, the contour plots for  $\phi_T = 0.8$  and  $\phi_T = 0.95$  are presented. Further, the hypoxic phase is shown inside the tumor. In Fig. 13, plots of TAF, MDE, ECM at  $t = 5$  in  $z = 0.8$  plane are shown.

The behavior of the tumor cells is similar to the two-vessel scenario. It seems that for the given parameter set the tumor cells are attracted by the nutrient rich blood vessels of the network. As can be observed in Fig. 11 (last row), the chemical potential of the tumor exhibits high gradients at the interface between tumor and healthy tissue. Therefore, the corresponding flux of the chemical potential given by (2) is potentially high at this location. As a result the tumor cells are pulled towards the interface between cancerous and

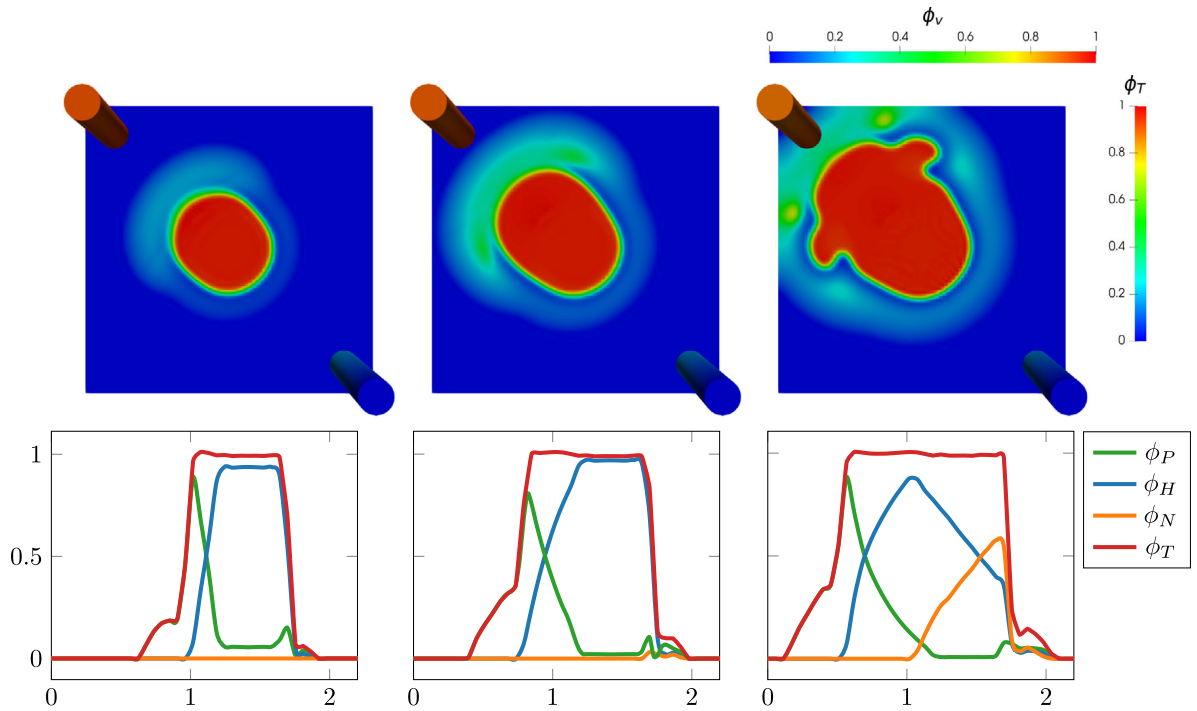


**Fig. 4.** Left: Evolution of the tumor volume fraction ( $\phi_T$ ) in the  $z = 1$  plane of the domain  $\Omega$ . Right: Plots of tumor ( $\phi_T$ ), prolific ( $\phi_P$ ), hypoxic ( $\phi_H$ ) and necrotic ( $\phi_N$ ) volume fractions along the line passing through the points  $(0, 0, 1)$  and  $(2, 2, 1)$  in the domain  $\Omega$ . From top row to bottom row, the plots correspond to time  $t \in \{3, 4, 5\}$ .

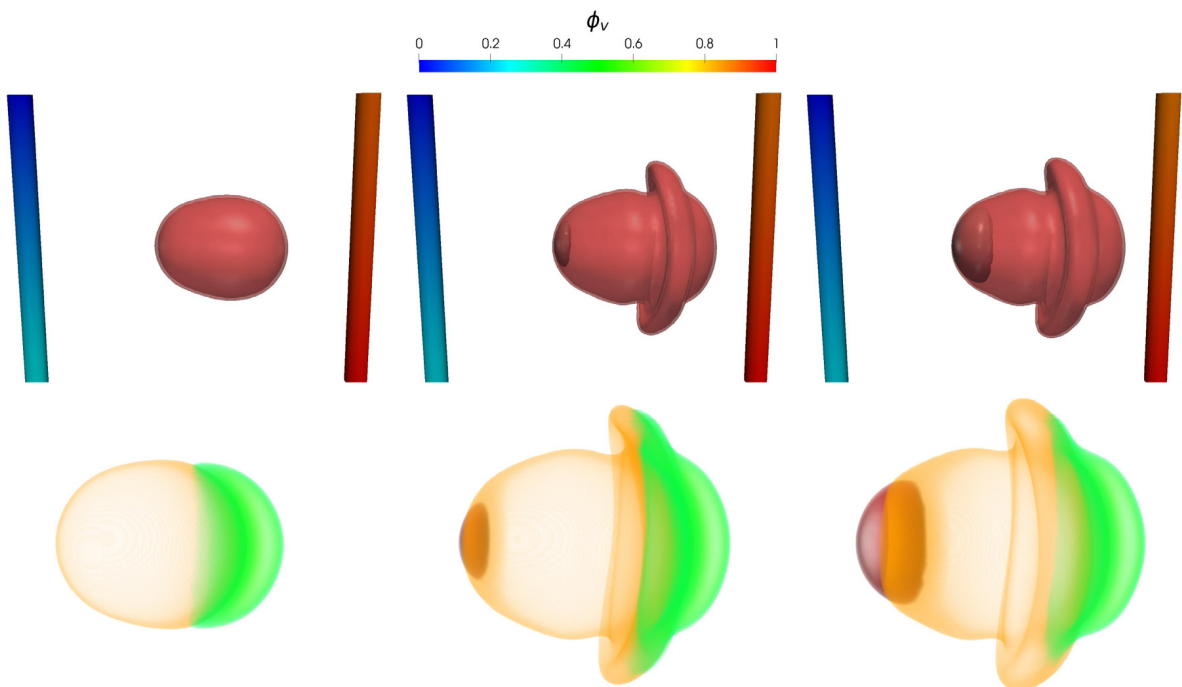


**Fig. 5.** Evolution of contour plots of the tumor volume fraction  $\phi_T$  with vessels (top) at 0.8 (light red) and 0.95 (red) at the time  $t \in \{4.25, 4.75, 5\}$  (left to right); the necrotic core is plotted at the contour line  $\phi_N = 0.42$  (black). Contour plots of the tumor phases without vessels (bottom) at  $\phi_P = 0.5$  (green),  $\phi_H = 0.45$  (orange),  $\phi_N = 0.4$  (dark red). (For interpretation of the references to color in this figure legend, the reader is referred to the web version of this article.)



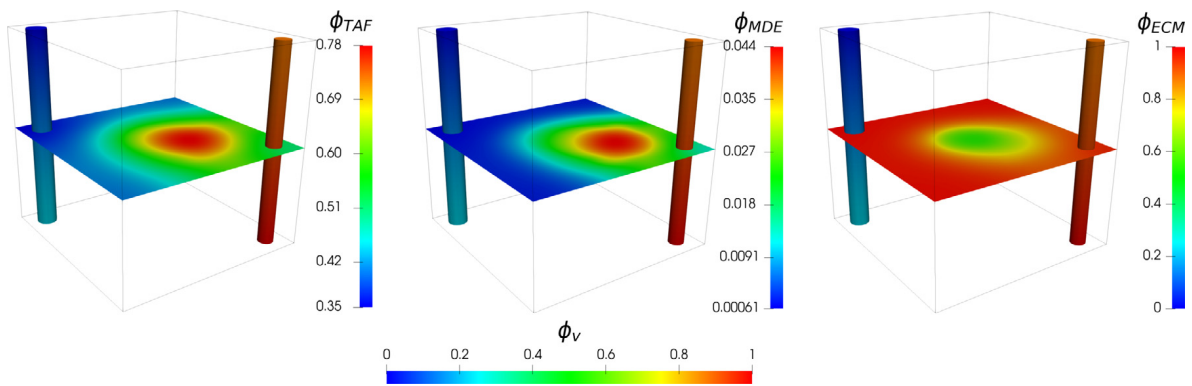


**Fig. 6.** Plots of  $\phi_{TAF}$  (left),  $\phi_{MDE}$  (middle), and  $\phi_{ECM}$  (right) at time  $t = 5$  in the  $z = 1$  plane of the domain  $\Omega$ . The colors (horizontal color bar) on the vessels show the transport of the 1D nutrient ( $\phi_v$ ). The production of TAF and MDE is maximal where the hypoxic tumor phase is located. The decay of ECM happens in the regions where MDE is produced. (For interpretation of the references to color in this figure legend, the reader is referred to the web version of this article.)

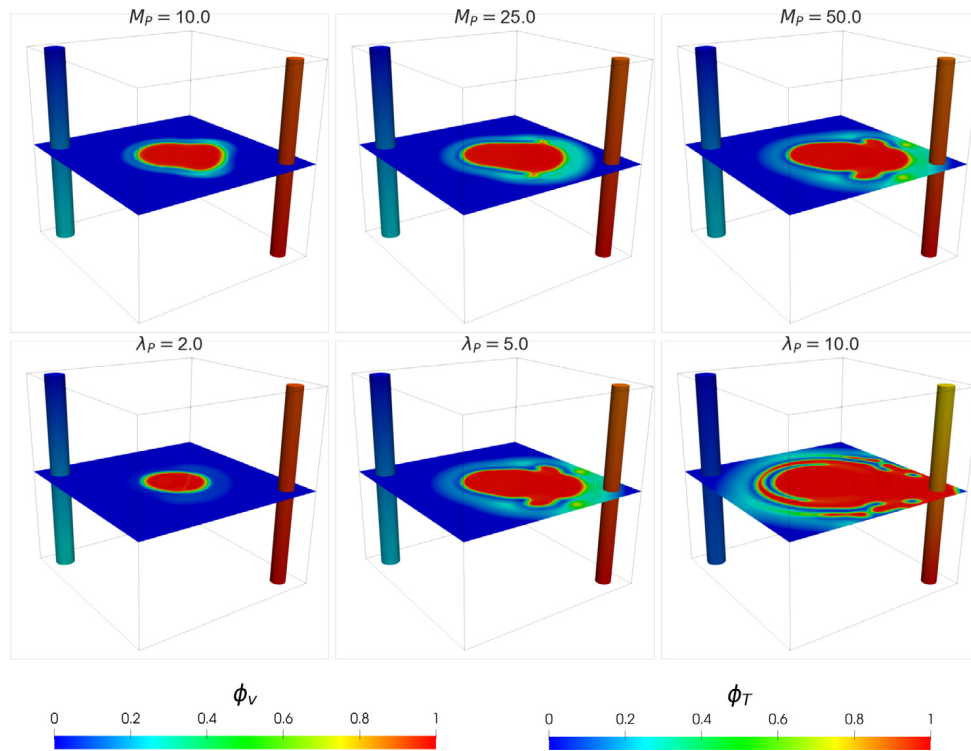


**Fig. 7.** Effect of the mobility  $M_P$  (top) for  $M_P \in \{10, 25, 50\}$  (left to right) and proliferation rate  $\lambda_P$  (bottom) for  $\lambda_P \in \{2, 5, 10\}$  (left to right) on the growth of the tumor volume. The color bar for 1D nutrients (left) and total tumor volume fraction (right) in included at the bottom. (For interpretation of the references to color in this figure legend, the reader is referred to the web version of this article.)

healthy tissue. Apparently, the flux is particularly high near the nutrient rich vessels such that the tumor cells move preferably towards the nutrient rich vessels.

Fig. 14 shows the tissue pressure and the corresponding velocity fields in  $z = 0.8$  plane. Just as in the two-vessel scenario, the pressure distribution induces a velocity field that goes from the high pressure region to the low pressure region.

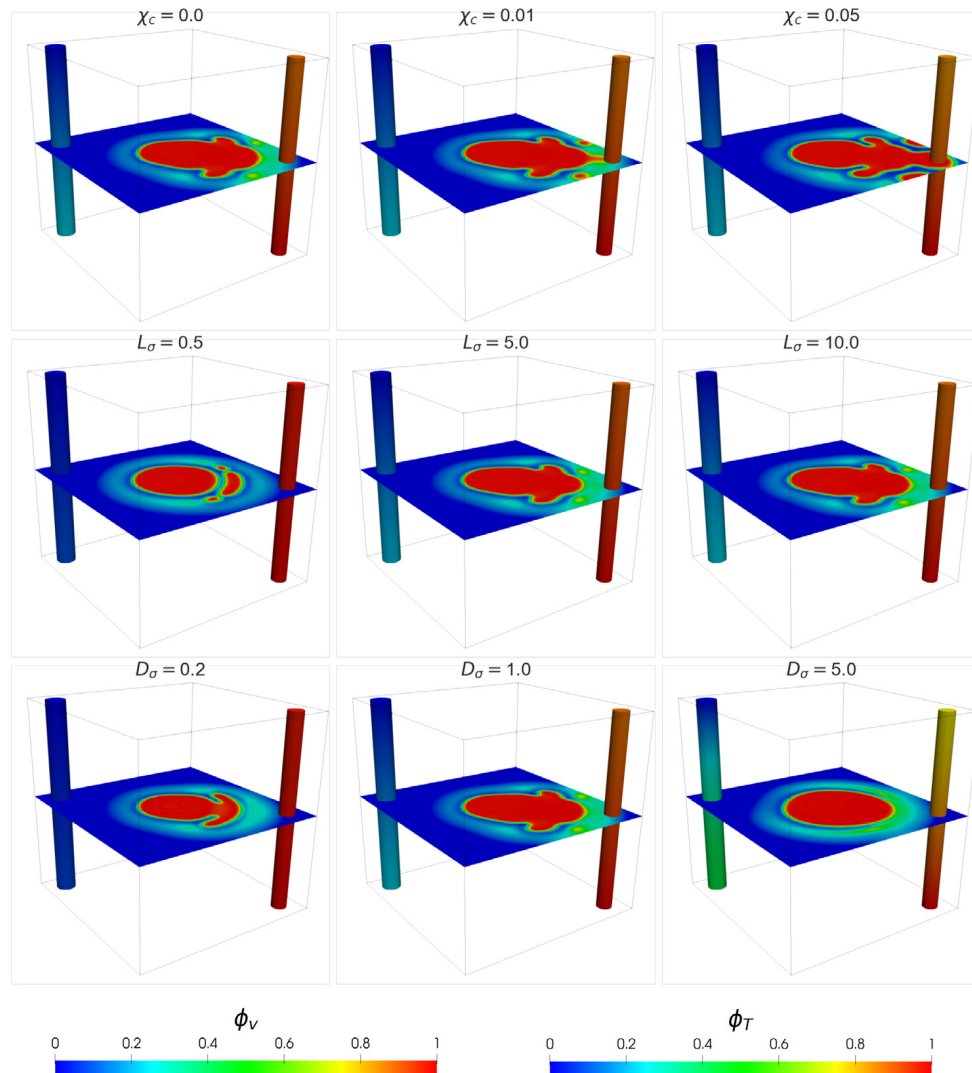


**Fig. 8.** Effect of the chemotactic constant  $\chi_c$  (top) for  $\chi_c \in \{0, 0.01, 0.05\}$  (left to right), permeability of the vessel wall  $L_\sigma$  (middle) for  $L_\sigma \in \{0.5, 5, 10\}$  (left to right), and diffusivity constant  $D_\sigma$  (bottom) for  $D_\sigma \in \{0.2, 1, 5\}$  (left to right) on the growth of the tumor volume. The color bar for 1D nutrients (left) and total tumor volume fraction (right) is included at the bottom. (For interpretation of the references to color in this figure legend, the reader is referred to the web version of this article.)

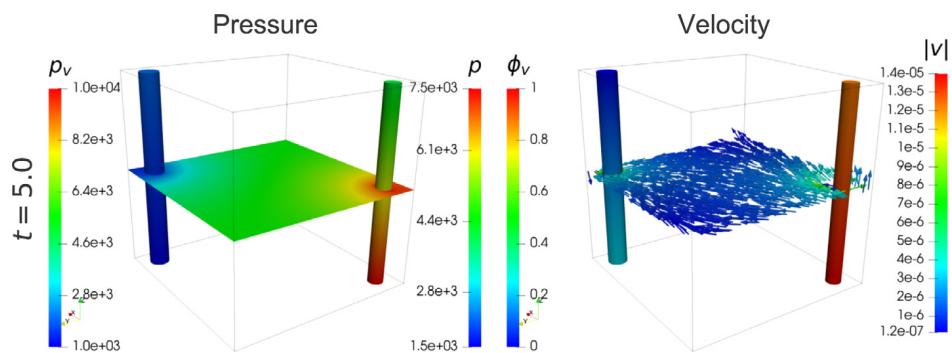


**Fig. 9.** Pressure (left) and velocity field (right) in a plane perpendicular to the  $z$ -axis (at  $z = 1$ ) of the domain  $\Omega$ . The artery is located in the right corner with a pressure decay from 10000 to 5000. The vein is located in the left corner with a pressure decay from 2000 to 1000. The velocity field induced by the pressure distribution is directed from the artery towards the vein.

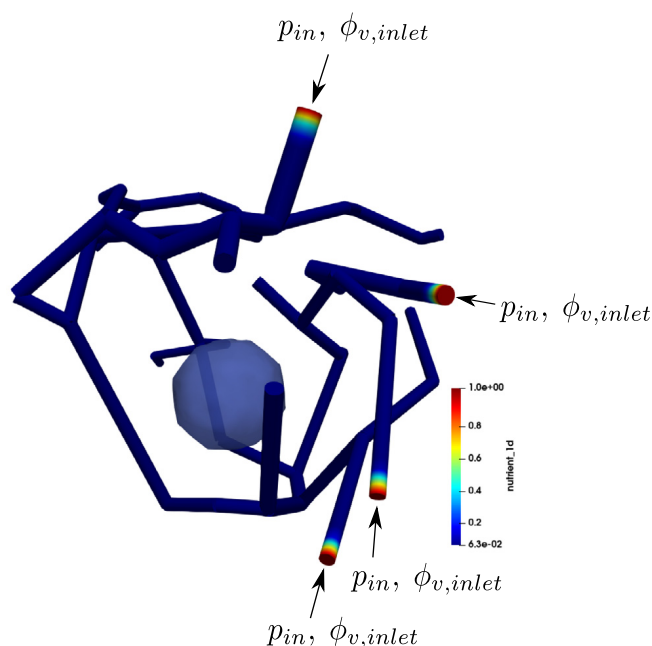


**Fig. 10.** Outline of the scaled blood vessel network with an initial tumor core. The tumor core is represented by a contour surface with respect to  $\phi_T$  (at  $\phi_T = 0.1$ ). At the four inlets, indicated by an arrow, nutrients are injected i.e. at these boundaries, we set  $\phi_v = \phi_{v,inlet} = 1$  and  $p_v = p_{in}$ .

## 7. Summary and outlook

In this work, we have presented a 3D–1D coupled multispecies model for tumor growth including the influence of nutrient transport in a vascular system that is located in the vicinity of a solid tumor. Flow and transport of nutrients within the vascular system are governed by one-dimensional partial differential equations. The corresponding flow and transport processes in the healthy and tumor tissue are based on Darcy’s law as well as a standard convection–diffusion equation. Coupling of the three-dimensional equations with their one-dimensional counterparts is done via filtration laws and source terms. In the source terms of the three-dimensional partial differential equations, Dirac measures occur. They are concentrated on the vessel surfaces of the vascular system, since there the exchange processes between the tissue and the vascular system take place. The remaining three-dimensional equations governing the distribution of the tumor cells are of Cahn–Hilliard type. The evolution of matrix degrading enzymes and the tumor angiogenesis factor are modeled by convection–diffusion equations. Lastly, the extracellular matrix density is described by an abstract ordinary differential equation.

The centerpiece of our work is a mathematical analysis of this model with a focus on the existence of solutions. We have shown the existence of weak solutions. Our proof is based on the Faedo–Galerkin method. Thereby, the system of partial differential equations is semi-discretized in space and reduced to a system of ordinary differential equations. Using the Cauchy–Peano theorem we show that the system of ordinary differential equations exhibits a solution. In a next step, the existence of weak solutions with respect to the partial differential equations is derived by means of the Banach–Alaoglu theorem. Finally, we present some simulation results for two different settings, illustrating the performance of our model. Our simulation results indicate that the tumor cells sense the vessels with an increased nutrient concentration and move towards them. Furthermore, the impact of several model parameters on the solution variables is discussed.

Among extensions and applications of the models described here are the simulation and optimal control of chemotherapy drug and radiation as well as modeling of the onset of metastasis. Simulation of these protocols and phenomena represent challenging goals for future work.

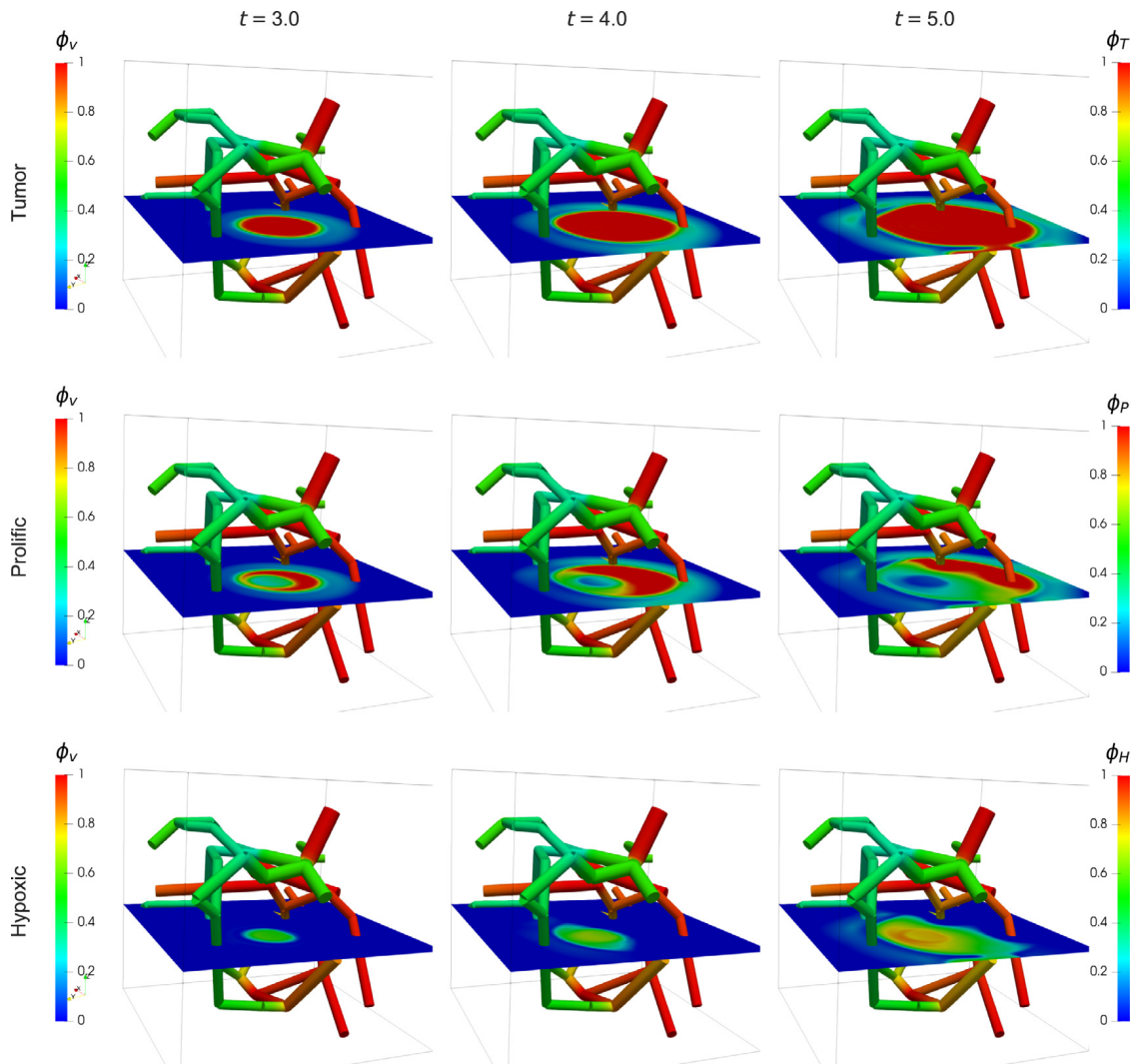


**Fig. 11.** Distribution of the tumor cell volume fraction  $\phi_T$  (top), proliferative cell volume fraction  $\phi_P$  (middle), and hypoxic cell volume fraction  $\phi_H$  (bottom) for  $t \in \{3, 4, 5\}$ . The tumor cells migrate towards to nutrient rich vessels.

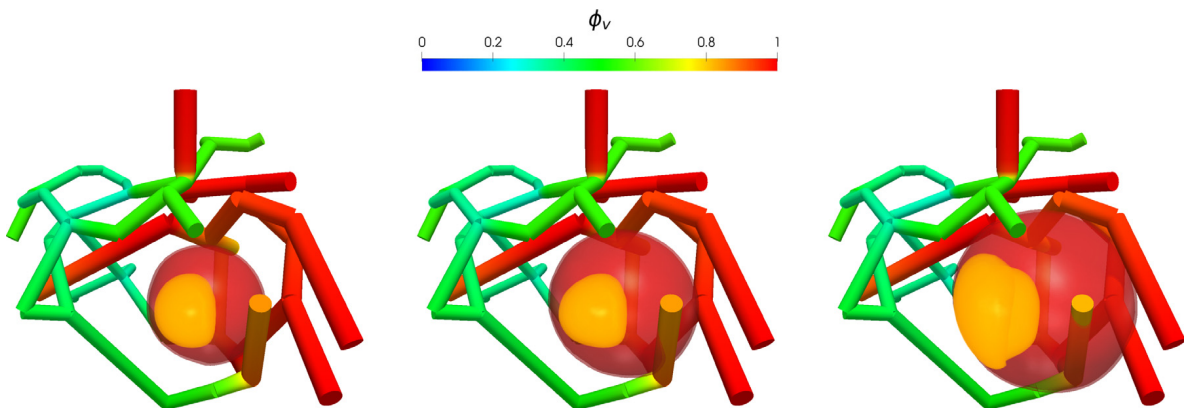


**Fig. 12.** Evolution of contour plots of the tumor volume fraction  $\phi_T$  at the values 0.8 (light red) and 0.95 (red), and of the hypoxic phase  $\phi_H$  at 0.35 at times  $t \in \{3, 3.5, 4\}$  (left to right). The tumor growth is directed towards the nutrient rich vessels. (For interpretation of the references to color in this figure legend, the reader is referred to the web version of this article.)

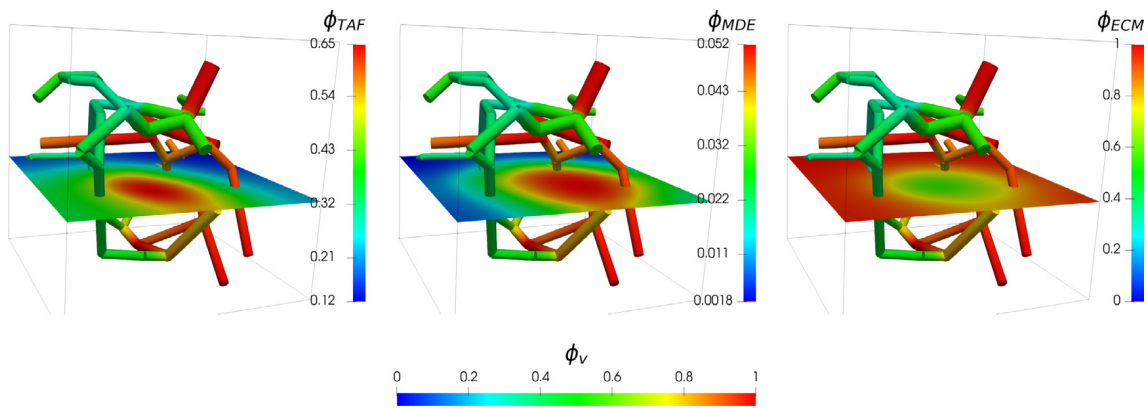


**Fig. 13.** Plots of  $\phi_{TAF}$  (left),  $\phi_{MDE}$  (middle), and  $\phi_{ECM}$  (right) at time  $t = 5$  in the  $z = 0.8$  plane of the domain  $\Omega$ . The colors (horizontal color bar) on the vessels show the transport of the 1D nutrient ( $\phi_v$ ). As in the case of two-vessels setting, the production of TAF and MDE is maximal where the hypoxic region is located. (For interpretation of the references to color in this figure legend, the reader is referred to the web version of this article.)

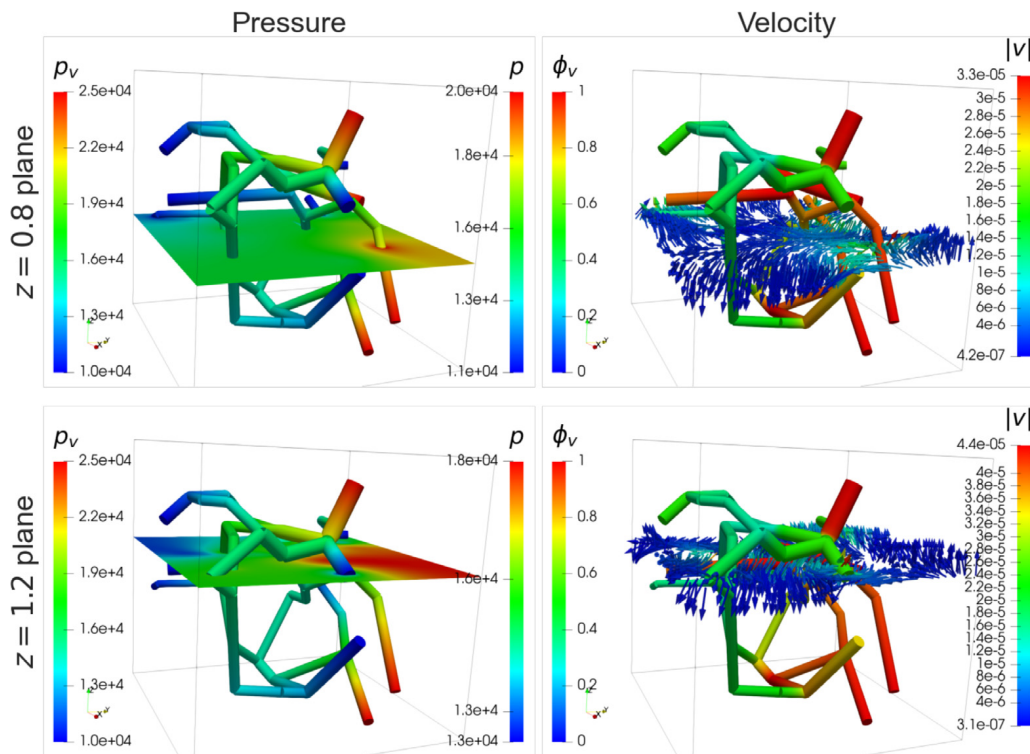


**Fig. 14.** Plots of pressure (left) and velocity field (right) in the  $z = 0.8$  (top) and  $z = 1.2$  (bottom) planes in the domain  $\Omega$ . The plots correspond to the simulation time  $t = 5$ . As in the two-vessel case, the velocity field is pointing from the high pressure region to the low pressure region.

### Acknowledgments

The authors thank the reviewer for the helpful comments and the careful review, which helped to further improve and clarify the article. We gratefully acknowledge the support of the German Science Foundation (DFG) for funding part of this work through grant WO 671/11-1. The work of PKJ and JTO was supported by the U.S. Department of Energy, Office of Science, Office of Advanced Scientific

Computing Research, Mathematical Multifaceted Integrated Capability Centers (MMICCS), under Award Number DE-SC0019303.

## References

- [1] H. Byrne, L. Preziosi, Modelling solid tumour growth using the theory of mixtures, *Math. Med. Biol. J. IMA* 20 (4) (2003) 341–366.
- [2] V. Cristini, X. Li, J.S. Lowengrub, S.M. Wise, Nonlinear simulations of solid tumor growth using a mixture model: invasion and branching, *J. Math. Biol.* 58 (4–5) (2009).
- [3] J.T. Oden, E. Lima, R.C. Almeida, Y. Feng, M.N. Rylander, D. Fuentes, D. Faghihi, M.M. Rahman, M. DeWitt, M. Gadde, et al., Toward predictive multiscale modeling of vascular tumor growth, *Arch. Comput. Methods Eng.* 23 (4) (2016) 735–779.
- [4] J.T. Oden, A. Hawkins, S. Prudhomme, General diffuse-interface theories and an approach to predictive tumor growth modeling, *Math. Models Methods Appl. Sci.* 20 (03) (2010) 477–517.
- [5] E. Lima, J.T. Oden, R. Almeida, A hybrid ten-species phase-field model of tumor growth, *Math. Models Methods Appl. Sci.* 24 (13) (2014) 2569–2599.
- [6] D. Hanahan, R.A. Weinberg, Hallmarks of cancer: The next generation, *Cell* 144 (5) (2011) 646–674.
- [7] B. Ginzburg, A. Katchalsky, The frictional coefficients of the flows of non-electrolytes through artificial membranes, *J. General Physiol.* 47 (2) (1963) 403–418.
- [8] H. Garcke, K.F. Lam, Global weak solutions and asymptotic limits of a Cahn–Hilliard–Darcy system modelling tumour growth, *AIMS Math.* 1 (2016) 318–360.
- [9] H. Garcke, K.F. Lam, Well-posedness of a Cahn–Hilliard system modelling tumour growth with chemotaxis and active transport, *European J. Appl. Math.* 28 (2) (2017) 284–316.
- [10] V. Cristini, J. Lowengrub, *Multiscale Modeling of Cancer: An Integrated Experimental and Mathematical Modeling Approach*, Cambridge University Press, 2010.
- [11] E. Lima, J.T. Oden, B. Wohlmuth, A. Shahmoradi, D. Hormuth II, T. Yankeelov, L. Scarabosio, T. Horger, Selection and validation of predictive models of radiation effects on tumor growth based on noninvasive imaging data, *Comput. Methods Appl. Mech. Engrg.* 327 (2017) 277–305.
- [12] M. Fritz, E. Lima, V. Nikolic, J.T. Oden, B. Wohlmuth, Local and nonlocal phase-field models of tumor growth and invasion due to ECM degradation, *Math. Models Methods Appl. Sci.* 29 (13) (2019) 2433–2468.
- [13] M. Fritz, E. Lima, J.T. Oden, B. Wohlmuth, On the unsteady Darcy–Forchheimer–Brinkman equation in local and nonlocal tumor growth models, *Math. Models Methods Appl. Sci.* 29 (09) (2019) 1691–1731.
- [14] A. Hawkins-Daarud, K.G. van der Zee, J.T. Oden, Numerical simulation of a thermodynamically consistent four-species tumor growth model, *Int. J. Numer. Methods Biomed. Eng.* 28 (1) (2012) 3–24.
- [15] H. Garcke, K.F. Lam, R. Nürnberg, E. Sitka, A multiphase Cahn–Hilliard–Darcy model for tumour growth with necrosis, *Math. Models Methods Appl. Sci.* 28 (03) (2018) 525–577.
- [16] S.M. Wise, J.S. Lowengrub, H.B. Frieboes, V. Cristini, Three-dimensional multispecies nonlinear tumor growth – I: Model and numerical method, *J. Theoret. Biol.* 253 (3) (2008) 524–543.
- [17] H.B. Frieboes, F. Jin, Y.-L. Chuang, S.M. Wise, J.S. Lowengrub, V. Cristini, Three-dimensional multispecies nonlinear tumor growth – II: Tumor invasion and angiogenesis, *J. Theoret. Biol.* 264 (4) (2010) 1254–1278.
- [18] J. Xu, G. Vilanova, H. Gomez, A mathematical model coupling tumor growth and angiogenesis, *PLoS One* 11 (2) (2016).
- [19] J. Xu, G. Vilanova, H. Gomez, Full-scale, three-dimensional simulation of early-stage tumor growth: The onset of malignancy, *Comput. Methods Appl. Mech. Engrg.* 314 (2017) 126–146.
- [20] J. Xu, G. Vilanova, H. Gomez, Phase-field model of vascular tumor growth: Three-dimensional geometry of the vascular network and integration with imaging data, *Comput. Methods Appl. Mech. Engrg.* 359 (2020) 112648.
- [21] R. Santagiuliana, M. Ferrari, B. Schrefler, Simulation of angiogenesis in a multiphase tumor growth model, *Comput. Methods Appl. Mech. Engrg.* 304 (2016) 197–216.
- [22] R. Santagiuliana, M. Milosevic, B. Milicevic, G. Sciumè, V. Simic, A. Ziemys, M. Kojic, B.A. Schrefler, Coupling tumor growth and bio distribution models, *Biomed. Microdev.* 21 (2) (2019) 33.
- [23] J. Kremheller, A.-T. Vuong, B.A. Schrefler, W.A. Wall, An approach for vascular tumor growth based on a hybrid embedded/homogenized treatment of the vasculature within a multiphase porous medium model, *Int. J. Numer. Methods Biomed. Eng.* 35 (2019) e3253.
- [24] T. Köppl, E. Vidotto, B. Wohlmuth, P. Zunino, Mathematical modeling, analysis and numerical approximation of second-order elliptic problems with inclusions, *Math. Models Methods Appl. Sci.* 28 (05) (2018) 953–978.
- [25] A.R. Anderson, M.A.J. Chaplain, Continuous and discrete mathematical models of tumor-induced angiogenesis, *Bull. Math. Biol.* 60 (5) (1998) 857–899.
- [26] E. Lima, R.C. Almeida, J.T. Oden, Analysis and numerical solution of stochastic phase-field models of tumor growth, *Numer. Methods Partial Differential Equations* 31 (2) (2015) 552–574.
- [27] N. Nargis, R. Aldredge, Effects of matrix metalloproteinase on tumour growth and morphology via haptotaxis, *J. Bioeng. Biomed. Sci.* 6 (207) (2016).
- [28] T. Hillen, K.J. Painter, M. Winkler, Convergence of a cancer invasion model to a logistic chemotaxis model, *Math. Models Methods Appl. Sci.* 23 (01) (2013) 165–198.
- [29] Y. Tao, Global existence for a haptotaxis model of cancer invasion with tissue remodeling, *Nonlinear Anal. RWA* 12 (1) (2011) 418–435.

- [30] S. Frigeri, K.F. Lam, E. Rocca, G. Schimperna, On a multi-species Cahn–Hilliard–Darcy tumor growth model with singular potentials, *Commun. Math. Sci.* 16 (3) (2018) 821–856.
- [31] L. Cherfils, A. Miranville, S. Zelik, The Cahn–Hilliard equation with logarithmic potentials, *Milan J. Math.* 79 (2) (2011) 561–596.
- [32] M.A. Chaplain, G. Lolas, Mathematical modelling of cancer cell invasion of tissue: The role of the urokinase plasminogen activation system, *Math. Models Methods Appl. Sci.* 15 (11) (2005) 1685–1734.
- [33] M.A. Chaplain, M. Lachowicz, Z. Szymańska, D. Wrzosek, Mathematical modelling of cancer invasion: the importance of cell–cell adhesion and cell–matrix adhesion, *Math. Models Methods Appl. Sci.* 21 (04) (2011) 719–743.
- [34] Y. Tao, M. Winkler, A chemotaxis–haptotaxis model: the roles of nonlinear diffusion and logistic source, *SIAM J. Math. Anal.* 43 (2) (2011) 685–704.
- [35] Y. Tao, M. Winkler, Energy-type estimates and global solvability in a two-dimensional chemotaxis–haptotaxis model with remodeling of non-diffusible attractant, *J. Differential Equations* 257 (3) (2014) 784–815.
- [36] C. Engwer, C. Stinner, C. Surulescu, On a structured multiscale model for acid-mediated tumor invasion: The effects of adhesion and proliferation, *Math. Models Methods Appl. Sci.* 27 (07) (2017) 1355–1390.
- [37] N. Sfakianakis, A. Madzvamuse, M.A. Chaplain, A hybrid multiscale model for cancer invasion of the extracellular matrix, *Multiscale Model. Simul.* 18 (2) (2020) 824–850.
- [38] T. Köppl, E. Vidotto, B. Wohlmuth, A 3D-1D coupled blood flow and oxygen transport model to generate microvascular networks, *Int. J. Numer. Methods Biomed. Eng.* 36 (10) (2020) e3386.
- [39] H. Brezis, *Functional Analysis, Sobolev Spaces and Partial Differential Equations*, Springer Science & Business Media, 2010.
- [40] T. Roubíček, *Nonlinear Partial Differential Equations with Applications*, Springer Science & Business Media, 2013.
- [41] L.C. Evans, *Partial Differential Equations*, American Mathematical Society, 2010.
- [42] J. Diestel, J. Uhl, *Vector Measures*, American Mathematical Society, 1977.
- [43] J. Simon, Compact sets in the space  $L^p(0, T; B)$ , *Ann. Matematica Pura Appl.* 146 (1) (1986) 65–96.
- [44] J.L. Lions, E. Magenes, *Non-Homogeneous Boundary Value Problems and Applications*, Springer Science & Business Media, 2012.
- [45] F. Boyer, P. Fabrie, *Mathematical Tools for the Study of the Incompressible Navier–Stokes Equations and Related Models*, Springer Science & Business Media, 2012.
- [46] F. Murat, C. Trombetti, A chain rule formula for the composition of a vector-valued function by a piecewise smooth function, *Boll. Unione Mat. Ital.* 6 (3) (2003) 581–595.
- [47] G. Leoni, M. Morini, Necessary and sufficient conditions for the chain rule in  $W_{loc}^{1,1}(\mathbb{R}^n; \mathbb{R}^d)$  and  $BV_{loc}(\mathbb{R}^n; \mathbb{R}^d)$ , *J. Eur. Math. Soc.* 9 (2) (2007) 219–252.
- [48] N. Große, C. Schneider, Sobolev spaces on Riemannian manifolds with bounded geometry: General coordinates and traces, *Math. Nachr.* 286 (16) (2013) 1586–1613.
- [49] H. Kim, Existence and regularity of very weak solutions of the stationary Navier–Stokes equations, *Arch. Ration. Mech. Anal.* 193 (1) (2009) 117–152.
- [50] C. D’Angelo, A. Quarteroni, On the coupling of 1d and 3d diffusion–reaction equations: application to tissue perfusion problems, *Math. Models Methods Appl. Sci.* 18 (08) (2008) 1481–1504.
- [51] W. Walter, *Ordinary Differential Equations*, Springer Science & Business Media, 1998.
- [52] S. Frigeri, M. Grasselli, E. Rocca, On a diffuse interface model of tumour growth, *European J. Appl. Math.* 26 (2) (2015) 215–243.
- [53] J. Jiang, H. Wu, S. Zheng, Well-posedness and long-time behavior of a non-autonomous Cahn–Hilliard–Darcy system with mass source modeling tumor growth, *J. Differential Equations* 259 (7) (2015) 3032–3077.
- [54] J. Lowengrub, E. Titi, K. Zhao, Analysis of a mixture model of tumor growth, *European J. Appl. Math.* 24 (5) (2013) 691–734.
- [55] H.W. Alt, *Linear Functional Analysis: An Application-Oriented Introduction*, Springer Science & Business Media, 2016.
- [56] F. Saedpanah, Well-posedness of an integro-differential equation with positive type kernels modeling fractional order viscoelasticity, *Eur. J. Mech. A Solids* 44 (2014) 201–211.
- [57] T. Secomb, R. Hsu, N. Beamer, B. Coull, Theoretical simulation of oxygen transport to brain by networks of microvessels: effects of oxygen supply and demand on tissue hypoxia, *Microcirculation* 7 (4) (2000) 237–247.
- [58] M. Fritz, P.K. Jha, T. Köppl, J.T. Oden, A. Wagner, B. Wohlmuth, Modeling and simulation of vascular tumors embedded in evolving capillary networks, 2020, arXiv preprint arXiv:2001.10183.
- [59] J. Reichold, M. Stampanoni, A.L. Keller, A. Buck, P. Jenny, B. Weber, Vascular graph model to simulate the cerebral blood flow in realistic vascular networks, *J. Cerebral Blood Flow Metabol.* 29 (8) (2009) 1429–1443.
- [60] E. Vidotto, T. Koch, T. Köppl, R. Helmig, B. Wohlmuth, Hybrid models for simulating blood flow in microvascular networks, *Multiscale Model. Simul.* 17 (3) (2019) 1076–1102.





## B. Further Articles

### B.1. On a subdiffusive tumor growth model with fractional time derivative

#### On a subdiffusive tumour growth model with fractional time derivative

Marvin Fritz, Christina Kuttler, Mabel L. Rajendran, Barbara Wohlmuth,  
Laura Scarabosio

---

In this publication, we provide a novel tumor development model based on RDEs with mechanical couplings and temporal fractional derivatives. The model is capable of modeling subdiffusion in tumor progression and considers the mechanical deformation of the tissue. Moreover, we consider the effects of chemotherapy on the tumor and introduce new source terms that can destroy the tumor cells. The suggested model is mathematically investigated, and we prove that the system is well-posed. That is, we show that a weak solution exists, it is unique, and it depends continuously on the data. The proof is based on a spatial discretization of the system and providing appropriate energy estimates. In particular, we point out the differences between the previous articles due to the new fractional derivative. Several steps have to be re-investigated, and new concepts have to be derived. Numerical simulations are presented in order demonstrate the effect of the fractional derivative and the influence of the fractional parameter on the model.

The work is structured as follows. The mathematical modeling of tumor progression with mechanical effects and fractional derivative is presented in Section 2. In Section 3, we introduce the notations and useful results that will be used in subsequent parts. In particular, we present a generalized Grönwall–Bellman lemma that can be applied to a convolved inequality. Moreover, we state a compactness result with fractional Sobolev spaces similar to the Aubin–Lions lemma. Section 4 deals with the mathematical analysis of the model that determines the existence, uniqueness, and continuous dependence of the weak solution using the Faedo–Galerkin techniques. In Section 5, the model is numerically discretized using the FEM for space and finite differences in time using a convolution quadrature formula for the fractional derivative. The numerical experiments in Section 6 illustrate how the fractional derivative and mechanical coupling in the model affect the model. We also provide chemotherapy in cycles and study its influence on the tumor cells.

I was heavily involved in the brainstorming process of the biological model and was in charge of proving the well-posedness of the coupled PDE system. In addition, I was in charge of writing the mathematical analysis, while the coauthors were responsible for the numerical implementation of the system.

## Permission to include:

Marvin Fritz, Christina Kuttler, Mabel L. Rajendran, Barbara Wohlmuth, Laura Scarabosio

**On a subdiffusive tumour growth model with fractional time derivative**

*IMA Journal of Applied Mathematics*, 86(04):688–729, 2021

(see also article [59] in the bibliography)

The following pages on copyright are excerpts from copies of the website

[https://academic.oup.com/journals/pages/access\\_purchase/rights\\_and\\_permissions/publication\\_rights](https://academic.oup.com/journals/pages/access_purchase/rights_and_permissions/publication_rights)

(Accessed on 21 November 2021)

[< Access and Purchase Resource Centre](#)[Collection sales enquiries](#)[Dispatch Dates](#)[Keep reading](#)[Leavers](#)[► Oxford Journals Archive](#)[► Pricing and Ordering](#)[▼ Rights and Permissions](#)[Author self archiving policy](#)[Accepted Manuscript  
Embargo Periods](#)[Image Permissions](#)**[Publication Rights](#)**[Rightslink](#)[Changes to list](#)

## Publication rights

### What is our policy?

For the majority of journals published by Oxford University Press, we have a policy of acquiring a sole and exclusive licence for all published content, rather than asking authors to transfer ownership of their copyright, which has been common practice in the past. We believe this policy more carefully balances the interests of our authors with our need to maintain the viability and reputation of the journals through which our authors are accorded status, recognition, and widespread distribution. In developing this policy we have been guided by the following principles:

- As a university press and not-for-profit academic publisher, we rely heavily on the good relationships we have with our authors. Having a licensing policy which enables an author to be identified as the owner of the copyright in an article is one of the key ways of demonstrating how highly we value these relationships.
- An exclusive licence enables the centralised and efficient management of permissions and licencing, ensuring the widest dissemination of the content through intermediaries;
- Exclusive rights also enable OUP to take measures on behalf of our authors against infringement, inappropriate use of an article, libel or plagiarism;
- At the same time, by maintaining exclusive rights, in all media for all published content, we can monitor and uphold the integrity of an article once refereed and accepted for publication to be maintained;

Please note - Although the majority of the journals published by Oxford University Press operate exclusive copyright agreements, some of our society journal may require an assignment of copyright. For further information, please refer to the Authors Guidelines sections of the Journal's homepage.

### Copyright agreements

OUP cannot publish your article until a completed copyright agreement has been received. You should receive a link to our online licencing system or a hardcopy form as soon as your article is accepted for publication.

### Government employees

- If you are or were a UK Crown servant and the article has been written in that capacity, we have an arrangement with HMSO to enable us to publish it while acknowledging that it is Crown Copyright. Please inform the Editorial office or Oxford University Press at the time of acceptance or as soon as possible that the article is Crown Copyright, so that we can ensure the appropriate acknowledgement and copyright line are used, as required by our arrangement with HMSO.
- If you are a US Government employee and the article has been written in that capacity, we acknowledge that the Licence to Publish applies only to the extent allowable by US law.

### Re-use of third party content as part of your Oxford Journals article

- As part of your article, you may wish to reuse material sourced from third parties such as other publishers, authors, museums, art galleries etc. To assist with this process, we have a Permission Request form and accompanying Guidelines that specifies the rights required in order for third party material to be published as part of your Article. For a copy of this form, please email.
- Responsibility for clearing these third party permissions must be borne by the Author, and this process completed as soon as possible – preferably before acceptance of the manuscript, but if not possible, before the Article reaches the Production stage of the process.

## Rights retained by ALL Oxford Journal authors

---

- The right, after publication by Oxford Journals, to use all or part of the Article and abstract, for their own personal use, including their own classroom teaching purposes;
- The right, after publication by Oxford Journals, to use all or part of the Article and abstract, in the preparation of derivative works, extension of the article into book-length or in other works, provided that a full acknowledgement is made to the original publication in the journal;
- The right to include the article in full or in part in a thesis or dissertation, provided that this is not published commercially;

For the uses specified here, please note that there is no need for you to apply for written permission from Oxford University Press in advance. Please go ahead with the use ensuring that a full acknowledgment is made to the original source of the material including the journal name, volume, issue, page numbers, year of publication, title of article and to Oxford University Press and/or the learned society.

The only exception to this is for the re-use of material for commercial purposes, e.g. republication or distribution of an article by a for-profit publisher or medical communications company etc. Permission for this kind of re-use is required and can be obtained by using Rightslink.

With Copyright Clearance Center's Rightslink® service it's faster and easier than ever before to secure permission from OUP titles to be republished in a coursepack, book, CD-ROM/DVD, brochure or pamphlet, journal or magazine, newsletter, newspaper, make a photocopy, or translate.

- Simply visit: [Oxford Academic](#) and locate your desired content.
- Click on (Order Permissions) within the table of contents and/ or at the bottom article's abstract to open the following page:
- Select the way you would like to reuse the content
- Create an account or login to your existing account
- Accept the terms and conditions and permission is granted

For questions about using the Rightslink service, please contact Customer Support via phone 877/622-5543 (toll free) or 978/777-9929, or email Rightslink customer care.

## Author self-archiving policies

---

Oxford Journals also offer a range of author self-archiving policies, permitting authors to share and distribute various versions of their articles. For full details of our self-archiving policies please see our [Author self-archiving](#) page.

## Permissions

---






- All requests to reuse the article, in whole or in part, in another publication will be handled by Oxford Journals. Unless otherwise stated, any permission fees will be retained by the Journal concerned. Where possible, any requests to reproduce substantial parts of the article (including in other Oxford University Press publications) will be subject to your approval (which is deemed to be given if we have not heard from you within 4 weeks of the permission being granted).
- If copyright of the article is held by someone other than the Author, e.g. the Author's employer, Oxford Journals requires non-exclusive permission to administer any requests from third parties.

requests from third parties.

- The Journal is registered with the Copyright Licensing Agency (London) and the Copyright Clearance Center (Danvers, Massachusetts), and other Reproduction Rights Organizations. These are non-profit organizations which offer centralised licensing arrangements for photocopying on behalf of publishers such as Oxford University Press.
- Please forward requests to re-use all or part of your article, or to use figures contained within it, to the [Rights and New Business Development Department](#).

---

## Connect

-  Facebook
-  Join our mailing list
-  Twitter
-  Blog
-  YouTube

## Useful links

- [Changes to our list](#)
- [Dispatch dates](#)
- [Frequently asked questions](#)

---

[About Us](#)

[Contact Us](#)

[Careers](#)

[Help](#)

[Access & Purchase](#)

[Rights & Permissions](#)

[Open Access](#)

[Potentially offensive content](#)

### Connect

[Join Our Mailing List](#)

[OUPblog](#)

[Twitter](#)

[Facebook](#)

[YouTube](#)

[Tumblr](#)

### Resources

[Authors](#)

[Librarians](#)

[Societies](#)

[Sponsors & Advertisers](#)

[Press & Media](#)

[Agents](#)

### Explore

[Shop OUP Academic](#)

[Oxford Dictionaries](#)

[Epigeum](#)

[OUP Worldwide](#)

[University of Oxford](#)

*Oxford University Press is a department of the University of Oxford. It furthers the University's objective of excellence in research, scholarship, and education by publishing worldwide*

**OXFORD**  
UNIVERSITY PRESS

Copyright © 2021 Oxford University Press

[Cookie Policy](#)

[Privacy Policy](#)

[Legal Notice](#)

[Site Map](#)

[Accessibility](#)

## **Notice of publication and copyright**

First Published in "On a subdiffusive tumour growth model with fractional time derivative" in IMA Journal of Applied Mathematics, 86(04):688–729 (2021), published by Oxford University Press.

DOI: <https://doi.org/10.1093/imamat/hxab009>

## On a subdiffusive tumour growth model with fractional time derivative

MARVIN FRITZ, CHRISTINA KUTTLER, MABEL L. RAJENDRAN\*, BARBARA WOHLMUTH  
*Department of Mathematics, Technical University of Munich, Garching, Germany*

\*Corresponding author: rajendrm@ma.tum.de

AND

LAURA SCARABOSIO  
*Institute for Mathematics, Astrophysics and Particle Physics, Radboud University,  
Nijmegen, The Netherlands*

[Received on 19 June 2020; revised on 10 February 2021; accepted on 31 March 2021]

In this work, we present and analyse a system of coupled partial differential equations, which models tumour growth under the influence of subdiffusion, mechanical effects, nutrient supply and chemotherapy. The subdiffusion of the system is modelled by a time fractional derivative in the equation governing the volume fraction of the tumour cells. The mass densities of the nutrients and the chemotherapeutic agents are modelled by reaction diffusion equations. We prove the existence and uniqueness of a weak solution to the model via the Faedo–Galerkin method and the application of appropriate compactness theorems. Lastly, we propose a fully discretized system and illustrate the effects of the fractional derivative and the influence of the fractional parameter in numerical examples.

*Keywords:* subdiffusive tumour growth; mechanical deformation; fractional time derivative; nonlinear partial differential equation; well posedness.

### 1. Introduction

Mathematical modelling to understand the development of tumour cells and their dynamics is of great importance as it in turn helps in devising appropriate treatment methods. In this study, we introduce fractional time derivatives in a tumour growth model with mechanical coupling. The fractional derivatives have the role of accounting for anomalous diffusion, more precisely subdiffusion, seen in tumour growth.

The tumour microenvironment has a strong influence on tumour cell proliferation and migration (Balkwill *et al.*, 2012; Wang *et al.*, 2017; Yuan *et al.*, 2016). Depending on the environment of the surrounding host tissue, tumour not only migrates using typical Fickian diffusion, but it also migrates more generally using subdiffusion, superdiffusion and even ballistic diffusion. Haptotaxis and chemotaxis, which are initiated by extracellular matrix and nutrient supply, respectively, and cell–cell adhesion all drastically affect a tumour’s diffusion mode when a tumour invades its surrounding host tissue and proliferates. In particular, experimental results by Jiang *et al.* (2014) both from *in vitro* and *in vivo* show evidence of anomalous diffusion in cancer growth. Taking the average radius of the tumour to be an indicator of the root-mean-squared displacement of the cells, they observed anomalous diffusion in *in vitro* experiments of growing cultured cells from the breast line and in the clinical data from patients with adrenal tumour and liver tumour.

Anomalous diffusion is a diffusion process with a nonlinear relation between mean squared displacement and time, unlike the normal diffusion process where the relation is linear. In the

microscopic setting, the diffusion processes are presented by the continuous time random walk (CTRW) model (Tahir-Kheli & Elliott, 1983), wherein the particle jumps in random directions and the waiting time before the next jump and jump lengths are given by random processes. We have the following three relevant examples of CTRW. When the mean of the probability density function (PDF) of the waiting time (first moment) and the variance of the PDF of the jump length (second moment) are finite, in the long-time limit we have a behaviour described by an integer-order diffusion equation. In this case, the solution for a point initial condition is a Gaussian PDF, and the mean square displacement (MSD) has a linear dependence on time. A PDF of the waiting time  $\sim t^{-1-\alpha}$  as  $t \rightarrow \infty$  with  $0 < \alpha < 1$ , results, in the continuum limit, in a time fractional diffusion equation, represented by a power-law dependence of MSD on time of the form  $\langle x^2(t) \rangle \sim t^\alpha$  leading to subdiffusive behaviour. A PDF of jump length  $\sim |x|^{-1-\beta}$  as  $|x| \rightarrow \infty$  with  $0 < \beta < 2$  gives us in the long-time limit a behaviour described by fractional diffusion equations in space, leading to superdiffusive behaviour. Fractional differential equations were obtained from the CTRW formulation in Compte (1996) and Metzler & Klafter (2000). The description of reactions that take place in systems with anomalous diffusion is discussed in Henry *et al.* (2006), Seki *et al.* (2003), Yuste *et al.* (2004) and Nepomnyashchy (2016). These examples of CTRW discussed above are adapted to cancer modelling by the migration proliferation dichotomy observed in the development of cancer cells in Iomin (2005b), Iomin (2005a), Iomin (2007) and Fedotov & Iomin (2007). We consider a subdiffusion limited reaction equation for the density of tumour cells, in contrast to the normal reaction diffusion for nutrients and chemotherapeutic density, to take into account the memory effects of cells. This involves the introduction of the Riemann–Liouville fractional derivative, which has the memory kernel in its definition, in the flux and reaction terms in the equation concerning tumour density, as seen in Iomin (2015), resulting in a multi-order system of fractional differential equations. The model can be modified to the one with Caputo fractional derivative assuming sufficient regularity as seen in Yuste *et al.* (2004).

It is important to incorporate mechanical effects in tumour growth model since the growth of the tumour increases mechanical stress due to the surrounding host tissues, which in turn impede the further growth of the tumour. Experimental evidence can be seen in Helmlinger *et al.* (1997), where multicellular spheroids were grown in agar gel concentrations ranging from 0% to 1% and increasing the agar concentration resulted in the inhibited expansion of the spheroid as the substrate stiffness increased. In the literature, reaction-diffusion models with mechanical coupling are seen in Lima *et al.* (2016), Lima *et al.* (2017), Faghihi *et al.* (2020) and Hormuth *et al.* (2018) for modelling tumour growth. In our model, we incorporate the mechanical effects in a similar way to the aforementioned papers.

After having introduced the mathematical model, we proceed with analysing existence and uniqueness of a weak solution. We remark that, while the mathematical analysis of Cahn–Hilliard equations with mechanical effects is well addressed in the literature—see, e.g. Miranville (2001), Carrive *et al.* (1999), Garcke (2003), Garcke (2005a) and Garcke *et al.* (2019)—the analysis of reaction-diffusion equations with mechanical coupling is not straightforward. The traditional Caputo derivative, which is valid for absolutely continuous functions, is extended to a wider class of functions through various generalizations in the study of weak solutions to fractional differential equations. For instance, some generalizations of the Caputo derivative in the literature are given in Kilbas *et al.* (2006), Allen *et al.* (2016), Gorenflo *et al.* (2015), Li & Liu (2018a) and Akilandeewari *et al.* (2017), and they all reduce to the traditional one under the assumption of sufficient regularity of the function. In the analysis, we use the one in Kilbas *et al.* (2006) and Diethelm (2010), which relies on Riemann–Liouville derivatives and is, in contrast to the traditional one, also valid for some functions that do not necessarily have the first derivative. Using Galerkin methods for showing the existence of weak solution to partial fractional differential equations is quite popular and it is seen for instance in Djilali & Rougirel (2018), Ouedjedi *et al.* (2019), Zacher (2009), Zacher (2019), McLean *et al.* (2019), McLean *et al.* (2020), Li



& Liu (2018b) and Manimaran *et al.* (2019) and for tumour growth models in Garcke & Lam (2017), Fritz *et al.* (2019b) and Fritz *et al.* (2019a). The key variations from that of integer-order in the analysis are the fractional Gronwall Lemma (McLean *et al.*, 2020), some special estimates due to the lack of chain rule for fractional derivatives (Vergara & Zacher, 2008) and compactness theorems similar to the Aubin–Lions theorem (Li & Liu, 2018b). The multi-order ordinary fractional differential system is well addressed (Diethelm, 2010); however, there is not much in the literature on the multi-order partial differential system.

The main novelties of our work can be summarized as follows: (a) we consider a nonlinear reaction-diffusion system with a fractional time derivative, capable of modelling subdiffusion in tumour progression, and we illustrate, by numerical simulations, its flexibility in describing the tumour dynamics by varying the fractional exponent; (b) we provide a rigorous mathematical analysis of the existence and uniqueness of a weak solution to this model, the original aspects consisting in the treatment of the fractional time derivative and of the mechanical coupling.

This exposition has the following structure: Section 2 gives the mathematical modelling of the tumour growth with mechanical effects and fractional derivative. In Section 3, we introduce the notations and preliminary results needed in the later sections. The mathematical analysis of the model giving existence and uniqueness of the weak solution using Galerkin methods is worked out in Section 4. The numerical discretization of the model using finite element method for space and finite differences in time with a convolution quadrature formula for the fractional derivative is given in Section 5. The results of the numerical experiments in Section 6 show the effects of the fractional derivative and the mechanical coupling in the model.

## 2. Mathematical modelling

We consider a material body  $\mathcal{B}$  composed of two constituents, tumour cells and healthy cells, which occupy a common portion of a bounded Lipschitz domain  $\Omega \subset \mathbb{R}^d$ ,  $d = 2$ , during the time  $t \in [0, T]$ . Nutrients such as oxygen and glucose in  $\Omega$  nourish both the healthy and tumour cells. The increasing number of tumour cells by the intake of nutrients and interaction with the surrounding healthy cells increases the mechanical stress, which in turn affects the mobility of the tumour. Treatment for cancer is given by chemotherapy in which the drug diffuses through the region  $\Omega$  and kills the fast growing cancerous cells. The quantities of interest to us are as follows: the mass density of the tumour cells per unit volume  $\rho\phi$ , where  $\phi : \Omega \times [0, T] \rightarrow [0, 1]$  is the volume fraction of the tumour cells in  $\mathcal{B}$  and  $\rho$  is the mass density of the tumour cells, the displacement field  $\mathbf{u} : \Omega \times [0, T] \rightarrow \mathbb{R}^d$ , the mass density of the nutrients  $\psi : \Omega \times [0, T] \rightarrow \mathbb{R}$  and the mass density of the chemotherapeutic agents  $\chi : \Omega \times [0, T] \rightarrow \mathbb{R}$ .

### 2.1 Evolution of tumour

Time evolution of the physical system must obey the laws of conservation of mass, linear and angular momentum, energy and the second law of thermodynamics. We ignore the temperature and thermal effects and proceed as done in Lima *et al.* (2016).

- *Conservation of mass:*

$$\partial_t(\rho\phi) + \nabla \cdot (\rho\phi\mathbf{v}) = \rho(S - \nabla \cdot \mathbf{J}), \quad (2.1)$$

where  $\mathbf{v}$  is the velocity field,  $\rho S$  is the mass density supplied by other constituents, which encompasses proliferation of tumour cells and their death due to chemotherapy treatment, and  $\rho\mathbf{J}$  is the mass flux over the boundary of  $\Omega$ , which we denote by  $\partial\Omega$ .

- Conservation of linear and angular momentum:

$$\begin{aligned} \partial_t(\rho\phi\mathbf{v}) + \nabla \cdot (\rho\phi\mathbf{v} \otimes \mathbf{v}) &= \nabla \cdot \mathbf{T} + \rho\phi\mathbf{b} + \mathbf{p}, \\ \mathbf{T} - \mathbf{T}^t &= \mathbf{m}, \end{aligned} \tag{2.2}$$

where  $\mathbf{T}$  is the Cauchy stress tensor for the tumour,  $\mathbf{b}$  is the body force,  $\mathbf{p}$  momentum supplied by other constituents,  $\mathbf{m}$  is the intrinsic moment of momentum, and  $\mathbf{T}^t$  denotes the transpose of  $\mathbf{T}$ .

The total energy of the system  $\tilde{\Psi}$  consists of the Ginzburg–Landau component  $\Psi(\phi, \nabla\phi)$  depending only on  $\phi$  and its gradient  $\nabla\phi$ , and the stored energy potential  $W(\phi, \boldsymbol{\varepsilon}(\mathbf{u}))$  depending on  $\phi$  and the strain measure  $\boldsymbol{\varepsilon}(\mathbf{u})$ . Assuming small deformations, we consider the potentials

$$\begin{aligned} \tilde{\Psi} &= \int_{\Omega} \Psi(\phi, \nabla\phi) + W(\phi, \boldsymbol{\varepsilon}(\mathbf{u})) \, dx, \\ \Psi(\phi, \nabla\phi) &= \frac{c}{2}\phi^2, \quad W(\phi, \boldsymbol{\varepsilon}(\mathbf{u})) = \frac{1}{2}\boldsymbol{\varepsilon} : \mathbf{C}(\phi)\boldsymbol{\varepsilon} + \boldsymbol{\varepsilon} : \bar{\mathbf{T}}(\phi), \end{aligned}$$

where  $c > 0$  is a constant,  $\boldsymbol{\varepsilon}(\mathbf{u}) = \frac{1}{2}(\nabla\mathbf{u} + \nabla\mathbf{u}^t)$ ,  $\bar{\mathbf{T}}(\phi) = \lambda\phi\mathbb{I}$  is the symmetric compositional stress tensor,  $\lambda > 0$  depending on the tumour growth rate and  $\mathbb{I}$  being the identity matrix,  $\mathbf{C}(\phi)$  is the linear elastic inhomogeneous material tensor, and the operator  $:$  denotes the inner product for second-order tensors.

The first variations of the energy functional with respect to  $\phi$  and  $\boldsymbol{\varepsilon}$  define the chemical potential, and the stress tensor, respectively,

$$\mu = \frac{\delta\Psi}{\delta\phi} + \frac{\delta W}{\delta\phi}, \quad \mathbf{T} = \frac{\delta W}{\delta\boldsymbol{\varepsilon}}. \tag{2.3}$$

The effects of the elastic deformation on the movement of tumour cells is prescribed by the term  $\lambda\nabla \cdot \mathbf{u}$  in the chemical potential.

To incorporate subdiffusion, we introduce fractional derivatives in the mass flux and mass sources. Modelling the subdiffusion and proliferation of cancer cells can lead to a linear fractional partial differential equation through a comb model with proliferation in one dimension (Iomin, 2015). On a microscopic level, subdiffusion-limited reaction is modelled in Seki *et al.* (2003) and Yuste *et al.* (2004) by having fractional derivatives in flux and reaction terms.

Motivated by the previous models, the subdiffusion limited reaction for tumour mass density takes the form,

$$\mathbf{J} = -M_{\phi}(\mathbf{x})\partial_t^{1-\alpha}\nabla\mu, \quad S = N_{\phi}\partial_t^{1-\alpha}f(\phi, \psi) - P_{\phi}\partial_t^{1-\alpha}g(\phi, \chi), \tag{2.4}$$

for  $\alpha \in (0, 1)$ , where  $M_{\phi} : \Omega \rightarrow \mathbb{R}^+$  is such that  $cM_{\phi}$  is the mobility of tumour cells,  $f, g : \Omega \times [0, T] \rightarrow \mathbb{R}$  model the uptake of nutrient and chemotherapeutic by the tumour cells,  $N_{\phi} > 0$  is the rate at which the tumour cells proliferate by using the nutrients, and  $P_{\phi} > 0$  is the rate at which the tumour cells die due to the chemotherapy treatment. The operator  $\partial_t^{1-\alpha}$  is the Riemann–Liouville fractional derivative and is

defined for a function  $\varphi : \Omega \times [0, T] \rightarrow \mathbb{R}$ , as

$$\partial_t^\alpha \varphi(t) = \partial_t(g_{1-\alpha} * \varphi)(t), \tag{2.5}$$

where the kernel is defined by

$$g_\alpha(t) := \begin{cases} t^{\alpha-1}/\Gamma(\alpha), & \alpha > 0, \\ \delta(t), & \alpha = 0, \end{cases}$$

where  $\delta(t)$  is the Dirac delta distribution and  $*$  denotes the convolution on the positive halfline with respect to the time variable, i.e.  $(g_\alpha * \varphi)(t) = \int_0^t g_\alpha(t-s)\varphi(s) ds$ . If  $\varphi$  is sufficiently smooth, then we have

$$\partial_t^\alpha (\varphi(t) - \varphi_0) = g_{1-\alpha} * \partial_t \varphi(t), \tag{2.6}$$

where  $\varphi_0$  is a given initial value. The right-hand side is the classical Caputo fractional derivative. The formulation on the left-hand side, which expresses the Caputo fractional derivative in terms of Riemann–Liouville fractional derivative, has the advantage that it requires less regularity of  $\varphi$  than the classical definition.

We reduce the complexity of the system by using the common simplifying assumptions as in Lima *et al.* (2016): the tumour and healthy cells have constant mass density  $\rho = \rho_0$ ,  $\mathbf{m} = \mathbf{0}$ , i.e. the material is monopolar, no body force, i.e.  $\mathbf{b} = \mathbf{0}$ , we neglect the terms with  $\mathbf{v} \otimes \mathbf{v}$  and  $\mathbf{p}$  by not considering the inertial effects, and we further assume that the mechanical equilibrium is attained on a much faster time scale than diffusion takes place, i.e. the term  $\rho_0 \mathbf{v} \partial_t \phi$  on the left-hand side in the linear momentum equation vanishes. For ease of technical difficulties, we assume that the tumour is an isotropic and homogeneous  $\mathbf{C}(\phi) \equiv \mathbf{C}$  material, and so  $\mathbf{C}$  takes the form  $\mathbf{C}\boldsymbol{\varepsilon} = 2G\boldsymbol{\varepsilon} + \frac{2G\nu}{1-2\nu} \text{tr}(\boldsymbol{\varepsilon})\mathbb{I}$ , where  $G > 0$  denotes the shear modulus, while  $\nu < \frac{1}{2}$  is the Poisson’s ratio. This assumption assures that the energy functional  $W(\phi, \boldsymbol{\varepsilon})$  is convex in both its variables, which is required in using Lemma 3.1, which is an analogous result to the chain rule in fractional derivatives for providing estimates for  $\phi$ . A more general energy functional is considered in Garcke (2003) with integer-order derivatives.

Along with these assumptions, we integrate (2.1), take  $\partial_t^\alpha$  on both sides of equation (2.1) and use the semigroup property of the kernel  $g_{1-\alpha} * g_\alpha = g_1 = 1$  in the following way

$$g_{1-\alpha} * \partial_t(g_\alpha * \varphi) = \partial_t(g_{1-\alpha} * g_\alpha * \varphi) - g_{1-\alpha}(t)(g_\alpha * \varphi)(0) = \partial_t(1 * \varphi) = \varphi,$$

assuming sufficient smoothness on the functions, to obtain from (2.1)–(2.4) the system

$$\partial_t^\alpha (\phi - \phi_0) = \nabla \cdot \left( M_\phi(\mathbf{x}) \nabla \mu \right) + N_\phi f(\phi, \psi) - P_\phi g(\phi, \chi), \tag{2.7a}$$

$$\mu = c\phi + \lambda \nabla \cdot \mathbf{u}, \tag{2.7b}$$

$$\mathbf{0} = \nabla \cdot \left( 2G\boldsymbol{\varepsilon}(\mathbf{u}) + \frac{2G\nu}{1-2\nu} \text{tr}(\boldsymbol{\varepsilon}(\mathbf{u}))\mathbb{I} + \lambda\phi\mathbb{I} \right), \tag{2.7c}$$

where  $\phi_0$  is a given data, playing the role of initial condition.

REMARK 2.1 If we assume smoothness on all involved variables, we can formally take the divergence in the deformation equation (2.7c) and conclude that

$$\left(G + \frac{G}{1 - 2\nu}\right) \Delta(\nabla \cdot \mathbf{u}) = -\lambda \Delta\phi.$$

If  $M_\phi$  is a constant, then, by substitution into (2.7a)–(2.7b), we obtain

$$\partial_t^\alpha(\phi - \phi_0) = M_\phi \left(c - \frac{\lambda^2(1 - 2\nu)}{2G(1 - \nu)}\right) \Delta\phi + N_\phi f(\phi, \psi) - P_\phi g(\phi, \chi).$$

We note that in this case the equation for  $\phi$  is independent of  $\mathbf{u}$ . Further, this also suggests that we require at least  $c > \frac{\lambda^2(1-2\nu)}{2G(1-\nu)}$  to conclude the existence of a solution. We indeed see in Section 4 that we require a slightly stronger condition on  $c$ .

### 2.2 Evolution of nutrient

The nutrient mass density is assumed to obey a reaction-diffusion equation, as standard (Preziosi, 2003, Ch. 5 and 10)

$$\frac{\partial \psi}{\partial t} = \nabla \cdot (M_\psi(\mathbf{x}) \nabla \psi) + S_\psi(\mathbf{x}, t) - N_\psi f(\phi, \psi), \tag{2.8}$$

$M_\psi : \Omega \rightarrow \mathbb{R}^+$  is the mobility of the nutrients,  $S_\psi : \Omega \times [0, T] \rightarrow \mathbb{R}$  denotes the external source of nutrients over the volume,  $N_\psi > 0$  denotes the rate at which nutrients are consumed by the tumour cells,  $f(\phi, \psi) = \frac{\phi(1-\phi)\psi}{K_\psi + \psi}$  is a monod equation combined with the term  $(1 - \phi)$  that ensures that  $\phi$ , which is a volume fraction, does not take values greater than 1. The parameter  $K_\psi > 0$  is the monod half saturation constant, corresponding to that nutrient mass density, where the nutrient-dependent growth takes its half maximum value.

### 2.3 Evolution of chemotherapy

The mass density of chemotherapy is assumed to be governed by a reaction-diffusion equation

$$\frac{\partial \chi}{\partial t} = \nabla \cdot (M_\chi(\mathbf{x}) \nabla \chi) - N_\chi \chi + S_\chi(\mathbf{x}, t) - P_\chi g(\phi, \chi), \tag{2.9}$$

where  $M_\chi : \Omega \rightarrow \mathbb{R}^+$  is the mobility of chemotherapeutic agents,  $S_\chi : \Omega \times [0, T] \rightarrow \mathbb{R}$  is the external supply of chemotherapeutic over the domain,  $N_\chi > 0$  is the rate at which the chemotherapeutic agents are degraded,  $P_\chi > 0$  denotes the rate at which chemotherapeutic agents act and are blocked later by killing tumour cells. The term  $g(\phi, \chi) = \frac{\phi(1-\phi)\chi}{K_\chi + \chi}$  includes, analogously to the nutrient uptake, a saturation effect, including also that mainly cells in a certain growth phase are sensible to the chemotherapy. The parameter  $K_\chi > 0$  is the density of chemotherapeutic agents when they reach their half maximum value.

Finally, collecting (2.7)–(2.9), the tumour evolution is governed by the system

$$\partial_t^\alpha(\phi - \phi_0) = \nabla \cdot (M_\phi(\mathbf{x})\nabla\mu) + N_\phi f(\phi, \psi) - P_\phi g(\phi, \chi), \quad (2.10a)$$

$$\mu = c\phi + \lambda \nabla \cdot \mathbf{u}, \quad (2.10b)$$

$$\mathbf{0} = \nabla \cdot \left( 2G\boldsymbol{\varepsilon}(\mathbf{u}) + \frac{2G\nu}{1-2\nu} \text{tr}(\boldsymbol{\varepsilon}(\mathbf{u}))\mathbb{I} + \lambda\phi\mathbb{I} \right), \quad (2.10c)$$

$$\frac{\partial\psi}{\partial t} = \nabla \cdot (M_\psi(\mathbf{x})\nabla\psi) + S_\psi(\mathbf{x}, t) - N_\psi f(\phi, \psi), \quad (2.10d)$$

$$\frac{\partial\chi}{\partial t} = \nabla \cdot (M_\chi(\mathbf{x})\nabla\chi) - N_\chi \chi + S_\chi(\mathbf{x}, t) - P_\chi g(\phi, \chi), \quad (2.10e)$$

in  $\Omega$ . We add to this system the following initial and boundary conditions

$$(\phi, \psi, \chi) = (\phi_0, \psi_0, \chi_0) \text{ on } \Omega \times \{t = 0\}, \quad (2.11a)$$

$$\nabla\mu \cdot \mathbf{n} = 0 \text{ on } \partial\Omega \times (0, T), \quad (2.11b)$$

$$\mathbf{u} = 0 \text{ on } \Sigma_1 \times (0, T), |\Sigma_1| > 0, \quad (2.11c)$$

$$\left( 2G\boldsymbol{\varepsilon}(\mathbf{u}) + \frac{2G\nu}{1-2\nu} \text{tr}(\boldsymbol{\varepsilon}(\mathbf{u}))\mathbb{I} + \lambda\phi\mathbb{I} \right) \cdot \mathbf{n} = \mathbf{0} \text{ on } \partial\Omega \setminus \Sigma_1 \times (0, T), \quad (2.11d)$$

$$\psi = \tilde{\psi}_b, \chi = \tilde{\chi}_b \text{ on } \Sigma_2 \times (0, T), \quad (2.11e)$$

$$M_\psi \nabla\psi \cdot \mathbf{n} = \psi_b, M_\chi \nabla\chi \cdot \mathbf{n} = \chi_b \text{ on } \partial\Omega \setminus \Sigma_2 \times (0, T), \quad (2.11f)$$

where  $\mathbf{n}$  denotes the outer normal to  $\Omega$  and  $\Sigma_1, \Sigma_2 \subset \partial\Omega$  are parts of the boundary  $\partial\Omega$  with non-zero measures. We assume no-flux boundary conditions for the chemical potential and Dirichlet–Neumann mixed boundary condition for the displacement, density of nutrient and chemotherapy. The homogeneous Dirichlet condition on the part of the boundary  $\Sigma_1$  for displacement accounts for the presence of a rigid part of the body such as bone, which prevents the variations of the displacement. The non-homogeneous Dirichlet condition on part of the boundary  $\Sigma_2$  for density of nutrient and chemotherapy accounts for the concentration supply from blood vessels. In the rest of the boundary, the more natural Neumann boundary condition is applied. The problem with non-homogeneous Dirichlet condition for density of nutrient and chemotherapy can be converted to a problem to have homogeneous Dirichlet boundary conditions by taking  $\tilde{\psi} = \psi - \tilde{\psi}_b$  and similarly for  $\chi$ . Therefore we assume  $\tilde{\psi}_b = \tilde{\chi}_b = 0$ .

**REMARK 2.2** We assumed that the displacement  $\mathbf{u}$  vanishes on  $\Sigma_1 \subset \partial\Omega$ , that means we imposed a homogeneous Dirichlet boundary on  $\Sigma_1$ —see also [Garcke et al. \(2019\)](#), [Faghihi et al. \(2020\)](#) and [Bartkowiak & Pawłow \(2005\)](#) for the same choice of boundary behaviour. This allows us to apply the well-known Korn inequality directly in the proof of existence. In the case of pure Neumann boundary conditions, one has to consider a different solution space for  $\mathbf{u}$  (see [Garcke, 2005b](#); [Miranville, 2001, 2003](#), for more details).

### 3. Preliminaries

In this section, we introduce the spaces along with the embedding results, and the useful inequalities and auxiliary results, which are used in the Section 4.

#### 3.1 Notation and embedding results

Let  $\mathcal{W}_p^k(\Omega; \mathbb{R}^d)$  denote the Sobolev space of order  $k$  with weak derivatives in the space  $\mathcal{L}_p(\Omega; \mathbb{R}^d)$  of  $p$ -integrable functions having value in  $\mathbb{R}^d$ . Shortly, we write  $\mathcal{W}_p^k(\Omega; \mathbb{R}) = \mathcal{W}_p^k(\Omega)$ ,  $\mathcal{H}^1(\Omega) = \mathcal{W}_2^1(\Omega)$  and  $\mathcal{H}_{0,\Sigma}^1(\Omega; \mathbb{R}^d)$  denotes the space of  $\mathcal{H}^1(\Omega; \mathbb{R}^d)$  functions with vanishing trace on  $\Sigma \subset \partial\Omega$ , see [Brezis \(2010\)](#) for more details. For notational simplicity, we denote  $\|\cdot\|_{\mathcal{L}_2(\Omega; \mathbb{R}^d)}$  and  $\|\cdot\|_{\mathcal{L}_2(\Sigma; \mathbb{R}^d)}$  by  $\|\cdot\|$  and  $\|\cdot\|_\Sigma$ , respectively,  $(\cdot, \cdot)_{\mathcal{L}_2(\Omega; \mathbb{R}^d)}$  and  $(\cdot, \cdot)_{\mathcal{L}_2(\Sigma; \mathbb{R}^d)}$  by  $(\cdot, \cdot)$  and  $(\cdot, \cdot)_\Sigma$ , respectively, and the brackets  $\langle \cdot, \cdot \rangle$  denote the duality pairing on  $\mathcal{H}^{-1}(\Omega) \times \mathcal{H}^1(\Omega)$ . The symbol  $\mathcal{C}^k(\cdot)$  denotes the space of  $k$ -times continuously differentiable functions and  $\mathcal{C}_b(\cdot)$  denotes the space of bounded continuous functions. Let  $\mathcal{H}$  be a real separable Hilbert space with norm  $\|\cdot\|_{\mathcal{H}}$  and  $\mathcal{V}$  be a Hilbert space such that  $\mathcal{V} \hookrightarrow \mathcal{H} \hookrightarrow \mathcal{V}'$  is a Gelfand triple. We define the Bochner space

$$\mathcal{L}_p(0, T; \mathcal{H}) := \left\{ \varphi : (0, T) \rightarrow X : \varphi \text{ Bochner measurable and } \|\varphi\|_{\mathcal{L}_p(0, T; \mathcal{H})}^p := \int_0^T \|\varphi(t)\|_{\mathcal{H}}^p dt < \infty \right\},$$

where  $p \in [1, \infty)$ . For  $p = \infty$  we modify it in the usual sense with the Bochner norm

$$\|\varphi\|_{\mathcal{L}_\infty(0, T; \mathcal{H})} := \operatorname{ess\,sup}_{t \in (0, T)} \|\varphi(t)\|_{\mathcal{H}}.$$

We introduce the Sobolev–Bochner space

$$\mathcal{W}_{p,q}^1(0, T; \mathcal{V}, \mathcal{V}') := \{ \varphi \in \mathcal{L}_p(0, T; \mathcal{V}) : \partial_t \varphi \in \mathcal{L}_q(0, T; \mathcal{V}') \},$$

and its fractional counter-part

$$\mathcal{W}_{p,q}^\alpha(0, T; \varphi_0, \mathcal{V}, \mathcal{V}') := \{ \varphi \in \mathcal{L}_p(0, T; \mathcal{V}) : g_{1-\alpha} * (\varphi - \varphi_0) \in {}_0\mathcal{W}_{p,q}^1(0, T; \mathcal{V}, \mathcal{V}') \},$$

where  $\varphi_0 \in \mathcal{H}$  and  ${}_0\mathcal{W}_{p,q}^1$  denotes functions in  $\mathcal{W}_{p,q}^1$  with vanishing trace at  $t = 0$ . This definition of the fractional Sobolev–Bochner space indeed corresponds to the space of integrable fractional time-derivatives.

In the existence proof we typically apply compactness results. A special case of the Aubin–Lions compactness theorem ([Simon, 1986](#), Corollary 4) states the following compact embedding

$$p \in [1, \infty), \quad \mathcal{W}_{p,1}^1(0, T; \mathcal{V}, \mathcal{V}') \hookrightarrow \mathcal{L}_p(0, T; \mathcal{H}). \tag{3.1}$$

In the fractional setting, we have the following analogous result

$$p \in [1, \infty), r \in \left( \frac{p}{1 + p\alpha}, \infty \right) \cap [1, \infty), \quad \mathcal{W}_{p,r}^\alpha(0, T; \varphi_0, \mathcal{V}, \mathcal{V}') \hookrightarrow \mathcal{L}_p(0, T; \mathcal{H}), \tag{3.2}$$

where  $\varphi_0 \in \mathcal{H}$  is given. The proof follows the lines of Li & Liu (2018b, Theorem 4.2) using the estimates from Li & Liu (2018b, Proposition 3.4).

We also employ the following continuous embedding into the time-continuous function space to establish additional regularity of the solutions of the partial differential equations,

$$\mathcal{W}_{2,2}^1(0, T; \mathcal{V}, \mathcal{V}') \hookrightarrow \mathcal{C}([0, T]; [\mathcal{V}, \mathcal{V}']_{1/2}), \quad (3.3)$$

where  $[\mathcal{V}, \mathcal{V}']_{1/2}$  denotes the interpolation space of order 1/2 of  $\mathcal{V}$  and  $\mathcal{V}'$ , see Lions & Magenes (2012, Theorem 3.1, Chapter 1), e.g.  $[\mathcal{H}_0^1(\Omega), \mathcal{H}^{-1}(\Omega)]_{1/2} = \mathcal{L}_2(\Omega)$ . In the fractional setting, we have a continuous embedding analogous to the one above. Indeed,

$$\varphi_0 \in \mathcal{H}, \varphi \in \mathcal{W}_{2,2}^\alpha(0, T; \varphi_0, \mathcal{V}, \mathcal{V}') \implies g_{1-\alpha} * (\varphi - \varphi_0) \in \mathcal{C}([0, T]; \mathcal{H}), \quad (3.4)$$

after possibly being redefined on a set of measure zero, see Zacher (2009, Theorem 2.1).

Throughout the whole paper, we denote by  $C$  a generic positive constant, which is independent of the unknowns  $\phi, \mu, \mathbf{u}, \psi$  and  $\chi$ .

### 3.2 Useful inequalities and auxiliary results

We recall the Poincaré–Wirtinger, Poincaré, Korn and Sobolev inequalities, see Brezis (2010) and Ciarlet (2013),

$$\begin{aligned} \|\varphi - \bar{\varphi}\| &\leq C \|\nabla \varphi\| && \text{for all } \varphi \in \mathcal{H}^1(\Omega), \\ \|\varphi\| &\leq C \|\nabla \varphi\| && \text{for all } \varphi \in \mathcal{H}_{0,\Sigma}^1(\Omega), \\ \|\varphi\|_{\mathcal{H}^1(\Omega; \mathbb{R}^d)} &\leq C \|\boldsymbol{\varepsilon}(\varphi)\| && \text{for all } \varphi \in \mathcal{H}_{0,\Sigma}^1(\Omega; \mathbb{R}^d), \\ \|\varphi\|_{\mathcal{W}_q^m(\Omega; \mathbb{R}^d)} &\leq C \|\varphi\|_{\mathcal{W}_p^k(\Omega; \mathbb{R}^d)} && \text{for all } \varphi \in \mathcal{W}_p^k(\Omega; \mathbb{R}^d), \quad k - \frac{d}{p} \geq m - \frac{d}{q}, \quad k \geq m, \end{aligned} \quad (3.5)$$

where  $\bar{\varphi} = \frac{1}{|\Omega|} \int_{\Omega} \varphi(\mathbf{x}) \, dx$  denotes the mean of  $\varphi$ . Also, we often make use of the  $\epsilon$ -Young and the Young convolution inequalities, given by

$$\begin{aligned} ab &\leq \epsilon a^p + \frac{b^q}{\mathbf{q}(\epsilon p)^{q/p}} && \text{for all } a, b \geq 0, \quad \frac{1}{p} + \frac{1}{q} = 1, \quad \epsilon > 0, \\ \|\varphi_1 * \varphi_2\|_{\mathcal{L}_r(\Omega)} &\leq \|\varphi_1\|_{\mathcal{L}_p(\Omega)} \|\varphi_2\|_{\mathcal{L}_q(\Omega)} && \text{for all } \varphi_1 \in \mathcal{L}_p(\Omega), \varphi_2 \in \mathcal{L}_q(\Omega), \quad \frac{1}{p} + \frac{1}{q} = \frac{1}{r} + 1, \end{aligned} \quad (3.6)$$

and Hölder's inequality, given by

$$\|\varphi_1 \varphi_2\|_{\mathcal{L}_1(\Omega)} \leq \|\varphi_1\|_{\mathcal{L}_p(\Omega)} \|\varphi_2\|_{\mathcal{L}_q(\Omega)} \quad \text{for all } \varphi_1 \in \mathcal{L}_p(\Omega), \varphi_2 \in \mathcal{L}_q(\Omega), \quad \frac{1}{p} + \frac{1}{q} = 1, \quad (3.7)$$

see Evans (2010, Appendix B).

The following inequality, which is analogous to the chain rule, is required to obtain a priori estimates to prove the existence of weak solutions of a time-fractional partial differential equation.

LEMMA 3.1 Suppose  $\varphi \in \mathcal{L}_2(0, T; \mathcal{L}_2(\Omega, \mathbb{R}^d))$ , and there exists  $\varphi_0 \in \mathcal{L}_2(\Omega, \mathbb{R}^d)$  such that  $g_{1-\alpha} * (\varphi - \varphi_0) \in {}_0\mathcal{W}_{2,2}^1(0, T; \mathcal{L}_2(\Omega, \mathbb{R}^d), \mathcal{L}_2(\Omega, \mathbb{R}^d))$ . Let  $H \in \mathcal{C}^1(\mathbb{R}^d)$  be a convex function such that  $g_{1-\alpha} * \int_{\Omega} H(\varphi) \, dx \in {}_0\mathcal{W}_1^1(0, T)$ . Then for almost all  $t \in (0, T)$ , we have

$$\begin{aligned} (H'(\varphi(t)), \partial_t(g_{1-\alpha} * \varphi)(t)) &\geq \partial_t \left( g_{1-\alpha} * \int_{\Omega} H(\varphi) \, dx \right) (t) \\ &+ \left( - \int_{\Omega} H(\varphi(t)) \, dx + (H'(\varphi(t)), \varphi(t)) \right) g_{1-\alpha}(t). \end{aligned} \tag{3.8}$$

*Proof.* Let  $k \in \mathcal{W}_1^1(0, T)$ . Then from a straightforward computation, we have the following identity for almost all  $t \in [0, T]$

$$\begin{aligned} \int_{\Omega} H'(\varphi(t)) : \partial_t(k * \varphi)(t) \, dx &= \partial_t \left( k * \int_{\Omega} H(\varphi) \, dx \right) (t) + k(t) \left( \int_{\Omega} -H(\varphi(t)) + H'(\varphi(t)) : \varphi(t) \, dx \right) \\ &- \int_0^t \frac{d}{ds} k(s) \left( \int_{\Omega} H(\varphi(t-s)) - H(\varphi(t)) - H'(\varphi(t)) : (\varphi(t-s) - \varphi(t)) \, dx \right) \, ds. \end{aligned} \tag{3.9}$$

We remark that the identity for functions with values in  $\mathbb{R}$  can be seen in [Kemppainen et al. \(2016, Lemma 6.1\)](#) and the integrated form for functions in  $\mathbb{R}^d$  can be seen in [Gripenberg et al. \(1990, Lemma 18.4.4\)](#). We note that if  $k$  is non-negative and non-increasing then the last term is positive, since  $H$  is a convex functional. The inequality (3.8) follows as in [Vergara & Zacher \(2008, Theorem 2.1\)](#) by approximating  $g_{1-\alpha}$  with a more regular kernel  $k_n \in \mathcal{W}^{1,1}(0, T)$ , using the above identity and taking the limit.  $\square$

A particular form of Lemma 3.1 with  $H(\varphi) = \frac{1}{2}\varphi^2$  is proved in [Vergara & Zacher \(2008, Theorem 2.1\)](#) with functionals having value in any Hilbert space, and we have for almost all  $t \in [0, T]$

$$\frac{1}{2} \frac{d}{dt} (g_{1-\alpha} * \|\varphi\|^2)(t) + \frac{1}{2} g_{1-\alpha}(t) \|\varphi(t)\|^2 \leq (\varphi(t), \partial_t(g_{1-\alpha} * \varphi)(t)). \tag{3.10}$$

REMARK 3.1 The first term in (3.10) is well-posed for  $\varphi \in \mathcal{W}_{2,2}^\alpha(0, T; \varphi_0, \mathcal{L}_2(\Omega, \mathbb{R}^d), \mathcal{L}_2(\Omega, \mathbb{R}^d))$  because of the following implication, which indeed holds true for a wide class of kernels and is proved in [Vergara & Zacher \(2008, Proposition 2.1\)](#),

$$\varphi \in \mathcal{L}_2(0, T; \mathcal{H}), g_{1-\alpha} * \varphi \in {}_0\mathcal{H}^1(0, T; \mathcal{H}) \implies g_{1-\alpha} * \|\varphi\|_{\mathcal{H}}^2 \in {}_0\mathcal{W}_1^1(0, T). \tag{3.11}$$

The following are the Gronwall–Bellman and generalized Gronwall–Bellman with singularity, used for providing explicit bounds on solutions.



LEMMA 3.2 (Gronwall–Bellman, cf. Evans (2010, Appendix B)). Assume  $C_1, C_2 \geq 0$  are constants. If  $\varphi(t)$  is a non-negative, integrable function on  $[0, T]$ , satisfying

$$\varphi(t) \leq C_1 + C_2 \int_0^t \varphi(s) \, ds,$$

for almost all  $t \in [0, T]$ , then it holds that

$$\varphi(t) \leq C_1 e^{C_2 T},$$

for almost all  $t \in [0, T]$ .

LEMMA 3.3 (Generalized Gronwall–Bellman, cf. Ye et al. (2007, Corollary 1)). Assume that  $a(t)$  is a non-negative integrable function on the interval  $[0, T]$ , and  $b > 0$  is a constant. If  $\varphi(t)$  is a non-negative, integrable function satisfying

$$\varphi(t) \leq a(t) + \frac{b}{\Gamma(\alpha)} \int_0^t (t-s)^{\alpha-1} \varphi(s) \, ds,$$

for almost all  $t \in [0, T]$ , then for almost all  $t \in [0, T]$  the following holds true,

$$\varphi(t) \leq a(t) + \int_0^t b \Gamma(\alpha) (t-s)^{\alpha-1} E_{\alpha,\alpha}(b \Gamma(\alpha) (t-s)^\alpha) a(s) \, ds,$$

where  $E_{\alpha,\alpha}(x) = \sum_{k=0}^\infty \frac{x^k}{\Gamma(\alpha k + \alpha)}$  is the two-paramater Mittag–Leffler function.

LEMMA 3.4 (Fractional integration by parts, cf. Djilali & Rougirel (2018, Proposition 3.1)). Let  $\varphi_1 \in \mathcal{L}_2(0, T; \mathcal{H})$  and  $\varphi_2 \in \mathcal{H}^1(0, T; \mathcal{H})$ . Then

$$\int_0^T (\partial_t (g_{1-\alpha} * \varphi_1)(t), \varphi_2) \, dt = - \int_0^T (\varphi_1, (g_{1-\alpha} *' \partial_t \varphi_2)(t)) \, dt + ((g_{1-\alpha} * \varphi_1)(t), \varphi_2) \Big|_{t=0}^{t=T},$$

where the convolution  $*'$  is defined by  $(g_\alpha *' \varphi)(t) = \int_t^T g_\alpha(t-s) \varphi(s) \, ds$ .

#### 4. Mathematical analysis

In this section, we provide the existence and uniqueness of the weak solution to the model (2.10) using the Galerkin approximation approach.

DEFINITION 4.1 We say that  $(\phi, \mu, \mathbf{u}, \psi, \chi)$  satisfying

$$\begin{aligned} \phi &\in \mathcal{W}_{2,2}^\alpha(0, T; \phi_0, \mathcal{L}_2(\Omega), \mathcal{L}_2(\Omega)), & \mu &\in \mathcal{L}_2(0, T; \mathcal{H}^1(\Omega)), \\ \mathbf{u} &\in \mathcal{L}_2(0, T; \mathcal{H}_{0,\Sigma_1}^1(\Omega; \mathbb{R}^d)), & \psi, \chi &\in \mathcal{W}_{2,2}^1(0, T; \mathcal{H}_{0,\Sigma_2}^1(\Omega), \mathcal{H}^{-1}(\Omega)), \end{aligned}$$

is a weak solution to the system (2.10) with data (2.11), if the initial conditions  $g_{1-\alpha} * (\phi - \phi_0)(0) = 0$ ,  $\psi(0) = \psi_0$ ,  $\chi(0) = \chi_0$  holds in the weak sense and the solution satisfies the variational form

$$\begin{aligned}
 (\partial_t^\alpha (\phi - \phi_0), \xi_1) + (M_\phi \nabla \mu, \nabla \xi_1) &= N_\phi(f(\phi, \psi), \xi_1) - P_\phi(g(\phi, \chi), \xi_1), \\
 (\mu, \xi_2) &= c(\phi, \xi_2) + \lambda(\nabla \cdot \mathbf{u}, \xi_2), \\
 2G(\boldsymbol{\varepsilon}(\mathbf{u}), \boldsymbol{\varepsilon}(\boldsymbol{\xi}_3)) + \frac{2G\nu}{1-2\nu}(\nabla \cdot \mathbf{u}, \nabla \cdot \boldsymbol{\xi}_3) &= -\lambda(\phi, \nabla \cdot \boldsymbol{\xi}_3), \\
 \langle \partial_t \psi, \xi_4 \rangle + (M_\psi \nabla \psi, \nabla \xi_4) &= (S_\psi, \xi_4) - N_\psi(f(\phi, \psi), \xi_4) + (\psi_b, \xi_4)_{\partial\Omega \setminus \Sigma_2}, \\
 \langle \partial_t \chi, \xi_4 \rangle + (M_\chi \nabla \chi, \nabla \xi_4) &= (S_\chi, \xi_4) - N_\chi(\chi, \xi_4) - P_\chi(g(\phi, \chi), \xi_4) + (\chi_b, \xi_4)_{\partial\Omega \setminus \Sigma_2},
 \end{aligned}
 \tag{4.1}$$

for all  $\xi_1 \in \mathcal{H}^1(\Omega)$ ,  $\xi_2 \in \mathcal{L}_2(\Omega)$ ,  $\boldsymbol{\xi}_3 \in \mathcal{H}_{0,\Sigma_1}^1(\Omega; \mathbb{R}^d)$  and  $\xi_4 \in \mathcal{H}_{0,\Sigma_2}^1(\Omega)$ .

**THEOREM 4.2** (Well-posedness of global weak solutions). Let the following assumptions hold:

- (A1)  $\phi_0, \psi_0, \chi_0 \in \mathcal{L}_2(\Omega)$ ,  $\psi_b, \chi_b \in \mathcal{L}_2(0, T; \mathcal{L}_2(\partial\Omega \setminus \Sigma_2))$ ,
- (A2)  $f, g \in \mathcal{C}_b(\mathbb{R}^2)$  such that  $0 \leq f \leq C_f$  and  $0 \leq g \leq C_g$ , for positive constants  $C_f, C_g$ ,
- (A3)  $M_\phi, M_\psi, M_\chi \in \mathcal{C}_b(\Omega)$  such that  $M_0 \leq M_\phi(\mathbf{x}), M_\psi(\mathbf{x}), M_\chi(\mathbf{x}) \leq M_\infty$  for positive constants  $M_0, M_\infty$ ,
- (A4)  $S_\psi, S_\chi \in \mathcal{L}_2(0, T; \mathcal{L}_2(\Omega))$ ,
- (A5)  $c > \frac{\lambda^2(1-2\nu)}{2G\nu}$ ,

then there exists a weak solution  $(\phi, \mu, \mathbf{u}, \psi, \chi)$  in the sense of Definition 4.1. Additionally, the solution satisfies the estimate

$$\begin{aligned}
 &\|\phi\|_{\mathcal{L}_2(0,T;\mathcal{L}_2(\Omega))}^2 + \|\mu\|_{\mathcal{L}_2(0,T;\mathcal{H}^1(\Omega))}^2 + \|\mathbf{u}\|_{\mathcal{L}_2(0,T;\mathcal{H}^1(\Omega;\mathbb{R}^d))}^2 + \|\psi\|_{\mathcal{L}_2(0,T;\mathcal{H}^1(\Omega))}^2 + \|\chi\|_{\mathcal{L}_2(0,T;\mathcal{H}^1(\Omega))}^2 \\
 &\leq C(\text{IC} + C_f + C_g + \|S_\psi\|_{\mathcal{L}_2(0,T;\mathcal{L}_2(\Omega))}^2 + \|S_\chi\|_{\mathcal{L}_2(0,T;\mathcal{L}_2(\Omega))}^2 + \|\psi_b\|_{\mathcal{L}_2(0,T;\mathcal{L}_2(\partial\Omega \setminus \Sigma_2))}^2 \\
 &\quad + \|\chi_b\|_{\mathcal{L}_2(0,T;\mathcal{L}_2(\partial\Omega \setminus \Sigma_2))}^2),
 \end{aligned}
 \tag{4.2}$$

where  $\text{IC} = \|\phi_0\|^2 + \|\psi_0\|^2 + \|\chi_0\|^2$ . Furthermore, the solution is unique if the nonlinear functions  $f, g$  are Lipschitz continuous with Lipschitz constants  $L_f, L_g > 0$ , respectively.

*Proof.* In order to prove the existence of weak solution, we first use the Faedo-Galerkin method and semi-discretize the original problem in space in Section 4.1. The discretized model can be formulated as a system of nonlinear mixed-order fractional differential equations in a finite dimensional space whose existence of a solution is then obtained by fixed point theorem in Appendix A. We obtain the required energy estimates in Section 4.2. In Section 4.3, we deduce from the Banach–Alaoglu theorem and compactness theorems, the existence of limit functions that yield a weak solution to the nonlinear system (2.10) in the sense of Definition 4.1 and show the weak solution satisfies the estimate (4.2). Finally, we show in Section 4.4 that the Lipschitz continuity assumption on the nonlinear functions  $f$  and  $g$  gives uniqueness of the solution. □

4.1 *Faedo–Galerkin approximation*

We first choose discrete spaces  $\mathbb{Y}^m, \mathbb{Z}^m$  and  $\mathbb{W}^m$  such that their unions over  $m \in \mathbb{N}$  are dense in  $\mathcal{H}^1(\Omega), \mathcal{H}_{0, \Sigma_2}^1(\Omega)$  and  $\mathcal{H}_{0, \Sigma_1}^1(\Omega; \mathbb{R}^d)$ , respectively. We construct approximate solutions in these discrete spaces. We see that the semi-discretized model of Problem (4.1) can be formulated as a system of multi-order fractional ordinary differential equations.

**Discrete spaces.** We introduce the discrete spaces

$$\mathbb{Y}^m = \text{span}\{y_1, \dots, y_m\}, \quad \mathbb{Z}^m = \text{span}\{z_1, \dots, z_m\}, \quad \mathbb{W}^m = \text{span}\{\mathbf{w}^1, \dots, \mathbf{w}^m\},$$

where  $y_k, z_k : \Omega \rightarrow \mathbb{R}, \mathbf{w}_k : \Omega \rightarrow \mathbb{R}^d$  for  $k = 1, \dots, m$  are eigenfunctions to the eigenvalues  $\lambda_k^y, \lambda_k^z, \lambda_k^w$  of the following respective problems

$$\begin{aligned} -\Delta y_k &= \lambda_k^y y_k & \text{in } \Omega, & & -\Delta z_k &= \lambda_k^z z_k & \text{in } \Omega, & & -\Delta \mathbf{w}_k &= \lambda_k^w \mathbf{w}_k & \text{in } \Omega, \\ \nabla y_k \cdot \mathbf{n} &= 0 & \text{on } \partial\Omega, & & z_k &= 0 & \text{on } \partial\Sigma_2, & & \mathbf{w}_k &= 0 & \text{on } \partial\Sigma_1, \\ \nabla z_k \cdot \mathbf{n} &= 0 & \text{on } \partial\Omega \setminus \partial\Sigma_2, & & \nabla \mathbf{w}_k \cdot \mathbf{n} &= 0 & \text{on } \partial\Omega \setminus \partial\Sigma_1. \end{aligned}$$

Since the Laplace operator is a compact, self-adjoint, injective operator, we conclude by the spectral theorem (Boyer & Fabrie, 2013; Brezis, 2010; Robinson, 2001) that

$$\begin{aligned} \{y_k\}_{k=1}^\infty, \{z_k\}_{k=1}^\infty &\text{ are orthonormal bases in } \mathcal{L}_2(\Omega) \text{ and orthogonal bases in } \mathcal{H}^1(\Omega), \\ \{\mathbf{w}_k\}_{k=1}^\infty &\text{ is an orthonormal basis of } \mathcal{L}_2(\Omega; \mathbb{R}^d) \text{ and orthogonal basis in } \mathcal{H}^1(\Omega; \mathbb{R}^d). \end{aligned}$$

Exploiting the orthonormality of the eigenfunctions, we deduce that  $\mathbb{Y}^m, \mathbb{Z}^m$  are dense in  $\mathcal{L}_2(\Omega)$ , and  $\mathbb{W}^m$  is dense in  $\mathcal{L}_2(\Omega; \mathbb{R}^d)$ . We introduce the orthogonal projection,  $\Pi_{\mathbb{Y}^m} : \mathcal{L}_2(\Omega) \rightarrow \mathbb{Y}^m$ , which can be written as

$$\Pi_{\mathbb{Y}^m} \varphi = \sum_{k=1}^m (\varphi, y_k) y_k,$$

and by the properties of orthogonal projections, we have  $\|\Pi_{\mathbb{Y}^m} \varphi\| \leq \|\varphi\|$ . Analogously, we can define  $\Pi_{\mathbb{Z}^m}$  and  $\Pi_{\mathbb{W}^m}$ .

**Faedo–Galerkin system:** Fix  $m > 0$  and consider the Faedo–Galerkin approximations  $\phi^m, \mu^m : [0, T] \rightarrow \mathbb{Y}^m, \mathbf{u}^m : [0, T] \rightarrow \mathbb{W}^m$  and  $\psi^m, \chi^m : [0, T] \rightarrow \mathbb{Z}^m$  with the representations

$$\begin{aligned} \phi^m(t) &:= \sum_{k=1}^m \vartheta_k^m(t) y_k, & \mu^m(t) &:= \sum_{k=1}^m \varrho_k^m(t) y_k, & \mathbf{u}^m(t) &:= \sum_{k=1}^m \zeta_k^m(t) \mathbf{w}_k, \\ \psi^m(t) &:= \sum_{k=1}^m \mathcal{X}_k^m(t) z_k, & \chi^m(t) &:= \sum_{k=1}^m \varpi_k^m(t) z_k, \end{aligned} \tag{4.3}$$

where  $\vartheta_k^m, \varrho_k^m, \varsigma_k^m, \chi_k^m, \varpi_k^m : (0, T) \rightarrow \mathbb{R}$  are coefficient functions for  $k = 1, \dots, m$ . To simplify notations, we set

$$\begin{aligned} f^m &= f(\phi^m, \psi^m), \quad g^m = g(\phi^m, \chi^m), \quad \psi_b^m = \Pi_{\mathbb{Z}^m} \psi_b, \quad \chi_b^m = \Pi_{\mathbb{Z}^m} \chi_b, \\ \phi_0^m &= \Pi_{\mathbb{Y}^m} \phi_0, \quad \psi_0^m = \Pi_{\mathbb{Z}^m} \psi_0, \quad \chi_0^m = \Pi_{\mathbb{Z}^m} \chi_0. \end{aligned}$$

The Faedo–Galerkin system of the model reads

$$(\partial_t^\alpha (\phi^m - \phi_0^m), y_k) + (M_\phi \nabla \mu^m, \nabla y_k) = N_\phi(f^m, y_k) - P_\phi(g^m, y_k), \quad (4.4a)$$

$$(\mu^m, y_k) = c(\phi^m, y_k) + \lambda(\nabla \cdot \mathbf{u}^m, y_k), \quad (4.4b)$$

$$2G(\boldsymbol{\varepsilon}(\mathbf{u}^m), \boldsymbol{\varepsilon}(\mathbf{w}_k)) + \frac{2G\nu}{1-2\nu}(\nabla \cdot \mathbf{u}^m, \nabla \cdot \mathbf{w}_k) = -\lambda(\phi^m, \nabla \cdot \mathbf{w}_k), \quad (4.4c)$$

$$(\partial_t \psi^m, z_k) + (M_\psi \nabla \psi^m, \nabla z_k) = (S_\psi, z_k) - N_\psi(f^m, z_k) + (\psi_b^m, z_k)_{\partial\Omega \setminus \Sigma_2}, \quad (4.4d)$$

$$(\partial_t \chi^m, z_k) + (M_\chi \nabla \chi^m, \nabla z_k) = (S_\chi, z_k) - N_\chi(\chi^m, z_k) - P_\chi(g^m, z_k) + (\chi_b^m, z_k)_{\partial\Omega \setminus \Sigma_2}, \quad (4.4e)$$

for all  $k = 1, \dots, m$ , along with the initial conditions

$$g_{1-\alpha} * (\phi^m - \phi_0^m)(0) = 0, \quad \psi^m(0) = \psi_0^m, \quad \chi^m(0) = \chi_0^m.$$

After inserting the Galerkin ansatz functions (4.3) into the system (4.6) and introducing the following notations

$$\begin{aligned} (\mathbf{A}_\mu^m)_{kl} &:= (M_\phi \nabla y_l, \nabla y_k), & (\mathbf{A}_\psi^m)_{kl} &:= (M_\psi \nabla z_l, \nabla z_k), & (\mathbf{A}_\chi^m)_{kl} &:= (M_\chi \nabla z_l, \nabla z_k), \\ (\mathbf{A}_\mathbf{u}^m)_{kl} &:= (\boldsymbol{\varepsilon}(\mathbf{w}_l), \boldsymbol{\varepsilon}(\mathbf{w}_k)), & (\mathbf{B}^m)_{kl} &:= (\nabla \cdot \mathbf{w}_l, \nabla \cdot \mathbf{w}_k), & (\mathbf{C}^m)_{kl} &:= (y_l, \nabla \cdot \mathbf{w}_k), \\ \boldsymbol{\vartheta}^m(t) &:= (\vartheta_1^m, \dots, \vartheta_m^m)^T, & \boldsymbol{\varrho}^m(t) &:= (\varrho_1^m, \dots, \varrho_m^m)^T, & \boldsymbol{\varsigma}^m(t) &:= (\varsigma_1^m, \dots, \varsigma_m^m)^T, \\ \boldsymbol{\chi}^m(t) &:= (\chi_1^m, \dots, \chi_m^m)^T, & \boldsymbol{\varpi}^m(t) &:= (\varpi_1^m, \dots, \varpi_m^m)^T, & \boldsymbol{\vartheta}_0^m &:= ((\phi_0, y_1), \dots, (\phi_0, y_m))^T, \end{aligned}$$

$$\begin{aligned} \mathbf{S}_\psi^m(t) &:= ((S_\psi, z_1), \dots, (S_\psi, z_m))^T, & \mathbf{S}_\chi^m(t) &:= ((S_\chi, z_1), \dots, (S_\chi, z_m))^T, \\ \boldsymbol{\psi}_b^m &:= ((\psi_b^m, z_1), \dots, (\psi_b^m, z_m))^T, & \boldsymbol{\chi}_b^m(t) &:= ((\chi_b^m, z_1), \dots, (\chi_b^m, z_m))^T, \\ \mathbf{f}_y^m(t) &:= ((f^m, y_1), \dots, (f^m, y_m))^T, & \mathbf{g}_y^m(t) &:= ((g^m, y_1), \dots, (g^m, y_m))^T, \\ \mathbf{f}_z^m(t) &:= ((f^m, z_1), \dots, (f^m, z_m))^T, & \mathbf{g}_z^m(t) &:= ((g^m, z_1), \dots, (g^m, z_m))^T, \end{aligned}$$

we obtain a more compact form of the Faedo–Galerkin system

$$\frac{d}{dt} (g_{1-\alpha} * (\vartheta^m(t) - \vartheta_0^m)) (t) + \mathbf{A}_\mu^m \varrho^m(t) = N_\phi \mathbf{f}_y^m(t) - P_\phi \mathbf{g}_y^m(t), \quad (4.5a)$$

$$\varrho^m(t) = c\vartheta^m(t) + \lambda(\mathbf{C}^m)^t \zeta^m(t), \quad (4.5b)$$

$$(2GA_u^m + \frac{2Gv}{1-2v} \mathbf{B}^m) \zeta^m(t) = -\lambda \mathbf{C}^m \vartheta^m(t), \quad (4.5c)$$

$$\frac{d}{dt} \boldsymbol{\chi}^m(t) + \mathbf{A}_\psi^m \boldsymbol{\chi}^m(t) = \mathbf{S}_\psi^m(t) - N_\psi \mathbf{f}_z^m(t) + \boldsymbol{\psi}_b^m, \quad (4.5d)$$

$$\frac{d}{dt} \boldsymbol{\omega}^m(t) + \mathbf{A}_\chi^m \boldsymbol{\omega}^m(t) = \mathbf{S}_\chi^m(t) - N_\chi \boldsymbol{\omega}^m(t) - P_\chi \mathbf{g}_z^m(t) + \boldsymbol{\chi}_b^m. \quad (4.5e)$$

The matrix  $\mathbf{F}^m := 2GA_u^m + \frac{2Gv}{1-2v} \mathbf{B}^m$  is positive definite by Korn's inequality (3.5) and hence, it is invertible. From (4.5b) and (4.5c), we can write  $\varrho^m(t)$ ,  $\zeta^m(t)$  in terms of  $\vartheta^m(t)$ .

$$\varrho^m(t) = (c\mathbb{I} - \lambda^2 (\mathbf{C}^m)^t (\mathbf{F}^m)^{-1} \mathbf{C}^m) \vartheta^m(t), \quad (4.6a)$$

$$\zeta^m(t) = -\lambda (\mathbf{F}^m)^{-1} \mathbf{C}^m \vartheta^m(t). \quad (4.6b)$$

Then we obtain a system of nonlinear multi-order fractional differential equations in the  $3m$  unknowns  $\{\vartheta_k, \boldsymbol{\chi}_k, \boldsymbol{\omega}_k\}_{1 \leq k \leq m}$

$$\frac{d}{dt} (g_{1-\alpha} * (\vartheta^m(t) - \vartheta_0^m)) (t) + \mathbf{A}_\mu^m (c\mathbb{I} - \lambda^2 (\mathbf{C}^m)^t (\mathbf{F}^m)^{-1} \mathbf{C}^m) \vartheta^m(t) = N_\phi \mathbf{f}_y^m(t) - P_\phi \mathbf{g}_y^m(t),$$

$$\frac{d}{dt} \boldsymbol{\chi}^m(t) + \mathbf{A}_\psi^m \boldsymbol{\chi}^m(t) = \mathbf{S}_\psi^m(t) - N_\psi \mathbf{f}_z^m(t) + \boldsymbol{\psi}_b^m,$$

$$\frac{d}{dt} \boldsymbol{\omega}^m(t) + \mathbf{A}_\chi^m \boldsymbol{\omega}^m(t) = \mathbf{S}_\chi^m(t) - N_\chi \boldsymbol{\omega}^m(t) - P_\chi \mathbf{g}_z^m(t) + \boldsymbol{\chi}_b^m,$$

along with the initial conditions, for  $k = 1, \dots, m$ ,

$$(g_{1-\alpha} * ((\vartheta^m)_k - (\phi_0, y_k))) (0) = 0, \quad (\boldsymbol{\chi}^m)_k(0) = (\psi_0, z_k), \quad (\boldsymbol{\omega}^m)_k(0) = (\chi_0, z_k).$$

The theory of ordinary fractional differential equations in Appendix A ensures the existence of solution to the nonlinear multi-order fractional differential system, and we obtain

$$\vartheta^m, \varrho^m, \zeta^m \in \mathcal{W}_{2,2}^\alpha(0, T; \vartheta_0^m, \mathbb{R}^m, \mathbb{R}^m), \quad \boldsymbol{\chi}^m, \boldsymbol{\omega}^m \in \mathcal{W}_{2,2}^1(0, T; \mathbb{R}^m, \mathbb{R}^m).$$

We further see from (4.6a) and (4.6b) that

$$\begin{aligned} \varrho_k^m(t) - \sum_{l=1}^m \left( c\mathbb{I} - \lambda^2 (\mathbf{C}^m)^t (\mathbf{F}^m)^{-1} \mathbf{C}^m \right)_{kl} (\phi_0, y_l) &= \sum_{l=1}^m \left( c\mathbb{I} - \lambda^2 (\mathbf{C}^m)^t (\mathbf{F}^m)^{-1} \mathbf{C}^m \right)_{kl} (\vartheta_l^m(t) - (\phi_0, y_l)), \\ \varsigma_k^m(t) + \lambda \sum_{l=1}^m \left( (\mathbf{F}^m)^{-1} \mathbf{C}^m \right)_{kl} (\phi_0, y_l) &= -\lambda \sum_{l=1}^m \left( (\mathbf{F}^m)^{-1} \mathbf{C}^m \right)_{kl} (\vartheta_l^m(t) - (\phi_0, y_l)). \end{aligned}$$

Taking convolution with  $g_{1-\alpha}$  on both sides of the above two equations, multiplying by  $y_k$  and  $\mathbf{w}_k$ , respectively, and taking summation over  $k = 1$  to  $m$ , we have

$$(g_{1-\alpha} * (\mu^m - \mu_0^m))(0) = 0, \quad (g_{1-\alpha} * (\mathbf{u}^m - \mathbf{u}_0^m))(0) = 0,$$

where  $\mu_0^m = \sum_{k,l=1}^m (c\mathbb{I} - \lambda^2 (\mathbf{C}^m)^t (\mathbf{F}^m)^{-1} \mathbf{C}^m)_{kl} (\phi_0, y_l) y_k$  and  $\mathbf{u}_0^m = -\lambda \sum_{l,k=1}^m ((\mathbf{F}^m)^{-1} \mathbf{C}^m)_{kl} (\phi_0, y_l) \mathbf{w}_k$  and they satisfy

$$(\mu_0^m, y_k) = c(\phi_0^m, y_k) + \lambda(\nabla \cdot \mathbf{u}_0^m, y_k), \tag{4.7a}$$

$$2G(\boldsymbol{\varepsilon}(\mathbf{u}_0^m), \boldsymbol{\varepsilon}(\mathbf{w}_k)) + \frac{2G\nu}{1-2\nu} (\nabla \cdot \mathbf{u}_0^m, \nabla \cdot \mathbf{w}_k) = -\lambda(\phi_0^m, \nabla \cdot \mathbf{w}_k). \tag{4.7b}$$

Therefore, we conclude

$$\begin{aligned} \phi^m &\in \mathcal{W}_{2,2}^\alpha(0, T; \phi_0^m, \mathbb{Y}^m, \mathbb{Y}^m), \quad \mu^m \in \mathcal{W}_{2,2}^\alpha(0, T; \mu_0^m, \mathbb{Y}^m, \mathbb{Y}^m), \\ \mathbf{u}^m &\in \mathcal{W}_{2,2}^\alpha(0, T; \mathbf{u}_0^m, \mathbb{W}^m, \mathbb{W}^m), \quad \psi^m, \chi^m \in \mathcal{W}_{2,2}^1(0, T, \mathbb{Y}^m, \mathbb{Y}^m). \end{aligned}$$

We obtain from (4.4b) (and (4.4c)) and (4.7a) (and (4.7b)) that  $\mu^m$  (and  $\mathbf{u}^m$ ) satisfy the following equations:

$$(\partial_t^\alpha (\mu^m - \mu_0^m), y_k) = c(\partial_t^\alpha (\phi^m - \phi_0^m), y_k) + \lambda(\partial_t^\alpha (\nabla \cdot \mathbf{u}^m - \nabla \cdot \mathbf{u}_0^m), y_k), \tag{4.8a}$$

$$2G(\partial_t^\alpha (\boldsymbol{\varepsilon}(\mathbf{u}^m) - \boldsymbol{\varepsilon}(\mathbf{u}_0^m)), \boldsymbol{\varepsilon}(\mathbf{w}_k)) + \frac{2G\nu}{1-2\nu} (\partial_t^\alpha (\nabla \cdot \mathbf{u}^m - \nabla \cdot \mathbf{u}_0^m), \nabla \cdot \mathbf{w}_k) = -\lambda(\partial_t^\alpha (\phi^m - \phi_0^m), \nabla \cdot \mathbf{w}_k). \tag{4.8b}$$

Further, we also get from the way discrete spaces are defined the following equation

$$\frac{-1}{\lambda_k^y} (\mu_0^m, \Delta y_k) = (\mu_0^m, y_k) = c(\phi_0^m, y_k) + \lambda(\nabla \cdot \mathbf{u}_0^m, y_k),$$

and taking integration by parts we get

$$(\nabla \mu_0^m, \nabla y_k) = \lambda_k^y c(\phi_0^m, y_k) + \lambda_k^y \lambda (\nabla \cdot \mathbf{u}_0^m, y_k). \tag{4.9}$$

## 4.2 Energy estimates

**Estimates for  $\mu^m$ .** Multiplying (4.4b) with  $\varrho_k^m(t)$  and summing from  $k = 1$  to  $m$ , we have, using Hölder's inequality (3.7),

$$\|\mu^m\|^2 = c(\phi^m, \mu^m) + \lambda(\nabla \cdot \mathbf{u}^m, \mu^m) \leq (c\|\phi^m\| + \lambda\|\nabla \cdot \mathbf{u}^m\|) \|\mu^m\|,$$

and thus

$$\|\mu^m\| \leq c\|\phi^m\| + \lambda\|\nabla \cdot \mathbf{u}^m\| \leq c\|\phi^m\| + \lambda\|\mathbf{u}^m\|_{\mathcal{H}^1(\Omega; \mathbb{R}^d)}. \quad (4.10)$$

Multiplying (4.7a) with  $(\mu_0^m, y_k)$ , summing from  $k = 1$  to  $m$  and using Hölder's inequality (3.7), we have the estimate

$$\|\mu_0^m\| \leq c\|\phi_0^m\| + \lambda\|\nabla \cdot \mathbf{u}_0^m\| \leq c\|\phi_0^m\| + \lambda\|\mathbf{u}_0^m\|_{\mathcal{H}^1(\Omega; \mathbb{R}^d)}. \quad (4.11)$$

**Estimates for  $\mathbf{u}^m$ .** Multiplying (4.4c) with  $\zeta_k^m(t)$ , and summing from  $k = 1$  to  $m$ , we have

$$2G\|\boldsymbol{\varepsilon}(\mathbf{u}^m)\|^2 + \frac{2G\nu}{1-2\nu}\|\nabla \cdot \mathbf{u}^m\|^2 = -\lambda(\phi^m, \nabla \cdot \mathbf{u}^m).$$

Using  $\epsilon$ -Young's (3.6) and Korn's inequality (3.5), we have

$$C\|\mathbf{u}^m\|_{\mathcal{H}^1(\Omega; \mathbb{R}^d)}^2 \leq 2G\|\boldsymbol{\varepsilon}(\mathbf{u}^m)\|^2 + \frac{G\nu}{1-2\nu}\|\nabla \cdot \mathbf{u}^m\|^2 \leq \frac{\lambda^2(1-2\nu)}{4G\nu}\|\phi^m\|^2. \quad (4.12)$$

Multiplying (4.7b) with  $(\mathbf{u}_0^m, \mathbf{w}_k)$ , and summing from  $k = 1$  to  $m$ , we estimate as before to get

$$C\|\mathbf{u}_0^m\|_{\mathcal{H}^1(\Omega; \mathbb{R}^d)}^2 \leq 2G\|\boldsymbol{\varepsilon}(\mathbf{u}_0^m)\|^2 + \frac{G\nu}{1-2\nu}\|\nabla \cdot \mathbf{u}_0^m\|^2 \leq \frac{\lambda^2(1-2\nu)}{4G\nu}\|\phi_0^m\|^2. \quad (4.13)$$

**Estimates for  $\phi^m$ .** Multiplying (4.4a) with  $\varrho_k^m(t)$ , (4.4b) with  $-\frac{d}{dt}(g_{1-\alpha} * (\vartheta_k^m - (\phi_0, y_k)))(t)$ , (4.4c) with  $\frac{d}{dt}(g_{1-\alpha} * (\zeta_k^m - (\mathbf{u}_0^m, \mathbf{w}_k)))(t) + \zeta_k^m(t)$ , and summing from  $k = 1$  to  $m$ , we have

$$(\partial_t^\alpha(\phi^m - \phi_0^m), \mu^m) + (M_\phi \nabla \mu^m, \nabla \mu^m) = N_\phi(f^m, \mu^m) - P_\phi(g^m, \mu^m), \quad (4.14a)$$

$$-(\mu^m, \partial_t^\alpha(\phi^m - \phi_0^m)) = -c(\phi^m, \partial_t^\alpha(\phi^m - \phi_0^m)) - \lambda(\nabla \cdot \mathbf{u}^m, \partial_t^\alpha(\phi^m - \phi_0^m)), \quad (4.14b)$$

$$2G(\boldsymbol{\varepsilon}(\mathbf{u}^m), \partial_t^\alpha(\boldsymbol{\varepsilon}(\mathbf{u}^m) - \boldsymbol{\varepsilon}(\mathbf{u}_0^m))) + \frac{2G\nu}{1-2\nu}(\nabla \cdot \mathbf{u}^m, \partial_t^\alpha(\nabla \cdot \mathbf{u}^m - \nabla \cdot \mathbf{u}_0^m)) = -\lambda(\phi^m, \partial_t^\alpha(\nabla \cdot \mathbf{u}^m - \nabla \cdot \mathbf{u}_0^m)), \quad (4.14c)$$

$$2G(\boldsymbol{\varepsilon}(\mathbf{u}^m), \boldsymbol{\varepsilon}(\mathbf{u}^m)) + \frac{2G\nu}{1-2\nu}(\nabla \cdot \mathbf{u}^m, \nabla \cdot \mathbf{u}^m) = -\lambda(\phi^m, \nabla \cdot \mathbf{u}^m). \quad (4.14d)$$

Upon adding (4.14a)–(4.14c), we obtain

$$c(\phi^m, \partial_t^\alpha(\phi^m - \phi_0^m)) + (\partial_\phi W(\phi^m, \boldsymbol{\varepsilon}(\mathbf{u}^m)), \partial_t^\alpha(\phi^m - \phi_0^m)) + (\partial_\varepsilon W(\phi^m, \boldsymbol{\varepsilon}(\mathbf{u}^m)), \partial_t^\alpha(\boldsymbol{\varepsilon}(\mathbf{u}^m) - \boldsymbol{\varepsilon}(\mathbf{u}_0^m))) \\ + (M_\phi \nabla \mu^m, \nabla \mu^m) = N_\phi(f^m, \mu^m) - P_\phi(g^m, \mu^m),$$

where we have, from Section 2,

$$W(\phi, \boldsymbol{\varepsilon}) = \frac{1}{2} \boldsymbol{\varepsilon} : \mathbf{C} \boldsymbol{\varepsilon} + \boldsymbol{\varepsilon} : \lambda \phi \mathbb{I}, \quad \mathbf{C} \boldsymbol{\varepsilon} = 2G \boldsymbol{\varepsilon} + \frac{2G\nu}{1-2\nu} \operatorname{tr} \boldsymbol{\varepsilon} \mathbb{I},$$

$$\partial_\phi W(\phi, \boldsymbol{\varepsilon}(\mathbf{u})) = \boldsymbol{\varepsilon}(\mathbf{u}) : \lambda \mathbb{I} = \lambda \nabla \cdot \mathbf{u}, \quad \partial_\varepsilon W(\phi, \boldsymbol{\varepsilon}(\mathbf{u})) = \mathbf{C} \boldsymbol{\varepsilon}(\mathbf{u}) + \lambda \phi \mathbb{I} = 2G \boldsymbol{\varepsilon}(\mathbf{u}) + \frac{2G\nu}{1-2\nu} \nabla \cdot \mathbf{u} \mathbb{I} + \lambda \phi \mathbb{I}.$$

We see that the convex functional  $W(\phi^m, \boldsymbol{\varepsilon}(\mathbf{u}^m))$  satisfies the assumptions in Lemma 3.1 by noticing that

$$\int_\Omega W(\phi^m, \boldsymbol{\varepsilon}(\mathbf{u}^m)) \, d\mathbf{x} = -G \|\boldsymbol{\varepsilon}(\mathbf{u}^m)\|^2 - \frac{G\nu}{1-2\nu} \|\nabla \cdot \mathbf{u}^m\|^2, \quad (4.15)$$

which is obtained using (4.14d). We now apply Lemma 3.1 with  $H(\varphi) = W(\phi^m, \boldsymbol{\varepsilon}(\mathbf{u}^m))$  and (3.10), and get the following estimate

$$\frac{d}{dt} \left( g_{1-\alpha} * \left( \frac{c}{2} \|\phi^m\|^2 + \int_\Omega W(\phi^m, \boldsymbol{\varepsilon}(\mathbf{u}^m)) \, d\mathbf{x} \right) \right) (t) + \left( c(\phi^m, \phi^m - \phi_0^m) - \frac{c}{2} \|\phi^m\|^2 \right) g_{1-\alpha}(t) \\ + \left( (\partial_\phi W(\phi^m, \boldsymbol{\varepsilon}(\mathbf{u}^m)), \phi^m - \phi_0^m) + (\partial_\varepsilon W(\phi^m, \boldsymbol{\varepsilon}(\mathbf{u}^m)), \boldsymbol{\varepsilon}(\mathbf{u}^m) - \boldsymbol{\varepsilon}(\mathbf{u}_0^m)) - \int_\Omega W(\phi^m, \boldsymbol{\varepsilon}(\mathbf{u}^m)) \, d\mathbf{x} \right) g_{1-\alpha}(t) \\ + (M_\phi \nabla \mu^m, \nabla \mu^m) \leq N_\phi(f^m, \mu^m) - P_\phi(g^m, \mu^m).$$

Using the convexity of the functionals  $W(\phi^m, \boldsymbol{\varepsilon}(\mathbf{u}^m))$  and  $\frac{c}{2}(\phi^m)^2$ , (A3), (4.10), (4.12) and (4.13), we have

$$\frac{d}{dt} \left( g_{1-\alpha} * \left( \frac{c}{2} \|\phi^m\|^2 + \int_\Omega W(\phi^m, \boldsymbol{\varepsilon}(\mathbf{u}^m)) \, d\mathbf{x} \right) \right) (t) + M_0 \|\nabla \mu^m\|^2 \leq C \left( \|\phi_0^m\|^2 g_{1-\alpha}(t) + \|\phi^m\|^2 \right) \\ + \frac{N_\phi}{2} \|f^m\|^2 + \frac{P_\phi}{2} \|g^m\|^2. \quad (4.18)$$

All the terms in the above estimate belong to  $\mathcal{L}_1(0, T)$ , and so we convolve with  $g_\alpha$  to get a bound for  $\phi^m$  in the space  $\mathcal{L}_2(0, T; \mathcal{L}_2(\Omega))$ . Using the fact that  $g_{1-\alpha} * \left( \frac{c}{2} \|\phi^m\|^2 + \int_\Omega W(\phi^m, \boldsymbol{\varepsilon}(\mathbf{u}^m)) \, d\mathbf{x} \right) (0) = 0$  and the auxiliary result  $g_\alpha * g_{1-\alpha} = g_1$ , see Diethelm (2010, Theorem 2.2), we have

$$g_\alpha * \frac{d}{dt} \left( g_{1-\alpha} * \left( \frac{c}{2} \|\phi^m\|^2 + \int_\Omega W(\phi^m, \boldsymbol{\varepsilon}(\mathbf{u}^m)) \, d\mathbf{x} \right) \right) \\ = \frac{d}{dt} \left( g_\alpha * g_{1-\alpha} * \left( \frac{c}{2} \|\phi^m\|^2 + \int_\Omega W(\phi^m, \boldsymbol{\varepsilon}(\mathbf{u}^m)) \, d\mathbf{x} \right) \right) = \frac{c}{2} \|\phi^m\|^2 + \int_\Omega W(\phi^m, \boldsymbol{\varepsilon}(\mathbf{u}^m)) \, d\mathbf{x}.$$



Convolving (4.18) with  $g_\alpha$ , we have for almost all  $t \in [0, T]$ ,

$$\begin{aligned} \frac{c}{2} \|\phi^m\|^2 + \int_{\Omega} W(\phi^m, \boldsymbol{\varepsilon}(\mathbf{u}^m)) \, dx + M_0 \left( g_\alpha * \|\nabla \mu^m\|^2 \right) (t) &\leq C \|\phi_0^m\|^2 + C \left( g_\alpha * \|\phi^m\|^2 \right) (t) \\ &+ \frac{N_\phi}{2} \left( g_\alpha * \|f^m\|^2 \right) (t) + \frac{P_\phi}{2} \left( g_\alpha * \|g^m\|^2 \right) (t). \end{aligned}$$

Further, using (4.15) and (4.12), we have

$$\begin{aligned} \frac{1}{2} \left( c - \frac{\lambda^2(1-2\nu)}{2G\nu} \right) \|\phi^m\|^2 + M_0 \left( g_\alpha * \|\nabla \mu^m\|^2 \right) (t) &\leq C \|\phi_0^m\|^2 + C \left( g_\alpha * \|\phi^m\|^2 \right) (t) \\ &+ \frac{N_\phi}{2} \left( g_\alpha * \|f^m\|^2 \right) (t) + \frac{P_\phi}{2} \left( g_\alpha * \|g^m\|^2 \right) (t), \end{aligned}$$

where the constant in the first term is positive by (A5). Using the generalised Gronwall–Bellman Lemma 3.3, integrating from 0 to  $T$ , using Young’s inequality for convolution (3.6) and the property of orthogonal projection, we obtain the upper bound

$$\|\phi^m\|_{\mathcal{L}_2(0,T;\mathcal{L}_2(\Omega))}^2 \leq C \left( \|\phi_0\|^2 + C_f + C_g \right). \tag{4.17}$$

Moreover, integrating (4.18) from 0 to  $T$ , using (4.17) and the fact that  $g_{1-\alpha}$  is positive yields

$$\|\nabla \mu^m\|_{\mathcal{L}_2(0,T;\mathcal{L}_2(\Omega))}^2 \leq C \left( \|\phi_0\|^2 + C_f + C_g \right). \tag{4.18}$$

**Estimates for  $\psi^m$ .** We have stated in (4.4d) the following Faedo–Galerkin equation for  $\psi^m$ ,

$$\left( \partial_t \psi^m, z_k \right) + \left( M_\psi \nabla \psi^m, \nabla z_k \right) = \left( S_\psi, z_k \right) - N_\psi \left( f^m, z_k \right) + \left( \psi_b^m, z_k \right)_{\partial\Omega \setminus \Sigma_2},$$

and by multiplying this equation by  $x_k^m(t)$  and taking summation over  $k = 1$  to  $m$  and using (A4), we arrive at

$$\left( \partial_t \psi^m, \psi^m \right) + M_0 \|\nabla \psi^m\|^2 \leq N_\psi \left( f^m, \psi^m \right) + \left( S_\psi, \psi^m \right) + \left( \psi_b^m, \psi^m \right)_{\partial\Omega \setminus \Sigma_2}.$$

Using the inequalities (3.7) and (3.6), we estimate the right-hand side and get the following upper bound

$$\frac{1}{2} \frac{d}{dt} \|\psi^m\|^2 + M_0 \|\nabla \psi^m\|^2 \leq \left( \frac{N_\psi}{2} + \frac{1}{2} \right) \|\psi^m\|^2 + \frac{N_\psi}{2} \|f^m\|^2 + \frac{1}{2} \|S_\psi\|^2 + \|\psi_b^m\|_{\partial\Omega \setminus \Sigma_2} \|\mathcal{Y} \psi^m\|_{\partial\Omega \setminus \Sigma_2},$$

where  $\mathcal{Y} : \mathcal{H}^1(\Omega) \rightarrow \mathcal{L}_2(\partial\Omega \setminus \Sigma_2)$  is the trace operator. Since the trace operator is continuous, we have  $\|\mathcal{Y} \varphi\|_{\partial\Omega \setminus \Sigma_2} \leq C \|\varphi\|_{\mathcal{H}^1(\Omega)}$  for every  $\varphi \in \mathcal{H}^1(\Omega)$ , see Evans (2010, Section 5.5, Theorem 1). Applying

$\epsilon$ -Young’s inequality (3.6), we find

$$\frac{1}{2} \frac{d}{dt} \|\psi^m\|^2 + \frac{M_0}{2} \|\nabla \psi^m\|^2 \leq \left(\frac{N_\psi}{2} + 1\right) \|\psi^m\|^2 + \frac{N_\psi}{2} \|f^m\|^2 + \frac{1}{2} \|S_\psi\|^2 + C \|\psi_b^m\|_{\partial\Omega \setminus \Sigma_2}^2.$$

Finally, the Gronwall–Bellman Lemma 3.2, yields the estimate,

$$\|\psi^m\|_{\mathcal{L}_2(0,T;\mathcal{L}_2(\Omega))}^2 + \|\nabla \psi^m\|_{\mathcal{L}_2(0,T;\mathcal{L}_2(\Omega))}^2 \leq C(\|\psi_0\|^2 + C_f + \|S_\psi\|_{\mathcal{L}_2(0,T;\mathcal{L}_2(\Omega))}^2 + \|\psi_b\|_{\mathcal{L}_2(0,T;\mathcal{L}_2(\partial\Omega \setminus \Sigma_2))}^2). \tag{4.19}$$

**Estimates for  $\chi^m$ .** Multiplying (4.4e) with  $\varpi_k^m(t)$  and taking summation over  $k = 1$  to  $m$ , using the typical inequalities and proceeding as in the estimates for  $\psi$ , we have the estimate

$$\|\chi^m\|_{\mathcal{L}_2(0,T;\mathcal{L}_2(\Omega))}^2 + \|\nabla \chi^m\|_{\mathcal{L}_2(0,T;\mathcal{L}_2(\Omega))}^2 \leq C(\|\chi_0\|^2 + C_g + \|S_\chi\|_{\mathcal{L}_2(0,T;\mathcal{L}_2(\Omega))}^2 + \|\chi_b\|_{\mathcal{L}_2(0,T;\mathcal{L}_2(\partial\Omega \setminus \Sigma_2))}^2). \tag{4.20}$$

Summing the equations (4.10), (4.12) and (4.19)–(4.22), we arrive at the energy estimate

$$\begin{aligned} & \|\phi^m\|_{\mathcal{L}_2(0,T;\mathcal{L}_2(\Omega))}^2 + \|\mu^m\|_{\mathcal{L}_2(0,T;\mathcal{H}^1(\Omega))}^2 + \|\mathbf{u}^m\|_{\mathcal{L}_2(0,T;\mathcal{H}^1(\Omega;\mathbb{R}^d))}^2 + \|\psi^m\|_{\mathcal{L}_2(0,T;\mathcal{H}^1(\Omega))}^2 \\ & + \|\chi^m\|_{\mathcal{L}_2(0,T;\mathcal{H}^1(\Omega))}^2 \leq C(\text{IC} + C_f + C_g + \|S_\psi\|_{\mathcal{L}_2(0,T;\mathcal{L}_2(\Omega))}^2 + \|S_\chi\|_{\mathcal{L}_2(0,T;\mathcal{L}_2(\Omega))}^2 \\ & \quad + \|\psi_b\|_{\mathcal{L}_2(0,T;\mathcal{L}_2(\partial\Omega \setminus \Sigma_2))}^2 + \|\chi_b\|_{\mathcal{L}_2(0,T;\mathcal{L}_2(\partial\Omega \setminus \Sigma_2))}^2). \end{aligned} \tag{4.21}$$

**Estimates for the time derivatives.** Since our equations in which we wish to pass to the limit have nonlinear functions in  $\phi^m, \psi^m, \chi^m$ , we need the strong convergence of these sequences. For this purpose we bound the time derivatives and use the compactness results (3.1) and (3.2). We first obtain the estimate of time derivative of  $\phi^m$  using the estimates from the time derivatives of  $\mu^m$  and  $\mathbf{u}^m$ . Multiplying (4.8a) with  $\frac{d}{dt} g_{1-\alpha} * (\varrho_k^m(t) - (\mu_0^m, y_k))$ , summing from  $k = 1$  to  $m$ , and estimating using Hölder’s inequality (3.7), we have

$$\|\partial_t^\alpha (\mu^m - \mu_0^m)\| \leq c \|\partial_t^\alpha (\phi^m - \phi_0^m)\| + \lambda \|\partial_t^\alpha (\nabla \cdot \mathbf{u}^m - \nabla \cdot \mathbf{u}_0^m)\|. \tag{4.22}$$

Multiplying (4.8b) with  $\frac{d}{dt} g_{1-\alpha} * (\varsigma_k^m(t) - (\mathbf{u}_0^m, \mathbf{w}_k))$ , summing from  $k = 1$  to  $m$ , we have

$$2G \|\partial_t^\alpha (\boldsymbol{\varepsilon}(\mathbf{u}^m) - \boldsymbol{\varepsilon}(\mathbf{u}_0^m))\|^2 + \frac{2G\nu}{1-2\nu} \|\partial_t^\alpha (\nabla \cdot \mathbf{u}^m - \nabla \cdot \mathbf{u}_0^m)\|^2 = -\lambda (\partial_t^\alpha (\phi^m - \phi_0^m), \partial_t^\alpha (\nabla \cdot \mathbf{u}^m - \nabla \cdot \mathbf{u}_0^m)).$$

Using Hölder’s inequality (3.7) gives us

$$\frac{2G\nu}{1-2\nu} \|\partial_t^\alpha (\nabla \cdot \mathbf{u}^m - \nabla \cdot \mathbf{u}_0^m)\|^2 \leq \lambda \|\partial_t^\alpha (\phi^m - \phi_0^m)\|^2. \tag{4.23}$$

Multiplying (4.9) with  $(\mu_0^m, y_k)$  and summing from  $k = 1$  to  $m$ , we obtain

$$\|\nabla \mu_0^m\|^2 \leq \lambda_k^y c(\phi_0^m, \mu_0^m) + \lambda_k^y \lambda (\nabla \cdot \mathbf{u}_0^m, \mu_0^m).$$

Using Hölder's (3.7), (4.11) and (4.13), we have

$$\|\nabla\mu_0^m\|^2 \leq C\|\phi_0^m\|^2. \quad (4.24)$$

We now use the above two estimates to obtain the estimate of time derivative of  $\phi^m$ . Multiplying (4.4a) with  $\frac{d}{dt}g_{1-\alpha} * (\vartheta_k^m - (\phi_0, y_k))$  and (4.8a) with  $\frac{d}{dt}g_{1-\alpha} * (\varrho_k^m(t) - (\mu_0^m, y_k))$ , and summing we get

$$\begin{aligned} c \|\partial_t^\alpha(\phi^m - \phi_0^m)\|^2 + \left( M_\phi \nabla\mu^m, \nabla\partial_t^\alpha(\mu^m - \mu_0^m) \right) &= N_\phi(f^m, \partial_t^\alpha(\mu^m - \mu_0^m)) - P_\phi(g^m, \partial_t^\alpha(\mu^m - \mu_0^m)) \\ &\quad - \lambda \left( \partial_t^\alpha(\nabla \cdot \mathbf{u}^m - \nabla \cdot \mathbf{u}_0^m), \partial_t^\alpha(\phi^m - \phi_0^m) \right). \end{aligned}$$

Using (3.10) and Hölder's inequality (3.7), we have

$$\begin{aligned} c \|\partial_t^\alpha(\phi^m - \phi_0^m)\|^2 + \frac{M_0}{2} \frac{d}{dt} \left( g_{1-\alpha} * \|\nabla\mu^m\|^2 \right) (t) &\leq \left( N_\phi \|f^m\| + P_\phi \|g^m\| \right) \|\partial_t^\alpha(\mu^m - \mu_0^m)\| \\ &\quad + g_{1-\alpha}(t) \|\nabla\mu_0^m\| + \lambda \|\partial_t^\alpha(\nabla \cdot \mathbf{u}^m - \nabla \cdot \mathbf{u}_0^m)\| \|\partial_t^\alpha(\phi^m - \phi_0^m)\|. \end{aligned}$$

Using (4.22) and (4.23), we have, for every  $\epsilon_1, \epsilon_2 > 0$ ,

$$\begin{aligned} c \|\partial_t^\alpha(\phi^m - \phi_0^m)\|^2 + \frac{M_0}{2} \frac{d}{dt} \left( g_{1-\alpha} * \|\nabla\mu^m\|^2 \right) (t) &\leq \left( \frac{\epsilon_1 + \epsilon_2}{4\epsilon_1\epsilon_2} \right) \left( N_\phi \|f^m\|^2 + P_\phi \|g^m\|^2 \right) \\ &\quad + g_{1-\alpha}(t) \|\nabla\mu_0^m\|^2 + \left( \epsilon_1 c + (\epsilon_2 + 1) \frac{\lambda^2(1-2\nu)}{2G\nu} \right) \|\partial_t^\alpha(\phi^m - \phi_0^m)\|^2. \end{aligned}$$

Choosing  $\epsilon_1$  and  $\epsilon_2$  appropriately, using assumption (A5) and integrating from 0 to  $T$ , using  $g_{1-\alpha}$  is positive and (4.24), we get an upper bound

$$\frac{1}{2} \left( c - \frac{\lambda^2(1-2\nu)}{2G\nu} \right) \|\partial_t^\alpha(\phi^m - \phi_0^m)\|_{\mathcal{L}_2(0,T;\mathcal{L}_2(\Omega))}^2 \leq C(\|\phi_0^m\|^2 + C_f + C_g). \quad (4.25)$$

We now obtain the estimates of time derivatives of  $\psi^m$  and  $\chi^m$ . Let  $\zeta_1 \in \mathcal{L}_2(0, T; \mathcal{H}_{0,\Sigma_2}^1(\Omega))$ , such that  $\Pi_{\mathbb{Z}^m}\zeta_1 = \sum_{k=1}^m \zeta_{1,k} z_k$ . We use the boundedness of the projection and the invariance of the time derivatives under the adjoint operator of  $\Pi_{\mathbb{Z}^m}$ , i.e.

$$\langle \partial_t \psi^m, \zeta_1 \rangle = \langle \partial_t \psi^m, \Pi_{\mathbb{Z}^m} \zeta_1 \rangle,$$

see Boyer & Fabrie (2013, Lemma V.1.6). Multiplying the Faedo–Galerkin equations (4.4d) with  $\zeta_{1,k}$  yields

$$\begin{aligned} \int_0^T \langle \partial_t \psi^m, \zeta_1 \rangle dt &= - \int_0^T (M_\psi \nabla \psi^m, \nabla \Pi_{\mathbb{Z}^m} \zeta_1) dt - \int_0^T N_\psi (f^m, \Pi_{\mathbb{Z}^m} \zeta_1) dt \\ &\quad + \int_0^T (S_\psi, \Pi_{\mathbb{Z}^m} \zeta_1) dt + \int_0^T (\psi_b, \Pi_{\mathbb{Z}^m} \zeta_1)_{\partial\Omega \setminus \Sigma_2} dt, \\ &\leq C(\|\psi_0\| + C_f + \|S_\psi\|_{\mathcal{L}_2(0,T;\mathcal{L}_2(\Omega))}) \|\nabla \Pi_{\mathbb{Z}^m} \zeta_1\|_{\mathcal{L}_2(0,T;\mathcal{L}_2(\Omega))}, \\ &\leq C(\|\psi_0\| + C_f + \|S_\psi\|_{\mathcal{L}_2(0,T;\mathcal{L}_2(\Omega))} + \|\psi_b\|_{\mathcal{L}_2(0,T;\mathcal{L}_2(\partial\Omega \setminus \Sigma_2))}) \|\zeta_1\|_{\mathcal{L}_2(0,T;\mathcal{H}^1(\Omega))}, \end{aligned} \tag{4.26}$$

and

$$\int_0^T \langle \partial_t \chi^m, \zeta_1 \rangle dt \leq C(T, g, S_\chi, \chi_0, \chi_b) \|\zeta_1\|_{\mathcal{L}_2(0,T;\mathcal{H}^1(\Omega))}. \tag{4.27}$$

### 4.3 Existence of a weak solution

We now prove that there is a subsequence of  $\phi^m, \mu^m, \mathbf{u}^m, \psi^m, \chi^m$ , which converges to the weak solution of our model (2.10) in the sense of Definition 4.1. We prove this by showing that the limit functions satisfy the variational form (4.1) and also satisfy the initial conditions.

**Weak Convergence.** The energy estimate (4.21) provides us the following

$$\begin{aligned} \{\phi^m\} &\text{ bounded in } \mathcal{L}_2(0, T; \mathcal{L}_2(\Omega)), \\ \{\mu^m\}, \{\psi^m\}, \{\chi^m\} &\text{ bounded in } \mathcal{L}_2(0, T; \mathcal{H}^1(\Omega)), \\ \{\mathbf{u}^m\} &\text{ bounded in } \mathcal{L}_2(0, T; \mathcal{H}^1(\Omega; \mathbb{R}^d)). \end{aligned} \tag{4.28}$$

By the Banach–Alaoglu theorem, these bounded sequences have weakly convergent subsequences, which we indicate with the same index. Hence, there exist functions  $\phi, \mu, \psi, \chi : (0, T) \times \Omega \rightarrow \mathbb{R}$  and  $\mathbf{u} : (0, T) \times \Omega \rightarrow \mathbb{R}^d$  such that as  $m \rightarrow \infty$  we have the following weak convergences

$$\begin{aligned} \phi^m &\rightharpoonup \phi \quad \text{in } \mathcal{L}_2(0, T; \mathcal{L}_2(\Omega)), \\ \mu^m &\rightharpoonup \mu, \psi^m \rightharpoonup \psi, \chi^m \rightharpoonup \chi \quad \text{in } \mathcal{L}_2(0, T; \mathcal{H}^1(\Omega)), \\ \mathbf{u}^m &\rightharpoonup \mathbf{u} \quad \text{in } \mathcal{L}_2(0, T; \mathcal{H}^1(\Omega; \mathbb{R}^d)). \end{aligned} \tag{4.29}$$

**Strong Convergence.** From the inequalities (4.25)–(4.27), we conclude that

$$\begin{aligned} \{\phi^m\} &\text{ bounded in } \mathcal{W}_{2,2}^\alpha(0, T; \phi_0, \mathcal{L}_2(\Omega), \mathcal{L}_2(\Omega)), \\ \{\psi^m\}, \{\chi^m\} &\text{ bounded in } \mathcal{W}_{2,2}^1(0, T; \mathcal{H}^1(\Omega), \mathcal{H}^{-1}(\Omega)). \end{aligned}$$

Using the Aubin–Lions compactness theorem and compactness results similar for fractional differential equations, see (3.1) and (3.2), we have

$$\begin{aligned} \mathcal{W}_{2,2}^\alpha(0, T; \phi_0, \mathcal{L}_2(\Omega), \mathcal{L}_2(\Omega)) &\hookrightarrow \mathcal{L}_2(0, T; \mathcal{L}_2(\Omega)), \\ \mathcal{W}_{2,2}^1(0, T; \mathcal{H}^1(\Omega), \mathcal{H}^{-1}(\Omega)) &\hookrightarrow \mathcal{L}_2(0, T; \mathcal{L}_2(\Omega)), \end{aligned}$$

and therefore we have the strong convergences (as  $m \rightarrow \infty$ )

$$\phi^m \rightarrow \phi, \psi^m \rightarrow \psi, \chi^m \rightarrow \chi \quad \text{in } \mathcal{L}_2(0, T; \mathcal{L}_2(\Omega)). \tag{4.30}$$

**Variational form.** We now show the limit functions satisfy the variational form (4.1). Let  $\eta \in C_0^\infty(0, T)$ , multiplying the Faedo–Galerkin system (4.6) by  $\eta$  and integrating from 0 to  $T$ , we have

$$\begin{aligned} &\int_0^T (\partial_t^\alpha(\phi^m - \phi_0^m), \eta(t)y_k) \, dt + \int_0^T (M_\phi \nabla \mu^m, \eta(t)\nabla y_k) \, dt \\ &= N_\phi \int_0^T (f^m, \eta(t)y_k) \, dt - P_\phi \int_0^T (g^m, \eta(t)y_k) \, dt, \end{aligned} \tag{4.31a}$$

$$\int_0^T (\mu^m, \eta(t)y_k) \, dt = c \int_0^T (\phi^m, \eta(t)y_k) \, dt + \lambda \int_0^T (\nabla \cdot \mathbf{u}^m, \eta(t)y_k) \, dt, \tag{4.31b}$$

$$2G \int_0^T (\boldsymbol{\varepsilon}(\mathbf{u}^m), \eta(t)\boldsymbol{\varepsilon}(\mathbf{w}_k)) \, dt + \frac{2G\nu}{1-2\nu} \int_0^T (\nabla \cdot \mathbf{u}^m, \eta(t)\nabla \cdot \mathbf{w}_k) \, dt = - \int_0^T \lambda(\phi^m, \eta(t)\nabla \cdot \mathbf{w}_k) \, dt, \tag{4.31c}$$

$$\begin{aligned} &\int_0^T (\partial_t \psi^m, \eta(t)z_k) \, dt + \int_0^T (M_\psi \nabla \psi^m, \eta(t)\nabla z_k) \, dt \\ &= \int_0^T (S_\psi, \eta(t)z_k) \, dt - N_\psi \int_0^T (f^m, \eta(t)z_k) \, dt + \int_0^T (\psi_b^m, z_k)_{\partial\Omega \setminus \Sigma_2} \, dt, \end{aligned} \tag{4.31d}$$

$$\begin{aligned} &\int_0^T (\partial_t \chi^m, \eta(t)z_k) \, dt + \int_0^T (M_\chi \nabla \chi^m, \eta(t)\nabla z_k) \, dt \\ &= \int_0^T (S_\chi, \eta(t)z_k) \, dt - N_\chi \int_0^T (\chi^m, \eta(t)z_k) \, dt - P_\chi \int_0^T (g^m, \eta(t)z_k) \, dt + \int_0^T (\chi_b^m, z_k)_{\partial\Omega \setminus \Sigma_2} \, dt. \end{aligned} \tag{4.31e}$$

The convergence of the linear terms follows directly from the definition of weak convergence. For instance, the functional

$$\mu^m \mapsto \int_0^T (\nabla \mu^m, \eta(t)\nabla y_k) \, dt \leq \|\mu^m\|_{\mathcal{L}_2(0,T;\mathcal{H}^1(\Omega))} \|\eta\|_{\mathcal{L}_2(0,T)} \|\nabla y_k\|,$$

is linear and continuous on  $\mathcal{L}_2(0, T; \mathcal{H}^1(\Omega))$  and therefore, we get from (4.29) that

$$\int_0^T (\nabla \mu^m, \eta(t) \nabla y_k) dt \rightarrow \int_0^T (\nabla \mu, \eta(t) \nabla y_k) dt,$$

for  $m \rightarrow \infty$ . The terms with time derivatives follow from integration by parts, change of integration and the definition of the weak convergence. The functionals

$$\begin{aligned} \phi^m &\mapsto \int_0^T (\partial_t (g_{1-\alpha} * (\phi^m - \phi_0^m))(t), \eta(t) y_k) dt = - \int_0^T ((\phi^m - \phi_0^m), (g_{1-\alpha}^{*'} \partial_t \eta)(t) y_k) dt, \\ &\leq \|\phi^m - \phi_0^m\|_{\mathcal{L}_2(0, T; \mathcal{L}_2(\Omega))} \|g_{1-\alpha}\|_{\mathcal{L}_1(0, T)} \|\eta'\|_{\mathcal{L}_2(0, T)} \|y_k\|, \\ \psi^m &\mapsto \int_0^T (\partial_t \psi^m, \eta(t) z_k) dt = - \int_0^T (\psi^m, \eta'(t) z_k) dt \leq \|\psi^m\|_{\mathcal{L}_2(0, T; \mathcal{L}_2(\Omega))} \|\eta'\|_{\mathcal{L}_2(0, T)} \|z_k\|, \\ \chi^m &\mapsto \int_0^T (\partial_t \chi^m, \eta(t) z_k) dt = - \int_0^T (\chi^m, \eta'(t) w_k) dt \leq \|\chi^m\|_{\mathcal{L}_2(0, T; \mathcal{L}_2(\Omega))} \|\eta'\|_{\mathcal{L}_2(0, T)} \|z_k\|, \end{aligned}$$

as we see are linear and continuous on  $\mathcal{L}_2(0, T; \mathcal{L}_2(\Omega))$ , and so by weak convergence and reapplying the integration by parts, we obtain the limit for the terms with time derivatives in (4.33).

The strong convergence results in (4.30) give us the limits of the terms involving nonlinear functions. From the strong convergence, we have

$$\phi^m \rightarrow \phi, \psi^m \rightarrow \psi \quad \text{in } \mathcal{L}_2(0, T; \mathcal{L}_2(\Omega)) \cong \mathcal{L}_2((0, T) \times \Omega), \quad \text{as } m \rightarrow \infty.$$

This implies there exist subsequences such that they converge almost everywhere on  $(0, T) \times \Omega$ . Since almost everywhere convergence is preserved under composition of a continuous functional, we have

$$f^m = f(\phi^m, \psi^m) \rightarrow f(\phi, \psi) \quad \text{a.e. in } (0, T) \times \Omega, \quad \text{as } m \rightarrow \infty.$$

Since  $\{f^m\}$  is bounded, we have by the Lebesgue dominated convergence theorem

$$f^m \eta(t) y_k \rightarrow f(\phi, \psi) \eta(t) y_k \quad \text{in } \mathcal{L}_1(0, T \times \Omega), \quad \text{as } m \rightarrow \infty.$$

Convergence of the terms involving  $g^m$  follow analogously.

By the above convergence results, we have that (4.33) holds true with the limit functions for all  $\eta \in C_0^\infty(0, T)$ . By the Lemma of du Bois-Reymond, we get that the limit functions  $(\phi, \mu, \mathbf{u}, \psi, \chi)$

satisfy

$$\begin{aligned}
 (\partial_t^\alpha (\phi(t) - \phi_0), y_k) + (M_\phi \nabla \mu, \nabla y_k) &= N_\phi(f(\phi, \psi), y_k) - P_\phi(g(\phi, \chi), y_k), \\
 (\mu, y_k) &= c(\phi, y_k) + \lambda(\nabla \cdot \mathbf{u}, y_k), \\
 \langle \partial_t \psi, z_k \rangle + (M_\psi \nabla \psi, \nabla z_k) &= (S_\psi, z_k) - N_\psi(f(\phi, \psi), z_k) + (\psi_b, z_k)_{\partial\Omega \setminus \Sigma_2}, \\
 \langle \partial_t \chi, z_k \rangle + (M_\chi \nabla \psi, \nabla z_k) &= (S_\chi, z_k) - N_\chi(\chi, z_k) - P_\chi(g(\phi, \chi), z_k) + (\chi_b, z_k)_{\partial\Omega \setminus \Sigma_2}, \\
 -\lambda(\phi, \nabla \cdot \mathbf{w}_k) &= 2G(\boldsymbol{\varepsilon}(\mathbf{u}), \boldsymbol{\varepsilon}(\mathbf{w}_k)) + \frac{2G\nu}{1-2\nu}(\nabla \cdot \mathbf{u}, \nabla \cdot \mathbf{w}_k),
 \end{aligned}$$

for almost all  $t \in (0, T)$  and for all  $k \geq 1$ . Using the density of  $\cup_{m \in \mathbb{N}} \mathbb{Y}^m, \cup_{m \in \mathbb{N}} \mathbb{Z}^m, \cup_{m \in \mathbb{N}} \mathbb{W}^m$  in  $\mathcal{H}^1(\Omega), \mathcal{H}_{0, \Sigma_2}^1(\Omega), \mathcal{H}_{0, \Sigma_1}^1(\Omega; \mathbb{R}^d)$ , respectively, we obtain a solution  $(\phi, \mu, \mathbf{u}, \psi, \chi)$  to the system (2.10) in the sense of Definition 4.1, provided they satisfy the initial conditions.

**Initial conditions.** We now prove that the limit functions satisfy the initial conditions. From the continuous embedding results (3.3) and (3.4), we have

$$\begin{aligned}
 \mathcal{W}_{2,2}^1(0, T; \mathcal{H}^1(\Omega), \mathcal{H}^{-1}(\Omega)) &\hookrightarrow \mathcal{C}([0, T]; \mathcal{L}_2(\Omega)), \\
 \phi \in \mathcal{W}_{2,2}^\alpha(0, T; \phi_0, \mathcal{L}_2(\Omega), \mathcal{L}_2(\Omega)) &\implies (g_{1-\alpha} * (\phi - \phi_0))(t) \in \mathcal{C}([0, T]; \mathcal{L}_2(\Omega)),
 \end{aligned}$$

yields  $\psi, \chi \in \mathcal{C}([0, T]; \mathcal{L}_2(\Omega))$  and  $(g_{1-\alpha} * (\phi - \phi_0))(t) \in \mathcal{C}([0, T]; \mathcal{L}_2(\Omega))$ . Let  $\eta \in \mathcal{C}^1([0, T]; \mathbb{R})$  with  $\eta(T) = 0$  and  $\eta(0) = 1$ . Then for all  $\xi_1 \in \mathcal{H}^1(\Omega), \xi_4 \in \mathcal{H}_{0, \Sigma_2}^1(\Omega)$ , we have

$$\begin{aligned}
 \int_0^T (\partial_t (g_{1-\alpha} * (\phi - \phi_0))(t), \eta(t)\xi_1) dt &= - \int_0^T ((g_{1-\alpha} * (\phi - \phi_0))(t), \eta'(t)\xi_1) dt \\
 &\quad - ((g_{1-\alpha} * (\phi - \phi_0))(0), \xi_1), \\
 \int_0^T \langle \partial_t \psi, \eta(t)\xi_4 \rangle dt &= - \int_0^T (\psi(t), \eta'(t)\xi_4) dt - (\psi(0), \xi_4).
 \end{aligned}$$

Taking the limit  $m \rightarrow \infty$ , we have

$$\begin{aligned}
 &- \int_0^T ((g_{1-\alpha} * (\phi^m - \phi^m(0)))(t), \eta'(t)\xi_1) dt - ((g_{1-\alpha} * (\phi^m - \phi^m(0)))(0), \xi_1) \\
 &\rightarrow - \int_0^T ((g_{1-\alpha} * (\phi - \phi_0))(t), \eta'(t)\xi_1) dt - (0, \xi_1), \\
 &- \int_0^T (\psi^m(t), \eta'(t)\xi_4) dt - (\psi^m(0), \xi_4) \rightarrow - \int_0^T (\psi(t), \eta'(t)\xi_4) dt - (\psi_0, \xi_4).
 \end{aligned}$$

Comparing, we have  $(g_{1-\alpha} * (\phi - \phi_0))(0) = 0$  and  $\psi(0) = \psi_0$ . Analogously, we get  $\chi(0) = \chi_0$ .

**REMARK 4.1** The result  $(g_{1-\alpha} * (\phi - \phi_0))(0) = 0$  does not imply  $\phi(0) = \phi_0$ . However, the function  $\phi_0$  plays the role of an initial data for  $\phi$  in a weak sense. Suppose,  $\phi$  and  $\partial_t (g_{1-\alpha} * (\phi - \phi_0))(t)$  are in

$\mathcal{C}([0, T]; \mathcal{L}_2(\Omega))$  and  $(g_{1-\alpha} * (\phi - \phi_0))(0) = 0$ , then we have  $\phi \in \mathcal{C}([0, T]; \mathcal{L}_2(\Omega))$  and  $\phi(0) = \phi_0$ , see Zacher (2009).

**Estimates for the weak solution.** We know that norms are weakly (also weakly-\*) lower semicontinuous and using the weak convergences in (4.29)

$$\begin{aligned} & \|\phi\|_{\mathcal{L}_2(0,T;\mathcal{L}_2(\Omega))}^2 + \|\mu\|_{\mathcal{L}_2(0,T;\mathcal{H}^1(\Omega))}^2 + \|\mathbf{u}\|_{\mathcal{L}_2(0,T;\mathcal{H}^1(\Omega;\mathbb{R}^d))}^2 + \|\psi\|_{\mathcal{L}_2(0,T;\mathcal{H}^1(\Omega))}^2 + \|\chi\|_{\mathcal{L}_2(0,T;\mathcal{H}^1(\Omega))}^2 \\ & \leq \liminf_{m \rightarrow \infty} \left( \|\phi^m\|_{\mathcal{L}_2(0,T;\mathcal{L}_2(\Omega))}^2 + \|\mu^m\|_{\mathcal{L}_2(0,T;\mathcal{H}^1(\Omega))}^2 + \|\mathbf{u}^m\|_{\mathcal{L}_2(0,T;\mathcal{H}^1(\Omega;\mathbb{R}^d))}^2 \right. \\ & \quad \left. + \|\psi^m\|_{\mathcal{L}_2(0,T;\mathcal{H}^1(\Omega))}^2 + \|\chi^m\|_{\mathcal{L}_2(0,T;\mathcal{H}^1(\Omega))}^2 \right), \\ & \leq C \left( \text{IC} + C_f + C_g + \|S_\psi\|_{\mathcal{L}_2(0,T;\mathcal{L}_2(\Omega))}^2 + \|S_\chi\|_{\mathcal{L}_2(0,T;\mathcal{L}_2(\Omega))}^2 + \|\psi_b\|_{\mathcal{L}_2(0,T;\mathcal{L}_2(\partial\Omega \setminus \Sigma_2))}^2 \right. \\ & \quad \left. + \|\chi_b\|_{\mathcal{L}_2(0,T;\mathcal{L}_2(\partial\Omega \setminus \Sigma_2))}^2 \right), \end{aligned}$$

where the final bound is obtained from (4.21), and IC is as defined in the theorem statement.

#### 4.4 Uniqueness

Now we prove the uniqueness of the weak solution under the assumption of Lipschitz continuity of the nonlinear functions. We assume that there exist two weak solutions  $(\phi_1, \mu_1, \mathbf{u}_1, \psi_1, \chi_1)$  and  $(\phi_2, \mu_2, \mathbf{u}_2, \psi_2, \chi_2)$  to the system and prove that these two solutions have to be identical. Introducing the following notations:

$$\begin{aligned} \tilde{\phi} &:= \phi_1 - \phi_2, \quad \tilde{\mu} := \mu_1 - \mu_2, \quad \tilde{\mathbf{u}} := \mathbf{u}_1 - \mathbf{u}_2, \\ \tilde{\psi} &:= \psi_1 - \psi_2, \quad \tilde{\chi} := \chi_1 - \chi_2, \\ f_1 - f_2 &:= f(\phi_1, \psi_1) - f(\phi_2, \psi_2), \quad g_1 - g_2 := g(\phi_1, \chi_1) - g(\phi_2, \chi_2), \end{aligned}$$

we see that  $(\tilde{\phi}, \tilde{\mu}, \tilde{\mathbf{u}}, \tilde{\psi}, \tilde{\chi})$  satisfies

$$(\partial_t^\alpha \tilde{\phi}, \xi_1) + (M_\phi \nabla \tilde{\mu}, \nabla \xi_1) = N_\phi(f_1 - f_2, \xi_1) - P_\phi(g_1 - g_2, \xi_1), \tag{4.32a}$$

$$(\tilde{\mu}, \xi_2) = c(\tilde{\phi}, \xi_2) + \lambda(\nabla \cdot \tilde{\mathbf{u}}, \xi_2), \tag{4.32b}$$

$$2G(\boldsymbol{\varepsilon}(\tilde{\mathbf{u}}), \boldsymbol{\varepsilon}(\xi_3)) + \frac{2G\nu}{1-2\nu}(\nabla \cdot \tilde{\mathbf{u}}, \nabla \cdot \xi_3) = -\lambda(\tilde{\phi}, \nabla \cdot \xi_3), \tag{4.32c}$$

$$\langle \partial_t \tilde{\psi}, \xi_4 \rangle + (M_\psi \nabla \tilde{\psi}, \nabla \xi_4) = -N_\psi(f_1 - f_2, \xi_4), \tag{4.32d}$$

$$\langle \partial_t \tilde{\chi}, \xi_4 \rangle + (M_\chi \nabla \tilde{\chi}, \nabla \xi_4) = -N_\chi(\tilde{\chi}, \xi_4) - P_\chi(g_1 - g_2, \xi_4). \tag{4.32e}$$



By choosing the test functions  $\tilde{\mu}(t), \partial_t^\alpha \tilde{\phi}(t) + \tilde{\mu}(t), \partial_t^\alpha \tilde{\mathbf{u}}(t) + \tilde{\mathbf{u}}, \tilde{\psi}(t), \tilde{\chi}(t)$  for equations (4.34a)-(4.34e), respectively, and proceeding as in the existence part, we have

$$\begin{aligned} \frac{c}{2} \|\tilde{\phi}(t)\|^2 + M_0 \left( g_\alpha * \|\nabla \tilde{\mu}\|^2 \right) (t) &\leq C \left( g_\alpha * \|\tilde{\phi}\|^2 \right) (t) + \frac{N_\phi}{2} \left( g_\alpha * \|f_1 - f_2\|^2 \right) (t) \\ &\quad + \frac{P_\phi}{2} \left( g_\alpha * \|g_1 - g_2\|^2 \right) (t), \end{aligned} \tag{4.33a}$$

$$\|\tilde{\mu}\| \leq c\|\tilde{\phi}\| + \lambda\|\nabla \cdot \tilde{\mathbf{u}}\|, \tag{4.33b}$$

$$2G\|\boldsymbol{\varepsilon}(\tilde{\mathbf{u}})\|^2 + \frac{G\nu}{1-2\nu}\|\nabla \cdot \tilde{\mathbf{u}}\|^2 \leq \frac{\lambda^2(1-2\nu)}{4G\nu}\|\tilde{\phi}\|^2, \tag{4.33c}$$

$$\frac{1}{2}\|\tilde{\psi}(t)\|^2 + M_0 \int_0^t \|\nabla \tilde{\psi}(s)\|^2 ds \leq \left( \frac{N_\psi}{2} + 1 \right) \int_0^t \|\tilde{\psi}(s)\|^2 ds + \frac{N_\psi}{2} \int_0^t \|f_1 - f_2\|^2 ds, \tag{4.33d}$$

$$\frac{1}{2}\|\tilde{\chi}(t)\|^2 + M_0 \int_0^t \|\nabla \tilde{\chi}(s)\|^2 ds \leq \left( N_\chi + \frac{P_\chi}{2} + \frac{1}{2} \right) \int_0^t \|\tilde{\chi}(s)\|^2 ds + \frac{P_\chi}{2} \int_0^t \|g_1 - g_2\|^2 ds. \tag{4.33e}$$

We observe that

$$\int_0^t \|\varphi(s)\|^2 ds \leq t^{1-\alpha} \Gamma(\alpha) (g_\alpha * \|\varphi\|^2)(t).$$

Adding (4.35a), (4.35d) and (4.35e), using the Lipschitz condition on the nonlinear functions and the above estimate, we have

$$\|\tilde{\phi}(t)\|^2 + \|\tilde{\psi}(t)\|^2 + \|\tilde{\chi}(t)\|^2 \leq C \left( g_\alpha * \left( \|\tilde{\phi}\|^2 + \|\tilde{\psi}\|^2 + \|\tilde{\chi}\|^2 \right) \right) (t).$$

Applying the generalized Gronwall-Bellman Lemma 3.3, we have  $\|\tilde{\phi}(t)\| = \|\tilde{\psi}(t)\| = \|\tilde{\chi}(t)\| = 0$ , almost everywhere in  $[0, T]$ . Further, we have from (4.35c) using Korn’s inequality (3.5), and from (4.35b) that that  $\|\tilde{\mathbf{u}}\|_{\mathcal{H}^1(\Omega)} = \|\tilde{\mu}\| = 0$ , almost everywhere in  $[0, T]$ .

### 5. Numerical discretization

The system (2.10) can be written in the form

$$\partial_t^\alpha (\mathbf{X} - \mathbf{X}_0) = \mathbf{F}(t, \mathbf{X}(t)), \quad \mathbf{X} = (\phi, \psi, \chi), \quad \boldsymbol{\alpha} = (\alpha, 1, 1), \tag{5.1}$$

with

$$\partial_t^\alpha (\mathbf{X} - \mathbf{X}_0) = \begin{bmatrix} \partial_t^\alpha (\phi - \phi_0) \\ \partial_t \psi \\ \partial_t \chi \end{bmatrix}, \quad \mathbf{F}(t, \mathbf{X}(t)) = \begin{bmatrix} \nabla \cdot (M_\phi(\phi, \psi, \chi) \nabla \mu) + N_\phi f(\phi, \psi) - P_\phi g(\phi, \chi) \\ \nabla \cdot (M_\psi(\phi, \psi, \chi) \nabla \psi) + S_\psi - N_\psi f(\phi, \psi) \\ \nabla \cdot (M_\chi(\phi, \psi, \chi) \nabla \chi) - N_\chi \chi + S_\chi - P_\chi g(\phi, \chi) \end{bmatrix} \tag{5.2}$$

and  $\mu = \mu(\phi)$  implicitly defined via (2.10b)-(2.10c). In (5.1),  $X_0 = (\phi_0, \psi_0, \chi_0)$  is the initial condition.

In our simulations, time discretization is performed using a first order quadrature scheme, of which we now recall the main features.

For ease of presentation, we focus on a single scalar equation. Convolution quadrature schemes approximate the Riemann–Liouville derivative  $\partial_t^\alpha \varphi$  (2.6) of some function  $\varphi = \varphi(t)$  by a discrete convolution, see for instance Lubich (1986, 1988) for seminal papers and Zeng *et al.* (2013) and Jin *et al.* (2016) for application to partial differential equations. Let  $t_n = nT/N_t$ , for  $n \in \{0, 1, \dots, N_t\}$ , be a subdivision of  $[0, T]$  in  $N_t$  equispaced time intervals of size  $\Delta t := T/N_t$ . Assuming  $\varphi(0) = 0$ , we approximate the Riemann–Liouville time derivative of a function  $\varphi$  by

$$\partial_t^\alpha \varphi \approx \bar{\partial}_t^\alpha \varphi := \frac{1}{(\Delta t)^\alpha} \sum_{j=0}^{N_t} b_j \varphi_{n-j}, \tag{5.3}$$

where  $\varphi_{n-j}$  is the approximation to  $\varphi(t_{n-j})$ . The quadrature weights  $(b_j)_{j \geq 1}$  are the coefficients in the power series expansion of  $\omega^\alpha(\zeta)$ , with  $\omega(\zeta) = \frac{\sigma(1/\zeta)}{\rho(1/\zeta)}$  the generating function of a linear multistep method (Lubich, 1988). When  $\varphi(0) = \varphi_0 \neq 0$ , we have a discretization to the Caputo derivative by applying (5.3) to  $\varphi - \varphi_0$ . From (5.3) we see that the memory effect of the fractional time derivative translates, numerically, to the fact that the value of the solution at some time step depends on its values at all previous time steps. In the backward differentiation formula of first order, also known as Grünwald–Letnikov approximation (Dumitru *et al.*, 2012, Section 2.1.2), the quadrature weights are defined recursively by

$$b_0 = 1, \quad b_j = -\frac{\alpha - j + 1}{j} b_{j-1} \quad \text{for } j \geq 1. \tag{5.4}$$

For  $\alpha = 1$ ,  $b_j = 0$  for  $j \geq 2$ , (5.3) coincides with the implicit Euler method. We refer to Jin *et al.* (2016, Section 4) for a detailed summary on the derivation of higher order convolution quadrature schemes together with their convergence properties.

Applying the scheme (5.3)–(5.4) to (5.1) and denoting by  $\phi_n \approx \phi(t_n)$ ,  $\psi_n \approx \psi(t_n)$ ,  $\chi_n \approx \chi(t_n)$  the approximate solutions at time  $t_n$ ,  $n = 1, \dots, N_t$ , we arrive at the following system of equations:

$$\sum_{j=0}^n b_j (\phi_{n-j} - \phi_0) = (\Delta t)^\alpha \nabla \cdot (M_\phi \nabla \mu_n) + (\Delta t)^\alpha N_\phi f(\phi_n, \psi_n) - (\Delta t)^\alpha P_\phi g(\phi_n, \chi_n) \tag{5.5a}$$

$$\psi_n - \psi_{n-1} = (\Delta t) \nabla \cdot (M_\psi \nabla \psi_n) - (\Delta t) N_\psi f(\phi_n, \psi_n) + (\Delta t) S_\psi \tag{5.5b}$$

$$\chi_n - \chi_{n-1} = (\Delta t) \nabla \cdot (M_\chi \nabla \chi_n) - (\Delta t) N_\chi \chi_n - (\Delta t) P_\chi g(\phi_n, \chi_n) + S_\chi, \tag{5.5c}$$

where

$$\mu_n = c\phi_n + \lambda \nabla \cdot \mathbf{u}_n, \tag{5.5d}$$

$$0 = \nabla \cdot \left( 2G\boldsymbol{\varepsilon}(\mathbf{u}_n) + \frac{2G\nu}{1-2\nu} \text{tr}(\boldsymbol{\varepsilon}(\mathbf{u}_n))\mathbb{I} + \lambda\phi_n\mathbb{I} \right). \tag{5.5e}$$

We obtain an algebraic system using a Galerkin approach with linear finite elements. Namely, let  $\mathcal{T}^h$  be a quasiuniform family of triangulations of  $\Omega$ ,  $h$  denoting the mesh width. For simplicity, we assume that  $\cup_{T \in \mathcal{T}^h} \bar{T} = \bar{\Omega}$ , which holds in all our numerical experiments. The piecewise linear finite element space is defined as

$$\mathcal{V}^h = \{\varphi \in \mathcal{C}(\bar{\Omega}) : \varphi|_T \in P_1(T), \forall T \in \mathcal{T}^h\} \subset \mathcal{H}^1(\Omega),$$

where  $P_1(T)$  denotes the set of all affine functions on  $T$ . As in the previous section, we assume that  $\tilde{\psi}_b \equiv 0$  and  $\tilde{\chi}_b \equiv 0$ . We formulate the discrete problem as follows: at the  $n$ -th time step, find

$$\phi_n, \mu_n \in \mathcal{V}^h, \mathbf{u}_n \in \left(\mathcal{V}^h \cap \mathcal{H}_{0,\Sigma_1}^1(\Omega)\right)^d, \psi_n, \chi_n \in \mathcal{V}^h \cap \mathcal{H}_{0,\Sigma_2}^1(\Omega)$$

such that, for all test functions  $\varphi_1, \varphi_4 \in \mathcal{V}^h, \varphi_2, \varphi_3 \in \mathcal{V}^h \cap \mathcal{H}_{0,\Sigma_2}^1(\Omega)$  and  $\varphi_5 \in \left(\mathcal{V}^h \cap \mathcal{H}_{0,\Sigma_1}^1(\Omega)\right)^d$ ,

$$\begin{aligned} (\psi_n, \varphi_2) + (\Delta t)(M_\psi \nabla \psi_n, \nabla \varphi_2) &= (\psi_{n-1}, \varphi_2) - (\Delta t)N_\psi(f(\phi_n, \psi_n), \varphi_2) \\ &\quad + (\Delta t)(S_\psi, \varphi_2) + (\Delta t)(\psi_b, \varphi_2)_{\partial\Omega \setminus \Sigma_2} \end{aligned} \quad (5.6a)$$

$$\begin{aligned} (\chi_n, \varphi_3) + (\Delta t)(M_\chi \nabla \chi_n, \nabla \varphi_3) + (\Delta t)N_\chi(\chi_n, \varphi_3) &= (\chi_{n-1}, \varphi_3) - (\Delta t)P_\chi(g(\phi_n, \chi_n), \varphi_3) + (\Delta t)(S_\chi, \varphi_3) \\ &\quad + (\Delta t)(\chi_b, \varphi_3)_{\partial\Omega \setminus \Sigma_2} \end{aligned} \quad (5.6b)$$

$$\begin{aligned} b_0(\phi_n, \varphi_1) + (\Delta t)^\alpha (M_\phi \nabla \mu_n, \nabla \varphi_1) &= - \sum_{j=1}^{n-1} b_j((\phi_{n-j} - \phi_0), \varphi_1) + (\Delta t)^\alpha (b_0 \phi_0, \varphi_1) \\ &\quad + (\Delta t)^\alpha N_\phi(f(\phi_n, \psi_n), \varphi_1) - (\Delta t)^\alpha P_\phi(g(\phi_n, \chi_n), \varphi_1) \end{aligned} \quad (5.6c)$$

$$(\mu_n, \varphi_4) - c(\phi_n, \varphi_4) - \lambda(\nabla \cdot \mathbf{u}_n, \varphi_4) = 0 \quad (5.6d)$$

$$2G(\boldsymbol{\varepsilon}(\mathbf{u}_n), \boldsymbol{\varepsilon}(\varphi_5)) + \frac{2G\nu}{1-2\nu}(\nabla \cdot \mathbf{u}_n, \nabla \cdot \varphi_5) = -\lambda(\phi_n, \nabla \cdot \varphi_5) \quad (5.6e)$$

(here we have rearranged the order of the equations for easier explanation in the upcoming remarks). This is a non-linear, coupled algebraic system with unknowns  $\phi_n, \mu_n, \mathbf{u}_n, \psi_n, \chi_n$ . At each time step, we solve this system with a fixed point iteration. In our experiments, we set the termination criteria for the latter to be a maximum of 50 iterations and a maximum tolerance for the relative error between two iterates of  $\text{TOL}=10^{-6}$ . For all experiments in the next section, this tolerance was always reached within less than 10 fixed point iterations.

The procedure described in this section has been implemented in FEniCS (Alnæs *et al.*, 2015), using version 2019.1.0. of the DOLFIN library (Logg *et al.*, 2012), to obtain the numerical results shown in the next section.

**REMARK 5.1** Equations (5.6a)-(5.6b) are decoupled from (5.6d)-(5.6e) and they are coupled with (5.6c) just through the non-linear terms on the right-hand side involving the functions  $f$  and  $g$ , respectively. This can be exploited to improve efficiency when solving the non-linear system: in the spirit of a Gauss-Seidel method, at each fixed point iteration one can first update  $\psi_n$  and  $\chi_n$  with (5.6a)-(5.6b) using the

TABLE 1 *Parameter values used in the simulations of Section 6, unless otherwise stated*

Equation	Parameter values													
	$M_\phi$	$N_\phi$	$K_\psi$	$P_\phi$	$c$	$\lambda$	$G$	$\nu$	$M_\psi$	$N_\psi$	$M_\chi$	$N_\chi$	$P_\chi$	$K_\chi$
(2.10a)	0.0001	0.6	2	1.1										
(2.10b)					0.4	0.002								
(2.10c)							0.4615	0.3						
(2.10d)									1	40				
(2.10e)											1	3	30	0.6

previous iterate of  $\phi_n$  on the right-hand side, and then insert these updated values in the right-hand side of (5.6c) and solve the last three coupled equations to update  $\phi_n, \mu_n$  and  $\mathbf{u}_n$ .

REMARK 5.2 When using first order finite elements, further efficiency can be gained by using mass lumping (Quarteroni & Valli, 2008, Sect.11.4) in (5.6d). More precisely, if in the first two terms in (5.6d) we approximate the mass matrix by its lumped version (which is diagonal), the latter can be inverted cheaply and we can express explicitly the coefficients vector of  $\mu_n$  (with respect to the finite element basis functions) in terms of the coefficient vectors for  $\phi_n$  and  $\mathbf{u}_n$ . Using the resulting expression for the coefficient vector of  $\mu_n$  in (5.6c) allows to eliminate (5.6d) from the system of equations and thus to reduce the system’s size.

### 6. Numerical simulations

In this section, we present the numerical approximations of the variables  $\phi, \mu, \mathbf{u}, \psi, \chi$  in the model (2.10) with a two-dimensional domain  $\Omega = (0, 1)^2$ . In Section 6.1, we study the effects of introducing the fractional time derivative in the reaction–diffusion model, neglecting mechanical effects and in absence of treatment. We next introduce, in Section 6.2, the coupling with mechanical forces, still in absence of treatment. Finally, in Section 6.3, we consider the effect of chemotherapeutic agents, including a periodic source for the treatment.

Where not otherwise stated, we choose the parameters to have the dimensionless values listed in Table 1. We have  $M_\phi \ll M_\psi, M_\chi$  because the tumour diffuses at a much lower speed compared to how fast the nutrient and chemotherapeutic agents diffuse. We set  $N_\phi \ll N_\psi$  because the nutrient rate of decrease is much faster than the proliferation rate of the tumour due to the nutrient consumption (usually a tumour can at most double its size in one day) and, for similar reasons, we have  $P_\phi \ll P_\chi$ . The half maximum value  $K_\psi$  has been chosen to be lower than the maximum concentration reached by the nutrient, in order to observe both effects of low-density limited and maximum capacity-limited growth of the tumour. Accordingly,  $K_\chi$  has been chosen to be lower than the maximum concentration reached by the chemotherapeutic agents. The degradation rate  $N_\chi$  is large compared to the other coefficients in the reaction terms of the equation for the chemotherapeutic substances because the latter degrade quite fast (their half-time is usually a couple of hours). The parameters  $c, \lambda, G$  and  $\nu < 0.5$  have been selected to be in the ranges considered in (Lima et al., 2016).

In the simulations, we have set  $\Delta t = 1/15$  for the time stepping and we have discretized the domain  $\Omega$  using a regular, triangular mesh with mesh size  $h = \sqrt{2}/150$  for all simulations but those in Figs 1 and 2, where we have used a finer mesh with  $h = \sqrt{2}/200$  to have a more precise computation of the radius of the tumour.

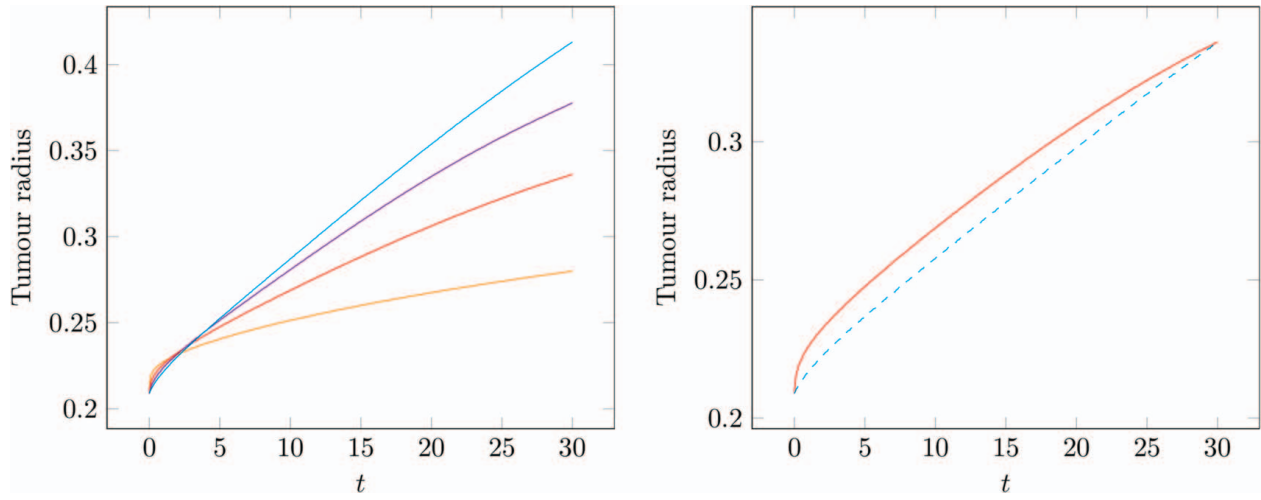


FIG. 1. Reaction–diffusion model and circular initial condition (6.1) with  $a = 0.22$  and  $b = 0.05$ . Left: evolution of radius of the tumour over time with parameters as in Table 1 and  $\alpha = 0.25$ (orange—),  $\alpha = 0.5$  (red—),  $\alpha = 0.75$  (violet—) and  $\alpha = 1$  (cyan—). Right: evolution of the radius over time for parameters as in Table 1 and  $\alpha = 0.5$  (red—), same line as in the left plot, and  $M_\phi = 0.0001/1.803, N_\phi = 0.6/1.803$  and  $\alpha = 1$  (cyan—)

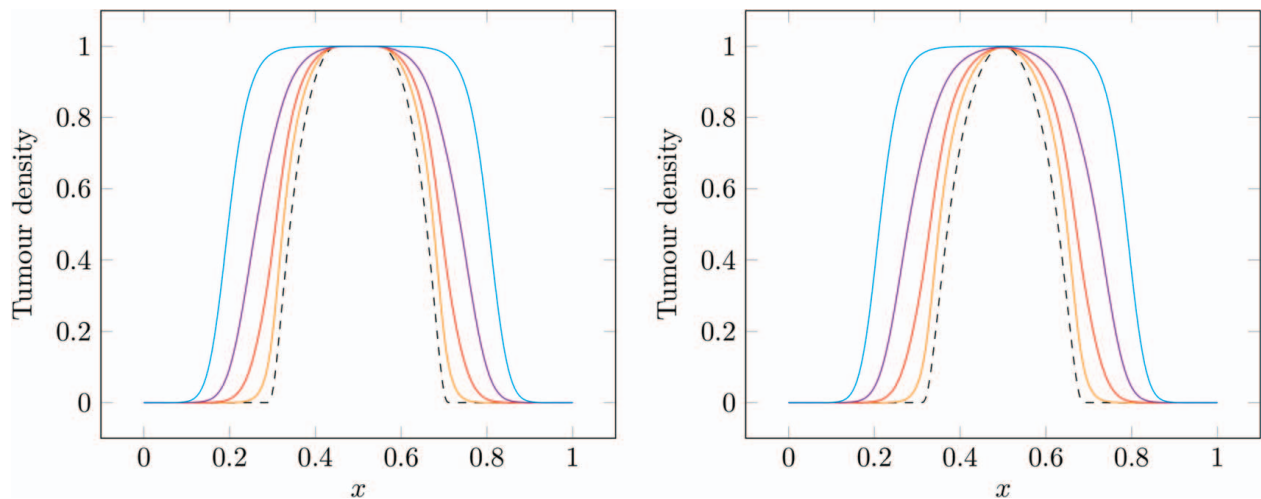


FIG. 2. Reaction–diffusion model and circular initial condition. Cross-section of the tumour density along the  $x$ -axis at  $T = 30$  for  $\alpha = 0.25$  (orange—),  $\alpha = 0.5$  (red—),  $\alpha = 0.75$  (violet—) and  $\alpha = 1$  (cyan—). Left: results for initial condition (6.1) with  $a = 0.22$  and  $b = 0.05$ . Right: results for initial condition (6.1) with  $a = 0.2$  and  $b = 0$ . In both plots, the dashed line depicts the initial condition.

We refer to the quantities  $\int_\Omega \phi(\mathbf{x}, t) d\mathbf{x}$ ,  $\int_\Omega \psi(\mathbf{x}, t) d\mathbf{x}$  and  $\int_\Omega \chi(\mathbf{x}, t) d\mathbf{x}$  as the tumour, nutrient and chemotherapy mass, respectively. Since  $\phi$  is a volume fraction, the mass of the tumour is technically given by  $\int_\Omega \rho \phi(\mathbf{x}, t) d\mathbf{x}$ , but, since we assume  $\rho$  to be constant,  $\int_\Omega \phi(\mathbf{x}, t) d\mathbf{x}$  is the mass up to rescaling.

### 6.1 Reaction-diffusion system without treatment

The goal of this section is to show the basic effects of introducing a fractional time derivative and the new modelling possibilities that it offers. For this, we consider the reaction–diffusion model (2.10a),

(2.10b) and (2.10d) with the parameters  $\lambda = 0, P_\phi = 0$ , in which case we have two variables  $\phi$  and  $\psi$ . For both  $\phi$  and  $\psi$  we impose homogeneous Neumann boundary conditions and a constant nutrient is supplied over the whole domain by setting  $S_\psi \equiv 0.5$ .

We first consider the evolution of a circular tumour and then of a tumour concentration having, initially, two disconnected components.

For the circular tumour, we consider the initial conditions

$$\phi_0(\mathbf{x}) = \begin{cases} 1 & \text{if } \|\mathbf{x} - \mathbf{c}\| \leq b, \\ \exp\left(1 - \frac{(a-b)^2}{(a-b)^2 - (\|\mathbf{x} - \mathbf{c}\| - b)^2}\right) & \text{if } b < \|\mathbf{x} - \mathbf{c}\| \leq a, \\ 0 & \text{otherwise,} \end{cases} \quad (6.1)$$

and  $\psi_0 \equiv 0$ . We first set  $\mathbf{c} = (0.5, 0.5), a = 0.22$  and  $b = 0.05$ . A cross section of (6.1) along the  $x$ -axis is depicted in the left plot of Fig. 2, dashed line.

Experiments with *in vitro* cell cultures as well as *in vivo* data (Jiang *et al.*, 2014) have shown that the growth of the tumour size over time can have different power law exponents depending on the type of cells and the surrounding environment. For this reason, we have tracked the radius of the tumour over time for different values of  $\alpha$ , whose results are shown in Fig. 1, left plot. Here we have defined the radius of the tumour as

$$R(t) = \operatorname{argmax}_{\|\mathbf{x} - \mathbf{c}\|, \mathbf{x} \in \Omega} \{ \phi(\mathbf{x}, t) \geq R_{thresh} \},$$

with  $R_{thresh}$  a threshold value that we have set to  $10^{-3}$ . The left plot in Fig. 1 clearly shows that, by varying  $\alpha$ , the radius grows with different power laws. This means that, if one is only interested in predicting the tumour size at a certain time, then a reaction-diffusion model with properly tuned diffusion and reaction coefficients would be sufficient. However, if one is interested in the dynamics, then the model with fractional exponent can express behaviours that cannot be modelled with an integer order model with time-constant coefficients. To show this, we have taken  $\alpha = 1$  and tuned  $M_\phi$  and  $N_\phi$  in order to obtain the same radius at  $t = 30$  as the one obtained with  $\alpha = 0.5$  and parameters as in Table 1. The results are shown in the right plot in Fig. 1, where, for  $\alpha = 1$ , we have taken  $M_\phi = 0.0001/1.803$  and  $N_\phi = 0.6/1.803$ . We see that, with the new values for  $M_\phi$  and  $N_\phi$ , the model with integer order time derivative can predict the same radius for the tumour at  $t = 30$  as  $\alpha = 0.5$  and the parameters in Table 1. However, the dynamics is quite different in the two cases.

The left plot in Fig. 2 shows a cross section along the  $x$  axis of the density of the tumour at final time  $T = 30$ . For reference, the dashed line is the initial condition. We observe that the spreading of the tumour is very sensitive to  $\alpha$ , and when  $\alpha$  is large, the spreading is faster. When  $\alpha$  is smaller, not only the tumour grows more slowly, but the interface between the tumour and the surrounding tissue is less sharp. The initial condition (6.1) has a plateau around the centre of the domain where the tumour density is 1. A question that can arise is what happens when we start with an initial condition, which has no plateau. To test this, we have run a second experiment with  $b = 0$  and  $a = 0.2$ . The cross section of the tumour density at  $T = 30$  is shown in the right plot of Fig. 2, where again the dashed line refers to the initial condition. Here we can observe that, for  $\alpha < 1$ , the tumour grows over time without forming a plateau in the centre, which happens for  $\alpha = 1$ . Such different behaviour is not surprising if one notices that varying the fractional exponent is not a simple re-scaling of the time variable and it introduces instead different nonlinear behaviours in the model.

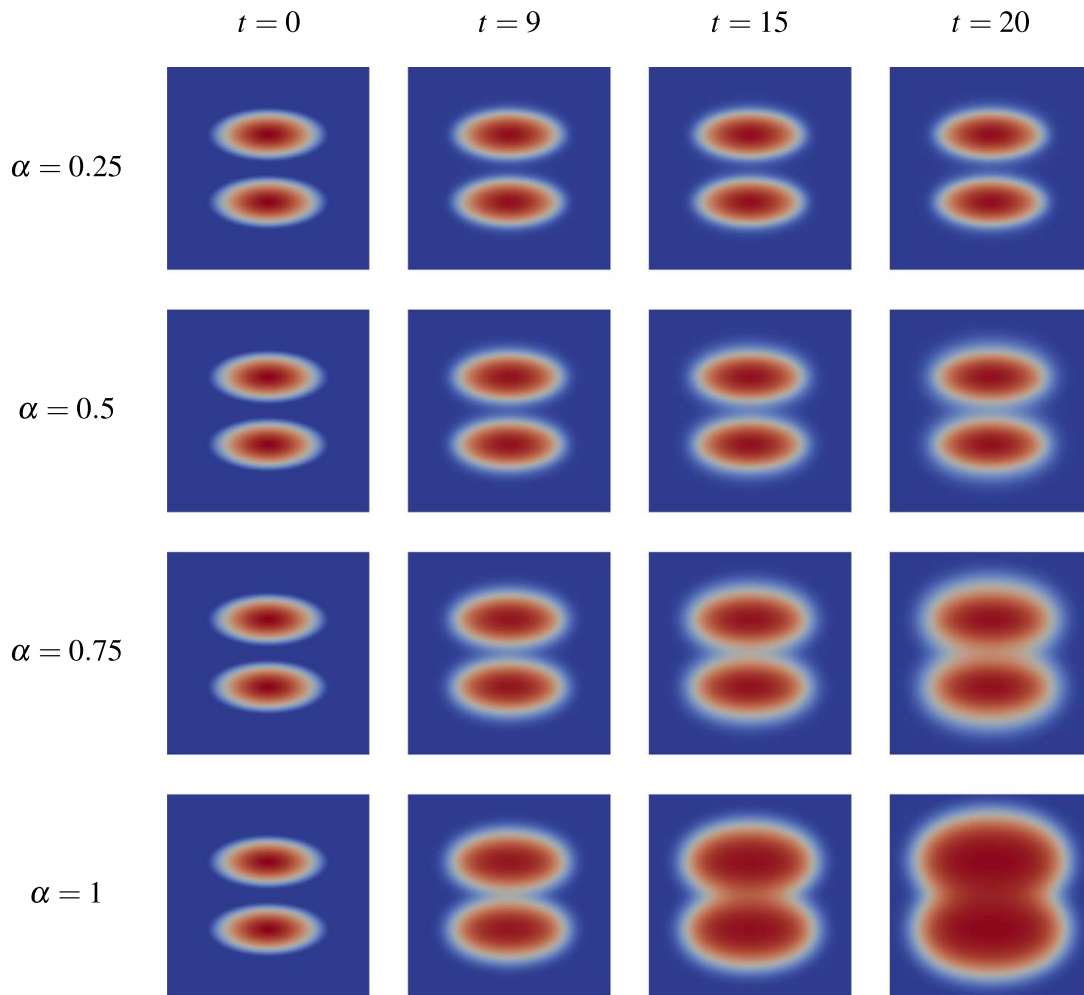


FIG. 3. Reaction–diffusion model with two ellipses as initial condition. Zoom in  $[0.2, 0.8]^2$  of tumour volume fraction for different values of  $\alpha$  at different times using a constant nutrient source  $S_\psi \equiv 0.5$ . The range for the colorbar has been fixed to be  $[0, 1]$  for all plots.

We now consider an initial condition with two disconnected components, namely, two initially separated elliptical tumour masses:

$$\phi_0(\mathbf{x}) = \begin{cases} \exp\left(1 - \frac{a^2}{a^2 - \|A(\mathbf{x} - \mathbf{c}_1)\|^2}\right) & \text{if } \|A(\mathbf{x} - \mathbf{c}_1)\| \leq a, \\ \exp\left(1 - \frac{a^2}{a^2 - \|A(\mathbf{x} - \mathbf{c}_2)\|^2}\right) & \text{if } \|A(\mathbf{x} - \mathbf{c}_2)\| \leq a, \\ 0 & \text{otherwise,} \end{cases} \quad (6.2)$$

with  $A = \begin{pmatrix} 1 & 0 \\ 0 & \gamma \end{pmatrix}$ ,  $\gamma = \sqrt{5}$ ,  $\mathbf{c}_1 = (0.5, 0.6)$ ,  $\mathbf{c}_2 = (0.5, 0.4)$  and  $a = 0.2$ . This initial condition is depicted in the first column of Fig. 3. As before, we take  $\psi_0 \equiv 0$ . The evolutions of the tumour for four values of  $\alpha$  are depicted in Fig. 3. There, we can see that different values of the fractional exponent affect the coalescence speed of the two ellipses: the smaller the  $\alpha$ , the lower the speed at which they merge. Moreover, as in the circular tumour case, we see that, the larger the  $\alpha$ , the sharper the interface

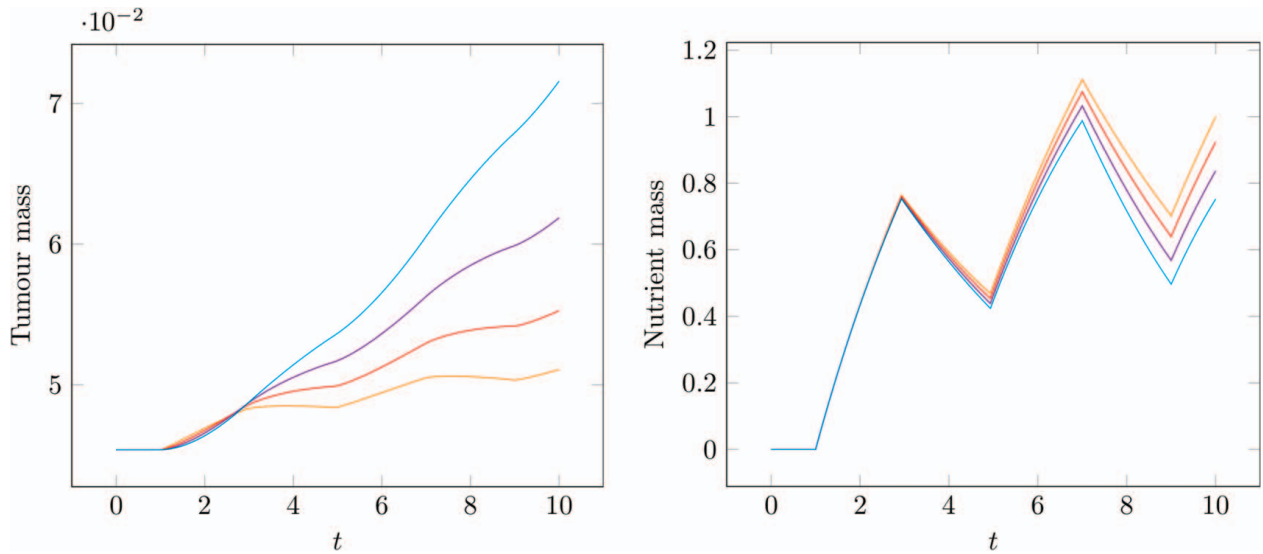


FIG. 4. Reaction–diffusion model with two ellipses as initial condition. Tumour mass ( $\int_{\Omega} \phi \, dx$ ) and nutrient mass ( $\int_{\Omega} \psi \, dx$ ) over time obtained by giving a periodic nutrient source (6.3), for different values of the fractional exponent: orange— $\alpha = 0.25$ , red— $\alpha = 0.5$ , violet— $\alpha = 0.75$ , cyan— $\alpha = 1$ .

between the tumour and the healthy tissue (compare for instance  $\alpha = 1$  at  $t = 9$  with  $\alpha = 0.75$  at  $t = 15$  and  $t = 20$ ). Similar observations were made in Liu *et al.* (2018) in a fractional phase-field model for porous media applications.

In the experiments shown so far, we have used a time-constant supply of nutrient, meaning a strictly increasing tumour mass over time. To observe the effects of varying  $\alpha$  in a more dynamic setting, we still consider the initial condition (6.2) but now a periodic source of nutrient, i.e. we set:

$$S_{\psi}(t) = \begin{cases} 0.5 & \text{if } 1 < t \leq 3 \text{ or } 5 < t \leq 7 \text{ or } 9 < t \leq 10, \\ 0 & \text{otherwise.} \end{cases} \quad (6.3)$$

The mass of the tumour and nutrient up to  $T = 10$  are depicted in Fig. 4, left and right plot, respectively. Regarding the tumour evolution, we observe conservation of mass up to  $t = 1$ , because of no nutrient supply and homogeneous Neumann boundary conditions. For  $1 < t \leq 3$ , we can see that, in the beginning, the tumour grows faster over time when  $\alpha$  is smaller and it grows faster for  $\alpha$  larger as time passes. We notice that, when the nutrient is again not provided, for  $3 < t \leq 5$  (and for  $7 < t \leq 9$ ), the tumour keeps growing nevertheless, because there is still some nutrient in the domain, and it grows faster for larger  $\alpha$ . Regarding the nutrient, we see that, for  $1 < t \leq 3$ , the nutrient consumption is approximately the same for all values of  $\alpha$ , while, for longer times, the larger the  $\alpha$ , the larger the nutrient uptake. This can be expected from the fact, that, for later times, the tumour mass is larger for  $\alpha$  large and therefore it consumes more nutrient.

## 6.2 Reaction-diffusion system with mechanical coupling in absence of treatment

The goal of this section is to show results of the reaction-diffusion model with a mechanical coupling as given in (2.10c), and (2.10d) with  $P_{\phi} = 0$ , in which case we have four variables. We use homogeneous Neumann boundary conditions for  $\phi, \mu, \psi$ , for  $\mathbf{u}$  we use homogeneous Dirichlet boundary condition on



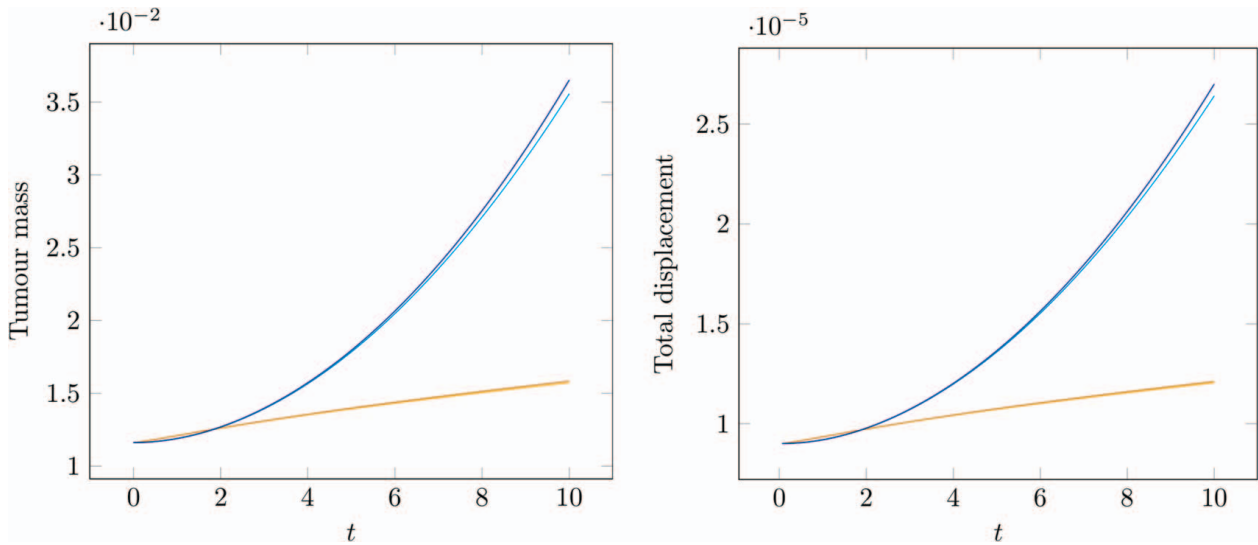


FIG. 5. Reaction–diffusion model with mechanical coupling and initial condition (6.4). Evolution of tumour mass ( $\int_{\Omega} \phi \, dx$ ) and of total displacement ( $\int_{\Omega} |\mathbf{u}| \, dx$ ) over time: yellow  $(0, 0.35, 1, 0)$ —  $\alpha = 0.25$  and constant coefficients, orange  $(0.8, 0.5, 0.2)$ —  $\alpha = 0.25$  and spatially varying coefficients, cyan—  $\alpha = 1$  and constant coefficients, blue  $(0, 0, 0.6)$ —  $\alpha = 1$  and spatially varying coefficients.

the left boundary and homogeneous Neumann elsewhere. We give a constant nutrient source  $S_{\psi} \equiv 0.5$ . We consider both constant coefficients  $M_{\phi}, M_{\psi}$  as from Table 1 and spatially varying ones, given by  $\tilde{M}_{\phi} = M_{\phi} \exp(5(y - 0.5)), \tilde{M}_{\psi} = M_{\psi} \exp(5(y - 0.5))$ , with again  $M_{\phi}, M_{\psi}$  as from Table 1. We note that both constants and non-constant coefficients take the same value at the centre of the domain, where we locate the irregularly shaped initial tumour mass

$$\begin{cases} \exp\left(1 - \frac{1}{1-f(x)}\right) & \text{if } f(x) < 1, -0.45 < x < 0.2, -0.4 < y < 0.35, \\ 0 & \text{otherwise,} \end{cases} \tag{6.4}$$

where  $f(x) = \sin(6x + 2y + 1)(7x - 0.2)^2 + \sin(-8x + 10y + 1.1)(9x - 0.1)^2$ . This initial condition is depicted in the left plot of Fig. 7. As in the previous experiments,  $\psi_0 \equiv 0$ . In this section, we compare the results when using  $\alpha = 0.25$  and  $\alpha = 1$ .

Figure 5 shows the evolution of tumour mass and of the total displacement  $\int_{\Omega} |\mathbf{u}| \, dx$  over time, when using constant and non-constant coefficients. In both cases, we observe that, apart from the very beginning, the tumour grows faster for  $\alpha = 1$ , and consequently, the displacement of the tumour is larger in this case. It is then for  $\alpha = 1$  that, for later times, we can observe some difference between the case of constant and non-constant coefficients. The fact that the tumour grows more when  $\alpha = 1$  can also be seen in the cross sections along the  $y$ -axis at time  $T = 10$  in Fig. 6 (tumour density in the left plot and modulus of the displacement in the right plot), where the dotted lines denote the corresponding initial conditions: we note that for  $\alpha = 0.25$  the shapes of the solutions at  $T = 10$  are closer to the initial conditions than for  $\alpha = 1$ , for both constant and spatially-varying coefficients. Furthermore, in Fig. 6 we see that the spatial variability of the coefficients (in the  $y$ -direction) translates in a more pronounced asymmetry of the solution with respect to the  $y$ -axis. Regarding the displacement, the asymmetry is

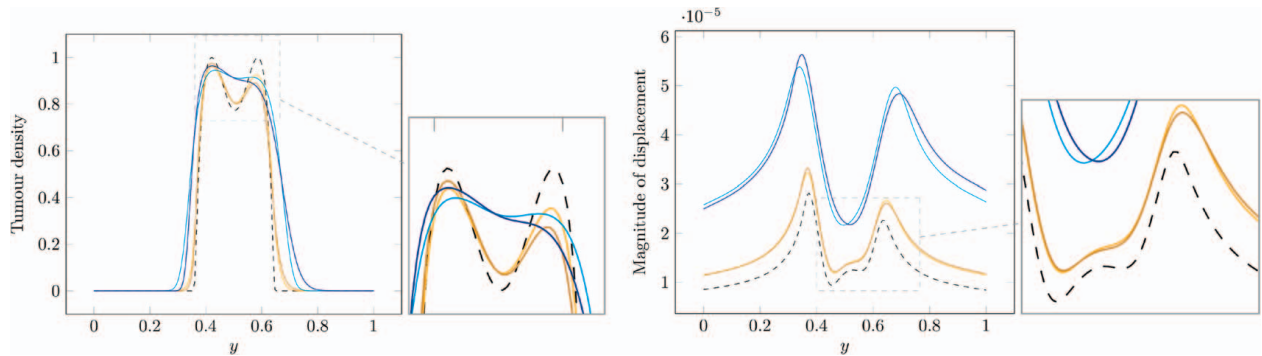


FIG. 6. Reaction–diffusion model with mechanical coupling and initial condition (6.4). Cross-sections along the  $y$ -axis at  $T = 10$ : yellow— $\alpha = 0.25$ , constant coefficients, orange— $\alpha = 0.25$ , spatially varying coefficients cyan— $\alpha = 1$ , constant coefficients, blue— $\alpha = 1$ , spatially varying coefficients. Left: cross section of the tumour volume fraction. Right: cross-section of the modulus of the displacement. The dashed lines denote the corresponding initial conditions.

more evident when  $\alpha = 1$ , because there the magnitude of the displacement is larger compared to when  $\alpha = 0.25$ .

### 6.3 Reaction-diffusion system with mechanical coupling and chemotherapy

In this section, we show simulations of a more realistic situation and include the treatment of cancer by giving chemotherapeutic agents. In all, we have five unknowns, solving (2.10a)-(2.10e). In the previous sections, nutrient supply with a source term for the nutrient could be thought as a situation close to an *in vitro* setting, where nutrients are added directly in the wells. Here, we assume nutrients and chemotherapeutic agents to be supplied through some blood vessels, which are around the tumour area, and so we take zero source functions  $S_\psi = S_\chi \equiv 0$  and non-homogeneous Dirichlet boundary conditions for  $\psi$  and  $\chi$ , over the whole boundary. We take  $\tilde{\psi}_b \equiv 2$  as Dirichlet boundary condition for the nutrient and

$$\tilde{\chi}_b(t) = \begin{cases} 1 & \text{if } t \leq 2 \text{ or } 6 < t \leq 8 \text{ or } 12 < t \leq 14, \\ 0 & \text{otherwise,} \end{cases}$$

for the chemotherapeutic agents, which are usually administered in cycles.

The boundary conditions for  $\phi$ ,  $\mu$  and  $\mathbf{u}$  are as in the previous section. We plot the mass of the tumour and chemotherapy for different values of  $\alpha$ . The initial condition for the tumour is the one with irregular shape as in the previous section and in the left plot of Fig. 7. We take  $\chi_0 \equiv 0$  for the chemotherapeutic agents. For the nutrient, we take an initial condition with values close to the concentration of the nutrient at equilibrium, namely, we take  $\psi_0(\mathbf{x}) = 2 - 0.5x(1 - x)y(1 - y)$ .

The tumour densities at  $T = 20$  for  $\alpha = 0.25$  and  $\alpha = 1$  are shown in the centre and right plot of Fig. 7, respectively (the left plot showing the initial condition). Figure 8 shows the evolution of the tumour mass (left) and of the mass of chemotherapeutic agents for different values of the fractional exponent. From the left plot, we see that the response of the tumour to the therapy in the model depends sensitively on  $\alpha$ : the smaller the  $\alpha$ , the more nonlinear the responses to applying or removing the supply of chemotherapeutic substances. One could also think about using a piecewise constant  $\alpha$ , one for when chemotherapy is supplied, one when it is not, in order to model a different response of the tumour in

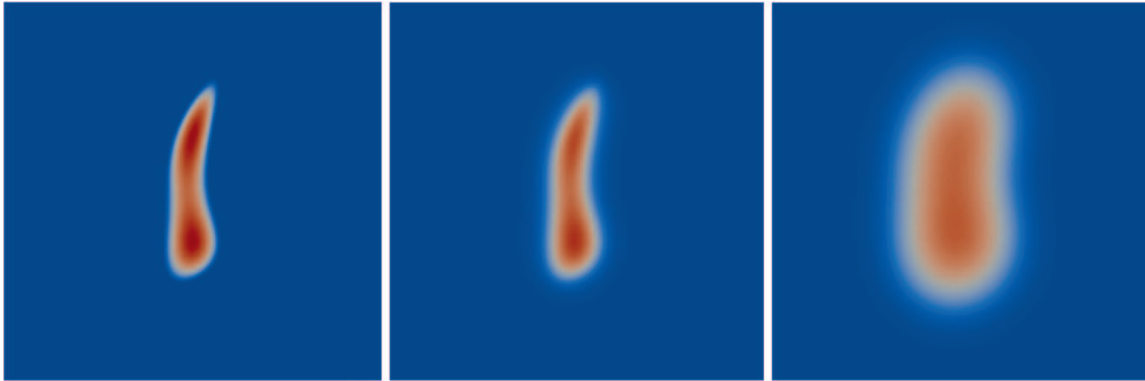


FIG. 7. Left: zoom in  $[0.2, 0.8]^2$  of initial condition for the tumour with irregular shape. Centre and right: reaction–diffusion model with mechanical coupling and treatment, zoom in  $[0.2, 0.8]^2$  of tumour density at  $T = 20$  for  $\alpha = 0.25$  (centre) and  $\alpha = 1$  (right). The range for the colorbar has been fixed to be  $[0, 1]$  for all plots.

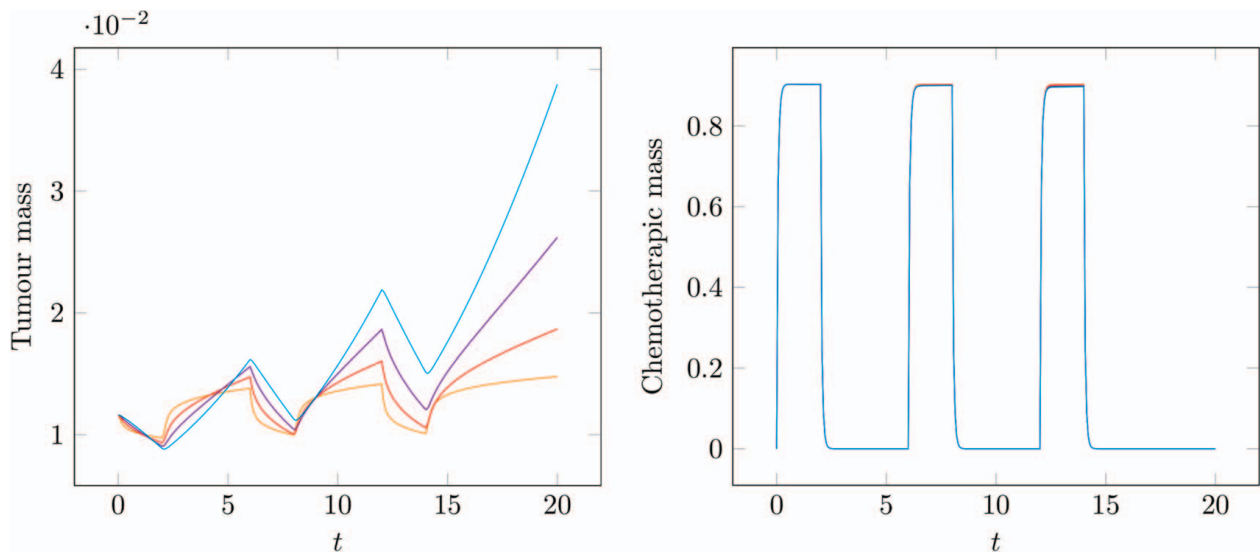


FIG. 8. Reaction–diffusion model with mechanical coupling and treatment and initial condition (6.4). Tumour mass ( $\int_{\Omega} \phi \, dx$ ) and chemotherapy mass ( $\int_{\Omega} \chi \, dx$ ) over time: orange— $\alpha = 0.25$ , red— $\alpha = 0.5$ , violet— $\alpha = 0.75$ , cyan— $\alpha = 1$ .

these two scenarios. The mass of chemotherapy over time is instead very similar for all values of  $\alpha$ . In particular, when administration of the chemotherapeutic agents is interrupted, their concentration drops quickly to 0 because of the degradation term ( $-N_{\chi} \chi$ ) in (2.10e).

## 7. Conclusions

We have presented a new model for tumour growth with fractional time derivatives, including mechanical effects and treatment by chemotherapy. Existence and uniqueness of a weak solution to the coupled, nonlinear model are obtained by a Galerkin method. Numerical experiments, based on low order finite elements in space and convolution quadrature in time, show that the order of the fractional time derivative influences strongly the evolution. Using the fractional order as an additional parameter

results in a larger model class. This can be of future interest for calibration of the model parameters by experimental data.

### Acknowledgements

The authors would like to thank Prof. Rico Zacher (University of Ulm) for very insightful discussions.

### Funding

Deutsche Forschungsgemeinschaft (DFG) through TUM International Graduate School of Science and Engineering (GSC 81); Laura Bassi Postdoctoral Fellowship (Technical University of Munich; to M.L.R.); and DFG (WO-671 11-1 to M.F., L.S. and B.W.).

### Conflict of interest

The authors declare that there is no conflict of interest.

### REFERENCES

- AKILANDEESWARI, A., BALACHANDRAN, K. & ANNAPOORANI, N. (2017) Solvability of hyperbolic fractional partial differential equations. *J. Appl. Anal. Comput.*, **7**, 1570–1585.
- ALLEN, M., CAFFARELLI, L. & VASSEUR, A. (2016) A parabolic problem with a fractional time derivative. *Arch. Ration. Mech. Anal.*, **221**, 603–630.
- ALNÆS, M., BLECHTA, J., HAKE, J., JOHANSSON, A., KEHLET, B., LOGG, A., RICHARDSON, C., RING, J., ROGNES, M. E. & WELLS, G. N. (2015) The FEniCS project version 1.5. *Arch. Numer. Softw.*, **3**.
- BALKWILL, F. R., CAPASSO, M. & HAGEMANN, T. (2012) The tumor microenvironment at a glance. *J. Cell Sci.*, **125**, 5591–5596.
- BARTKOWIAK, E. & PAWŁOW, I. (2005) The Cahn-Hilliard-Gurtin system coupled with elasticity. *Control Cybern.*, **34**, 1005–1043.
- BOYER, F. & FABRIE, P. (2013) *Mathematical Tools for the Study of the Incompressible Navier–Stokes Equations and Related Models*. New York: Springer.
- BREZIS, H. (2010) *Functional Analysis, Sobolev Spaces and Partial Differential Equations*. New York: Springer.
- CARRIVE, M., MIRANVILLE, A., PIÉTRUS, A. & RAKOTOSON, J. (1999) The Cahn-Hilliard equation for an isotropic deformable continuum. *Appl. Math. Lett.*, **12**, 23–28.
- CIARLET, P. G. (2013) *Linear and Nonlinear Functional Analysis with Applications*. Philadelphia: SIAM.
- COMPTE, A. (1996) Stochastic foundations of fractional dynamics. *Phys. Rev. E*, **53**, 4191.
- DIETHELM, K. (2010) *The Analysis of Fractional Differential Equations: An Application-Oriented Exposition using Differential Operators of Caputo Type*. Berlin: Springer.
- DJILALI, L. & ROUGIREL, A. (2018) Galerkin method for time fractional diffusion equations. *J. Elliptic Parabol. Equ.*, **4**, 349–368.
- DUMITRU, B., KAI, D. & ENRICO, S. (2012) *Fractional Calculus: Models and Numerical Methods*. New Jersey: World Scientific.
- EVANS, L. C. (2010) *Partial Differential Equations*. Providence: American Mathematical Society.
- FAGHIHI, D., FENG, X., LIMA, E., ODEN, J. T. & YANKEELOV, T. E. (2020) A coupled mass transport and deformation theory of multi-constituent tumor growth. *J. Mech. Phys. Solids*, **139**, 1–13.
- FEDOTOV, S. & IOMIN, A. (2007) Migration and proliferation dichotomy in tumor-cell invasion. *Phys. Rev. Lett.*, **98**, 118101.
- FRTZ, M., LIMA, E., NIKOLIC, V., ODEN, J. T. & WOHLMUTH, B. (2019a) Local and nonlocal phase-field models of tumor growth and invasion due to ECM degradation. *Math. Models Methods Appl. Sci.*, **29**, 2433–2468.

- FRITZ, M., LIMA, E., ODEN, J. T. & WOHLMUTH, B. (2019b) On the unsteady Darcy-Forchheimer-Brinkman equation in local and nonlocal tumor growth models. *Math. Models Methods Appl. Sci.*, **29**, 1691–1731.
- GARCKE, H. (2003) On Cahn–Hilliard systems with elasticity. *Proceedings of the Royal Society of Edinburgh Section A: Mathematics*, **133**, 307–331.
- GARCKE, H. (2005a) Mechanical effects in the Cahn-Hilliard model: a review on mathematical results. *Mathematical Methods and Models in Phase Transitions* (A. MIRANVILLE ed). Nova Science Publ, pp. 43–77.
- GARCKE, H. (2005b) *On a Cahn-Hilliard Model for Phase Separation with Elastic Misfit*, vol. **22**, pp. 165–185.
- GARCKE, H. & LAM, K. F. (2017) Well-posedness of a Cahn–Hilliard system modelling tumour growth with chemotaxis and active transport. *Eur. J. Appl. Math.*, **28**, 284–316.
- GARCKE, H., LAM, K. F. & SIGNORI, A. (2019) On a phase field model of Cahn-Hilliard type for tumour growth with mechanical effects. *Nonlinear Analysis: Real World Applications*, **57**, 1–28.
- GORENFLO, R., LUCHKO, Y. & YAMAMOTO, M. (2015) Time-fractional diffusion equation in the fractional Sobolev spaces. *Frac. Calc. Appl. Anal.*, **18**, 799–820.
- GRIPENBERG, G., LONDEN, S. O. & STAFFANS, O. (1990) *Volterra Integral and Functional Equations. Encyclopedia of Mathematics and Its Applications*. Cambridge: Cambridge University Press.
- HELMLINGER, G., NETTI, P. A., LICHTENBELD, H. C., MELDER, R. J. & JAIN, R. K. (1997) Solid stress inhibits the growth of multicellular tumor spheroids. *Nat. Biotechnol.*, **15**, 778–783.
- HENRY, B., LANGLANDS, T. & WEARNE, S. (2006) Anomalous diffusion with linear reaction dynamics: from continuous time random walks to fractional reaction-diffusion equations. *Phys. Rev. E*, **74**, 031116.
- HORMUTH, D. A., ELDRIDGE, S. L., WEIS, J. A., MIGA, M. I. & YANKEELOV, T. E. (2018) Mechanically coupled reaction-diffusion model to predict glioma growth: methodological details. *Cancer Systems Biology*. Springer, pp. 225–241.
- IOMIN, A. (2005a) Fractional transport of tumor cells. *WSEAS Trans. Biol. Biomed.*, **2**, 82–86.
- IOMIN, A. (2005b) Superdiffusion of cancer on a comb structure. *Journal of Physics: Conference Series*, vol. 7. IOP Publishing, p. 57.
- IOMIN, A. (2007) Fractional transport of cancer cells due to self-entrapment by fission. *Mathematical Modeling of Biological Systems*. Springer, vol. I. pp. 193–203.
- IOMIN, A. (2015) Continuous time random walk and migration–proliferation dichotomy of brain cancer. *Biophys. Rev. Lett.*, **10**, 37–57.
- JIANG, C., CUI, C., LI, L. & SHAO, Y. (2014) The anomalous diffusion of a tumor invading with different surrounding tissues. *PLoS One*, **9**, e109784:1–16.
- JIN, B., LAZAROV, R. & ZHOU, Z. (2016) Two fully discrete schemes for fractional diffusion and diffusion-wave equations with nonsmooth data. *SIAM J. Sci. Comput.*, **38**, A146–A170.
- KEMPPAINEN, J., SILJANDER, J., VERGARA, V. & ZACHER, R. (2016) Decay estimates for time-fractional and other non-local in time subdiffusion equations in  $\mathbb{R}^d$ . *Math. Annal.*, **366**, 941–979.
- KILBAS, A. A., SRIVASTAVA, H. M. & TRUJILLO, J. J. (2006) *Theory and Applications of Fractional Differential Equations*, vol. 204 (North-Holland Mathematics Studies). Amsterdam: Elsevier.
- LI, L. & LIU, J.-G. (2018a) A generalized definition of Caputo derivatives and its application to fractional ODEs. *SIAM J. Math. Anal.*, **50**, 2867–2900.
- LI, L. & LIU, J.-G. (2018b) Some compactness criteria for weak solutions of time fractional PDEs. *SIAM J. Math. Anal.*, **50**, 3963–3995.
- LIMA, E., ODEN, J. T., HORMUTH, D., YANKEELOV, T. & ALMEIDA, R. (2016) Selection, calibration, and validation of models of tumor growth. *Math. Models Methods Appl. Sci.*, **26**, 2341–2368.
- LIMA, E., ODEN, J. T., WOHLMUTH, B., SHAHMORADI, A., HORMUTHII, D., YANKEELOV, T., SCARABOSIO, L. & HORGER, T. (2017) Selection and validation of predictive models of radiation effects on tumor growth based on noninvasive imaging data. *Comput. Methods Appl. Mech. Eng.*, **327**, 277–305.
- LIONS, J. L. & MAGENES, E. (2012) *Non-homogeneous Boundary Value Problems and Applications I*. Berlin: Springer.
- LIU, H., CHENG, A., WANG, H. & ZHAO, J. (2018) Time-fractional Allen–Cahn and Cahn–Hilliard phase-field models and their numerical investigation. *Comput. Math. Appl.*, **76**, 1876–1892.

- LOGG, A., WELLS, G. N. & HAKE, J. (2012) DOLFIN: A C++/Python finite element library. *Automated Solution of Differential Equations by the Finite Element Method*. Springer, pp. 173–225.
- LUBICH, C. (1986) Discretized fractional calculus. *SIAM J. Math. Anal.*, **17**, 704–719.
- LUBICH, C. (1988) Convolution quadrature and discretized operational calculus. I. *Numerische Mathematik*, **52**, 129–145.
- MANIMARAN, J., SHANGERGANESH, L., DEBBOUCHE, A. & ANTONOV, V. (2019) Numerical solutions for time-fractional cancer invasion system with nonlocal diffusion. *Front. Phys.*, **7**, 93. doi: [10.3389/fphy](https://doi.org/10.3389/fphy).
- MCLEAN, W., MUSTAPHA, K., ALI, R. & KNIO, O. (2019) Well-posedness of time-fractional advection-diffusion-reaction equations. *Fract. Calc. Appl. Anal.*, **22**, 918–944.
- MCLEAN, W., MUSTAPHA, K., ALI, R. & KNIO, O. M. (2020) Regularity theory for time-fractional advection-diffusion-reaction equations. *Comput. Math. Appl.*, **79**, 947–961.
- METZLER, R. & KLAFTER, J. (2000) The random walk's guide to anomalous diffusion: a fractional dynamics approach. *Phys. Rep.*, **339**, 1–77.
- MIRANVILLE, A. (2001) Long-time behavior of some models of Cahn-Hilliard equations in deformable continua. *Nonlinear Anal. Real World Appl.*, **2**, 273–304.
- MIRANVILLE, A. (2003) Generalized Cahn-Hilliard equations based on a microforce balance. *J. Appl. Math.*, **2003**, 165–185.
- NEPOMNYASHCHY, A. (2016) Mathematical modelling of subdiffusion-reaction systems. *Math. Model. Nat. Phenom.*, **11**, 26–36.
- OUEDJEDI, Y., ROUGIREL, A. & BENMERIEM, K. (2019) Galerkin method for time fractional semilinear equations. *Preprint*, HAL-02124150.
- PREZIOSI, L. E. (2003) *Cancer Modelling and Simulation*. Boca Raton: Chapman & Hall/CRC Mathematical Biology and Medicine Series.
- QUARTERONI, A. & VALLI, A. (2008) *Numerical Approximation of Partial Differential Equations*, vol. 23. Springer Science & Business Media. Berlin: Springer.
- ROBINSON, J. C. (2001) *Infinite-Dimensional Dynamical Systems: An Introduction to Dissipative Parabolic PDEs and the Theory of Global Attractors*, vol. 28. Cambridge: Cambridge University Press.
- SEKI, K., WOJCIK, M. & TACHIYA, M. (2003) Recombination kinetics in subdiffusive media. *J. Chem. Phys.*, **119**, 7525–7533.
- SIMON, J. (1986) Compact sets in the space  $L^p(0, T; B)$ . *Ann. Mat. Pur. Appl.*, **146**, 65–96.
- TAHIR-KHELI, R. & ELLIOTT, R. (1983) Correlated random walk in lattices: tracer diffusion at general concentration. *Phys. Rev. B*, **27**, 844.
- VERGARA, V. & ZACHER, R. (2008) Lyapunov functions and convergence to steady state for differential equations of fractional order. *Math. Z.*, **259**, 287–309.
- WANG, M., ZHAO, J., ZHANG, L., WEI, F., LIAN, Y., WU, Y., GONG, Z., ZHANG, S., ZHOU, J., CAO, K., et al. (2017) Role of tumor microenvironment in tumorigenesis. *J. Cancer*, **8**, 761.
- YE, H., GAO, J. & DING, Y. (2007) A generalized Gronwall inequality and its application to a fractional differential equation. *J. Math. Anal. Appl.*, **328**, 1075–1081.
- YUAN, Y., JIANG, Y.-C., SUN, C.-K. & CHEN, Q.-M. (2016) Role of the tumor microenvironment in tumor progression and the clinical applications. *Oncol. Rep.*, **35**, 2499–2515.
- YUSTE, S., ACEDO, L. & LINDENBERG, K. (2004) Reaction front in an  $A + B \rightarrow C$  reaction-subdiffusion process. *Phys. Rev. E*, **69**. doi: [036126](https://doi.org/10.1103/PhysRevE.69.036126).
- ZACHER, R. (2009) Weak solutions of abstract evolutionary integro-differential equations in Hilbert spaces. *Funkc. Ekvacioj*, **52**, 1–18.
- ZACHER, R. (2019) *Time Fractional Diffusion Equations: Solution Concepts, Regularity, and Long-time Behavior*. Fractional Differential Equations, p. 159.
- ZENG, F., LI, C., LIU, F. & TURNER, I. (2013) The use of finite difference/element approaches for solving the time-fractional subdiffusion equation. *SIAM J. Sci. Comput.*, **35**, A2976–A3000.

**A. Existence Result for Nonlinear Finite Dimensional System**

Consider the multi-order fractional differential system of the form

$$\begin{aligned} \frac{d}{dt} (g_{1-\alpha_k} * (X_k(t) - X_{k,0})) (t) &= F_k(t, X_1(t), \dots, X_m(t)), \quad k = 1, \dots, m, \\ (g_{1-\alpha_k} * (X_k - X_{k,0})) (0) &= 0, \quad k = 1, \dots, m, \end{aligned} \tag{A.1}$$

where  $0 < \alpha_k \leq 1, X_k : [0, T] \rightarrow \mathbb{R}, F_k : [0, T] \times \mathbb{R}^m \rightarrow \mathbb{R}$  is such that  $F_k(\cdot, X_1, \dots, X_m) \in \mathcal{L}_2(0, T)$  and it is Lipschitz in the other variables. Existence of a solution to a similar system with continuous function  $F_k$  is given in (Diethelm, 2010, Lemma 5.3), here we prove the result in the vector form. In the vector notation, the system (A.1) can be written as

$$\begin{aligned} D^\alpha (X - X_0) &= F(t, X(t)), \\ (\mathbf{k} * (X - X_0)) (0) &= \mathbf{0}, \end{aligned} \tag{A.2}$$

where

$$\begin{aligned} D^\alpha (X - X_0) &= \frac{d}{dt} (\mathbf{k} * (X - X_0)) (t), \quad X(t) = \begin{pmatrix} X_1(t) \\ \vdots \\ X_m(t) \end{pmatrix}, \quad X_0 = \begin{pmatrix} X_{1,0} \\ \vdots \\ X_{m,0} \end{pmatrix}, \\ \mathbf{k}(t) &= \begin{pmatrix} g_{1-\alpha_1} & 0 & \dots & 0 \\ \vdots & & & \\ 0 & \dots & 0 & g_{1-\alpha_m} \end{pmatrix}, \quad F(t, X(t)) = \begin{pmatrix} F_1(t, X_1(t), \dots, X_m(t)) \\ \vdots \\ F_m(t, X_1(t), \dots, X_m(t)) \end{pmatrix}. \end{aligned}$$

LEMMA A.1 Let  $F(\cdot, X) \in \mathcal{L}_2(0, T; \mathbb{R}^m)$  for any  $X \in \mathbb{R}^m$  and  $X(\cdot) \in \mathcal{L}_2(0, T; \mathbb{R}^m)$ . Then  $X(t)$  satisfies (A.2) if, and only if,  $X(t)$  satisfies the following Volterra integral equation

$$X(t) = X_0 + \int_0^t \mathbf{l}(t-s)F(s, X(s))ds, \tag{A.3}$$

where

$$\mathbf{l}(t) = \begin{pmatrix} g_{\alpha_1} & 0 & \dots & 0 \\ \vdots & & & \\ 0 & \dots & 0 & g_{\alpha_m} \end{pmatrix}.$$

*Proof.* First we prove necessity. Let  $X(\cdot) \in \mathcal{L}_2(0, T; \mathbb{R}^m)$  satisfy (A.2). With the initial condition  $(\mathbf{k} * (X - X_0)) (0) = 0$  and the result  $\mathbf{l} * \mathbf{k} = \mathbf{1}$ , we have

$$\mathbf{l} * \frac{d}{dt} (\mathbf{k} * (X - X_0))(t) = \frac{d}{dt} (\mathbf{l} * \mathbf{k} * (X - X_0))(t). \tag{A.4}$$

Taking a convolution with  $\mathbf{l}$  on both sides of (A.2), using (A.4), we obtain (A.3), and hence the necessity is proved.

Now we prove the sufficiency. Let  $X(\cdot) \in \mathcal{L}_2(0, T; \mathbb{R}^m)$  satisfy (A.3). Taking a convolution with  $\mathbf{k}$  and differentiating on both sides of (A.3), using  $\mathbf{l} * \mathbf{k} = \mathbf{1}$ , we arrive at (A.2). Further from the continuity of  $(\mathbf{1} * F(t, X)) (t)$ , we have  $(\mathbf{1} * F(t, X(t))) (0) = 0$ , which implies  $(\mathbf{k} * (X - X_0)) (0) = \mathbf{0}$ , and this proves the sufficiency part. □

LEMMA A.2 (Banach Fixed point theorem)[(Kilbas *et al.*, 2006, Theorem 1.9)] Let  $(\mathcal{U}, d)$  be a nonempty complete metric space, let  $0 \leq \omega < 1$ , and let  $\Lambda : \mathcal{U} \rightarrow \mathcal{U}$  be a map such that, for every  $\varphi_1, \varphi_2 \in \mathcal{U}$ , the relation

$$d(\Lambda\varphi_1, \Lambda\varphi_2) \leq \omega d(\varphi_1, \varphi_2)$$

holds. Then the operator  $\Lambda$  has a unique fixed point  $\varphi^* \in \mathcal{U}$ . Furthermore, if  $\{\Lambda^k\}_{k \in \mathbb{N}}$  is the sequence of operators defined by

$$\Lambda^1 = \Lambda, \quad \Lambda^k = \Lambda\Lambda^{k-1}, \quad \forall k \in \mathbb{N} \setminus \{1\},$$

then, for any  $\varphi_0 \in \mathcal{U}$ , the sequence  $\{\Lambda^k \varphi_0\}_{k=1}^\infty$  converges to the above fixed point  $\varphi^*$ .

THEOREM A.1 The initial value problem given by the system of multi-order fractional differential equations along with the initial condition (A.1) has a uniquely determined solution on the interval  $[0, T]$ .

*Proof.* To prove the existence for the nonlinear differential equation (A.2) it is enough to show the existence to its equivalent integral equation (A.3) as shown in Lemma A.1. The nonlinear integral equation is converted to a linear integral equation and Banach fixed point theorem is used to show the existence of the unique solution to (A.3). For a particular  $Y \in \mathcal{L}_2(0, T; \mathbb{R}^m)$ , we obtain the corresponding linear equation to (A.3) as

$$X(t) = X_0 + \int_0^t I(t-s)F(s, Y(s))ds. \tag{A.5}$$

Define the operator  $\Lambda$  on  $\mathcal{U} := \mathcal{L}_2(0, T_h; \mathbb{R}^m)$  for some  $T_h > 0$  as

$$\Lambda Y(t) := X_0 + \int_0^t I(t-s)F(s, Y(s))ds.$$

Using Young’s inequality for convolution (3.6), we have

$$\begin{aligned} \|\Lambda Y\|_{\mathcal{L}_2(0, T_h; \mathbb{R}^m)}^2 &\leq C (\|X_0\|_{\mathbb{R}^m} + \|I\|_{\mathcal{L}_1(0, T_h; \mathbb{R}^m)} \|F(t, Y)\|_{\mathcal{L}_2(0, T_h; \mathbb{R}^m)}), \\ &\leq C (\|X_0\|_{\mathbb{R}^m} + \|I\|_{\mathcal{L}_1(0, T; \mathbb{R}^m)} (L_F \|Y\|_{\mathcal{L}_2(0, T_h; \mathbb{R}^m)} + \|F(t, \mathbf{0})\|_{\mathcal{L}_2(0, T; \mathbb{R}^m)})), \\ &\leq C \|Y\|_{\mathcal{L}_2(0, T_h; \mathbb{R}^m)}. \end{aligned} \tag{A.6}$$

This means that  $\Lambda$  maps  $\mathcal{U}$  into itself. Further we get

$$\begin{aligned} \|\Lambda Y - \Lambda Z\|_{\mathcal{L}_2(0, T_h; \mathbb{R}^m)} &\leq \| (I * (F(t, Y) - F(t, Z))) (t) \|_{\mathcal{L}_2(0, T_h; \mathbb{R}^m)}, \\ &\leq L_F \|I\|_{\mathcal{L}_1(0, T_h; \mathbb{R}^m)} \|Y - Z\|_{\mathcal{L}_2(0, T_h; \mathbb{R}^m)}. \end{aligned}$$

We choose  $T_h > 0$  such that  $L_F \|I\|_{\mathcal{L}_1(0, T_h; \mathbb{R}^m)} < 1$ , which means  $\Lambda$  is a contraction. By Lemma A.2 there exists a unique solution  $X \in \mathcal{L}_2(0, T_h; \mathbb{R}^m)$  to (A.5) on the interval  $[0, T_h]$ . Further we see that for any  $\tau \in (0, T)$ , we have by proceeding as before in (A.6)

$$\|X\|_{\mathcal{L}_2(0, \tau; \mathbb{R}^m)} \leq C,$$

for some constant independent of  $\tau$ . Therefore we obtain  $X \in \mathcal{L}_2(0, T; \mathbb{R}^m)$ . Then  $F \in \mathcal{L}_2(0, T; \mathbb{R}^m)$ , and the initial condition implies  $X \in \mathcal{W}_{2,2}^\alpha(0, T; X_0, \mathbb{R}^m, \mathbb{R}^m)$ .  $\square$